

Appendix F10

DHI Water & Environment Pty Ltd 2009

Hydrodynamic Model Validation at Scott Reef and Surrounds



BROWSE FLNG DEVELOPMENT
Draft Environmental Impact Statement

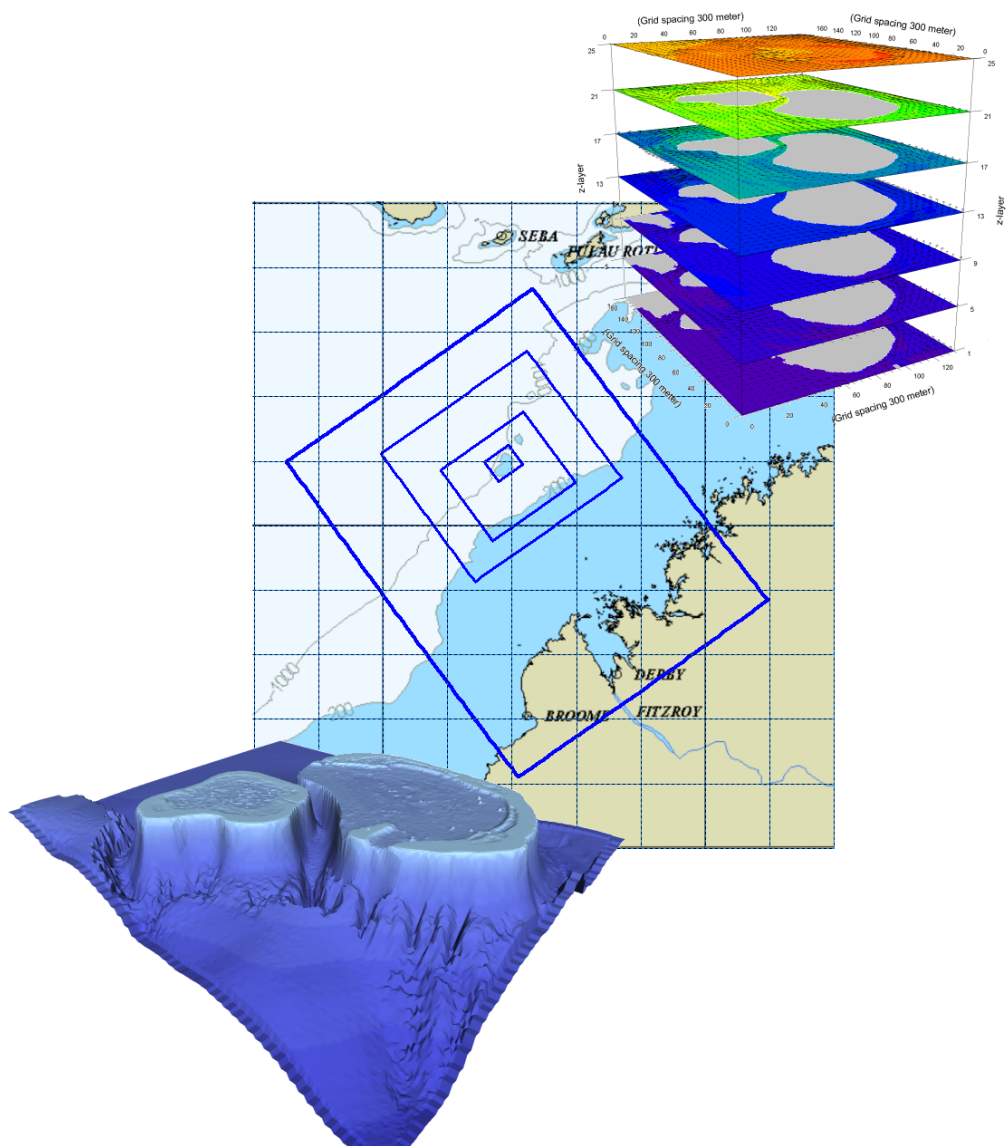
EPBC 2013/7079
November 2014

Browse Environmental Modelling – Phase 1

Hydrodynamic Model Validation at Scott Reef and Surrounds

Project No CTR9.301 and CTR9.303

Final Report, Revision 03





© DHI Water and Environment Pty Ltd 2009

The information contained in this document produced DHI Water and Environment Pty Ltd is solely for the use of the Client identified on the cover sheet for the purpose for which it has been prepared and DHI Water and Environment Pty Ltd undertakes no duty to or accepts any responsibility to any third party who may rely upon this document.

All rights reserved. No section or element of this document may be removed from this document, reproduced, electronically stored or transmitted in any form without the written permission of DHI Water and Environment Pty Ltd.

All hard copies of this document are "UNCONTROLLED DOCUMENTS". The "CONTROLLED" document is held in electronic form by DHI Water and Environment Pty Ltd.



CONTENTS

EXECUTIVE SUMMARY	III
1 INTRODUCTION.....	1
2 STUDY APPROACH	2
2.1 The Browse LNG Development	2
2.2 Scope of Study	4
2.3 Climate and Seasons	5
2.3.1 The Climate in the Northern Part of Australia.....	5
2.3.2 Seasonal Wind Patterns for the Study Area.....	5
2.4 Oceanographic and Meteorological Processes of Importance for Environmental Modelling of the Study Area.....	6
2.4.1 Overview	6
2.4.2 Wind, Waves and Currents.....	8
2.4.3 Internal Tides and Solitons.....	8
2.4.4 Large Scale Oceanographic Flows	10
3 MEASUREMENTS AVAILABLE FROM THE STUDY AREA	14
3.1 Requirements to a Measurement Programme	14
3.2 Browse Measurement Programme	16
3.3 Site Visit	21
4 SELECTION AND SET-UP OF 3-DIMENSIONAL MODEL	27
4.1 General.....	27
4.2 Overview of 3-Dimensional Models.....	27
4.2.1 DHI's 3-Dimensional Models	27
4.2.2 Other 3-Dimensional Models for the Study Area.....	29
4.3 Selection of 3-Dimensional Model	30
4.4 Model Set-up.....	35
4.4.1 General	35
4.4.2 Bathymetry and Computational Grid	35
4.4.3 Boundary Conditions.....	38
4.4.4 Initial Conditions	41
4.4.5 Meteorological Forcing and Heat Exchange	42
5 CALIBRATION AND VALIDATION OF 3-DIMENSIONAL MODEL.....	45
5.1 Selection of Calibration and Validation Periods.....	45
5.2 Basic Model Parameters	50
5.3 Calibration Parameters.....	50
5.4 Sensitivity Tests for Inclusion of Large Scale Eddies	51
5.5 Performance Criteria.....	52
5.6 Results of Model Calibration for Spring Period	53



5.7	Results of Model Validation for Summer Period	76
5.8	Results of Model Validation for Autumn Period.....	99
5.9	Results of Model Validation for Winter Period.....	108
5.10	Calibration With Surface Drifter Buoys	118
5.10.1	General	118
5.10.2	Comparison with Drifter Buoys Tracks within Scott Reef.....	119
5.10.3	Comparison with Drifter Buoys Tracks outside of Scott Reef.....	122
6	SUMMARY AND CONCLUSIONS	125
7	REFERENCES.....	129

APPENDIX A **SHORT DESCRIPTION OF MIKE 3 CLASSIC (FINITE DIFFERENCE VERSION) AND SHORT DESCRIPTION OF MIKE 3 FM (FINITE VOLUME VERSION)**

APPENDIX B **SPRING CALIBRATION PERIOD, COMPARISONS BETWEEN MEASUREMENTS AND MODEL SIMULATION AS ISOPLETH PLOTS, TIME SERIES PLOTS, Q-Q PLOTS AND FREQUENCY PLOTS**

APPENDIX C **SUMMER VALIDATION PERIOD, COMPARISONS BETWEEN MEASUREMENTS AND MODEL SIMULATION AS ISOPLETH PLOTS, TIME SERIES PLOTS, Q-Q PLOTS AND FREQUENCY PLOTS**

APPENDIX D **AUTUMN VALIDATION PERIOD, COMPARISONS BETWEEN MEASUREMENTS AND MODEL SIMULATION AS ISOPLETH PLOTS, TIME SERIES PLOTS, Q-Q PLOTS AND FREQUENCY PLOTS**

APPENDIX E **WINTER VALIDATION PERIOD, COMPARISONS BETWEEN MEASUREMENTS AND MODEL SIMULATION AS ISOPLETH PLOTS, TIME SERIES PLOTS, Q-Q PLOTS AND FREQUENCY PLOTS**

APPENDIX F **PEER REVIEW OF HYDRODYNAMIC MODEL AND BRECKNOCK-4 APPLICATION MODEL**

APPENDIX G **REPLY TO PEER REVIEW**



EXECUTIVE SUMMARY

The Browse LNG Development entails the development of three offshore gas-condensate fields in the Browse Basin. These fields are located on the North West Shelf, approximately 290 km from the Kimberley coast and 400 km north of Broome and in the vicinity of Scott Reef.

Woodside has commenced its environmental approval process for the upstream component of the development, and has identified that physical oceanographic modelling services will be required as part of the impact assessment for the Environmental Impact Statement.

The purpose of the present study has been to select, set-up, calibrate and validate a 3-dimensional hydrodynamic model for Scott Reef and the surrounding area in order to model the physical oceanography at Scott Reef and surrounds for the environmental approval process.

Wind, water level, current and water temperature measurements were available from a total of six locations within the study area covering periods of up to 12 months. This measurement duration was found to adequately capture the dominant physical phenomena that govern fluid transport and dispersion within the study region. Additionally, drifter buoy tracks were available.

The finite-difference non-hydrostatic version of DHI's 3-dimensional modelling system, MIKE 3 Classic, was selected and set-up with a resolution in the vertical of 20m (to a depth of about 500m) and in the horizontal resolution ranging from 300m at Scott Reef to 8100m in areas away from the study area.

The model was calibrated with the measurements for a 14 day period during the spring (or transition) season, and validated for a 14 day period during each of the other three seasons: summer (NW monsoon), autumn (transition) and winter (SE monsoon). The four periods were chosen to each cover a full spring-neap tidal period. The model results were compared to the measurements in a number of ways including time series plots, quantile-quantile plots and frequency plots. Additionally, a statistical analysis was carried out for key parameters. The drifter tracks were used for a calibration of the particle tracking module.

Modelling tides and temperature variations and the associated currents around two coral reef situated at the shelf break is a challenging task and raises the question about the importance of phenomena like upwelling between the reef, internal wave activity and large scale circulations. The model, which has been set-up and calibrated in the present study, has focussed on the ability to provide the 'Design' and environmental team with support in their decision making, and thus focussed on processes of importance for the modelling tasks required for this support.



1 INTRODUCTION

This report has been prepared for SKM/ERM (CES) by DHI Water & Environment Pty Ltd (DHI) and covers the scope of work as described in:

Browse LNG Development, CTR 9.301, Environmental Approvals, Phase 2B, Hydrodynamic Model for Scott Reef and Surrounds, Revision 0, dated 1/10/08

Plus an additional scope of work carried out as part of:

Browse LNG Development, CTR 9.303, Early Works and Approvals, Environmental Application Modelling for Scott Reef and Surrounds, Revision 0, dated 22/05/09

The end client for the study is Woodside Energy Ltd (WEL).

CTR 9.301 plus the additional scope of work covers the first part of the hydrodynamic modelling support services for the upstream component of the Browse LNG Development: The setup and validation of the hydrodynamic model for Scott Reef and Surrounds. It has been contracted under the Woodside CES Contract No. 0C00000246, and CES have sub-contracted the modelling component of these services to DHI.

The CTR 9.301 scope of work comprises three tasks:

- Task 1: Selection of appropriate hydrodynamic model
- Task 2: Validation of model with in-situ measurements
- Task 3: Validation of model with surface drifter buoys

While the additional scope of work under CTR 9.303 comprise:

- Inclusion of two additional validation periods
- An extended methodology and rationale
- Additional model sensitivity tests

The total scope of work is covered in the report as follows: This introduction (chapter 1) is followed by a description of the study approach in chapter 2 and a description of available measurements in chapter 3. The model selection and set-up are covered in chapter 4, while the calibration and validation is described in detail in chapters 5. Finally summary and conclusions are included in chapter 6.

The calibrated model shall be applied for engineering decision support and for the environmental approvals process as described in CTR 9.303.



2 STUDY APPROACH

2.1 The Browse LNG Development

The Browse LNG Development entails the development of three offshore gas-condensate fields in the Browse Basin, Torosa, Brecknock and Calliance. These fields are located on the North-west Shelf, approximately 290 km from the Kimberley coast and 400 km north of Broome in the vicinity of Scott Reef. An overview map and a more detailed map of the Notational Development Areas are shown in Fig 2.1 and Fig 2.2.

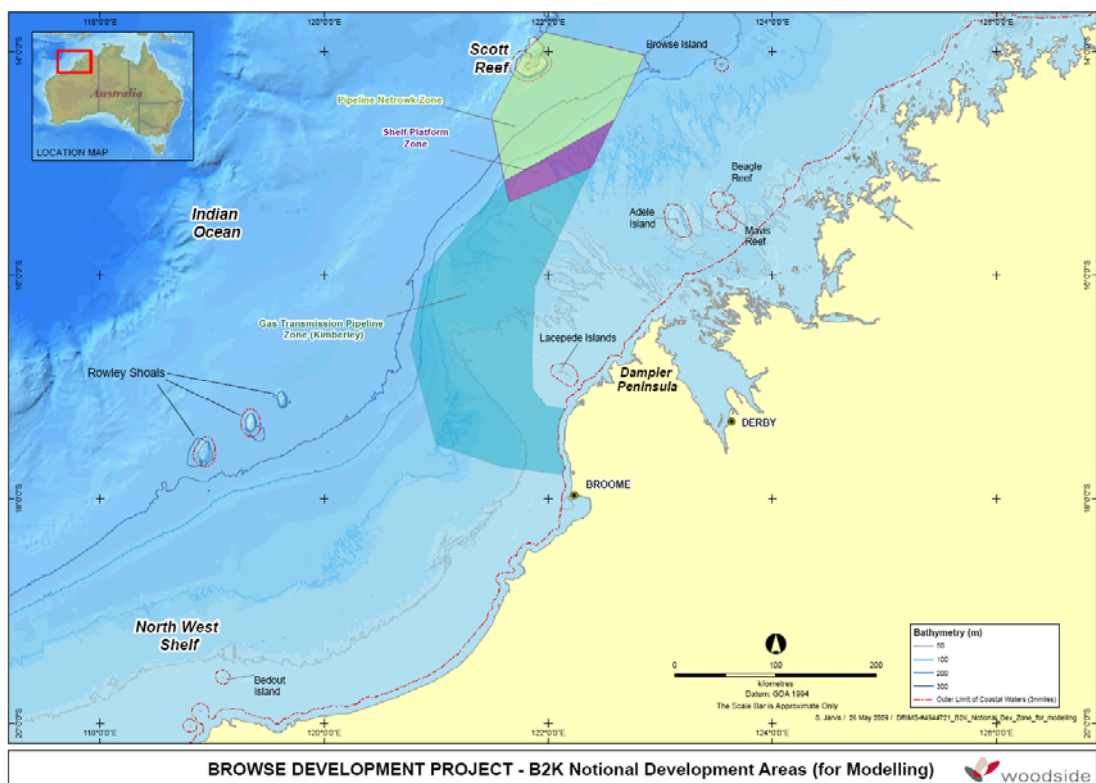


Fig 2.1 Overview map for Browse Development, Notional Development Areas (from DRIMS-#4944721_B2K_Notional_Dev_Zone_for_modelling.pdf)

Woodside is currently considering three onshore based development themes and two offshore based themes for the Browse LNG Development. For all themes, the upstream gas processing facilities are broadly similar and will include a gas collection system and necessary infrastructure to enable the production and transport of natural gas and associated products from the three separate reservoirs. The design of the downstream facilities will depend to a large degree on the final location of the LNG plant site.

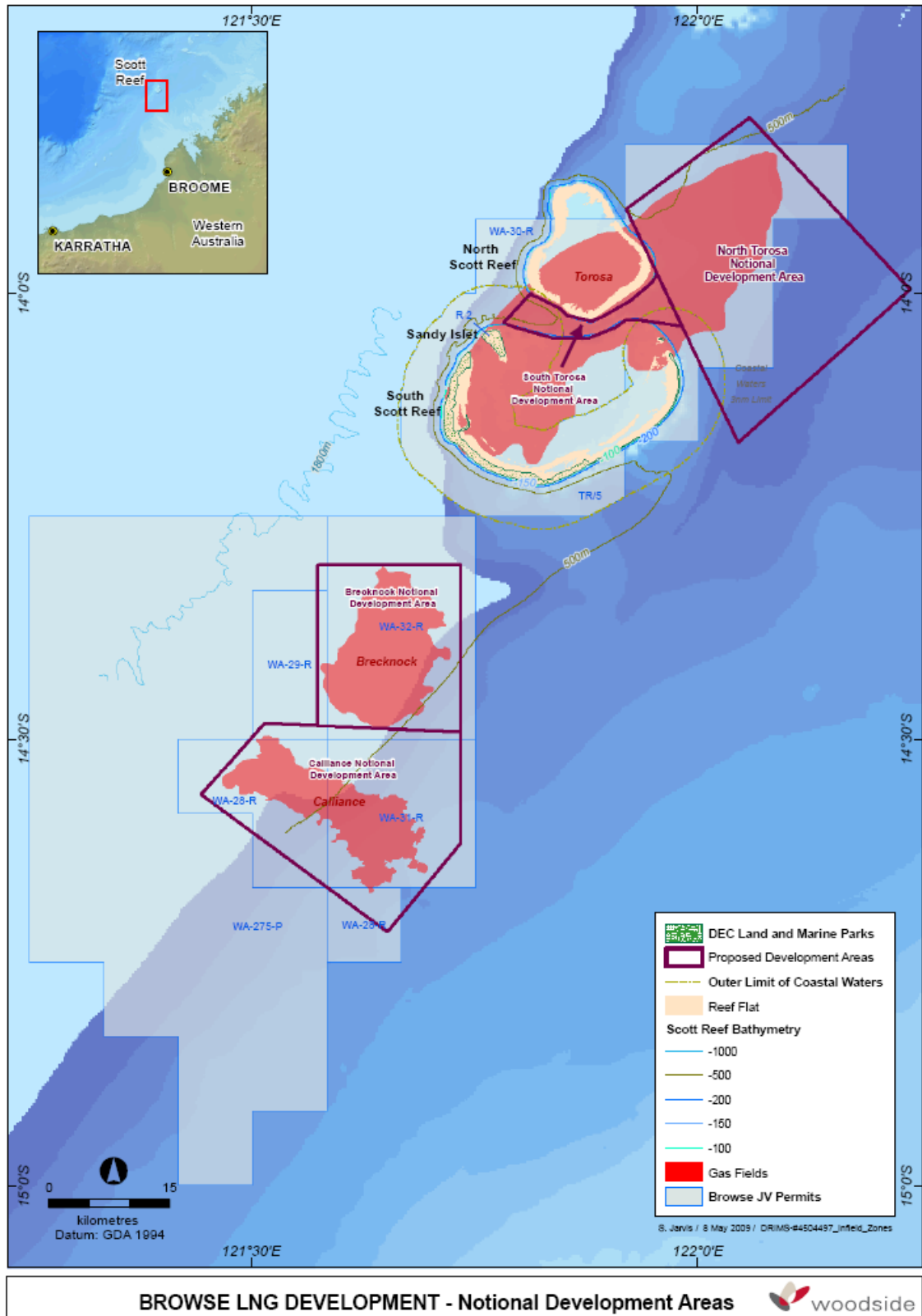


Fig 2.2 Browse Development, Notational Development Areas (from DRIMS-#4504497_Infield_Zones.pdf)



Woodside has commenced its environmental approval process for the upstream component of the development by submitting a referral to the Commonwealth Department of Environment, Water, Heritage and the Arts (DEWHA) who have assessed the referral and set a level of assessment at Environmental Impact Statement (EIS). Work has commenced on scoping for the requirement of the EIS and it has been identified that physical oceanographic modelling services will be required as part of the impact assessment process.

The components of the EIS that will require modelling support include:

- Inputs into the Design Process and Decision-Making:
 - Development of engineering mitigation options to reduce impacts;
 - Basis of Design (BOD); and
 - Front End Engineering and Design (FEED).
- Modelling of impacts for impacts assessment associated with:
 - Upstream environmental approvals;
 - Early activities approvals; and
 - Oil spill trajectory modelling.

The set-up and calibration of the hydrodynamic model required as a basis for these tasks are described in this report.

2.2 Scope of Study

The purpose of the present study is to set-up, calibrate and validate a hydrodynamic model covering the Notational Development Areas shown in Fig 2.1, so that it can be used for subsequent environmental modelling as described in section 2.1. With this in mind the scope was defined as follows:

1. Selection of appropriate hydrodynamic model, with suitable initial and boundary conditions, and include
 - Discussion of key assumptions for development of model.
 - Review of forcing mechanism and identification of dominant mechanisms.
2. Calibration and validation of the model for one two week period (in order to capture the spring-neap cycle) in each of the four seasons with in-situ measurements. Specifically comparison with WEL field measurements in and around the region surrounding Scott Reef at:
 - Brecknock (550m water depth B2-1 mooring).
 - North Scott Reef (475m water depth C1-1 mooring).
 - South Scott Reef (300m water depth, H2-1 mooring).
 - Channel between North and South Scott Reef (450m water depth, I1-1 mooring).
 - Shelf crossing (200m water depth, G2-1 mooring).



3. Calibration/validation of model by comparisons with surface drifter buoy trajectories.

The required scope for these tasks is described in detail in Section 5.1 of Ref /1/ with updates in Ref /19/.

It should be noted that the hydrodynamic model is not to be used for the engineering design process or for determining extreme loadings from cyclones, but for the environmental modelling as described in section 2.1.

2.3 Climate and Seasons

2.3.1 The Climate in the Northern Part of Australia

The area is affected by monsoonal winds and the occasional tropical cyclone. Over the Indian Ocean the subtropical anticyclone maintains a stabilising influence. The year divides into two main seasons, summer and winter defined by the prevailing winds, with transition periods in between.

In winter anticyclones move east in succession across the continent giving generally fine, hot, and dry weather in north and west Australia under the southeast trade winds (also known as the southeast monsoon). In summer warm, moist, tropical air is brought to the region by the west to northwest winds of the northwest monsoon. This gives uncomfortable, hot, and humid conditions with plentiful rain. The northwest monsoon may last from 2 weeks to 4-5 months. Break periods occur within the monsoon when a southeast flow is re-established. About 40 days is the normal time between such breaks. Tropical cyclones affect northwest and west Australia between November and April.

The seasons are determined by the annual north to south movement of the east to west high pressure belt which lies across, or just south of, Australia and extends west over the Indian Ocean. The axis of the high pressure belt moves to its summer position of 35° to 40°S in January and February.

2.3.2 Seasonal Wind Patterns for the Study Area

The seasons for the study area vary from year to year when defined on the basis of the prevailing wind. 4 years of wind measurements from Adele Island located 200 km to the southeast of Scott Reef has been analysed as shown in Table 2.1.



Table 2.1 Seasonal wind patterns at Adele Island

Wind Patterns and Season	1989	1993	1994	1995
SW-NW winds Northwest Monsoon Summer	October - March	September - March	October - February	October - February
Transitional Winds Autumn	April - May	April - May	March - April	March - April
SE winds Southeast Monsoon Winter	June - July	June - July	May - July	May - July
Transitional Winds Spring	August - September	August	August - September	August - September

Based on Table 2.1 typical seasons have been defined as listed below. But it should be kept in mind that these vary from year to year. For simplicity the two transitions periods have been termed autumn and spring.

Typical seasons based on wind patterns are:

Summer (Northwest monsoon):	October – February
Autumn (transitional):	March – April
Winter (Southwest monsoon):	May – July
Spring (transitional):	August – September

2.4 Oceanographic and Meteorological Processes of Importance for Environmental Modelling of the Study Area

2.4.1 Overview

From an environmental modelling point of view, it is essential that the physical processes and forcings that will determine the advection and dispersion of pollutants is understood. This is essential so the processes that dominate/force the transport can be identified to ensure that as a minimum requirement, it is these processes that are accurately reproduced in the hydrodynamic and environmental modelling. This, in turn, gives confidence in the environmental modelling output.

An overview of the important processes for both the hydrodynamic (oceanographic) modelling and for the subsequent environmental modelling is given in Table 2.2 and discussed in the following sections.



Table 2.2 Physical phenomena in oceanographic (hydrodynamic) modelling, their timescale of variation and their importance as input forcing into oceanographic and environmental modelling studies

Physical Phenomena	Driver	Typically observed phenomena	Timescale of variation	Importance for oceanographic modelling to be used for environmental dispersion studies	Importance for environmental dispersion studies
Wind	Atmospheric pressure gradients	Monsoonal winds	Months to weeks	High	High
		Cyclones	Hours to days	See note 2	See note 2
		Land Sea Breeze	Hours	High, but only in coastal areas	High, but only in coastal areas
Waves	Wind	Monsoonal winds	Months to weeks	Low except locally in the breaking zone	High
		Cyclones	Hours to days	See note 2	See note 2
		Land Sea Breeze	Hours	Low except locally in the breaking zone	High, but only in coastal areas
Currents (in top 50 m)	Wind	Monsoonal winds	Months to weeks	High	High
		Cyclones	Hours to days	See note 2	See note 2
		Land Sea Breeze	Hours	High, but only in coastal areas	High, but only in coastal areas
Currents (all depths)	Gravitational pull of moon and sun	Barotropic (depth-averaged) tide	Hours to weeks	High	High
		Baroclinic (internal) tide	Hours to weeks	Medium	Medium
		Solitons	Minutes to hours	Low (if present)	Low (if present)
	Oceanographic pressure gradients	Oceanographic Drift (large scale currents)	Months	Low (if present)	Low (if present)
		Eddies	Days to weeks	Low (if present)	Low (if present)

Note 1: Within one year the two monsoon wind patterns are well covered. However, the start and finish of the two monsoon seasons vary from year to year.

Note 2: Modelling of cyclones is not a part of the scope for the present study based on the assessment, that the small statistical probability of a cyclones hitting a given location combined with the small probability of discharge/spill occurring concurrently yields a very small probability of occurrence.



2.4.2 Wind, Waves and Currents

Physical processes that are typically in operation in marine environments include wind, waves and currents.

Winds tend to be local (e.g. land - sea breezes with spatial scales of 100s of kms that vary on a daily basis driven by differential heating over land and water) or synoptic (e.g. monsoonal winds with spatial scales of 1000s of kms that vary on scales of days or months driven by upper atmosphere pressure gradients). With Scott Reef being about 300 km away from the main land, the monsoonal winds are the dominating ones in the Scott Reef area.

Additionally, cyclones occur every year in waters north of Western Australia, but do not reach the Scott Reef area every year. Hydrodynamic modelling of cyclones for use in the environmental modelling has not been included as part of the present scope of work based on the assessment that the small statistical probability of a cyclones hitting a given location combined with the small probability of discharge/spill occurring concurrently at that location yields a very small probability of occurrence.

While waves are important for turbulent mixing processes, they do not contribute significantly to net fluid transport (rather causing fluid parcels to undergo a closed trajectory) leaving winds and currents as the two major contributors to fluid advection. This fluid motion is predominantly horizontal but may also occur in the vertical (due to turbulent mixing).

Currents can be induced by the wind or by pressure gradients due to gravity (that sets up barotropic tidal waves, which in turn can generate baroclinic (internal) tides and solitons) or large scale (1000s of kms) oceanographic flows (that induce oceanic drift and eddies that occur on time scales of weeks to months).

Additionally, small vertical flows are generated by temperature differences in the water column. These are generally very small compared to the horizontal currents.

All in all, the primary function of wind and currents is to disperse released pollutants laterally away from the source point (although turbulent mixing under rigorous forcing will also result in vertical transport).

2.4.3 Internal Tides and Solitons

While barotropic tide (i.e. the tidal wave normally experienced as diurnal or semidiurnal tide) is well understood and normally easily included in a hydrodynamic model, baroclinic tide (i.e. internal tidal waves) and solitons are more difficult to model. To assist in the evaluation of the importance of internal waves for the environmental modelling two (supplementary) definitions of internal tides and solitons are given below:



A shorter definition

Internal waves are a frequently encountered phenomena throughout the global ocean and on the continental shelf. Like “surface waves” “internal waves” is a generic term, which covers all types of waves within the ocean, some reoccurring on a regular basis like internal tides, while others only occur now and then like single solitary waves (called solitons). Internal waves typically are much longer and higher than surface gravity waves because the density differences (and therefore the restoring forces) within the sea are usually much smaller than the air-sea density difference. Internal waves are generated by disturbances to a stratified ocean by for example tides, varying winds and waves, and often in combination with variations in depth like a shelf break, an island or a sea mount.

A longer definition

Internal waves are a frequently encountered phenomena throughout the global ocean. Like “surface waves” “internal waves” is a generic term, which covers all types of waves within the ocean. Internal waves typically have much lower frequencies and higher amplitudes than surface gravity waves because the density differences (and therefore the restoring forces) within a fluid are usually much smaller than the air-fluid density difference. Internal waves are generated by disturbances to a stratified ocean (tides, wind stress fluctuations and wave action) at frequencies between the rotation of the earth (Coriolis frequency) and the local stratification (buoyancy frequency).

Internal waves are studied for a variety of reasons. They provide a mechanism for the removal of energy from the tide, via the linear internal tide, into internal solitary waves, eventually to be dissipated into turbulent motions when the waves break in shallow waters (Ref /16/). The strong horizontal currents and vertical shear associated with internal solitary waves may destabilize underwater platforms and drilling operations for oil exploration. The dissipation of internal solitary waves in shallow waters introduces bottom nutrients in the water column, thereby fertilizing the local region and modifying the biology therein (Ref /17/). The perturbations in the density field due to internal wave motions can cause large fluctuations in the sound speed and thus affect acoustic propagation which is of particular relevance to the design of sonar systems (Ref /14/).

On continental shelf and slope regions, a common generation source is the oscillating tidal flow over varying topography, which gives rise to the linear internal tide. Linear internal tides are generated by the interaction of tidal currents with sloping topography in the presence of density stratification at critical points when the slope of the internal wave characteristics equals the bottom slope (e.g. Ref /18/). These linear internal tides have length scales of 10's of km and periods of 12.4 hours (semidiurnal tide) or 24 hours (diurnal tide). Linear internal tides propagate horizontally as well as vertically in the ocean, and when intersecting the seasonal thermocline they produce internal solitary waves (ISW), also called large amplitude internal waves or nonlinear internal tides. The word “soliton” is also sometimes used, and refers to an



individual internal solitary wave that maintains in shape while travelling at constant speed. However, internal solitary waves constantly interact with topography while propagating, and change their shape accordingly. ISW packets will form by nonlinear steepening of the linear internal tide over the continental slope (Ref /18/). During the shoreward propagation of the ISW packet over the sloping bottom, the number of oscillations increases and the wave amplitude grows. The ISW have periods between approximately 10 minutes and 1 hour, are associated with length scales of a few hundred meters to a few kilometres and crest-to-trough displacements up to 160m have been observed (Ref /15/).

Solitons are thus important for design of pipelines in areas where they occur, while they have very little importance for dispersion of contaminants.

Internal tides are generally included in 3-dimensional hydrodynamic models when understanding internal tides as the variation of the water temperature at a given location and depth with the barotropic tide.

However, studying the generation of internal tide beams (called “linear internal tide” above), their propagation, transformation into solitons and their dissipation requires dedicated modelling with focus on these phenomena.

2.4.4 Large Scale Oceanographic Flows

The possible influence of large scale oceanographic currents on the dispersion of contaminants has been assessed, especially the possible influence of the Indonesian Through Flow and the Holloway Current.

Fig 2.3, Fig 2.4 and Fig 2.5 show the Indonesian Through Flow and the Holloway Current as described by different sources/authors.

These figures show that the Indonesian Through Flow is located to the north of the Browse development areas and doesn't directly influence Scott Reef. However, eddies are shed off and travel along the shelf break, but weaken as they come on to the shelf. These eddies can be seen in measurements from Brecknock, with generally small speeds, but occasionally with speeds up to 0.3 – 0.4 m/s.

As these eddies (but not the Indonesian Through Flow itself) may have some importance for the hydrodynamic and environmental modelling, a sensitivity test was carried out as a part of the model calibration. A discussion of this test is included in section 5.4. The conclusion was that it was not possible to include these large scale eddies into the hydrodynamic model (see section 5.4). And since the comparison of the model with measurements in general was satisfactory, the possible lack of the influence from the large scale eddies will not have a significant influence on the environmental modelling carried out on the basis of the hydrodynamic model.

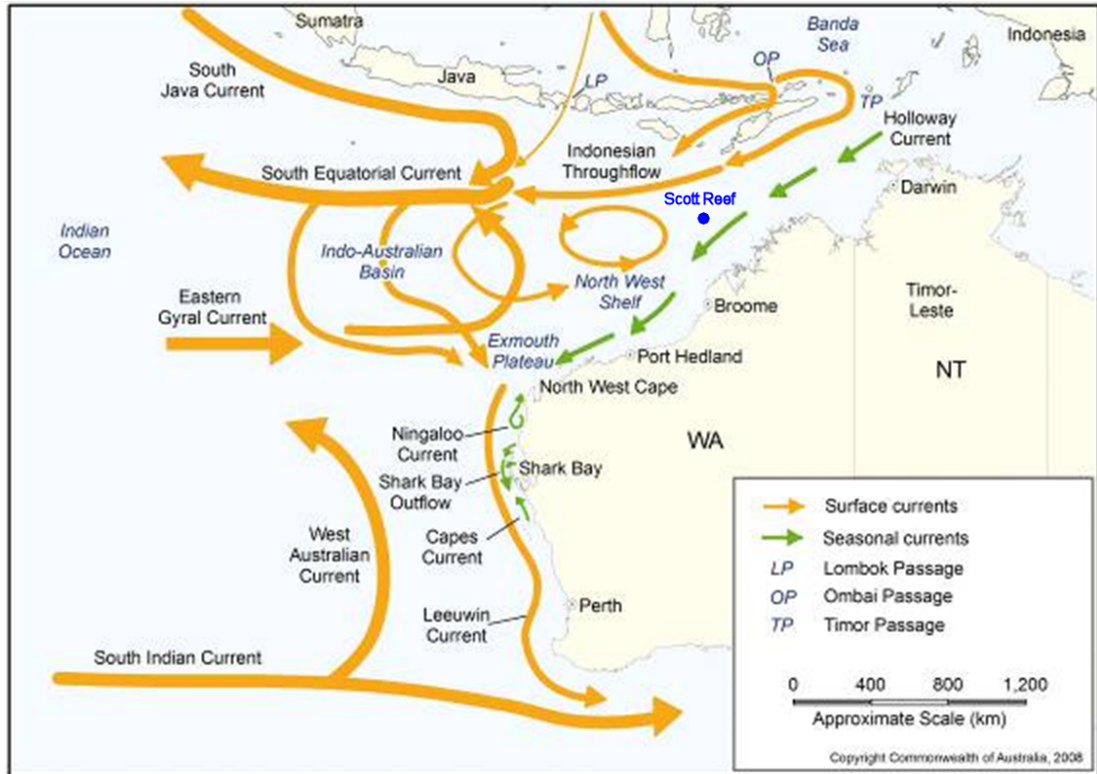


Fig 2.3 From "The North-west Marine Bioregional Plan, Bioregional Profile, A Description of the Ecosystems, Conservation Values and Uses of the North-west Marine Region, Department of the Environment, Water, Heritage and the Arts, 2008"

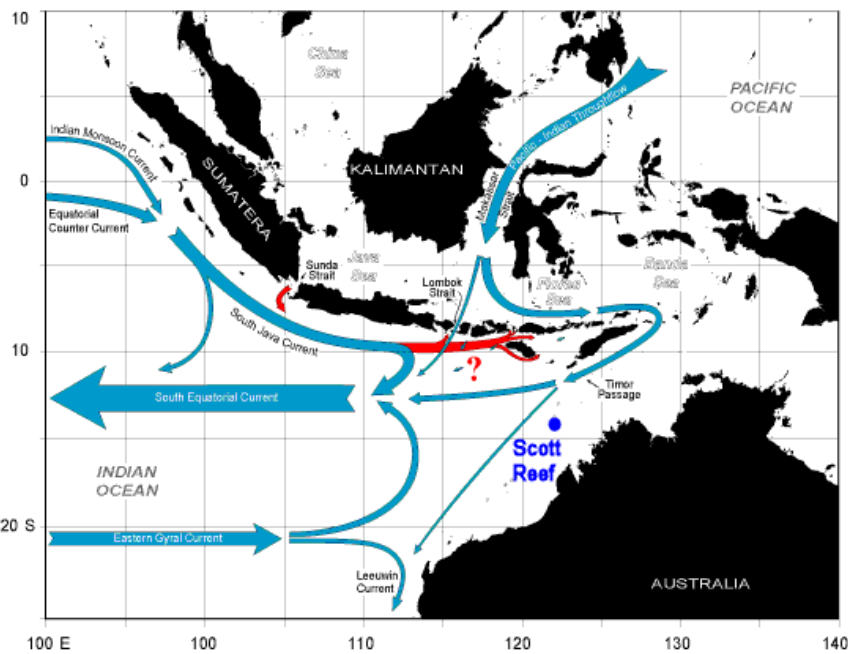


Fig 2.4 From "Teresa K. Chereskin, WOCE Indian Ocean Expedition, http://tryfan.ucsd.edu/woce_ioe/woce_ioe.htm"

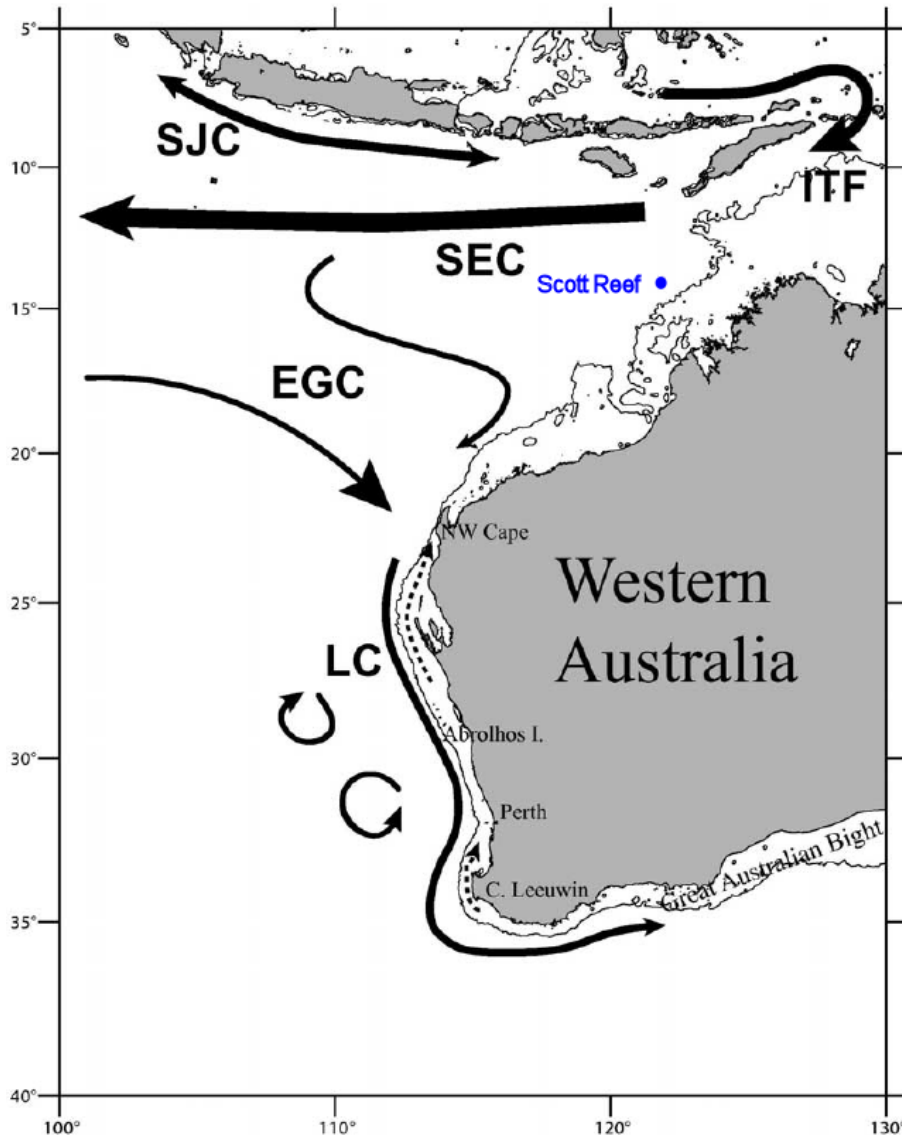


Fig 2.5 From "Ming Feng et al, Seasonal and interannual variations of upper ocean heat balance off the west coast of Australia, Journal of Geophysical Research, Vol 113, C12025, 2008"

Fig 2.6 show the location of the current stations on which Peter Holloway based his description of the Holloway current.

While the Holloway Current has been identified in measurements at North Rankin, we have not identified it in measurements at Brecknock. Holloway himself has only identified it in measurements further south (and possibly north of Darwin). It is therefore not envisaged to have any major importance for the environmental modelling of the area of interest in the present study.

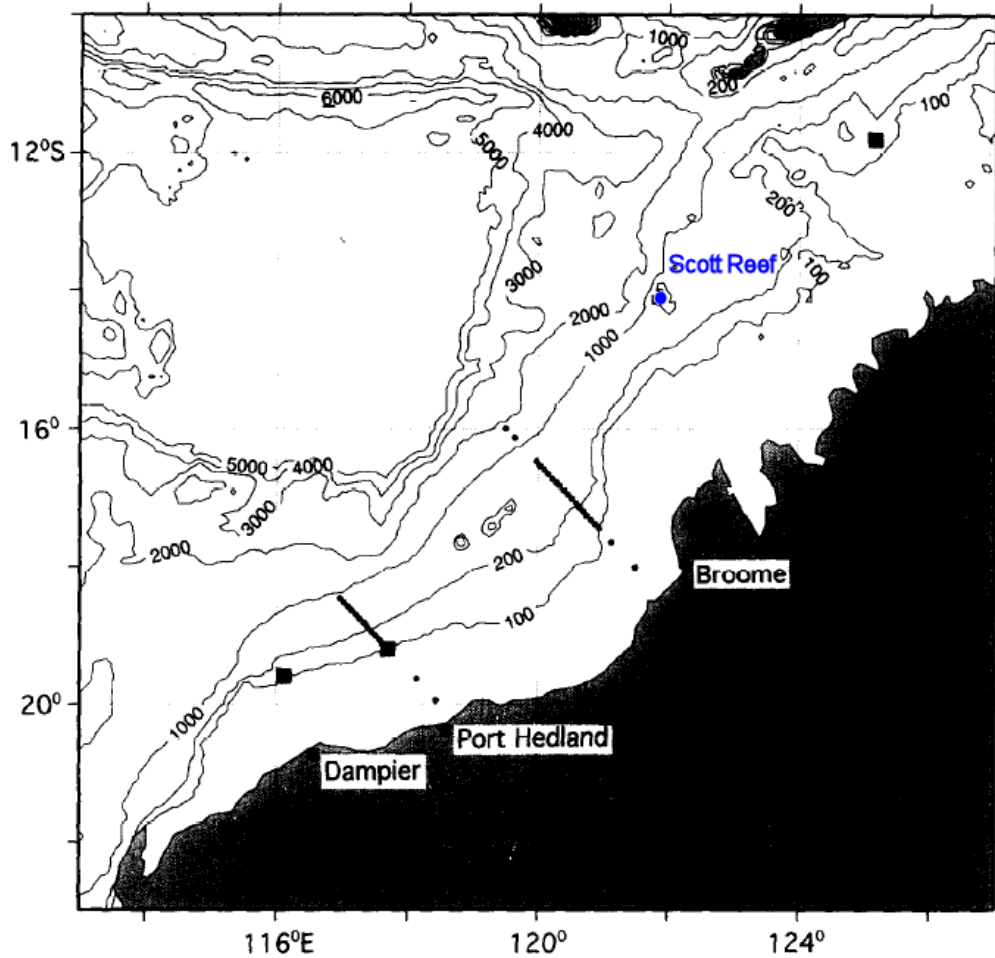


Fig. 1. Map of the Australian North West Shelf showing the locations of CTD/ADCP stations (●) and current meter moorings (■).

Fig 2.6 From "Peter E. Holloway, Leeuwin Current Observations on the Australian North West Shelf, May – June 1993, *Deep Sea Research*, Vol 42, No 3, pp285-305, 1995"



3 MEASUREMENTS AVAILABLE FROM THE STUDY AREA

3.1 Requirements to a Measurement Programme

The purpose of in-situ oceanographic and meteorological measurements at a site of interest is to understand the dominant physical processes that govern the advection (movement) of fluid (water and air).

Based on the description of the area of interest in Chapter 2, the physical phenomena, their time scale, variability and their importance for oceanographic modelling to be used for environmental dispersion studies are listed in Table 3.1. This table corresponds to Table 2.2 except that a column describing whether the variation of the physical phenomena within a year is larger than variation from year to year.

If the variation within a year (for example comparing January sea breezes to July sea breezes in a given year) is greater than the variation from year to year (for example comparing January sea breeze in consecutive years) then 12 months of measurements is adequate to understand this process.

For processes for which variations from year to year are greater than within one year (oceanographic drift for example) longer periods of measurements, oceanographic remote (satellite) sensing or numerical modelling hindcasts are required.

Ideally, in-situ measurements should be collected for 5-10 years to understand seasonal as well as inter-annual variations of winds, currents and seawater temperatures at a site of interest. This is not practicable from a cost as well as engineering schedule perspective.

Barotropic tidal processes, driven by the gravitational pull of the moon and the sun, are predominantly seasonally and annually independent. Typically only 3 months of measurements is required to adequately resolve the barotropic tidal currents.

In association with wind, wave and current measurements, seawater temperature through the water column is routinely measured. This allows determination of the density gradient through the water column (given that salinity is generally only a minor contributor to density in most offshore oceanic environments) which, in turn, plays a role in determining pollutant vertical migration if the pollutant density at the point of release differs from the density of the receiving fluid (e.g. oil, which is less dense than sea water, will float to the surface regardless of the release point in the water column).



Table 3.1 *Physical phenomena in oceanographic (hydrodynamic) modelling, their timescale of variation, relative importance of seasonal versus annual variability and their importance as input forcing into oceanographic modelling to be used for subsequent environmental modelling studies*

Physical Phenomena	Driver	Typically observed phenomena	Timescale of variation	Variation within a year larger than variation from year to year	Importance for oceanographic modelling to be used for environmental dispersion studies
Wind	Atmospheric pressure gradients	Monsoonal winds	Months to weeks	Yes and No See note 1	High
		Cyclones	Hours to days	No	See note 2
		Land Sea Breeze	Hours	Yes	High, but only in coastal areas
Waves	Wind	Monsoonal winds	Months to weeks	Yes and No See note 1	Low except locally in the breaking zone
		Cyclones	Hours to days	No	See note 2
		Land Sea Breeze	Hours	Yes	Low except locally in the breaking zone
Currents (in top 50 m)	Wind	Monsoonal winds	Months to weeks	Yes and No See note 1	High
		Cyclones	Hours to days	No	See note 2
		Land Sea Breeze	Hours	Yes	High, but only in coastal areas
Currents (all depths)	Gravitational pull of moon and sun	Barotropic (depth-averaged) tide	Hours to weeks	Yes	High
		Baroclinic (internal) tide	Hours to weeks	Yes	Medium
		Solitons	Minutes to hours	No	Low (if present)
	Oceanographic pressure gradients	Oceanographic Drift (large scale currents)	Months	No	Low (if present)
		Eddies	Days to weeks	No	Low (if present)

Note 1: Within one year the two monsoon wind patterns are well covered. However, the start and finish of the two monsoon seasons vary from year to year.

Note 2: Modelling of cyclones is not a part of the scope for the present study based on the assessment, that the small statistical probability of a cyclone hitting a given location combined with the small probability of discharge/spill occurring concurrently yields a very small probability of occurrence.



The measurement rationale is therefore to collect data for 12 months to understand those processes for which seasonal variability is dominant, use these 12 months of measurements to calibrate a numerical hindcast model, and then use this model to hindcast longer periods that aim to understand variations from year to year.

3.2 Browse Measurement Programme

With this in mind, an extensive measurement programme was conducted in and around Scott Reef (more than 70 instruments at a cost in excess of \$10 million AUD) with instruments to be deployed for 12 months. The data return on this very large field campaign was high with only 3 moorings not returning a full 12 months of information.

Current measurement locations (also in Fig 3.1) were located at:

- Brecknock, approximately 50 km to the South of Scott Reef in 550 m water.
- Torosa, approximately 20 km North East of Scott Reef in 475 m of water.
- Within the channel separating north and south Scott Reef, just south of South Scott Reef.
- On the continental shelf break in 100 m of water.

Water levels were also measured within South Scott Reef, while a meteorological station was placed at Scott Reef (see Fig 3.1).

Specifically the data collected consisted of (see Fig 3.1, Table 3.2 and Table 3.3):

- 12 months of wind measurements were collected within South Scott Reef
- 12 months of through water column currents and temperature were collected at Brecknock and Torosa.
- 6 months of through water column currents and temperature were collected from within the channel, south of Scott Reef and on the shelf (moorings were lost after 6 months).

Analysis of the measurements at these locations (Table 3.2) resulted in the following key findings:

Winds:

- Little evidence of land sea breeze at Scott Reef and surrounds with monsoonal winds dominant. This is also the case for Brecknock.

Currents:

- Surface currents influenced by the wind at all locations.
- Evidence of strong currents due to depth-averaged (barotropic) tides at all of the locations.
- No evidence of internal solitons at any of the locations.
- Evidence of weak currents due to internal (baroclinic) tides at all of the locations.
- Evidence of some influence of eddies/oceanic drift in deep water (550m water depth) during some months. This influence is limited to the surface



layer (top 50-100m) and has a maximum magnitude approximately half of that of the depth-averaged tide. No evidence of this effect in the channel or on the shelf (100m water depth).

Seawater temperature:

- Large seawater temperature fluctuations in both the deep water and on the shelf on a daily basis due to the action of the tides, particularly during spring (strong) tides.
- Season deepening of the thermocline during the winter months and re-stratification during spring an early summer at all locations.
- A slight horizontal temperature gradient between the Brecknock site and the shelf location due to tidally driven mixing of the water column on the shelf.

The 12 months of wind measurements at Scott Reef, in conjunction to Meteorological station operated at Scott Reef and nearby Adele Island over a number of years, and in conjunction with spatially varying wind fields available from meteorological models and satellites (see section 4.4.5), provide an excellent wind database for use in the model calibration/validation, and for later use in the environmental modelling.

From the analysis of the measurements it is seen that the currents are dominated by wind induced shear (near the surface) as well as depth-averaged (barotropic) currents. The other processes identified in Table 3.1 are either not evident (e.g. solitons) or of secondary importance (e.g. baroclinic tides, oceanic drift, eddies). As noted previously, 3 months of measurements of barotropic tidal processes are required to adequately quantify this process, thus the 6 months of measurements for all five locations and 12 months for two locations is more than sufficient to satisfy this criterion. And with 12 months of measurements for two locations the two distinct monsoonal seasons with transitions periods in between are also well covered.

The observed slight seawater temperature differences between Brecknock and the Shelf region does not materially contribute to the advection and dispersion of pollutants.



Table 3.2 List of measurements from Browse Measurement Programme (provided by WEL for the present study)

Station Name	Longitude (deg)	Latitude (deg)	Depth (mMSL)	Parameters used in study	Period
A2-1 Browse WL	121.8750	-14.1683	40	Water level	10/09/2006 - 14/09/2007*
A3-1 Browse Met	121.8874	-14.1629	43	Wind speed Wind direction	10/09/2006 - 24/08/2007
B2-1 Brecknock	121.5743	-14.5111	550	Water temperature velocity	17/09/2006 - 08/09/2007
C1-1 North Scott Reef	121.9974	-13.8954	475	Water temperature velocity	16/09/2006 - 13/09/2007
G2-1 Shelf Crossing	122.1924	-14.7309	197	Water temperature velocity	15/11/2006 – 21/03/2007
H2-1 South Scott Reef	121.8914	-14.1893	300	Water temperature velocity	14/09/2006 - 09/04/2007
I1-1 Channel	121.888611	-14.036667	447	Water temperature velocity	15/09/2006 - 18/02/2007**

*: Data file covering the period 10/09/2006 – 9/11/2006 is unreliable

** : Some of the sensors continued until 27/07/2007

Table 3.3 Sensor depths

Station Name	Parameter	Sensor depths (m Above Sea Bed)
B2-1 Brecknock	Temperature and currents	530*; 490; 450; 390; 330; 250; 130; 2.6
	Temperature only	510; 470; 430; 410; 370; 310*; 290; 270; 210; 170; 90; 50
C1-1 North Scott Reef	Temperature and currents	455, 395, 2.6
G2-1 Shelf Crossing	Temperature and currents	180, 100, 5** 2.6**, 1.5**
	Temperature only	160, 140, 120, 80, 60, 40
H2-1 South Scott Reef	Temperature and currents	280; 220; 140; 80; 2.6
	Temperature only	260; 240; 200; 180; 160; 120; 100; 60; 40; 20
I1-1 Channel	Temperature and currents	422; 382; 282; 142; 2.6

*: Sensor data unreliable

** : Only sensors above 5.0m ASB used in model comparisons



Fig 3.1 Location of measurements. Red pins: Water temperature/velocity stations.
Yellow pins: Water level station and meteorological station.

Additionally, drifter tracking was also carried out. The ones used for the model calibration are shown in Fig 3.2 (total track lengths).

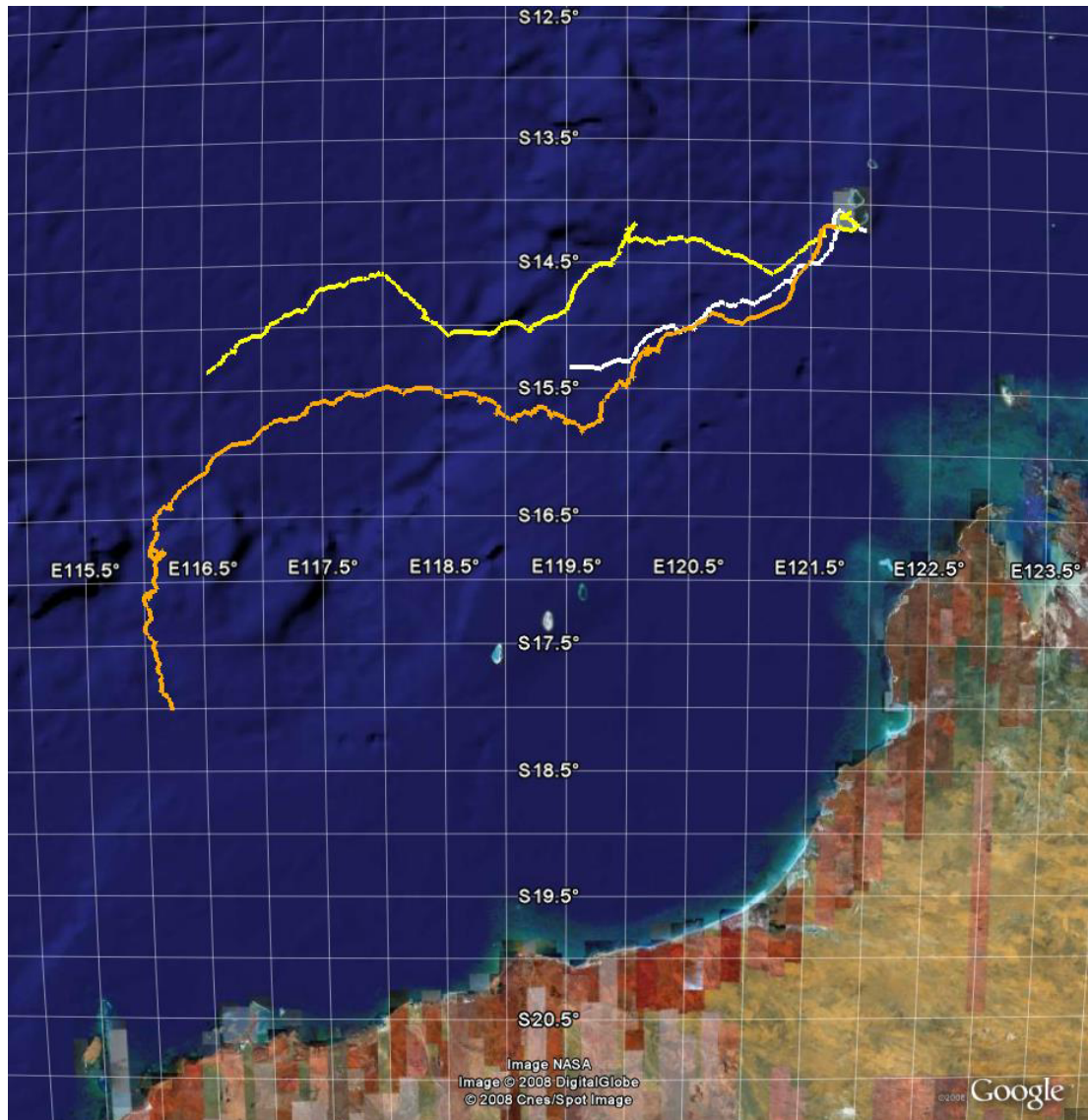


Fig 3.2 Tracks of drifters (heading to the southwest) shown in white (buoy no 227896), yellow (buoy no 223316) and orange (buoy no 223372).



3.3 Site Visit

From a whale survey flight over Scott Reef a number of photos were taken on 2 September 2008. The flight path is shown in Fig 3.3 which also indicates the position of the photos taken. The flight was conducted at 1000 ft which provided a good opportunity for viewing the reef in detail.

In particular when flying over the reef the scale of it was realised. The distance from the north edge of North Reef to the south edge of South Reef is 37 km, while the width of South Reef, which is the larger of the two, is 29 km.

Fig 3.4 to Fig 3.11 show 8 selected photos from the flight.

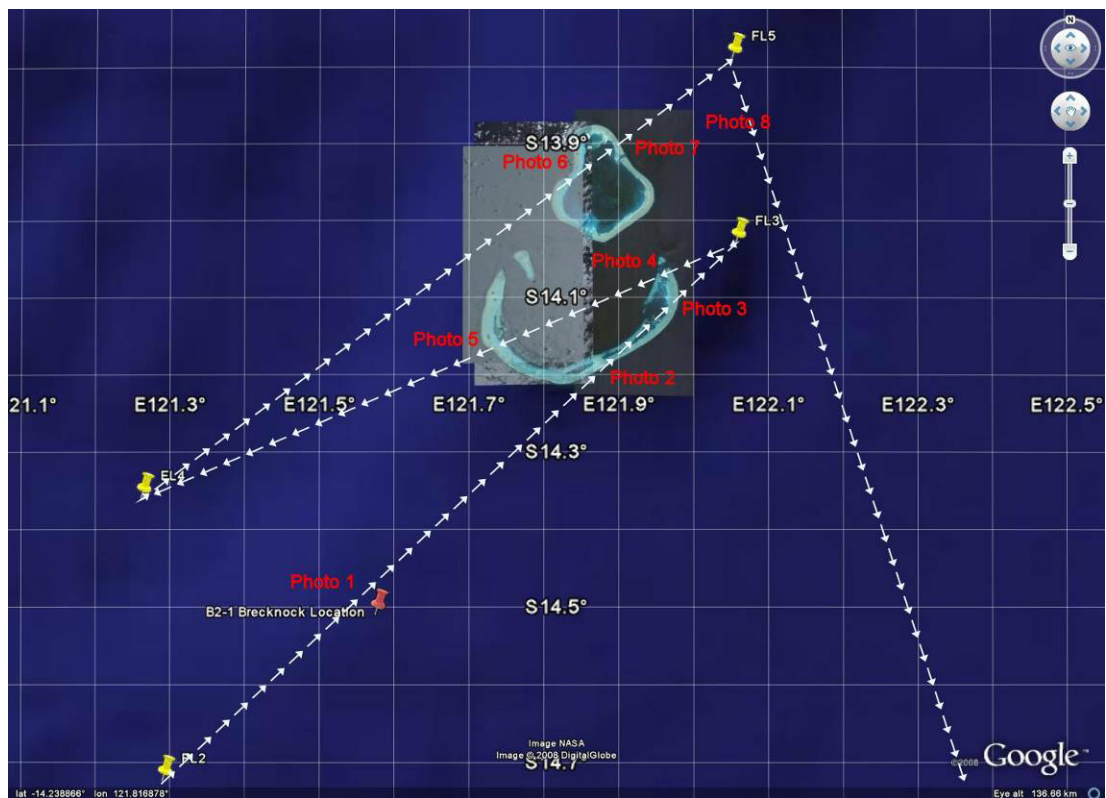


Fig 3.3 Flight path



Fig 3.4 Photo 1: Drill rig drilling in Brecknock reservoir



Fig 3.5 Photo 2: South Reef approaching from the southwest



Fig 3.6 Photo 3: South Reef lagoon

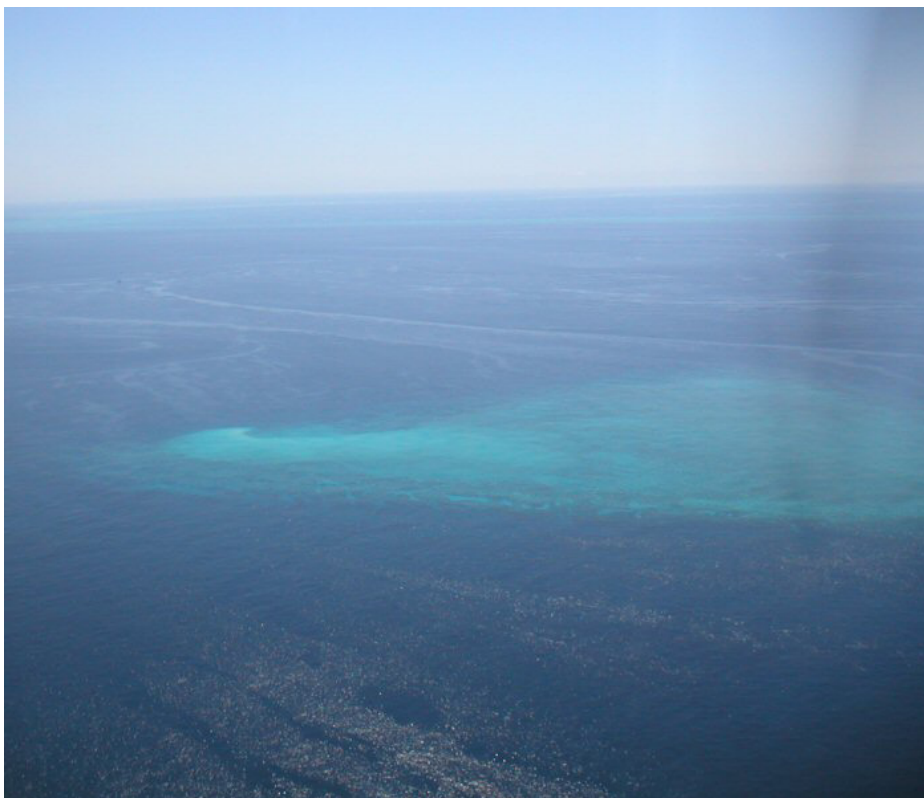


Fig 3.7 Photo 4: South Reef, entrance to channel between North and South Reef



Fig 3.8 Photo 5: South Reef looking north along the west side

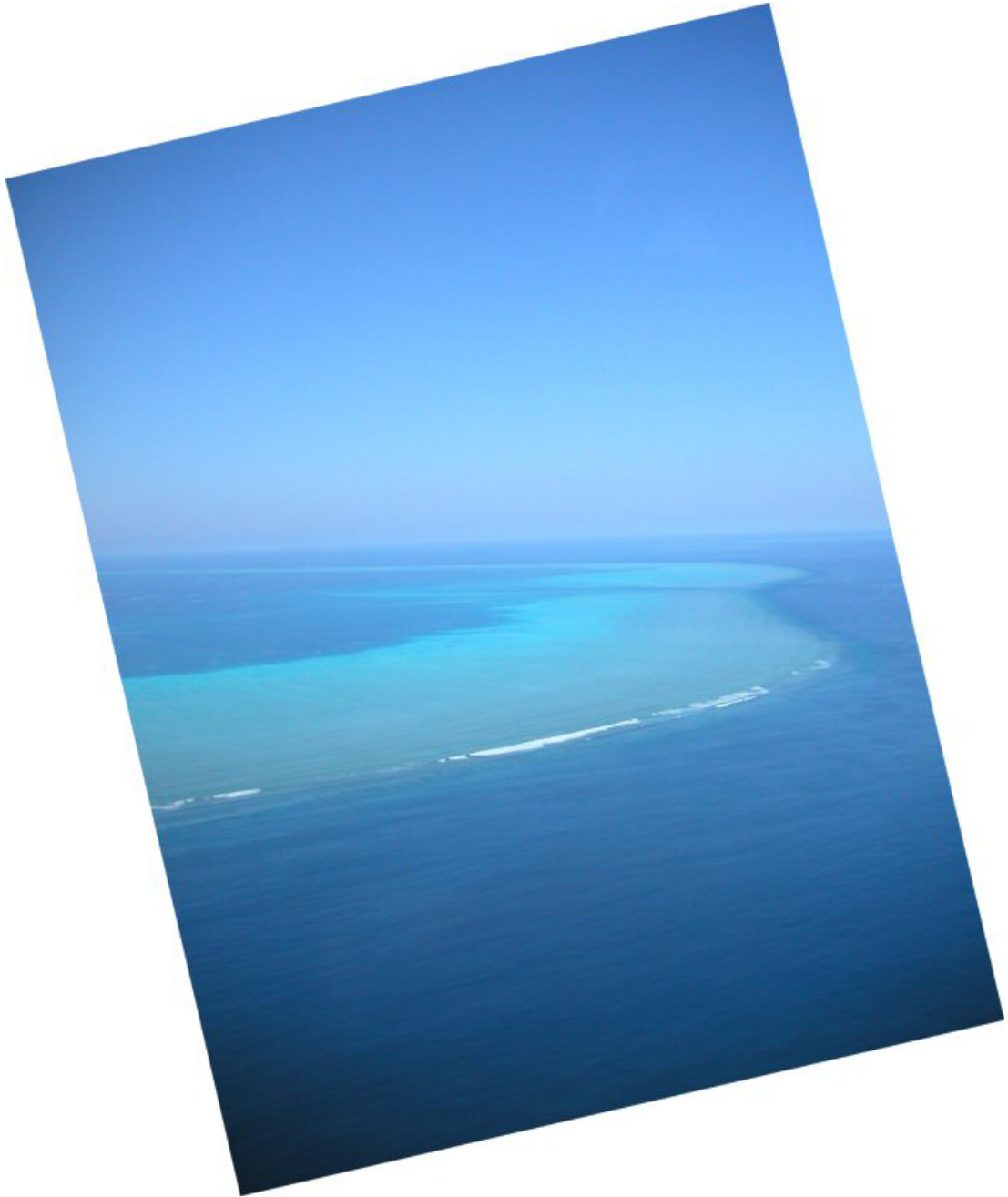


Fig 3.9 Photo 6: North Reef



Fig 3.10 Photo 7: North Reef, north-eastern lagoon entrance



Fig 3.11 Photo 8: North Reef



4 SELECTION AND SET-UP OF 3-DIMENSIONAL MODEL

4.1 General

The Browse development area is located on the edge of the continental shelf about 400 km north of Broome (see Fig 2.1) with depths varying from 200m in the shelf platform zone to more than 500m around Scott Reef. As described in the previous chapters the area is dominated by wind and by tide (with a spring tidal range of up to 4m). A thermal stratification in the water column in the area is also of importance for the currents experienced in the area. In order to model the water level and current variations a baroclinic hydrodynamic model taking into account the temperature variations was required.

A number of hydrodynamic models have already been set-up for the area including the profile model, GOTM (Ref /2/), the 3-dimensional model, ROMS (Ref /3/) and the 3-dimensional model, GCOM3D (Ref /8/).

As a part of the MIKE by DHI software suite a number of hydrodynamic models including 2-dimensional and 3-dimensional models are available. The selection of the 3-dimensional model applied in the present study is described below.

4.2 Overview of 3-Dimensional Models

4.2.1 DHI's 3-Dimensional Models

DHI's 3-dimensional hydrodynamic model is called MIKE 3.

MIKE 3 is a generalised mathematical modelling system designed for a wide range of applications in areas such as:

- oceanography
- coastal regions
- estuaries and lakes

The system is fully three-dimensional solving the momentum equation and continuity equations in the three directions.

MIKE 3 simulates unsteady flow taking into account density variations, bathymetry and external forcing such as meteorology, tidal elevations, currents and other hydrographic conditions.



MIKE 3 can be applied to:

- oceanographic studies
- coastal circulation studies
- water pollution studies
- environmental impact assessment studies
- heat and salt recirculation studies
- sedimentation studies

MIKE 3 exists in two basically different versions:

- MIKE 3 Classic, which is a finite difference model with a rectangular grid in the horizontal dimension and z-layers in the vertical. It can be run on a single grid or with dynamically nested grids. This version is described in detail in Appendix A.
- MIKE 3 FM, which is a finite volume model with an unstructured mesh with triangular and/or quadrangular elements in the horizontal dimension and sigma-layers or mixed sigma and z-layers in the vertical dimension. This version is also described in detail in Appendix A.

These two versions and their different types of grids are listed in Table 4.1.

The MIKE 3 HD (hydrodynamic) model forms the basis for the application models. These include advection-dispersion of conservative or linearly decaying substances (AD), a mud transport (MT) module simulating transport along with erosion and deposition of cohesive material, and a ECO Lab module simulating water quality (describing BOD-DO relations, nutrients and coliform bacteria problems), eutrophication (simulating algae growth and primary production) and other ecological processes. A Lagrangian based particle (PA) module can also be invoked for simulating plumes, tracers, sediment transport or the spreading and decay of E-Coli bacteria. Finally, a Lagrangian oil spill analysis module (SA) for describing spreading and decaying of oil spill can be invoked. The relationship is illustrated in Fig 4.1.

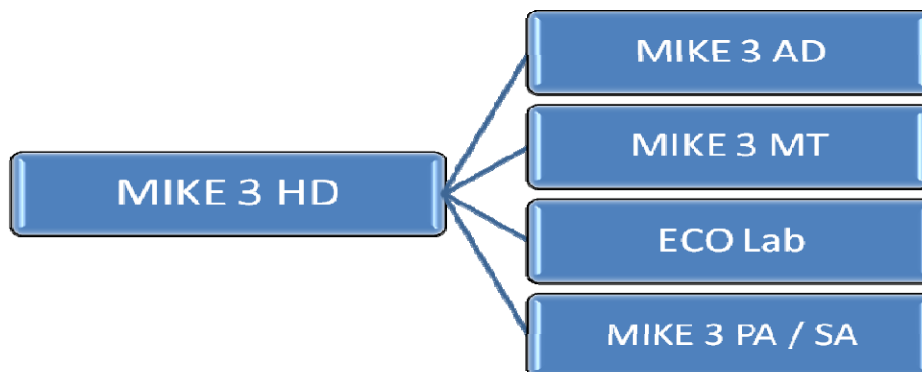


Fig 4.1 MIKE 3 modelling system



Table 4.1 MIKE 3 versions

	<p>Single Grid, MIKE 3 Classic with z-layers</p> <p>The full time-dependent non-linear equations of continuity and conservation of momentum in three dimensions are solved by finite difference techniques with the variables defined on a rectangular staggered grid in x, y and z-space. Two different hydrodynamic engines are included. One based on a non-hydrostatic pressure formulation and the other using a hydrostatic pressure assumption.</p>
	<p>Multiple Grid, MIKE 3 Classic Nested with z-layers</p> <p>This is basically the same as the single grid version. However, it provides the possibility of refining areas of special interest within the model area (nesting). All the domains within the model area are dynamically linked together thus ensuring high computational speed. The Multiple Grids version is also called the Nested version and includes a non-hydrostatic and a hydrostatic version.</p>
	<p>Flexible Mesh, MIKE 3 FM with sigma-layers or mixed sigma and z-layers</p> <p>The spatial discretisation of the governing equations is performed using a cell-centred finite volume method. In the horizontal plane an unstructured grid is used while sigma layers (fixed number of layers with varying size) or sigma layers combined with z-layers (below the sigma layers) are used in the vertical domain (3D). Cartesian as well as spherical coordinates can be used. An unstructured grid provides an optimal degree of flexibility in the representation of complex geometries and enables smooth representations of boundaries. Small elements may be used in areas where more detail is desired, and larger elements used where less detail is needed, optimising information for a given amount of computational time.</p>

4.2.2 Other 3-Dimensional Models for the Study Area

At the School of Environmental Systems Engineering (SESE), University of Western Australia (UWA), a ROMS (Regional Ocean Modelling System) model has been developed for the Scott Reef over the last couple of years (see e.g. Ref /3/). The model is a finite difference model with a curvilinear orthogonal grid in the horizontal and sigma-layers in the vertical.

In connection with the present study Michael Meuleners (from SESE), who has worked with and supervised work on the Scott Reef ROMS model at SESE, has



through meetings and discussions provided invaluable advice and support to DHI during DHI's Scott Reef model set-up.

4.3 Selection of 3-Dimensional Model

The selection of a 3-dimensional model took into account the following:

- A fine resolution in the horizontal grid was required around Scott Reef and surrounding areas, while a coarser resolution could be applied further away.
- In the ROMS model a vertical resolution of about 25m of the top 500m of the water column had proven to be adequate to resolve the thermal variation.
- The experience from the ROMS model would suggest that a hydrostatic model (which does not take the vertical accelerations into account) should be adequate describe the currents in the area (i.e. a non-hydrostatic model that includes the vertical accelerations would not be required).
- Although a sigma-grid (bottom fitted grid) will be less accurate in areas with steep slopes, like at Scott Reef, the ROMS model had shown that a sigma grid (in contrast to a finite difference staggered grid) would provide overall good results. One of the benefits of using a sigma-grid would be a good resolution within the reef lagoons.

Both MIKE 3 Classic and MIKE 3 FM were anticipated to be able to model the study area. But initially MIKE 3 FM was selected and set-up based on the following:

- The flexible mesh generation offers very good possibilities for having a fine mesh in areas where this is required, while a coarser mesh is used in other areas. This would result in fewer computational points.
- The vertical sigma-layers had been successful in the ROMS model. (This had been an area of concern.) Using sigma-layers would provide a good resolution within the reef lagoons.
- The tidal (barotropic) wave speed is generally better described in MIKE 3 FM than in MIKE 3 Classic allowing for an easier model calibration.
- A geographical (spherical) coordinate system could be applied (which is not available in MIKE 3 Classic) thus taking into account the curvature of the earth.
- The pre- and post-processing tools for MIKE 3 FM are faster to use than for MIKE 3 Classic.



MIKE 3 FM was set-up in the same way (i.e. with the same input data) as described in Section 4.4 for MIKE 3 classic with the only differences being:

- The model area and computational mesh, which is shown in Fig 4.2, and
- A time varying temperature boundary with no filtering, which in MIKE 3 classic was changed to a boundary with a 60 hour low-pass filtering, thus removing all tidal variations from the temperatures.

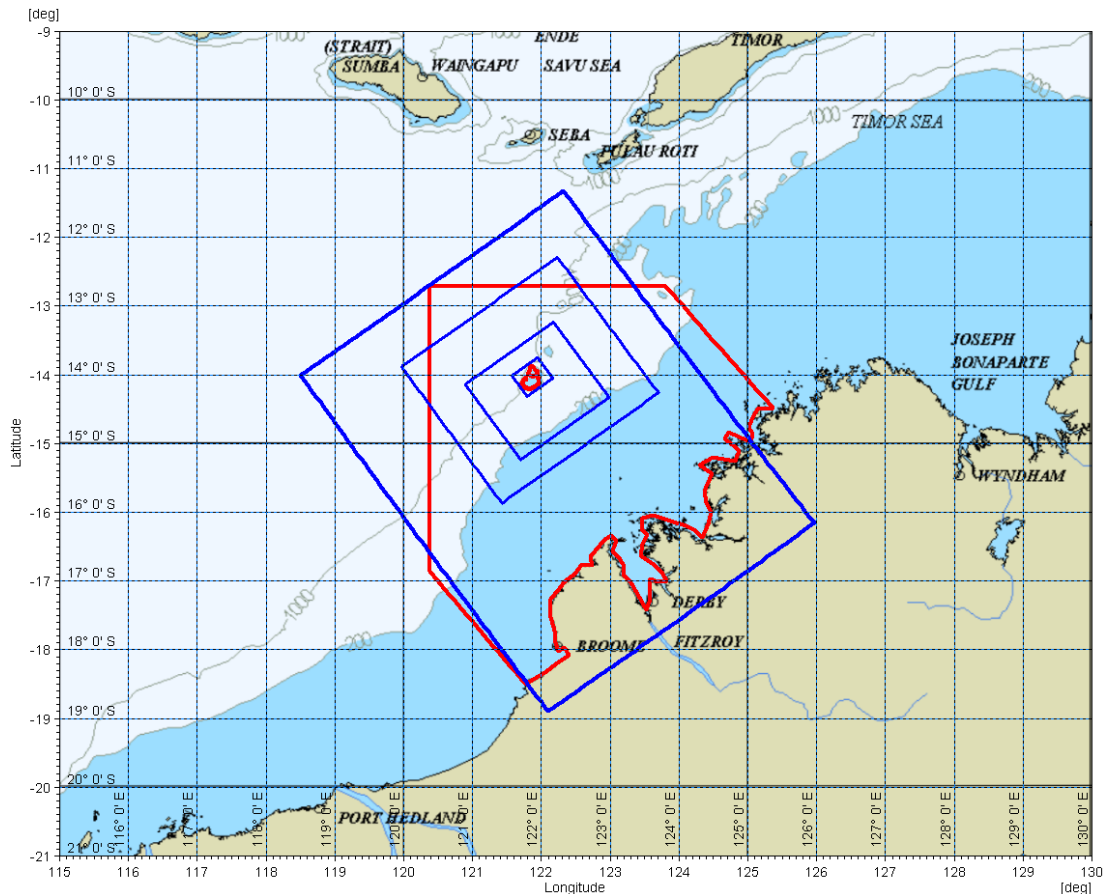


Fig 4.2 Areas covered by MIKE 3 FM (red line) and MIKE 3 classic, nested version (blue lines)

In general MIKE 3 FM behaved well and provided a very accurate description of the tidal variation in water levels, currents and temperatures. However, a number of short-comings were identified with no immediate short term solution at hand:

1. The extremely steep gradient on the reef edge made the model computations unstable.

Likely solution: With the 2009 release of MIKE 3 FM (in April 2009) mixed sigma-layers on top of z-layer became available, which is likely so solve this problem. However, this new version wasn't available at the time the present project work was carried out.



2. The computational requirements became very large (i.e. significantly more than one week of computational time which for this project is considered a practical limit), if a resolution in the order of 200m to 400m were to be achieved at and around Scott Reef. The time step depends on the tidal wave speed (celerity), which increases with depth and becomes very large when depths of 500m to 1500m are considered (as is the case close to Scott Reef). In MIKE 3 FM a maximum Courant-Friedrich-Levy number of 1 is required for stability, while MIKE 3 classic (with an implicit solution scheme) is stable for Courant numbers of up to 5 (or more). This means that for the same number of computational points (or elements) MIKE 3 classic runs significantly faster than MIKE 3 FM.

Likely solution: As MIKE 3 FM is parallelised (with shared memory) it will be possible to run with a fine mesh as cpu-clusters becomes larger and more accessible.

3. The fluctuation in the temperature as computed by the model only showed the tidal variation, while the remaining variability seen in the measurements were only partly reproduced. This is illustrated in Fig 4.3 (MIKE 3 FM) and Fig 4.4 (MIKE 3 classic), where the larger variability as computed by MIKE 3 classic is seen. MIKE 3 FM even has time varying temperature boundary conditions (with a large variability), while MIKE 3 classic only has constant (non-varying) temperature boundaries. This ability to reproduce the variability was very important in order to be able to simulate the upwelling seen during some periods in the measurements from the moorings in the channel between South and North Reef. (It should be noted that the ROMS modellers at UWA had not yet included these measurements in their comparisons as the channel had not been a focus area for their studies.)

Likely solution: The larger variability and better fit as seen for MIKE 3 classic likely results from one or more of a number of the following factors: A higher order scheme is applied in the MIKE 3 classic solution, the non-hydrostatic version of MIKE 3 classic was applied (as the hydrostatic version proved unstable), and a finer overall resolution could be achieved with MIKE 3 classic. With a non-hydrostatic version of MIKE 3 FM being planned and with access to high-speed computing becoming more accessible on commercial projects, MIKE 3 FM should also be able to overcome this present limitation.

Based on the above it was decided to apply MIKE 3 classic. With the hydrostatic version of MIKE 3 classic being unstable (even with filters applied), the final choice was MIKE 3 classic non-hydrostatic, which as shown in the Sections below, provided a good description of the measurements available for the model calibration.

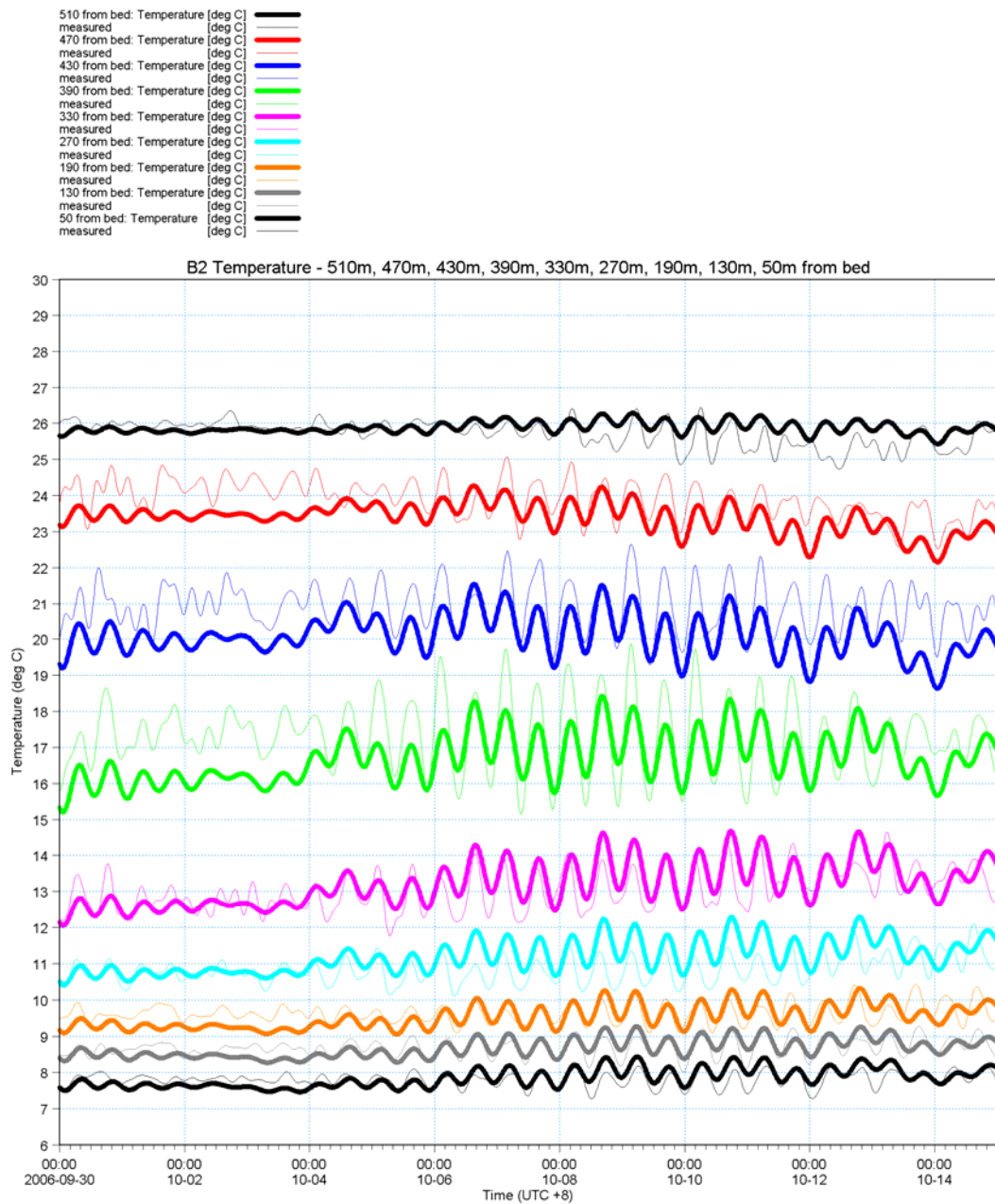


Fig 4.3 Temperatures as computed by MIKE 3 FM (thick lines) and as measured (thin lines) at Brecknock in 8 depths.



510m from bed: Temperature [C]	[deg C]	—
measured	[deg C]	—
470m from bed: Temperature [C]	[deg C]	—
measured	[deg C]	—
430m from bed: Temperature [C]	[deg C]	—
measured	[deg C]	—
390m from bed: Temperature [C]	[deg C]	—
measured	[deg C]	—
330m from bed: Temperature [C]	[deg C]	—
measured	[deg C]	—
270m from bed: Temperature [C]	[deg C]	—
measured	[deg C]	—
190m from bed: Temperature [C]	[deg C]	—
measured	[deg C]	—
130m from bed: Temperature [C]	[deg C]	—
measured	[deg C]	—
50m from bed: Temperature [C]	[deg C]	—
measured	[deg C]	—

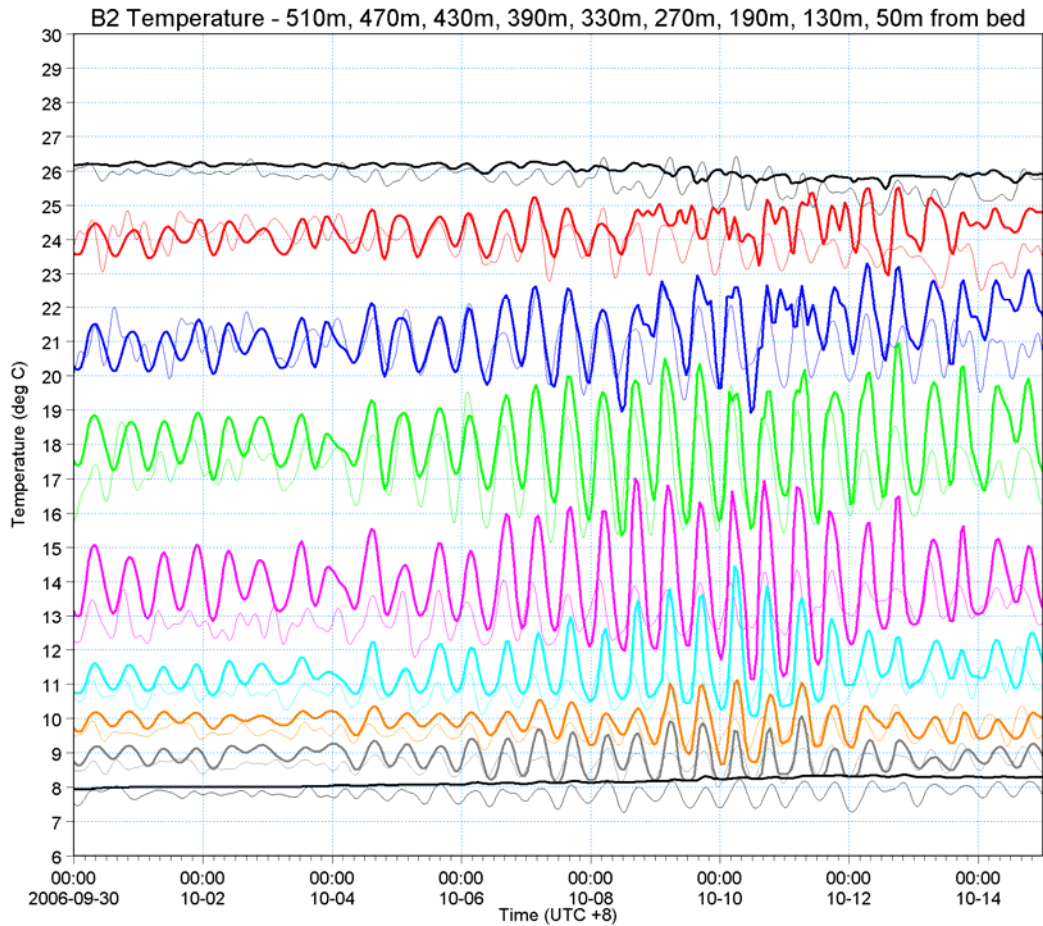


Fig 4.4 *Temperatures as computed by MIKE 3 classic (thick lines) and as measured (thin lines) at Brecknock in 8 depths.*



4.4 Model Set-up

4.4.1 General

The following is a description of the model set-up for the MIKE 3 classic nested rectangular grid model. Apart from a few differences as mentioned in Section 4.3 above this set-up is identical to the set-up for the MIKE 3 FM model.

4.4.2 Bathymetry and Computational Grid

The area covered by the model is shown in Fig 4.5 while the grid dimensions are listed in Table 4.2. The origin of the outer grid was located at 118.5°E and 14.5°S with an angle from North to the y-axis of 55°. For all grids the GDA 1994 MGA Zone 51 projection were applied.

25 z-layers with a thickness of 20m were applied with the top layer being 1½ times the general thickness. The extra thickness of the top layer is a standard feature in the model introduced in order to accommodate the tidal variation within the top layer. The bottom layer is bottom fitted representing depths below 490m. Flooding and drying (in the top layer) was applied.

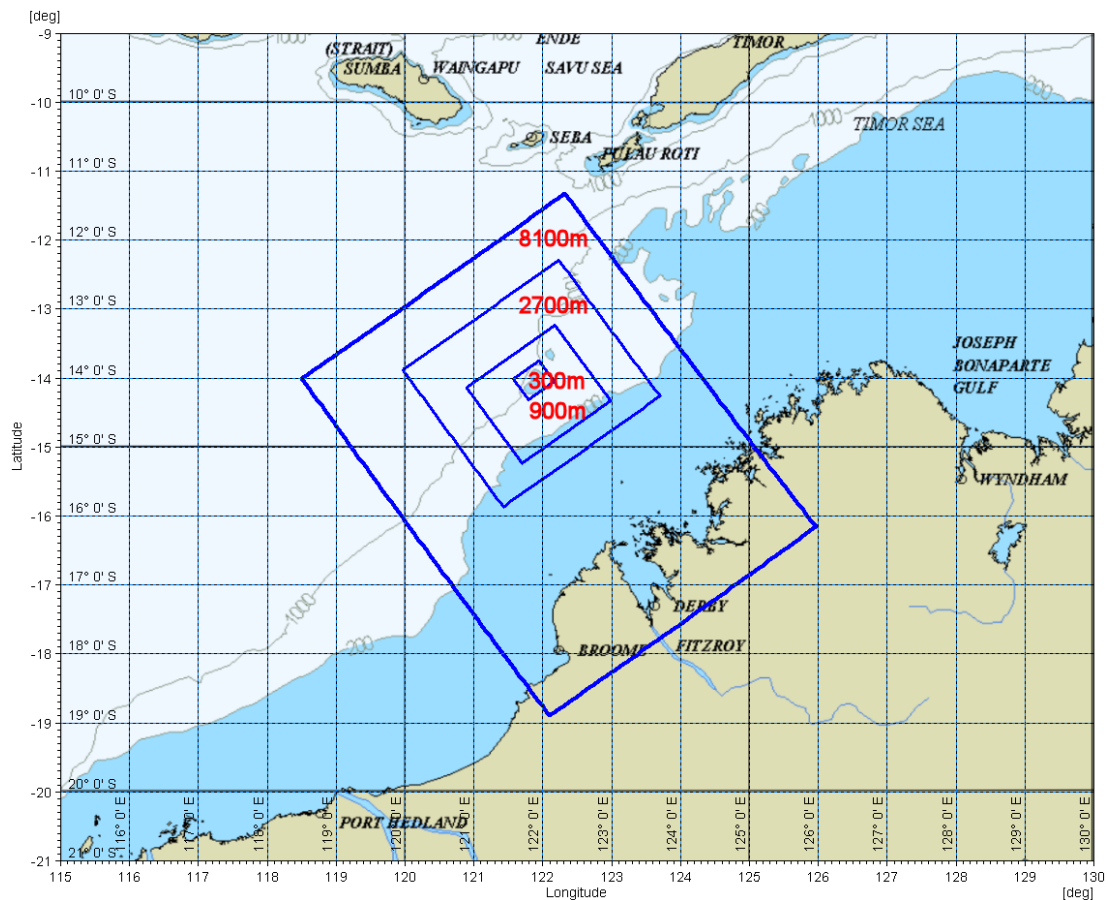


Fig 4.5 Area covered by MIKE 3 classic nested model with 8100m, 2700m, 900m, and 300m dynamically nested grids shown in blue



Table 4.2 MIKE 3 grid definitions

¹: Top layer thickness is 30m and bottom layer thickness varies with depth

Model grid spacing (m)	Grid dimensions (X by Y by Z)	No. of computational points
8100	82*8100m by 63*8100m by 25*20m ¹	39,567
2700	100*2700m by 112*2700m by 25*20m ¹	148,592
900	166*900m by 190*900m by 25*20m ¹	559,210
300	136*300m by 166*300m by 25*20m ¹	363,349
Total		1,110,718

The depths for each grid point were interpolated from the following two bathymetric data sources:

- Australian Bathymetry and Topography Grid, June 2005, Geoscience Australia. Coverage: 92° E – 172° E and 8° S –60° S, resolution: 9'' x 9'' (approximately 278m x 268m around Scott Reef).
- Browse Development Project, ROV/HDD Bathymetric Data – Rev A (incorporating Scott Reef Bathymetric Model – Revision 2), June 2007, Woodside Energy Pty Ltd. Coverage: Scott Reef and surroundings, resolution: 10m x 10m (reduced to 100m x 100m for use in model bathymetry generation).

The latter data set were used for the Scott Reef area, while the former were used elsewhere. The areas where the two met were smoothed out in order to avoid sudden steps in the bathymetry. The model bathymetries are shown in Fig 4.6 to Fig 4.8.

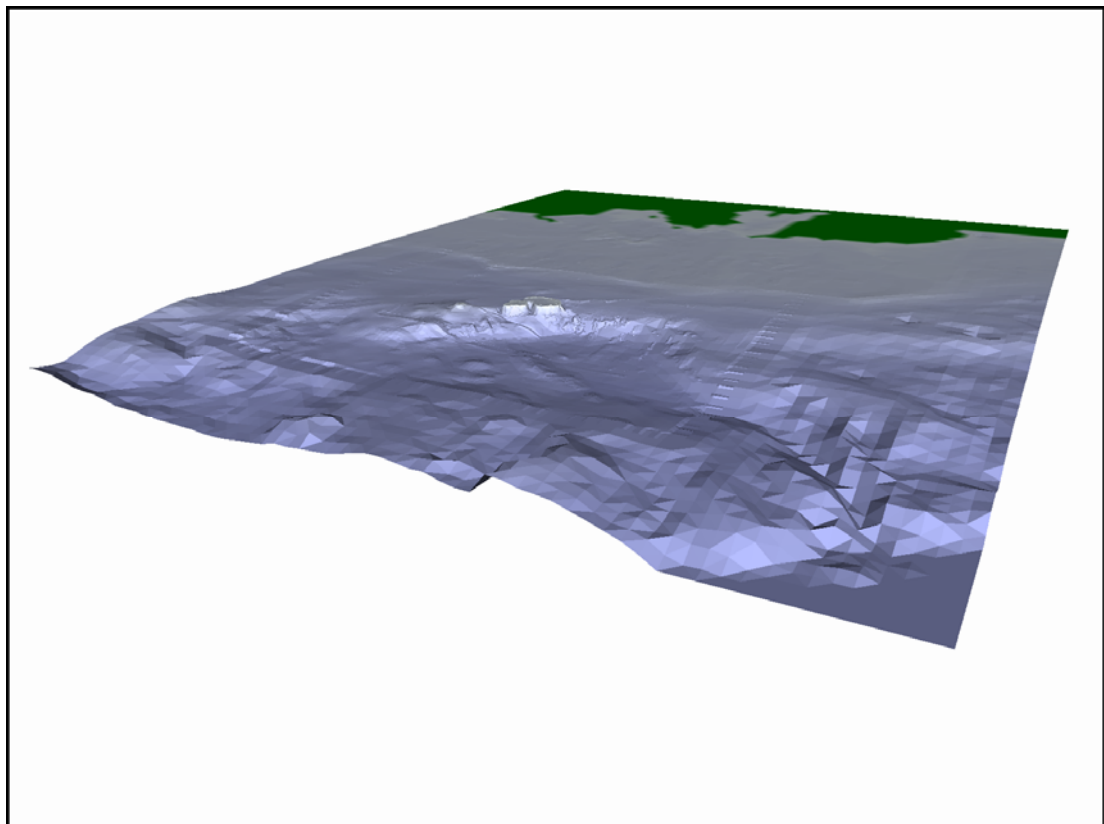


Fig 4.6 8100m model bathymetry seen from northwest

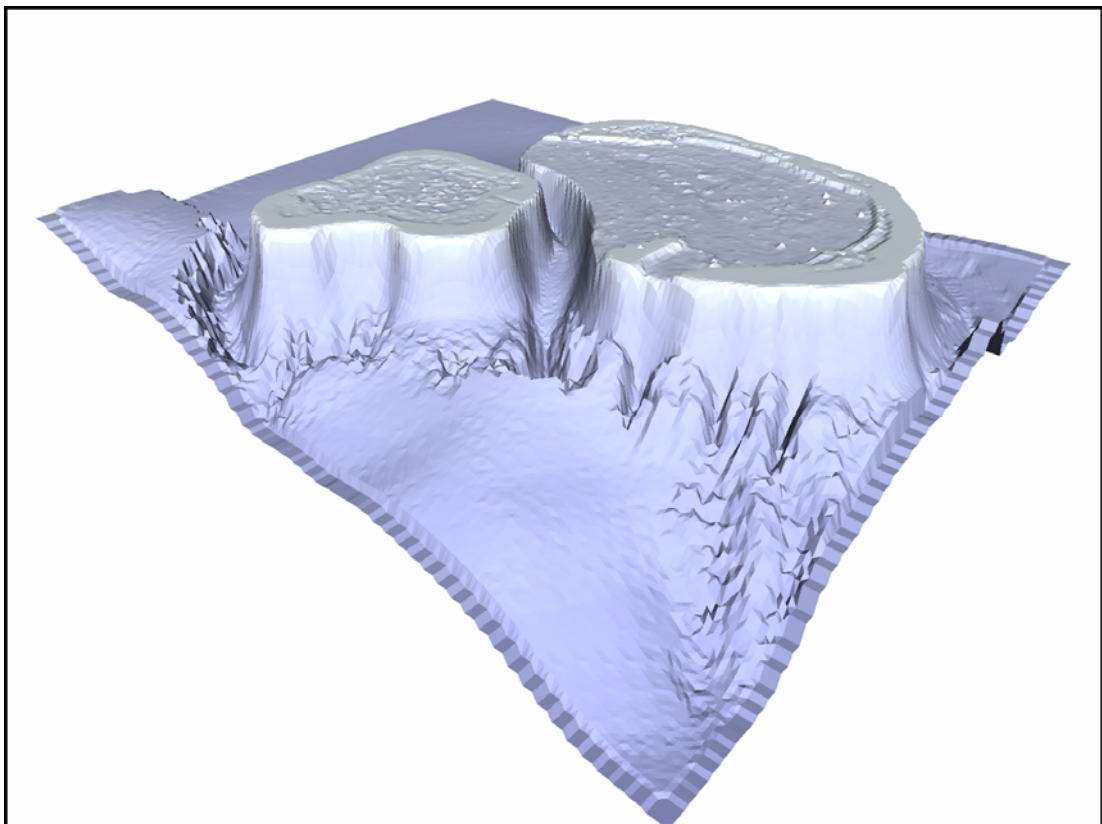
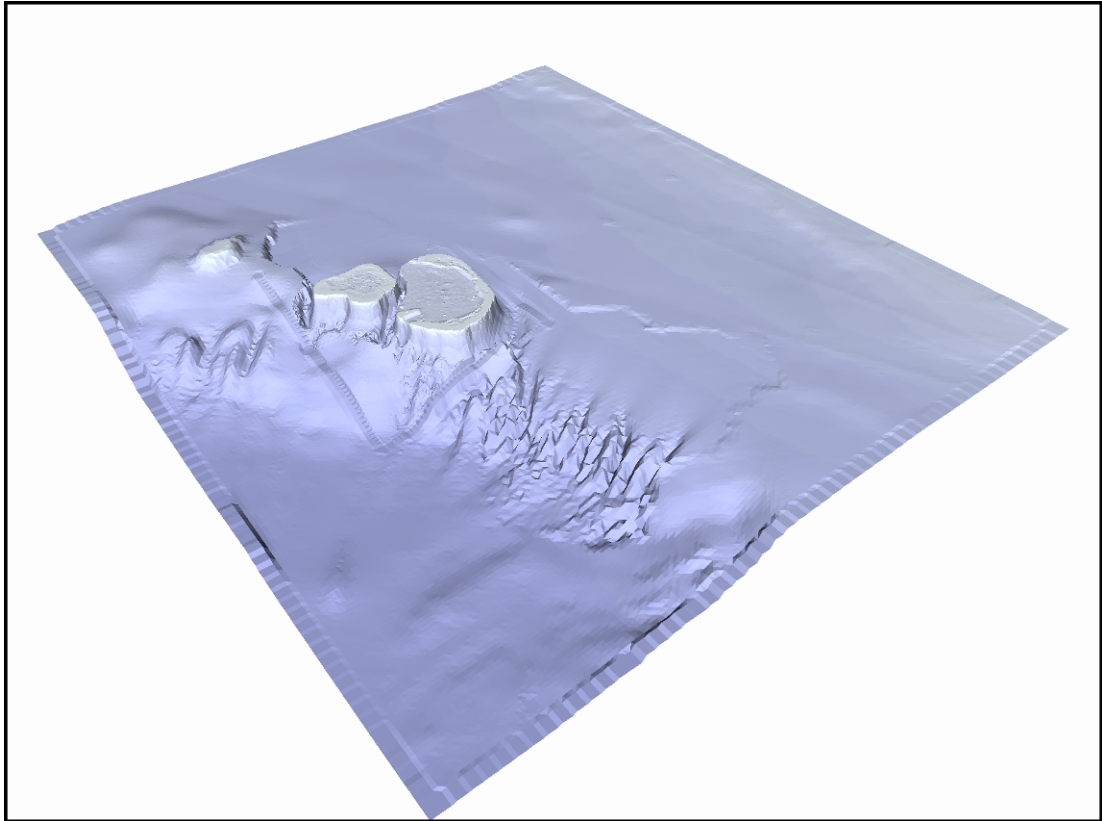


Fig 4.7 900m model bathymetry (top) and 300m model bathymetry (bottom) seen from west

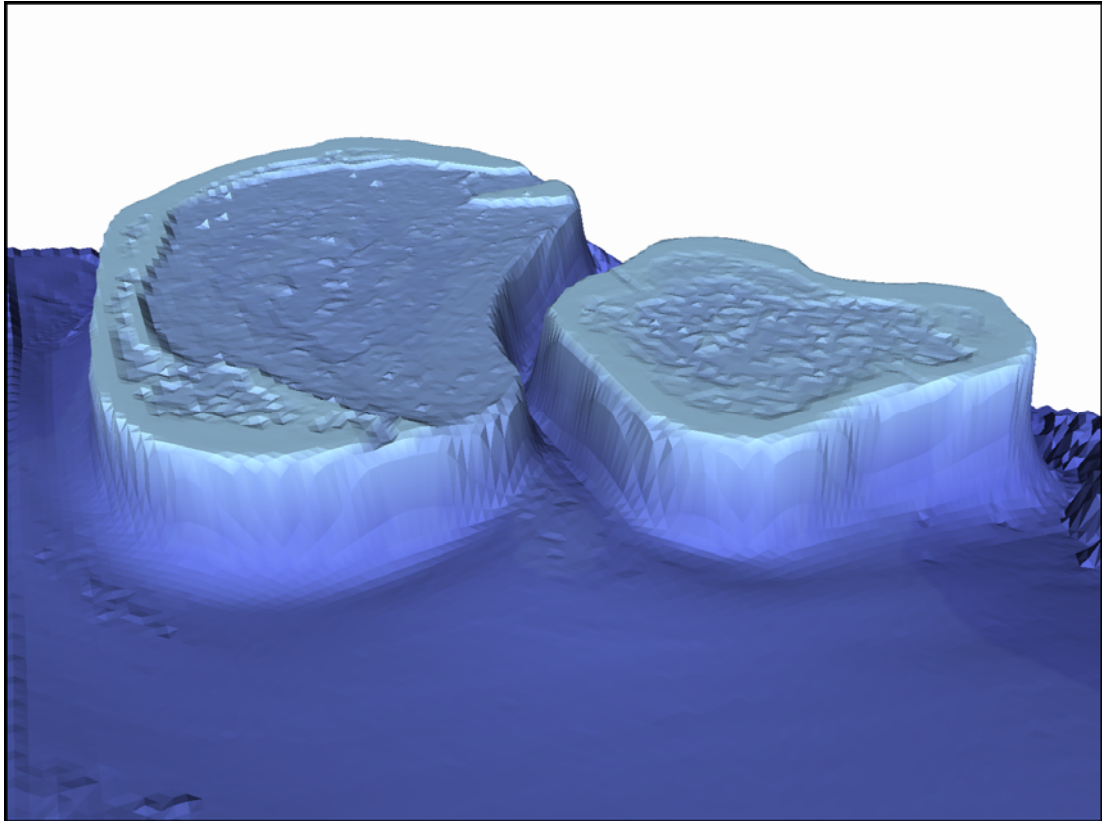


Fig 4.8 300m model bathymetry with channel seen from east

4.4.3 Boundary Conditions

Water levels

The tidal variation along the open sea boundaries to the southwest, the northwest and to the northeast were generated from tidal constants from a global tidal model with a resolution of 0.25 deg x 0.25 deg (see ref /4/). The following tidal constituents were applied:

$$M_2, S_2, K_2, N_2, O_1, K_1, P_1, Q_1$$

where subscript 2 refers to semi-diurnal tidal constituents and subscript 1 refers to diurnal tidal constituents, and where M_2 and S_2 are the principal lunar and solar semi-diurnal constituents respectively.

As an example maps showing the variation of the amplitude and the phase for M_2 are shown in Fig 4.9. The maps illustrate that the tidal wave enters the model area from the west and northwest, and that the amplitude is amplified as it approaches the Kimberley coast.

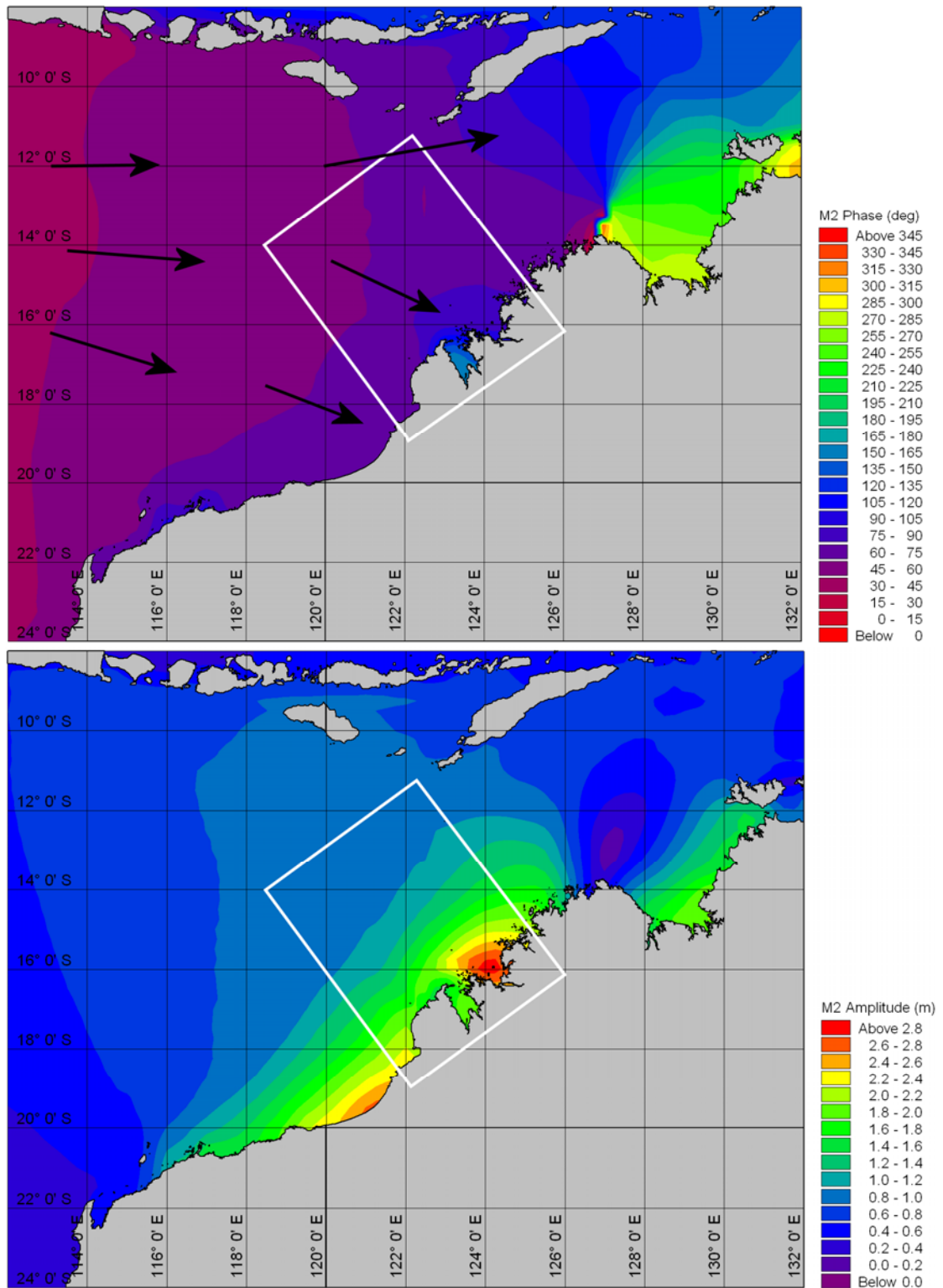


Fig 4.9 Phase (top) and amplitude (bottom) for M_2 constituent from global tidal model (ref /4/) with model boundaries shown in white and tidal wave direction indicated by arrows.



Temperatures

Based on the experience with the ROMS model at UWA the temperature measurements from the 18 sensors at Brecknock were used to produce a temperature profile at the three open boundaries. The profile and its variation throughout the entire measuring period is shown in Fig 4.10. A low pass filter was applied to remove all tidal variations (with a frequency corresponding to 60 hours and less). The four vertical lines in the figure correspond to the four periods selected for model calibration and validation (see section 5.1). At depths of more than 550m the temperature only decreased slightly (as verified by BLUElink data at UWA – see Ref /9/).

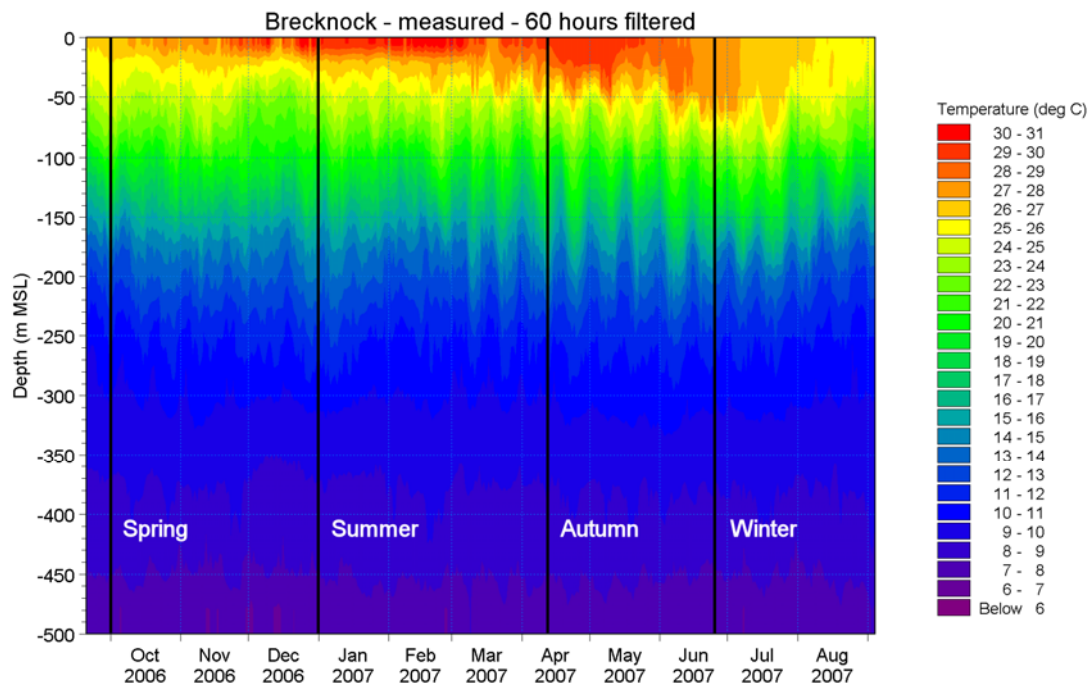


Fig 4.10 Temperature profile at Brecknock for the entire measuring period. Vertical lines correspond to the four selected calibration and validation periods, one for each season.

Alternatively the temperature variations could have been taken from a large ocean model like BLUElink (developed by Bureau of Meteorology, Royal Australian Navy and CSIRO). However, the experience at UWA as mentioned above indicated that measured data at Brecknock provided a better description of the temperature profile on the shelf than the model data from BLUElink did. Therefore the measured data at Brecknock were applied at the open boundary of the present model.

Salinities

In the ROMS model at UWA a constant salinity of 34.6 PSU was applied. Using a constant and not a varying salinity was based on the experience that only temperature differences contributed significantly to density differences and thus density driven currents.

This assumption was verified by WEL (Ref /10/) by comparing the density profile from the Browse area with and without taking the salinity variation into account. Fig



4.11 shows a comparison for the month of October for each year from 1993 to 2006, while the difference (in kg/m^3) month by month for the whole period 1993 to 2007 is shown in Fig 4.12.

Although the WEL analysis was carried out for a salinity of 34.5 PSU, it was decided to use the salinity applied in the ROMS model at UWA of 34.6 PSU in the present model.

Browse Bluelink mean density profiles with varying salinity (green) and constant salinity (34.5 PSU)(blue) for Oct.:1993-2006

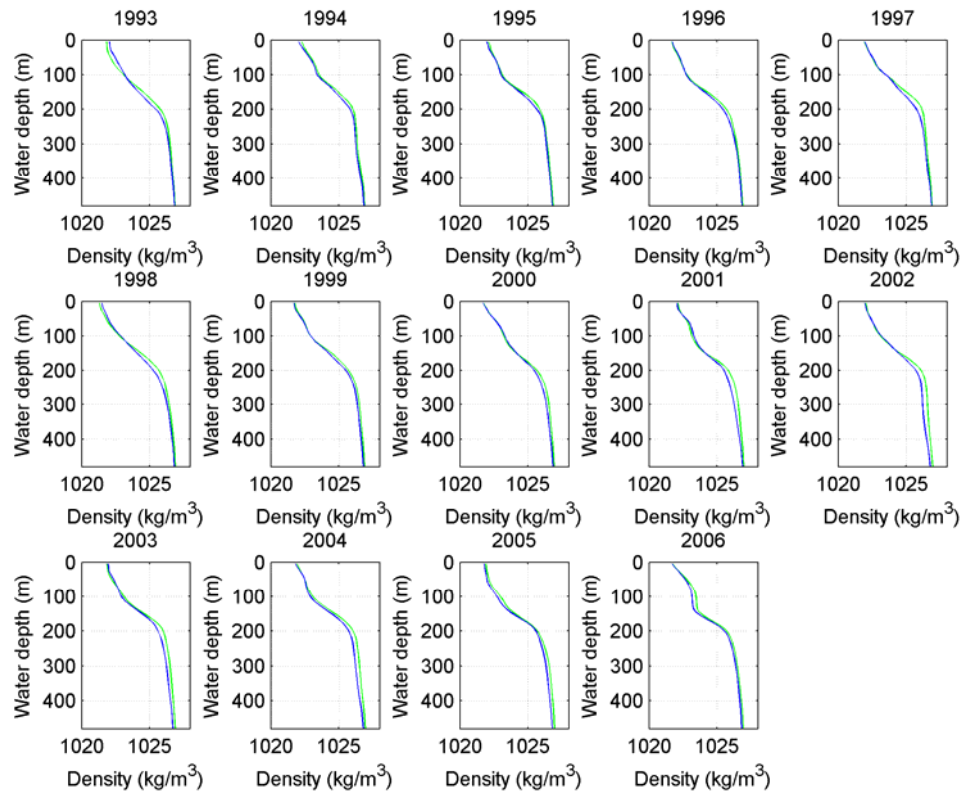


Fig 4.11 Density profiles at Browse with and without taking the salinity variation into account. Month of October. (provided by WEL)

4.4.4 Initial Conditions

A “cold start” with a constant water level of 0.0m (mean sea level), a constant salinity of 34.6 PSU, and a temperature profile for the whole model area corresponding to the Brecknock profile at the boundary (see Fig 4.10) was applied.

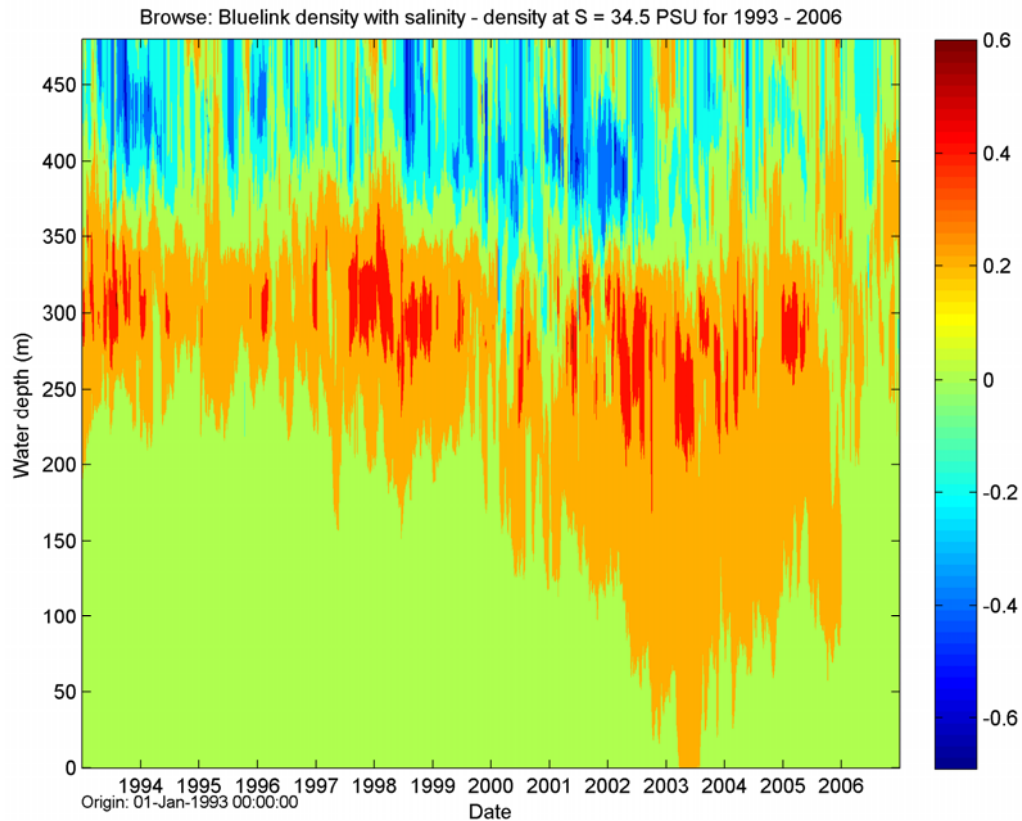


Fig 4.12 Density difference (in kg/m^3) between taking the salinity variation into account and keeping salinity constant at 34.5 PSU. 1993 - 2007. (provided by WEL)

4.4.5 Meteorological Forcing and Heat Exchange

Accurate hydrodynamic modelling of the area of interest requires accurate description of the following parameters varying in time and space:

- Wind speed and direction
- Atmospheric pressure

Additionally, for heat exchange with the atmosphere the following parameters are required:

- Wind speed
- Air temperature
- Clearness (or cloudiness)
- Relative humidity

Some or all of these parameters are also required for environmental modelling.

An overview of the availability of these parameters was prepared and is listed in Table 4.3. Based on this overview and with the aim of getting the highest possible resolution it was decided to use the wind data from SatOcean data (see Ref /13/) combined with the remaining five parameters from the global GFS model data from NCEP (see Ref /13/).

Table 4.3 Available sources of meteorological data varying in time and space



Data Name	Available at	Area available	Resolution	Period	Parameters
NCEP-40 40 years re-analysis from NCEP	NOAA: www.cdc.noaa.gov/data/gridded/data.ncep.reanalysis.html	Global	2.5 x 2.5 deg (cloudiness only 1.88 x 1.88 deg) 6 hourly	1948 to present	Winds, pressure, air temp, humidity and cloudiness
GFS from NCEP	Compiled at DHI Denmark from www.emc.ncep.noaa.gov/modelinfo/ (see Ref /11/)	Global	1 x 1 deg, (0.5x0.5 deg from 2008) 6 hourly	2002 to present (air temp, humidity and cloudiness from 2004-07)	Winds, pressure, air temp, humidity and cloudiness
NCDC blended NCEP/satellite winds (SEAWINDS)	NOAA / NCDC: www.ncdc.noaa.gov/oa/rsad/seawinds.html	Global	0.25 x 0.25 deg, 6 hourly	1987-07 to present	Winds
Meso-LAPS from BOM	Bureau of Meteorology: webclim@bom.gov.au	See note 1	0.125 x 0.125 deg, 6 hourly	2002 to present but only 5 years at a time	Winds, pressure, air temp, dew point
SatOcean blended satellite/NCEP winds and calibrated	Woodside Energy Ltd (see Ref /13/)	See note 2	0.0625 x 0.0625 deg, 3 hourly	2002-11 to 2007-11	Winds

Note 1: Covers all of Australia and adjacent areas: 4.875°N – 55.0°S and 95.0°E – 169.875°E

Note 2: Corners of area: (21.00°S,119.20°E), (15.05°S,127.35°E), (9.80°S,123.20°E) and (15.80°S,115.00°E). See also Fig 4.13.

Abbreviations:

NCEP	National Centers for Environmental Prediction
NOAA	National Oceanic and Atmospheric Administration
GFS	Global Forecast System
NCDC	National Climatic Data Center
LAPS	Limited Area Prediction System
BOM	Bureau of Meteorology

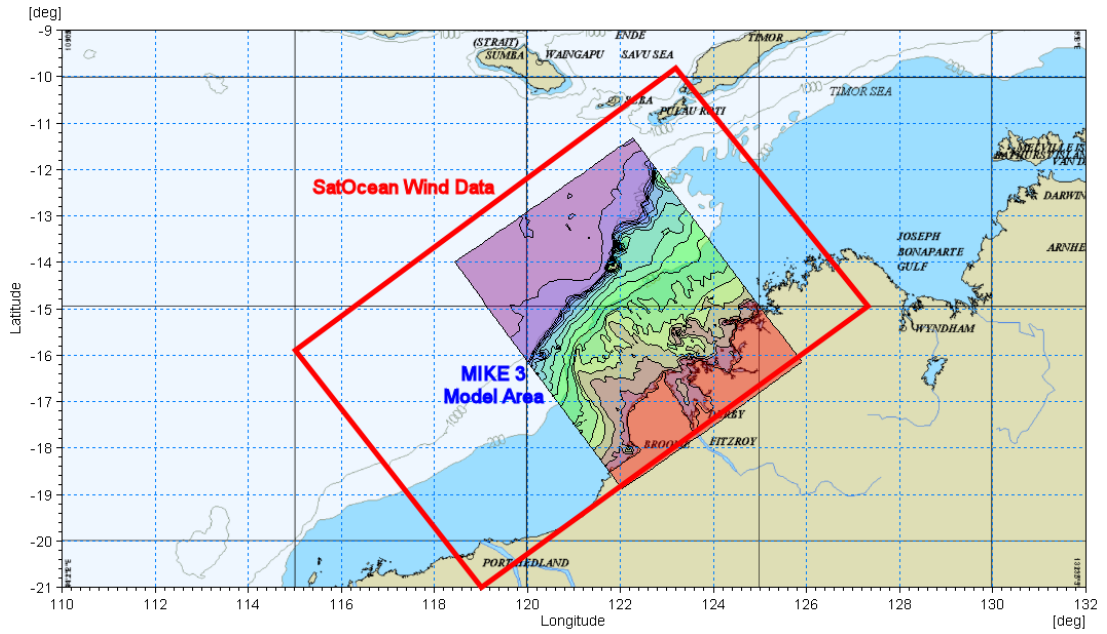


Fig 4.13 Area covered by SatOcean blended satellite and NCEP wind data (red box) relative to area covered by MIKE 3 model (coloured box)



5 CALIBRATION AND VALIDATION OF 3-DIMENSIONAL MODEL

5.1 Selection of Calibration and Validation Periods

The scope of work required four 14 day periods to be selected for the model calibration and validation, one period for each season. When selecting the four periods the following criteria were used:

- Each period should represent a season as defined by the wind.
- Each period should cover a 14 day neap-spring-neap tidal cycle.
- At station I1-1 (in Scott Reef Channel) one period should include a period with upwelling and another without upwelling.

To assist in the selection the wind speed and direction at Scott Reef (taken from the SatOcean wind data) covering the 12 months measurement period is shown in Fig 5.1 and Fig 5.2, while the predicted tidal water level variation at Scott Reef is shown in Fig 5.3. Furthermore, the temperature measurements at I1-1 are shown in Fig 5.4 as the data availability at this station should be taken into account when selecting the four periods.

Additionally, it is envisaged that each of the four periods should be extended to cover two consecutive 14 day neap-spring-neap tidal cycles. This would give about one month of hydrodynamic data for each season as a basis for the environmental modelling.

With these criteria in mind the four periods as listed in Table 5.1 were chosen. Note that one day and 16 hours were added at the start of the period for model warm-up.

Table 5.1 Periods selected for calibration and validation (UCT+8 hours = Western Standard Time)

Period	Start (UTC+8 hours)	End (UTC+8 hours)
Spring (Transition period)	2006-10-01 08:00	2006-10-17 00:00
Summer (NW monsoon)	2006-12-30 08:00	2007-01-15 00:00
Autumn (Transition period)	2007-04-11 08:00	2007-04-27 00:00
Winter (SE monsoon)	2007-06-25 08:00	2007-07-11 00:00

Arbitrarily the first period (spring) was used for model calibration (i.e. fine tuning the model parameters), while the three remaining periods were used as model validation periods (i.e. to show that the model parameters chosen during the calibration period are valid for other periods).

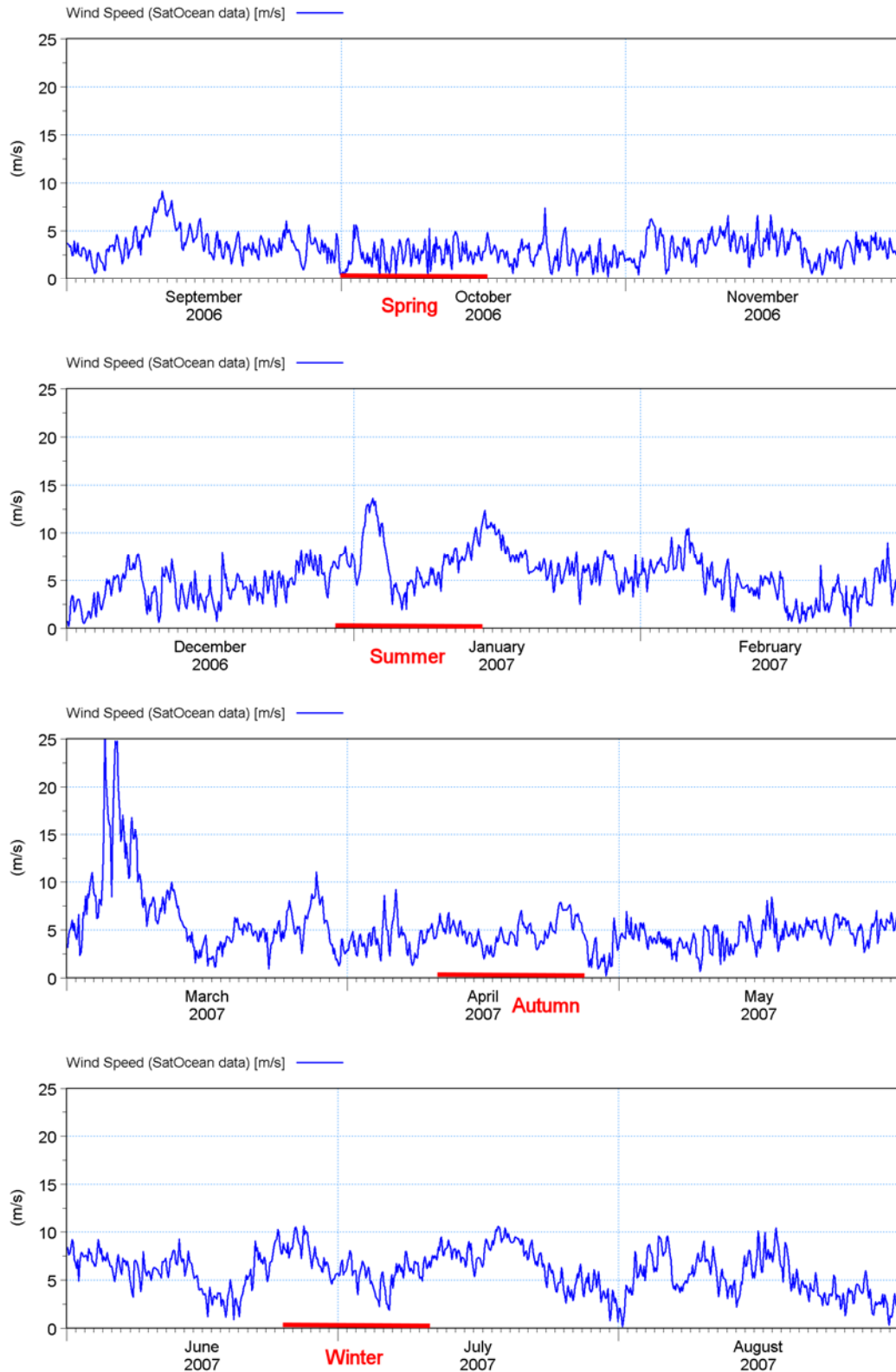


Fig 5.1 Wind speed at Scott Reef (from SatOcean wind data, Ref /13/)

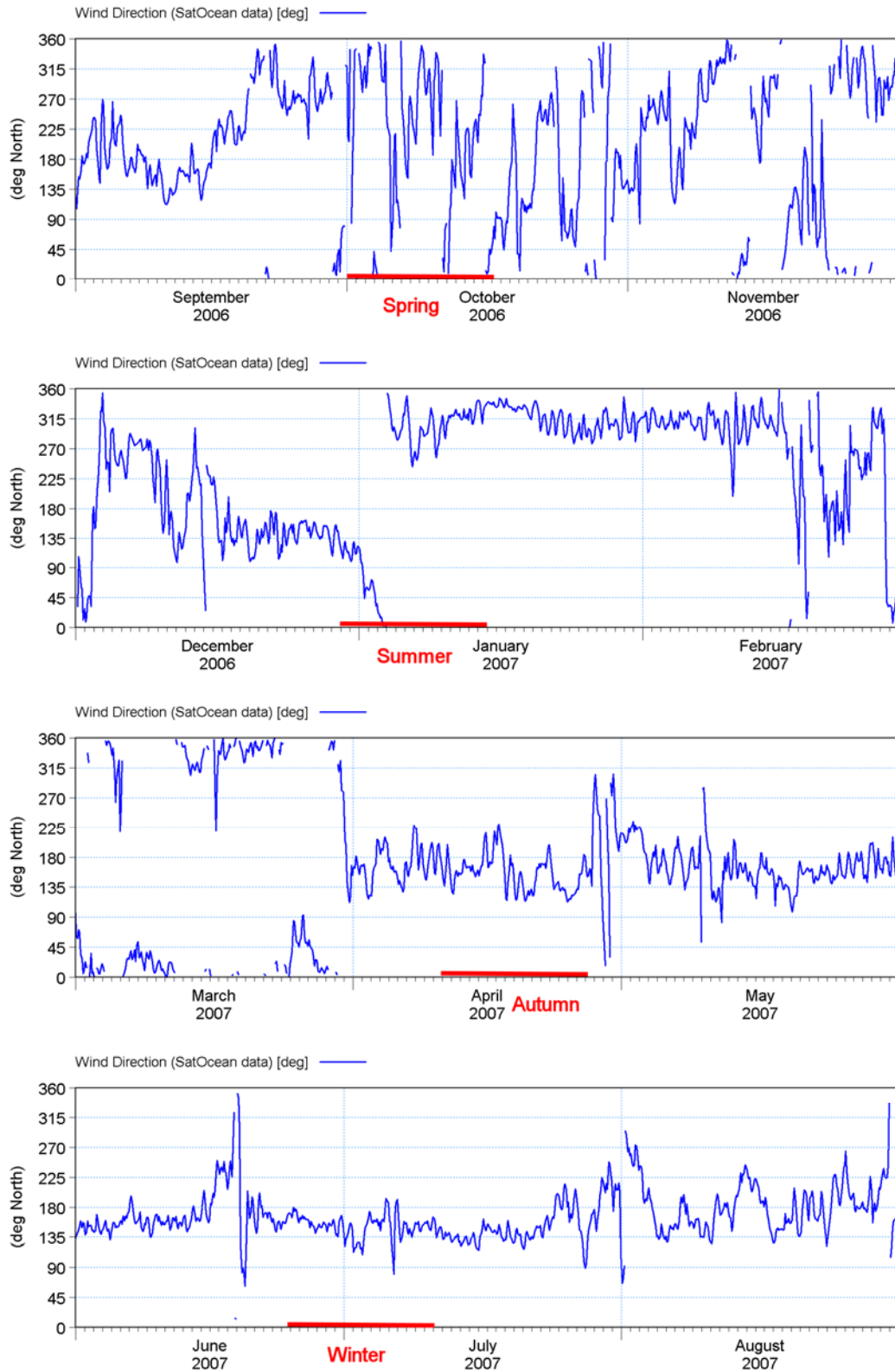


Fig 5.2 Wind direction at Scott Reef

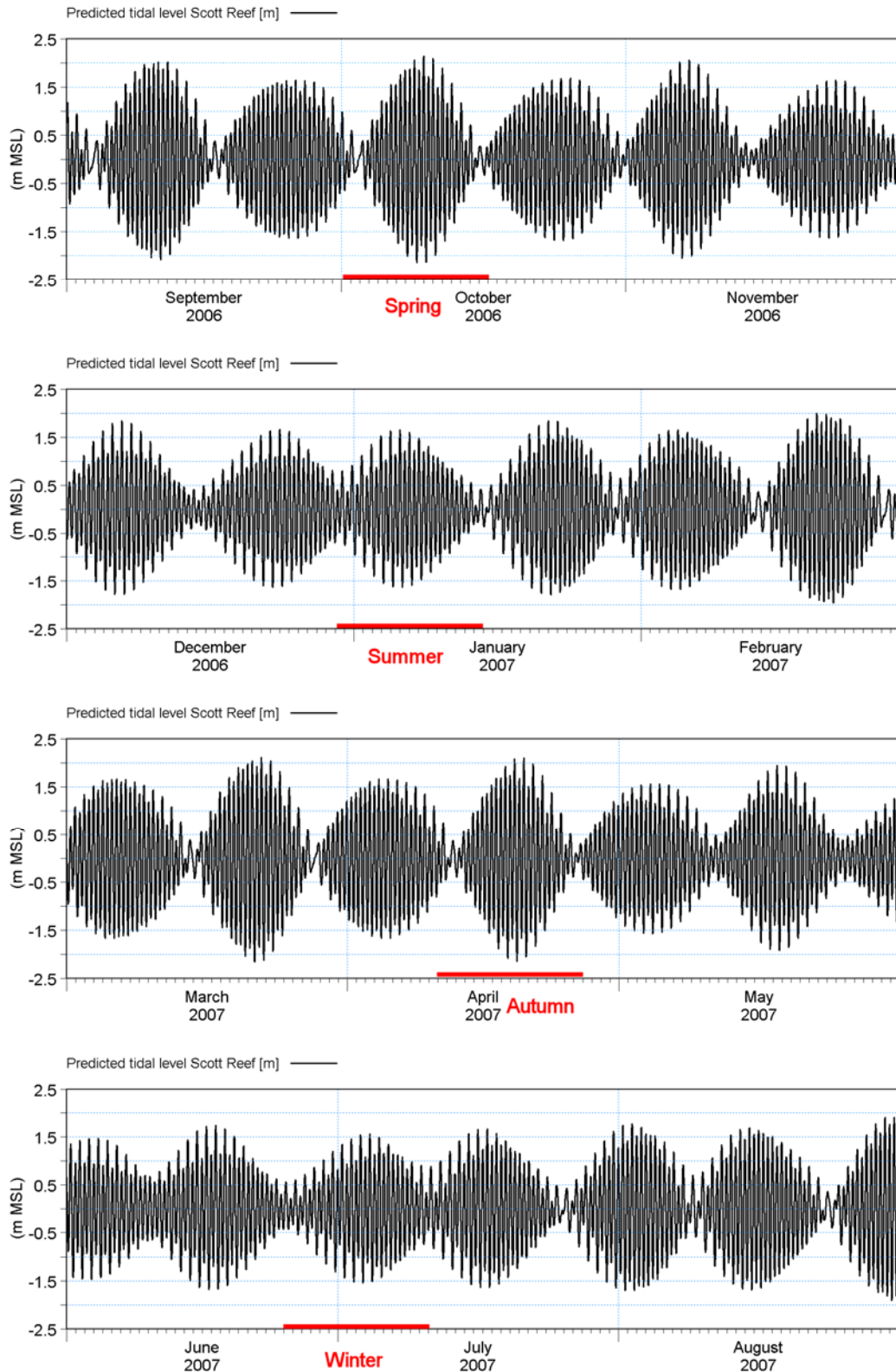


Fig 5.3 Predicted tidal level at Scott Reef

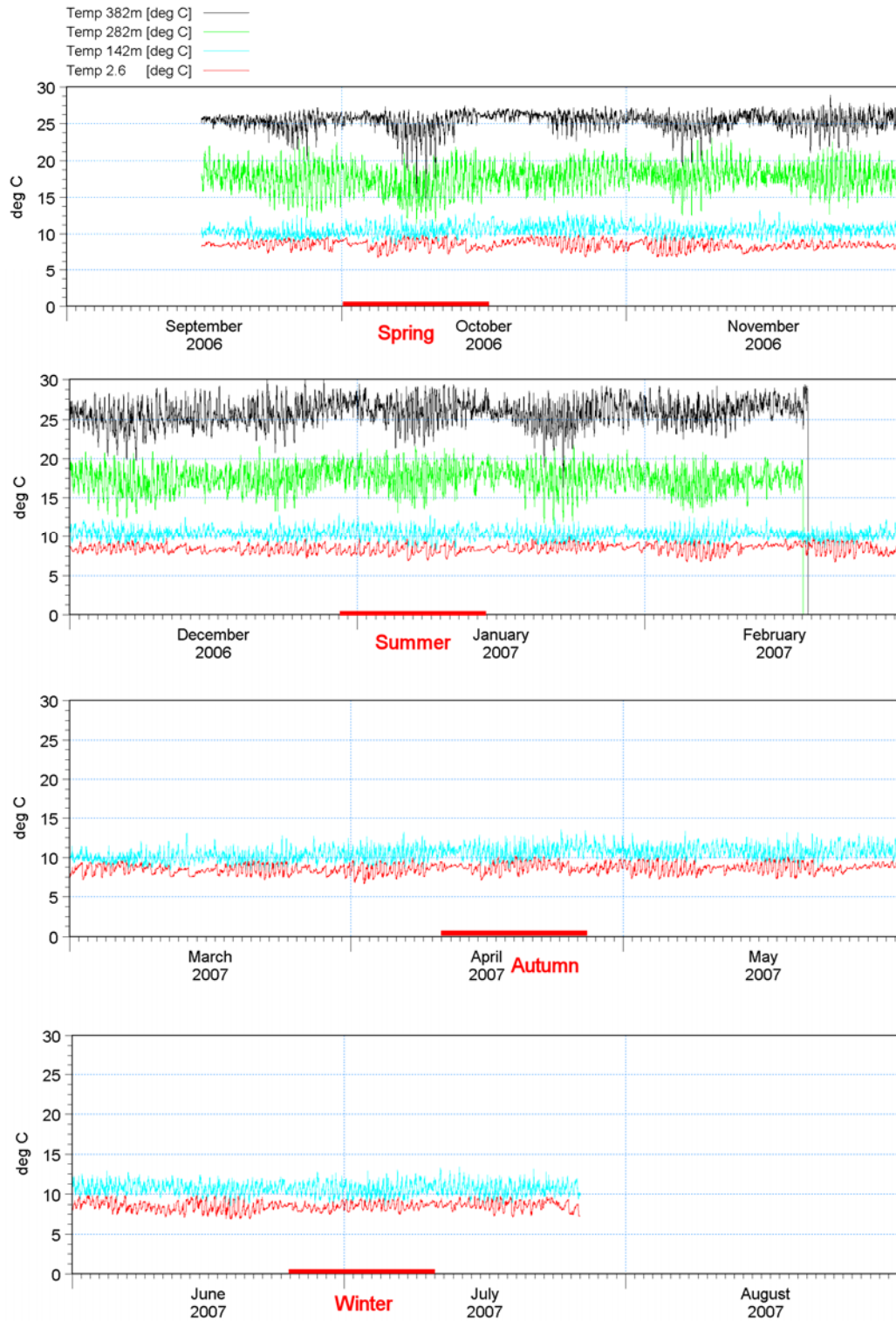


Fig 5.4 Measured water temperature at I1-1 (Note that the top two sensors failed 18/2/2007)



5.2 **Basic Model Parameters**

All model depths have been given relative to mean sea level (MSL), which is 2.3m above Scott Reef Datum (SRD) (see Ref /6/). The time zone applied was UTC+8 hours (Western Standard Time).

The time step applied in the simulations was 10 seconds giving a maximum Courant number of 4.8. The Courant Number expresses how fast the information travels in the computational grid in one time step. While many computational solution methods only allow for a Courant number up to 1, the solution scheme applied in MIKE 3 classic allows for Courant numbers up to 5 (or even 10 depending on the bathymetry) making it a relatively fast model.

5.3 **Calibration Parameters**

The model calibration initially focussed on the B2-1 (Brecknock) location as temperature profiles from this location was applied at the open model boundaries. Secondly, the model calibration concentrated on the other locations where measurements were available, especially location I1-1. For water levels A2-1 plus standard tidal stations at Browse Island and Adele Island were considered.

A number of parameters are available for the calibration of the 3-dimensional non-hydrostatic hydrodynamic model. They include:

- Turbulence scheme and coefficients
- Compressibility
- Wind stress
- Bottom friction
- Heat exchange

Their values as determined for the present calibration are described below. Note that the five parameters are listed with the most important ones at the top.

For a detailed description of the calibration parameters and for a detailed scientific description of MIKE 3 classic see Ref /5/.

Turbulence scheme

For the description of the turbulence a dynamic k- ϵ formulation was applied in the vertical and a Smagorinsky formulation with a constant of 0.4 (which is the default value) in the horizontal.

Compressibility

This parameter describes the “stiffness” of the system and is very important for the calibration. It depends on the depth, grid spacing and time step. After testing a number of approaches it was decided to use a constant compressibility of 668 m/s for the 8100m, 2700m and 900m grids, while a depth varying compressibility of 10 – 668 m/s was applied in the 300m grid.

Wind stress



The wind stress coefficient varies between 0.0016 for 0 m/s and 0.0026 for 24 m/s. This variation is the one normally used for open sea areas.

Bottom friction

For the bottom friction formulation a bed roughness length scale of 0.05m was applied. The bottom friction was not of importance for the model calibration.

Heat exchange

No changes to the supplied default parameters were made.

5.4 Sensitivity Tests for Inclusion of Large Scale Eddies

As mentioned in section 2.4.4 eddies which are shed off from the Indonesian Through Flow (located to the north of the area of interest) may influence the current in the study area, and have been identified in the measurements from Brecknock. They are, however, of secondary importance when compared to tide and wind (see Table 3.1).

Three possibilities for including them in the model set-up for the present study have been identified:

- Extend the model area to cover the Indonesian Through Flow, its sources and driving forces. This will be a major modelling job and will not be possible within the present project.
- Extract boundary data from a large scale model and apply to the model in the present study. One possibility for such a large scale model is the Bluelink model, which is being developed by the Bureau of Meteorology, the Royal Australian Navy and CSIRO. Data from Bluelink are, however, only available for research projects and not yet for commercial projects.
- Extract boundary data from satellite measurements. These large scale eddies can be seen in satellite measurements of sea surface temperatures (SST), and they also manifest themselves as changes in the sea surface as sea level anomalies (SLA). An example of both is shown in Fig 5.5.

This third possibility has been tested by extracting SLA's from satellite measurements and adding them to the tidal boundaries of the hydrodynamic model.

The method does, however, not reproduce eddies in the model as seen on the satellite measurements. The reason for this is most likely that the satellite SLA maps represent data collected over a period of 7-10 days, and thus represent an "overall" picture, but not an exact water level anomaly at a specific point in time.

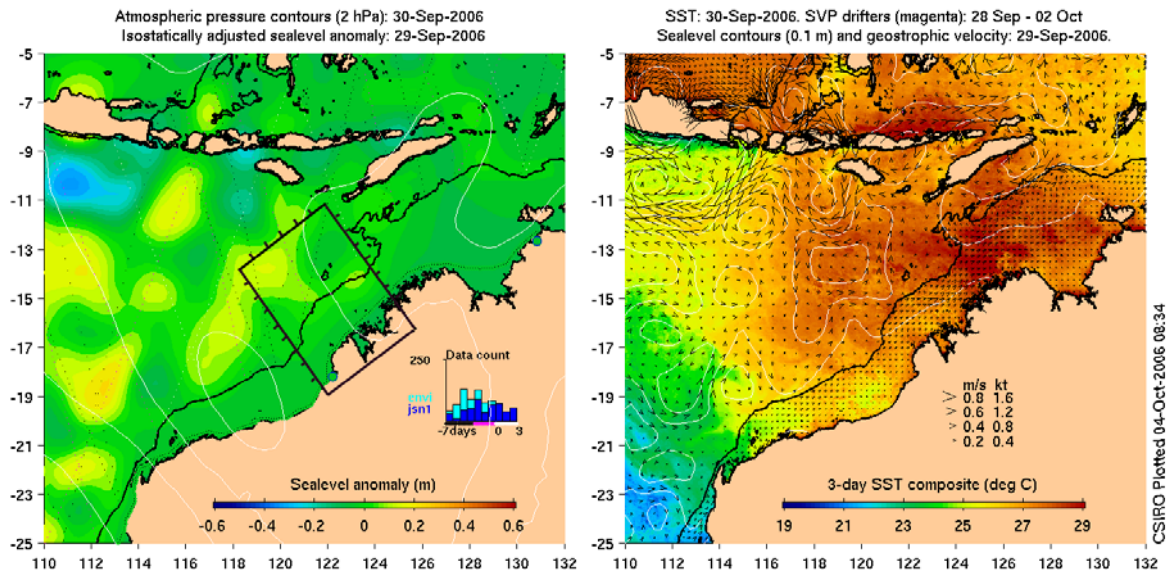


Fig 5.5 Sealevel anomaly (left) and sea surface temperature (right) from satellite measurements from a 10 day period around 30 September 2006 (from CSIRO www.marine.csiro.au/remotesensing/oceancurrents/NW/20060929.html)

It has thus not been possible to include these eddies in the present modelling. However, with the eddies only being of secondary importance (to tide and wind) and as the model in general reproduces the measured current speeds with only a very small bias (i.e. the mean current speed from the model and from the measurements only differ with few cm/s – see for example Table 5.2) it is concluded that the model even without these eddies represents the currents around Scott satisfactorily and is well suited to be applied in environmental modelling for Scott Reef and surrounds (see the following sections in this chapter).

5.5 Performance Criteria

The evaluation of whether a model provides a sufficiently accurate description of the environment depends in general on the specific objective for the individual model. Furthermore, in practice the achievable quality is dependent on several factors, such as:

- The basics of the numerical model, such as processes included and their formulations.
- The quality of the available forcing conditions, initial conditions and bathymetric information for the model domain.
- The quality of the calibration and validation data for comparison with model results.
- The complexity of the area and processes being simulated.

Finally, the model quality achieved depends on how much effort is put into the calibration exercise, which may be limited due to time constraints.



Traditionally, the evaluation of performance has been based on visual comparisons, e.g. by time series plots or instantaneous plan/transect plots of modelling results and monitoring data. However, a quantitative approach for the performance control has been introduced, where the general discrepancy (or match) between model and monitoring data is expressed numerically.

An appropriate internationally accepted standard for the validation of hydrodynamic model performance can be found in the UK Foundation for Water Research publication Ref FR0374 '*A framework for marine and estuarine model specification in the UK*' (Ref /12/).

In broad terms this can be categorised by the following performance limits:

- Tidal elevations: Root Mean Square (RMS) error < 15% on spring tide and 20% on neap tide ranges (maximum deviation 0.1 m at marine estuarine boundary, 0.3 m at estuary head);
- Current speed deviation RMS error < 10 to 20% (maximum deviation 0.2 m/s);
- Direction error RMS error < 20 deg; and
- Timing of high water at marine estuarine boundary 15 minutes, 25 minutes at estuary head.

The present model covers an offshore area (including a reef) and not an estuary. However, with no specific criteria available for offshore areas the estuarine values have been applied. This is seen as a valid approach as estuarine systems are structurally more complex than open ocean systems. In addition, quantile-quantile plots and frequency analysis plots have been produced to illustrate the model accuracy.

5.6 Results of Model Calibration for Spring Period

The results from the model calibration period comprise for each of the four grids (see Table 4.2) and for each time step a 3-dimensional matrix of temperature, velocities (called u, v and w) and excess pressure. Additionally a 2-dimensional matrix of water level was stored. These output data can be presented in a number of ways. An example of a surface velocity and temperature field is shown in Fig 5.6, while the initial temperature profile along X=74 and Y=65 and the temperature field at the time corresponding to Fig 5.6 are shown in Fig 5.7 and Fig 5.8 respectively. A 3-D plot of the whole area showing a selected number of layers are shown in Fig 5.9. Animations of surface plots and profile plots are also readily produced.

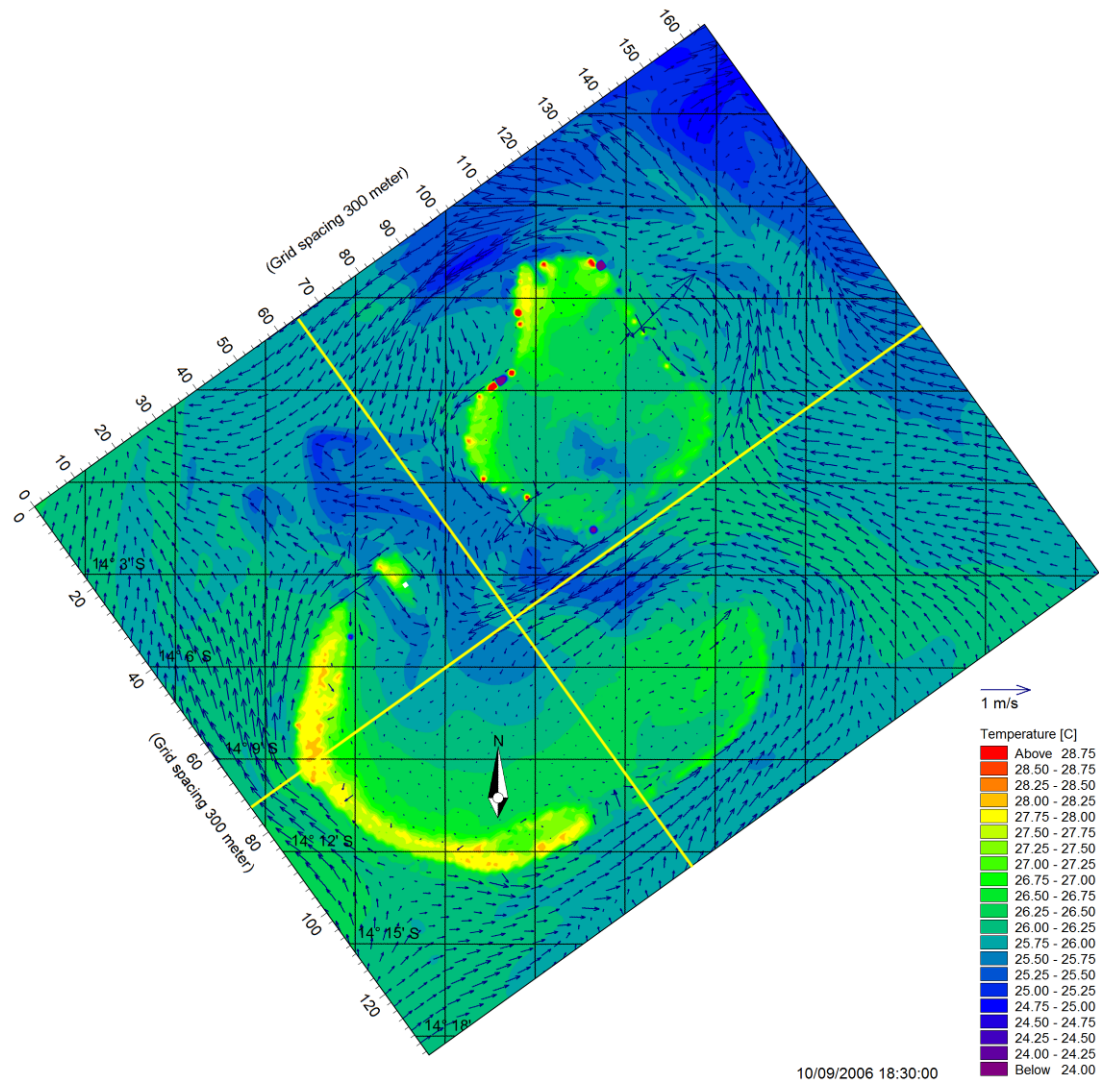


Fig 5.6 Surface velocity and temperature field in 300m grid on 9 Oct 2006 18:30. Yellow lines indicate location of X- and Y- profiles.

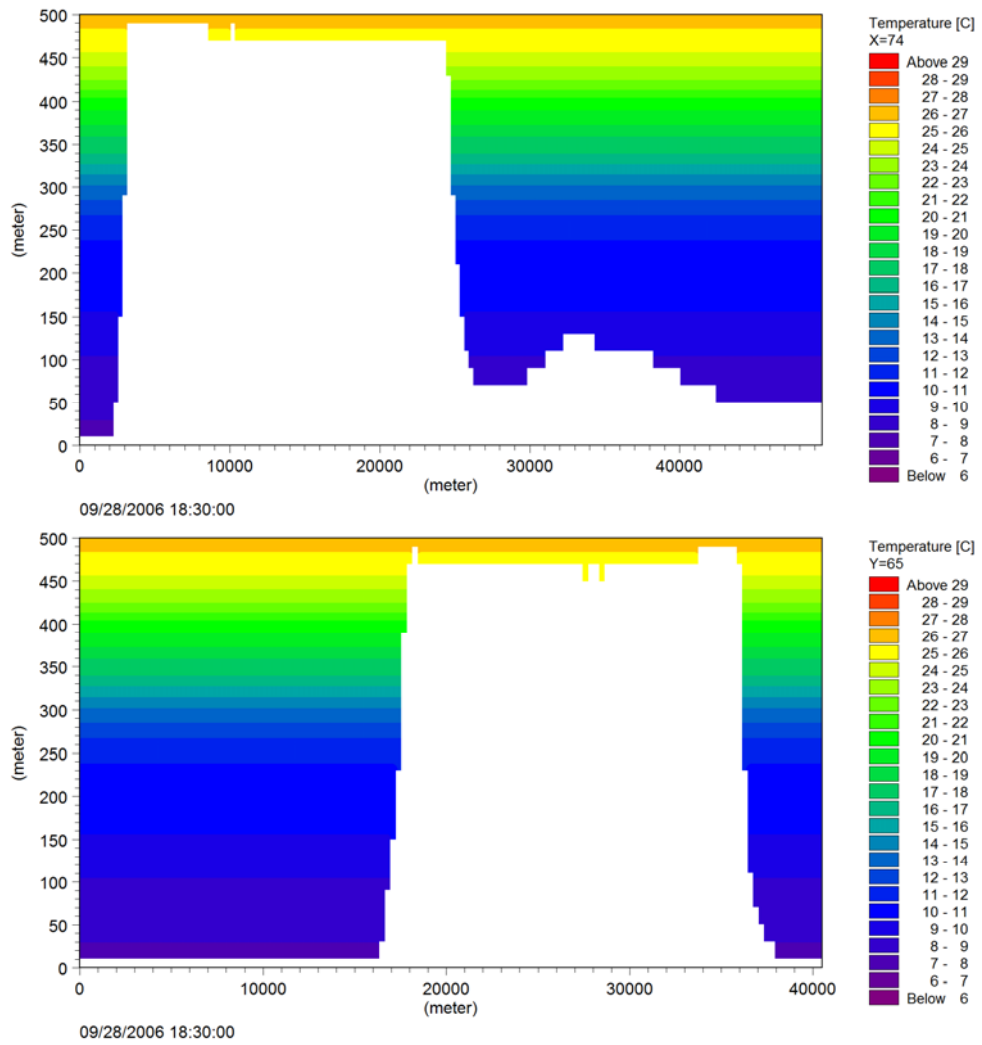


Fig 5.7 Profiles at start of simulation (initial field)

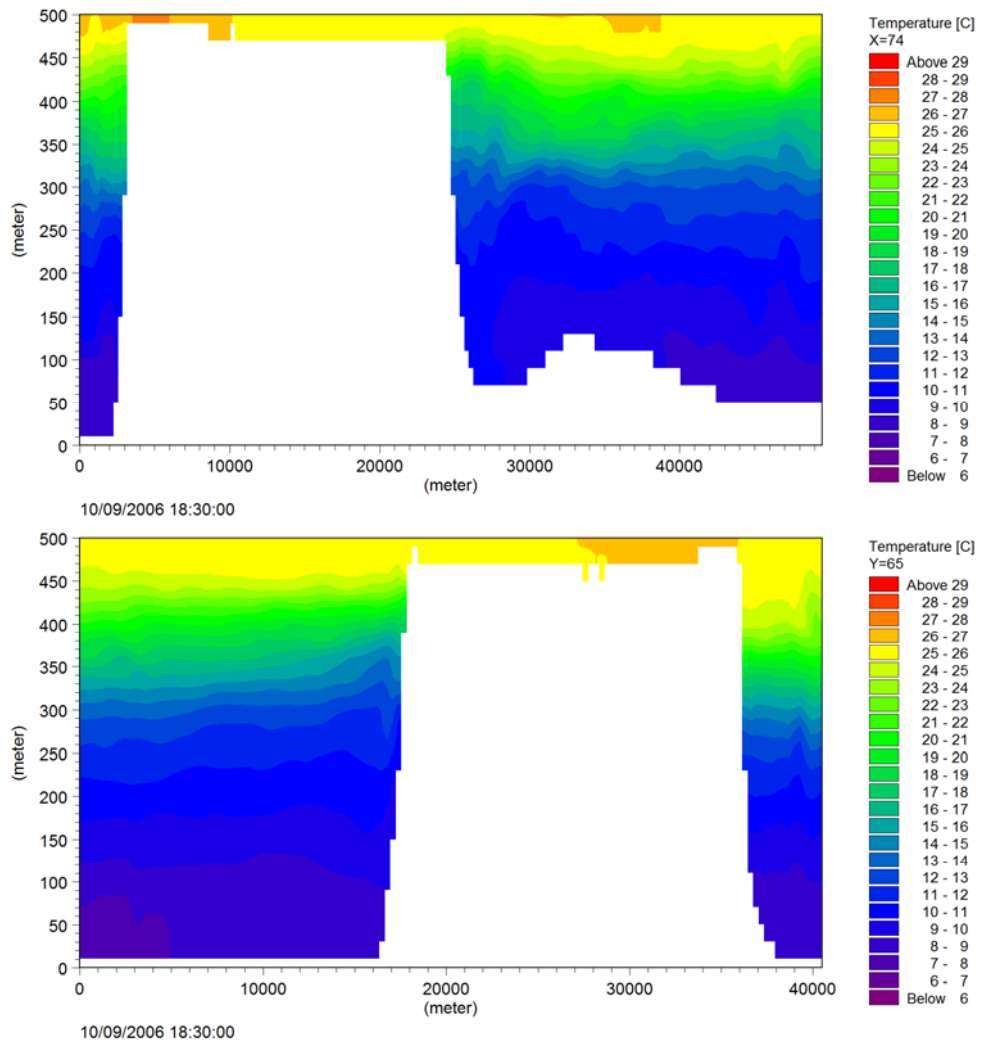


Fig 5.8 Profiles on 9 Oct 2006 18:30

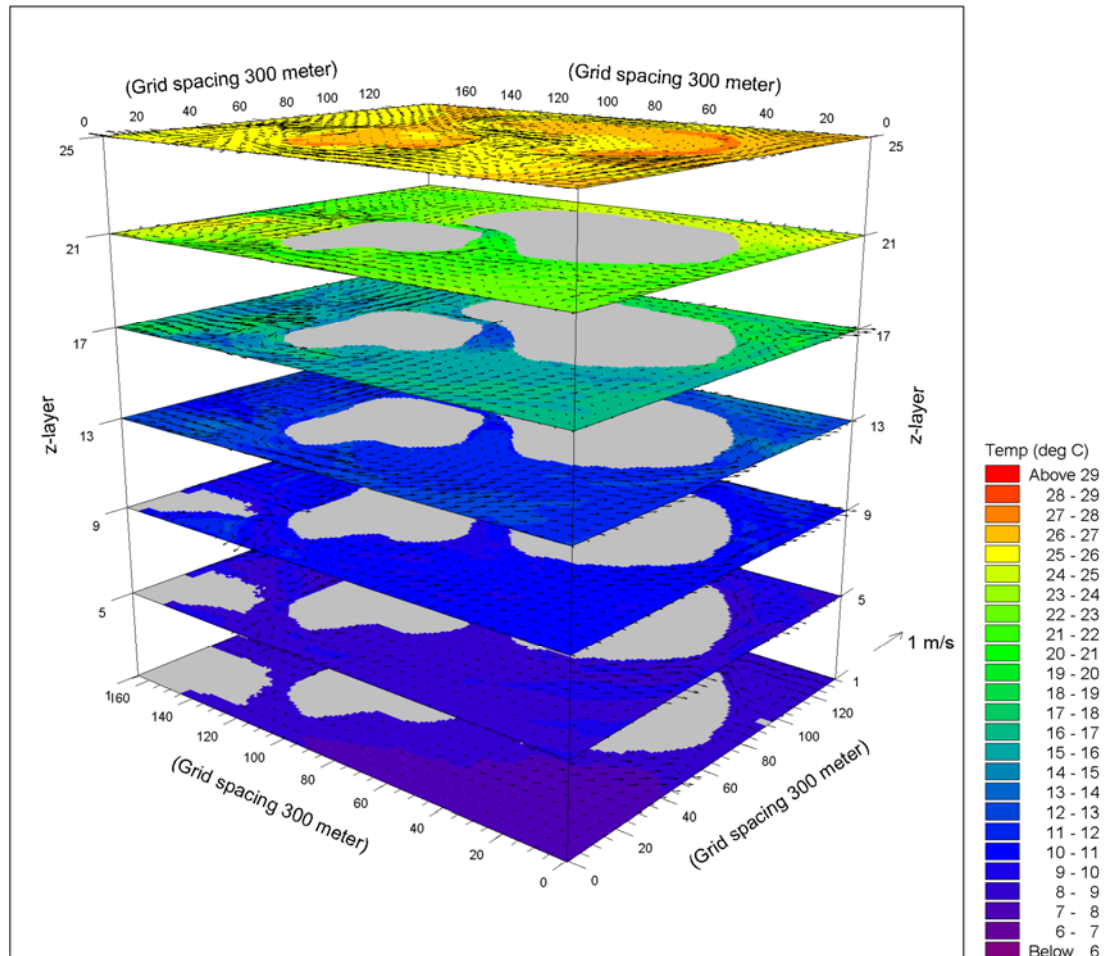


Fig 5.9 3-D view from the west of the inner-most grid showing temperature (in colour) and velocity (as arrows) 9 Oct 2006 18:30

Time series from the positions where measurements were available were extracted from the model results and compared to the measurements. The location of the measurement stations in the model grids are shown in Fig 5.10.

In addition to comparison of time series, quantile-quantile plots (Q-Q plots) and frequency plots were produced for visual assessment of the accuracy.

All comparisons are included in Appendix B, while the main plots are also included in this section.

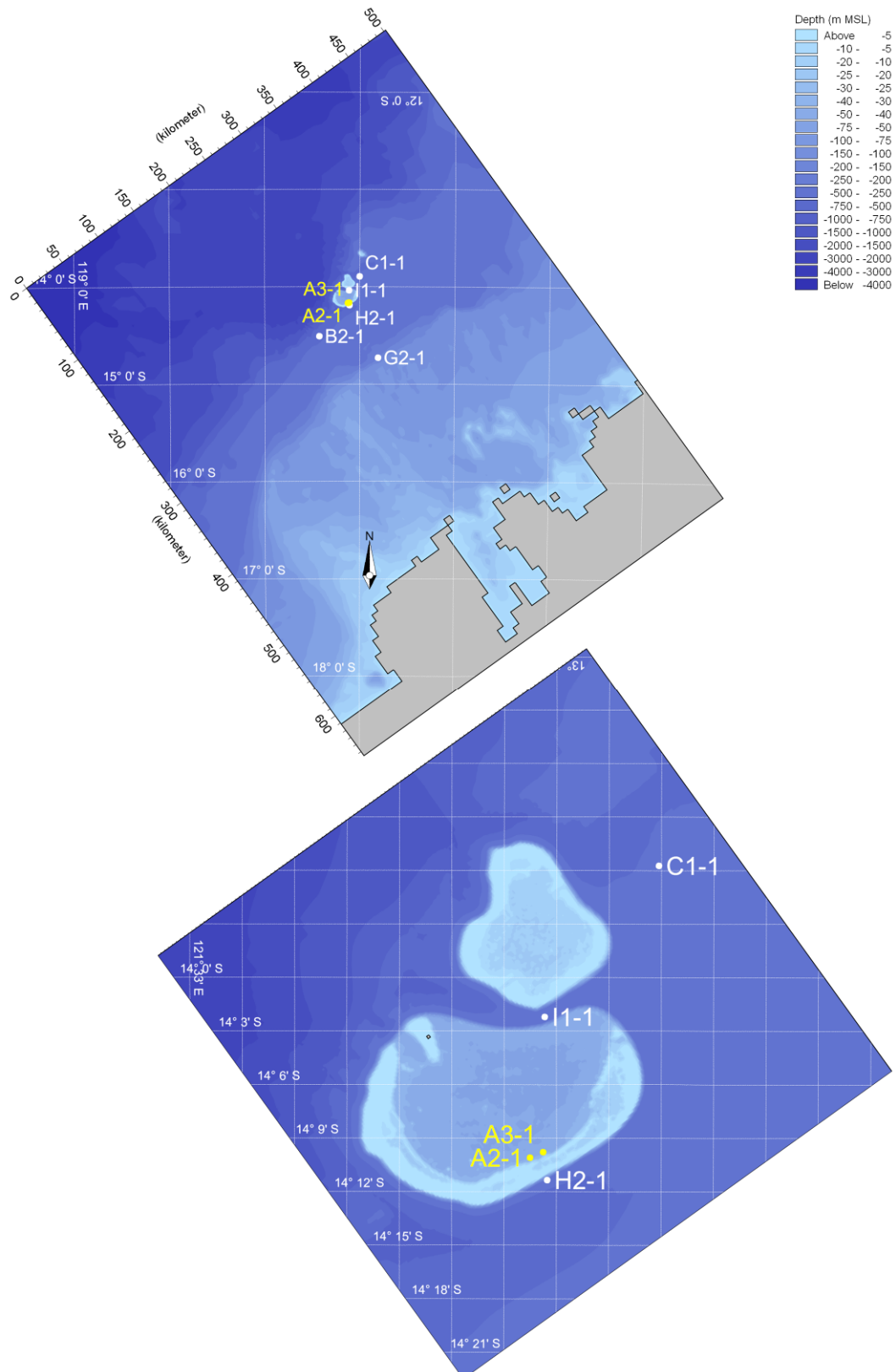


Fig 5.10 Locations where current and temperature measurements and model results have been compared are shown in white. Water level measurements have been compared for A2-1 while A3-1 is the meteorological station. Both of these stations are shown in yellow. Lower map shows details around Scott Reef (in 300m grid).



Of the many plots in the appendix B the plots of the depth averaged currents, the isopleth plots, the multi-time series plots showing temperatures and the Q-Q plots give a good overview of the model accuracy. These plots are shown in Fig 5.11 to Fig 5.14 for B2-1, in Fig 5.17 to Fig 5.20 for H2-1, and in Fig 5.21 to Fig 5.24 for I1-1.

Note that there are measurements at too few depths at C1-1 to compute the depth averaged currents and to produce an isopleths plot. Therefore only a plot showing temperatures and a Q-Q plot for temperatures are shown for C1-1 (Fig 5.15 and Fig 5.16).

A Q-Q plot for the depth-averaged current speed for all stations is shown in Fig 5.25.

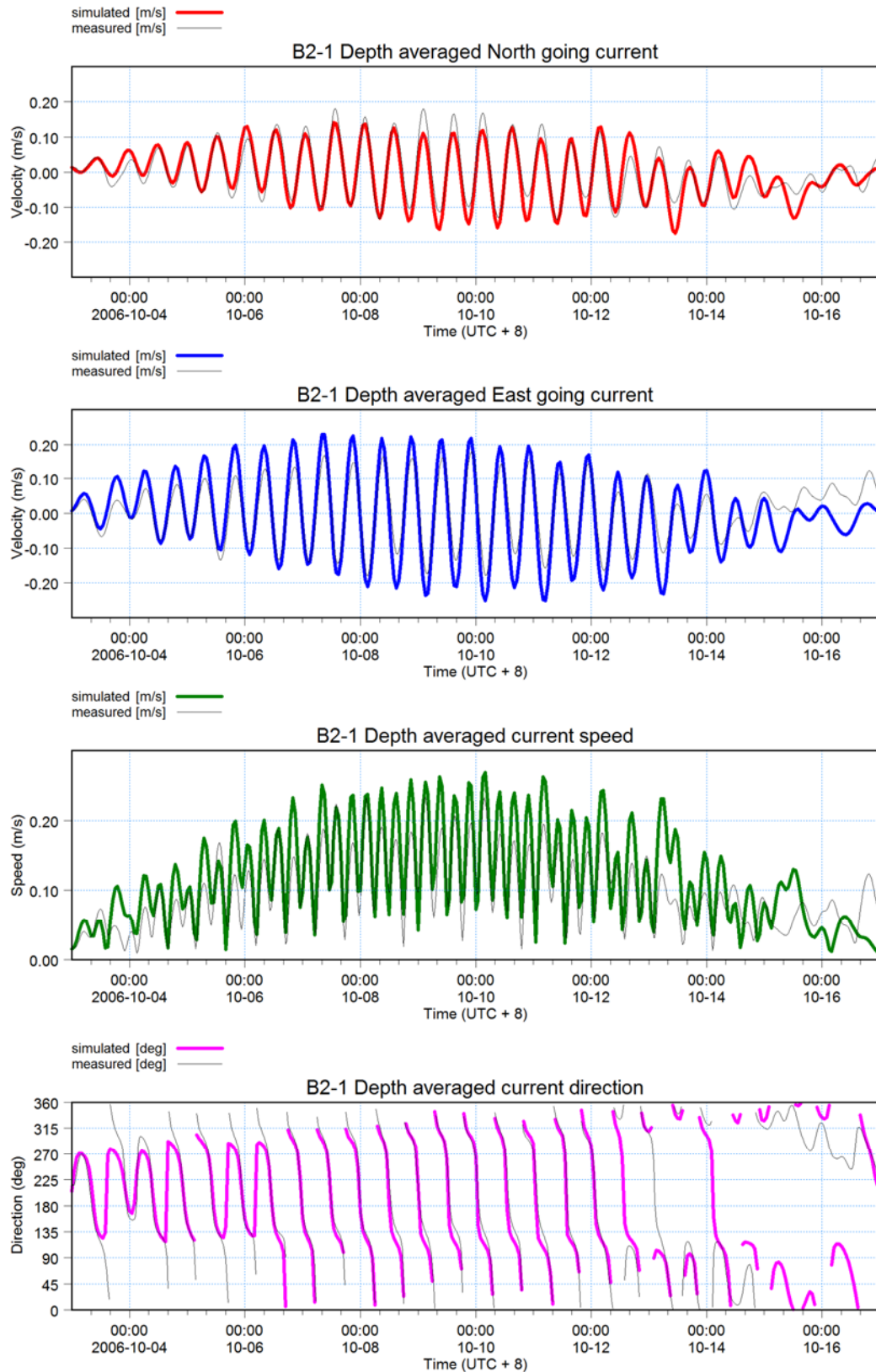


Fig 5.11 Depth averaged currents for B2-1, spring calibration period

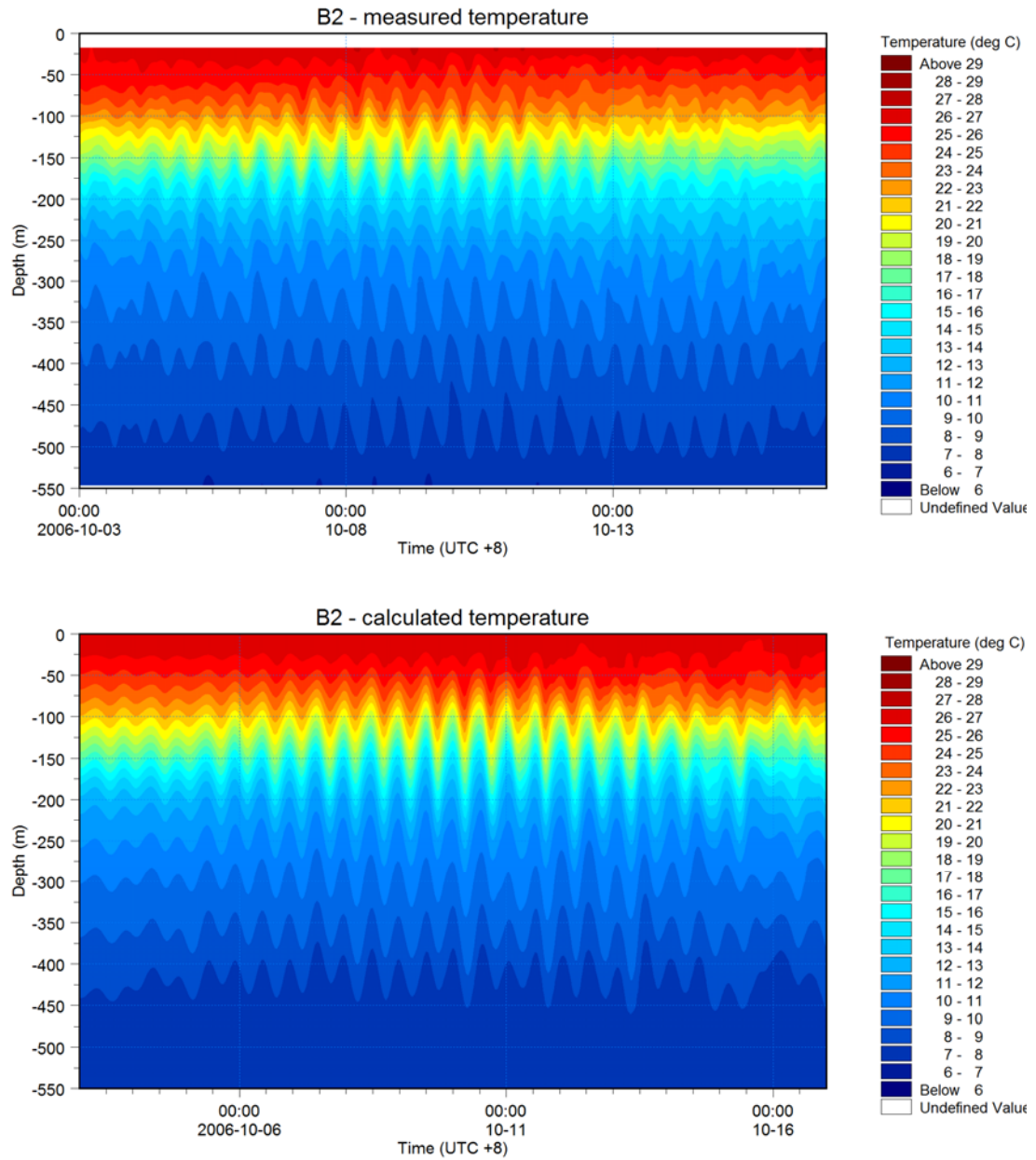


Fig 5.12 Isopleth plot for B2-1, spring calibration period

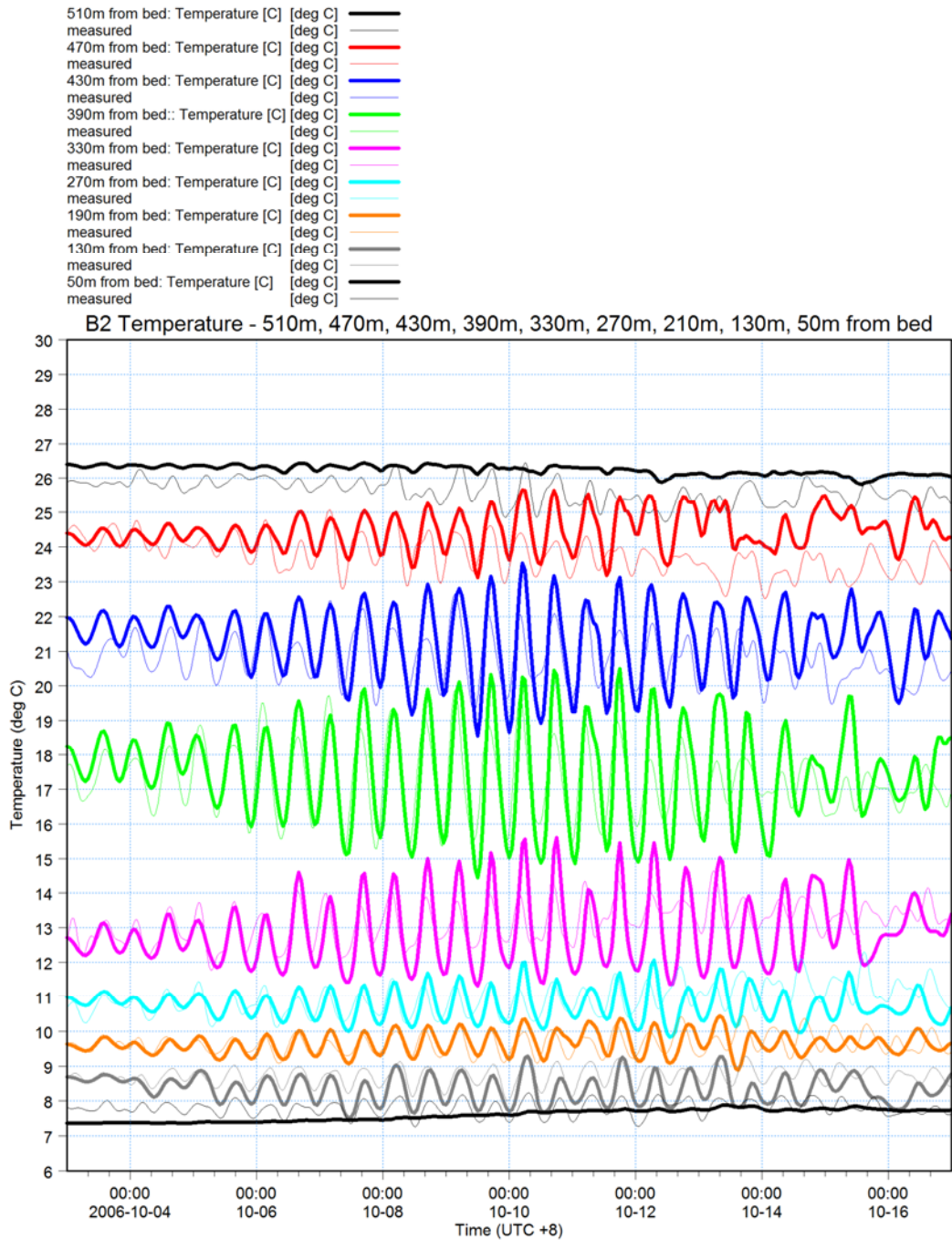


Fig 5.13 Multi-time series plot for B2-1, spring calibration period
 Thin lines: measured values, thick lines: model results



- T at 510m x x
- T at 470m x x
- T at 430m x x
- T at 390m x x
- T at 330m x x
- T at 270m x x
- T at 190m x x
- T at 130m x x
- T at 50m x x

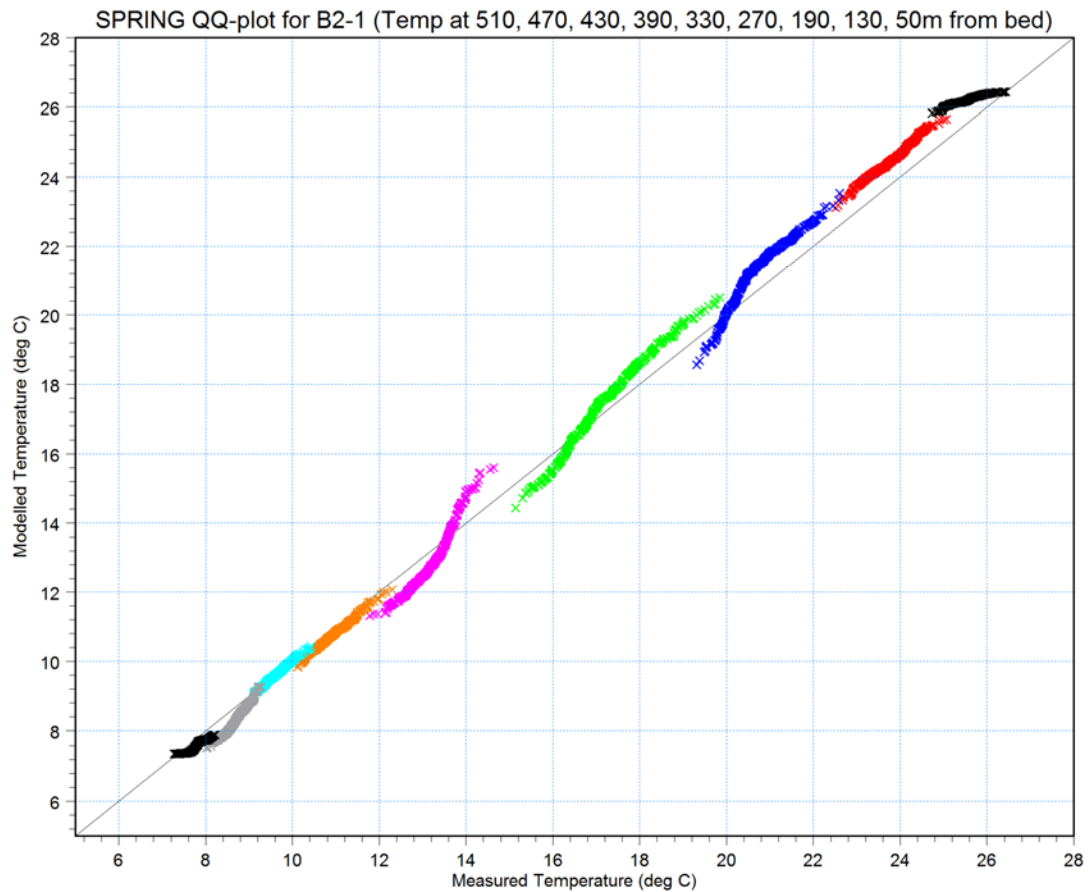


Fig 5.14 Q-Q plot for temperatures for B2-1, spring calibration period

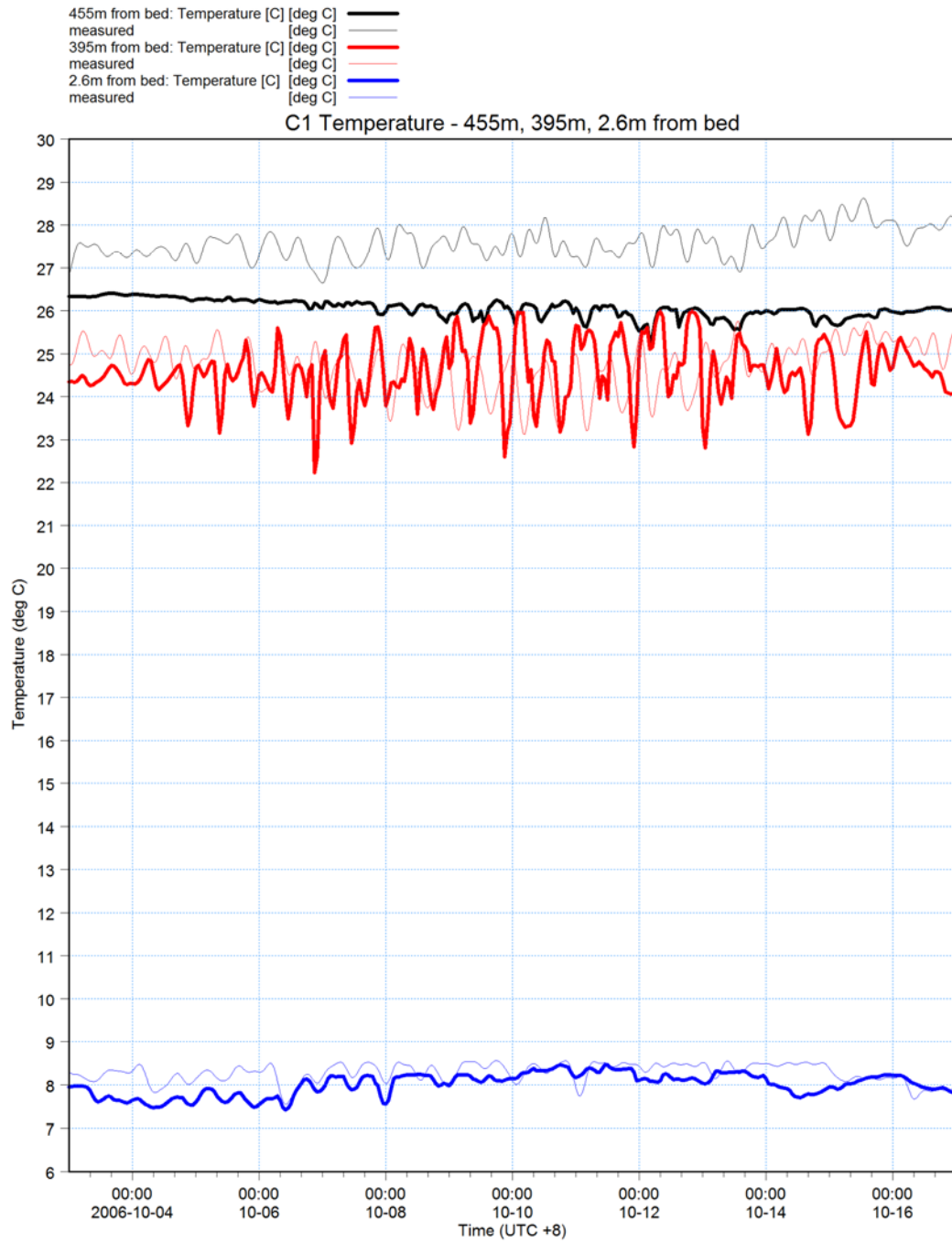


Fig 5.15 Multi-time series plot for C1-1, spring calibration period
Thin lines: measured values, thick lines: model results



T at 455m × ×
T at 395m × ×
T at 2.6m × ×

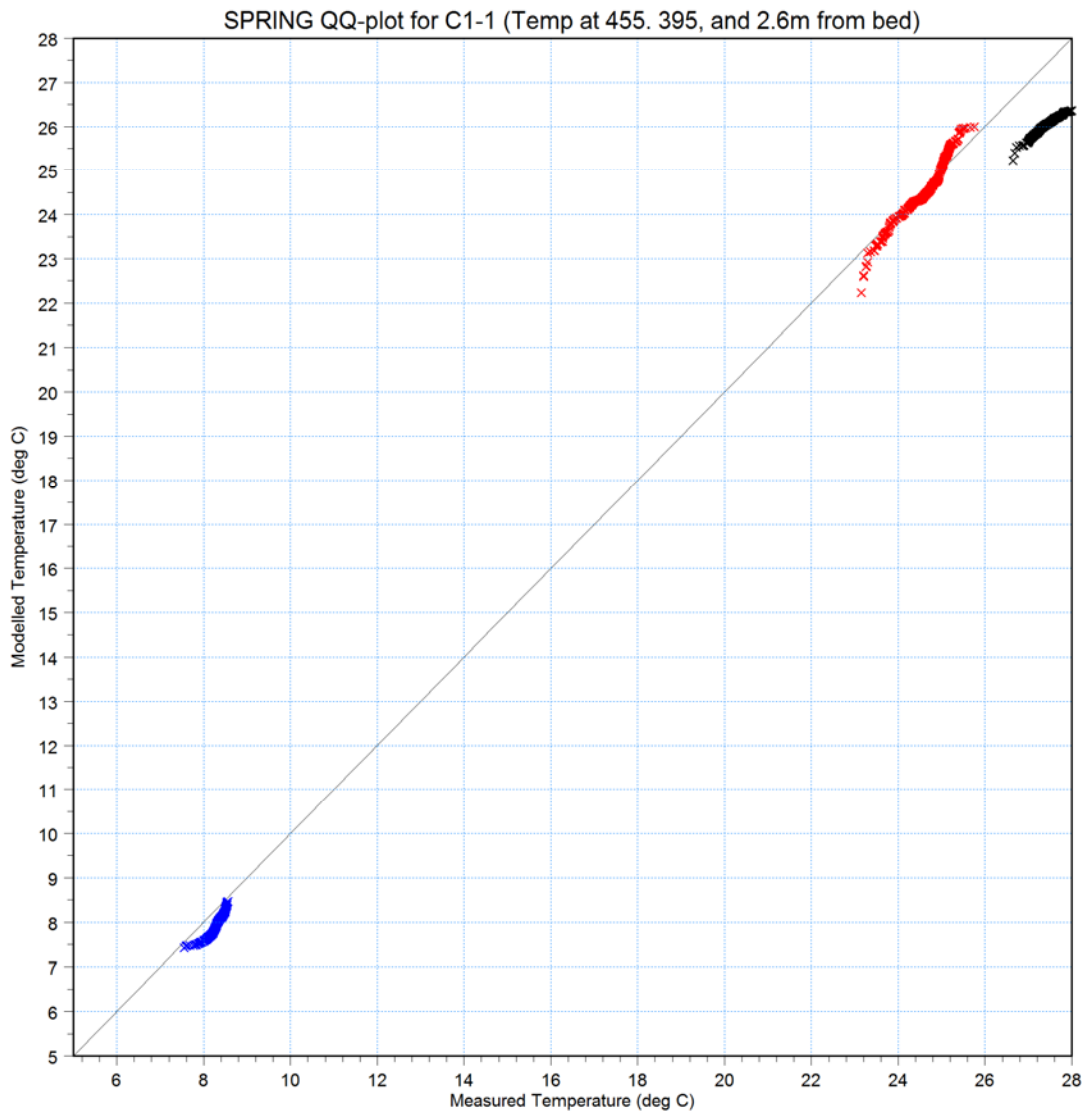


Fig 5.16 Q-Q plot for temperatures for C1-1, spring calibration period

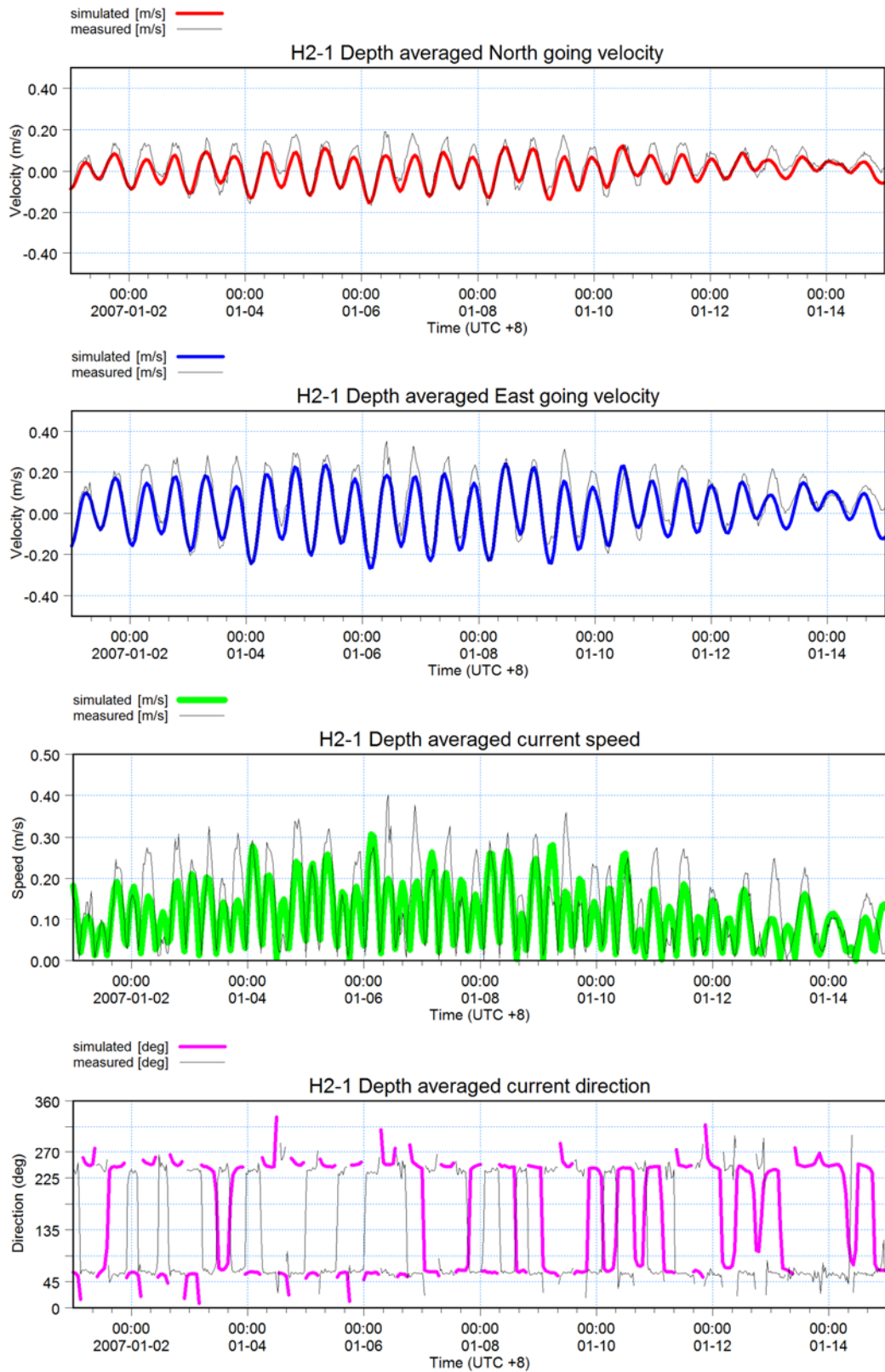


Fig 5.17 Depth averaged currents for H2-1, spring calibration period

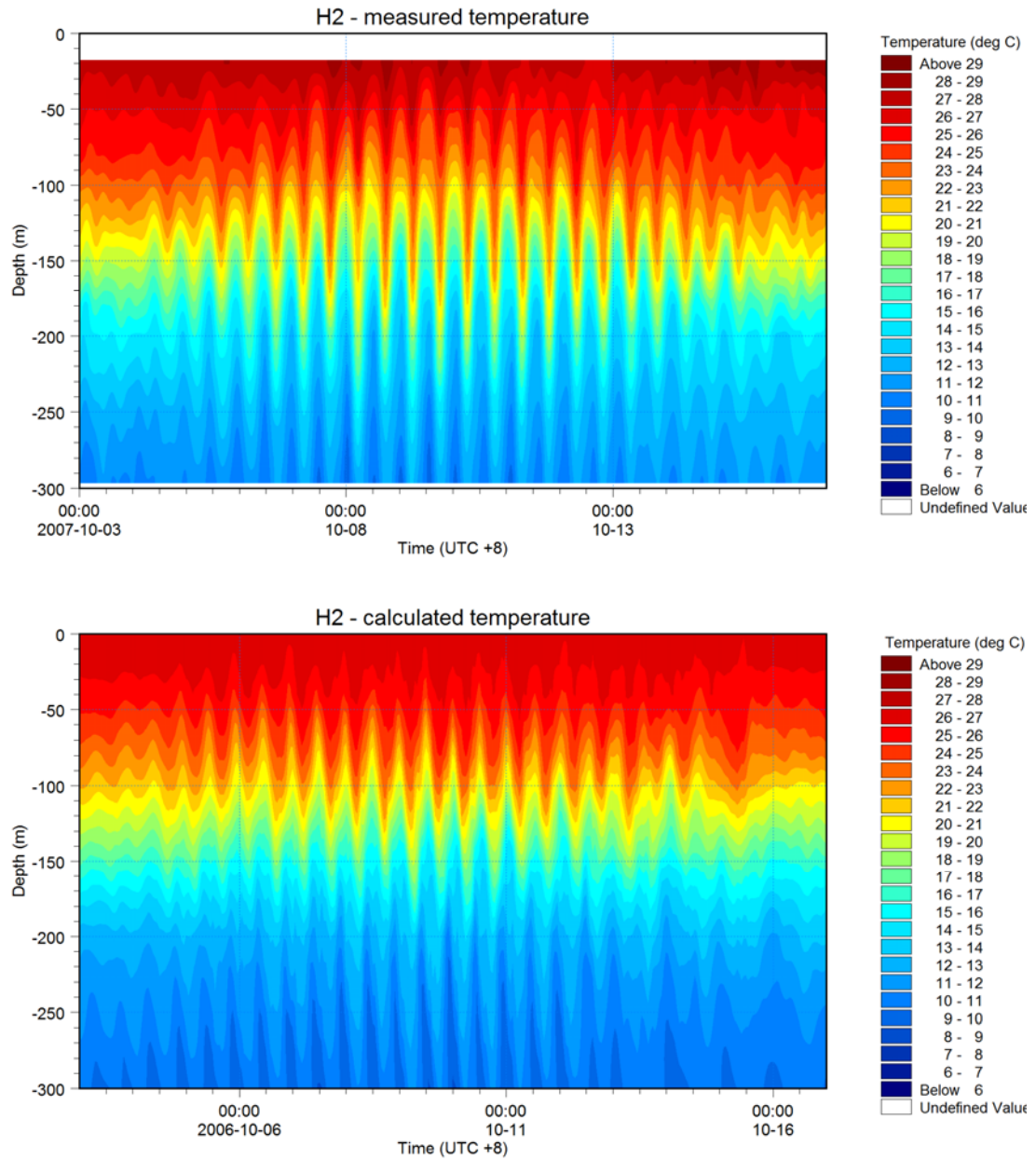


Fig 5.18 Isopleth plot for H2-1, spring calibration period

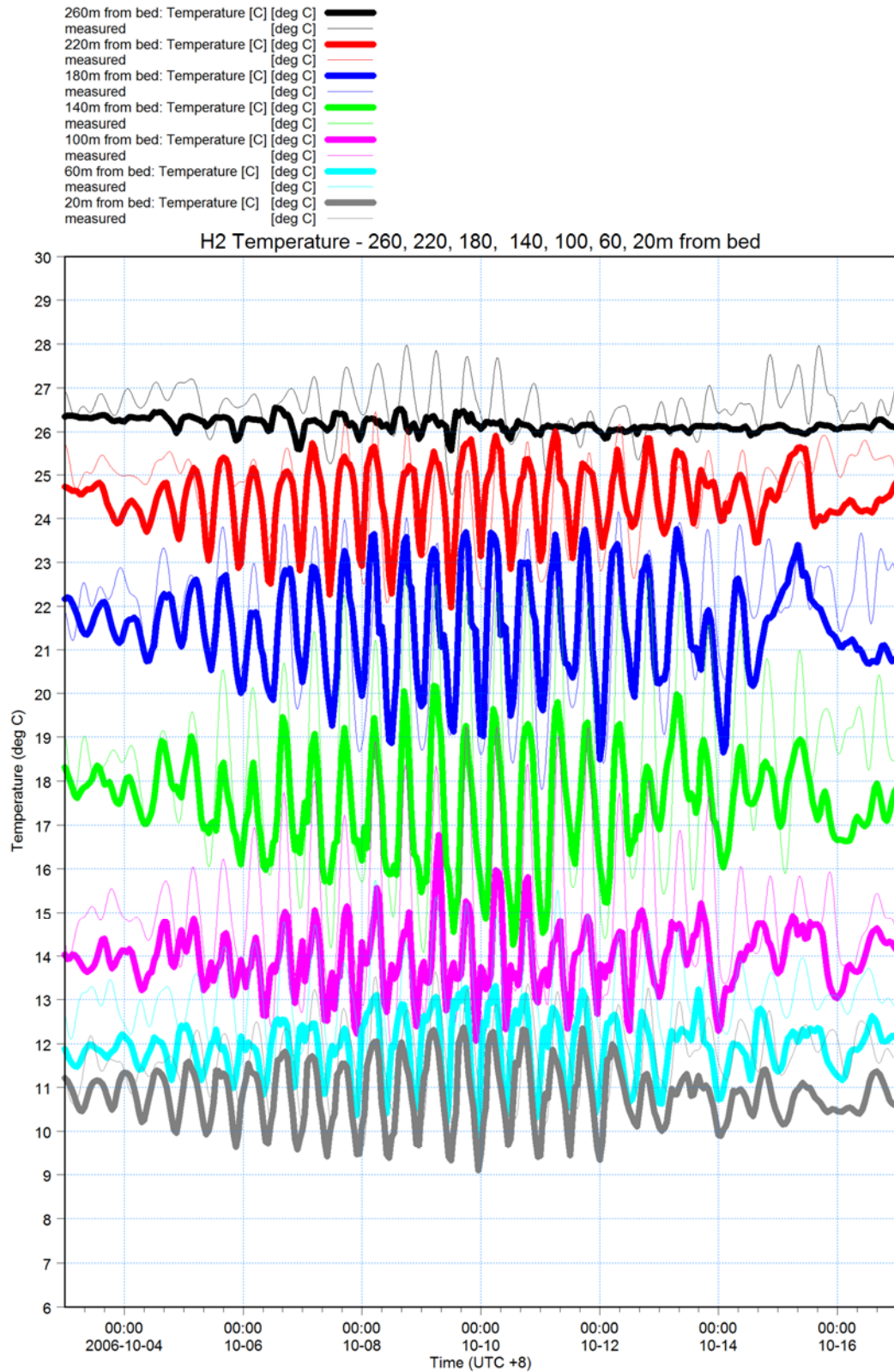


Fig 5.19 Multi-time series plot for H2-1, spring calibration period.
Thin lines: measured values, thick lines: model results



T at 260m	x	x
T at 220m	x	x
T at 180m	x	x
T at 140m	x	x
T at 100m	x	x
T at 60m	x	x
T at 20m	x	x

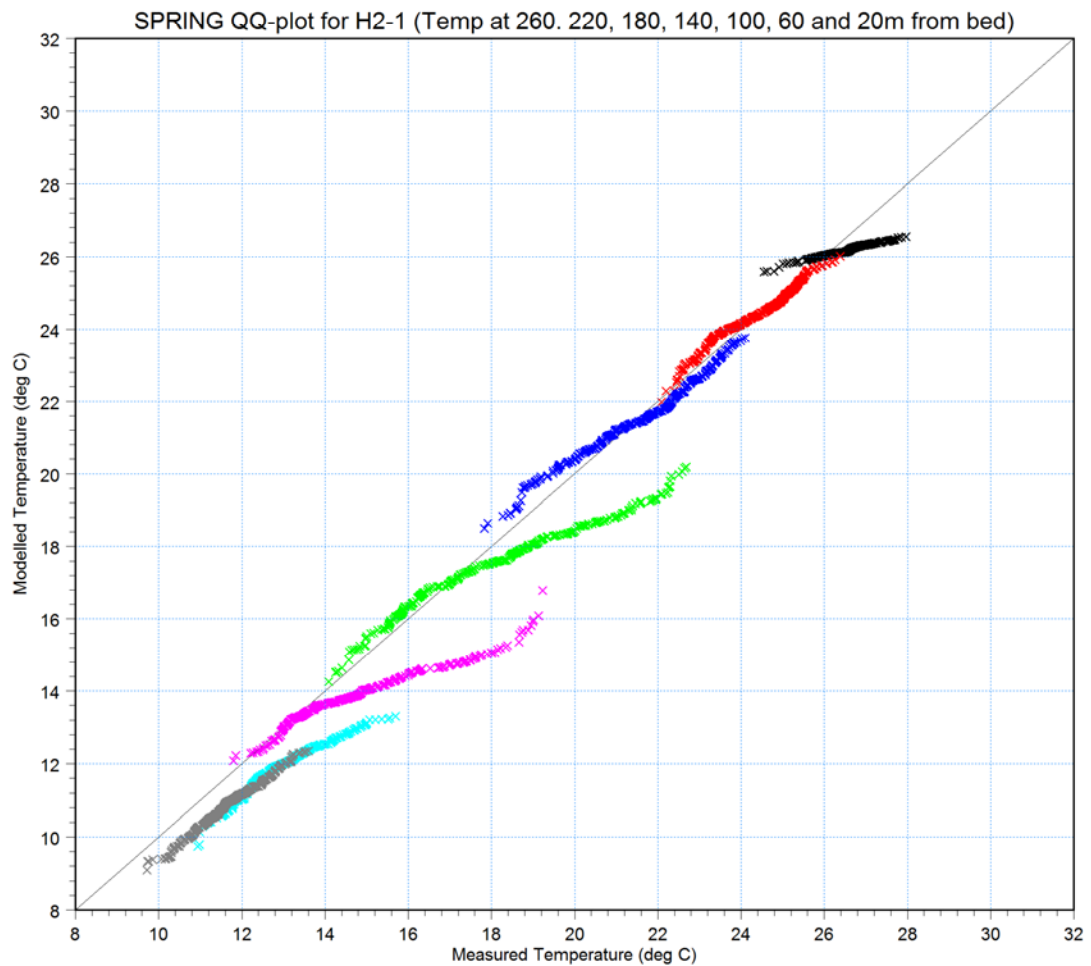


Fig 5.20 Q-Q plot for temperatures for H2-1, spring calibration period

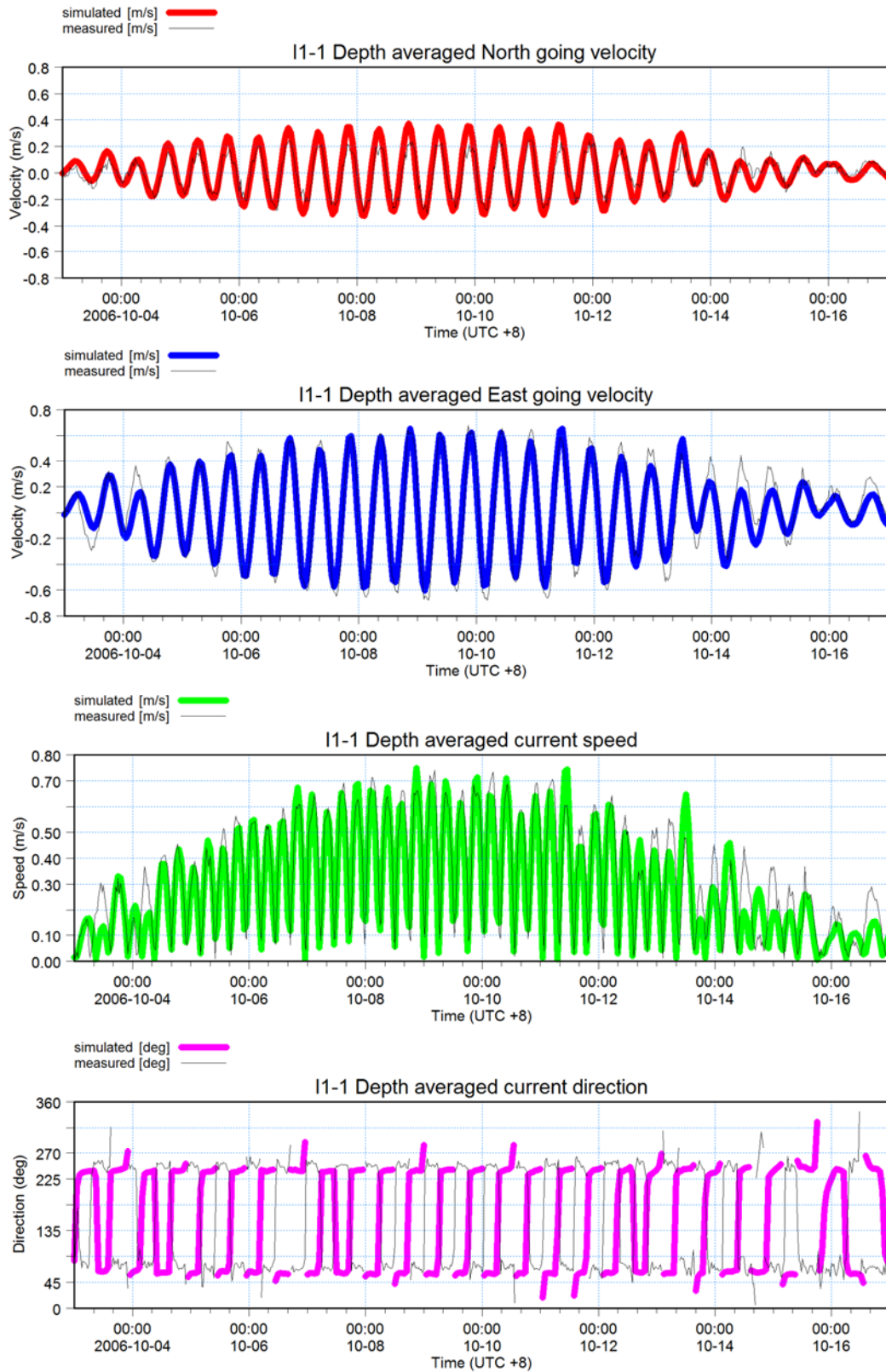


Fig 5.21 Depth averaged currents for I1-1, spring calibration period

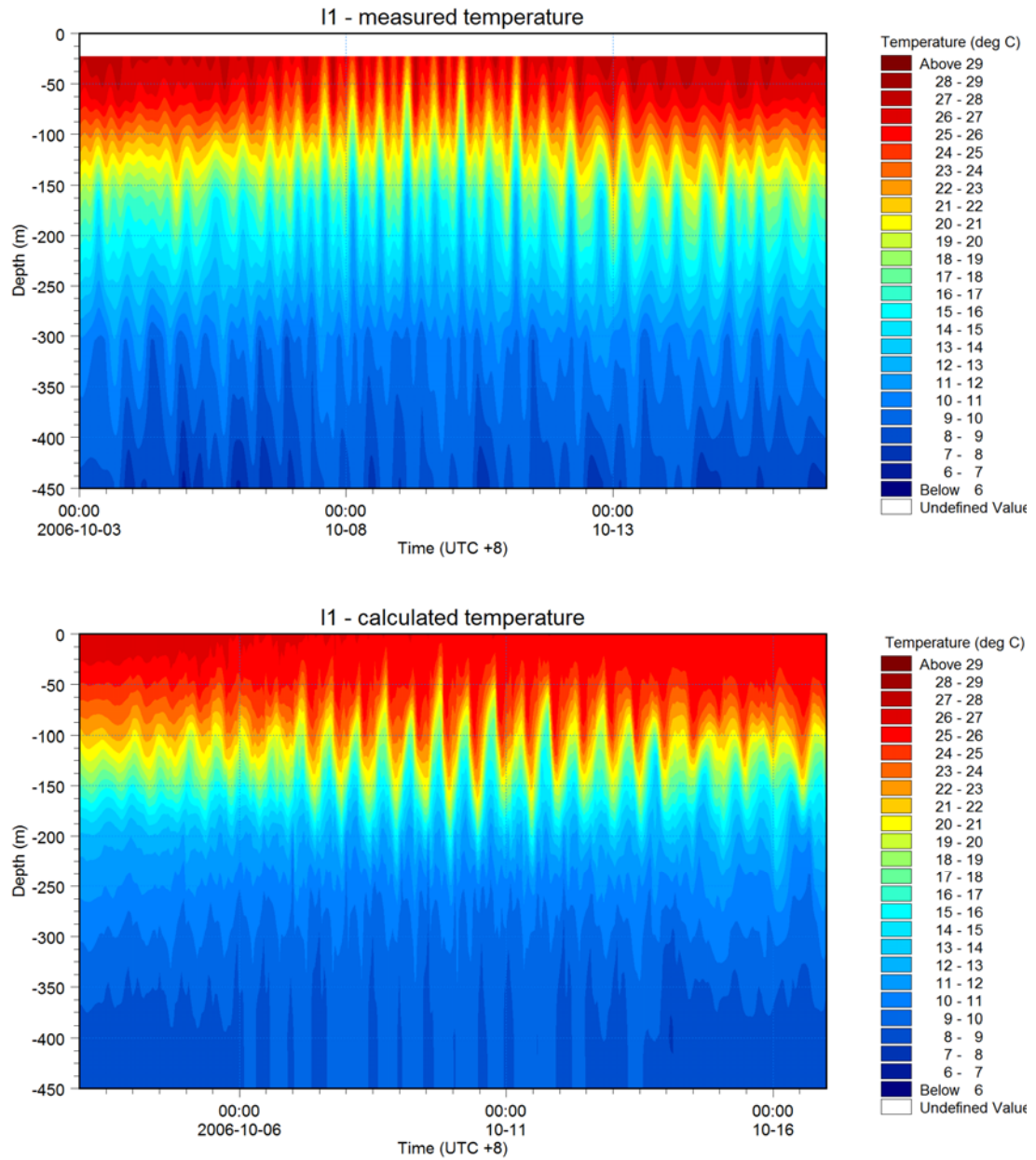


Fig 5.22 Isopleth plot for I1-1, spring calibration period

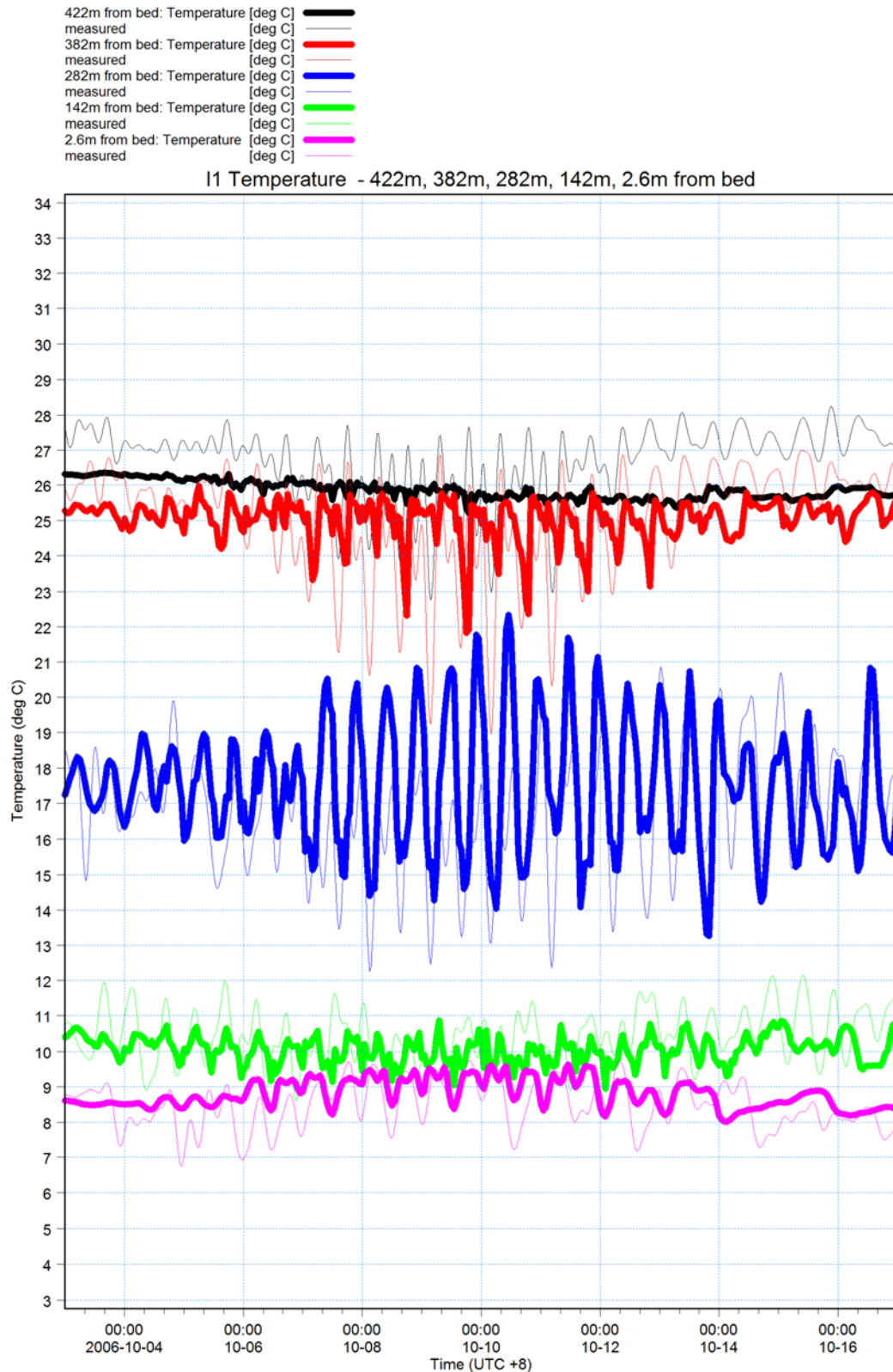


Fig 5.23 Multi-time series plot for I1-1, spring calibration period
Thin lines: measured values, thick lines: model results



T at 422m × ×
T at 382m × ×
T at 282m × ×
T at 142m × ×
T at 2.6m × ×

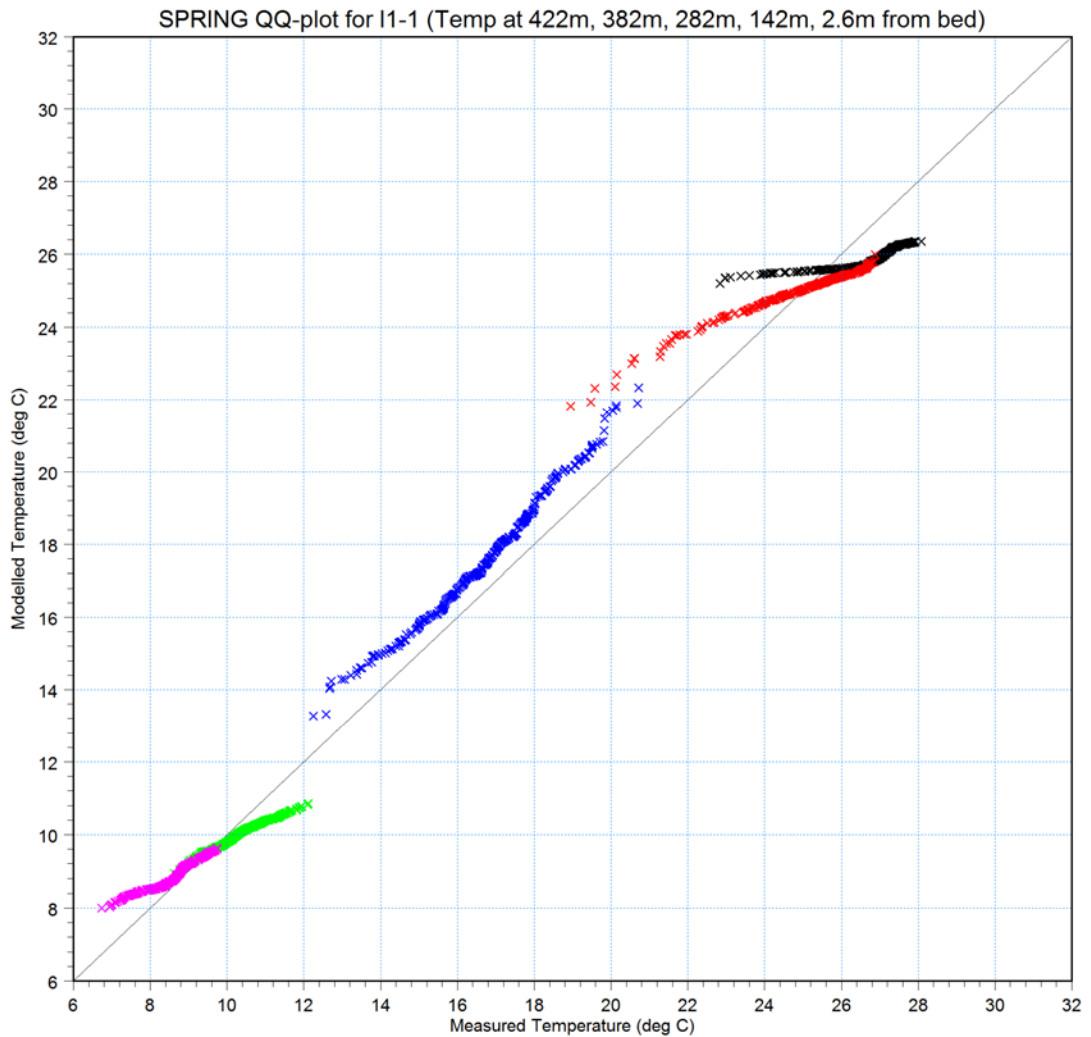


Fig 5.24 Q-Q plot for temperatures for I1-1, spring calibration period

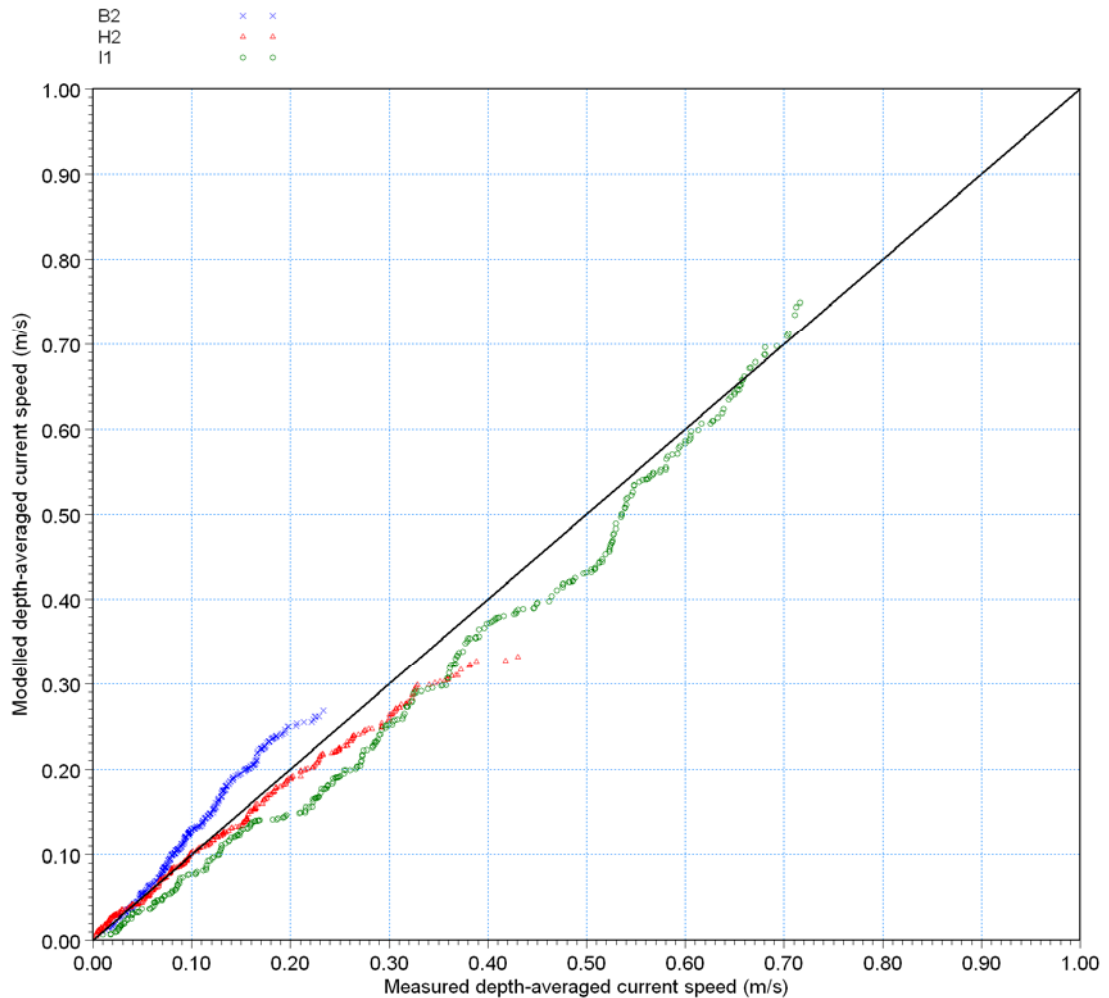


Fig 5.25 Q-Q plot for depth averaged currents for all stations, spring calibration

In addition to the visual comparison a statistical analysis as part of the model performance assessment has also been compiled. The results are listed in Table 5.2.

Table 5.2 Statistical analysis of key parameters for spring calibration period
 *: Defined as mean of model – mean of measurements results
 **: RMS Error / peak value * 100

Station	Parameter	Bias* [m/s]	RMS Error [m/s]	Peak value [m/s]	RMS Error [%]**
B2-1	Depth averaged current speed (m/s)	0.02	0.04	0.23	15
H2-1	Depth averaged current speed (m/s)	-0.01	0.06	0.43	14
I1-1	Depth averaged current speed (m/s)	-0.03	0.10	0.74	14

Referring to the performance criteria listed in Section 5.5 the RMS (Root Mean Square) error for currents should preferably be less than 10 to 20%, which is fulfilled for all stations. The bias listed in Table 5.2 gives an indication of whether the model over-predicts (positive value) or under-predicts (negative value) the current speeds. With all values being only a few cm/s these are considered acceptable.



The models ability to reproduce the current measurements is also visualised in Fig 5.25, where a good fit between model and measurements is seen.

In the following sub-sections the comparisons at each of the four stations where measurements are available for this calibration period are discussed.

Comments to comparisons at B2-1

In general the comparison of simulated and measured current speed and direction (Fig 5.11) show a good agreement with the model. Especially the phases are good, while the peak current magnitude is sometimes overestimated by 3-5 cm/s. The overall bias is, however, only 2 cm/s.

The temperatures (Fig 5.12 to Fig 5.14) are also well reproduced including the large variations experienced around spring tide (10-10-2006).

Comments to comparisons at C1-1

Except for the topmost temperature sensor (455m above sea bed) there is a good agreement between model and measurements (Fig 5.15 and Fig 5.16). With the top layer in the model being 30m thick it has not been possible to reproduce the temperature variation in the detail in the surface. The layers below seem, however, not to be affected by this.

Comments to comparisons at H2-1

At this location, which is located just south of South Reef and very close to the reef edge, the currents in the model are in general good although speeds at tidal peaks are slightly underestimated (Fig 5.17) with a general bias of 1 cm/s.

For the temperature (Fig 5.18 to Fig 5.20) the very large variations, especially during spring tide, are reproduced by the model. The detailed variations which may partly be sub-grid variations (i.e. requires a model with a finer resolution) are, however, less well reproduced.

Comments to comparisons at I1-1

The measured and simulated depth averaged currents compare very well at this station (see Fig 5.21).

The temperature comparisons (Fig 5.22 to Fig 5.24) show an acceptable agreement with very large variations during spring tide. The upwelling of cold water seen in the measurements 382m above seabed is also reproduced in the model although not as pronounced as in the measurements.

Conclusion

Based on the visual comparisons and the statistical analysis it is concluded that the model demonstrates a satisfactory reproduction of the complicated hydrodynamic conditions during the spring calibration period in the area around Scott Reef.



5.7 Results of Model Validation for Summer Period

The results for summer validation period are presented in the same way as for the spring calibration period with all comparisons included in Appendix C (except for the comparison of water levels at Scott Reef, which is shown in Fig 5.26 and Fig 5.27) and with key plots shown below.

For the summer validation period measurements were available for the same stations as for the spring calibration period: B2-1, C1-1, H2-1, and I1-1. Additionally, measurements were available from A2-1 (water levels) and G2-1 (currents and temperatures). The key plots for these five stations are shown in Fig 5.26 through Fig 5.46. Note that as for the spring period there are measurements at too few depths at C1-1 to compute the depth averaged currents for this station.

The results of the statistical analysis for the summer validation period are listed in Table 5.3.

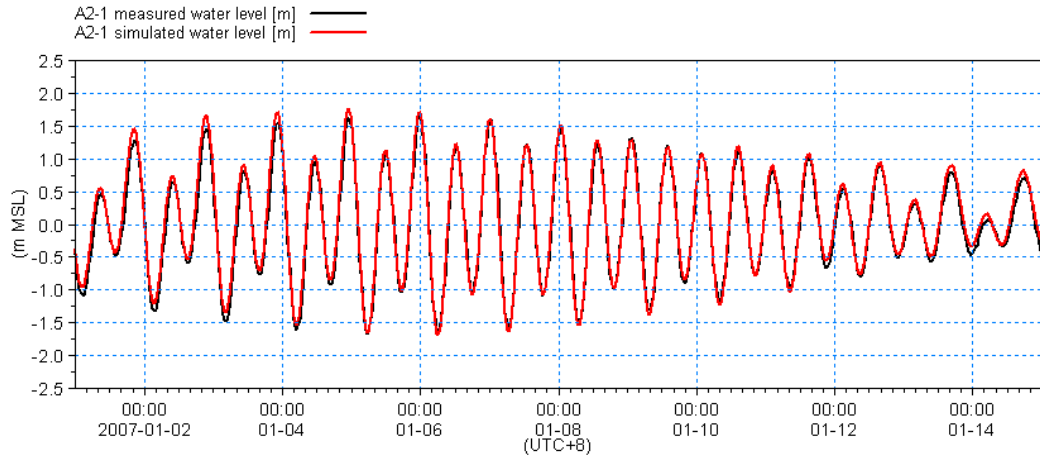


Fig 5.26 Comparison of measured and modelled water level for A2-1 Scott Reef, summer validation period.

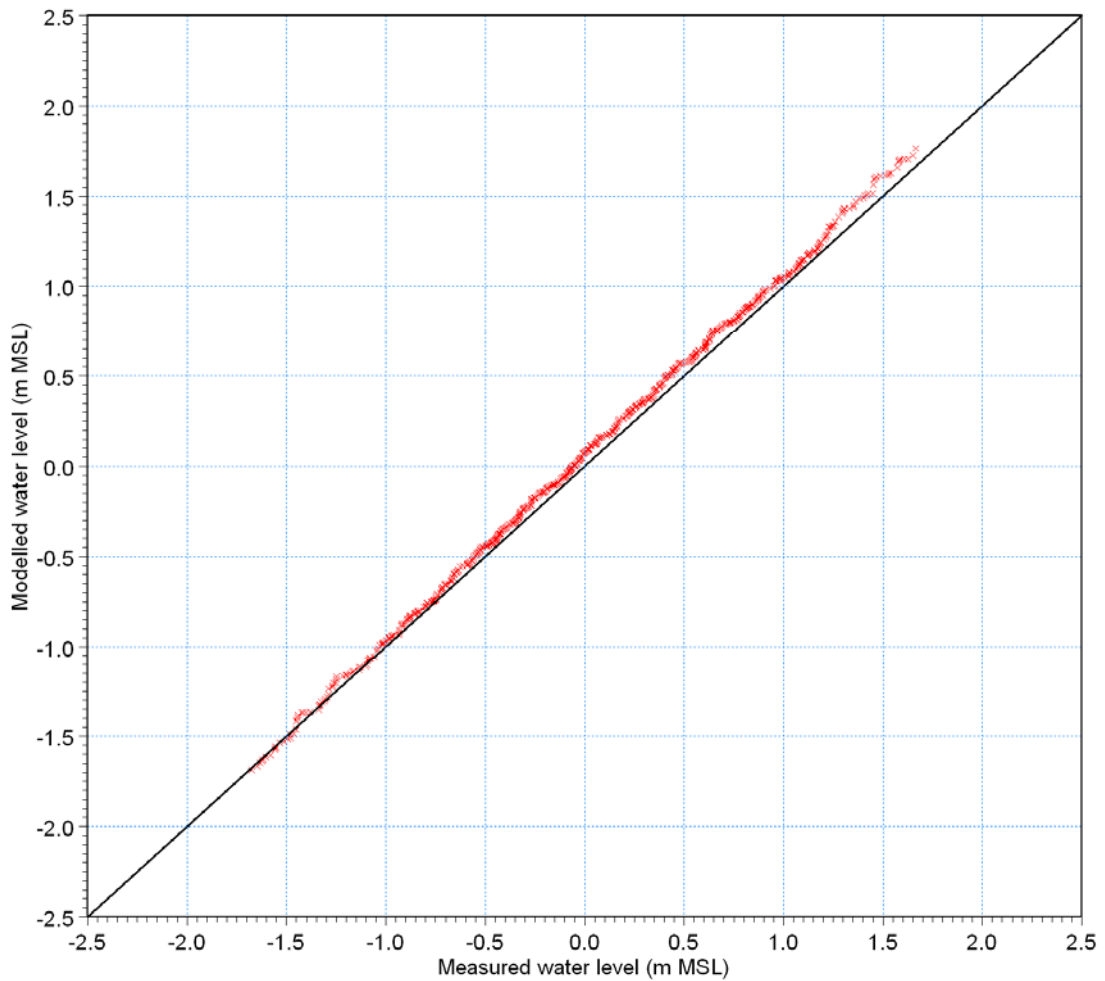


Fig 5.27 Q-Q plot for water levels at A2-1 Scott Reef, summer validation period.

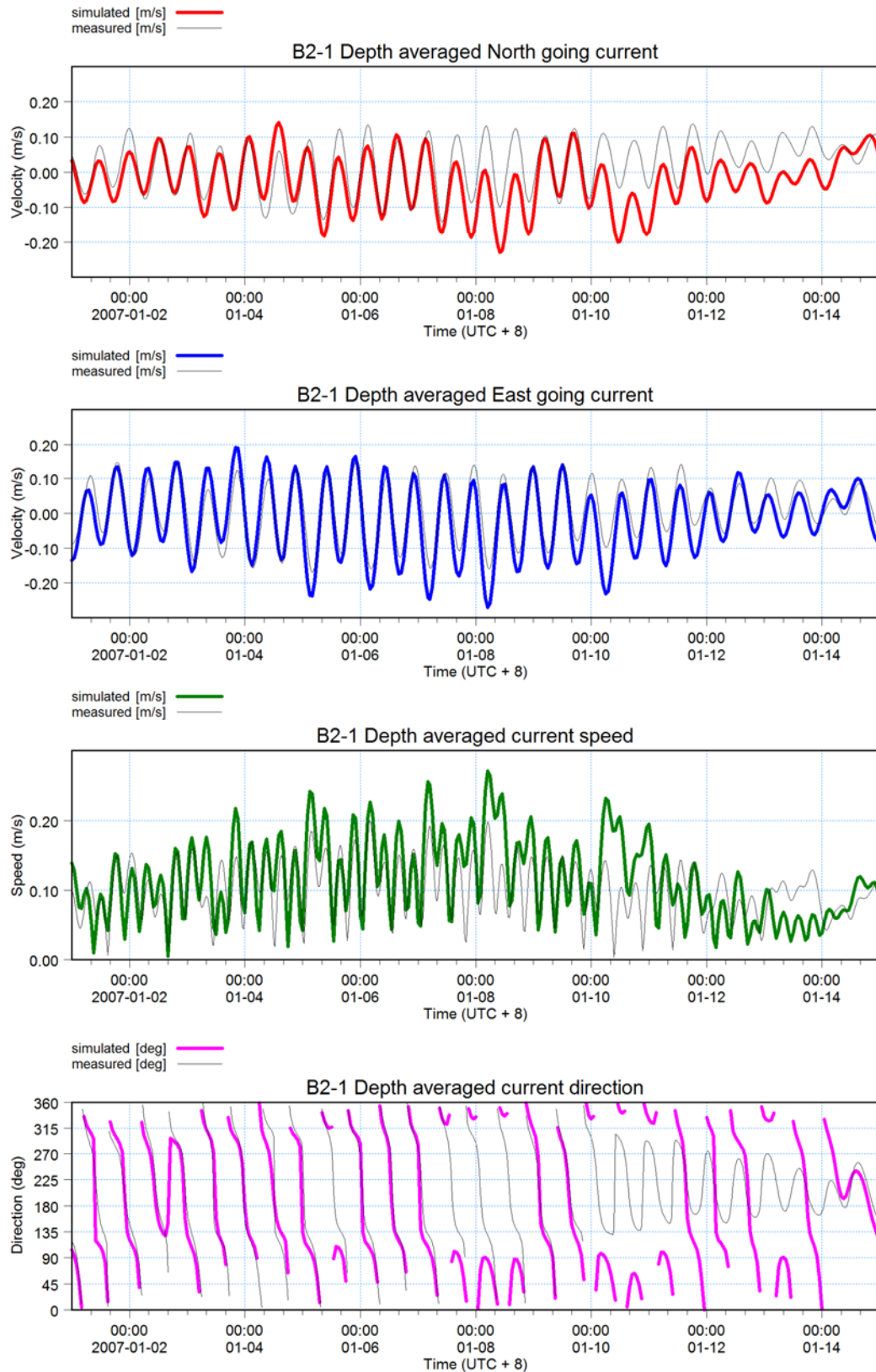


Fig 5.28 Depth averaged currents for B2-1, summer validation period

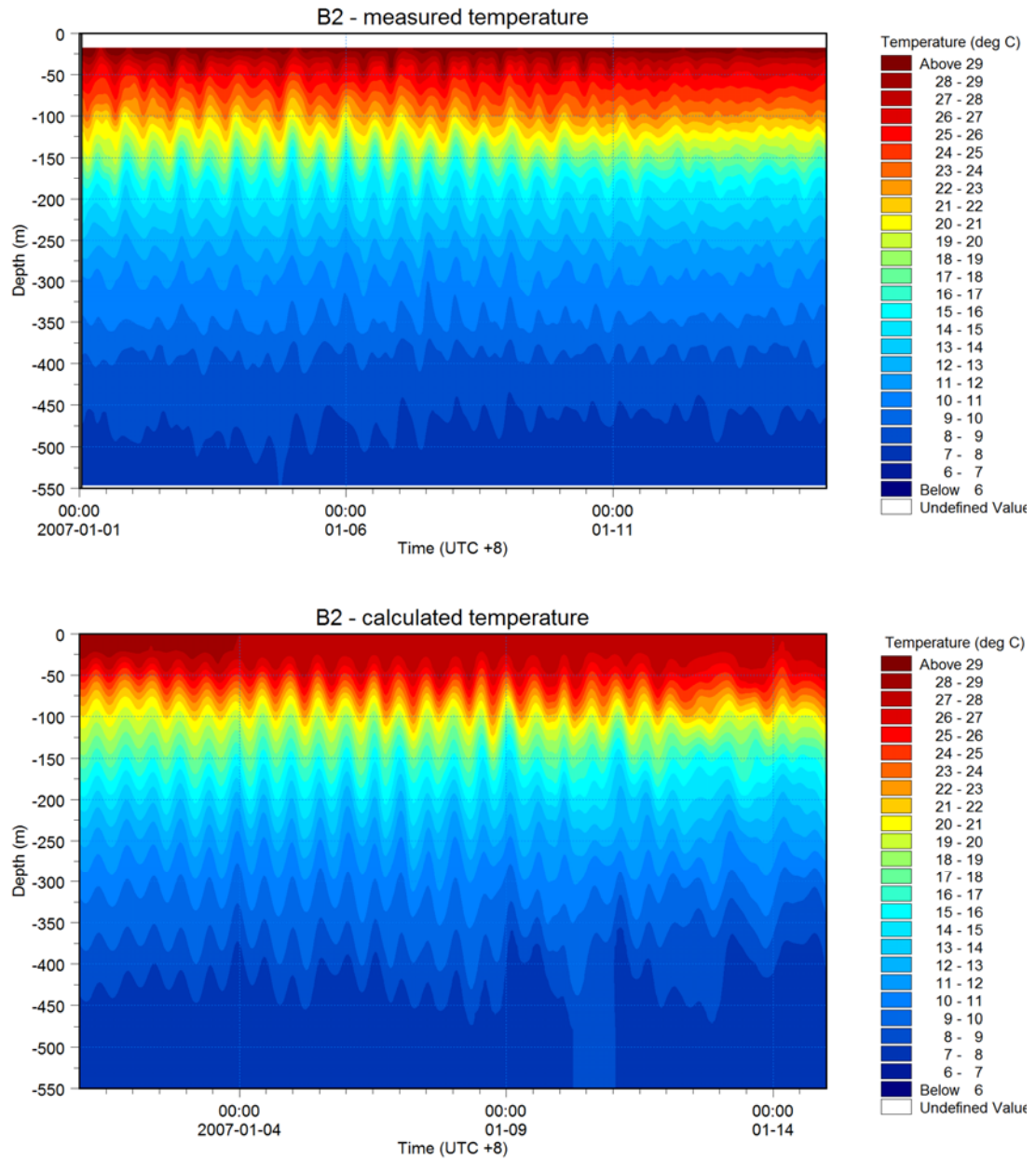


Fig 5.29 Isopleth plot for B2-1, summer validation period

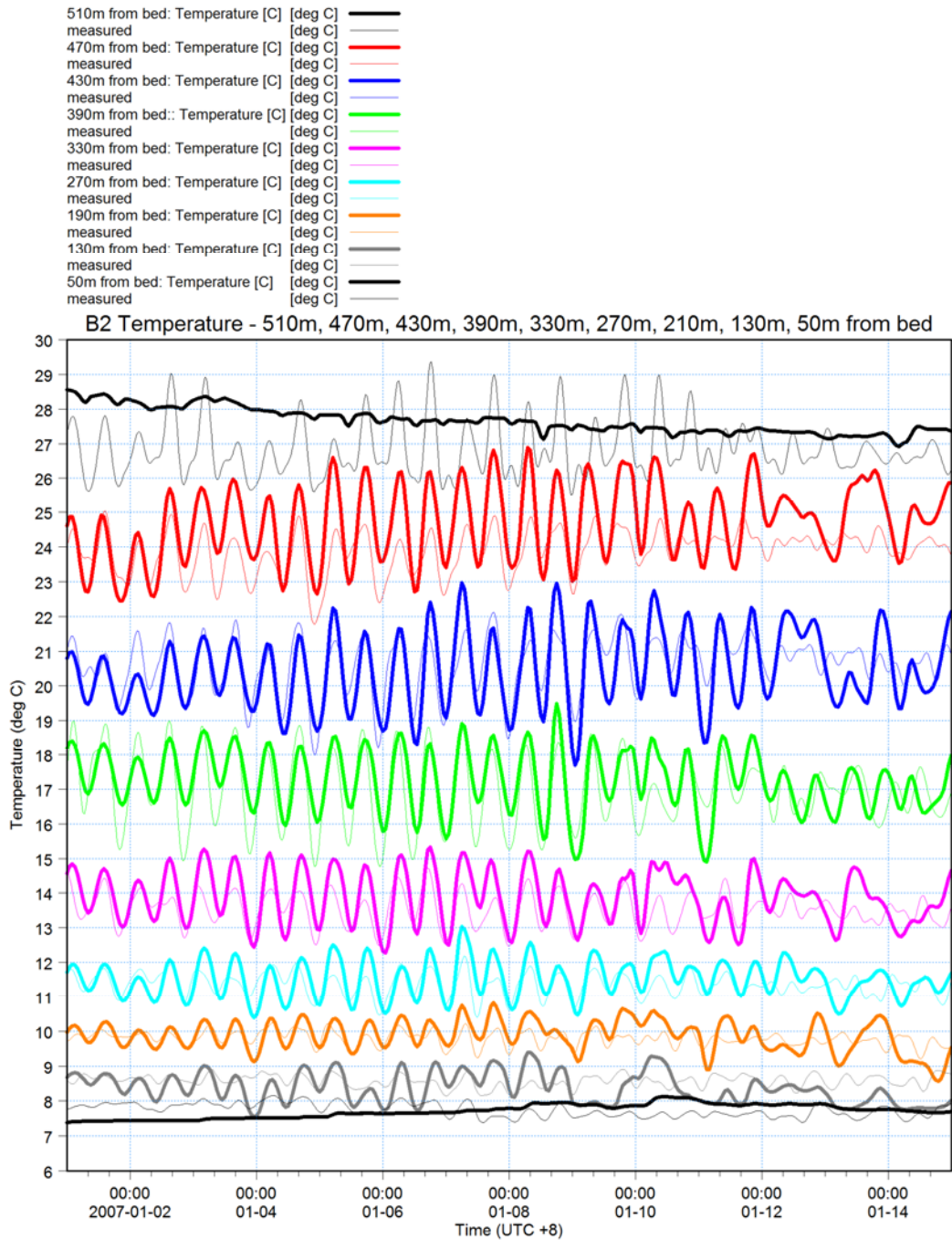


Fig 5.30 Multi-time series plot for B2-1, summer validation period
 Thin lines: measured values, thick lines: model results



- T at 510m x x
- T at 470m x x
- T at 430m x x
- T at 390m x x
- T at 330m x x
- T at 270m x x
- T at 190m x x
- T at 130m x x
- T at 50m x x

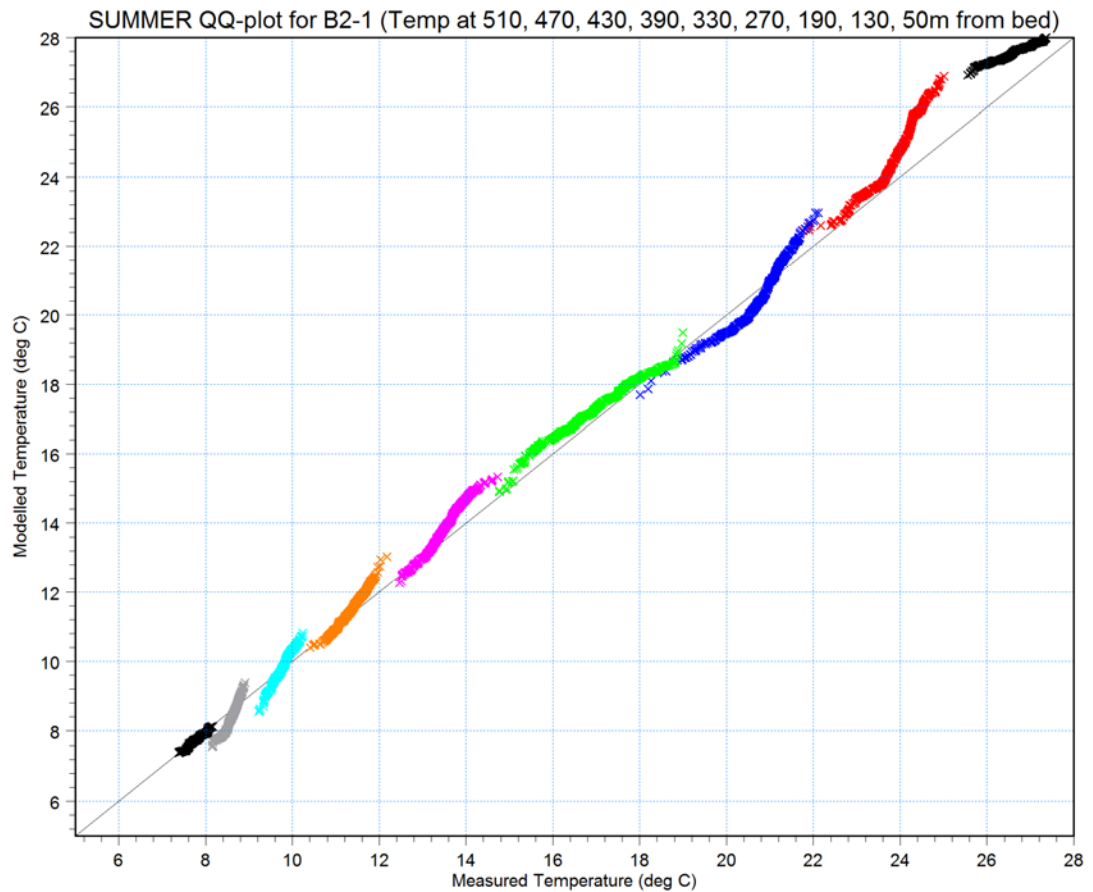


Fig 5.31 Q-Q plot for temperatures for B2-1, summer validation period

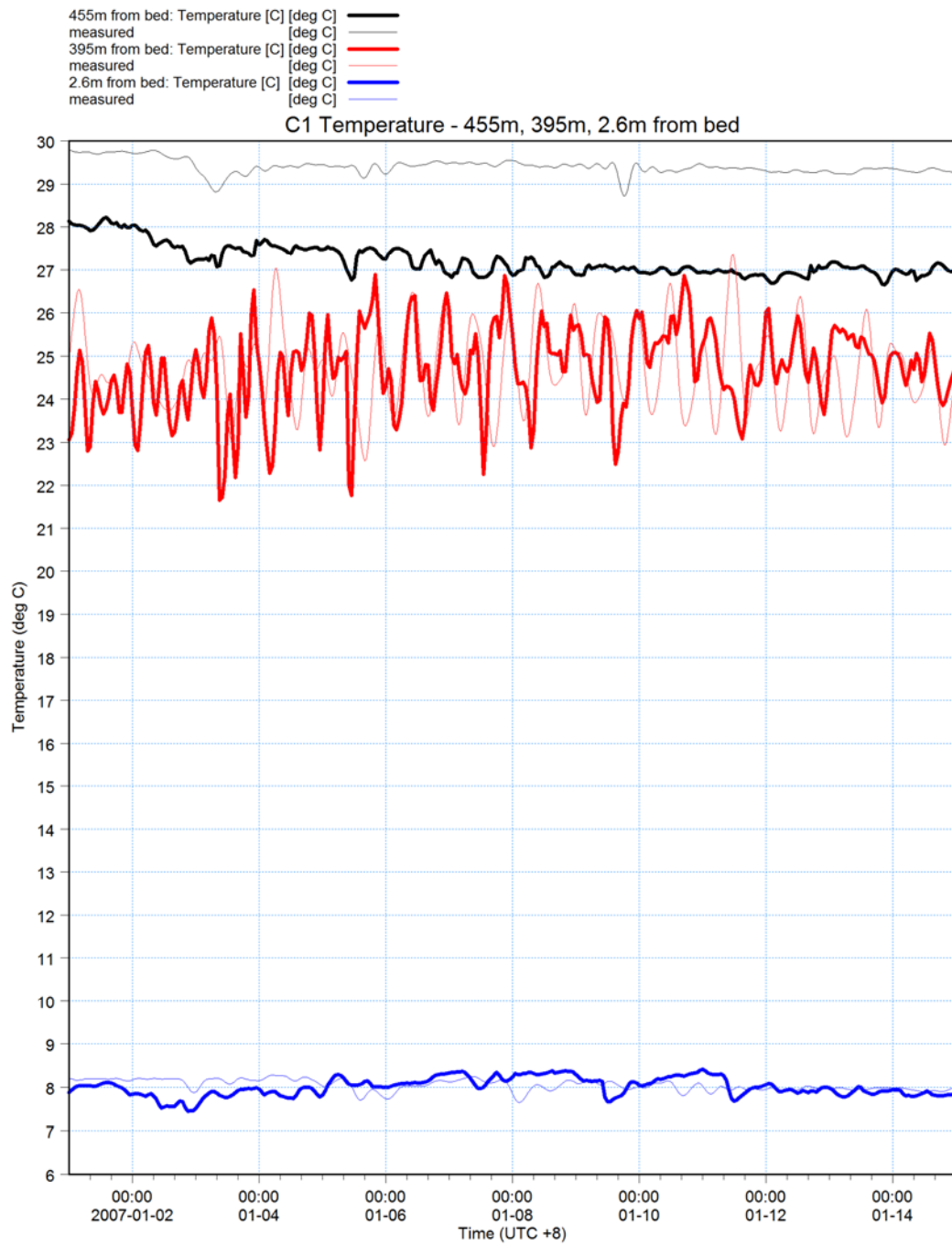


Fig 5.32 Multi-time series plot for C1-1, summer validation period
Thin lines: measured values, thick lines: model results



T at 455m x x
T at 395m x x
T at 2.6m x x

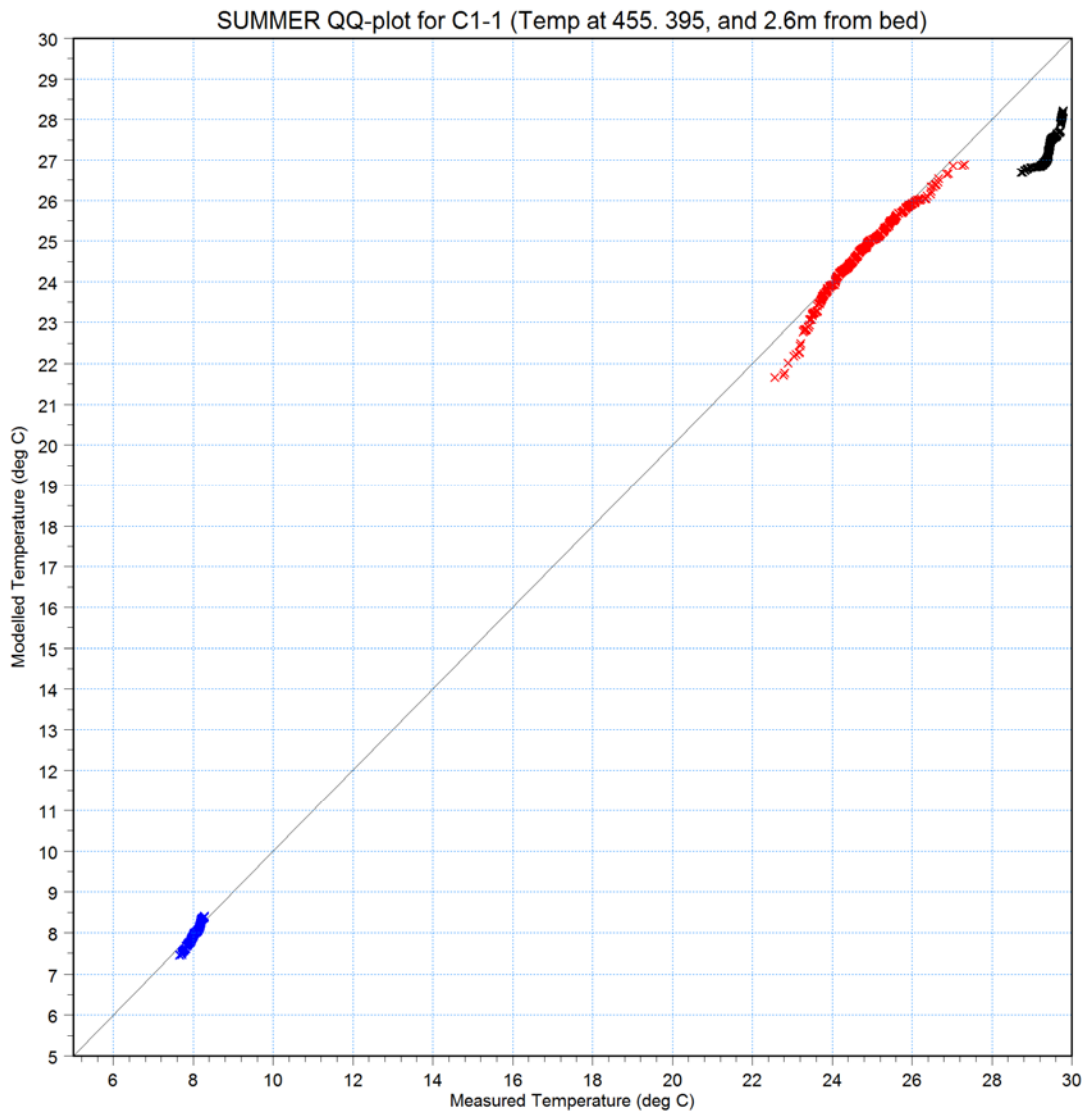


Fig 5.33 Q-Q plot for temperatures for C1-1, summer validation period

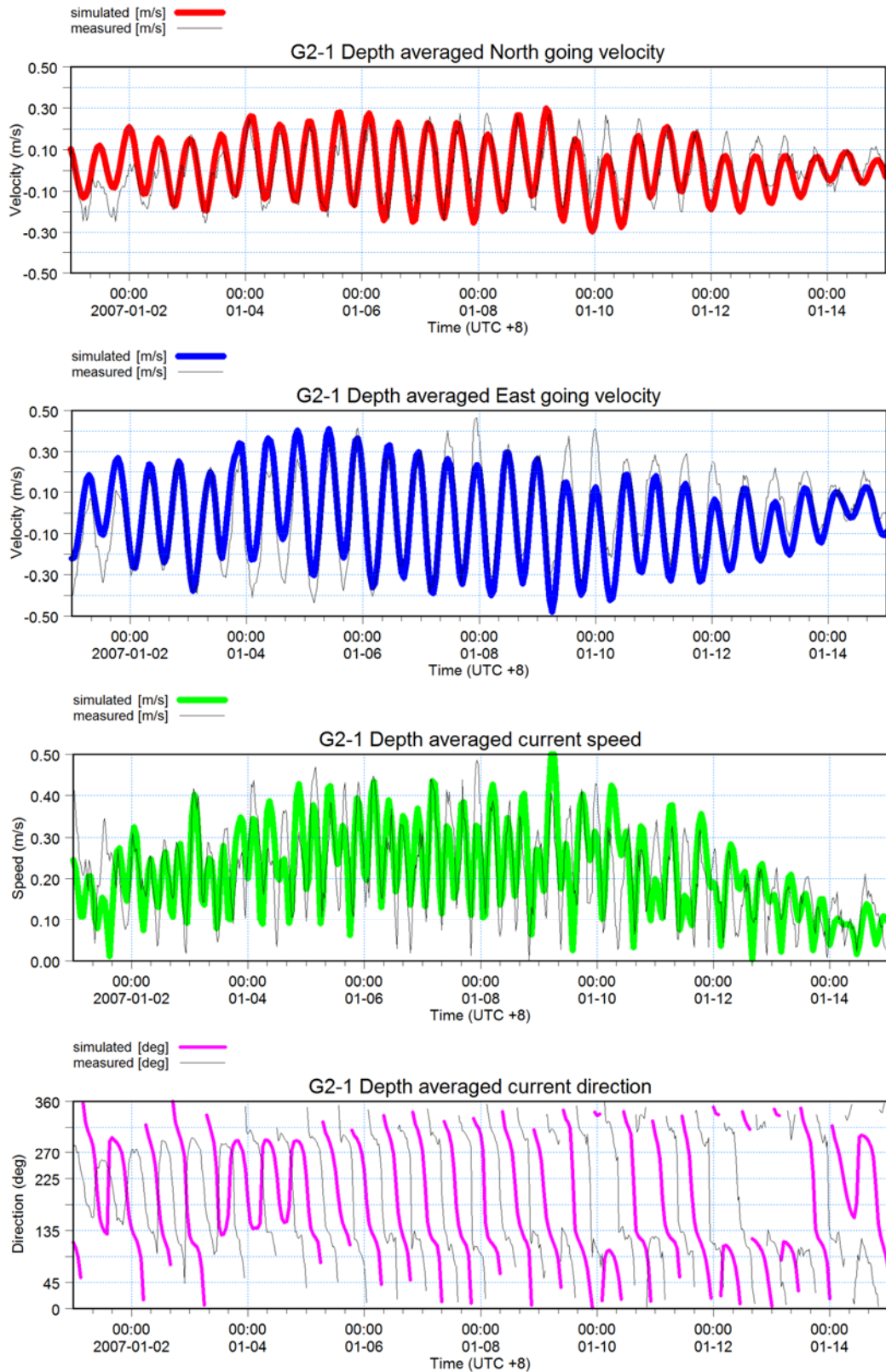


Fig 5.34 Depth averaged currents for G2-1, summer validation period

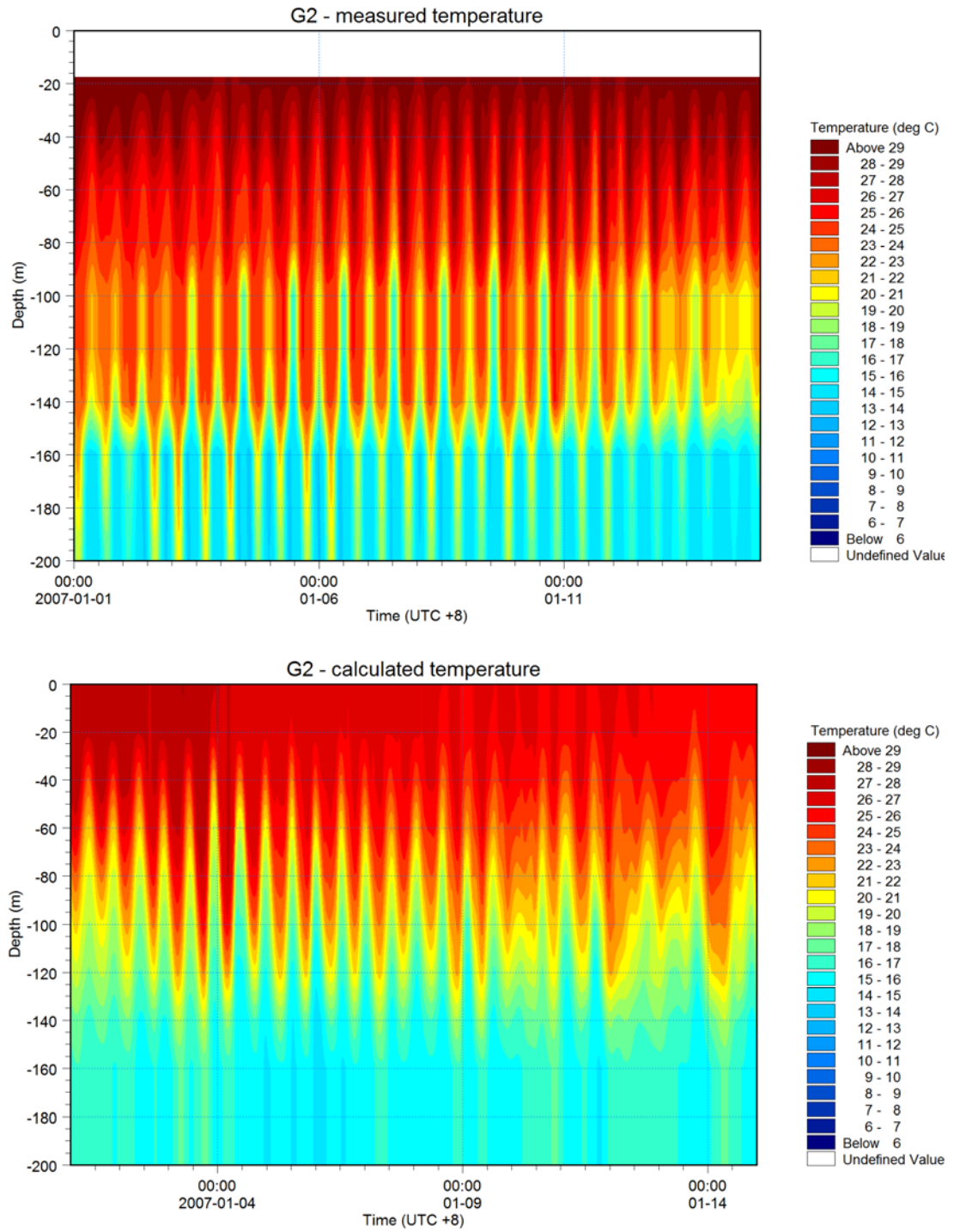


Fig 5.35 Isopleth plot for G2-1, summer validation period

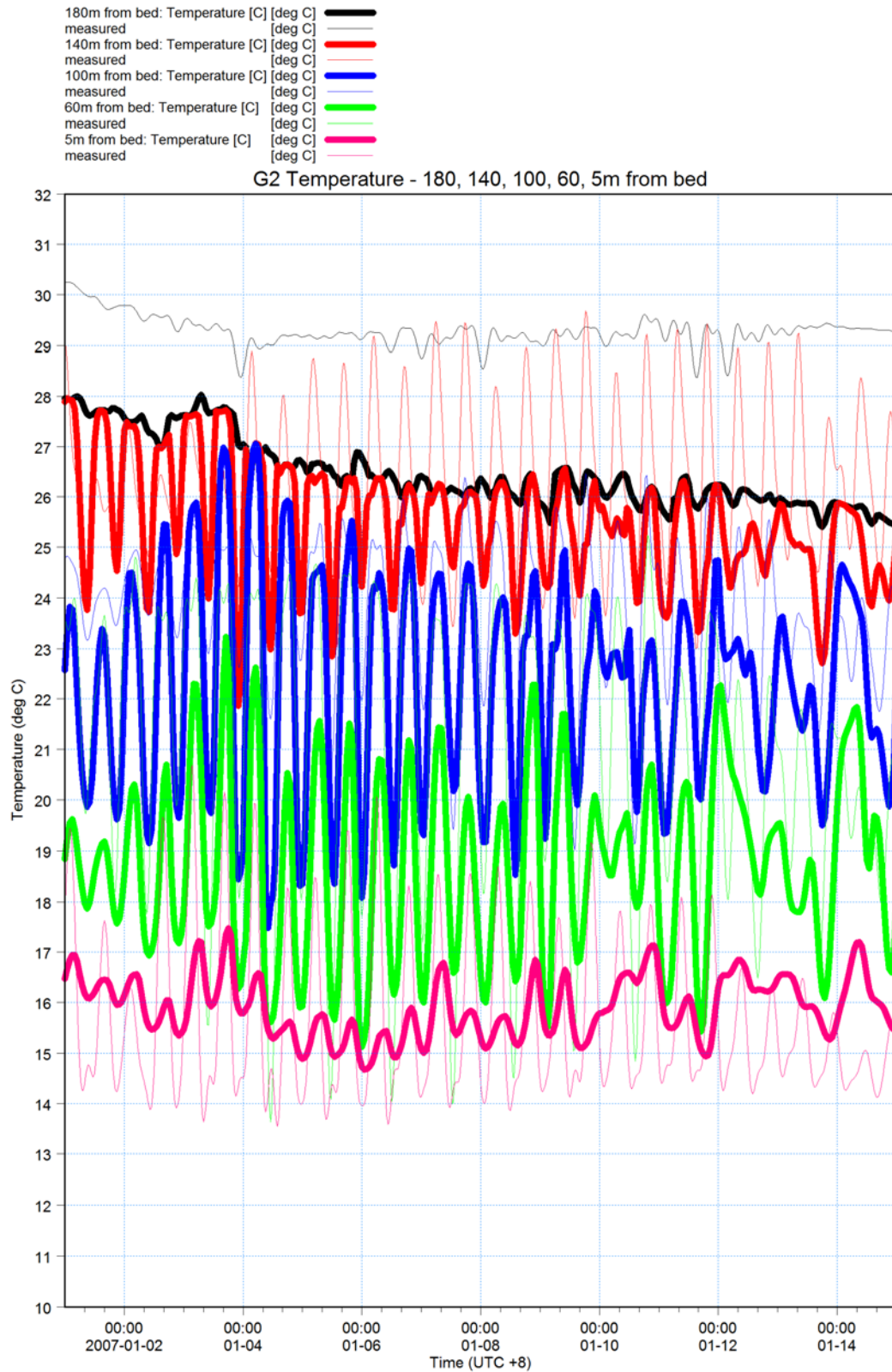


Fig 5.36 Multi-time series plot for G2-1, summer validation period
Thin lines: measured values, thick lines: model results



T at 180m x x
T at 140m x x
T at 100m x x
T at 60m x x
T at 5m x x

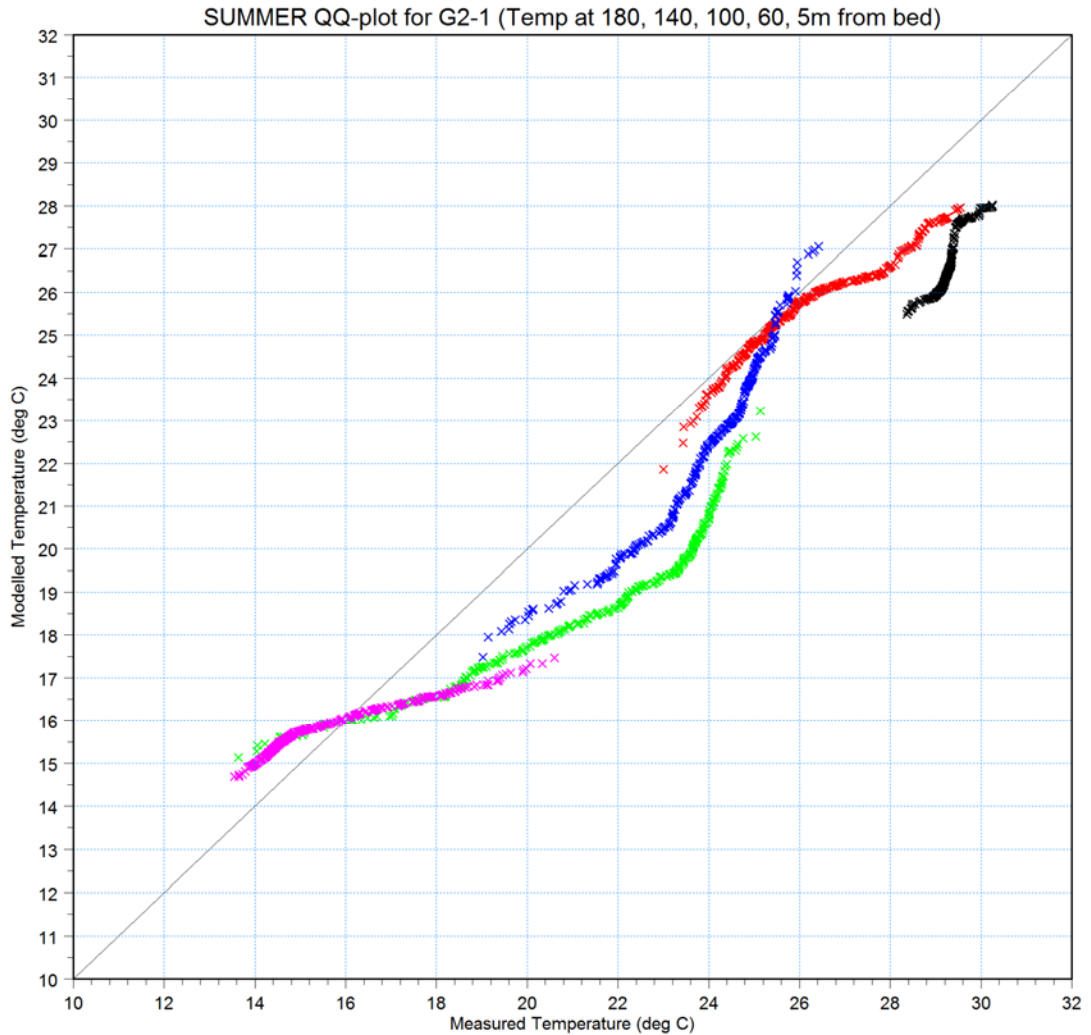


Fig 5.37 Q-Q plot for temperatures for G2-1, summer validation period

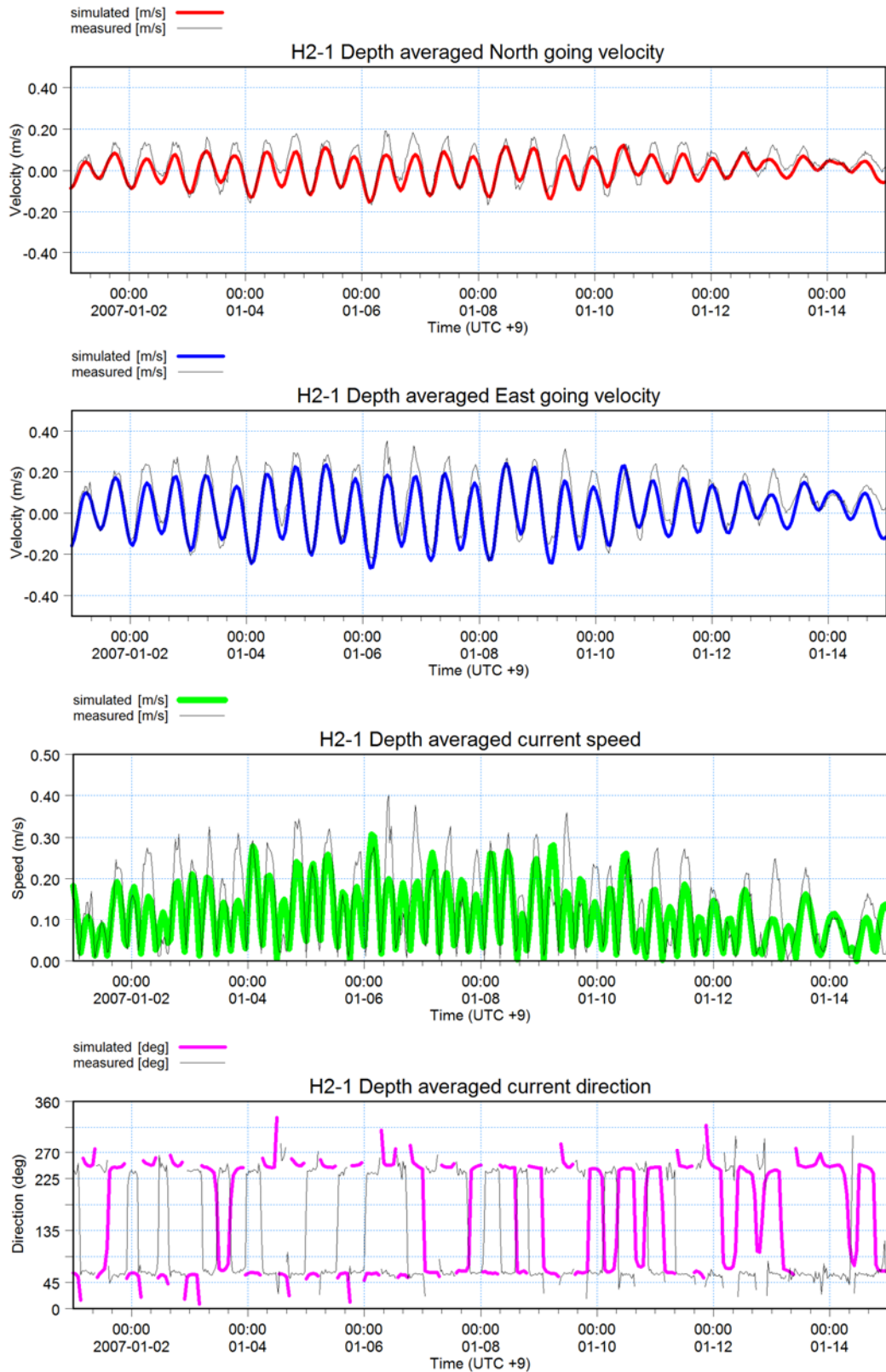


Fig 5.38 Depth averaged currents for H2-1, summer validation period

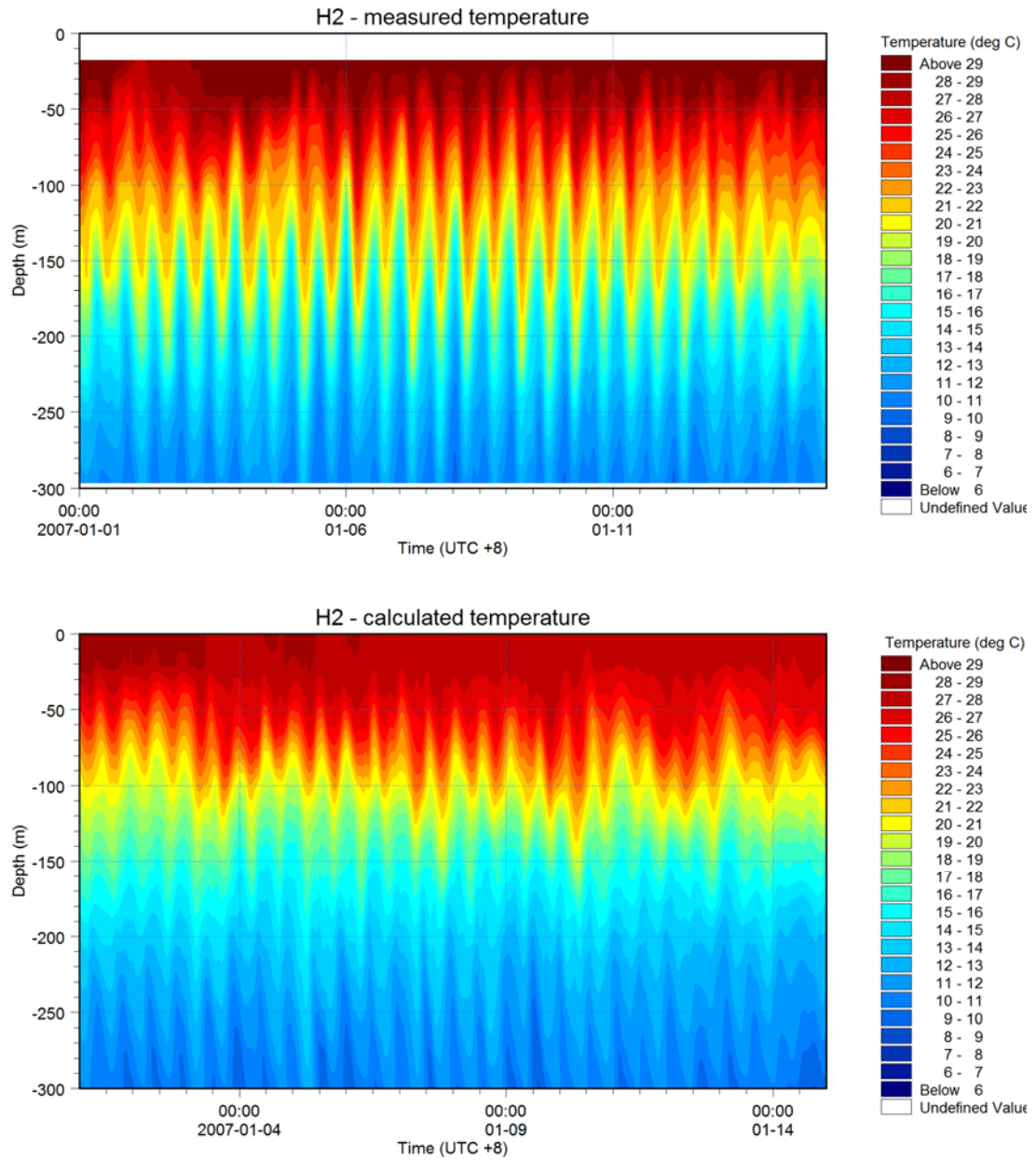


Fig 5.39 Isopleth plot for H2-1, summer validation period

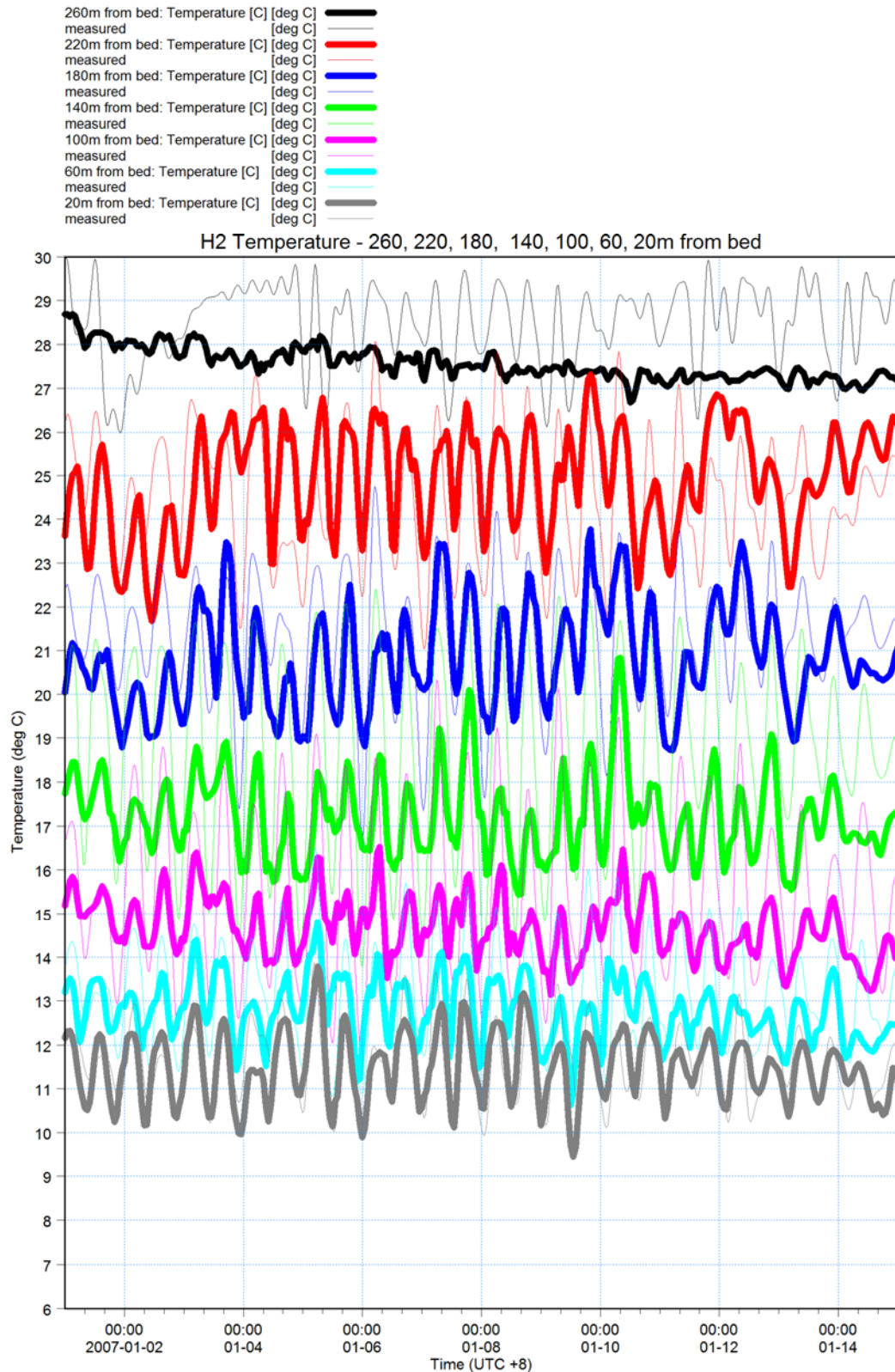


Fig 5.40 Multi-time series plot for H2-1, summer validation period
Thin lines: measured values, thick lines: model results



T at 260m	x	x
T at 220m	x	x
T at 180m	x	x
T at 140m	x	x
T at 100m	x	x
T at 60m	x	x
T at 20m	x	x

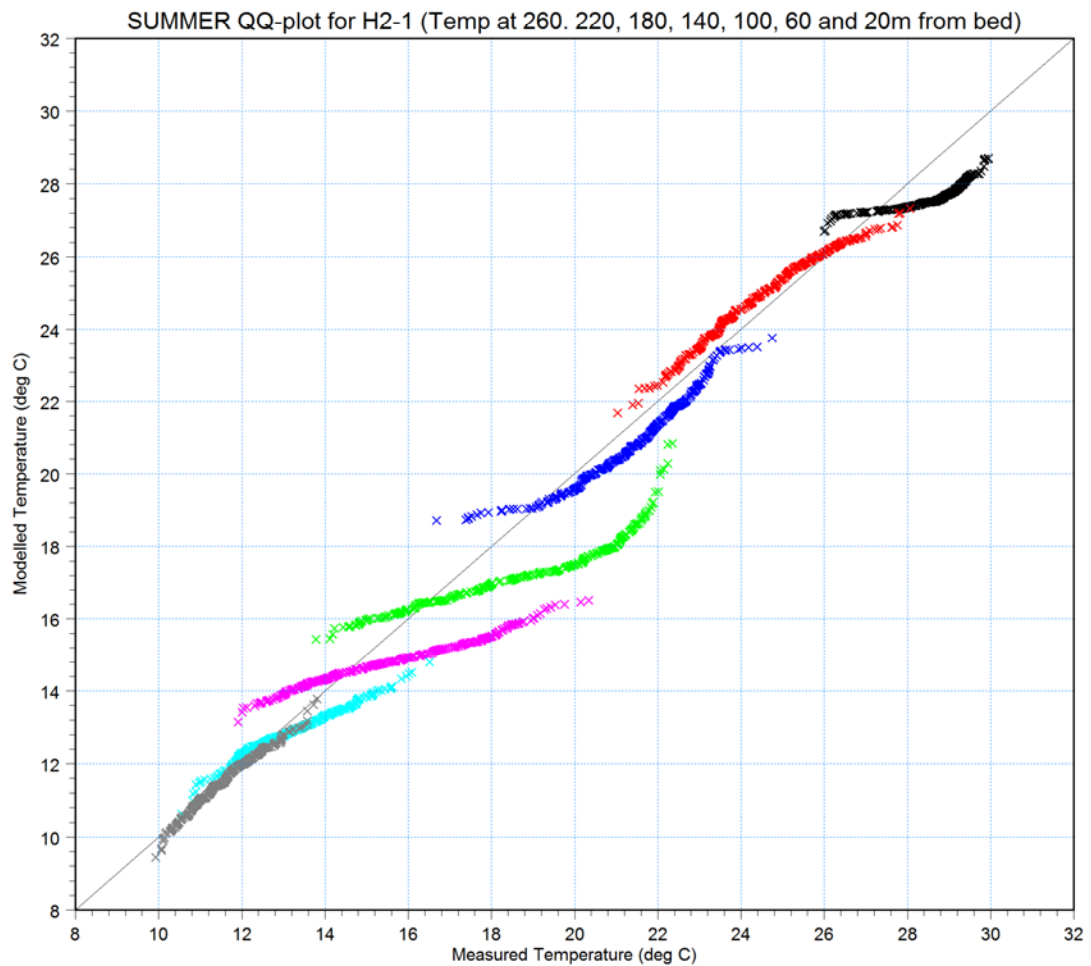


Fig 5.41 Q-Q plot for temperatures for H2-1, summer validation period

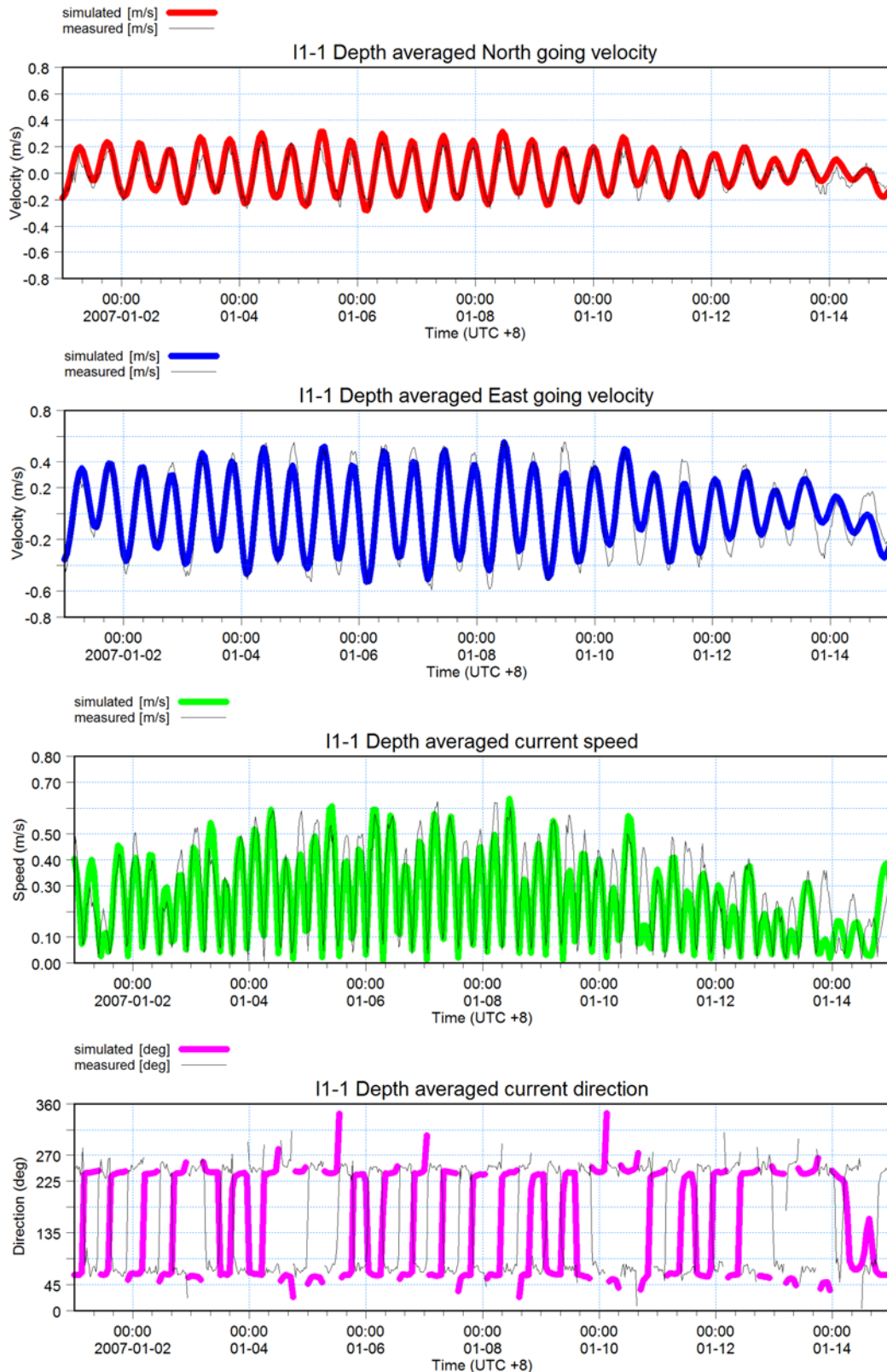


Fig 5.42 Depth averaged currents for I1-1, summer validation period

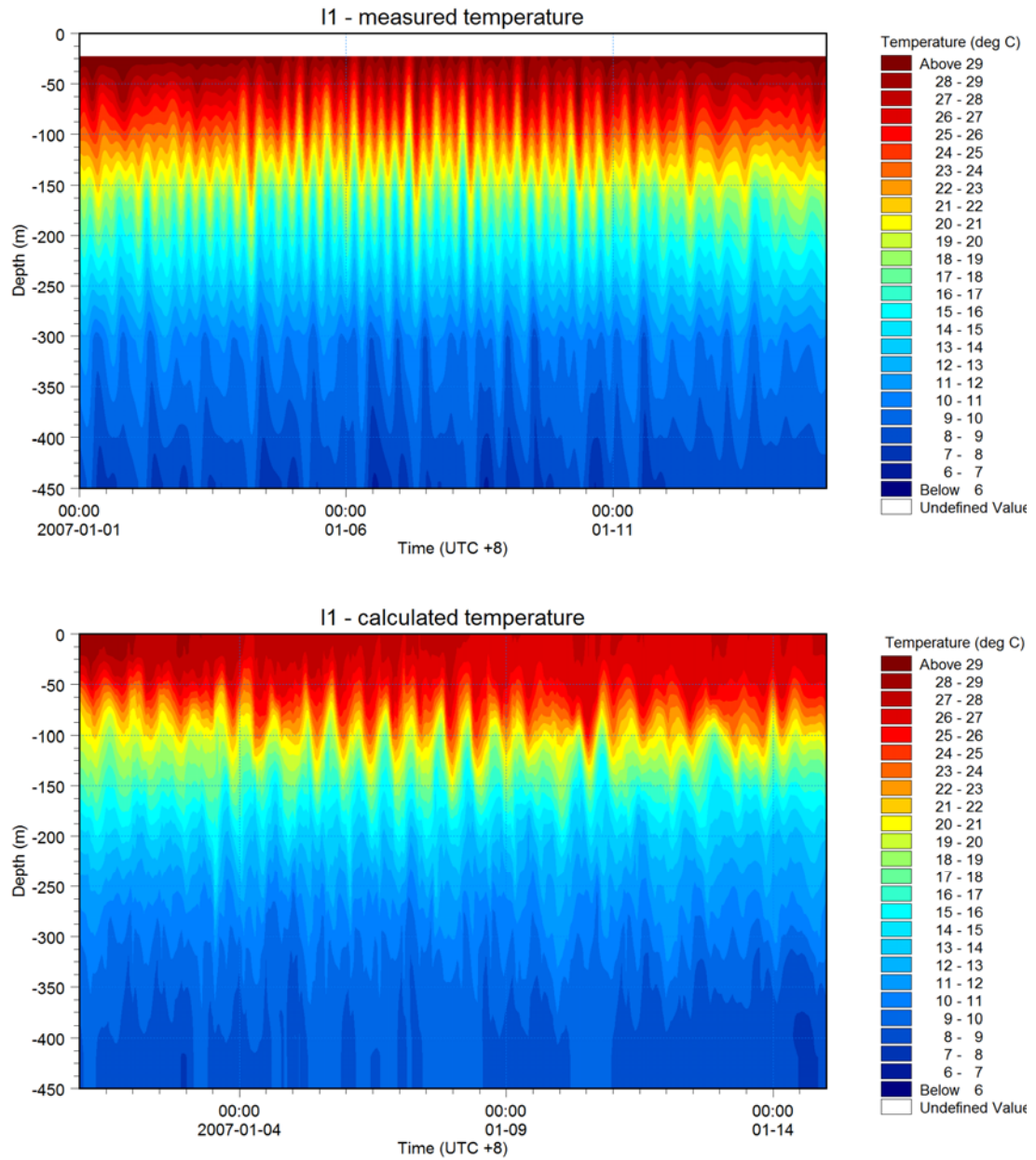


Fig 5.43 Isopleth plot for I1-1, summer validation period

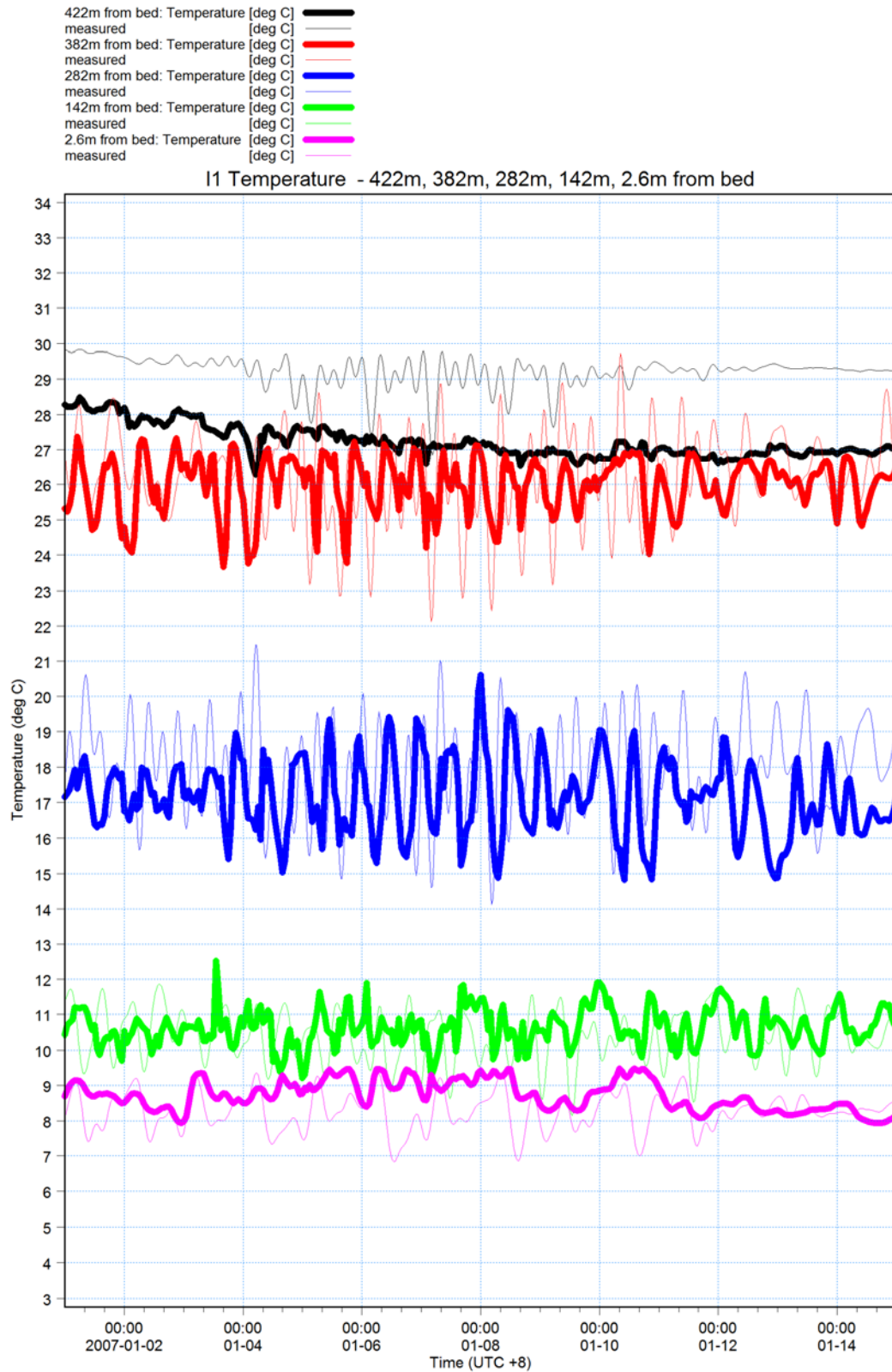


Fig 5.44 Multi-time series plot for I1-1, summer validation period
Thin lines: measured values, thick lines: model results



T at 422m x x
T at 382m x x
T at 282m x x
T at 142m x x
T at 2.6m x x

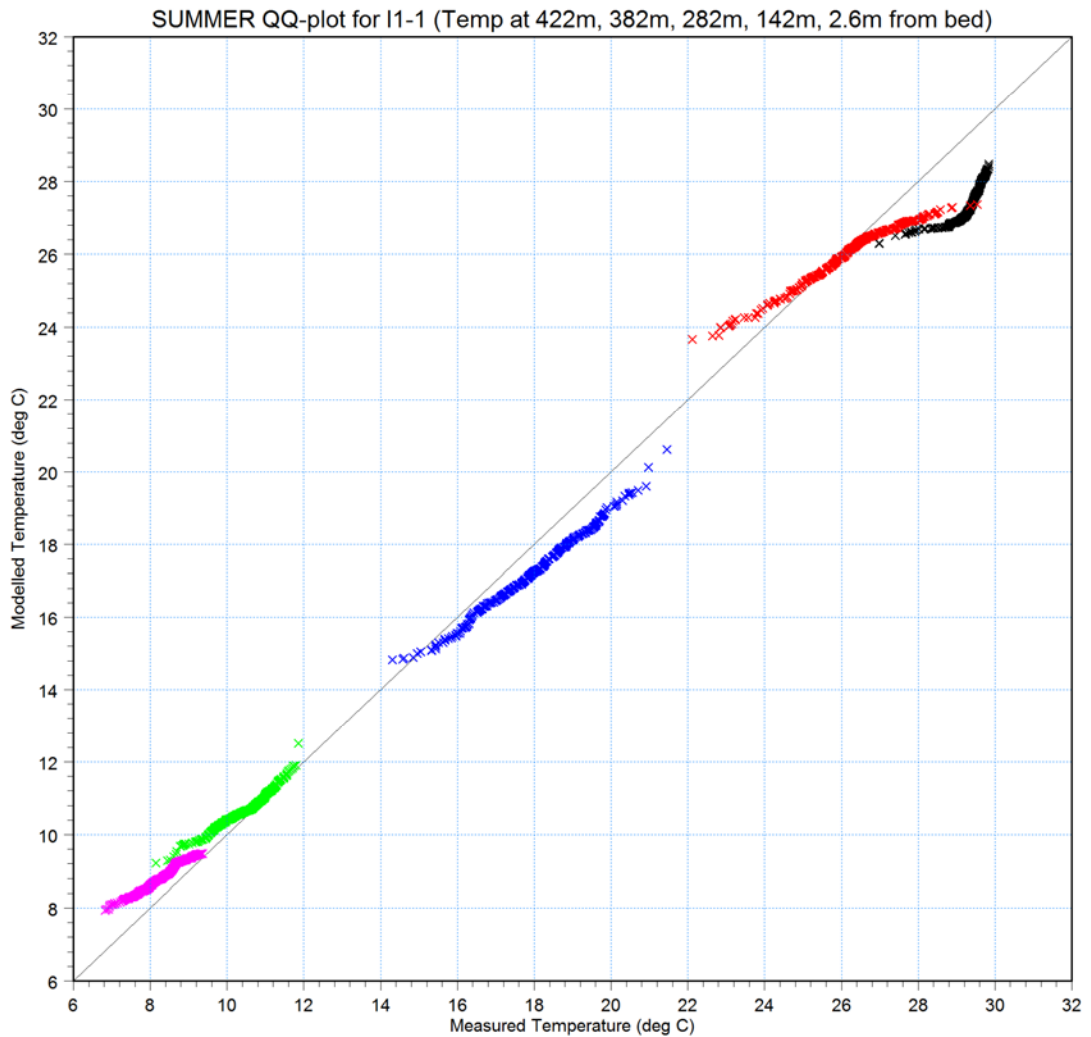


Fig 5.45 Q-Q plot for temperatures for I1-1, summer validation period

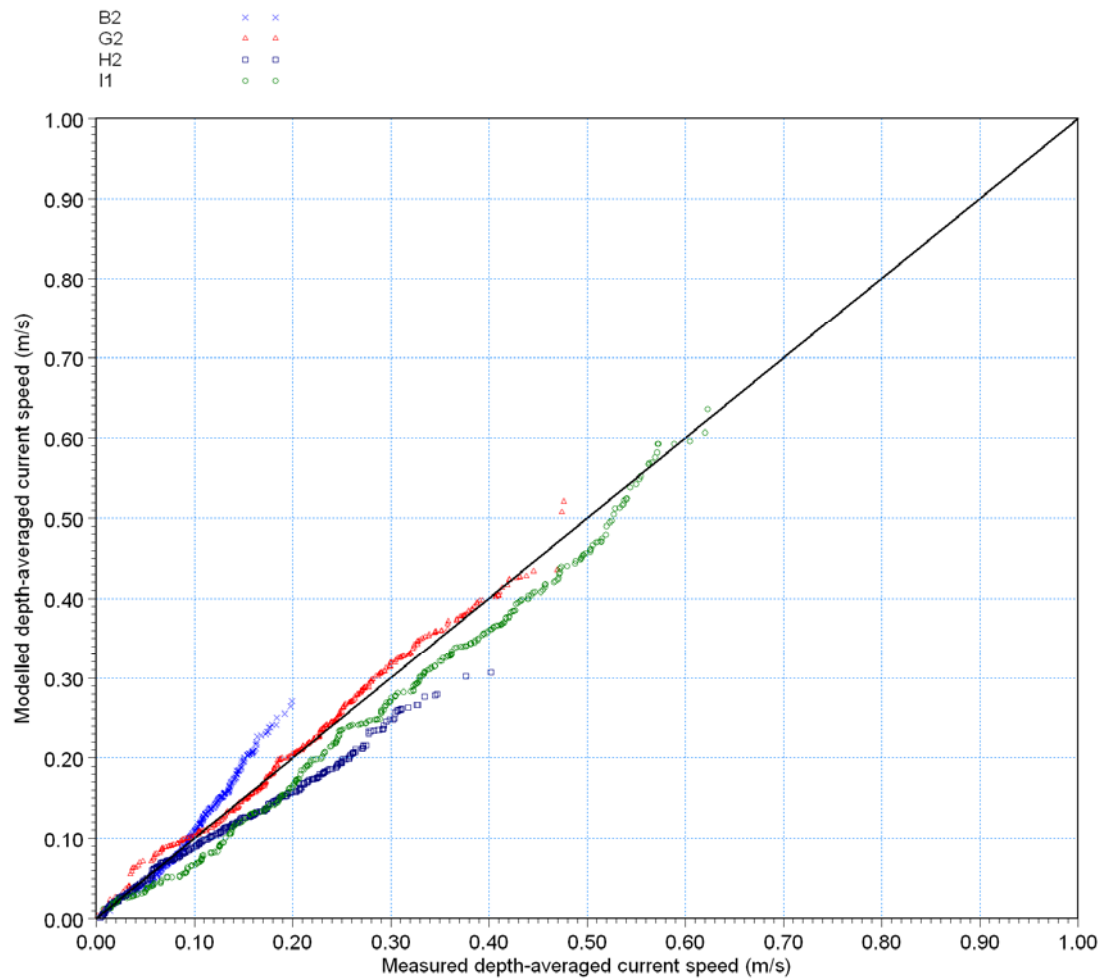


Fig 5.46 Q-Q plot for depth averaged currents for all stations, summer validation period

Table 5.3 Statistical analysis of key parameters for summer validation period

*: Defined as mean of model – mean of measurements results

**: defined as RMS / peak value * 100

Station	Parameter	Bias* [m/s]	RMS Error [m] or [m/s]	Peak value [m] or [m/s]	RMS Error [%]**
A2-1	Water level (m)	0.06	0.09	1.76	5
B2-1	Depth averaged current speed (m/s)	0.01	0.05	0.20	23
G2-1	Depth averaged current speed (m/s)	0.01	0.09	0.49	18
H2-1	Depth averaged current speed (m/s)	-0.02	0.07	0.40	17
I1-1	Depth averaged current speed (m/s)	-0.03	0.10	0.63	16

Based on the performance criteria listed in Section 5.5 the RMS error for currents should preferably be less than 10 to 20%, which is fulfilled for all stations except B2-1. However, with the peak current being only 20 cm/s 23% is acceptable. (see also the discussion of RMS values for the autumn period in section 5.8). For water levels RMS should be less than 15%, which is also fulfilled. The bias listed in Table 5.3 gives an indication of whether the model under-predict (positive value) or over-



predicts (negative value) the water levels and the current speeds. With all values being only a few cm or cm/s these biases are considered acceptable.

The models ability to reproduce the current measurements is also visualised in Fig 5.46, where a good fit between model and measurements is seen.

In the following sub-sections the comparisons at each of the six stations where measurements are available for this validation period are discussed.

Comments to comparisons at A2-1

The comparison of water levels at A2-1 (located within Scott Reef) is shown in Fig 5.26 and Fig 5.27 and demonstrates that the model reproduces the tidal water level variations very well. This is also underpinned by an RMS value of only 5%. A bias of 6 cm is not a serious error as part or all of this is likely to be caused by a datum shift.

Comments to comparisons at B2-1

In general a good agreement between simulated and measured current speed and direction is found although not as good as for the spring calibration period (Fig 5.28). Again a slight overproduction by the model is seen.

Looking at Fig 5.29 and Fig 5.31 the temperatures seems well represented in the model. However, looking at Fig 5.30 they are not as well reproduced as during the spring calibration period. The large variations seen in the measurements for the top-most sensor is, however, not reproduced by the model, which is likely caused by the model having a top layer of 30m.

Comments to comparisons at C1-1

The comparison of temperatures shown in Fig 5.32 and Fig 5.33 show the same pattern as for the spring calibration period, where a good agreement is seen at the seabed and 395m above seabed, while the steep temperature gradient close to the surface is not reproduced by the model. This is as earlier mentioned likely caused by the top layer being 30m thick.

Comments to comparisons at G2-1

The comparison of current shown in Fig 5.34 shows a good agreement between model and measurements, both with respect to phase and magnitude and during both neap tide and spring tide.

A comparison of temperatures is shown in Fig 5.35 to Fig 5.37. While the model reproduces the large variations also seen in the measurements (often up to 7 degrees within 6 hours), the general level of the temperature in the model is lower in the upper part of the water column. In other words the mixing in the model is too high at this location with too cold water being brought to the surface. This only happens in a belt along the 200m depth contour where G2-1 is located (see Fig 5.47). Changing initial conditions in the top layer to warmer water than at B2-1, or changing the top layer thickness to 10m does not change the high mixing found along the 200m contour and G2-1.

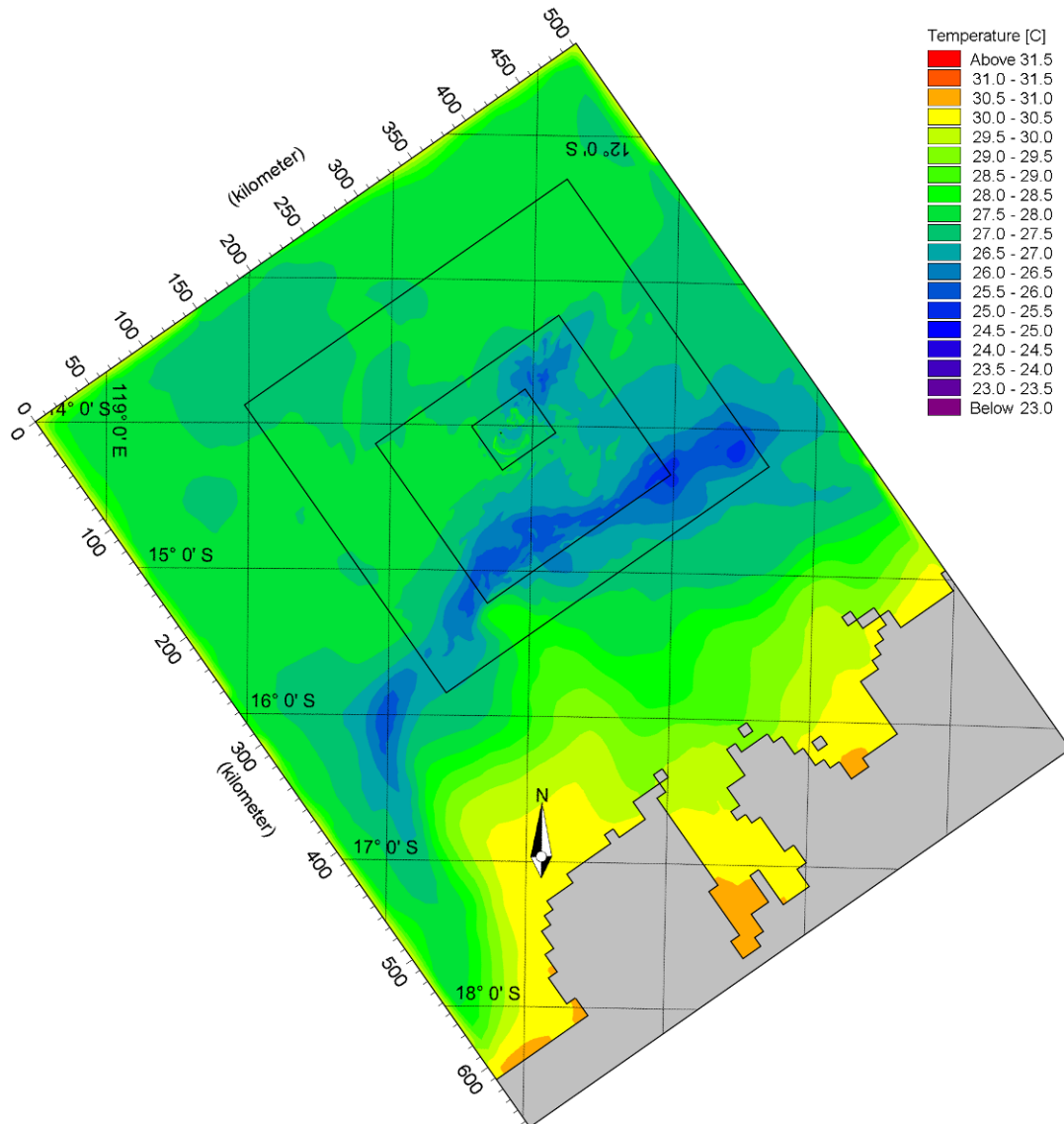


Fig 5.47 Temperature in surface layer with cold water seen around the 200m contour (refer Fig 5.10) at 2007-01-12 12:00

Comments to comparisons at H2-1

While the current phases are well reproduced by the model (Fig 5.38) the peak current magnitude at this station is somewhat underestimated in the model. The bias is, however, only 2 cm/s.

The temperature comparisons (Fig 5.39 to Fig 5.41) show a very dynamic area with the model reproducing only part of this variability as seen from the Q-Q plot.

Comments to comparisons at I1-1

Currents are generally very well reproduced (Fig 5.42) at this station.

Temperature comparisons (Fig 5.43 to Fig 5.45) show an acceptable agreement between model and measurements. The top layer in the model does, however,



generally have a lower temperature of 1-2 degrees. The model shows some upwelling, but not as much as the measurements.

Conclusion

Based on the visual comparisons and the statistical analysis it is concluded that the model demonstrates a satisfactory reproduction of the complicated hydrodynamic conditions during the summer validation period.

5.8 Results of Model Validation for Autumn Period

The results for autumn validation period are presented similar to the spring and summer periods with all comparisons included in Appendix D (except for the comparison of water levels at Scott Reef, which is shown in Fig 5.48 and Fig 5.49) and key figures shown below.

For the autumn validation period measurements were only available for A2-1 (water levels), B2-1 (currents and temperatures) and C1-1 (currents and temperatures). The key plots for these stations are shown in Fig 5.48 through Fig 5.56. Note that as for the other periods there are measurements at too few depths at C1-1 to compute the depth averaged currents for this station.

The results of the statistical analysis for the summer validation period are listed in Table 5.4.

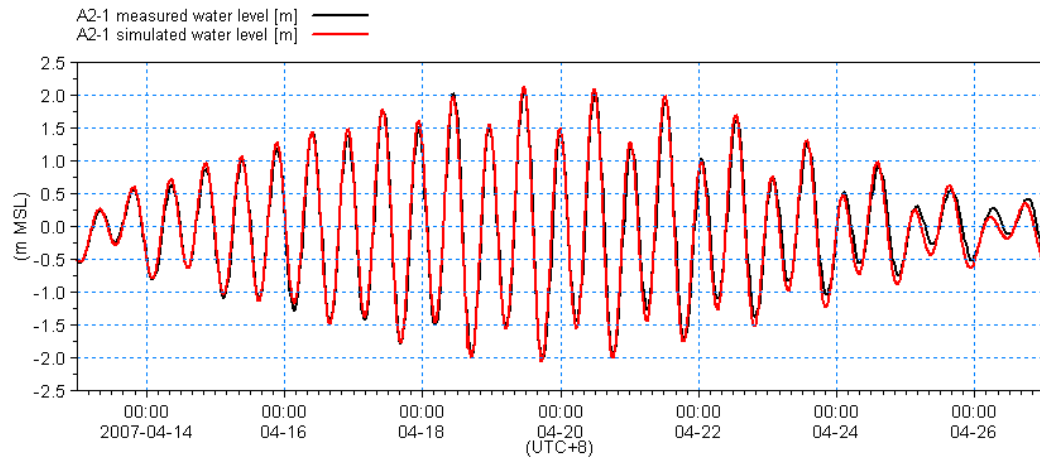


Fig 5.48 Comparison of measured and modelled water level for A2-1 Scott Reef, autumn validation period.

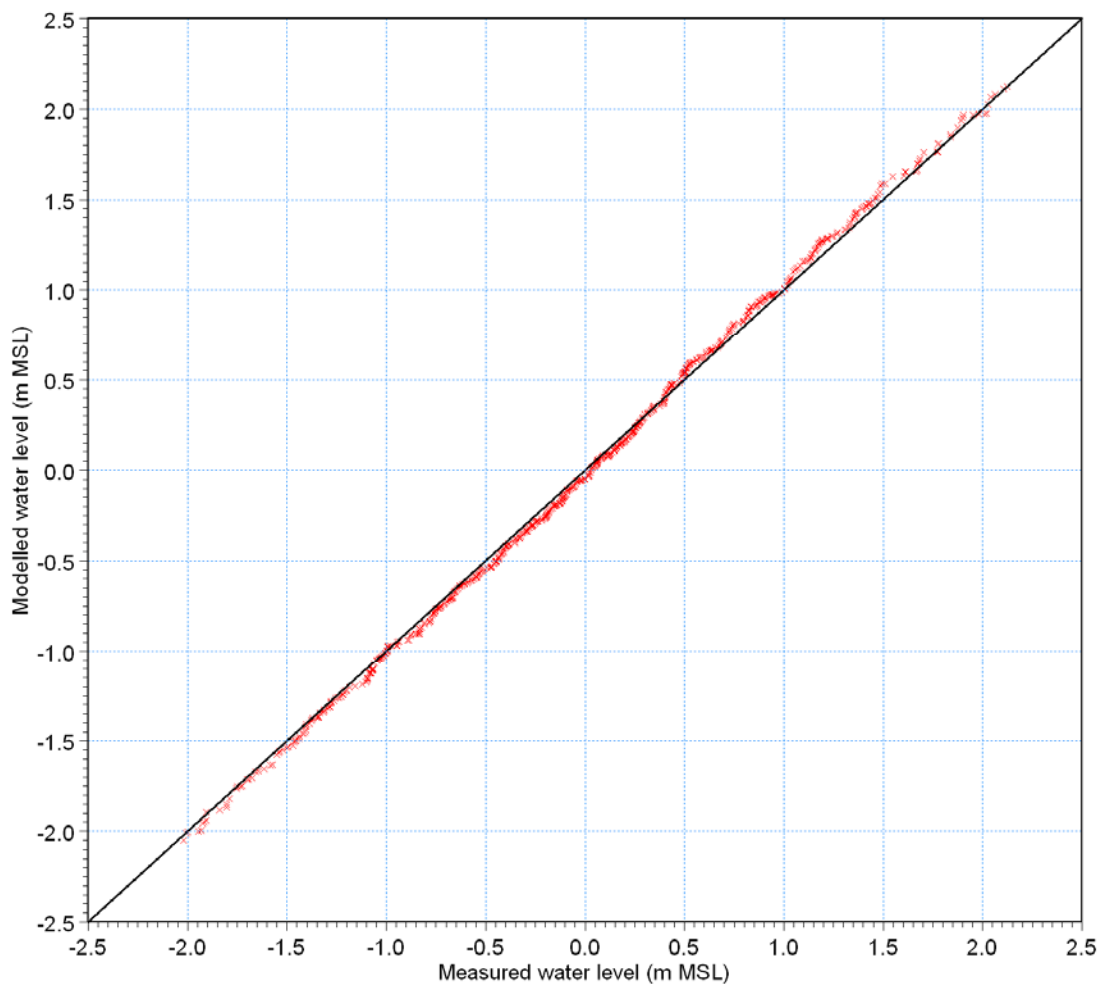


Fig 5.49 Q-Q plot for water levels at A2-1 Scott Reef, autumn validation period.

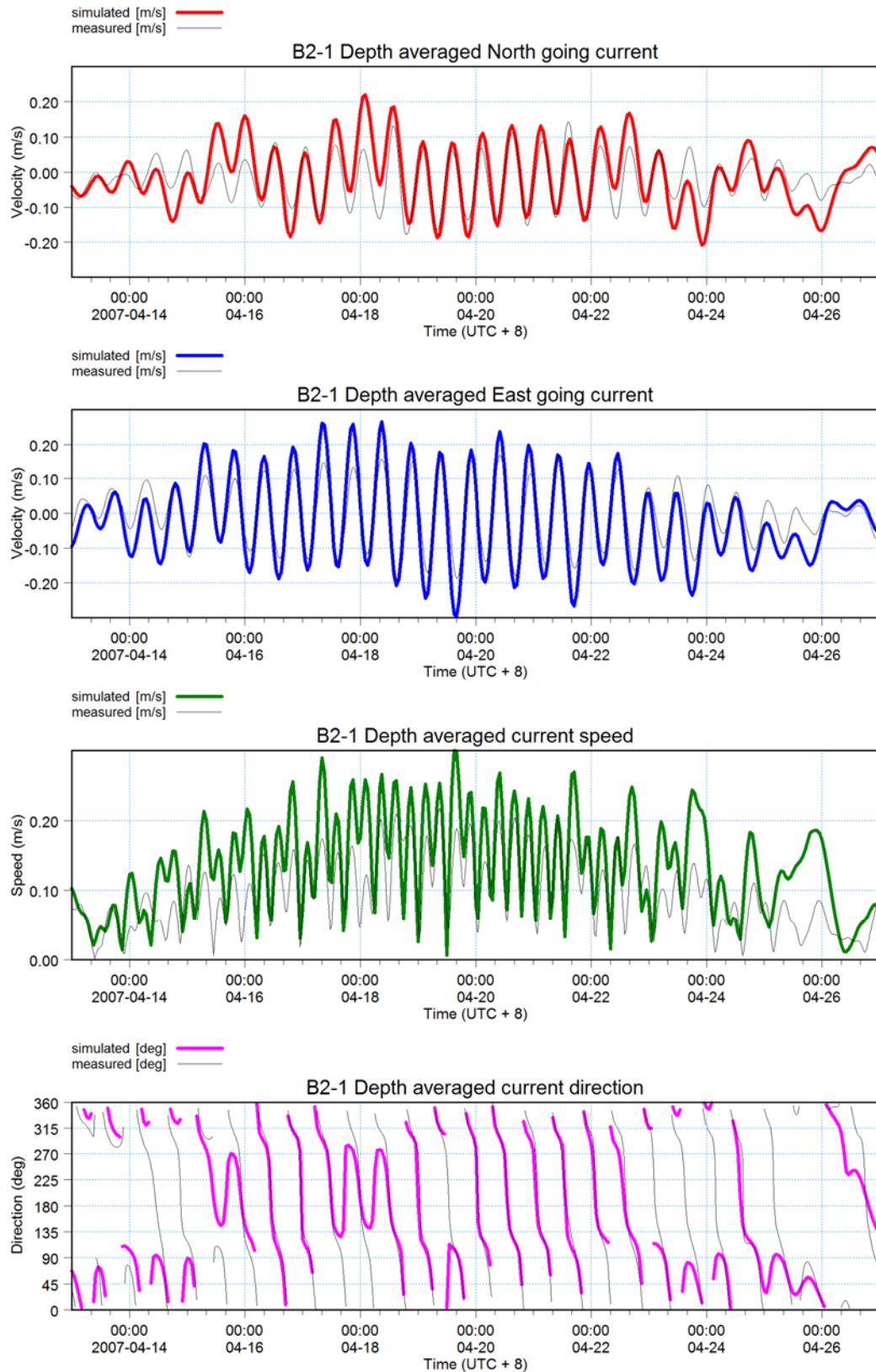


Fig 5.50 Depth averaged currents for B2-1, autumn validation period

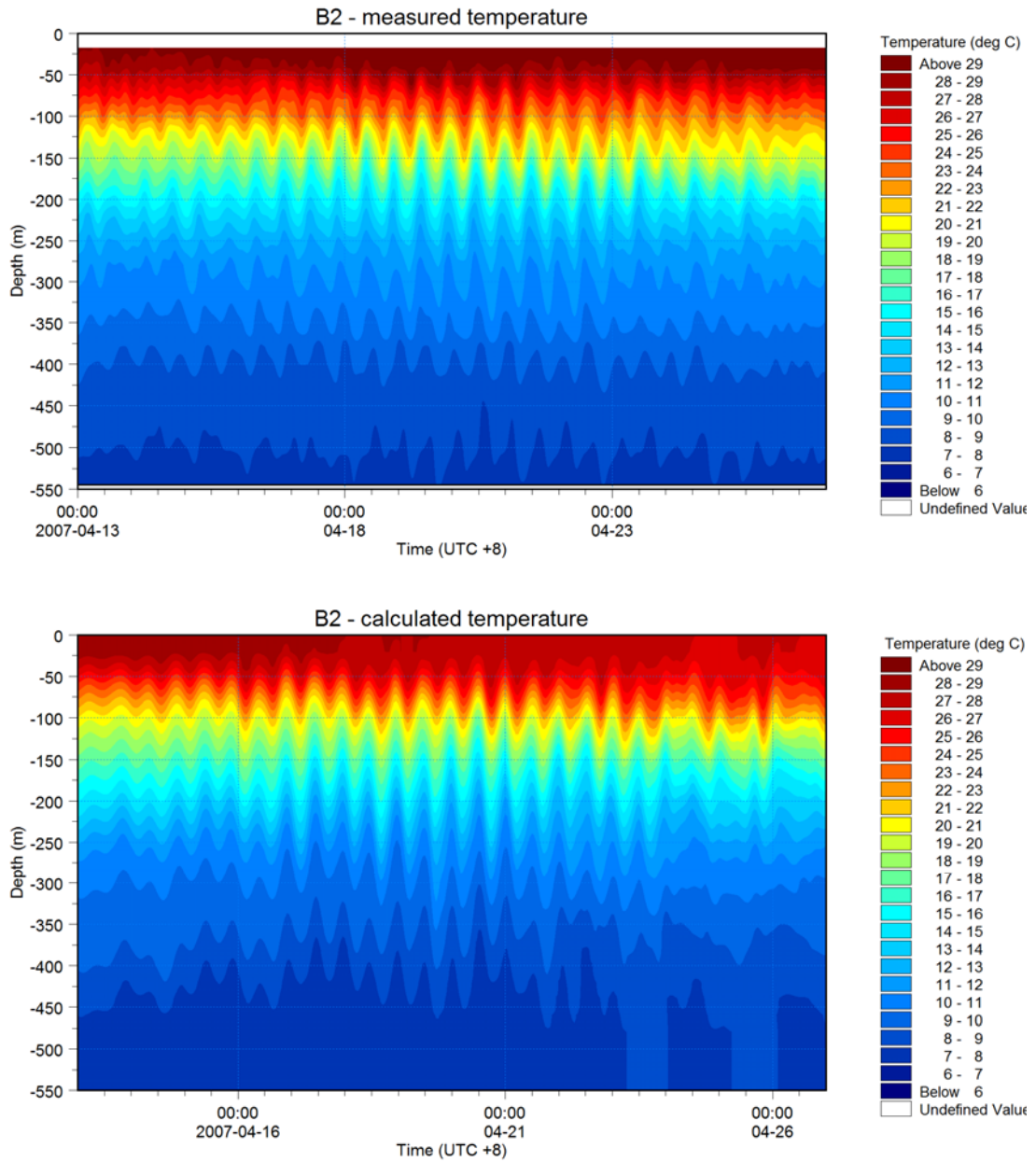


Fig 5.51 Isopleth plot for B2-1, autumn validation period

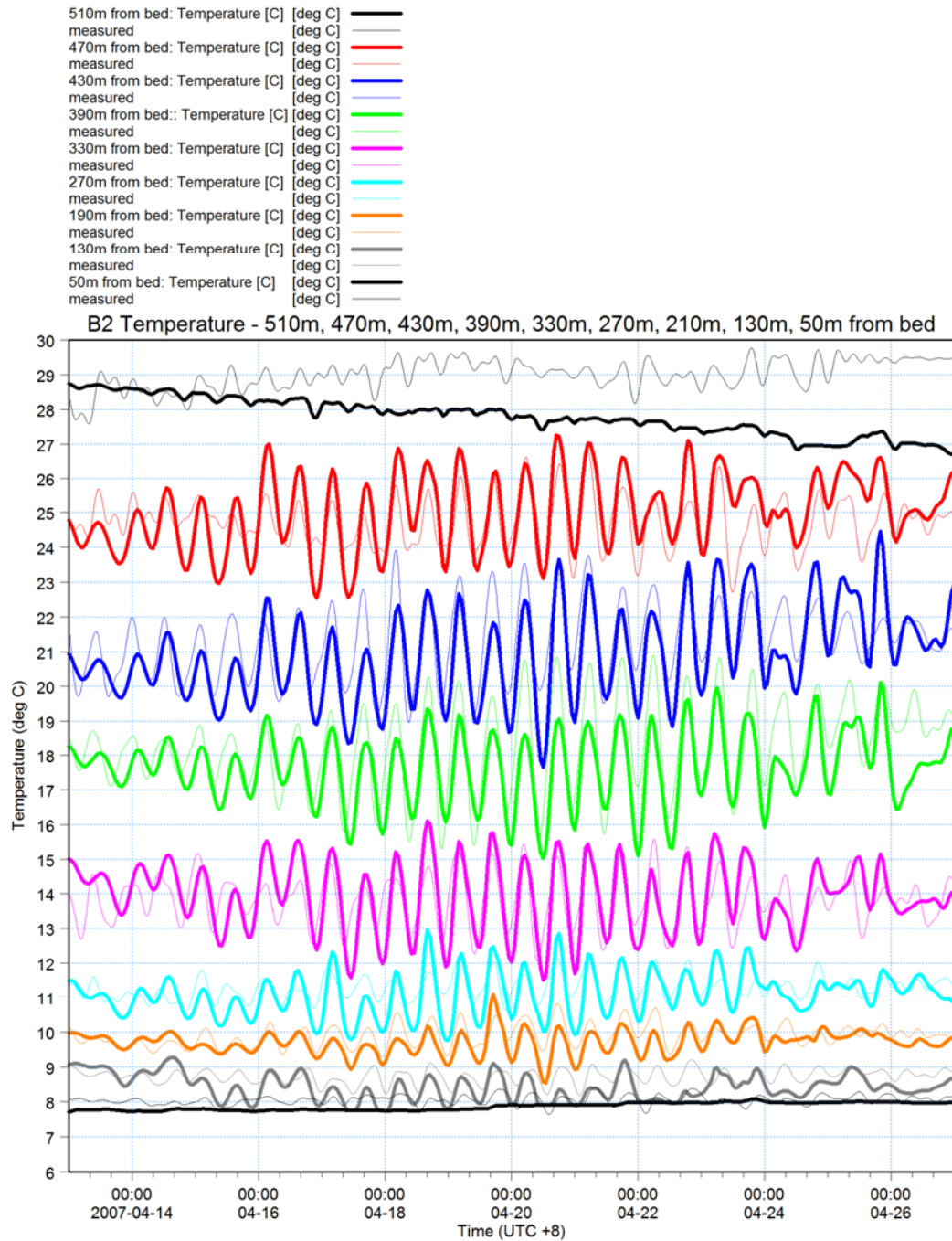


Fig 5.52 Multi-time series plot for B2-1, autumn validation period
Thin lines: measured values, thick lines: model results



- T at 510m x x
- T at 470m x x
- T at 430m x x
- T at 390m x x
- T at 330m x x
- T at 270m x x
- T at 190m x x
- T at 130m x x
- T at 50m x x

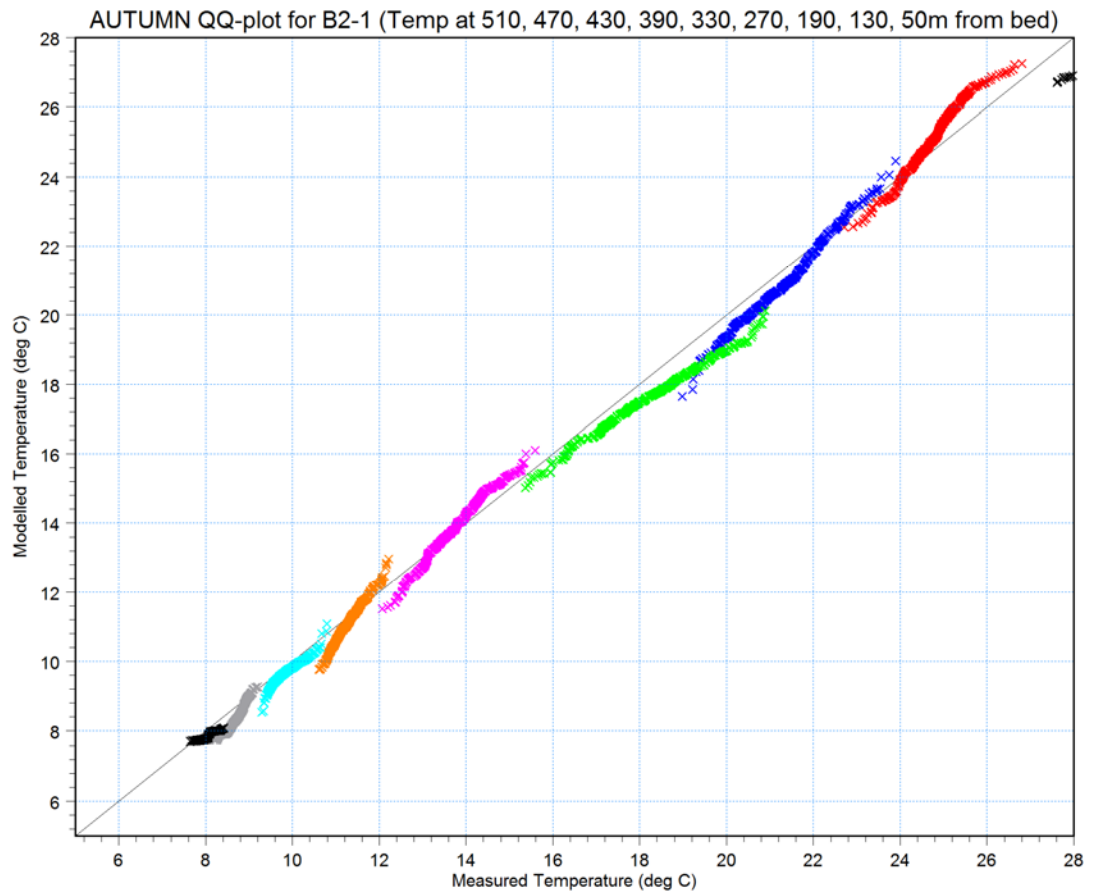


Fig 5.53 Q-Q plot for temperatures for B2-1, autumn validation period

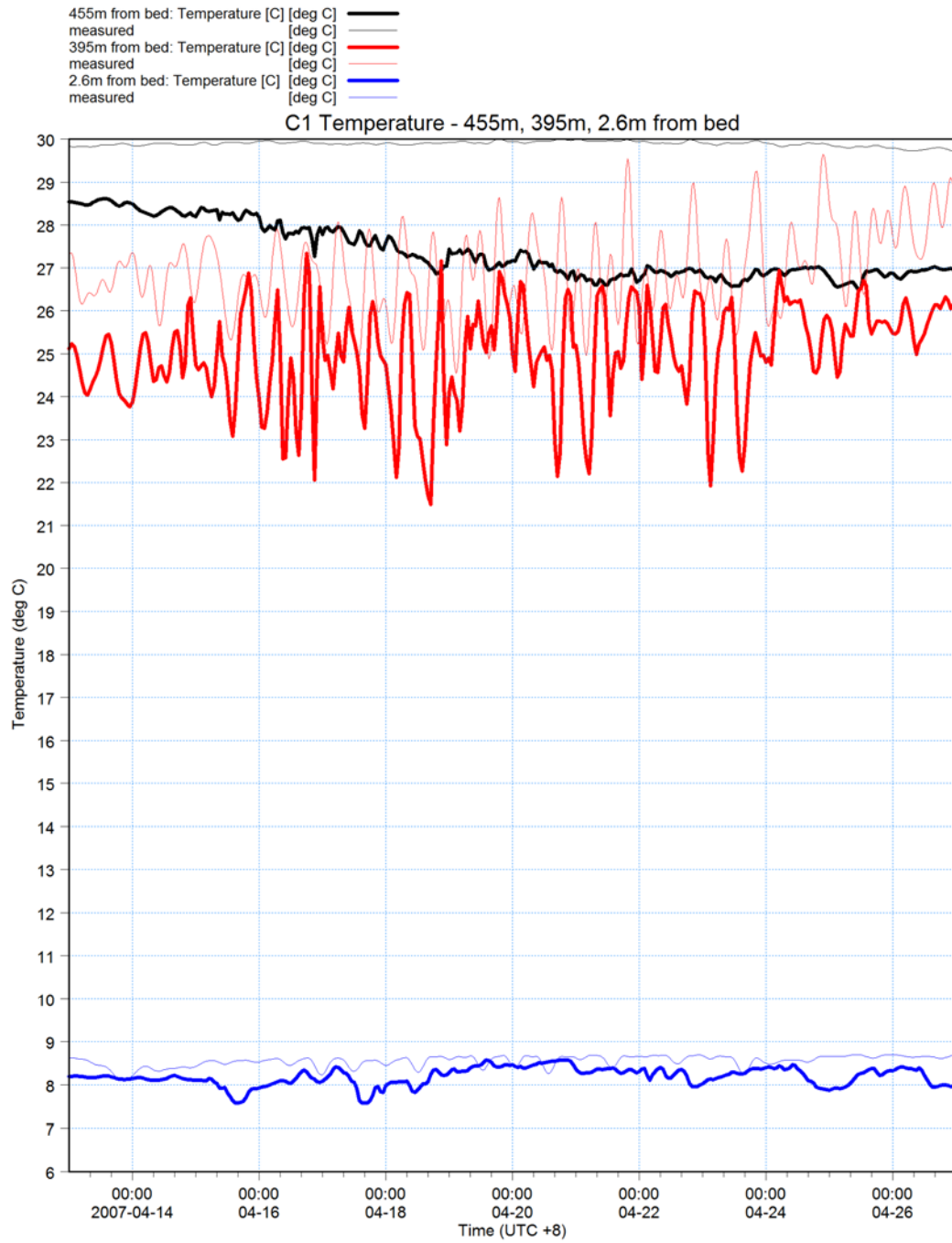


Fig 5.54 Multi-time series plot for C1-1, autumn validation period
Thin lines: measured values, thick lines: model results



T at 455m x x
T at 395m x x
T at 2.6m x x

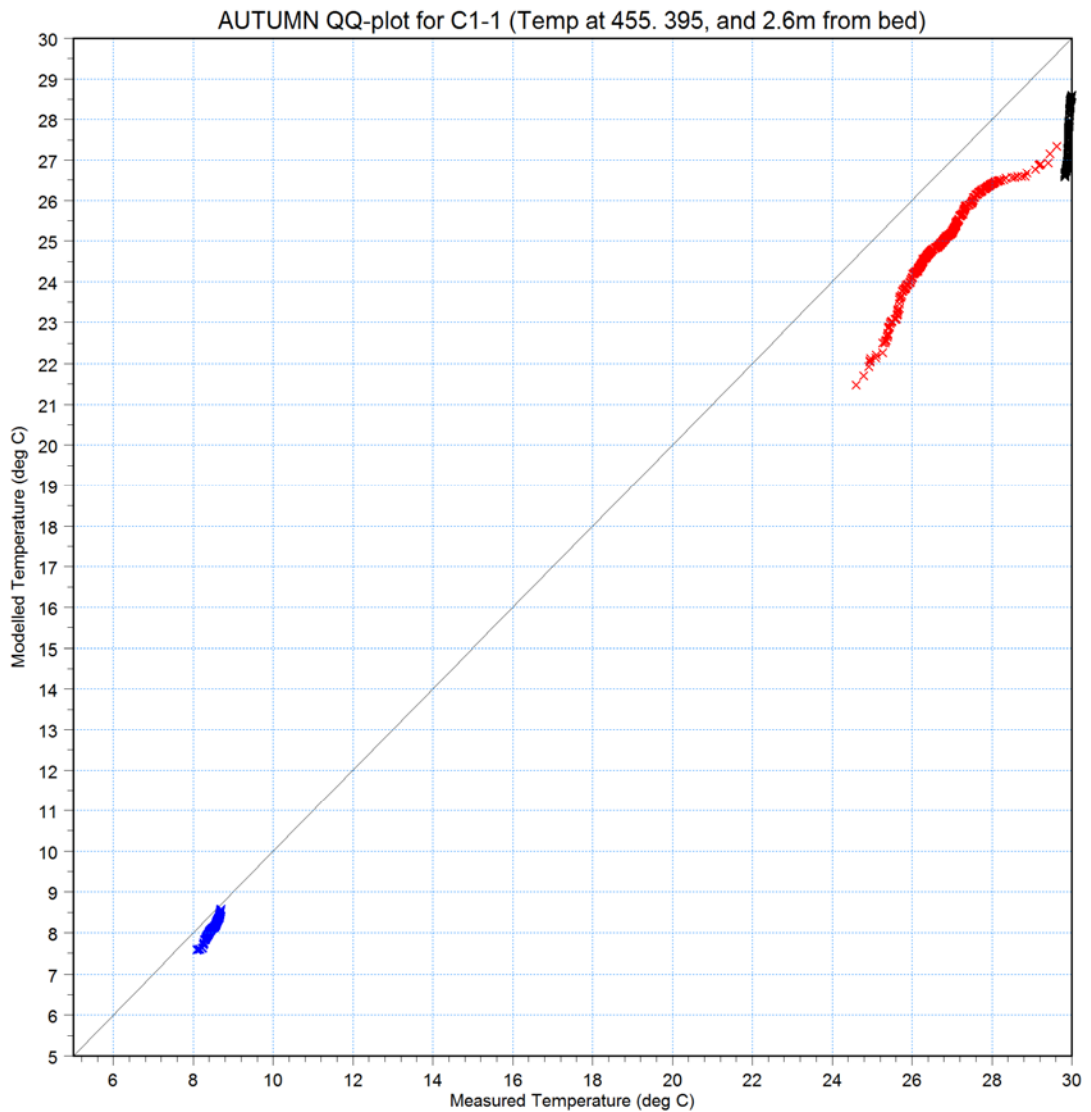


Fig 5.55 Q-Q plot for temperatures for C1-1, autumn validation period

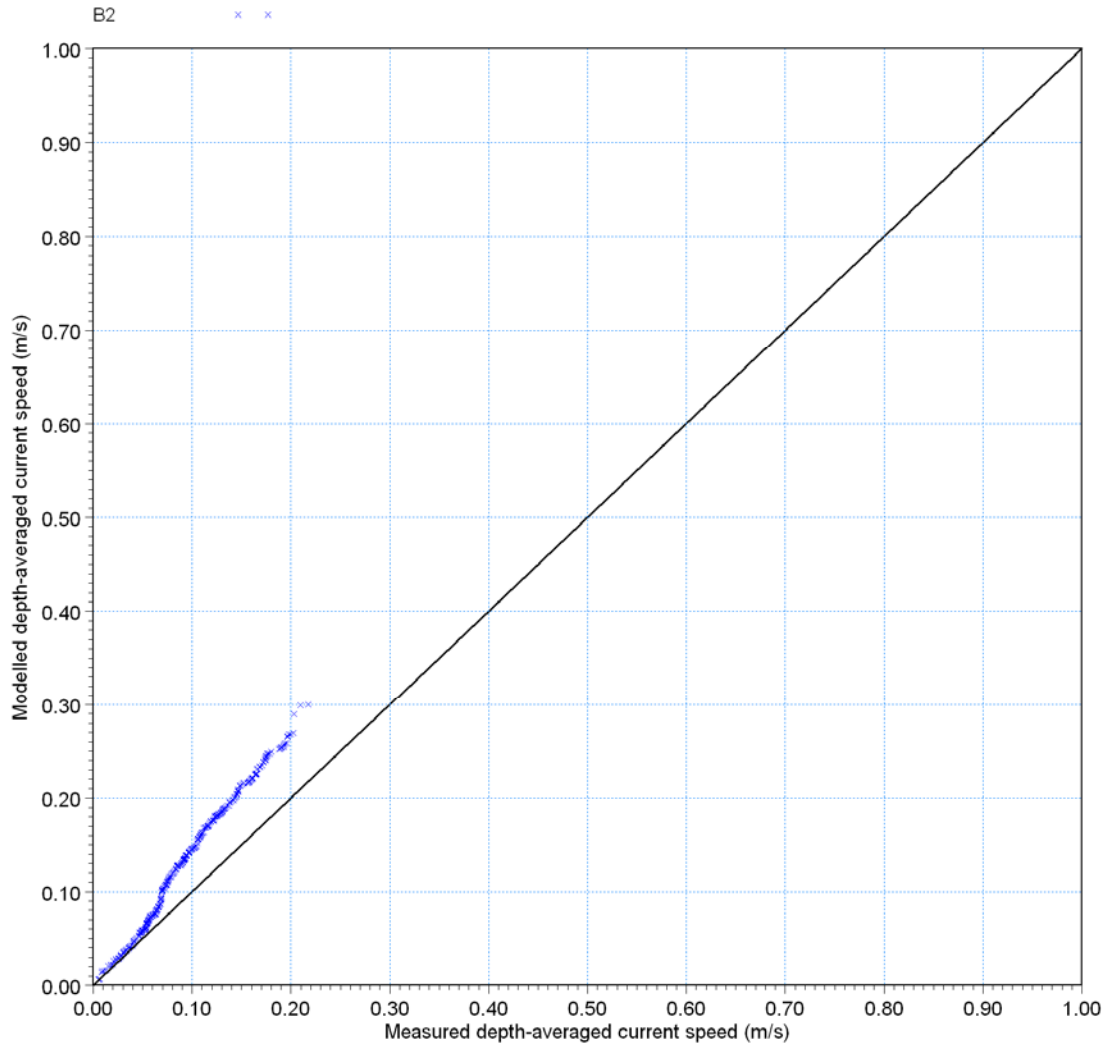


Fig 5.56 Q-Q plot for depth averaged currents for all stations (only B2-1 available), autumn validation period

Table 5.4 Statistical analysis of key parameters for autumn validation period
 *: Defined as mean of model – mean of measurements results
 **: defined as RMS / peak value * 100

Station	Parameter	Bias* [m/s]	RMS Error [m] or [m/s]	Peak value [m] or [m/s]	RMS Error [%]**
A2-1	Water level (m)	-0.01	0.10	2.12	5
B2-1	Depth averaged current speed (m/s)	0.04	0.06	0.22	25

The RMS error should be less than 15% for water levels, which is easily fulfilled at station A2-1, while the RMS error at B2-1 is 6 cm/s which corresponds to 25% as the peak speed is only 22 cm/s. As discussed below the phases at B2-1 are reproduced very well by the model, while the magnitude of the speed is over-predicted. This is also reflected in the bias of 4 cm/s. The over-prediction is most pronounced 250m above seabed (see page D-11 and D-14), where the magnitude of the measured currents is significantly smaller than in the measurements above and below. This may suggest some errors in the measurements as the temperature variation at this



depth (see page D-3) is well reproduced by the model. The same difference (250m above seabed) is seen in the winter period (page E-11 and E-14), while it is not present in the spring and summer period. This could be explained by the fact that the spring and summer period are covered by the first instrument deployment, while the autumn and winter period are covered by the second instrument deployment.

All three stations for which measurements were available for the autumn period are discussed below.

Comments to comparisons at A2-1

The comparison of water levels at A2-1 is shown in Fig 5.48 and Fig 5.49 and demonstrates that the model reproduces the tidal water level variations very well. This is also underpinned by an RMS value of only 5%.

Comments to comparisons at B2-1

As discussed above the phases are in good agreement, while the peak magnitude on the average is over-predicted by about 5-7 cm/s with a bias of 4 cm/s (Fig 5.50).

Temperatures (Fig 5.51 to Fig 5.53) are generally well reproduced except for the top layer where too much surface cooling is seen in the model results.

Comments to comparisons at C1-1

For C1-1 the cooling in the top layers in the model is too pronounced as for B2-1, while the very large temperature variations 395m above seabed are well reproduced (see Fig 5.54 and Fig 5.55).

Conclusion

Measurements were only available from three stations for the autumn period. The comparisons between measurements and model at the two stations with currents/temperatures show an acceptable although not perfect agreement. The water levels at A2-1 are, however, very well reproduced by the model. All in all an acceptable model validation.

5.9 Results of Model Validation for Winter Period

The results for winter validation period are presented similar to the other periods with all comparisons included in Appendix E (except for the comparison of water levels at Scott Reef, which is shown in Fig 5.57 and Fig 5.58) and key figures shown below.

For the winter validation period measurements were only available for A2-1 (water levels), B2-1 (currents and temperatures) and C1-1 (currents and temperatures) The key plots for these stations are shown in Fig 5.57 through Fig 5.65. Note that as for the other periods there are measurements at too few depths at C1-1 to compute the depth averaged currents for this station.

The results of the statistical analysis for the winter validation period are listed in Table 5.5.

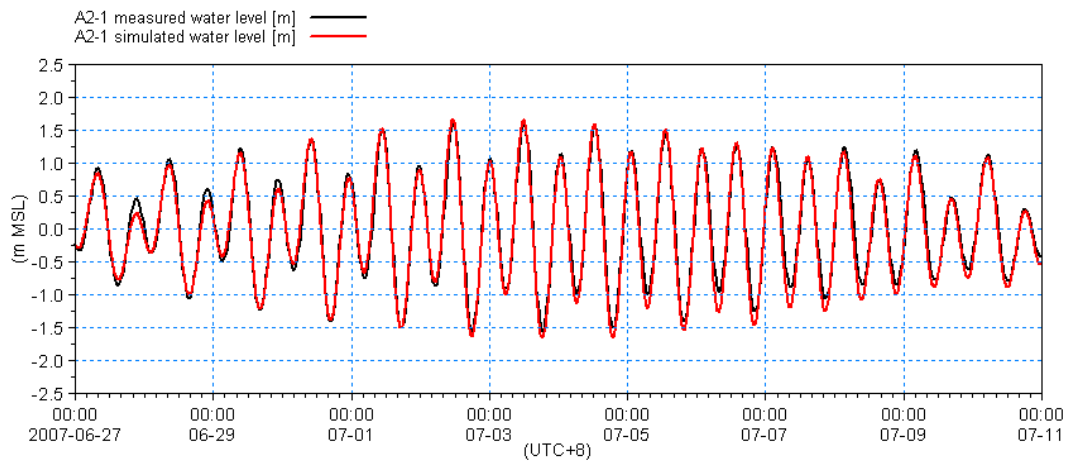


Fig 5.57 Comparison of measured and modelled water level for A2-1 Scott Reef, winter validation period.

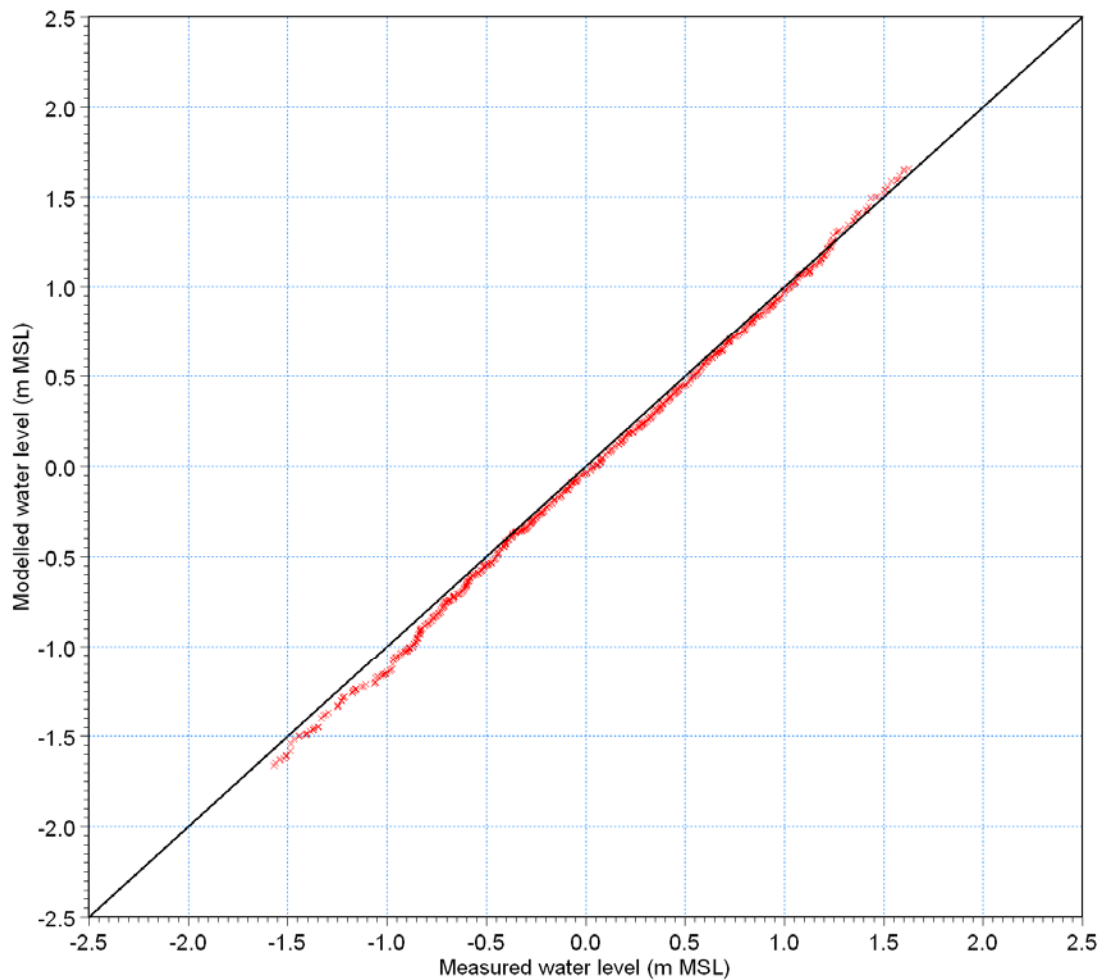


Fig 5.58 Q-Q plot for water levels at A2-1 Scott Reef, winter validation period.

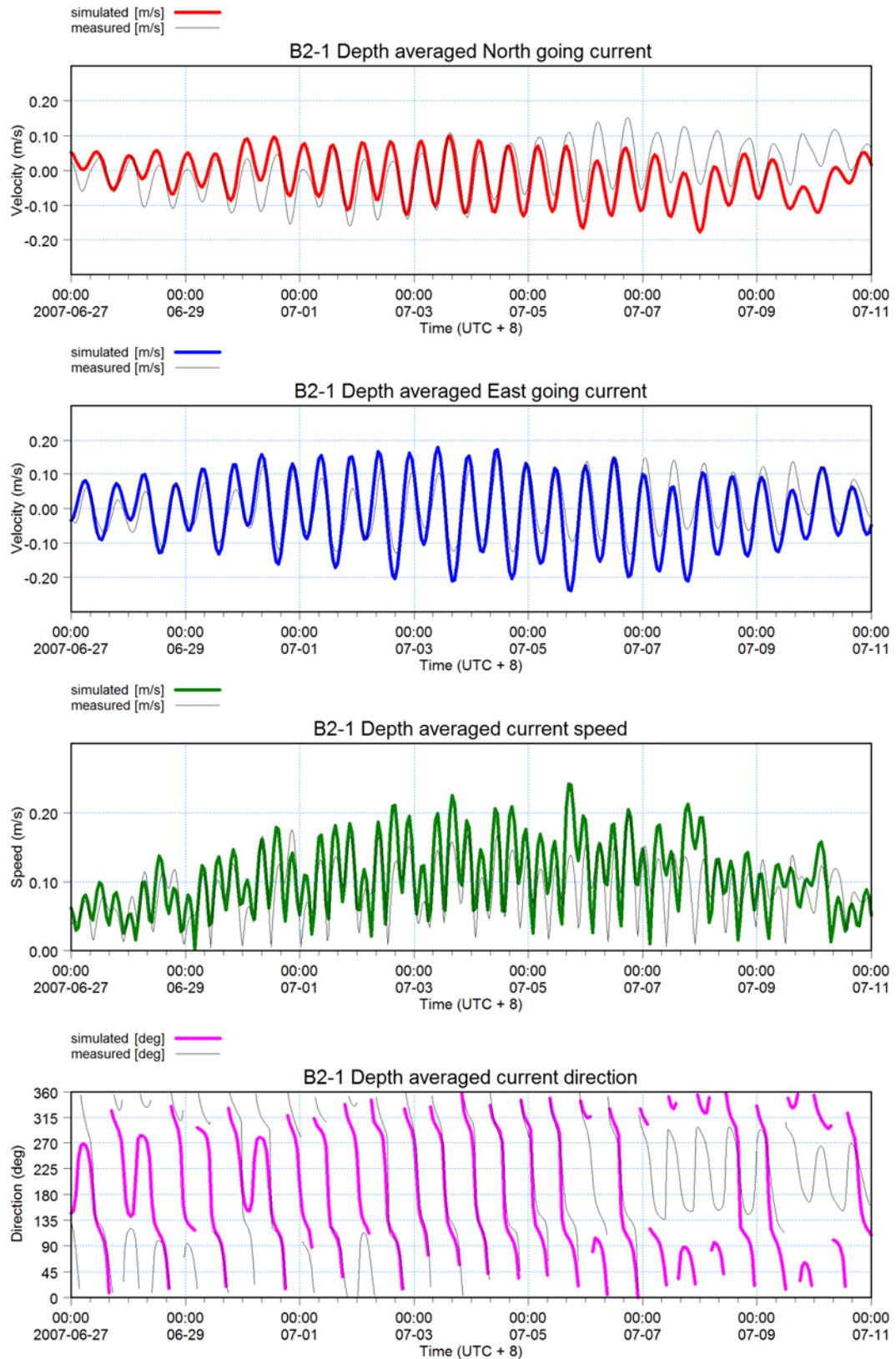


Fig 5.59 Depth averaged currents for B2-1, winter validation period

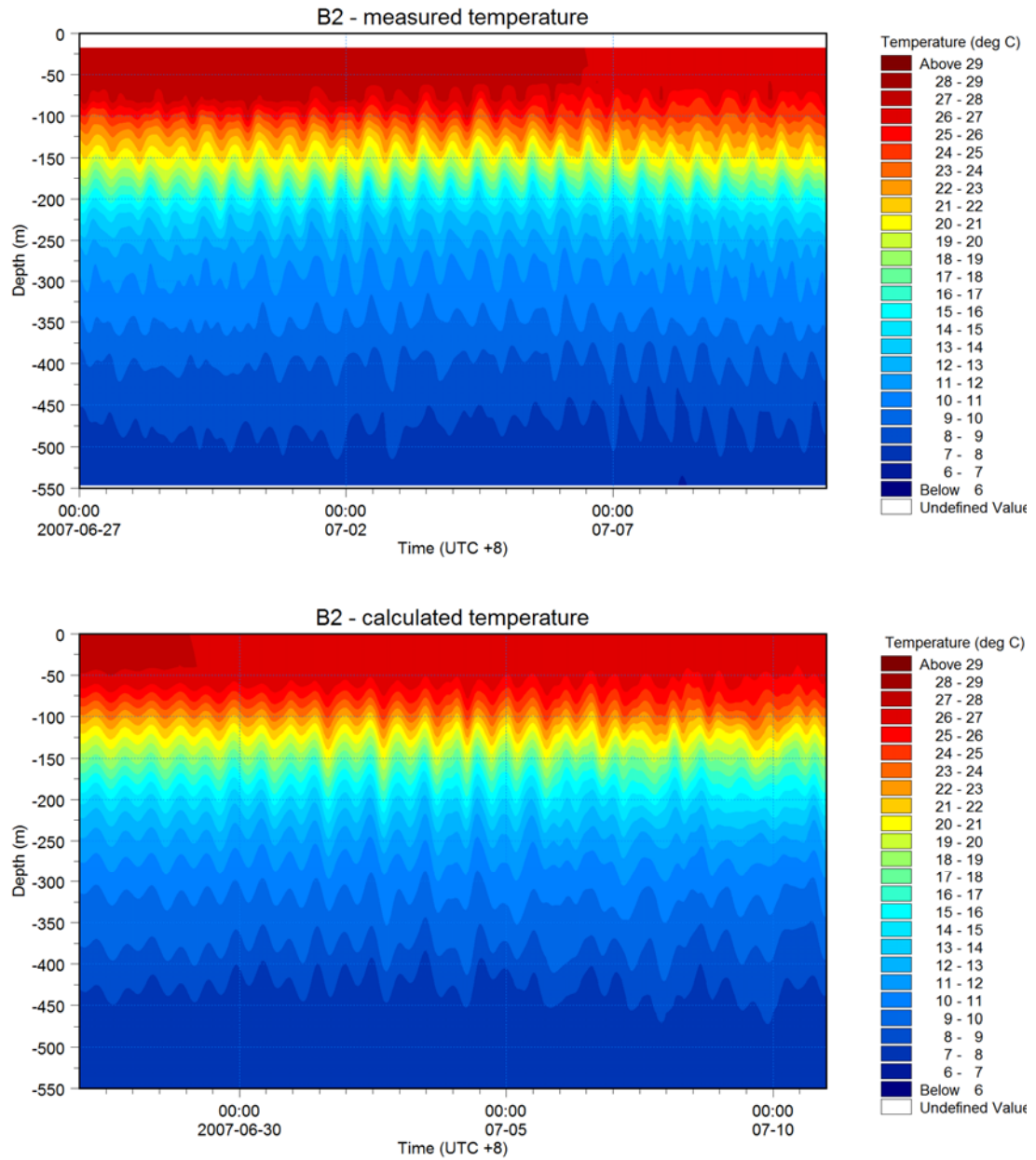


Fig 5.60 Isopleth plot for B2-1, winter validation period

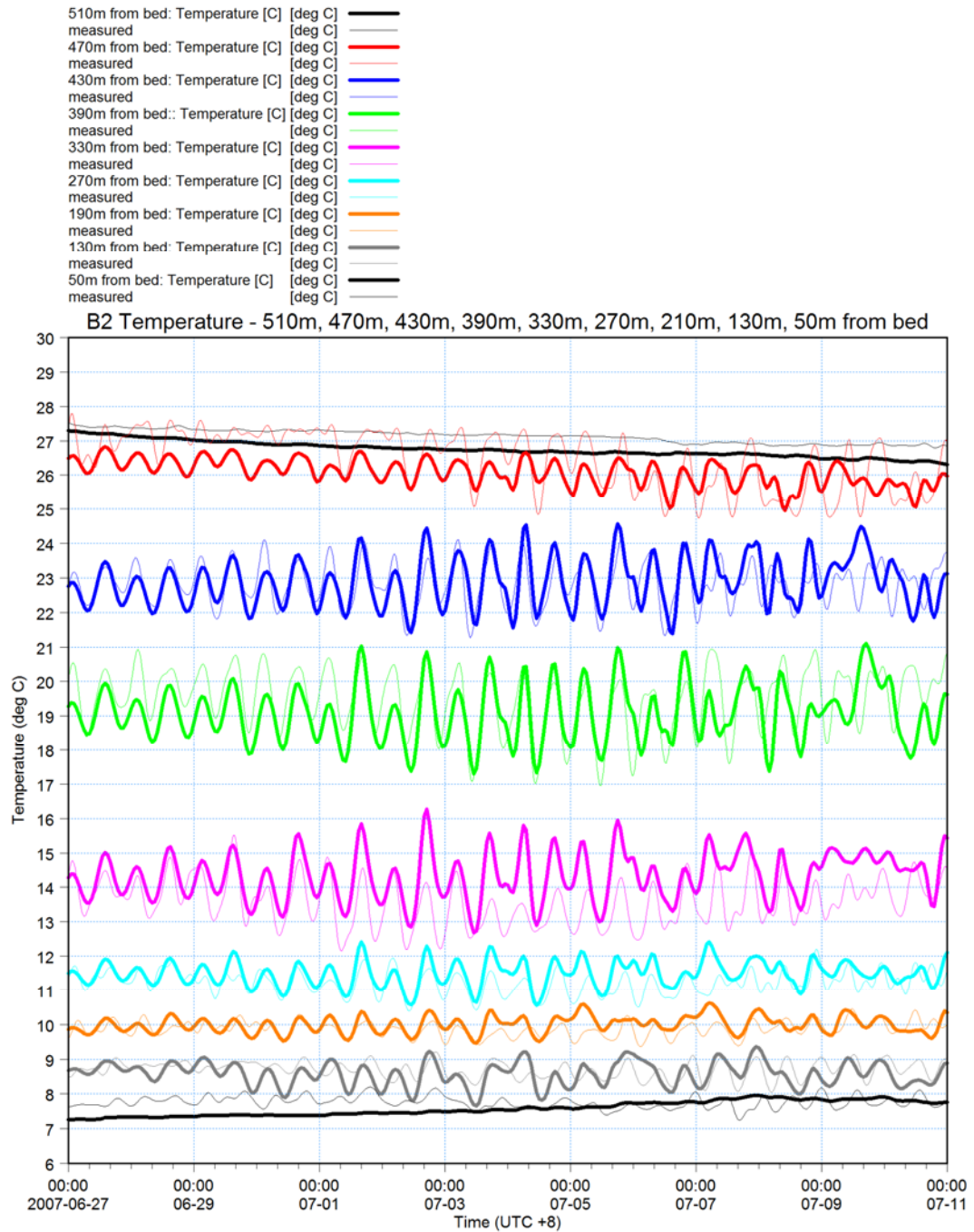


Fig 5.61 Multi-time series plot for B2-1, winter validation period
Thin lines: measured values, thick lines: model results



- T at 510m x x
- T at 470m x x
- T at 430m x x
- T at 390m x x
- T at 330m x x
- T at 270m x x
- T at 190m x x
- T at 130m x x
- T at 50m x x

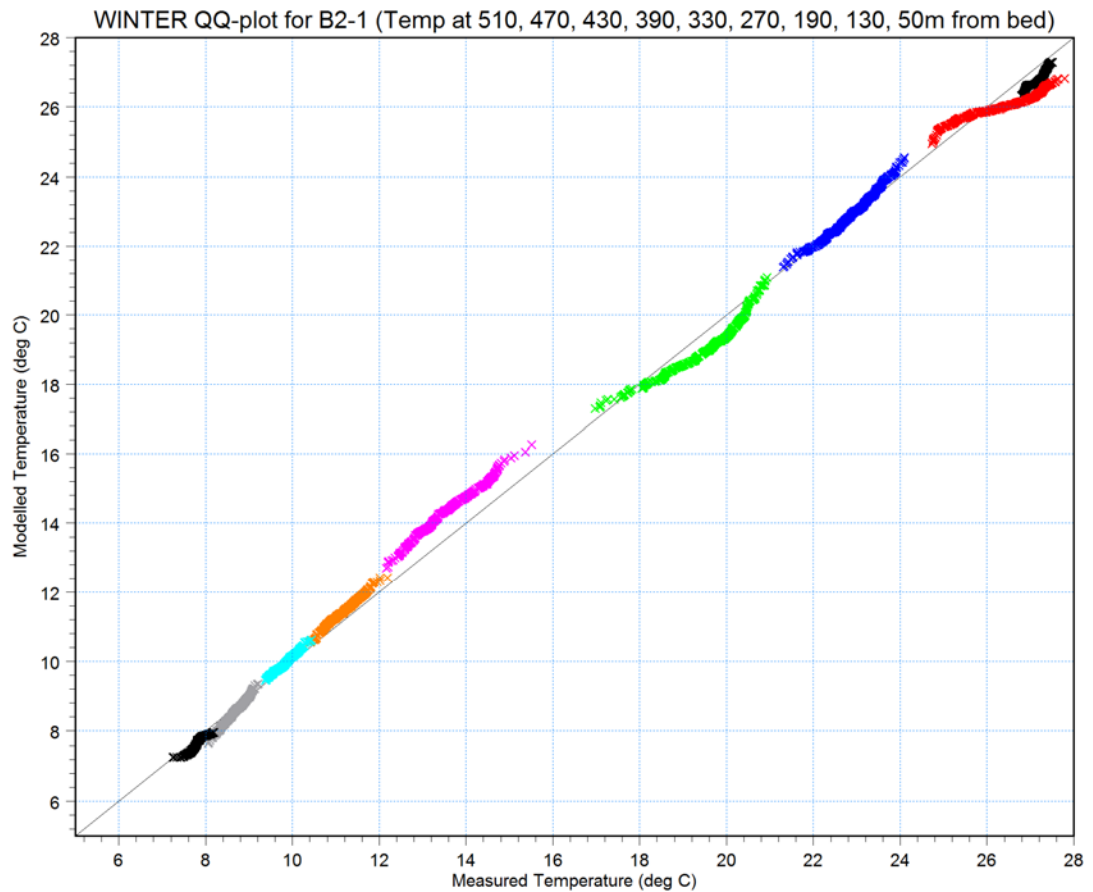


Fig 5.62 Q-Q plot for temperatures for B2-1, winter validation period

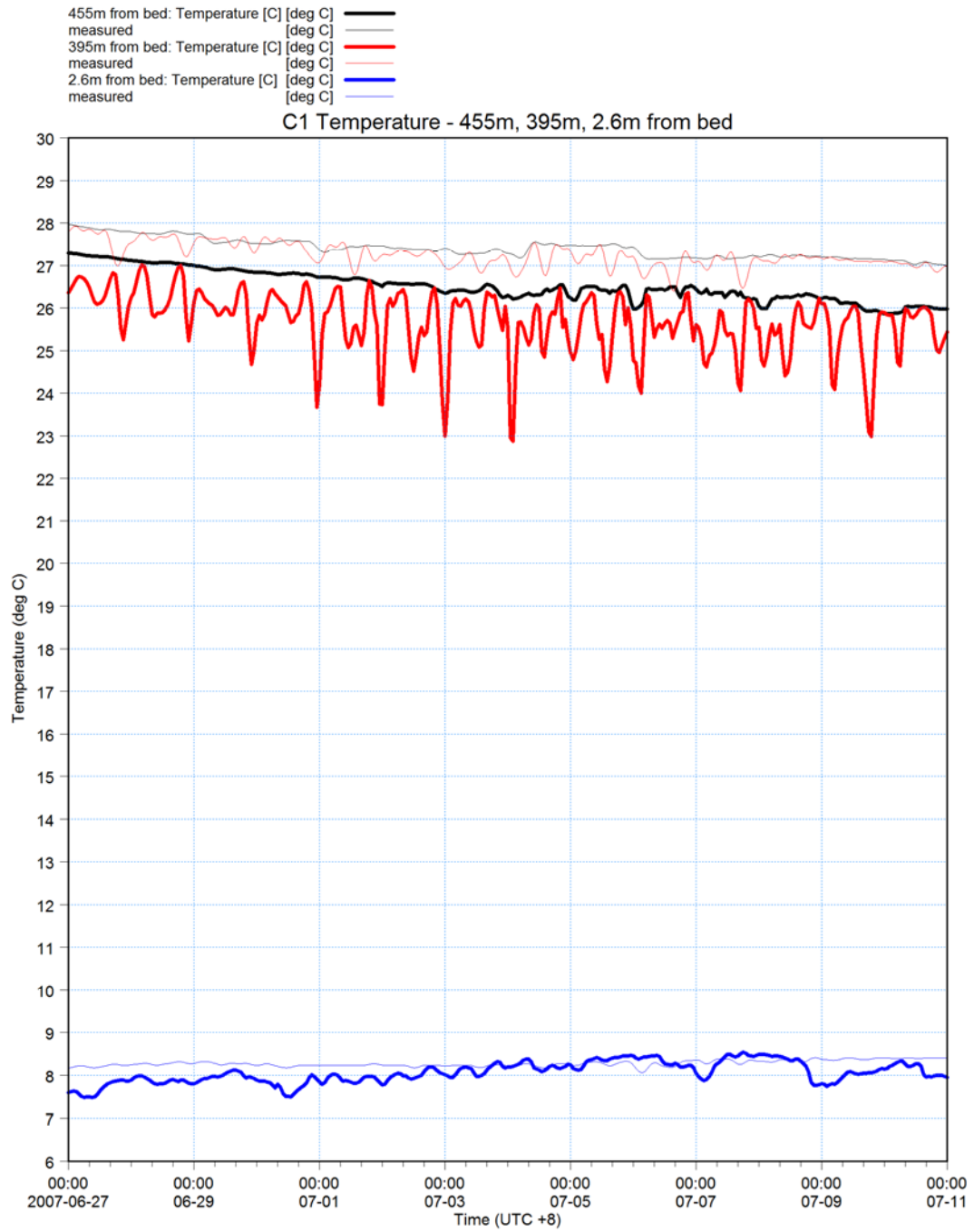


Fig 5.63 Multi-time series plot for C1-1, winter validation period
Thin lines: measured values, thick lines: model results



T at 455m x x
T at 395m x x
T at 2.6m x x

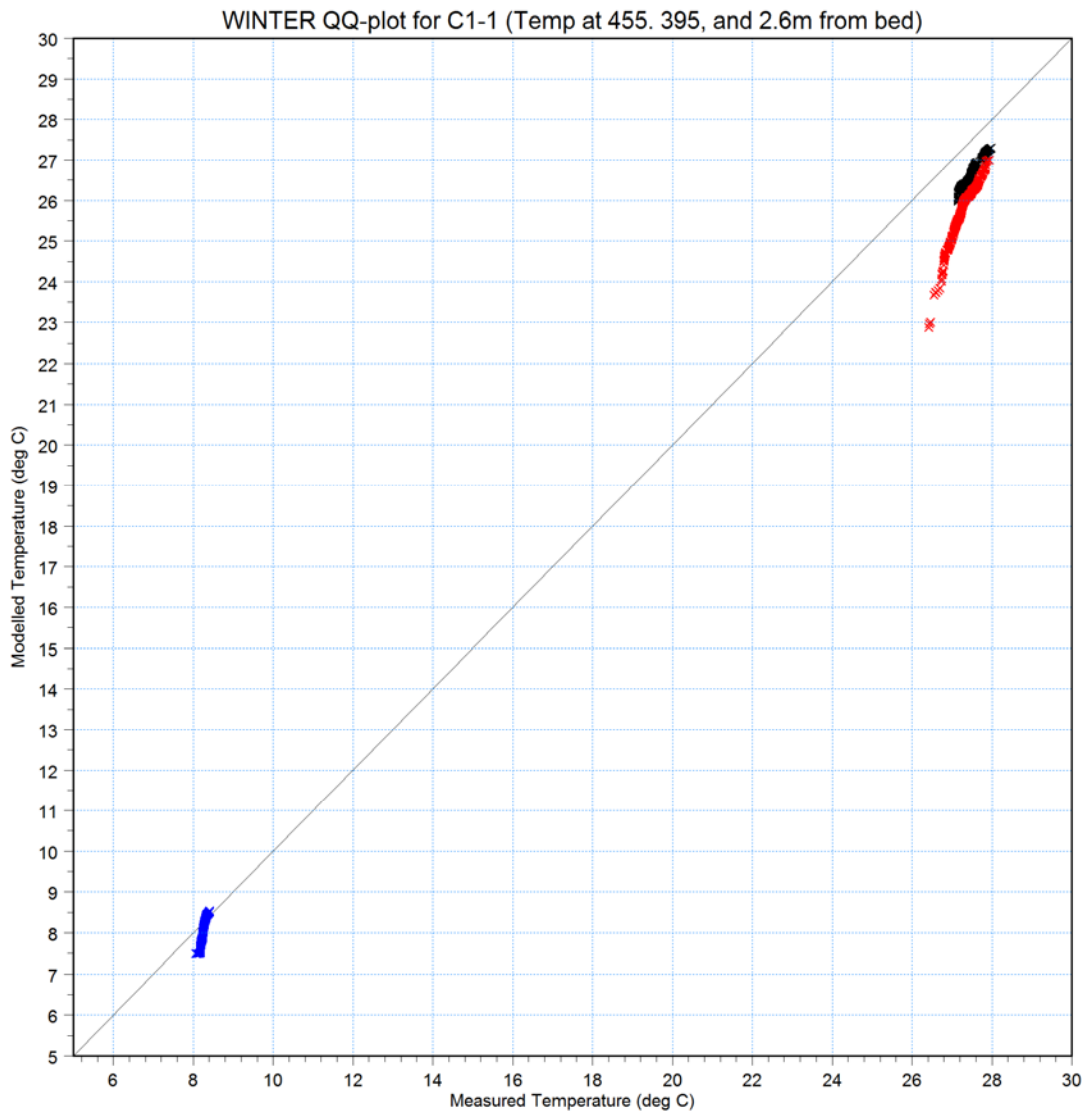


Fig 5.64 Q-Q plot for temperatures for C1-1, winter validation period

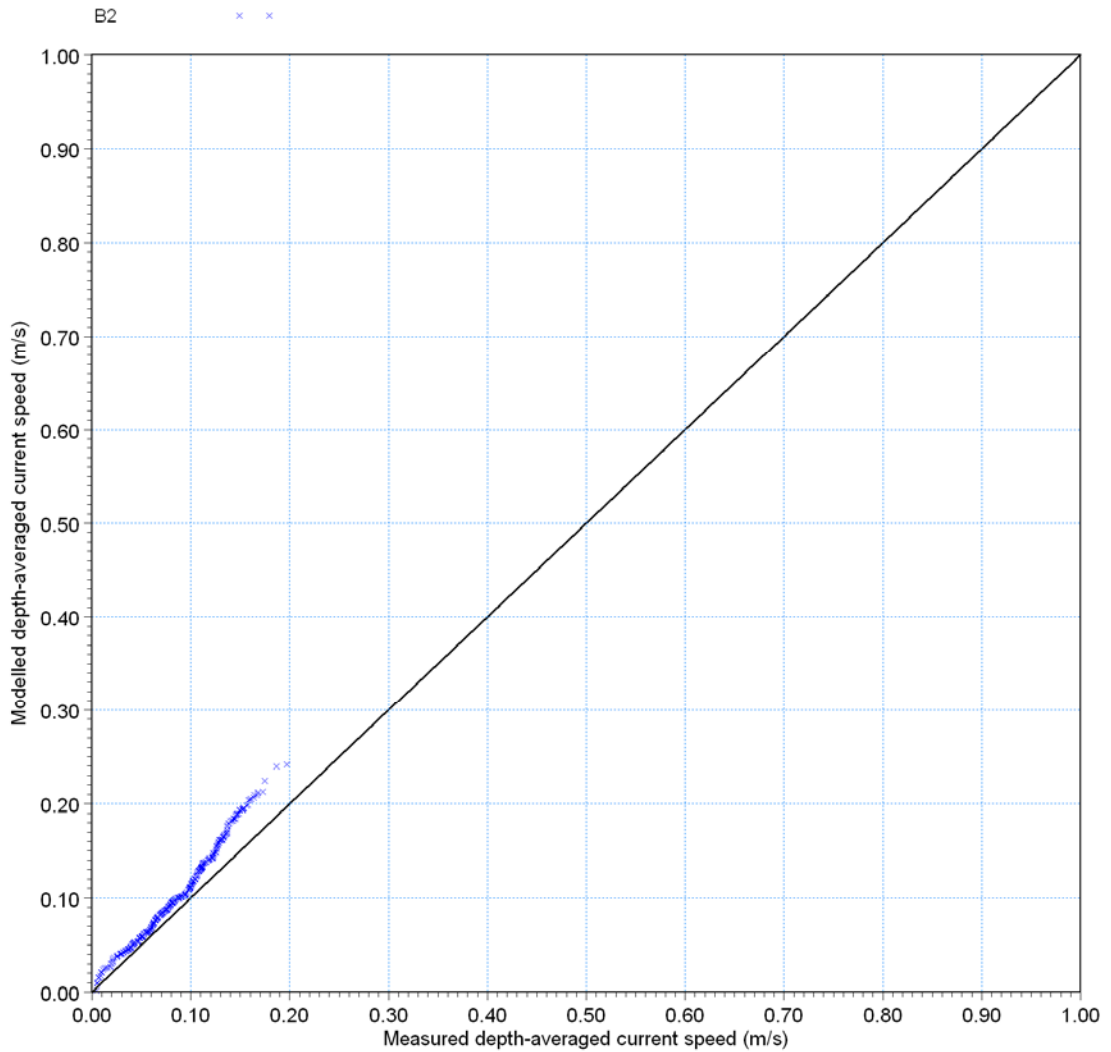


Fig 5.65 Q-Q plot for depth averaged currents for all stations (only B2-1 available), winter validation period

Table 5.5 Statistical analysis of key parameters for winter validation period
 *: Defined as mean of model – mean of measurements results
 **: defined as RMS / peak value * 100

Station	Parameter	Bias* [m/s]	RMS Error [m] or [m/s]	Peak value [m] or [m/s]	RMS Error [%]**
A2-1	Water level (m)	-0.04	0.10	1.66	6
B2-1	Depth averaged current speed (m/s)	0.02	0.04	0.20	18

The RMS error should be less than 15% for water levels, which is easily fulfilled at station A2-1. At station B2-1 the RMS error is also less than the recommended 20% although there might be an issue with the current meter 250m above seabed (see discussion for autumn validation period in section 5.8).



All three stations for which measurements were available for the winter period are discussed below.

Comments to comparisons at A2-1

The comparison of water levels at A2-1 is shown in Fig 5.57 and demonstrates that the model reproduces the tidal water level variations well with an RMS value of 6%.

Comments to comparisons at B2-1

As for the other period the current phases at B2-1 are in good agreement, while the peak current speeds are overestimated by the model often by about 5 cm/s. The general bias is, however, only 2 cm/s (Fig 5.59).

Temperatures (Fig 5.60 Fig 5.62) are impressively well reproduced by the model even in the top layer.

Comments to comparisons at C1-1

For C1-1 the cooling in the top layers in the model is only about 1 degree and not as pronounced as for the autumn period. However, some upwelling is seen in the model results 395m above seabed, while this is not found in the measurements (Fig 5.63 and Fig 5.64).

Conclusion

As for the autumn period measurements were only available from three stations for the winter period. The comparisons between measurements and model at the two stations with currents/temperatures show good agreement as does the comparison of the water levels at A2-1. All in all a good model validation.



5.10 Calibration With Surface Drifter Buoys

5.10.1 General

In order to illustrate the model's capability of simulating surface currents (which are important for many applications like oil spill modelling) a calibration by use of the post processing module for particle tracking and spill analysis, MIKE 3 PA/SA were carried out.

WEL provided a number of ARGOS drifter buoy tracks. The drifter buoy (or drogue) representing the conditions in a depth of 1 m is shown in Fig 5.66.

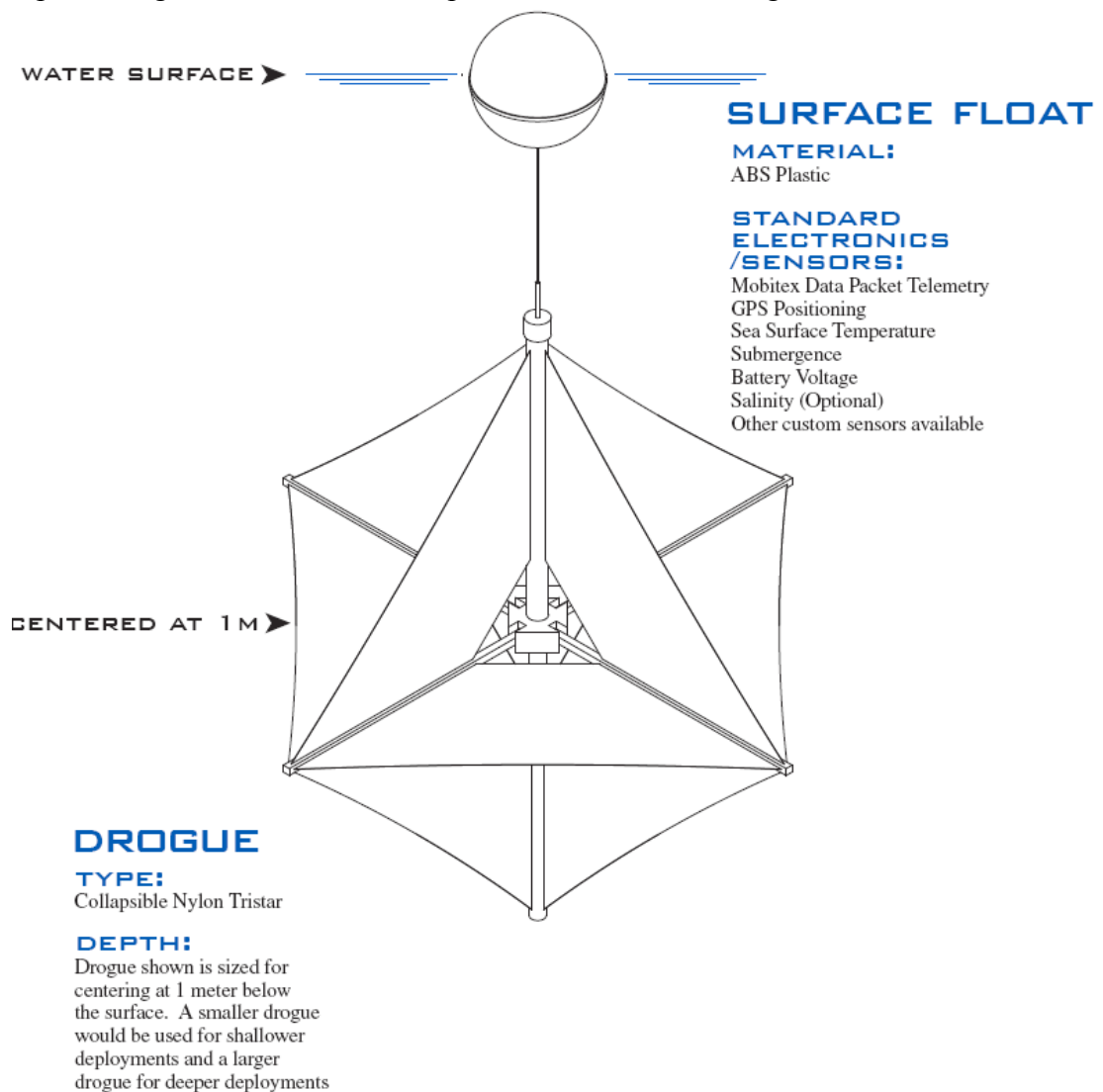


Fig 5.66 Surface drifter buoy (Microstar from Pacific Gyre)

Those tracks falling within the period where temperature data were available from Brecknock (for boundary conditions) are listed in Table 5.6 and shown in Fig 3.2.



Table 5.6 Drifter tracks falling within Brecknock data coverage period

File Name	Period	
	Start	End
argos_DRIFT_223316_mailbox_microstar223316.xlsx	10-02-2007	17-05-2007
argos_DRIFT_223372_mailbox_microstar223372.xlsx	06-04-2007	08-06-2007
argos_DRIFT_227896_mailbox_microstar227896.xlsx	08-04-2007	01-05-2007

For comparison with these tracks a hydrodynamic model simulation covering the period 04-04-2007 to 22-04-2004 (including two days for model warm-up) was carried out. The first track was selected for the model calibration away from Scott Reef while the third one was used for model calibration inside of Scott Reef. The second track was not used in this calibration.

5.10.2 Comparison with Drifter Buoy Tracks within Scott Reef

Drifter buoy no 227896 drifted into Scott Reef on 9/4/2007 and it drifted out again on 10/4/2007. The whole track for the buoy is shown in Fig 5.67 together with a close-up on Scott Reef.

The Lagrangian particle model, MIKE 3 PA, was then applied by releasing a particle on 9/4/2007 00:00 and on 10/4/2007 00:00 in the same location as the drifter buoy. The comparison between the measured and simulated drifter locations is shown in Fig 5.68, Fig 5.69 and Fig 5.70.

The particle model can take into account the wind drift (or acceleration) in the surface layer. As the top-most layer in the MIKE 3 hydrodynamic simulations is 30m thick, this surface wind drift has been included as a calibration factor.

Wind speed and direction were taken from the A3-1 met station.

The results shown in Fig 5.68, Fig 5.69 and Fig 5.70 were obtained using a deflection angle of -20° and a wind friction of 0.03. For details on the MIKE 3 PA model see Ref /7/.

It was concluded that using the calibration factors above a satisfactory comparison was obtained.

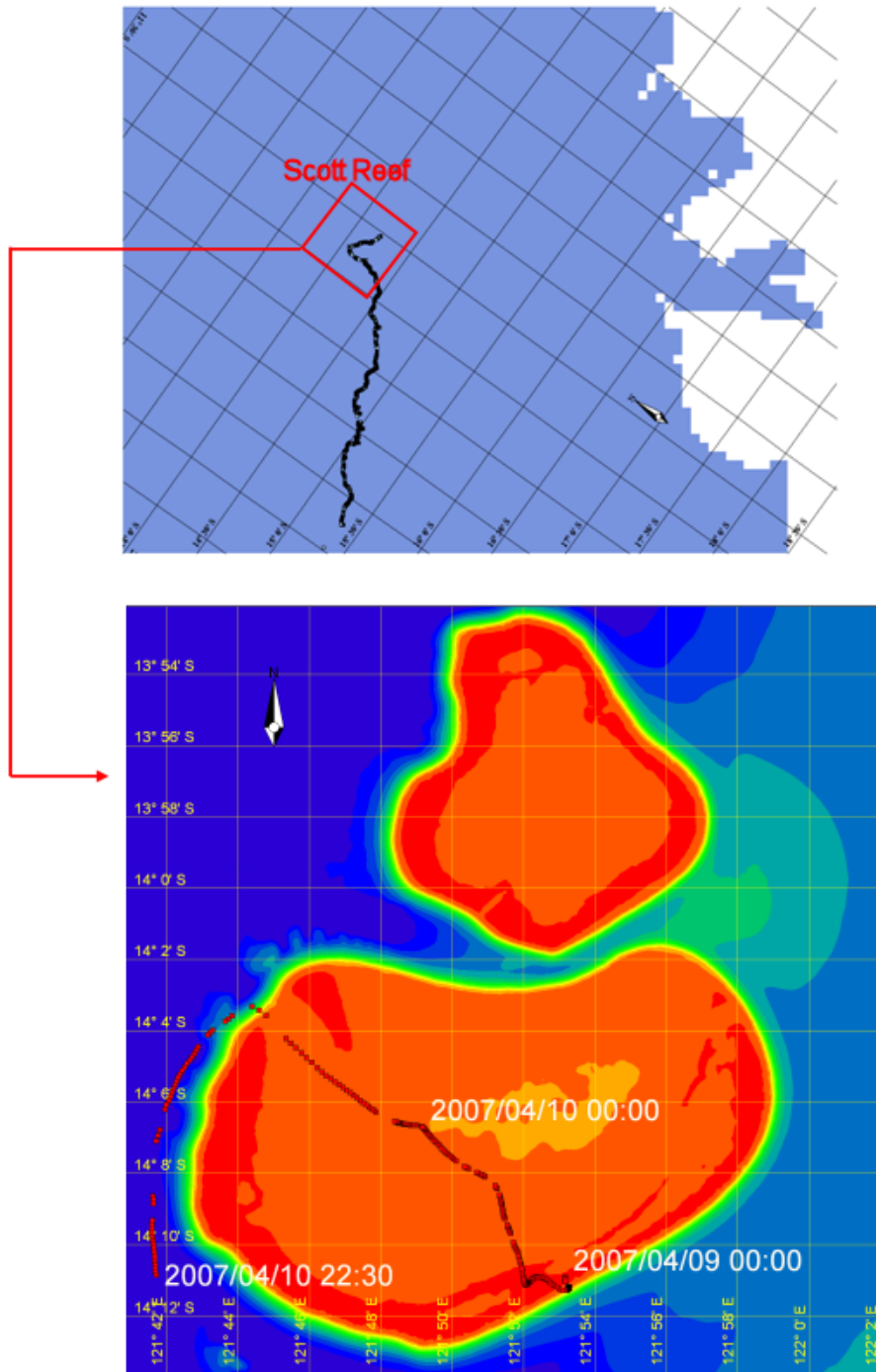


Fig 5.67 Measured track for drifter buoy no 227896

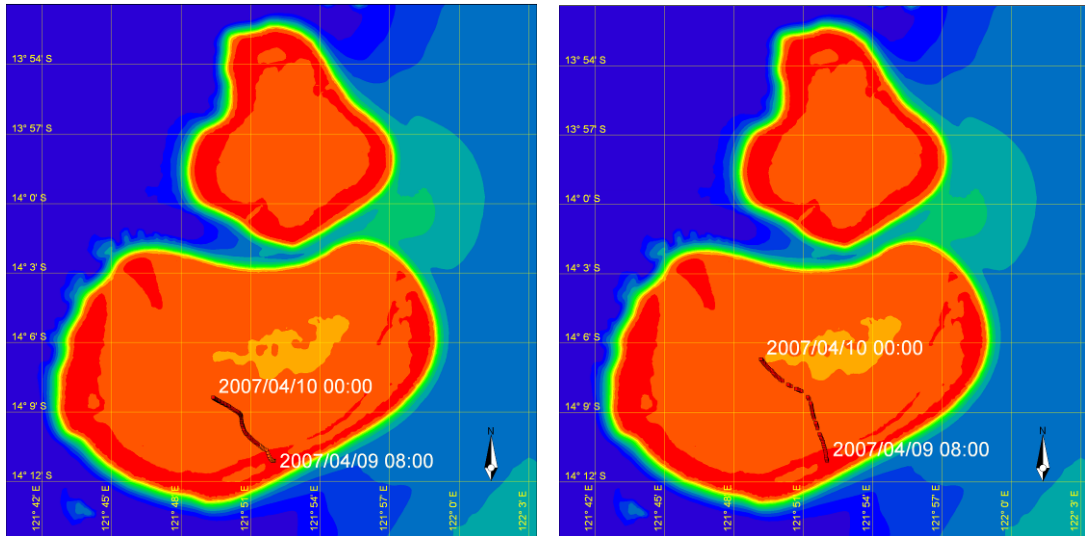


Fig 5.68 Simulated (left) and measured (right) track for drifter buoy no 227896 on 9/4/2007

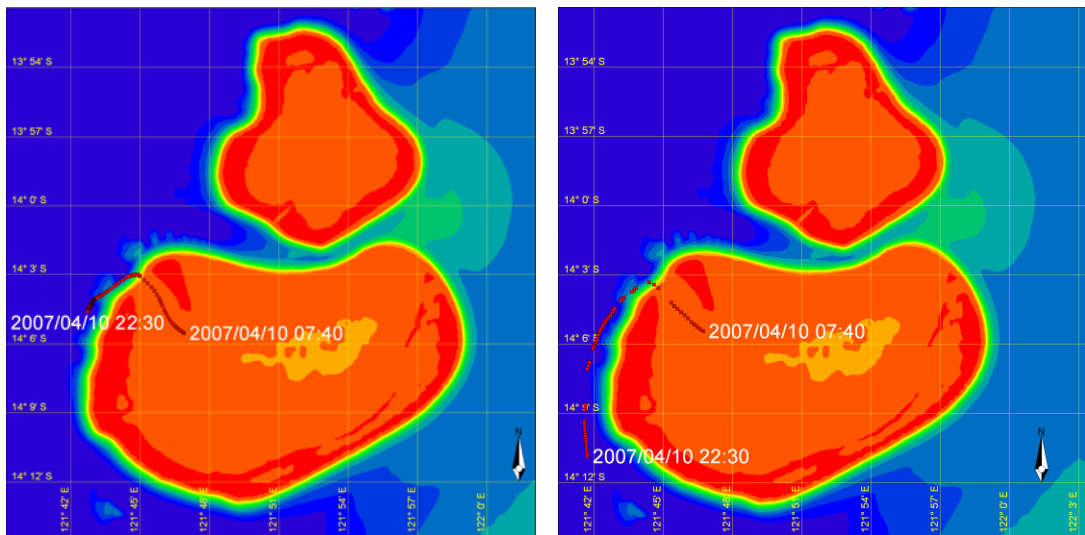


Fig 5.69 Simulated (left) and measured (right) track for drifter buoy no 227896 on 10/4/2007

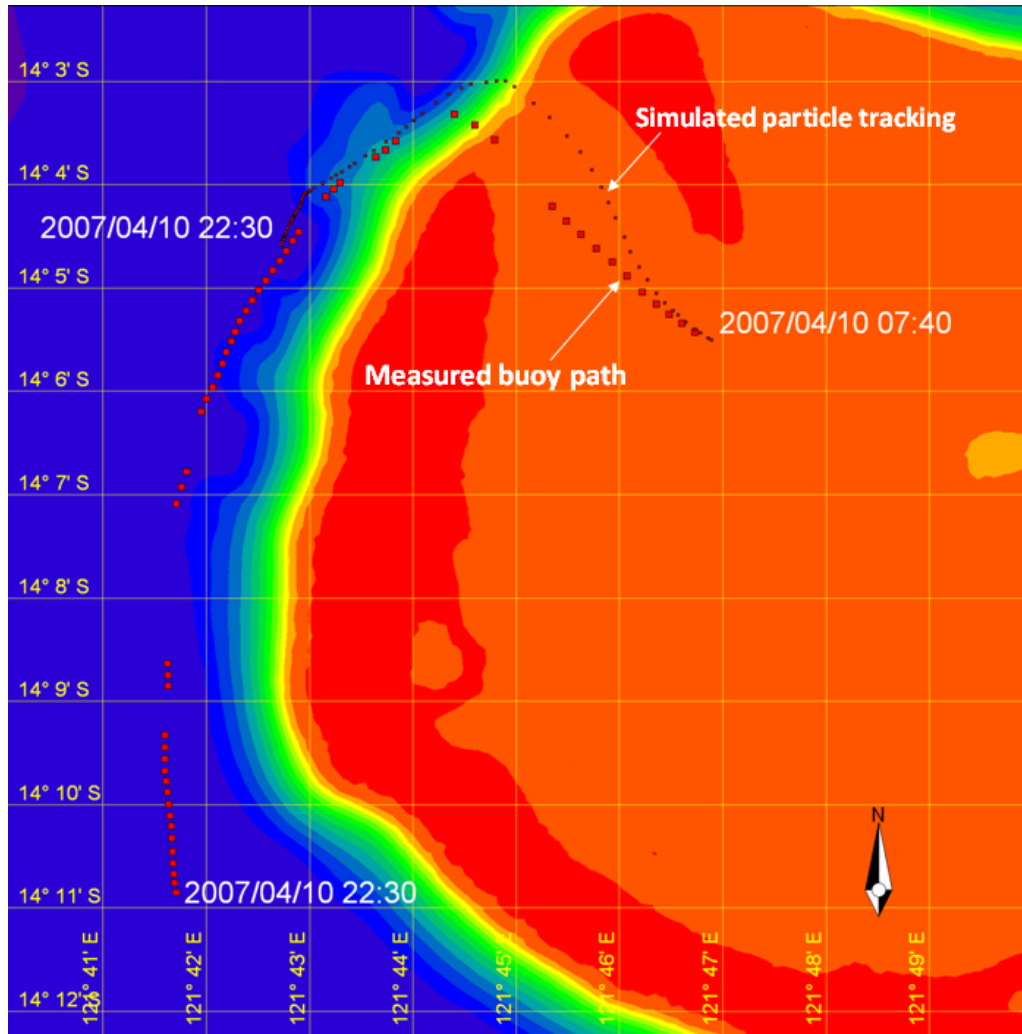


Fig 5.70 Measured and simulated track for drifter buoy no 227896 on 10/4/2007 (zoom)

5.10.3 Comparison with Drifter Buoy Tracks outside of Scott Reef

As an example of the drifter tracks outside Scott Reef drifter no 223316 was chosen and the particle model was applied by releasing a particle on 9/4/2007 00:00 in the same location as the drifter buoy. The total track is shown in Fig 5.71 while the comparison between the measured and simulated drifter locations for the period 9/4/2007 to 16/4/2007 is shown in Fig 5.72.

Again, additional wind drift in the top layer was included.

The results shown in Fig 5.72 were obtained using a deflection angle of -18° and a wind friction of 0.092, and are considered to be satisfactory.

However, while the deflection angle is similar to the one obtained from the calibration within Scott Reef, the wind friction was quite different. This difference is likely to be caused by the large difference in water depths for the two locations.

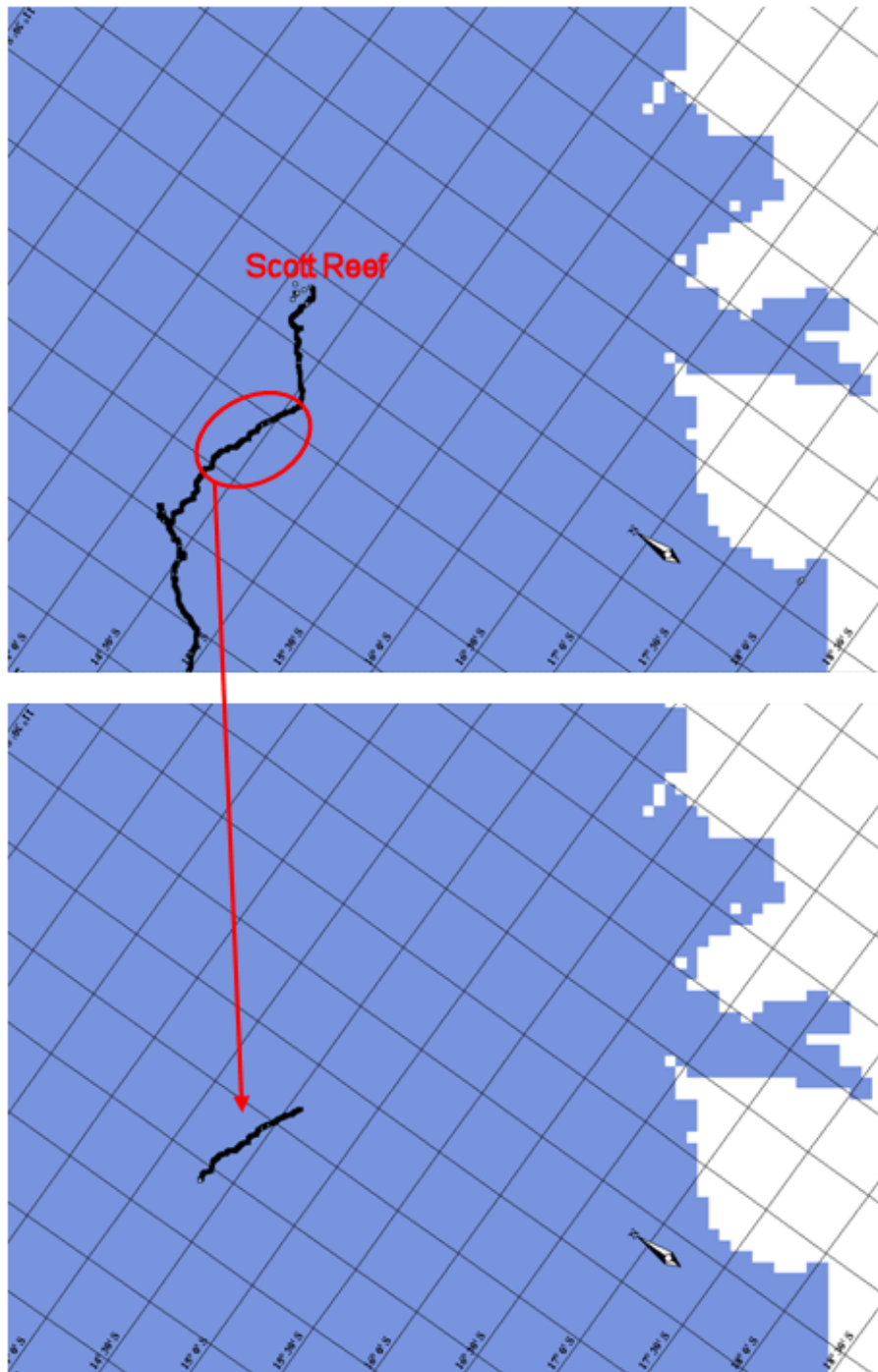


Fig 5.71 Measured track for drifter buoy no 223316

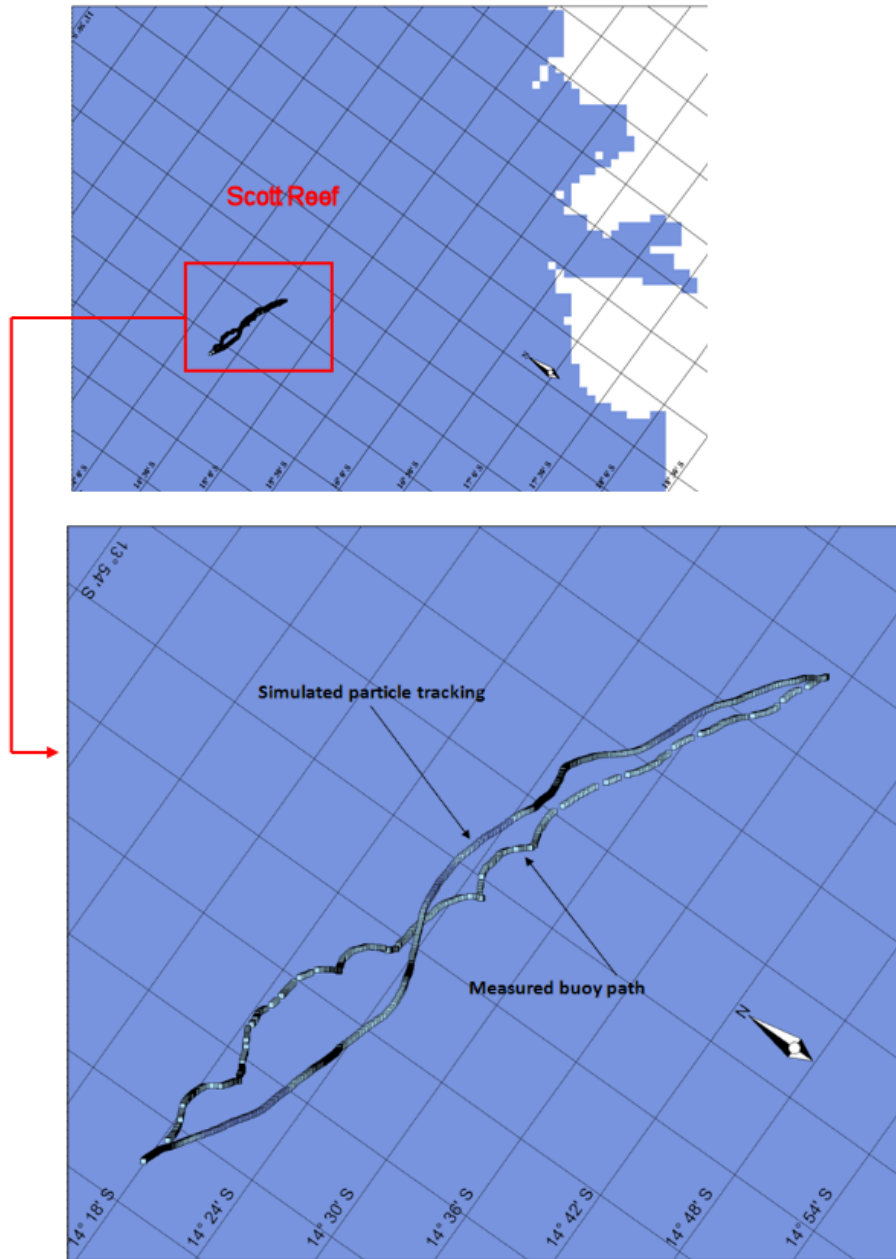


Fig 5.72 Measured and simulated track for drifter buoy no 223316 on 9/4/2007 to 16/4/2007



6 SUMMARY AND CONCLUSIONS

Woodside has commenced its environmental approval process for the upstream component of the Browse LNG Development near Scott Reef 400 km north of Broome, and has identified that physical oceanographic modelling services will be required as part of the impact assessment for the Environmental Impact Statement. Physical oceanographic modelling will also be required during the design process.

The purpose of the present study has been to select, set-up, calibrate and validate a 3-dimensional hydrodynamic/oceanographic model capable of describing the physical oceanography at Scott Reef and surrounds. This model will then subsequently be used as a basis for environmental modelling including dispersion of produced formation water, oil spills, hydrotest water, waste water, cooling water etc.

Before defining the calibration and validation periods, and in preparation for the subsequent environmental modelling, the important meteorological and oceanographic phenomena were identified. The main ones are the wind driven currents and the depth-averaged (barotropic) tide, while internal (baroclinic) tide also has some influence.

Oceanographic currents may have a minor influence (compared to tide and wind), but Scott Reef does not lie directly in the path of the Indonesian Through Flow, which may have influenced the area. The Indonesian Through Flow is located to the north of Scott Reef and does, on the other hand, shed off eddies, which reach Scott Reef and have been identified in measurements at Brecknock. Including these eddies in the model by applying satellite data (surface level anomalies) has been tested but not found feasible because of the satellite data being too scarce. With the eddies only being of having minor influence leaving out the eddies is not believed to be a major shortcoming of the study.

Another oceanographic current, which may have an influence, is the Holloway current. This current has, however, not been identified in the Brecknock measurements like the eddies from the Indonesian Through Flow. The Holloway current is not as well studied and understood as the Indonesian Through Flow, and no efforts have thus been made to include it in the model.

Based on the list of important phenomena, requirements to a measurement programme were identified. While tidal variations can be covered within a relatively short period of time (a number of months), the monsoonal winds with a NW monsoon during the summer and a SE monsoon during the winter, requires 6-12 months of measurements. Thus with 12 months of data seasonal variations are covered. Variations from year to year in the monsoonal wind pattern (like start and end dates) requires long records (say at least 5 years), which will have to be taken into account during the subsequent environmental modelling.



A large oceanographic data collection programme was carried out from September 2006 to September 2007 by Woodside, and a substantial number of current and water temperature measurements were thus available for the model calibration and validation from a number of locations in the study area and from a number of depths at each location.

With the seasonal variations in mind and with a substantial amount of measurements from a 12 months period, four periods were selected for the model calibration and validation, one for each of the two main monsoon seasons (“summer” and “winter”) and one for each of the two transition periods in-between (“spring” and “autumn”). Each period covered a tidal neap-spring-neap cycle, ie 14 days.

DHI’s 3-dimensional modelling system, MIKE 3, is available in a number of versions suitable for different types of model applications. The system is comprised of a number of modules, with the hydrodynamic module forming the basis for the application models. These include advection-dispersion of conservative or linearly decaying substances (AD), a mud transport (MT) module simulating transport along with erosion and deposition of cohesive material, and a ECO Lab module simulating water quality (describing BOD-DO relations, nutrients and coliform bacteria problems), eutrophication (simulating algae growth and primary production) and other ecological processes. A Lagrangian based particle (PA) module is also available for simulating plumes, tracers, sediment transport or the spreading and decay of different pollutants. Finally, a Lagrangian oil spill analysis module (SA) for describing spreading and decaying of oil spill can be invoked.

After substantial testing it was decided to use the finite-difference version of MIKE 3 (MIKE 3 Classic) with constantly spaced z-layers in the vertical and nested rectangular grids in the horizontal dimension. 25 layers with a spacing of 20m was applied in the vertical, while a horizontal resolution ranging from 300m around Scott Reef to 8100m away from the area of interest was applied.

The spring period was used for model calibration with the main calibration factors being: turbulence scheme, compressibility, wind stress, bottom friction and heat exchange factors.

The calibration factors were then applied in the validation simulations for the three remaining periods, summer, autumn and winter.

For each of the four periods comparisons of water levels, currents and seawater temperatures were carried out for up to six stations and for each station up to 18 levels. Comparisons were plotted as time series, isopleths plots, quantile-quantile plots and frequency plots. Additionally, performance characteristics were calculated (as root-mean-square and bias) and compared to hydrodynamic model standards. It should be noted that the performance criteria (taken from Ref /12/) are focussed on marine estuaries. However, as no similar criteria are available for offshore areas and coral islands, the values from marine estuaries have been adopted for this study.



A summary of the model performance at the six stations (one water level station, A2-1, and five stations with current and temperature string) is as follows:

A2-1 water level station located within Scott Reef: In general a very good agreement between modelled and measured water levels was found.

B2-1 current and temperature string located in the Brecknock area: In general the tidal phases are well reproduced while the current magnitude is slightly overestimated. However, the depth-averaged current speed is generally relatively low with a maximum of only 20-23 cm/s during spring tide.

C1-1 current and temperature string located in the Torosa area: For some of the periods the temperature at the top is too low in the model. Otherwise a good comparison is found. As C1-1 only has three current meters no depth-averaged currents have been computed.

G2-1 current and temperature string located in the Shelf area: While the depth-averaged current in general are adequately reproduced by the model (with a bias of only 1 cm/s and an acceptable RMS error of 18%), too much mixing throughout the water column with too much cold water coming to the top is seen. This strong mixing is almost only found in the model around the 200m depth contour, where G2-1 is located. In the measurements a large temperature variation is found just below the surface, but without providing the same strong mixing as seen in the model results. Even with a 10m top layer in the model (in contrast to a thickness of 30m otherwise applied) too strong mixing occurred in the model. However, with the depth-averaged currents being much more important for the subsequent environmental modelling, the comparisons are considered acceptable.

H2-1 current and temperature string located just south of Scott Reef: The phases for the depth-averaged currents are generally in good agreement, while the current magnitude is a bit on the low side, but acceptable. The temperatures in the model exhibit the very large variability seen in the measurements at H2-1, but are not as accurate as at for example B2-1 or I1-1.

I1-1 current and temperature string located in the channel between South and North Reef: The tidal currents are generally well reproduced by the model. The upwelling of cold water during spring tide is also partly reproduced by the model.

Summarising, it is concluded that the model demonstrates a satisfactory reproduction of the complicated hydrodynamic conditions in the area around Scott Reef during the four periods representative for the conditions that occur during a full year.

Additionally, the particle tracking module, MIKE 3 PA, was calibrated against a number of drifter tracks. Such a calibration can prove difficult as small scale variations like small eddies around the edge of Scott Reef can be difficult to simulate



in the model. However, in general a good agreement between simulated and measured tracks was found.

Finally, it should be mentioned that modelling tides and temperature variations and the associated currents around two coral islands situated at the shelf break is a very challenging task. Some of the phenomena occurring in the area, like internal waves, solitons and oceanographic current with associated eddies, are still focus areas for scientific research projects as these phenomena are far from fully described and understood. In the present study a pragmatic approach has been taken: Establish an oceanographic modelling tool that is capable of reproducing water level, current and temperature variations that include the phenomena which are important for the subsequent environmental modelling.



7 REFERENCES

- /1/ Browse LNG Development – Scope of Work for Hydrodynamic Model for Scott Reef and Surrounds by WEL, DRIMS #4338421, WEL Document No JB0006TH0001 Rev 0 dated 5/08/2008.
- /2/ Bird, J. C., Modeling Sub-Reef Thermodynamics to Predict Coral Bleaching: A Case Study at Scott Reef, WA, Master Thesis, James Cook University, 2005.
- /3/ Rayson, M, A Three Dimensional Hydrodynamic Model of Scott Reef, Western Australia, Bachelor of Engineering with Honours Thesis (partial), University of Western Australia, 2006.
- /4/ Andersen, Ole Baltazar, Global ocean tides from ERS 1 and TOPEX/POSEIDON altimetry, Journal. of Geophysical Research, Vol 100, C12, pp. 25249-25260, 1995.
- /5/ DHI, MIKE 3 Flow Model, Hydrodynamic Module, Scientific Documentation, 2008.
- /6/ Browse Development – Tidal Polity for Bathymetric Reduction by WEL, DRIMS #3121580-v2, WEL Document No JB0000RT0001 Rev 0 dated 3/09/2006.
- /7/ DHI, MIKE 21 & MIKE 3 PA/SA, Particle Analysis and Oil Spill Analysis Module, User Guide, 2008.
- /8/ Torosa South-1 Pilot Appraisal Well. EPBC Act Referral Supplementary Documentation, Woodside Energy Ltd, Appendix G.
- /9/ The BLUElink Project, Bureau of Meteorology, www.bom.gov.au/bluelink/
- /10/ Private correspondence with Geoff Wake, Metocean group, Woodside Energy Ltd. 2008
- /11/ NOAA/National Weather Service, National Centers for Environmental Prediction (NCEP), Environmental Modeling Center, Global Forecast System (GFS), www.emc.ncep.noaa.gov/modelinfo/
- /12/ Foundation for Water Research, Publication FR0374 “A Framework for Marine and Estuarine Model Specification in the UK” 1993
- /13/ SatOcean Services technical report, 2008, "Wind Statistics over the Northwest shelf, Offshore Australia" prepared for Woodside Energy Ltd.



- /14/ Duda, D.F. and J.C. Preisig (1999). A modeling study of acoustic propagation through moving shallow-water solitary wave packets. *IEEE J. Oceanic Eng.*, vol. 24, 16-32.
- /15/ Duda, T.F., Lynch, J.F., Irish, J.D., Beardsley, R.C., Ramp, S.R., Chiu,, C.-S., Tang T.Y. and Y.-J. Yang (2004). Internal tide and nonlinear internal wave behavior at the continental slope in the Northern South China Sea. *IEEE J. Oceanic Eng.*, vol. 29, 1105-1130.
- /16/ Kantha, L.H. and Tierney, C.C. (1997). Global baroclinic tides. *Prog. Oceanography*, 40, 163-178.
- /17/ Scotti, A. and J. Pineda (2004). Observations of very large and steep internal waves of elevation near the Massachusetts coast. *Geophys. Res. Let.*, vol. 31, L22307.
- /18/ Vlasenko, V., Stashchuk, N. and Hutter K. (2005). *Baroclinic tides: Theoretical modeling and observational evidence.* Cambridge University Press.
- /19/ Minutes of Meeting, CES/DHI Hydrodynamic Model Meeting, 20/5/09 at WEL, DRIMS-#4621092-v7-Browse_LNG_Development_-_Upstream_Modelling_Meeting_Minutes.DOC

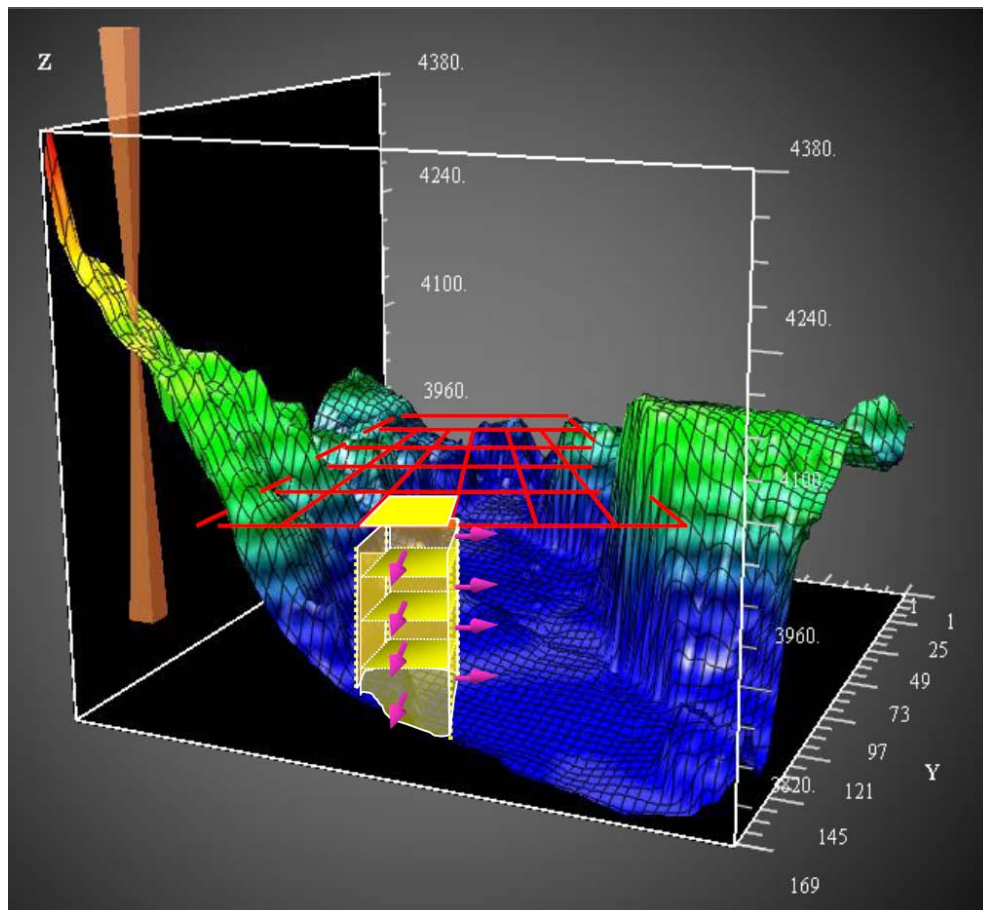


APPENDICES



APPENDIX A

Short Description of MIKE 3 Classic (Finite Difference Version) and Short Description of MIKE 3 FM (Finite Volume Version)



MIKE 3 FLOW MODEL CLASSIC

Short Description

DHI Water & Environment

5 Agern Allé

DK-2970 Hørsholm

Denmark

Tel: +45 45 16 92 00

Fax: +45 45 16 92 92

E-Mail: dhi@dhigroup.com

Web: www.dhigroup.com

INTRODUCTION

MIKE 3 is a generalised mathematical modelling system designed for a wide range of applications in areas such as:

- oceanography
- coastal regions
- estuaries and lakes

The system is fully three-dimensional solving the momentum equation and continuity equations in the three Cartesian directions.

MIKE 3 simulates unsteady flow taking into account density variations, bathymetry and external forcing such as meteorology, tidal elevations, currents and other hydrographic conditions.

MIKE 3 can be applied to:

- oceanographic studies
- coastal circulation studies
- water pollution studies
- environmental impact assessment studies
- heat and salt recirculation studies
- sedimentation studies

MIKE 3 is composed of three fundamental modules: The hydrodynamic (HD) module, the turbulence module and the advection-dispersion (AD) module. Various features such as free surface description, laminar flow description and density variations are optionally invoked within the three fundamental modules.

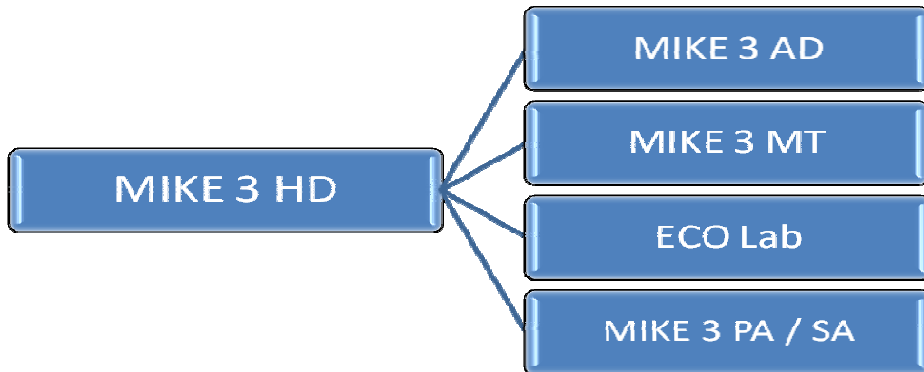
A number of application modules have been implemented and can be invoked optionally. These are advection-dispersion of conservative or linearly decaying substances (AD), a mud transport (MT) module simulating transport along with erosion and deposition of cohesive material, and a ECO Lab module simulating water quality (describing BOD-DO relations, nutrients and hygienic problems), eutrophication (simulating algae growth and primary production) and other ecological processes. A Lagrangian based particle (PA) module can also be invoked for simulating eg tracers, sediment transport or the spreading and decay of E-Coli bacteria. Finally, a Lagrangian oil spill analysis module (SA) for describing spreading and decaying of oil spill can be invoked.

The modelling system is based on the conservation of mass and momentum in three dimensions of a Newtonian fluid. The flow is decomposed into mean quantities and turbulent fluctuations. The closure problem is solved through the Boussinesq eddy viscosity concept relating the Reynold stresses to the mean velocity field. To handle density variations, the equations for conservation of salinity and temperature are included. An equation of state constitutes the relation between the density and the variations in salinity and temperature and – if the MT calculations are invoked – mud concentration.

In the hydrodynamic module, the prognostic variables are the velocity components in the three directions and the fluid pressure. The model equations are discretised in an implicit, finite difference scheme on a staggered grid and solved non-iteratively by use of the alternating directions' implicit technique. A phase and amplification analysis neglecting effects of viscosity, convective terms, rotation, density variations, etc has been performed. Under these circumstances, the finite difference scheme is unconditionally stable.

The transport of scalar quantities, such as salinity and temperature, is solved in the advection-dispersion module using an explicit, finite difference technique based on quadratic upstream interpolation in three dimensions. The finite difference scheme, which is accurate to fourth order, has attractive properties concerning numerical dispersion, stability and mass conservation.

The decomposition of the prognostic variables into a mean quantity and a turbulent fluctuation leads to additional stress terms in the governing equations to account for the non-resolved processes both in time and space. By the adoption of the eddy viscosity concept these effects are expressed through the eddy viscosity, which is optionally determined by one of the following five closure models: a constant eddy viscosity, the Smagorinsky sub-grid (zero-equation) model, the k - (one-equation) model, the standard k - ϵ (two-equation) model and, finally, a combination of the Smagorinsky model for the horizontal direction and a k - ϵ model for the vertical direction. The turbulence models are all solved in an explicit manner except for the one-dimensional (vertical) k - ϵ model, which is solved by an implicit scheme.



Design structure of the three-dimensional modelling system, MIKE 3

GOVERNING EQUATIONS

In a three-dimensional hydrodynamic model for flow of Newtonian fluids, the following elements are required:

- mass conservation
- momentum conservation
- conservation of salinity and temperature
- equation of state relating local density to salinity, temperature and pressure as well as to possible mud concentration

Thus, the governing equations consist of seven (possibly eight) equations with seven (eight) unknowns.

The mathematical foundation is the Reynolds-averaged Navier-Stoke's equations in three dimensions, including the effects of turbulence and variable density, together with the mass conservation equation:

$$\frac{\partial u_i}{\partial t} + \frac{\partial u_i u_j}{\partial x_j} + 2\Omega_{ij} u_j = -\frac{1}{\rho} \frac{\partial P}{\partial x_i} + g_i + \frac{\partial}{\partial x_j} \left(\nu_T \left\{ \frac{\partial u_i}{\partial x_j} + \frac{\partial u_j}{\partial x_i} \right\} - \frac{2}{3} \delta_{ij} k \right)$$

$$\frac{\partial \rho}{\partial t} + \frac{\partial}{\partial x_j} (\rho u_j) = 0$$

where ρ is the local density of the fluid, u_i the velocity in the x_i -direction, Ω_{ij} the Coriolis tensor P the fluid pressure, g_i the gravitational vector, ν_T the turbulent eddy viscosity, δ_{ij} Kronecker's delta, k the turbulent kinetic energy, and t denotes the time.

Coast contours and depth contours are described as accurately as possible with the selected grid size. The transport equations for salt and temperature are used together with an equation of state for the density of the water:

$$\frac{\partial S}{\partial t} + \frac{\partial}{\partial x_j} (u_j S) = \frac{\partial}{\partial x_j} \left(D_s \frac{\partial S}{\partial x_j} \right)$$

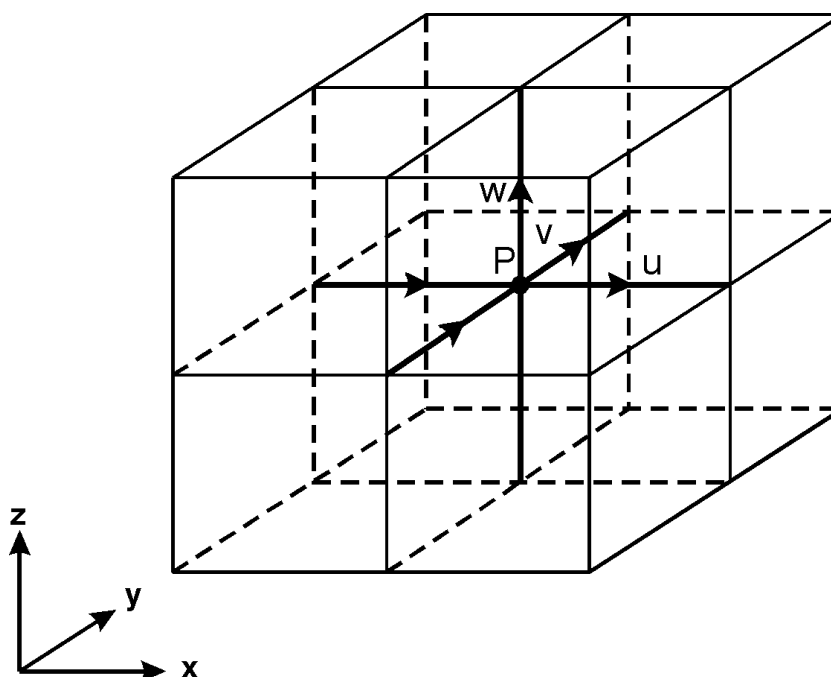
$$\frac{\partial T}{\partial t} + \frac{\partial}{\partial x_j} (u_j T) = \frac{\partial}{\partial x_j} \left(D_T \frac{\partial T}{\partial x_j} \right) + Q_H$$

where S is the salinity, T the temperature and Q_H the heat exchange with the atmosphere. D_s and D_T are the dispersion coefficients for salt and temperature, respectively. There are several types of equations of state for the density of seawater. In MIKE 3, the definition given by UNESCO has been adopted relating local density to salinity, temperature and pressure.

Heat exchange with the atmosphere is implemented with basis in the four physical processes:

- sensible heat flux (convection)
- latent heat flux (vaporisation)
- net short wave radiation
- net long wave radiation

The mass and momentum equations cannot be solved by a computer as they express a continuous change in both time and space. Thus, the equations need to be reformulated in terms of discrete changes in both time and space. A number of techniques for this reformulation are used in computational fluid dynamics of which the finite volume and finite difference are the most popular techniques.



The staggered grid adopted in MIKE 3

Traditionally, the finite difference technique has been used in the field of hydraulics, and almost all models developed at DHI up until 2000 have used this approach..

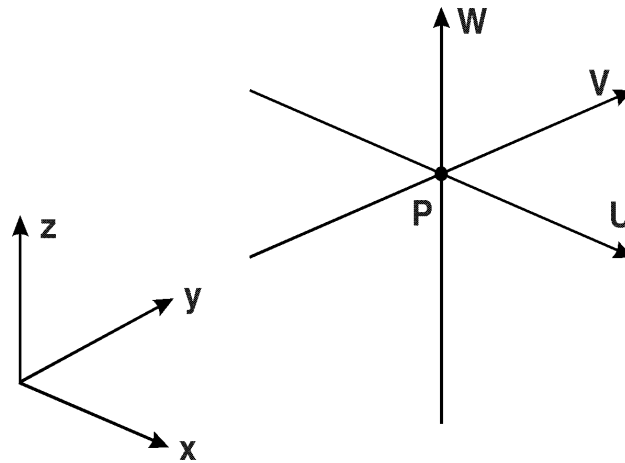
Before discretising the differential equations into a finite difference scheme, a spatial grid is required. The actual grid that has been adopted is the so-called Arakawa C staggered grid, see figure above.

The mesh size (or grid spacing) is defined as the distance between two nodes.

The velocities u , v and w are defined between the nodes, whereas scalar quantities such as the pressure, salinity, temperature, etc are defined in the

nodes. The prognostic variables used in the hydrodynamic part of MIKE 3 are shown in the figure below.

The adopted staggered grid allows for the spatial discretisation of the differential equations. The mass equation is space centred in every node, whereas the momentum equations are space centred in the corresponding velocity 'nodes' to form a huge set of equations. However, the time derivatives imply the definition of certain time levels, also, leading to either explicit or implicit schemes. In general, all prognostic variables in implicit schemes are defined at the same time level and then an iterative technique is applied to inverse the matrix to advance the solution one time step.



Definition of the prognostic variables used in the hydrodynamic part of MIKE 3

This inversion may be performed on the entire matrix in one step, which, due to the size of the matrix, is a costly way. Alternatively, the inversion may be split into three operations according to the three directions. In each operation, only the prognostic variables directly associated with the directions are considered as prognostic, whereas the other direction variables are locked, eg only the pressure and u-velocities during a x-direction operation. This technique is known as the Alternating Directions Implicit (ADI) algorithm.

In almost all of the modelling systems developed at the DHI up until around 2000, the ADI-technique has been adopted to inverse the matrices. Usually, iterative methods are required for the inversion of the matrices due to the non-linear terms in the momentum equations. However, applying two special techniques allows for a non-iterative ADI algorithm to be adopted. The first of these two techniques is called the 'fractioned-step' technique. Basically, the 'fractioned-step' technique is a time staggering of the prognostic variables. This technique has been described in detail by Leendertse (1967).

The second special technique is called 'side-feeding' and is basically a semi-linearisation of the

non-linear terms. Details on this side-feeding technique are given by Abbott (1979).

The primitive equations, as listed above, will mathematically form an ill-posed problem whenever the fluid pressure and the velocities constitute the prognostic variables due to a weak coupling between the pressure and the velocities. *This is the key issue in three-dimensional modelling.* The system is said to be stiff as both slow and fast processes are present, which inherently cause difficulties in the numerical algorithm. In free surface flows, however, only the slow processes are of interest and usually the fast processes (like shock

waves) have no substantial influence on the slow processes (like the free surface waves) suggesting that they may be removed without loss of information. The fast processes are easily eliminated by replacing the time derivative of the density in the mass conservation equation with the pressure term in the equation of state, whereby a compressibility of the fluid is introduced. The fast processes are then subsequently eliminated through an artificial compressibility whereby the system has become hyperbolic dominated. This approach is known as the artificial compressibility approach and was first proposed by Chorin, 1967.

Alternatively, so-called pressure correcting methods can be applied in which the divergence-free continuity equation is enforced through the solution of a Poisson equation for the pressure (cf Ferziger, 1987 and Patankar, 1980).

It is the artificial compressibility method that has been adopted in MIKE 3.

ADVECTION - DISPERSION

MIKE 3 is applicable to flow problems in which density variations and turbulence are important features. The mathematical modelling of such flows requires the solution of partial differential equations of the advective-diffusive type.

The flow modelling will require the solution of the transport equation for:

- Salinity
- Temperature (heat)
- Turbulent kinetic energy (k -equation)
- Dissipation of turbulent kinetic energy (ϵ -equation).

The latter two equations form the well-known k and k - ϵ turbulence models, see Section on Turbulence. For the k -model and the standard k - ϵ model, the non-linear transport equations are solved by explicit UPWIND scheme. The one-dimensional (vertical) k - ϵ model essentially forms two one-dimensional diffusion equations, which are efficiently solved by an implicit scheme.

The partial differential equations describing transport of salinity and temperature as well as transport of concentrations of substances, water

quality and eutrophication components and mud concentration are all linear advective-diffusive type equations, and accordingly the same solution scheme is applied to all these components.

A large number of methodologies for solving the advection-diffusion problem are reported in the literature. However, in order to be consistent with the HD module, a finite difference approach was chosen.

The QUICKEST (Quadratic Upstream Interpolation for Convective Kinematics with Estimated Streaming Terms, Leonard (1979)) is applied. The method is based on a conservative control-volume formulation. Upstream interpolation is used to determine higher order derivatives. This procedure avoids the stability problems of central differencing while remaining free of the inaccuracies of numerical diffusion associated with the usual upstream differencing.

The extension of this scheme to two and three dimensions is given in Justesen et al (1989), Ekebjærg and Justesen (1991) and Vested et al (1992). For use in situations where resolution of steep fronts are important, the scheme has been further improved by implementation of an exponential interpolation at steep fronts, the so-called QUICKEST-SHARP scheme, see also Leonard (1988).

Alternatively, the so-called QUICKEST-ULTIMATE scheme, using operator splitting, may optionally be invoked, see eg Leonard (1991). This scheme is advantageous in cases with more than one advection-diffusion component, since in MIKE 3 it has been implemented such that the CPU time consumption is practically independent of the number of components.

The equation to be solved in the AD model can be written as:

$$\frac{\partial c}{\partial t} + \frac{\partial}{\partial x}(uc) + \frac{\partial}{\partial y}(vc) + \frac{\partial}{\partial z}(wc) = \frac{\partial}{\partial x} \left(D_x \frac{\partial c}{\partial x} \right) + \frac{\partial}{\partial y} \left(D_y \frac{\partial c}{\partial y} \right) + \frac{\partial}{\partial z} \left(D_z \frac{\partial c}{\partial z} \right) + SOURCE / SINK$$

Considering the grid point (x_j, y_k, z_l) , the explicit, finite difference approximation for the equation above is written for the associated control volume

$$\left(x_j - \frac{1}{2} - \Delta x, x_j + \frac{1}{2} - \Delta x ; \right. \\ \left. y_k - \frac{1}{2} - \Delta y, y_k + \frac{1}{2} - \Delta y ; \right. \\ \left. z_l - \frac{1}{2} - \Delta z, z_l + \frac{1}{2} - \Delta z \right).$$

$$c_{j,k,l}^{n+1} = c_{j,k,l}^n - \frac{\Delta t}{\Delta x} \{ T_x(j+1, k, l) - T_x(j-1, k, l) \} \\ - \frac{\Delta t}{\Delta y} \{ T_y(j, k+1, l) - T_y(j, k-1, l) \} \\ - \frac{\Delta t}{\Delta z} \{ T_z(j, k, l+1) - T_z(j, k, l-1) \}$$

It is computationally more convenient and efficient to express the scheme by the use of transports. The transports through the control surface are the velocity perpendicular to the surface multiplied by the surface concentrations. These concentrations are located between nodes and have to be interpolated.

With the QUICKEST-SHARP scheme, eight points are used to calculate the transport through each control surface. With the QUICKEST-ULTIMATE scheme, three points are used corresponding to down-stream, up-stream and very-up-stream positions relative to each control surface. The interpolation weights are determined in such a way that truncation error terms up to third order are cancelled.

TURBULENCE

Today, calculations of mean flow properties of turbulent flows in 2D and 3D can be accomplished with a number of different mathematical models to provide closure, eg the k - ϵ model. Such calculations

are now standard in many industrial applications. Furthermore, in the scientific community, results of laboratory experiments are often compared with results from mathematical models. In such simulations it is usually possible to make a distinction between the 'mean flow' and the superimposed 'turbulent fluctuations' in an unambiguous way.

In geophysical systems, on the other hand, a variety of interacting motions at different time scales exist. The terms' grid scale processes and subgrid scale processes therefore apply to different physical phenomena depending upon the grid on which the system is resolved.

A number of processes are listed according to their time scale in the table below. The spectral window indicates the resolved time scales, whereas the smaller scale processes are given as filtered out processes. It is seen that depending upon which process one wants to resolve, a different, smaller scale process may be the most important to model.

Of course, there is a length scale associated with each of the time scales in the table below. It is observed that a larger time scale will generally correspond to a larger length scale.

The table below makes it apparent that the term turbulence model is inappropriate, because this model has to include the effects of processes that are usually not referred to as turbulence. Such processes include mesialscale and mesoscale processes such as internal waves, tides and surges. Generally, these motions would be placed at the 'mean flow' level, but in reality this will depend on the temporal resolution!

Time Scales in Oceanography. From Nihoul et al (1989)

Time scale	Frequency s ⁻¹	Spectral windows (highlighted processes)	Smaller scale fluctuations (filtered out processes)
1 second	1	Microscale processes 3D "eddy" turbulence (+surface waves)	Molecular diffusion
1 minute	10 ⁻²	Mesialscale processes Internal waves Vertical microstructure "Bliny" inhibited turbulence	Eddy turbulence
1 hour	10 ⁻⁴	Mesoscale processes Inertial oscillations Tides, storm surges	"Bliny turbulence"
1 day	10 ⁻⁵	Diurnal variations	
1 week	10 ⁻⁶	Synoptiscale processes Frontal currents Meanders, "rossby" turbulence	Mesoscale variability
1 month	10 ⁻⁷	Seasonalscale processes	"Rossby turbulence"
1 year	10 ⁻⁸	Globalscale processes Climatic processes (Paleo) climatiscale processes	Seasonal variability

Smagorinsky model

A turbulence closure model must prove its validity through the model calibration and the associated comparisons with measured data. Good turbulence models have extensive universality without being too complex. The most popular model for the subgrid scale eddy viscosity was proposed by Smagorinsky (1963). Here, the eddy viscosity is linked to the filter size (grid spacing) and the large eddy strain rate, ie velocity gradients of the resolved flow field,

$$\nu_T = \ell^2 \sqrt{2 S_{ji} S_{ij}}$$

in which

$$S_{ij} = -\frac{1}{2} \left[\frac{\partial u_i}{\partial x_j} + \frac{\partial u_j}{\partial x_i} \right]$$

is the stress tensor and ℓ is a characteristic length scale.

k model

The first important improvement of the mixing-length theory is to determine the velocity scale from a transport equation rather than from the mean flow field.

It is physically most reasonable to utilise \sqrt{k} as the velocity scale. k is a direct measure of the intensity of the turbulent fluctuations in all three directions (the turbulent kinetic energy). Since this energy is contained in the large-scale eddies, \sqrt{k} becomes a velocity scale for the large-scale motion.

Now, using this velocity scale together with a prescribed length scale ℓ , the eddy viscosity can be expressed as

$$\nu_T = c'_\mu \sqrt{k} \ell$$

This expression is known as the Kolmogorov-Prandtl relation. The distribution of k has to be deduced from the solution of a transport equation

for k . c'_μ is an empirical constant to be determined from experiments.

Turbulence models that consist of the flow equation, the transport equation for k , and a specified length scale are called one-equation models of turbulence and are normally based on the eddy viscosity concept.

The inclusion of the memory effect in the turbulence represents one step forward in comparison with the zero-equation models. However, when the effects of convection and diffusion are important, a transport equation for either the length scale or a related quantity must be added to the turbulence model. This may be relevant in recirculating flows or rapidly changing flows.

Standard k - ε model

The length scale specification inherent in the one-equation model can be replaced by a transport equation for a turbulent quantity

$$z = k^m \ell^n$$

where m and n can be any numbers. Several of these combinations have been proposed and tried so far. Little success has been gained using the length scale itself, see eg Launder and Spalding (1972). Instead, the isotropic energy dissipation rate has been used extensively:

$$\varepsilon = C_D \frac{k^{3/2}}{\ell}$$

A two-equation turbulence model may consist of the flow equation, the transport equation for the turbulent kinetic energy, the transport equation for the dissipation rate, and the Kolmogorov-Prandtl expression

$$v_T = c_\mu \frac{k^2}{\varepsilon}$$

to link the quantities together. Such a model is usually referred to as a k - ε model in the literature.

Within the framework of the eddy viscosity concept it is the most advanced turbulence model that can be

established. In many flows, however, when the individual Reynolds stresses play very important roles, transport equations can be derived that eliminate the need for the eddy viscosity.

Mixed 2D Smagorinsky, 1D k - ε model

Due to the large aspect ratio $\Delta x/\Delta z$ often used in applications of MIKE 3, different formulations are appropriate for the horizontal and the vertical directions. In the mixed Smagorinsky/ k - ε model, the horizontal eddy viscosity is determined as described above for the pure Smagorinsky model. For the vertical direction, the 1D k - ε model described by Burchard and Baumert (1995) is applied. This model uses transport equations for two quantities to describe the turbulent motion: the turbulent kinetic energy, k , and the dissipation rate of turbulent kinetic energy, ε . The Kolmogorov-Prandtl expression

$$v_T = c_\mu \frac{k^2}{\varepsilon}$$

couple the mean flow equations to the state variables of the turbulence model. The basic assumption of the present k - ε model is that vertical motions are mainly turbulent fluctuations and the mean component can be neglected. Due to the coarse horizontal resolutions, it is further assumed that advective processes are insignificant compared to the local balance. The transport equation for k and for ε then reads

$$\frac{\partial k}{\partial t} = \frac{\partial}{\partial z} \left(\frac{v_T}{\sigma_k} \frac{\partial k}{\partial z} \right) + P + G - \varepsilon$$

$$\frac{\partial \varepsilon}{\partial t} = \frac{\partial}{\partial z} \left(\frac{v_T}{\sigma_\varepsilon} \frac{\partial \varepsilon}{\partial z} \right) + c_{1\varepsilon} \frac{\varepsilon}{k} (P + c_{3\varepsilon} G) - c_{2\varepsilon} \frac{\varepsilon^2}{k}$$

where

$$P = v_T \left\{ \left(\frac{\partial u}{\partial z} \right)^2 + \left(\frac{\partial v}{\partial z} \right)^2 \right\}$$

is the production term due to velocity shear, and

$$G = \frac{g}{\rho} \frac{v_T}{\sigma_T} \frac{\partial \rho}{\partial z}$$

is the production term due to buoyancy, u and v are the horizontal velocity components, v_T is the effective eddy viscosity, g the gravity, ρ the density, and σ_T the Prandtl number. c_μ , σ_k , σ_ϵ , $c_{1\epsilon}$, $c_{2\epsilon}$ and $c_{3\epsilon}$ are empirical parameters.

Buoyancy Effects

A very important aspect of turbulence modelling is to incorporate the effects of buoyancy in a correct way. Although turbulence modelling has been a research area for more than 20 years, there is no universal modification for buoyancy, which can be applied to the existing turbulence models in all cases. This is mainly due to the fact that stratified flows in oceanography are often governed by instabilities and countergradient transport phenomena. Usually, turbulence models are based on gradient diffusion/ transport models, which will fail in such cases.

When a density gradient is present in eg the mixing layer in a stratified flow, the diffusion coefficient is damped. This means that entrainment and mixing will be overpredicted if the model does not account for this effect. The simplest way of introducing this is to reduce the eddy viscosity in areas with density gradients. The problem is how to parameterise the dampening.

Various suggestions on how to modify the Smagorinsky formulation of the eddy viscosity have been given. From the research on stratified flows, see eg Pedersen (1980), it has been established that such a dampening must be a function of the Richardson gradient number, Ri given by

$$Ri = -\frac{g}{\rho} \frac{\partial \rho}{\partial z} / \sqrt{\left(\frac{\partial u}{\partial z}\right)^2 + \left(\frac{\partial v}{\partial z}\right)^2}$$

For stable stratification, the Smagorinsky eddy viscosity can optionally be reduced as

$$\frac{v_T}{v_{T0}} = \frac{1}{(1 + \psi Ri)^\alpha}$$

where ψ and α are dimensionless constants. The Smagorinsky formulation of the eddy viscosity and modified to handle buoyancy effect has been implemented in an explicit manner.

In the k - ϵ closure model, the Prandtl number σ_T , which appears in the transport equations for k and ϵ , is modified explicitly by the expression

$$\sigma_T = \left\{ \frac{\left(1 + \frac{10}{3} Ri\right)^3}{1 + 10 Ri} \right\}^{1/2}$$

for stable stratification, while σ_T equals unity for unstable stratification. The eddy viscosity is modified implicitly through the k - ϵ equations and the Kolmogorov-Prandtl expression.

MUD TRANSPORT

Mud is typically defined as a fluid-sediment mixture consisting of saltwater, sands, silts, clays and organic materials. In the environment, a layered mud structure is often observed with a suspension layer near the surface, a fluid mud layer below and finally the settle mud bed, see table below. The fluid mud layer is defined as having a dry density

from 10 g/l to 325 g/l. This division is made due to the following reasons: A) mud with dry densities higher than 10 g/l shows beginning non-Newtonian behaviour, ie changing viscous properties; and B) mud with dry densities higher than 325 g/l will be 'frame-work supported' (an effective stress is present) and shows plastic behaviour

An overview of the division of fluid-sediment mixtures used in this document, see also van Rijn (1993)

Name	Dry density (g/l)	Wet density (g/l)	Consolidation stage	Rheological behaviour
Suspension	0-10	----	----	'Newtonian'
Fluid mud	10-100	----	freshly consolidated (1 day)	dilute fluid mud
	100-250	----	weakly consolidated (1 week)	fluid mud (Bingham)
	250-325	1150-1200	medium consolidated (1 month)	dense fluid mud (Bingham)
Soft settled mud bed	325-400	1200-1250	medium consolidated (1 month)	dense fluid mud (Bingham)
	400-550	1250-1350	highly consolidated (1 year)	fluid-solid
	550-650	1350-1400	stiff mud (10 years)	solid
Hard	>650	>1400	hard mud (100 years)	solid

The mud suspension shows Newtonian behaviour and may be approached by classical fluid mechanics, ie be immediately included in the hydrographic description. The fluid mud layer shows non-Newtonian behaviour and may be approached by fluid mechanics using the relevant rheologic constitutive equation. The (hard) settled mud bed may be approached by continuum mechanics (ie soil mechanics).

The mud transport module is coupled with the hydrodynamic module in MIKE 3. The suspended mud influences the hydrodynamics by changing the density and the kinematic viscosity of the mixture. The density of the mixture is by definition related to the concentration as follows:

$$\rho_m = \rho_{wat} + c \left(\frac{\rho_{sed} - \rho_{wat}}{\rho_{sed}} \right)$$

where ρ_m [g/l] is the density of the mixture, ρ_{wat} [~1000 g/l] is the density of the water, c [g/l] is the sediment concentration, and ρ_{sed} [~2600 g/l] is the density of the sediment. By altering the density due to suspended material damping of turbulence at lutoclines is automatically taken care of in the hydrodynamic modelling by a Richardson damping technique. The kinematic viscosity can be approximated by:

$$\frac{\nu_m}{\nu} \approx 100^{\frac{c}{600 \text{ g/l}}}$$

where ν_m [m²/s] is the kinematic viscosity of the mixture, and ν [m²/s] is the kinematic viscosity of the water.

The basis for the mud transport module is the mass conservation equation for mud, which is given by:

$$\frac{\partial c}{\partial t} + \frac{\partial}{\partial x_j} (c(u_j - w_{s,j})) = \frac{\partial}{\partial x_j} \left(D_c \frac{\partial c}{\partial x_j} \right) + S_c$$

where $w_{s,j} = (0, 0, w_s)$ [mm/s] is the settling velocity vector, D_c is the dispersion of cohesive sediment, and S_c is a local source (NOT erosion or deposition). The mass conservation equation resembles the conservation equation for temperature and salinity - the only difference is the inclusion of the settling velocity. The major problem in mud transport modelling is the description of the boundary condition at the bed and the description of the settling velocity. The solutions used in the MIKE 3 MT module are outlined in the following.

The settling velocity (w_s) used is related to concentration (hindered settling is taken into account) and to dissipation (the floc sizes depend on the dissipation) as follows:

$$w_s = w_{s0} \left(\frac{c}{c_{s0}} \right) \left(1 - \frac{c}{\frac{5+2n}{n} c_{s0MAX}} \right)^{5+n} \left(1 - \sqrt{\frac{\epsilon}{\epsilon_0}} \right)$$

where w_{s0} (~1 mm/s) is a reference settling velocity, c_{s0} (~1 g/l) is a reference sediment concentration, n (~1) is a dimensionless suspended material parameter, c_{s0MAX} (~7 g/l) is the concentration at maximum settling velocity, ϵ [m^2/s^3] is the dissipation, and ϵ_0 [m^2/s^3] is the 'floc destruction dissipation', ie the dissipation at which the flocs are destroyed. The present formulation relating the settling velocity to the dissipation is used in the entire water column.

The dissipation is taken into account throughout the water column, but only nearest to the bed is the dissipation from short period surface waves also taken into account.

The boundary condition used at the surface is that there is no mud material transport through the surface. The boundary condition at the bed is one of the major problems in mud transport modelling. At the bed we can have either erosion from the bed or deposition to the bed. If erosion (E [$g/m^2/s$]) takes place it is determined by:

$$E = e_0 \sqrt{\rho_b \tau_{ce}} \frac{\tau_b - \tau_{ce}}{\tau_{ce}}, \text{ when } \tau_{bmax} > \tau_{ce}$$

where e_0 (~ $5 \cdot 10^{-5}$) is a dimensionless bed material parameter, ρ_b [kg/m^3] is the dry density of the bed surface, τ_{ce} [N/m^2] is the critical shear stress for erosion, and τ_b [N/m^2] is the bed shear stress (index max gives that it is the maximum during a short period surface wave cycle).

If deposition (D [$g/m^2/s$]) of weak and/or strong flocs takes place on the mud bed it is determined by (ignoring possible dispersion of flocs):

$$D = c_b w_s \quad \text{when } \tau_{bmax} < \tau_{ce}$$

where c_b [g/l] is the concentration close to the bed and is thus determined from the solution of the mass conservation equation for the cohesive sediment.

The bed is described by multiple layers, where depositing material always enters the first layer.

In MIKE 3 HD, the influence of short surface waves is not considered directly (indirectly through calibrating the bed friction parameter). The short waves are, however, very important when describing the mud transport: time varying shear stress and liquefaction. Typically, the wave period and the wave height are possible to get, whereby the wave length and other information can be determined on the basis of the classical wave theory. Such parameters can be entered into the MT module, which then is able to take surface waves into account.

PARTICLE AND SPILL ANALYSIS

The Particle Analysis module (PA) and the Spill Analysis module (SA) are both Lagrangian particle models, where particles are followed instead of solving the Eulerian equations. This approach is generally very CPU time efficient.

The particles move due to the advective current and due to turbulent fluctuations. The advective velocities are obtained from the hydrodynamic simulation, whereas the turbulent contributions are controlled by the dispersion coefficients.

The particles are released from a source. The position and strength can vary with time. Up to 64 sources with different particle properties can be specified.

The structure of the particle cloud is described by

PA
Settling velocity, either constant or specified as a distribution of velocities or grain sizes

SA
The ratio between eight oil fractions characterized by density, vapour pressure, pour point etc.

The mass (PA) or volume (SA) of the particle cloud can change due to

PA
sedimentation / resuspension. Also non-buoyant conservative particles can be simulated

SA
weathering of the oil: emulsification (water uptake), evaporation, entrainment into the water column and dissolution

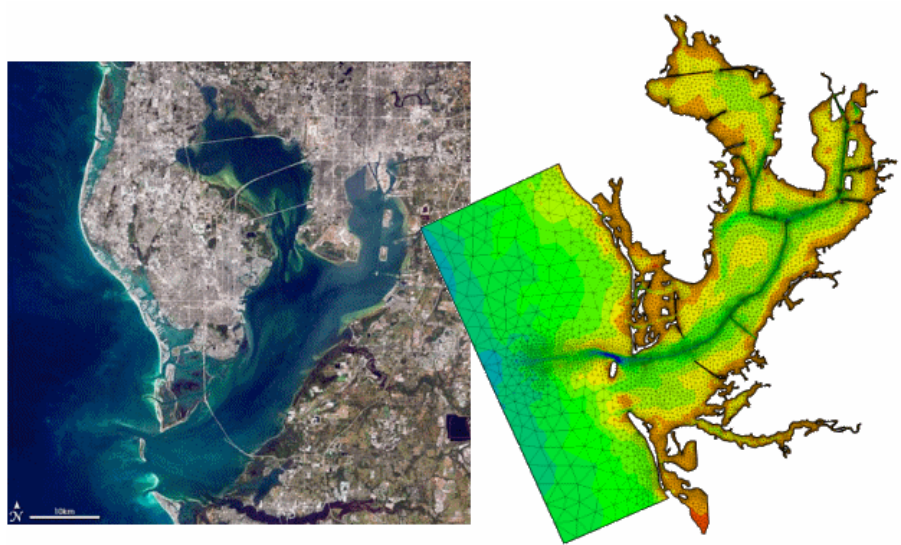
The output can be specified as instantaneous or averaged values. Among other items are

PA
<ul style="list-style-type: none"> • depth averaged concentration of mass in suspension (kg/m^3) • sedimentation/ resuspension (kg/m^2) • exceedance frequency (s^{-1})

SA
<ul style="list-style-type: none"> • oil slick thickness (mm) • thickness of each fraction (mm) • weatherings • exceedance frequency (s^{-1})

REFERENCES

- Abbott, M.B. (1979): "*Computational Hydraulics. Elements of the Theory of Free Surface Flows*", Pitman Publishing Ltd., London.
- Burchard, H. and H. Baumert (1995): "*On the performance of a mixed-layer model based on the $k-\epsilon$ turbulence closure*", J. Geophysical Research, Vol. 100, No. C5.
- Chorin, A.J. (1967): "*A Numerical Method for Solving Incompressible Viscous Flow Problems*", J. Comp. Physics, 2, 12-26.
- Ekebjærg, L.C. and Justesen, P. (1989): "*An explicit scheme for Advection-Diffusion Modelling in Two Dimensions*", Comput. Methods Appl. Mech. Engrg. 1991, 88, 287-297.
- Ferziger, J.H. (1987): "*Simulation of Incompressible Turbulent Flows*", J. Comp. Physics, 69, 1-48.
- Justesen, P., Olesen, K.W. and Vested, H.J. (1989): "*High-Accuracy Modelling of Advection in Two- and Three-Dimensions*", Proc. IAHR Congress, Ottawa, Canada.
- Lauder, B.E. and Spalding, D.B. (1972): "*Mathematical Models of Turbulence*", Academic Press, New York.
- Leendertse, J.J. (1967): "*Aspects of a Computational Model for Long Water Wave Propagation*", Rand Memorandum, RH-5299-PR, Santa Monica, California.
- Leonard, B.P. (1979): "*A Stable and Accurate Convective Modelling Procedure Based on Quadratic Upstream Interpolation*", Computational Methods on Applied Mechanics and Engineering, Vol. 19, pp. 59-98.
- Leonard, B.P. (1988): "*Simple high-accuracy resolution program for convective modelling of discontinuities*" Internat. J. Numer. Methods Fluids, 8, pp- 1291-1318.
- Leonard, B.P. (1991): "*The ULTIMATE conservative difference scheme applied to unsteady one-dimensional advection*", Computational Methods on Applied Mechanics and Engineering, Vol. 88, pp. 17-74.
- Nihoul, J.C.J, Deleersnijder, E. and Djenidi, S. (1989): "*Modelling the General Circulation of Shelf Seas by 3D $k-M$ Models*", Earth Science Reviews, Vol. 26, No. 3, p. 163.
- Patankar, S.V. (1980): "*Numerical Heat Transfer and Fluid Flow*", McGraw-Hill, New York.
- Pedersen, F.B. (1980): "*A Monograph on Turbulent Entrainment and Friction in Two Layer Stratified Flow*", Series Paper 25, Inst. of Hydrodynamics and Hydraulic Engineering, Technical University of Denmark.
- Smagorinsky, J. (1963): "*General Circulation Experiments with the Primitive Equations, 1, The Basic Experiment*", Mon. Weather Rev., Vol. 91, pp. 90-164.
- van Rijn, L. C. (1993): "*Principles of Sediment Transport in Rivers, Estuaries and Coastal Sea*." Aqua Publication.
- Vested, H.J., Justesen, P. and Ekebjærg, L.C. (1992): "*Advection-dispersion modelling in three dimensions*", Appl. Math. Modelling, Vol. 16, October 1992.



MIKE 21 & MIKE 3 FLOW MODEL FM

Hydrodynamic Module

Short Description



Agern Allé 5 Tel: +45 4516 9200
DK-2970 Hørsholm Support: +45 4516 9333
Denmark Fax: +45 4516 9292

E-mail: software@dhigroup.com
Web: www.dhigroup.com

WATER • ENVIRONMENT • HEALTH

MIKE213_FM_Short_Description_HD_.doc/HKH/BHM/AJS/2007Short_Descriptions.lsm/2007-11-19



MIKE 21 & MIKE 3 Flow Model FM

The Flow Model FM is a new comprehensive modelling system for two- and three-dimensional water modelling developed by DHI Water & Environment. The new 2D and 3D models carry the same names as the classic DHI model versions MIKE 21 & MIKE 3 with an 'FM' added that refers to the type of model grid - Flexible Mesh.

The modelling system has been developed for complex applications within oceanographic, coastal and estuarine environments. However, being a general modelling system for 2D and 3D free-surface flows it may also be applied for studies of inland surface waters, e.g. overland flooding and lakes or reservoirs.



MIKE 21 & MIKE 3 Flow Model FM is a new general hydrodynamic flow modelling system based on a finite volume method on an unstructured mesh

DHI's new Flexible Mesh (FM) series includes the following:

Flow Model FM modules:

- Hydrodynamic Module, HD
- Transport Module, TR
- Ecology and water quality Module, ECO Lab
- Sand Transport Module, ST
- Mud Transport Module, MT

Wave module:

- Spectral Wave Module, SW

The FM Series meets the increasing demand for realistic representations of nature, both with regard to 'look alike' and to its capability to model coupled processes, e.g. coupling between currents,

waves and sediments. Coupling of modules is managed in the Coupled Model FM.

All modules are supported by new advanced user interfaces including efficient and sophisticated tools for mesh generation, data management, 2D/3D visualization, etc. In combination with comprehensive documentation and support, the new FM series forms a unique professional software tool for consultancy services related to design, operation and maintenance tasks within the marine environment.

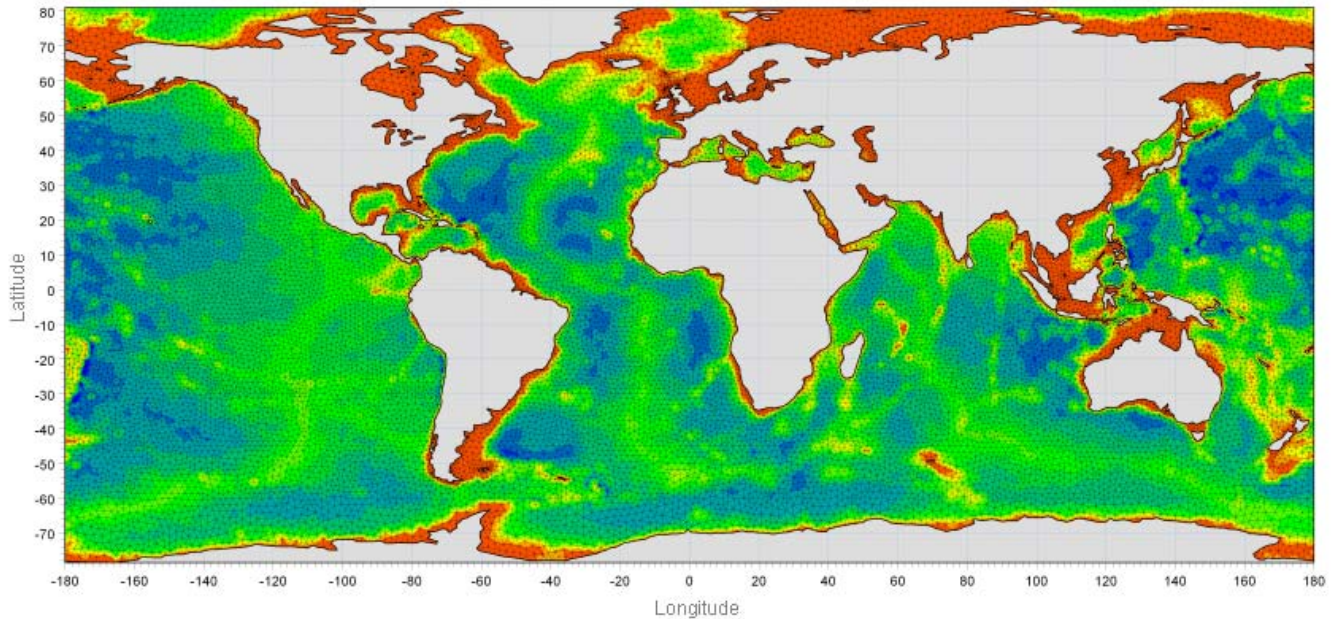
An unstructured grid provides an optimal degree of flexibility in the representation of complex geometries and enables smooth representations of boundaries. Small elements may be used in areas where more detail is desired, and larger elements used where less detail is needed, optimising information for a given amount of computational time.

The spatial discretisation of the governing equations is performed using a cell-centred finite volume method. In the horizontal plane an unstructured grid is used while a structured mesh is used in the vertical domain (3D).

This document provides a short description of the Hydrodynamic Module included in MIKE 21 & MIKE 3 Flow Model FM.



Example of computational mesh for Tamar Estuary, UK



MIKE 21 & MIKE 3 FLOW MODEL FM supports both Cartesian and spherical coordinates. Spherical coordinates are usually applied for regional and global sea circulation applications. The chart shows the computational mesh and bathymetry for the planet Earth generated by the MIKE Zero Mesh Generator

MIKE 21 & MIKE 3 Flow Model FM - Hydrodynamic Module

The Hydrodynamic Module provides the basis for computations performed in many other modules, but can also be used alone. It simulates the water level variations and flows in response to a variety of forcing functions on flood plains, in lakes, estuaries and coastal areas.

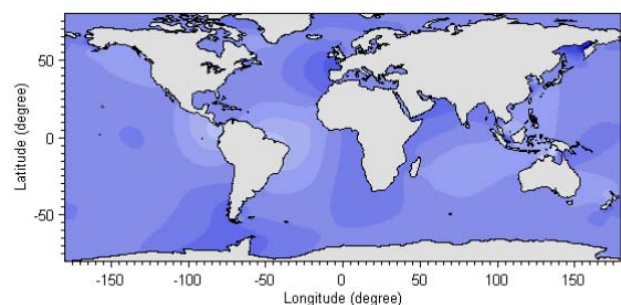
Application Areas

The Hydrodynamic Module included in MIKE 21 & MIKE 3 Flow Model FM simulates unsteady flow taking into account density variations, bathymetry and external forcings.

The choice between 2D and 3D model depends on a number of factors. For example, in shallow waters, wind and tidal current are often sufficient to keep the water column well-mixed, i.e. homogeneous in salinity and temperature. In such cases a 2D model can be used. In water bodies with stratification, either by density or by species (ecology), a 3D model should be used. This is also the case for enclosed or semi-enclosed waters where wind-driven circulation occurs.

Typical application areas are

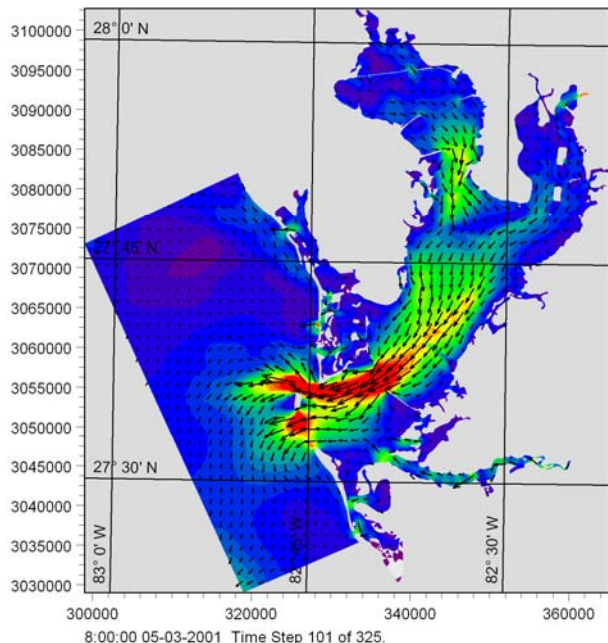
- Assessment of hydrographic conditions for design, construction and operation of structures and plants in stratified and non-stratified waters
- Environmental impact assessment studies
- Coastal and oceanographic circulation studies
- Optimization of port and coastal protection infrastructures
- Lake and reservoir hydrodynamics
- Cooling water, recirculation and desalination
- Coastal flooding and storm surge
- Inland flooding and overland flow modelling
- Forecast and warning systems



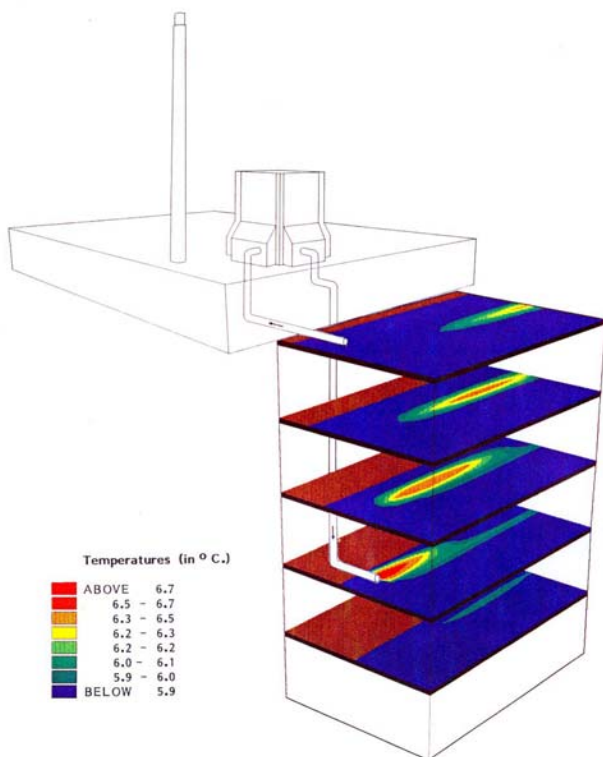
Example of a global tide application of MIKE 21 Flow Model FM. Results from such a model can be used as boundary conditions for regional scale forecast or hindcast models



The MIKE 21 & MIKE 3 Flow Model FM also support spherical coordinates, which makes both models particularly applicable for global and regional sea scale applications.



Example of a flow field in Tampa Bay, FL, simulated by MIKE 21 Flow Model FM

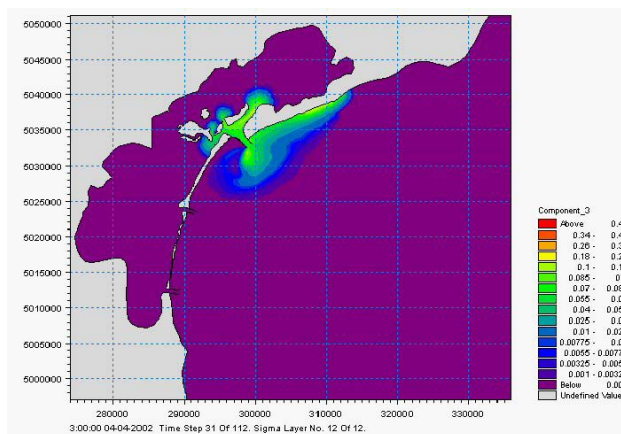


Study of thermal recirculation



Typical applications with the MIKE 21 & MIKE 3 Flow Model FM include cooling water recirculation and ecological impact assessment (eutrophication)

The Hydrodynamic Module is together with the Transport Module (TR) used to simulate the spreading and fate of dissolved and suspended substances. This module combination is applied in tracer simulations, flushing and simple water quality studies.



Tracer simulation of single component from outlet in the Adriatic, simulated by MIKE 21 Flow Model FM HD+TR

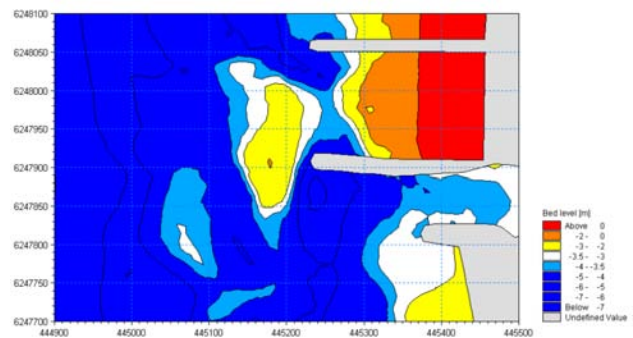


Prediction of ecosystem behaviour using the MIKE 21 & MIKE 3 Flow Model FM together with ECO Lab

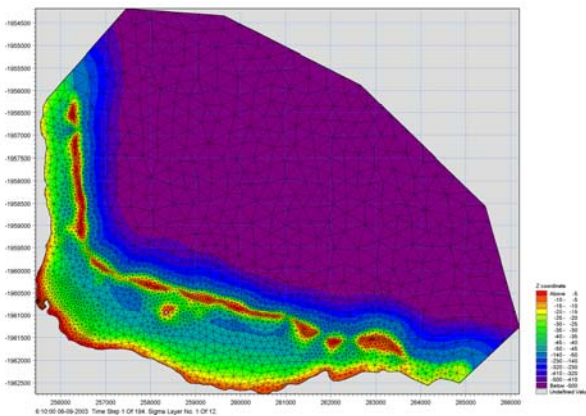
The Hydrodynamic Module can be coupled to the Ecological Module (ECO Lab) to form the basis for environmental water quality studies comprising multiple components.

Furthermore, the Hydrodynamic Module can be coupled to sediment models for the calculation of sediment transport. The Sand Transport Module and Mud Transport Module can be applied to simulate transport of non-cohesive and cohesive sediments, respectively.

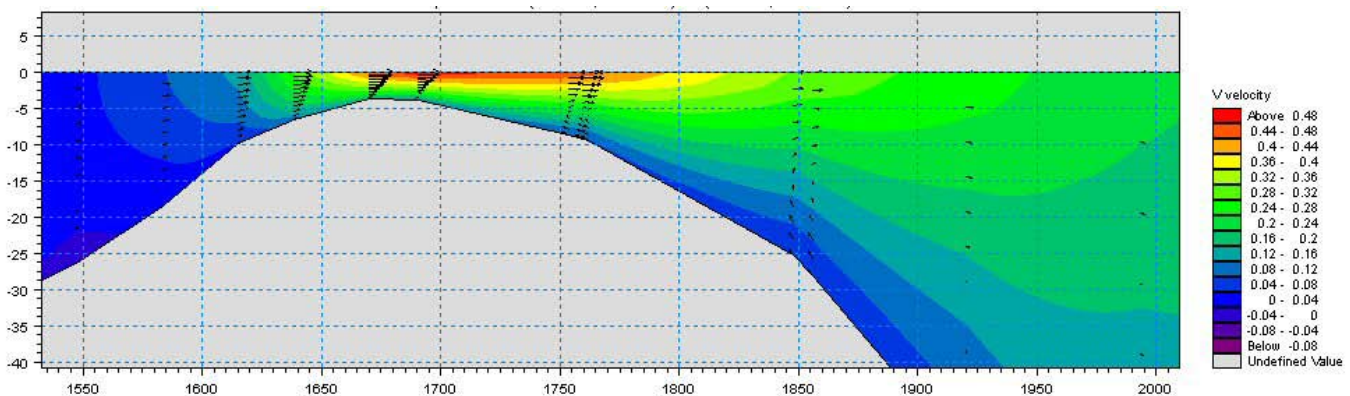
In the coastal zone the transport is mainly determined by wave conditions and associated wave-induced currents. The wave-induced currents are generated by the gradients in radiation stresses that occur in the surf zone. The Spectral Wave Module can be used to calculate the wave conditions and associated radiation stresses.



Coastal application (morphology) with coupled MIKE 21 HD, SW and ST, Torsminde harbour Denmark



Model bathymetry of Taravao Bay, Tahiti



Example of Cross reef currents in Taravao Bay, Tahiti simulated with MIKE 3 Flow Model FM. The circulation and renewal of water inside the reef is dependent on the tides, the meteorological conditions and the cross reef currents, thus the circulation model includes the effects of wave induced cross reef currents



Computational Features

The main features and effects included in simulations with the MIKE 21 & MIKE 3 Flow Model FM – Hydrodynamic Module are the following:

- Flooding and drying
- Momentum dispersion
- Bottom shear stress
- Coriolis force
- Wind shear stress
- Barometric pressure gradients
- Ice coverage
- Tidal potential
- Precipitation/evaporation
- Wave radiation stresses
- Sources and sinks

Model Equations

The modelling system is based on the numerical solution of the two/three-dimensional incompressible Reynolds averaged Navier-Stokes equations subject to the the assumptions of Boussinesq and of hydrostatic pressure. Thus, the model consists of continuity, momentum, temperature, salinity and density equations and it is closed by a turbulent closure scheme. The density does not depend on the pressure, but only on the temperature and the salinity.

For the 3D model, the free surface is taken into account using a sigma-coordinate transformation approach.

Below the governing equations are presented using Cartesian coordinates.

The local continuity equation is written as

$$\frac{\partial u}{\partial x} + \frac{\partial v}{\partial y} + \frac{\partial w}{\partial z} = S$$

and the two horizontal momentum equations for the x- and y-component, respectively

$$\frac{\partial u}{\partial t} + \frac{\partial u^2}{\partial x} + \frac{\partial vu}{\partial y} + \frac{\partial wu}{\partial z} = fv - g \frac{\partial \eta}{\partial x} -$$

$$\frac{1}{\rho_0} \frac{\partial p_a}{\partial x} - \frac{g}{\rho_0} \int_z^\eta \frac{\partial \rho}{\partial x} dz + F_u + \frac{\partial}{\partial z} \left(\nu_t \frac{\partial u}{\partial z} \right) + u_s S$$

$$\frac{\partial v}{\partial t} + \frac{\partial v^2}{\partial y} + \frac{\partial uv}{\partial x} + \frac{\partial wv}{\partial z} = -fu - g \frac{\partial \eta}{\partial y} -$$

$$\frac{1}{\rho_0} \frac{\partial p_a}{\partial y} - \frac{g}{\rho_0} \int_z^\eta \frac{\partial \rho}{\partial y} dz + F_v + \frac{\partial}{\partial z} \left(\nu_t \frac{\partial v}{\partial z} \right) + v_s S$$

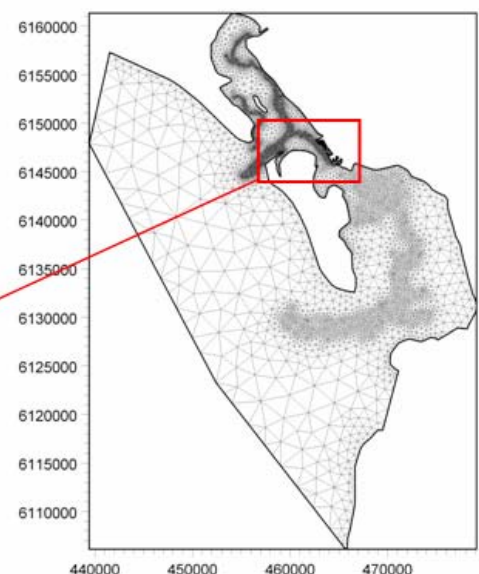
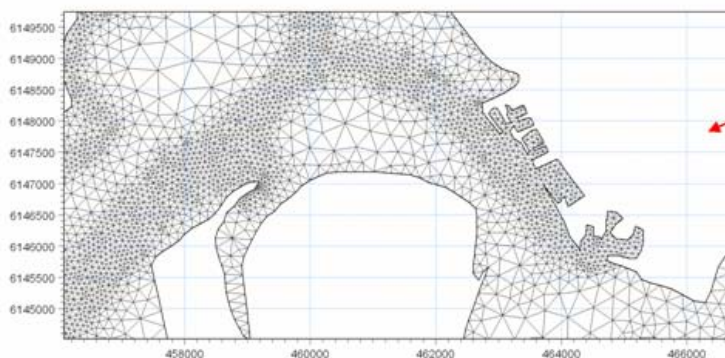
Temperature and salinity

In the Hydrodynamic Module, calculations of the transports of temperature, T , and salinity, s follow the general transport-diffusion equations as

$$\frac{\partial T}{\partial t} + \frac{\partial uT}{\partial x} + \frac{\partial vT}{\partial y} + \frac{\partial wT}{\partial z} = F_T + \frac{\partial}{\partial z} \left(D_v \frac{\partial T}{\partial z} \right) + \hat{H} + T_s S$$

$$\frac{\partial s}{\partial t} + \frac{\partial us}{\partial x} + \frac{\partial vs}{\partial y} + \frac{\partial ws}{\partial z} = F_s + \frac{\partial}{\partial z} \left(D_v \frac{\partial s}{\partial z} \right) + s_s S$$

Unstructured mesh technique gives the maximum degree of flexibility, for example: 1) Control of node distribution allows for optimal usage of nodes 2) Adoption of mesh resolution to the relevant physical scales 3) Depth-adaptive and boundary-fitted mesh. Below is shown an example from Ho Bay Denmark with the approach channel to the Port of Esbjerg



The horizontal diffusion terms are defined by

$$(F_T, F_s) = \left[\frac{\partial}{\partial x} \left(D_h \frac{\partial}{\partial x} \right) + \frac{\partial}{\partial y} \left(D_h \frac{\partial}{\partial y} \right) \right] (T, s)$$

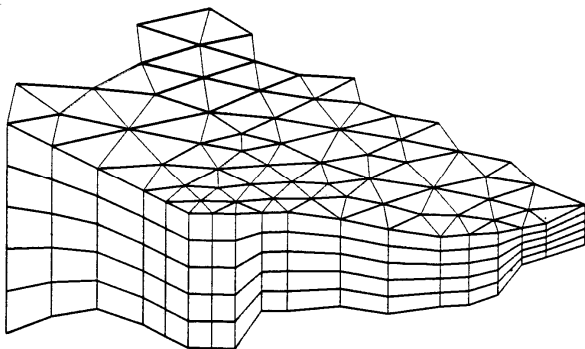
The equations for two-dimensional flow are obtained by integration of the equations over depth.

Heat exchange with the atmosphere is also included.

Symbol list	
t	time
x, y, z	Cartesian coordinates
u, v, w	flow velocity components
T, s	temperature and salinity
D_v	vertical turbulent (eddy) diffusion coefficient
\hat{H}	source term due to heat exchange with atmosphere
S	magnitude of discharge due to point sources
T_s, S_s	temperature and salinity of source
F_T, F_s, F_c	horizontal diffusion terms
D_h	horizontal diffusion coefficient
h	depth

Solution Technique

The spatial discretisation of the primitive equations is performed using a cell-centred finite volume method. The spatial domain is discretised by subdivision of the continuum into non-overlapping elements/cells.



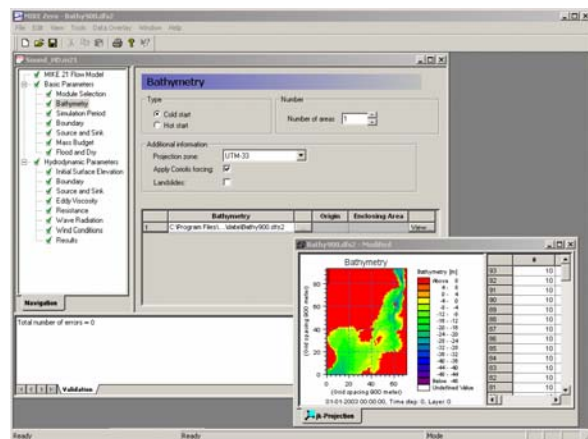
Principle of 3D mesh

In the horizontal plane an unstructured mesh is used while a structured mesh is used in the vertical domain of the 3D model. In the 2D model the elements can be triangles or quadrilateral elements. In the 3D model the elements can be prisms or bricks whose horizontal faces are triangles and quadrilateral elements, respectively.

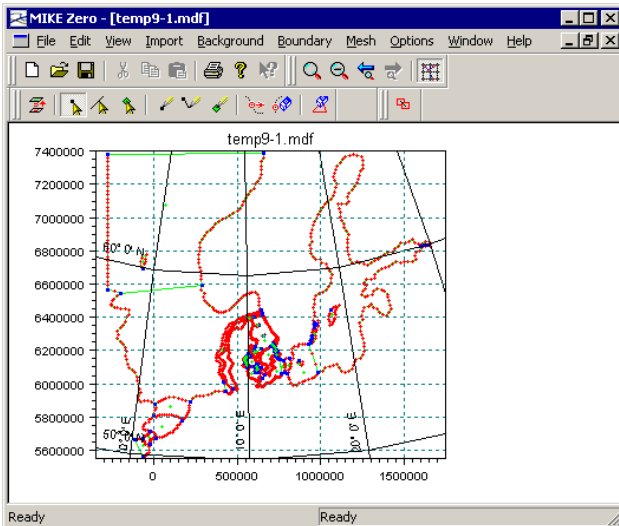
Model Input

Input data can be divided into the following groups:

- Domain and time parameters:
 - computational mesh (the coordinate type is defined in the computational mesh file) and bathymetry
 - simulation length and overall time step
- Calibration factors
 - bed resistance
 - momentum dispersion coefficients
 - wind friction factors
- Initial conditions
 - water surface level
 - velocity components
- Boundary conditions
 - closed
 - water level
 - discharge
- Other driving forces
 - wind speed and direction
 - tide
 - source/sink discharge
 - wave radiation stresses



View button on all the GUIs in MIKE 21 & MIKE 3 FM HD for graphical view of input and output files



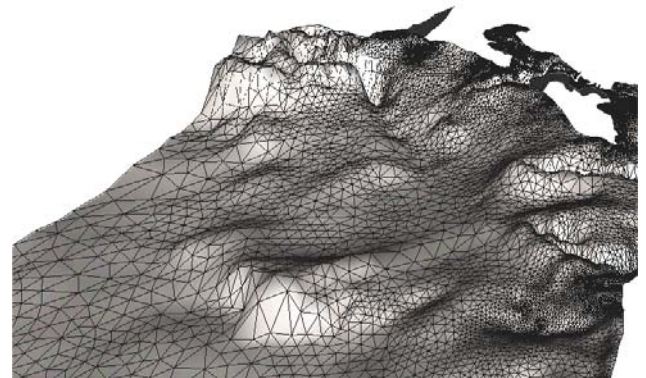
The Mesh Generator is an efficient MIKE Zero tool for the generation and handling of unstructured meshes, including the definition and editing of boundaries

Providing MIKE 21 & MIKE 3 Flow Model FM with a suitable mesh is essential for obtaining reliable results from the models. Setting up the mesh includes the appropriate selection of the area to be modelled, adequate resolution of the bathymetry, flow, wind and wave fields under consideration and definition of codes for defining boundaries.



2D visualization of a computational mesh (Odense Estuary)

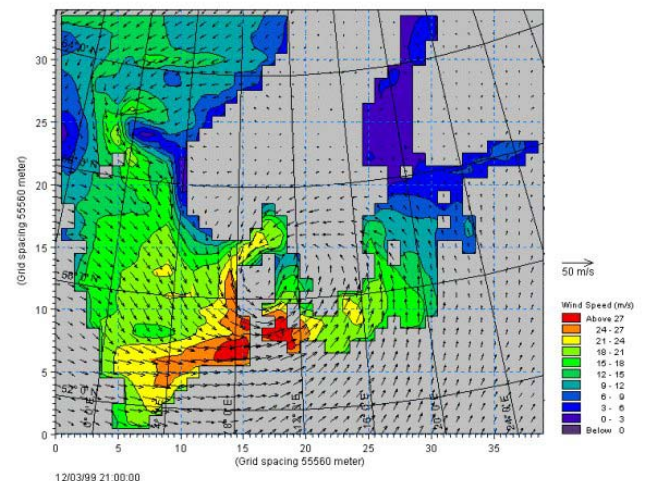
Bathymetric values for the mesh generation can e.g. be obtained from the DHI Software product MIKE C-Map. MIKE C-Map is an efficient tool for extracting depth data and predicted tidal elevation from the world-wide Electronic Chart Database CM-93 Edition 3.0 from C-Map Norway.



3D visualization of a computational mesh

If wind data is not available from an atmospheric meteorological model, the wind fields (e.g. cyclones) can be determined by using the wind-generating programs available in MIKE 21 Toolbox.

Global winds (pressure & wind data) can be downloaded for immediate use in your simulation. The sources of data are from GFS courtesy of NCEP, NOAA. By specifying the location, orientation and grid dimensions, the data is returned to you in the correct format as a spatial varying grid series or a time series. The link is: www.dhisoftware.com/mikemarine/online_data



The chart shows a hindcast wind field in the North Sea and Baltic Sea as wind speed and wind direction

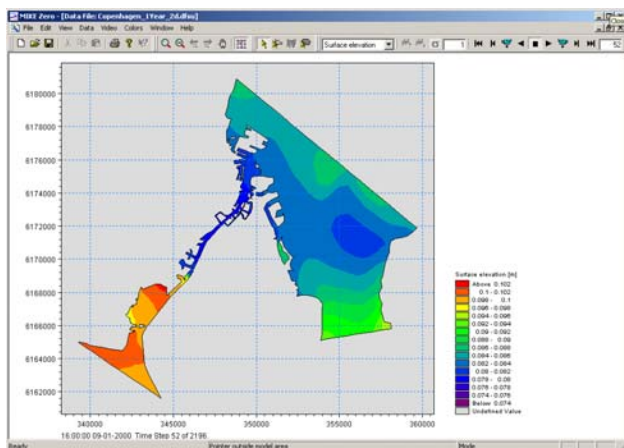
Model Output

Computed output results at each mesh element and for each time step consist of:

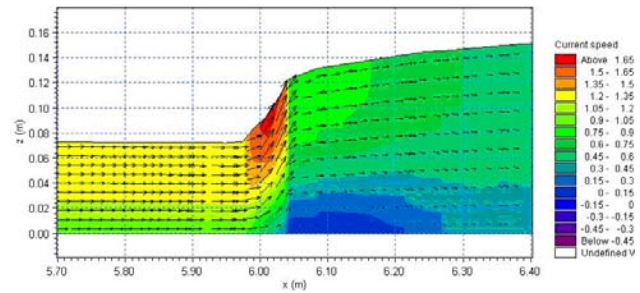
- Basic variables
 - water depth and surface elevation
 - flux densities in main directions
 - velocities in main directions
 - densities, temperatures and salinities
- Additional variables
 - Current speed and direction
 - Wind velocities
 - Air pressure
 - Drag coefficient
 - Precipitation/evaporation
 - Courant/CFL number
 - Eddy viscosity

The output results can be saved in defined points, lines and areas. In the case of 3D calculations the results are saved in a selection of layers.

Output from MIKE 21 & MIKE 3 Flow Model FM is typically post-processed using the Data Viewer available in the common MIKE Zero shell. The Data Viewer is a tool for analysis and visualization of unstructured data, e.g. to view meshes, spectra, bathymetries, results files of different format with graphical extraction of time series and line series from plan view and import of graphical overlays.



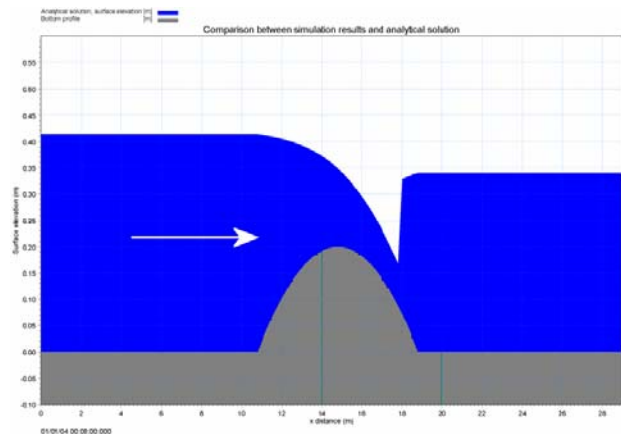
The Data Viewer in MIKE Zero – an efficient tool for analysis and visualization of unstructured data including processing of animations. Above screen dump shows surface elevations from a model setup covering Port of Copenhagen



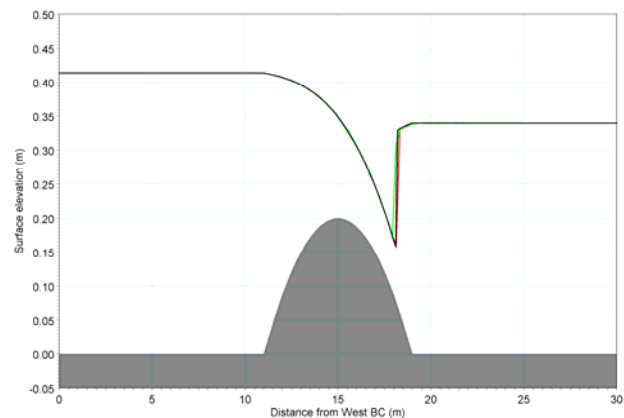
Vector and contour plot of current speed at a vertical profile defined along a line in Data Viewer in MIKE Zero

Validation

Before the first release of MIKE 21 & MIKE 3 Flow Model FM the model was successfully applied to a number of rather basic idealized situations for which the results can be compared with analytical solutions or information from the literature.

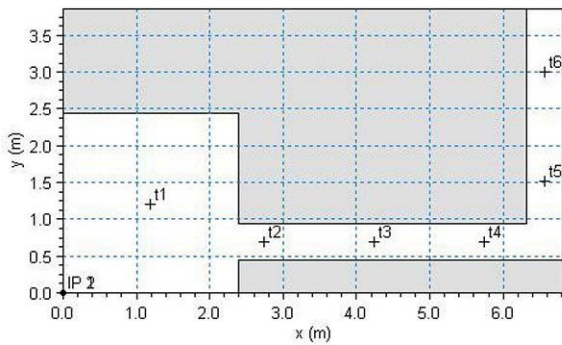


The domain is a channel with a parabola-shaped bump in the middle. The upstream (western) boundary is a constant flux and the downstream (eastern) boundary is a constant elevation. Below: the total depths for the stationary hydraulic jump at convergence. Red line: 2D setup, green line: 3D setup, black line: analytical solution

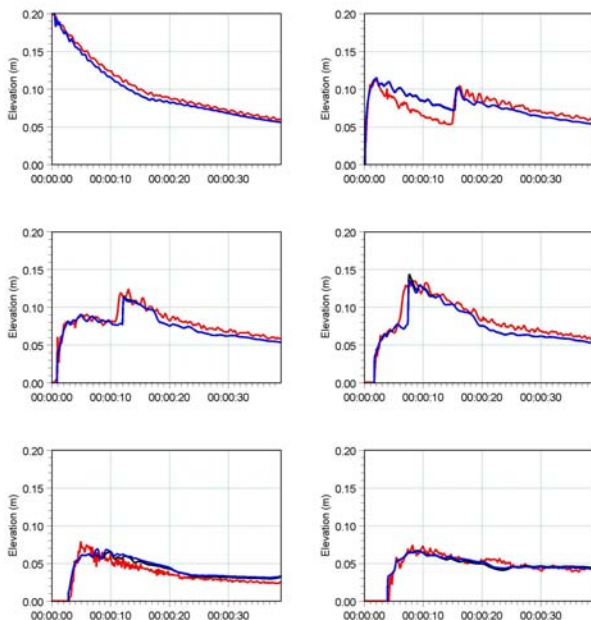




A dam-break flow in an L-shaped channel (a, b, c):

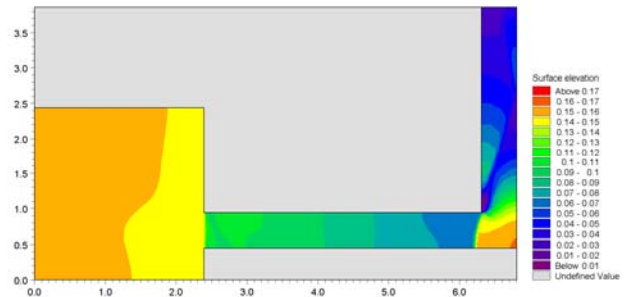
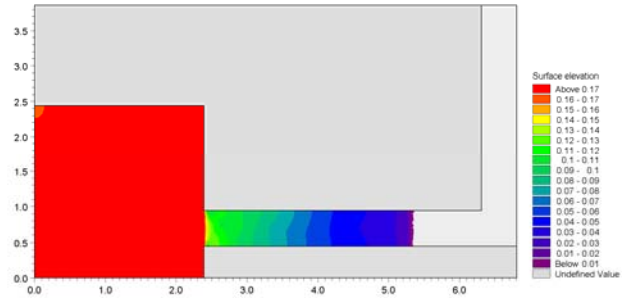


a) Outline of model setup showing the location of gauging points



b) Comparison between simulated and measured water levels at the six gauge locations. (Blue) coarse mesh (black) fine mesh and (red) measurements

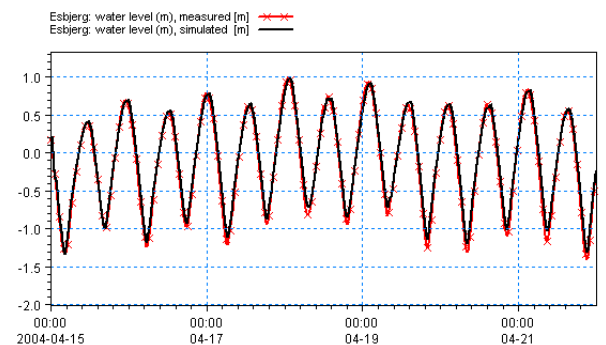
The model has also been applied and tested in more natural geophysical conditions; ocean scale, inner shelves, estuaries, lakes and overland, which are more realistic and complicated than academic and laboratory tests.

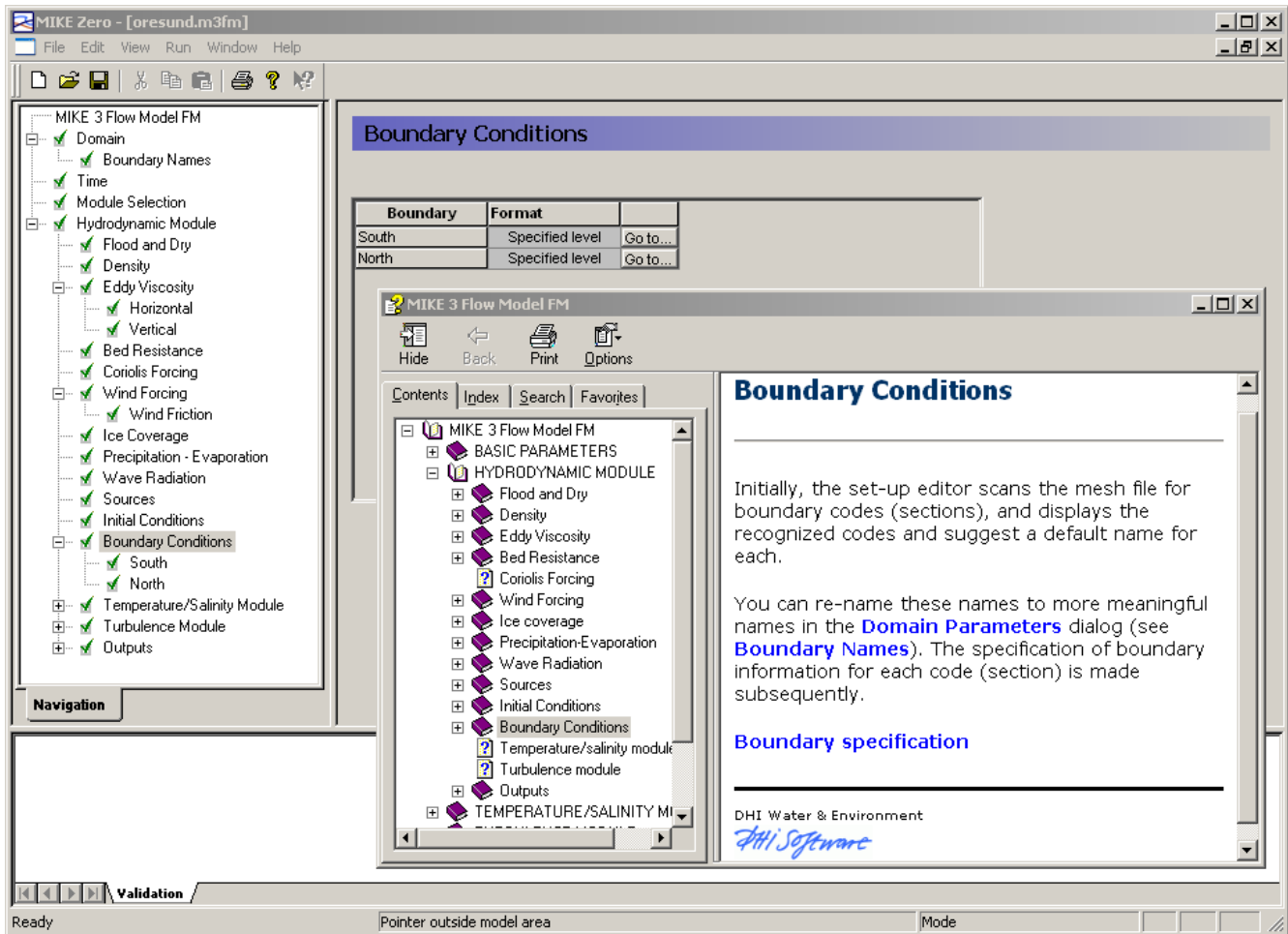


c) Contour plots of the surface elevation at $T = 1.6$ s (top) and $T = 4.8$ s (bottom)



Example from Ho Bay, a tidal estuary (barrier island coast) in South-West Denmark with access channel to the Port of Esbjerg. Below: Comparison between measured and simulated water levels



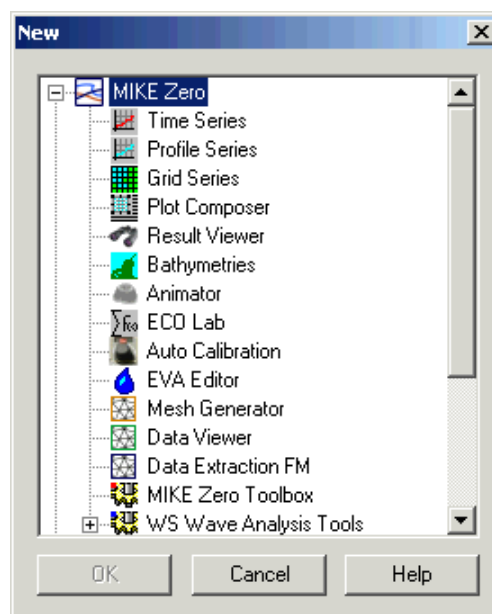


The user interface of the MIKE 21 and MIKE 3 Flow Model FM (Hydrodynamic Module), including an example of the extensive Online Help system

Graphical User Interface

The MIKE 21 & MIKE 3 Flow Model FM are operated through a fully Windows integrated graphical user interface (GUI). Support is provided at each stage by an Online Help system.

The common MIKE Zero shell provides entries for common data file editors, plotting facilities and a toolbox for/utilities as the Mesh Generator and Data Viewer.



Overview of the common MIKE Zero utilities



Hardware and Operating System Requirements

The MIKE 21 and MIKE 3 Flow Model FM Hydrodynamic Module supports Microsoft Windows XP and Microsoft Windows Vista. Microsoft Internet Explorer 5.0 (or higher) is required for network license management as well as for accessing the Online Help.

The recommended minimum hardware requirements for executing MIKE 21 & MIKE 3 Flow Model FM are listed below:

Processor:	2 GHz PC (or higher)
Memory (RAM):	1 GB (or higher)
Hard disk:	40 GB (or higher)
Monitor:	SVGA, resolution 1024x768
Graphic card:	32 MB RAM (or higher), 24 bit true colour
Media:	CD-ROM/DVD drive, 20 x speed (or higher)

Support

News about new features, applications, papers, updates, patches, etc. are available here:

<http://www.dhigroup.com/Software/Download/DocumentsAndTools.aspx>

For further information on MIKE 21 and MIKE 3 Flow Model FM software, please contact your local DHI agent or the Software Support Centre:

Software Support Centre
DHI

Agern Allé 5
DK-2970 Hørsholm
Denmark

Tel: +45 4516 9333

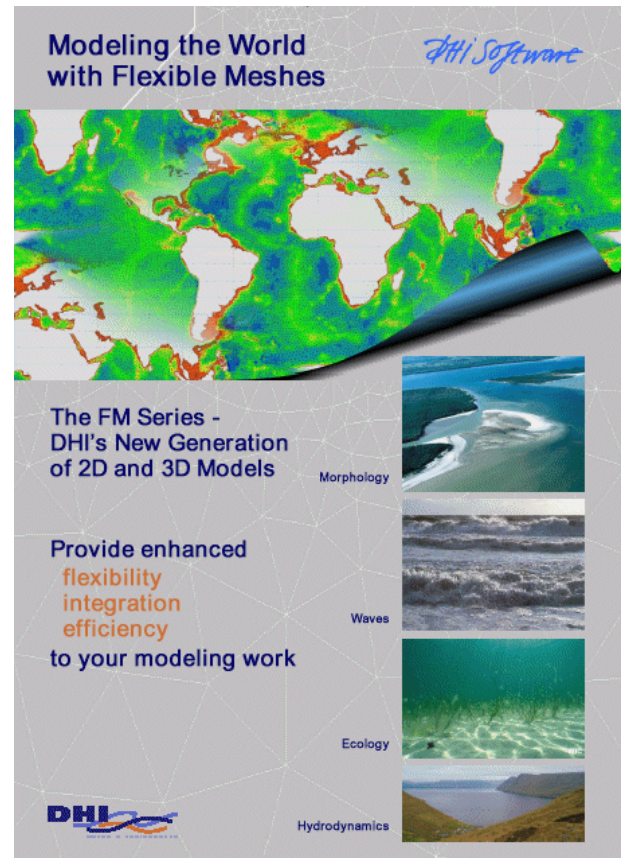
Fax: +45 4516 9292

<http://dhigroup.com/Software.aspx>
software@dhigroup.com

References

The MIKE 21 & MIKE 3 Flow Model FM are provided with comprehensive user guides, online help, scientific documentation, application examples and step-by-step training examples.

The MIKE 21 & MIKE 3 Flow Model FM have been, and are, extensively used in DHI consultancy services (some 50 studies in 20 different countries) and in several research projects.



Petersen, N.H., Rasch, P. "Modelling of the Asian Tsunami off the Coast of Northern Sumatra", presented at the 3rd Asia-Pacific DHI Software Conference in Kuala Lumpur, Malaysia, 21-22 February, 2005

French, B. and Kerper, D. Salinity Control as a Mitigation Strategy for Habitat Improvement of Impacted Estuaries. 7th Annual EPA Wetlands Workshop, NJ, USA 2004.

DHI Note, "Flood Plain Modelling using unstructured Finite Volume Technique" January 2004 – download from http://www.dhisoftware.com/mike21/Download/Papers_Docs/M21FM_Floodplain.pdf

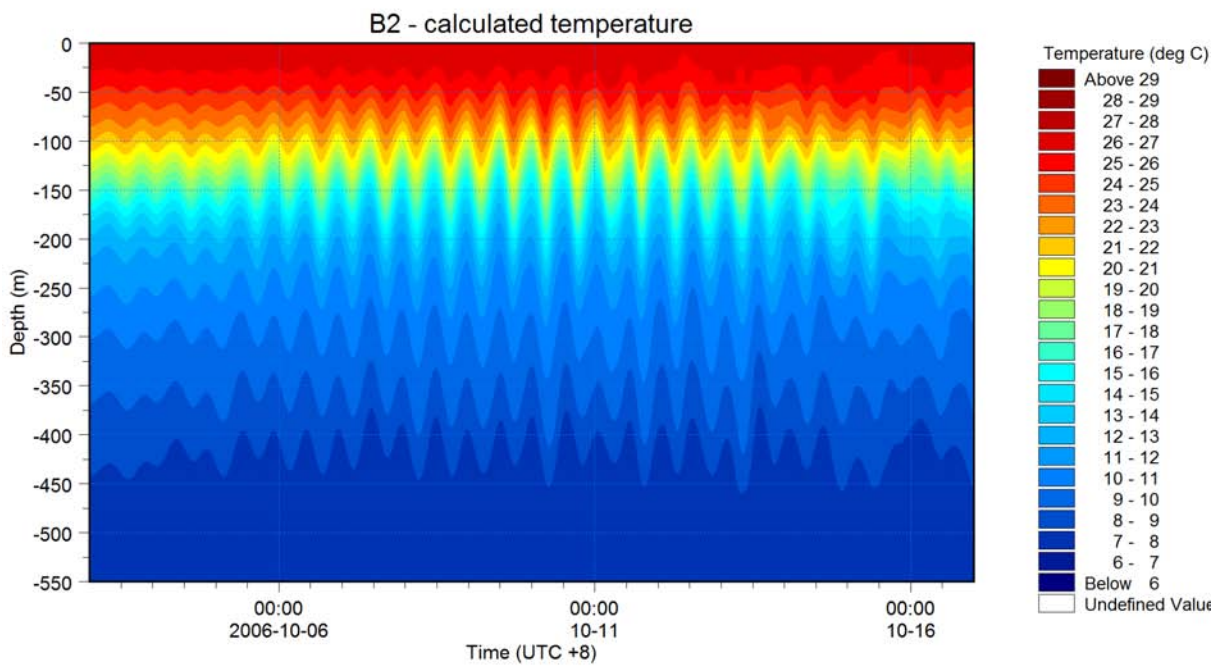
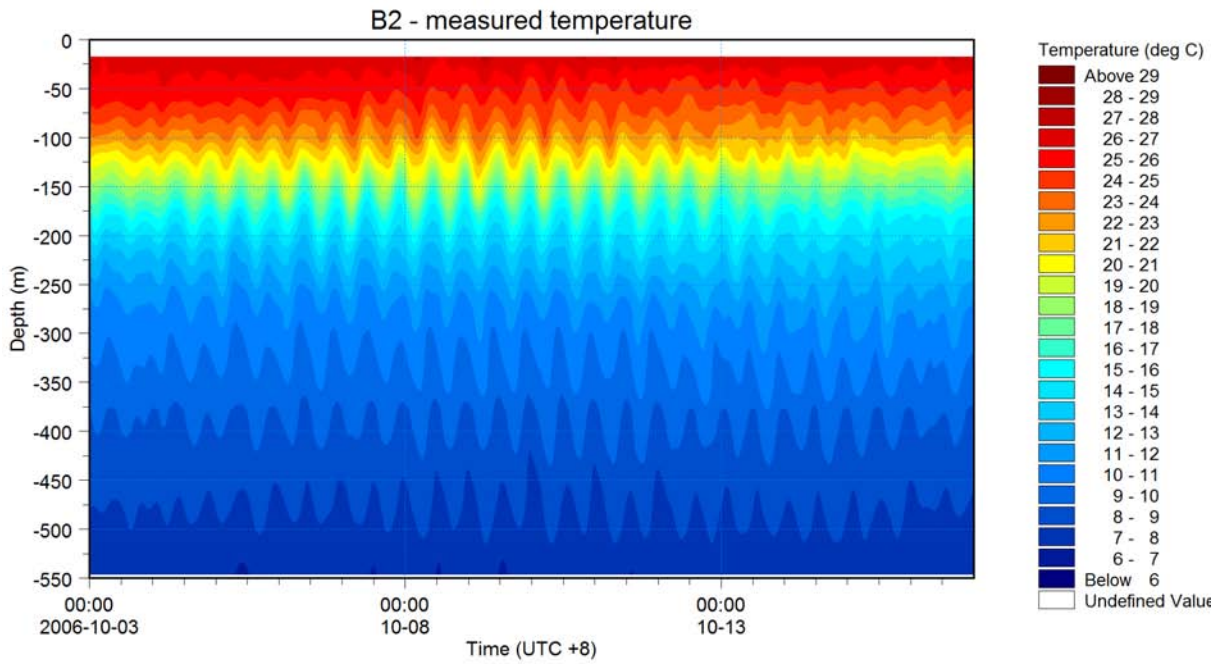




APPENDIX B

Spring Calibration Period

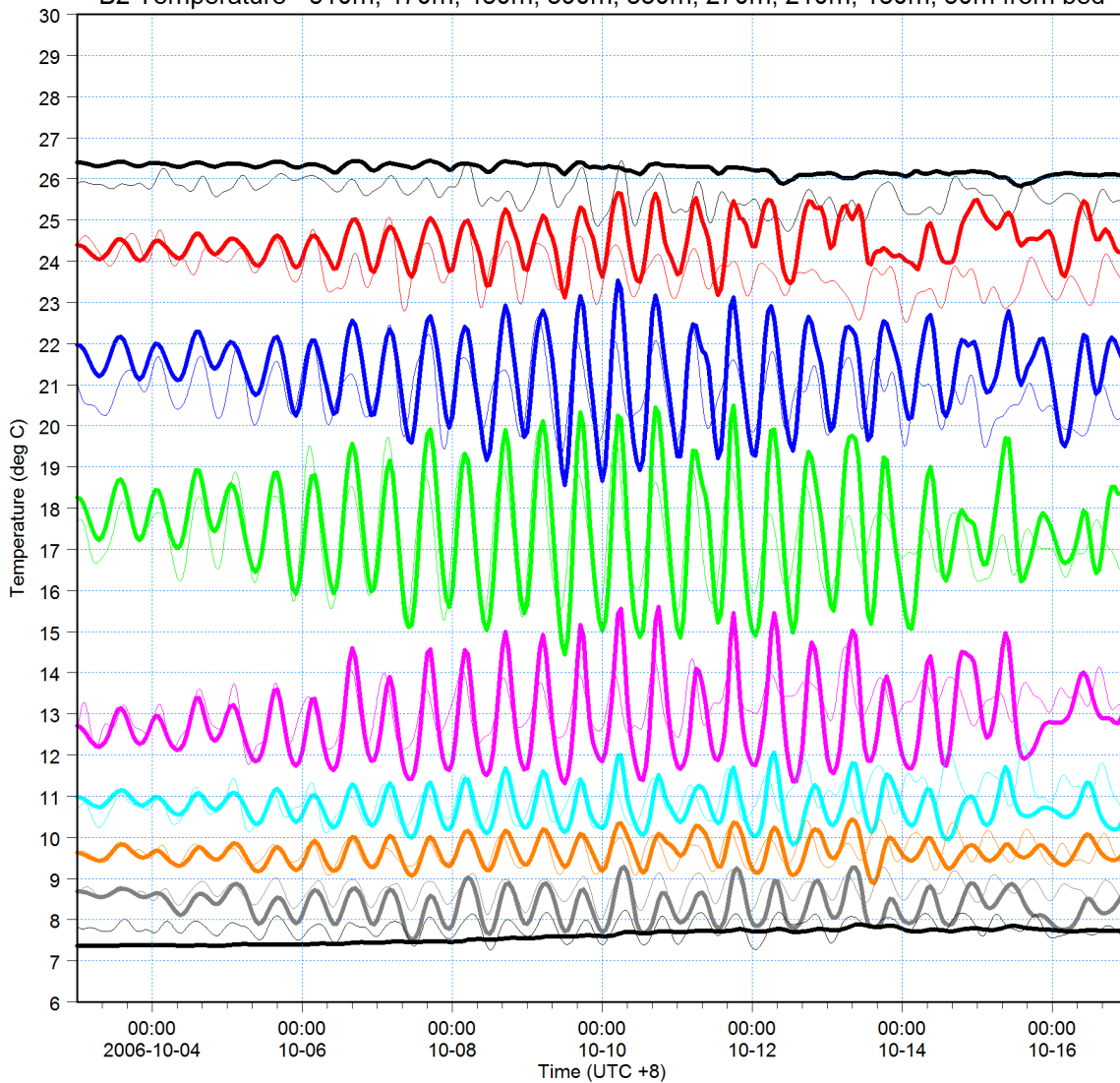
Comparisons between Measurements and Model Simulation as Isopleth Plots, Time Series Plots, Q-Q Plots and Frequency Plots





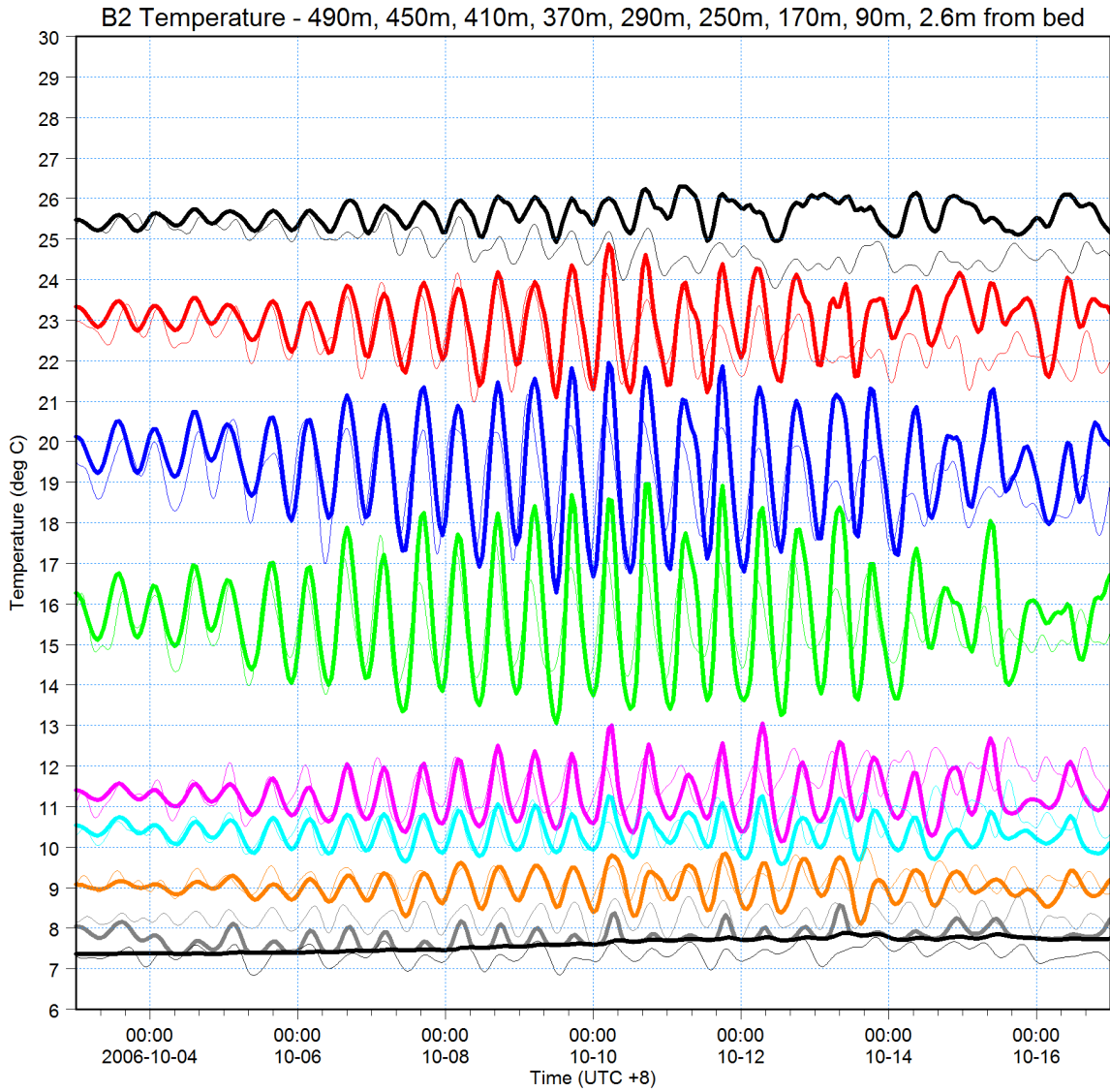
510m from bed: Temperature [C] [deg C] —
measured [deg C] —
470m from bed: Temperature [C] [deg C] —
measured [deg C] —
430m from bed: Temperature [C] [deg C] —
measured [deg C] —
390m from bed: Temperature [C] [deg C] —
measured [deg C] —
330m from bed: Temperature [C] [deg C] —
measured [deg C] —
270m from bed: Temperature [C] [deg C] —
measured [deg C] —
190m from bed: Temperature [C] [deg C] —
measured [deg C] —
130m from bed: Temperature [C] [deg C] —
measured [deg C] —
50m from bed: Temperature [C] [deg C] —
measured [deg C] —

B2 Temperature - 510m, 470m, 430m, 390m, 330m, 270m, 210m, 130m, 50m from bed



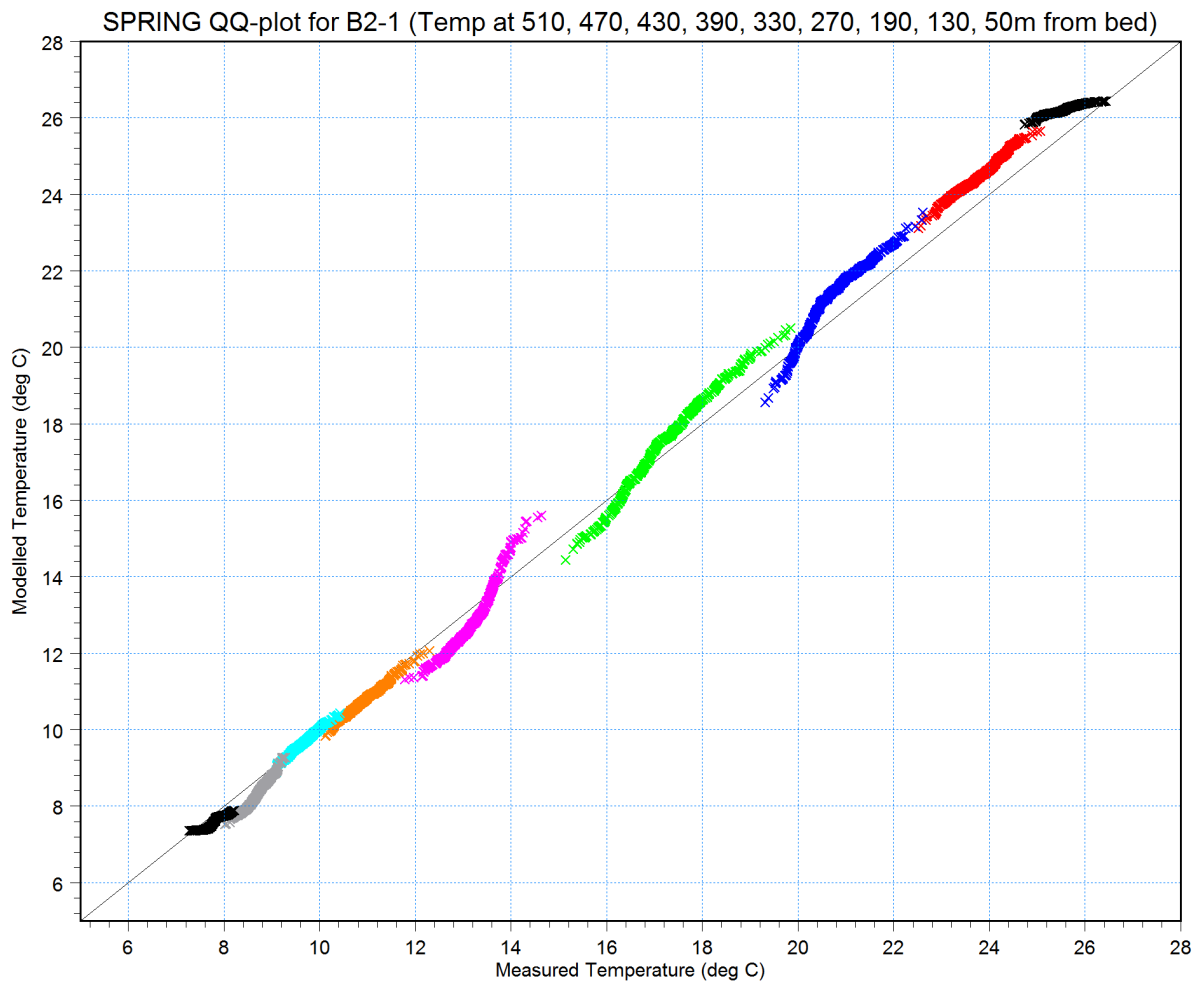


490m from bed: Temperature [C] [deg C] —
measured [deg C] —
450m from bed: Temperature [C] [deg C] —
measured [deg C] —
410m from bed: Temperature [C] [deg C] —
measured [deg C] —
370m from bed: Temperature [C] [deg C] —
measured [deg C] —
290m from bed: Temperature [C] [deg C] —
measured [deg C] —
250m from bed: Temperature [C] [deg C] —
measured [deg C] —
170m from bed: Temperature [C] [deg C] —
measured [deg C] —
130m from bed: Temperature [C] [deg C] —
measured [deg C] —
2.6m from bed: Temperature [C] [deg C] —
measured [deg C] —



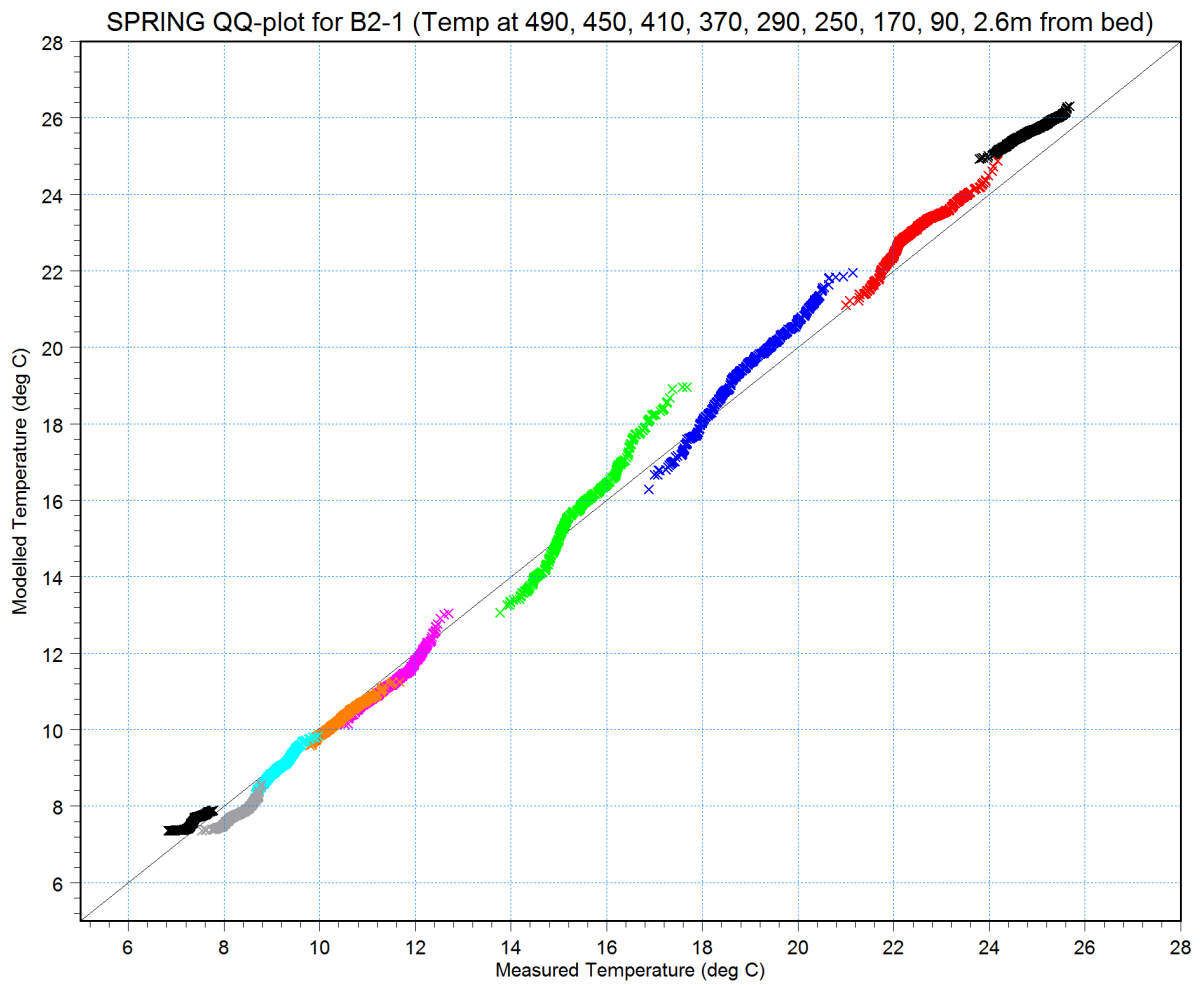


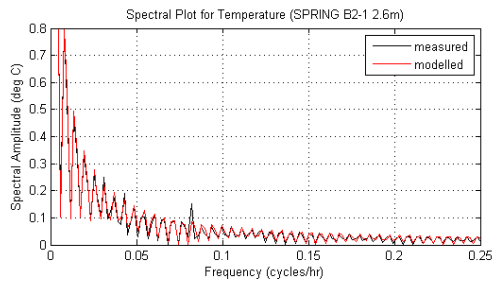
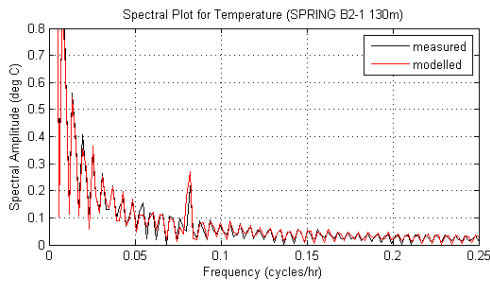
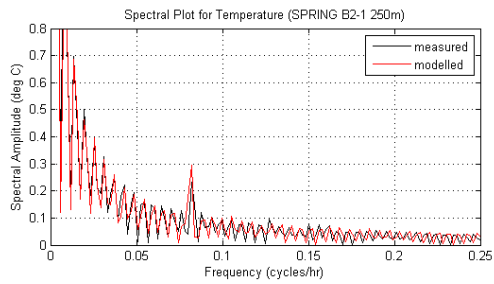
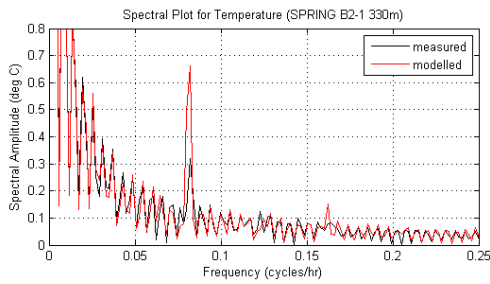
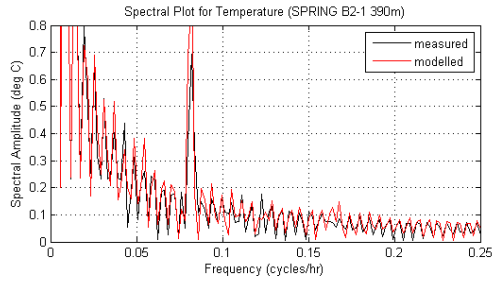
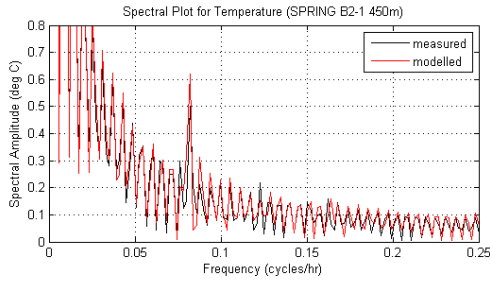
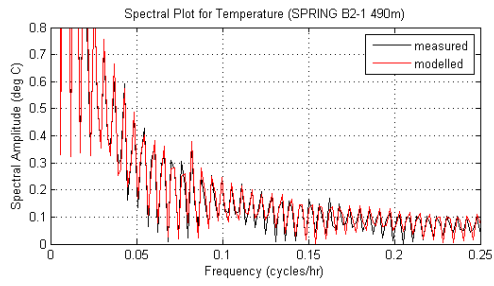
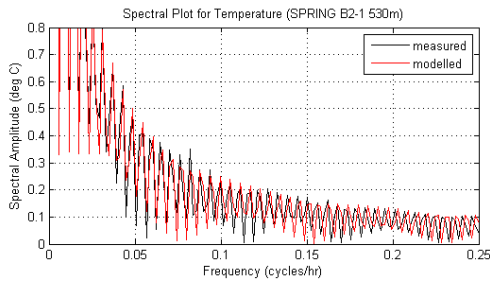
- T at 510m × ×
- T at 470m × ×
- T at 430m × ×
- T at 390m × ×
- T at 330m × ×
- T at 270m × ×
- T at 190m × ×
- T at 130m × ×
- T at 50m × ×

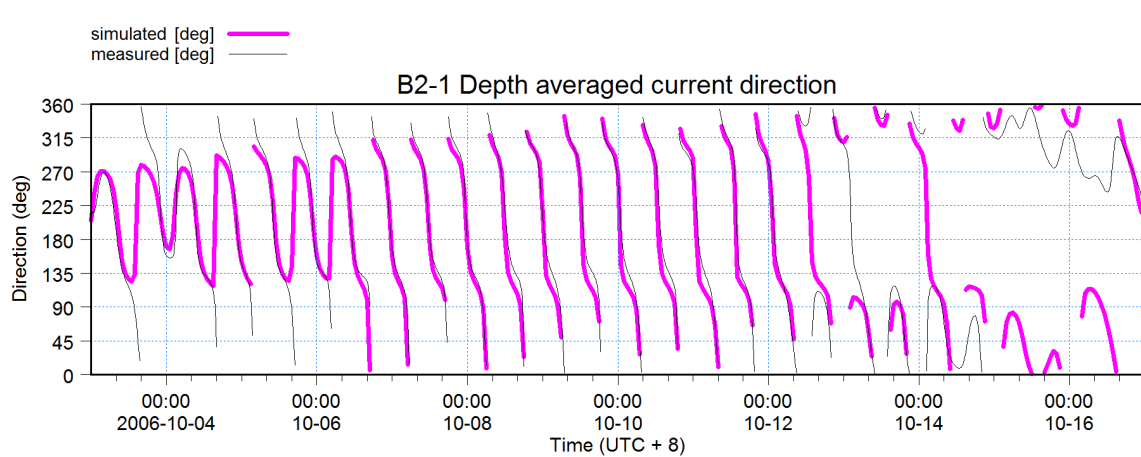
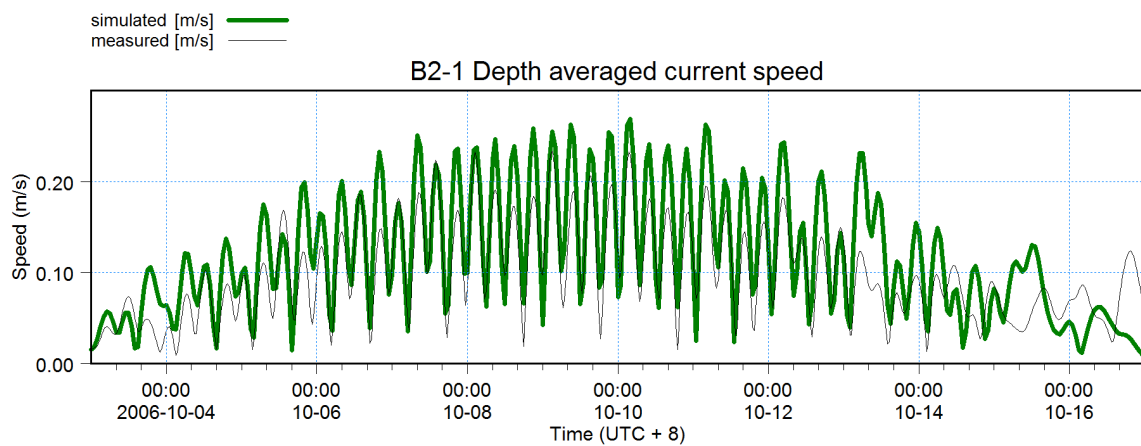
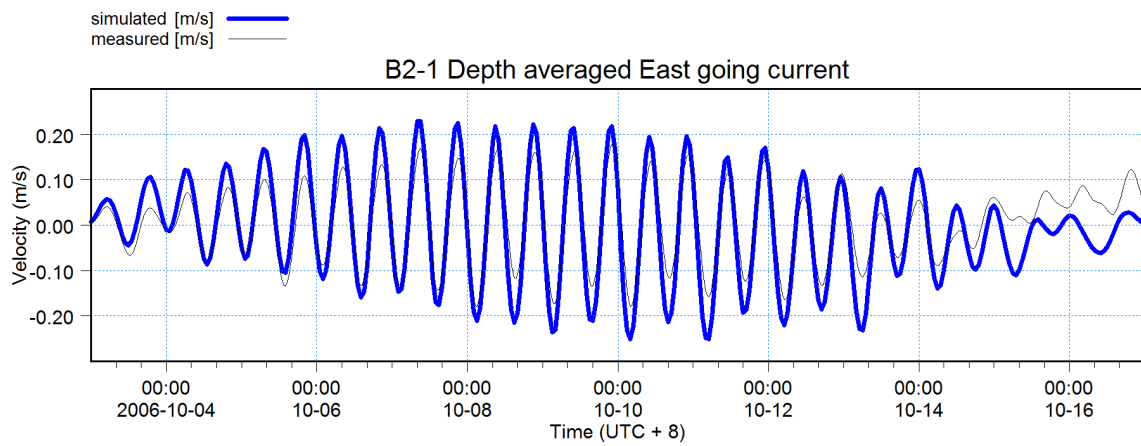
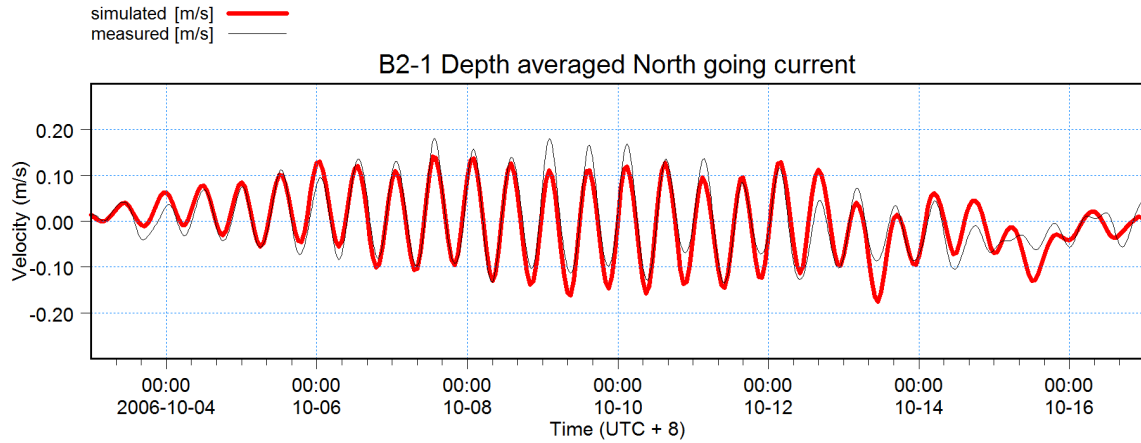




- T at 490m × ×
- T at 450m × ×
- T at 410m × ×
- T at 370m × ×
- T at 290m × ×
- T at 250m × ×
- T at 170m × ×
- T at 90m × ×
- T at 2.6m × ×

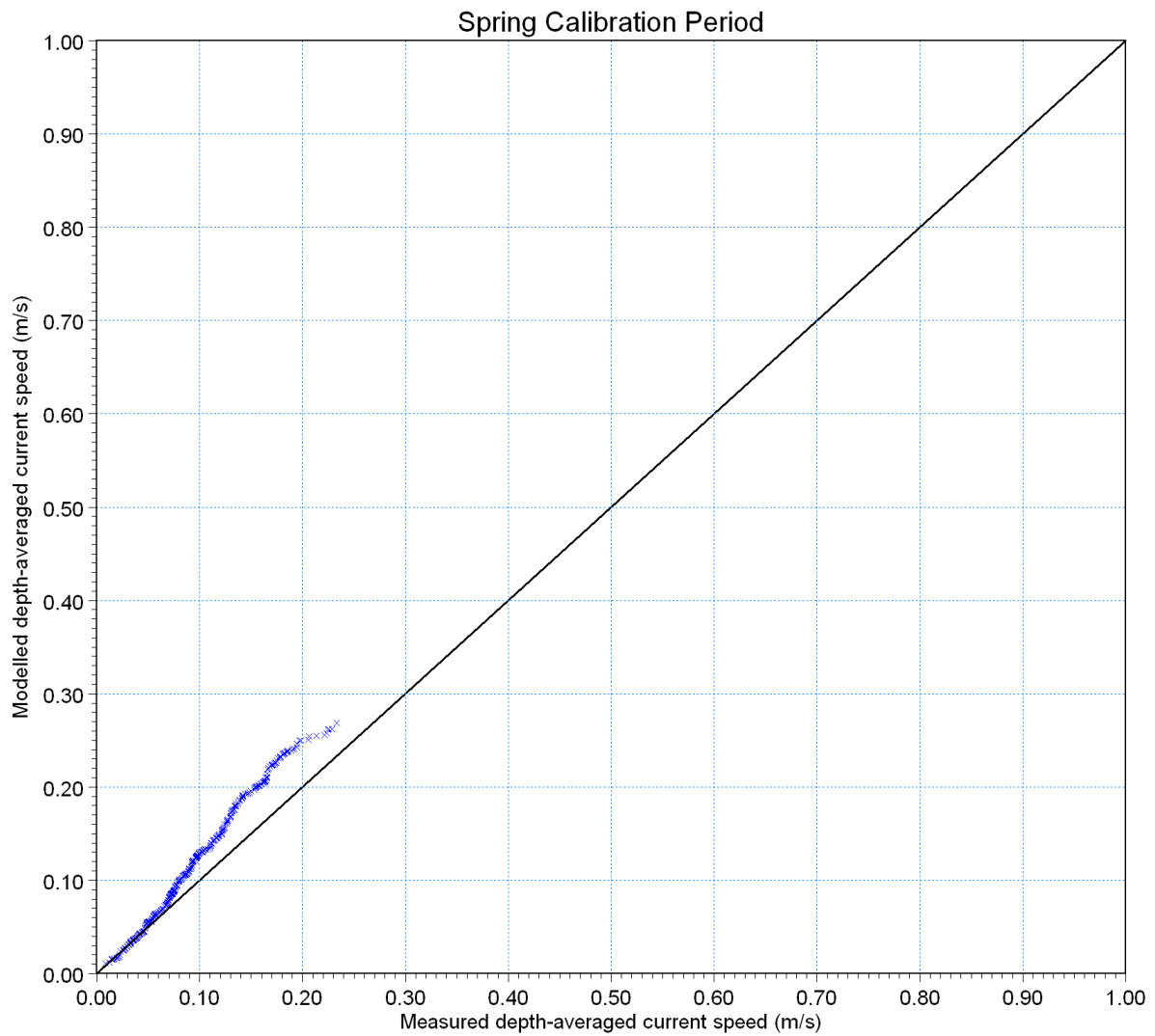


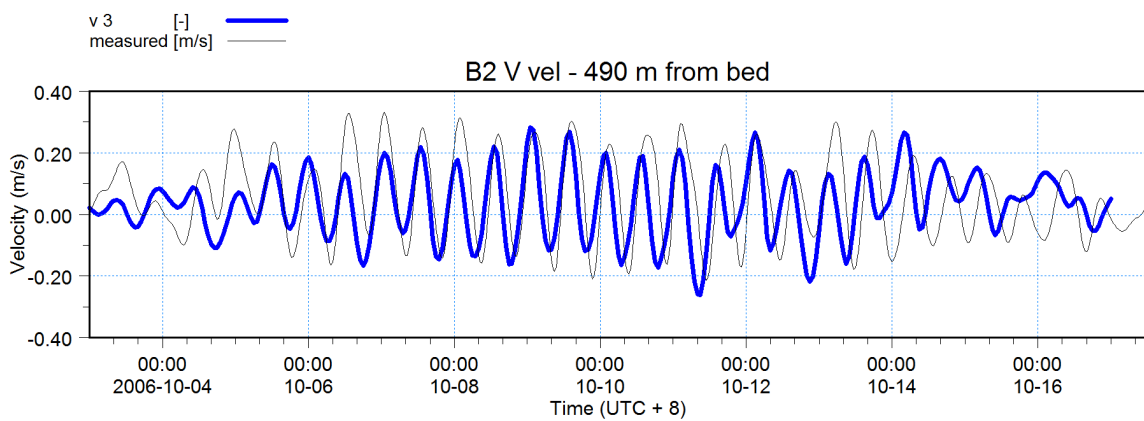
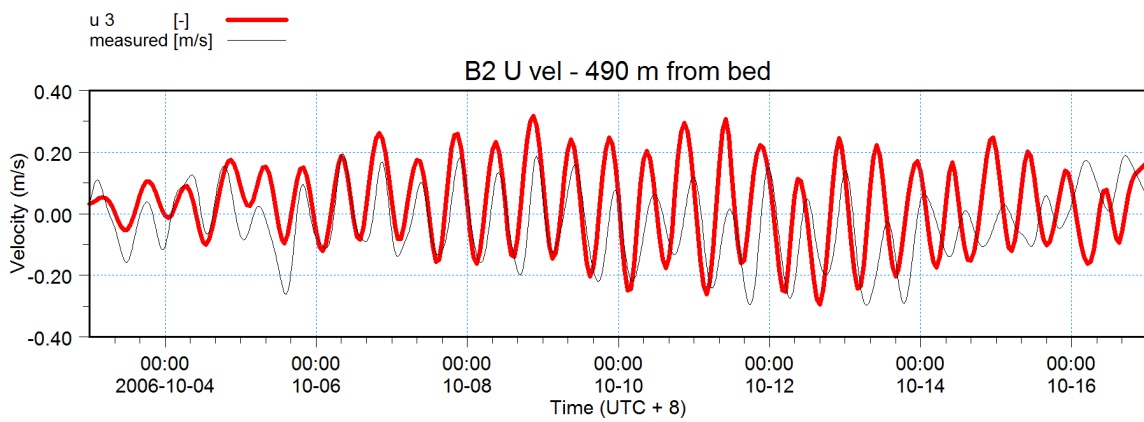
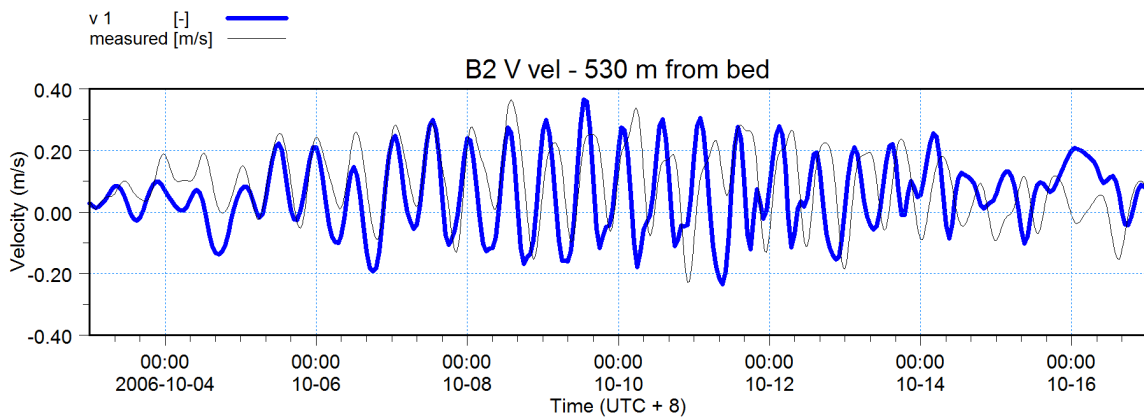
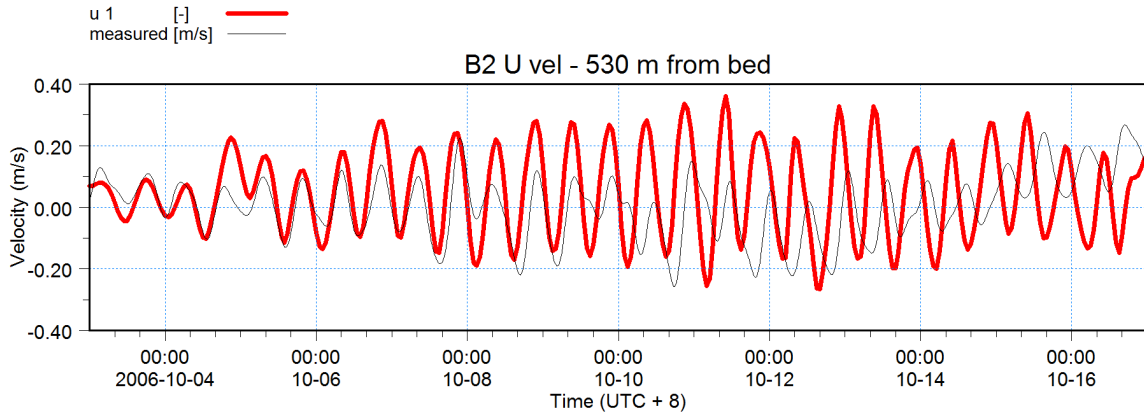


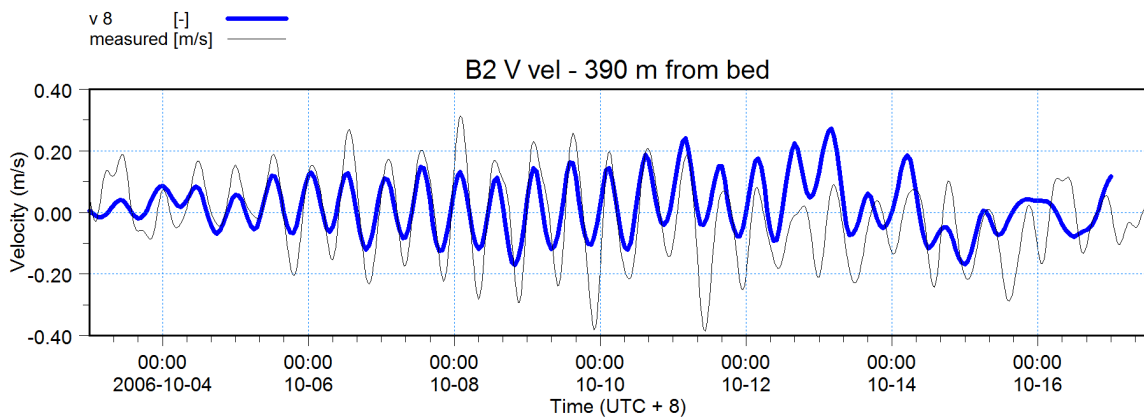
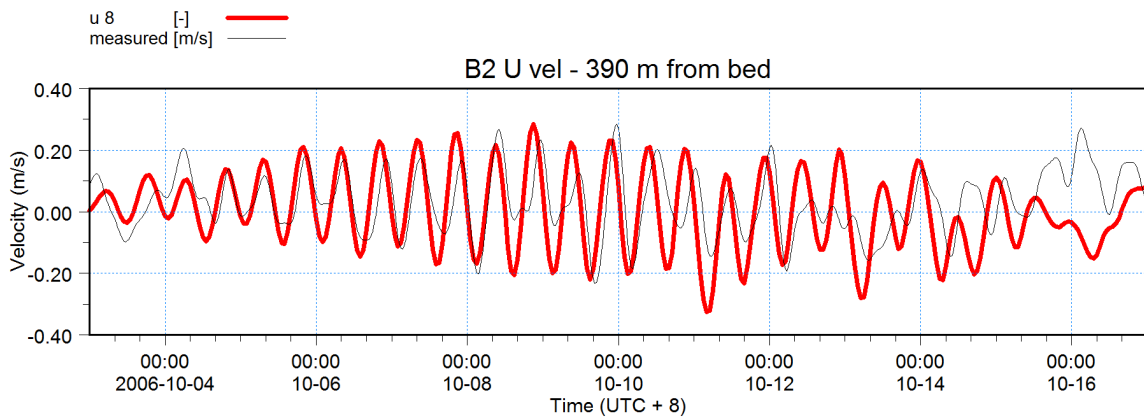
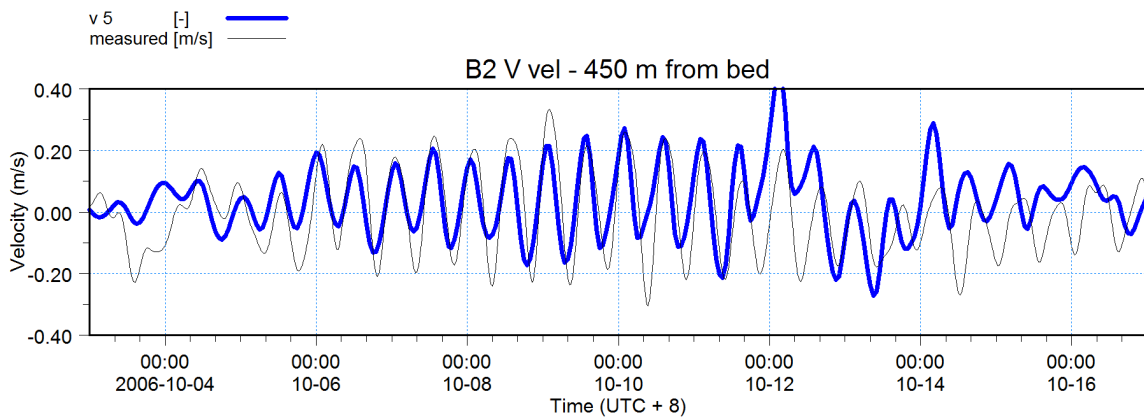
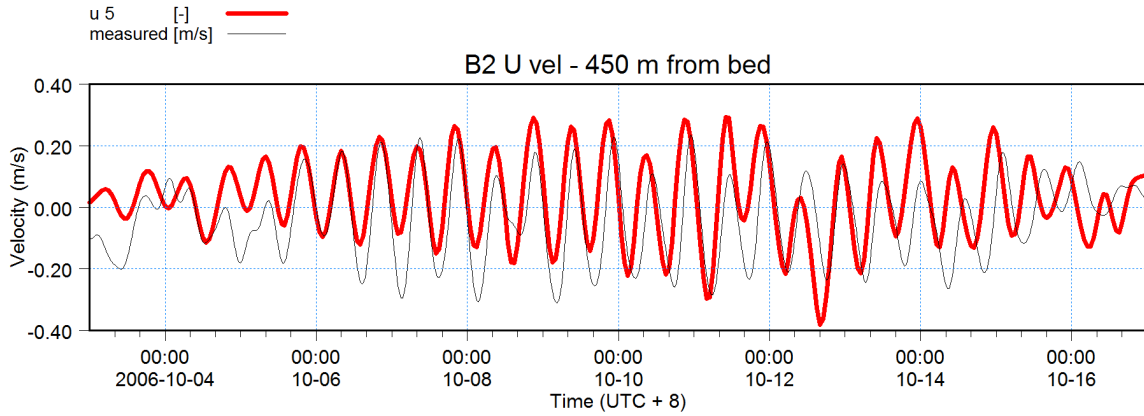


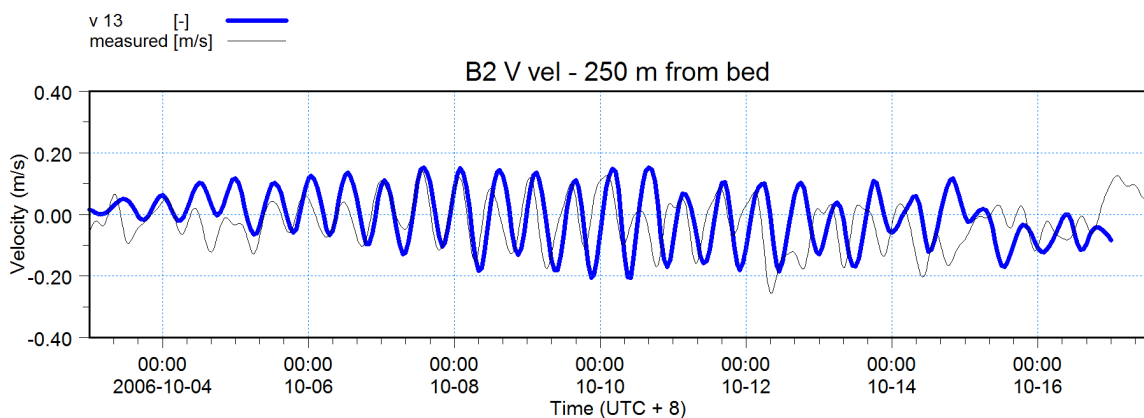
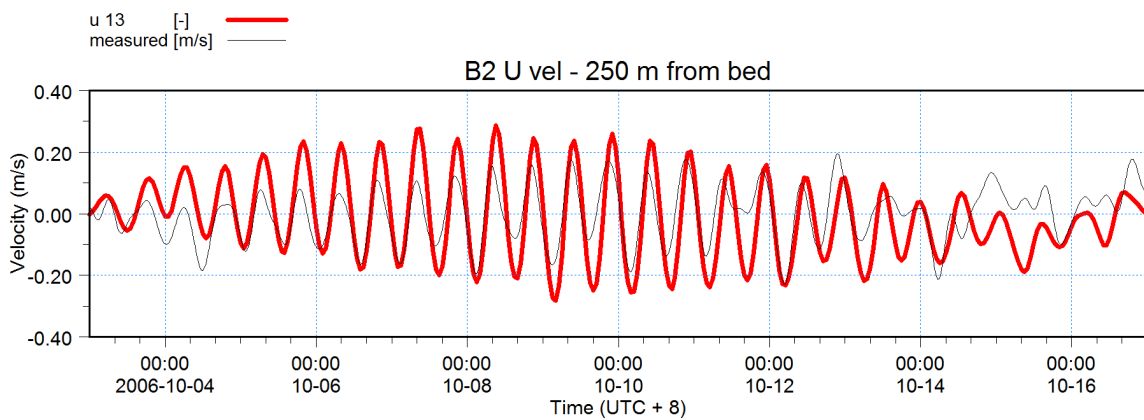
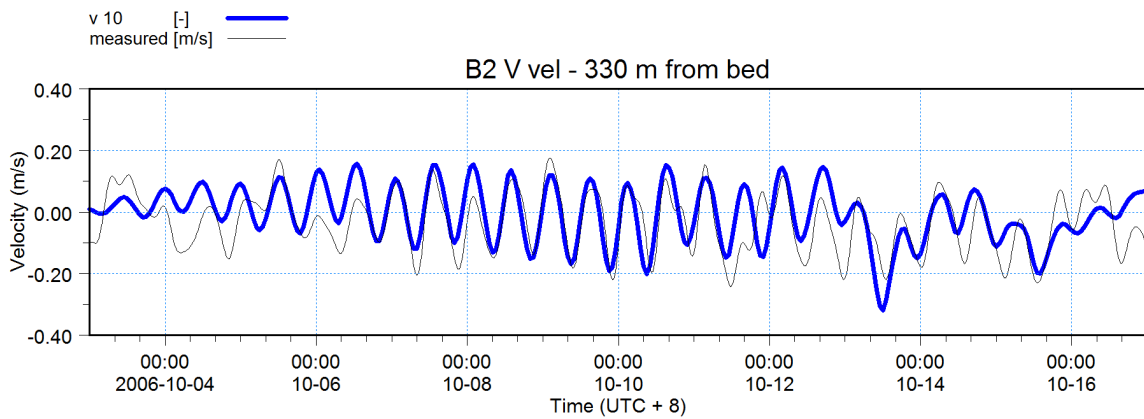
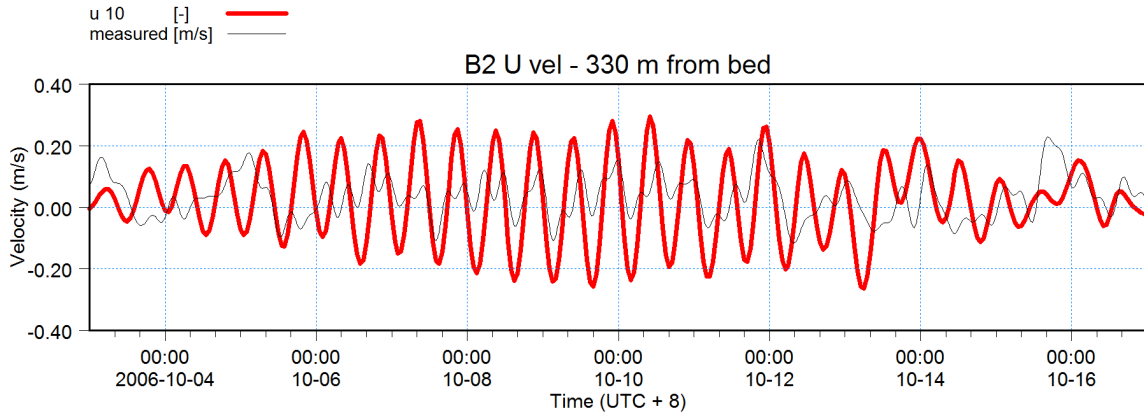


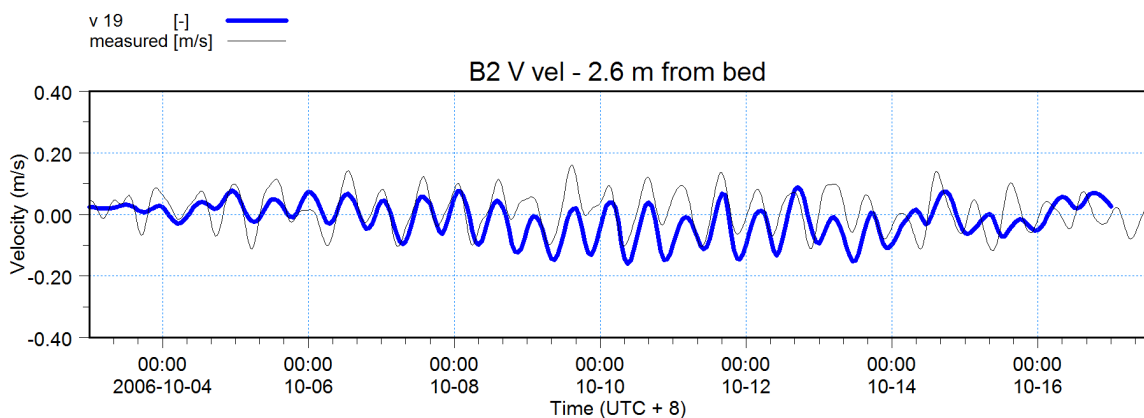
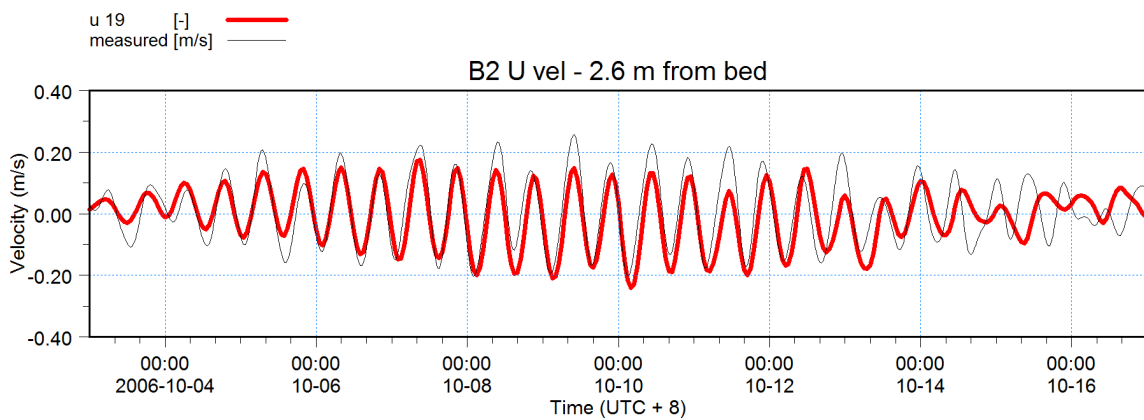
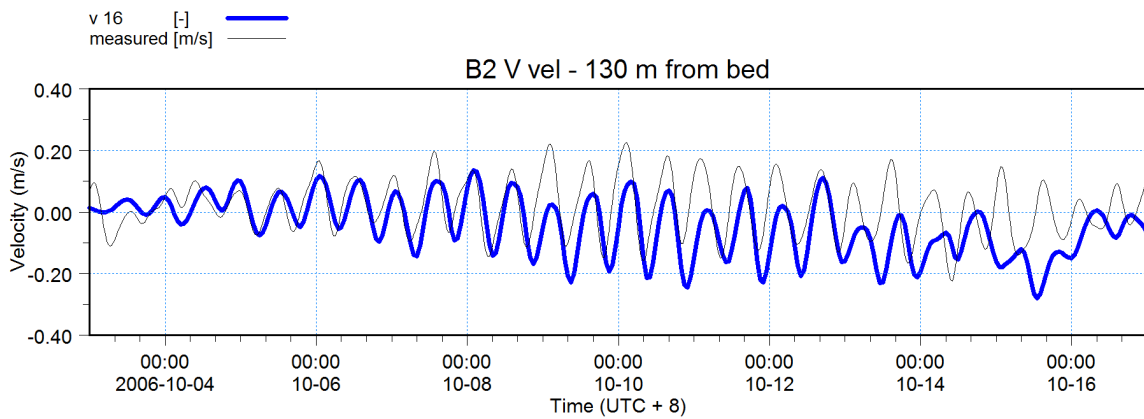
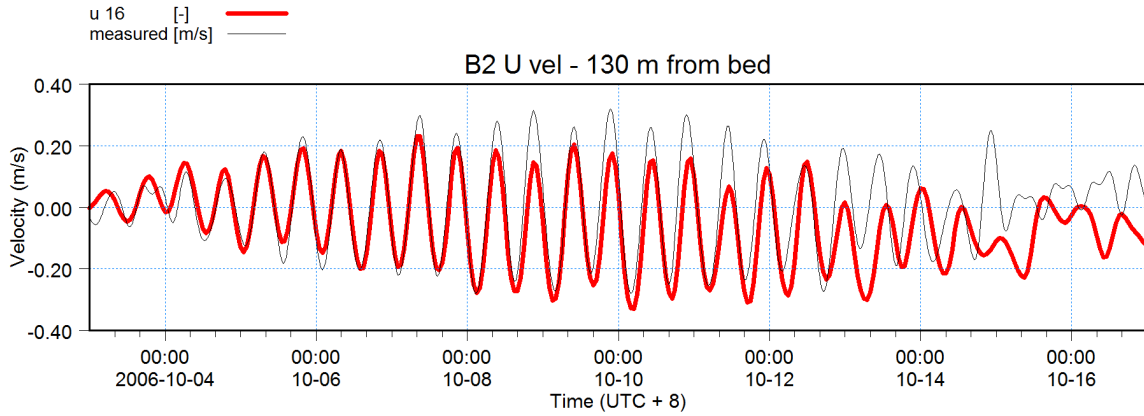
B2 × ×

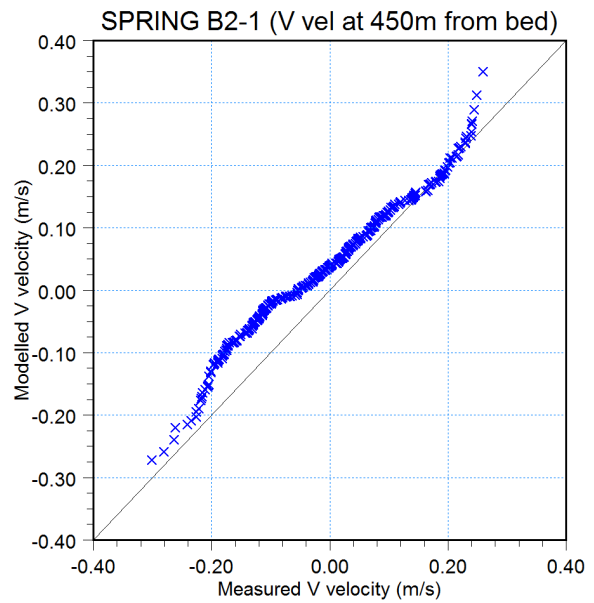
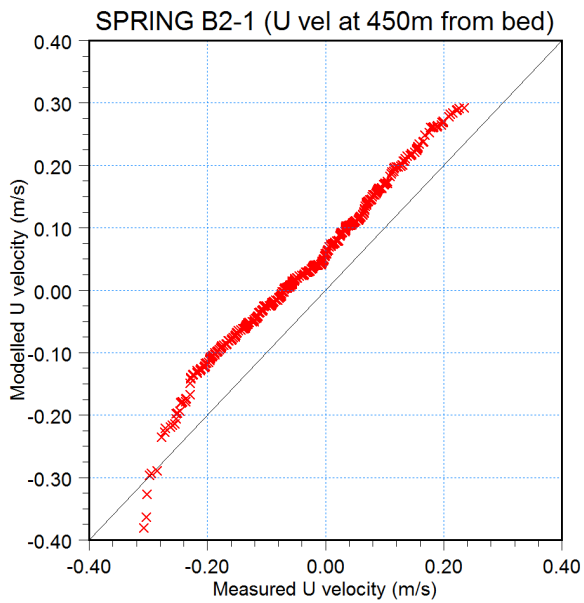
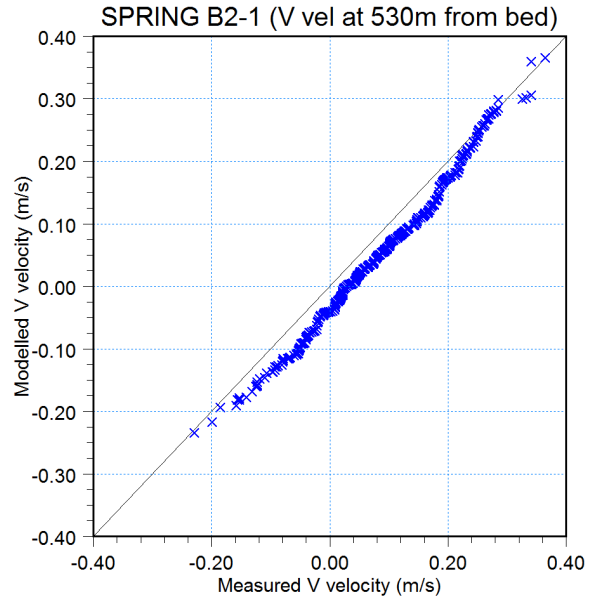
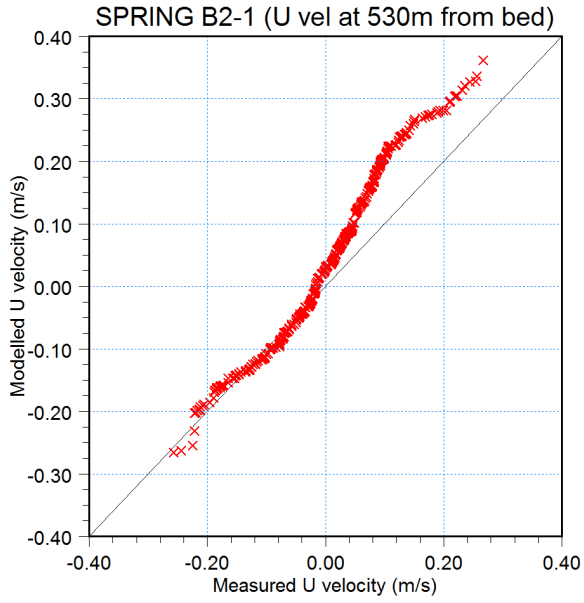


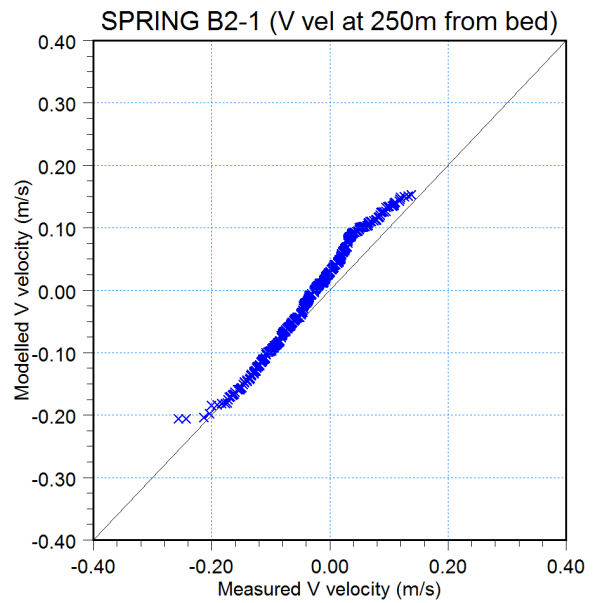
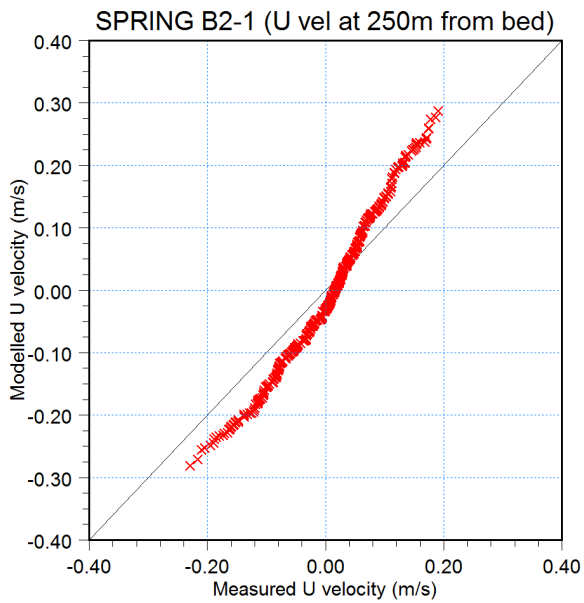
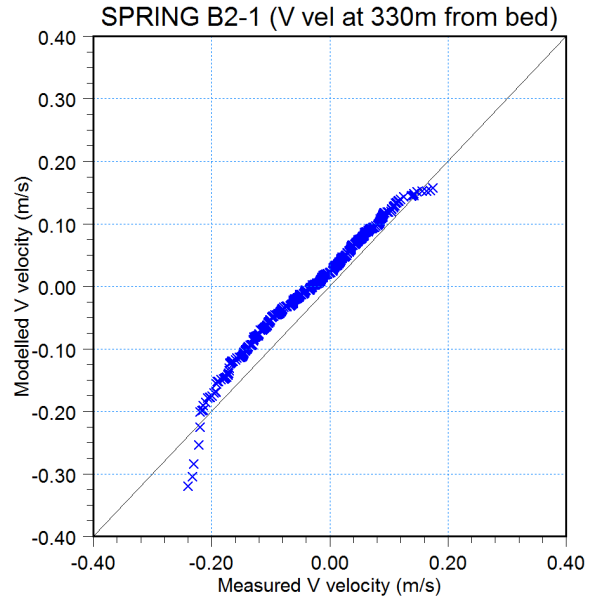
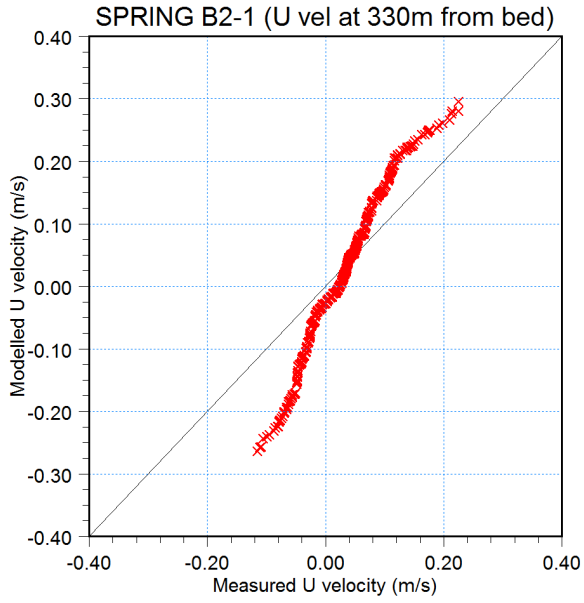


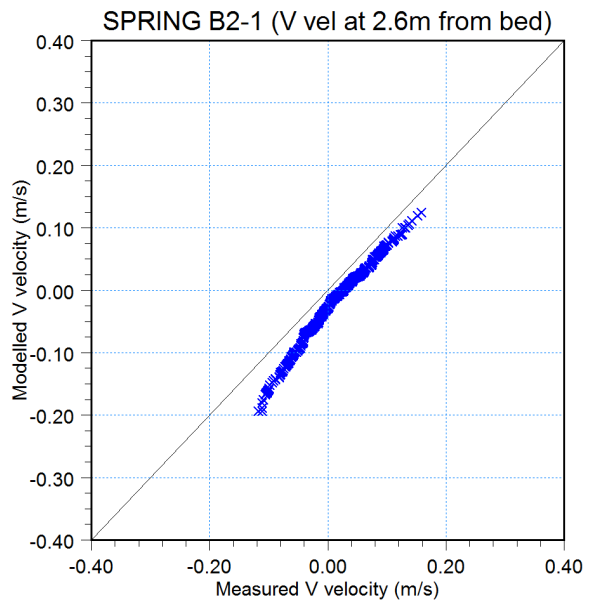
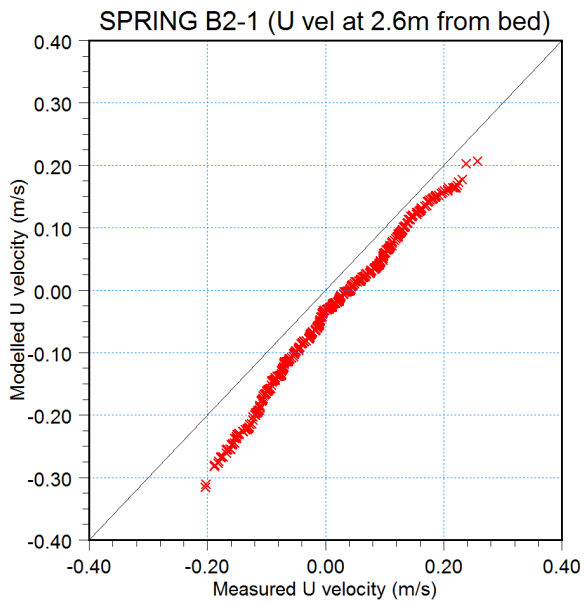
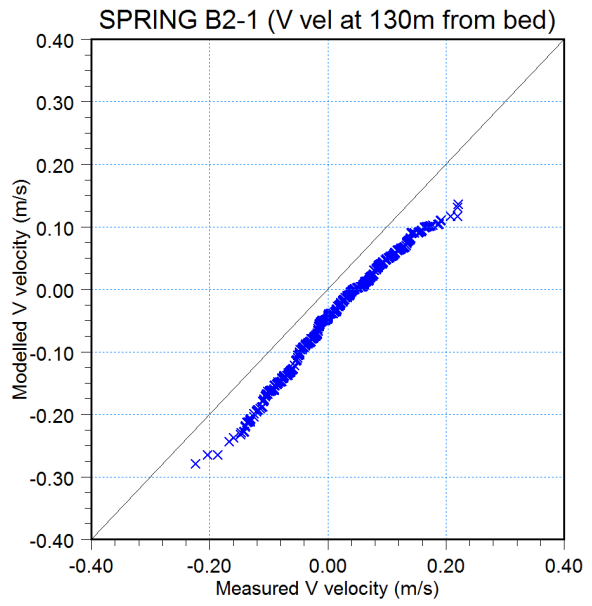
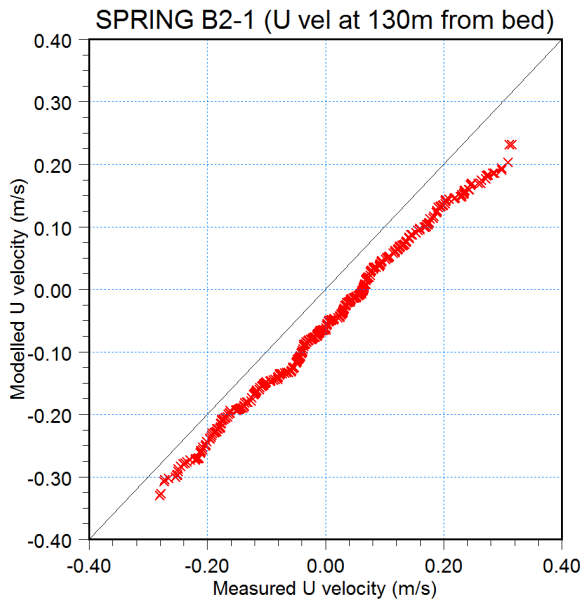


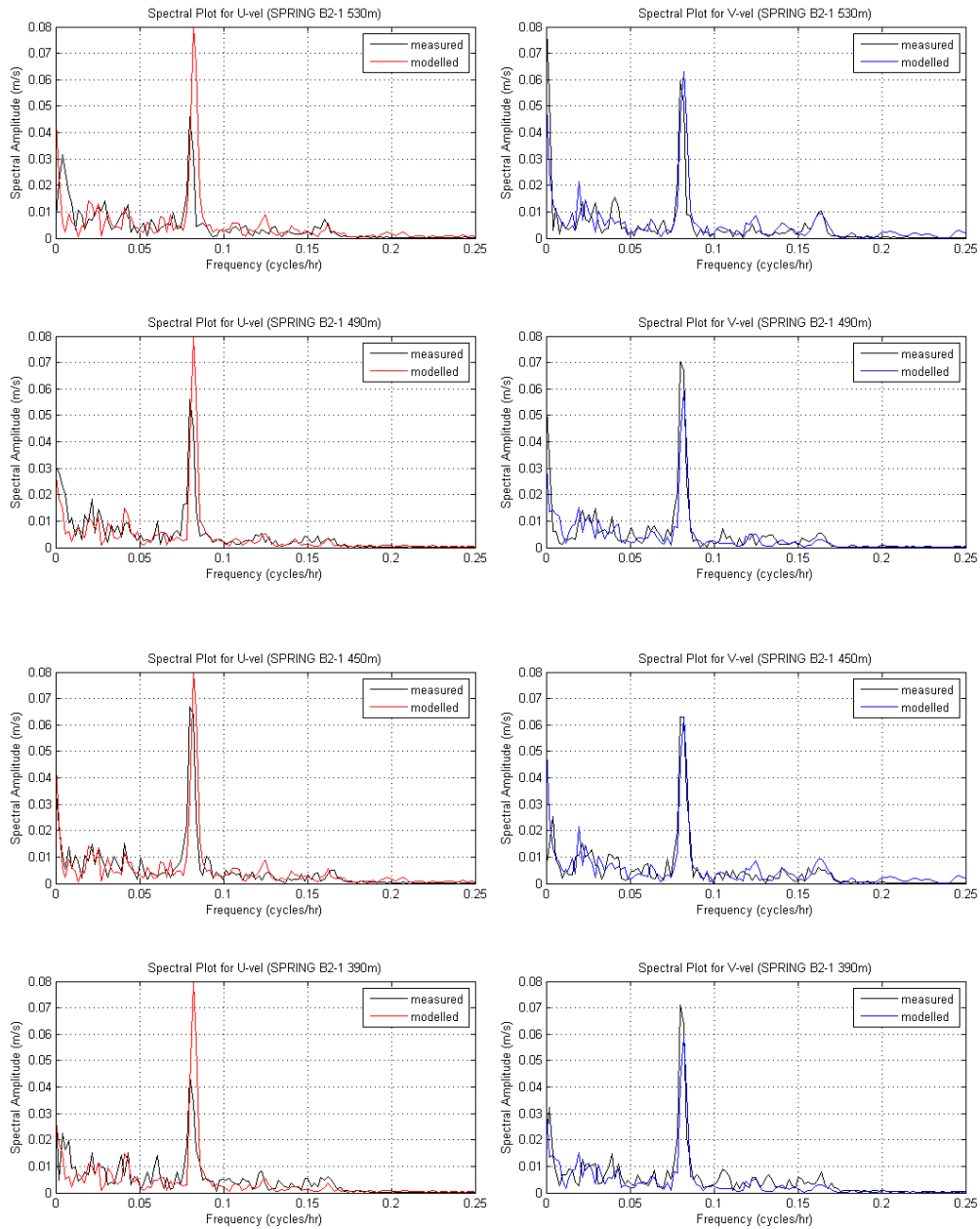


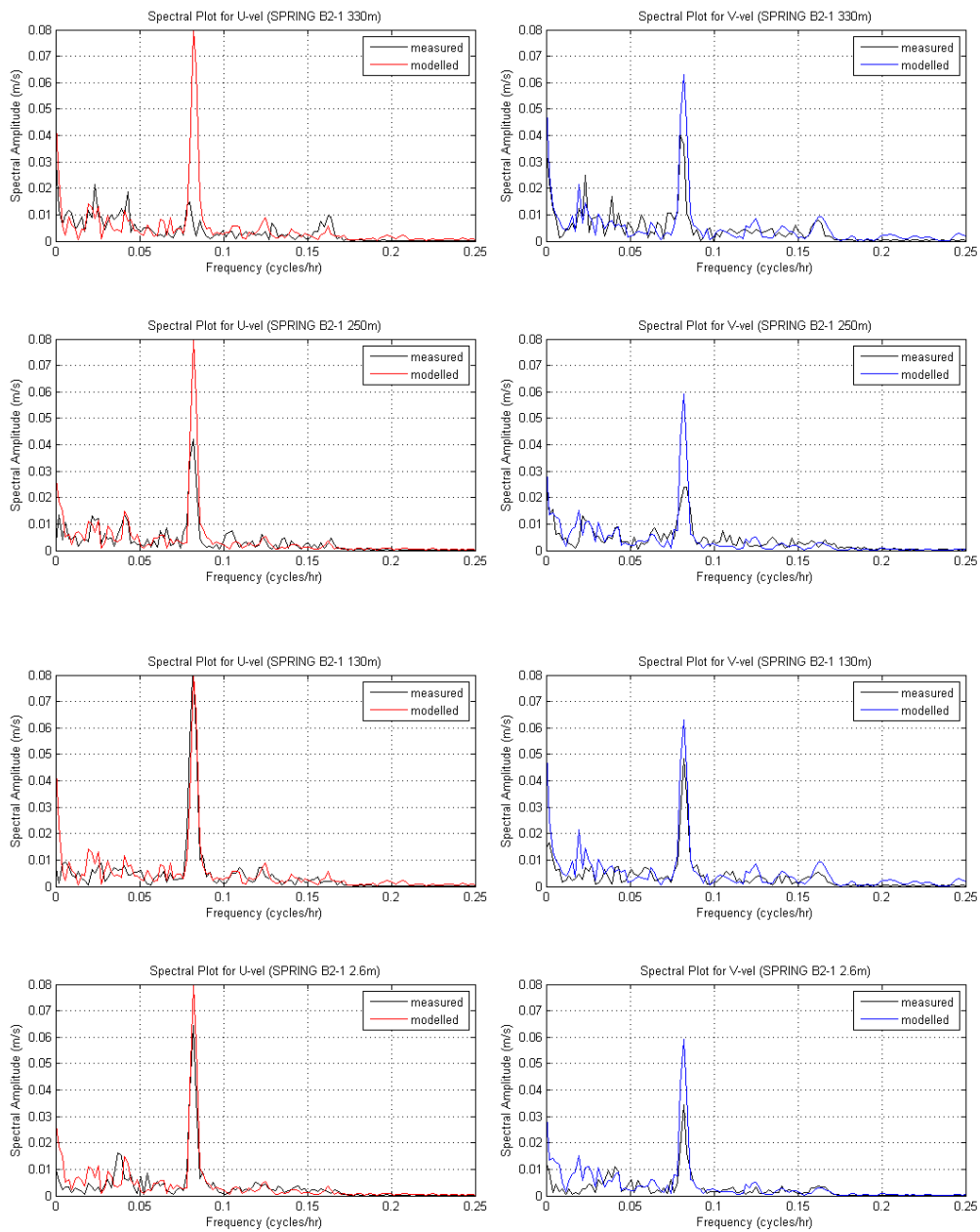








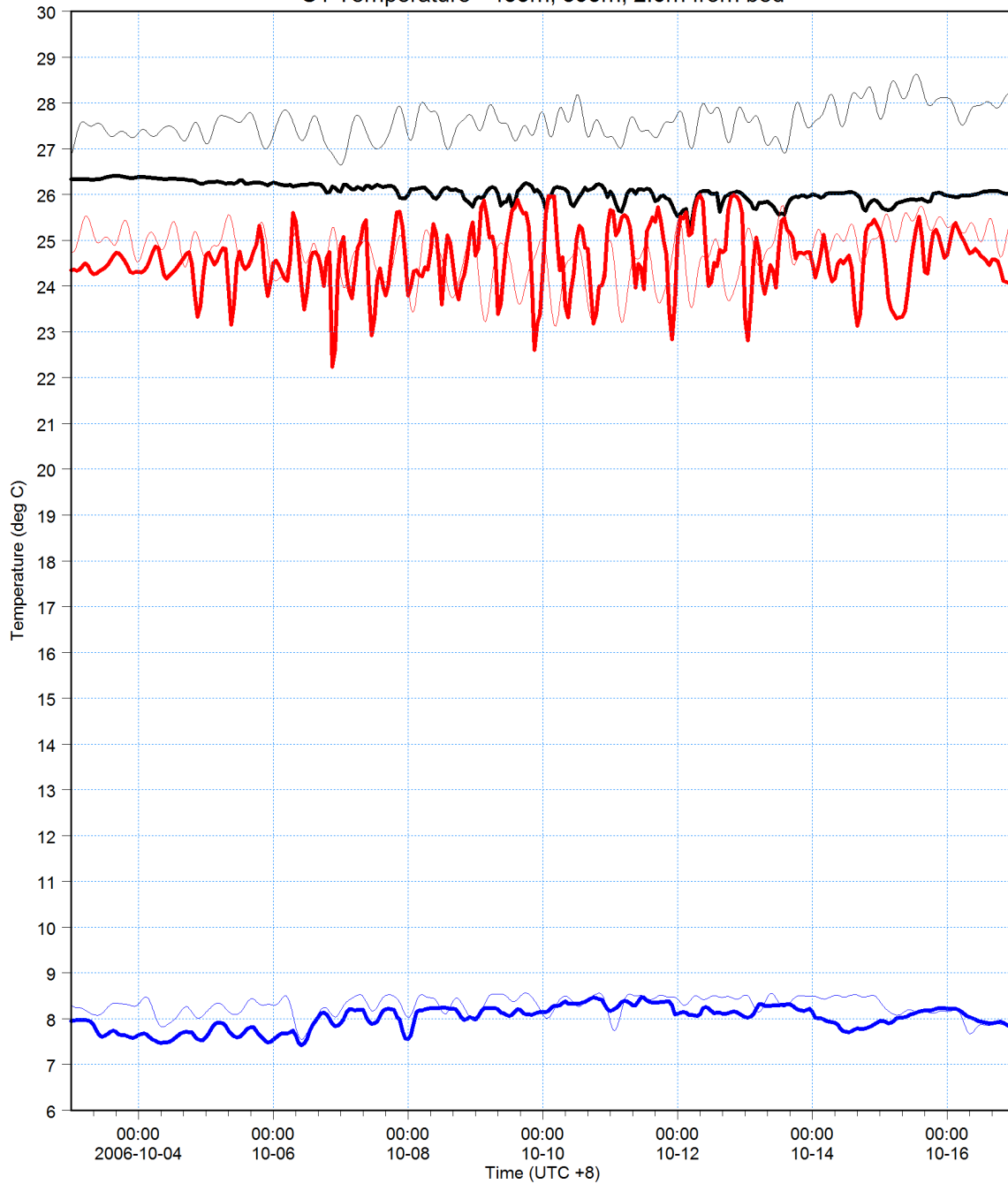






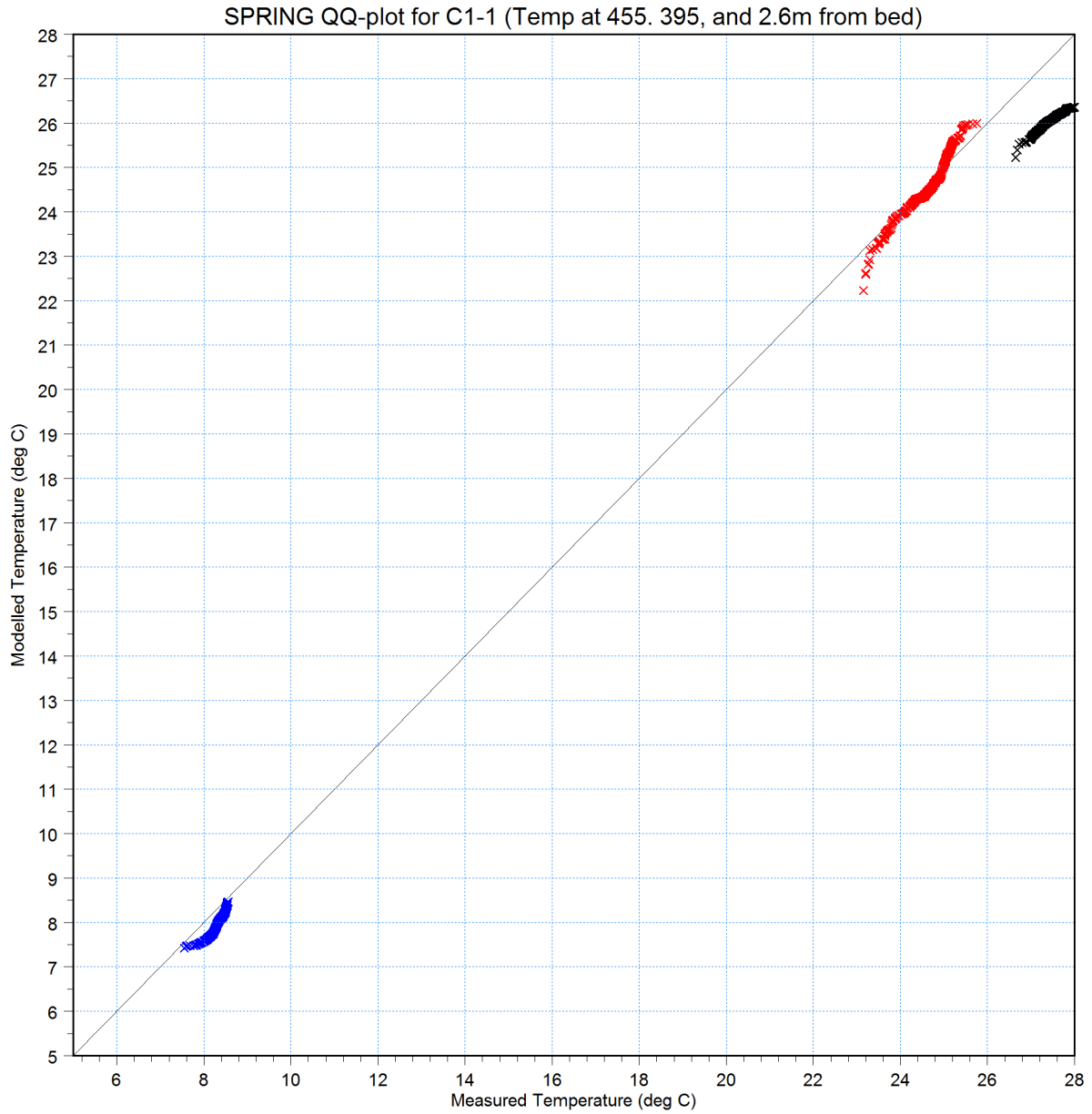
455m from bed: Temperature [C] [deg C] ———
measured [deg C] ———
395m from bed: Temperature [C] [deg C] ———
measured [deg C] ———
2.6m from bed: Temperature [C] [deg C] ———
measured [deg C] ———

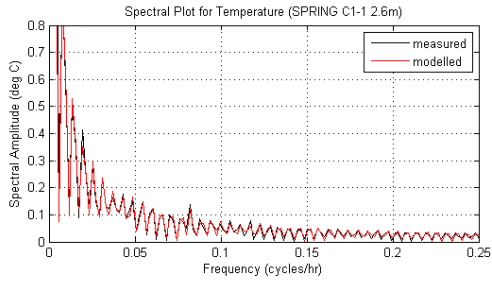
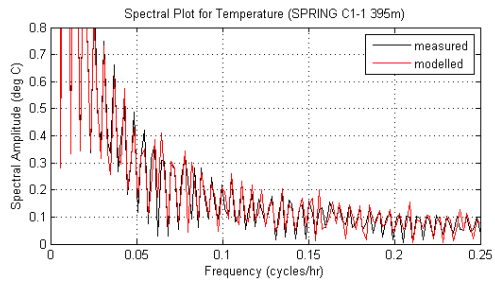
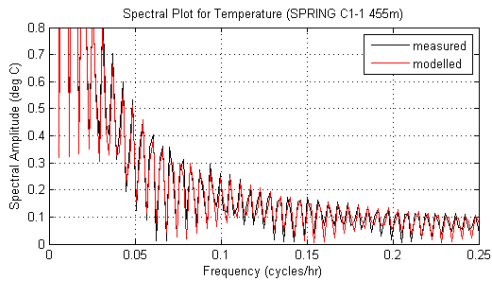
C1 Temperature - 455m, 395m, 2.6m from bed

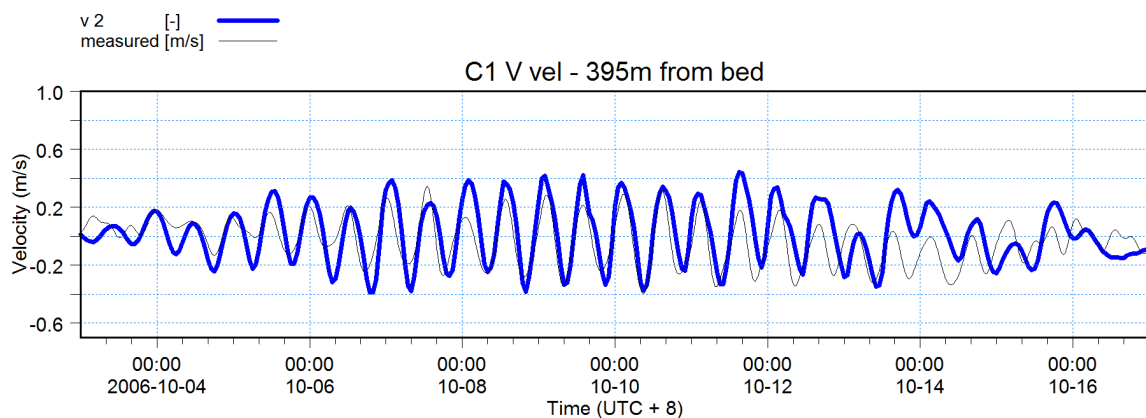
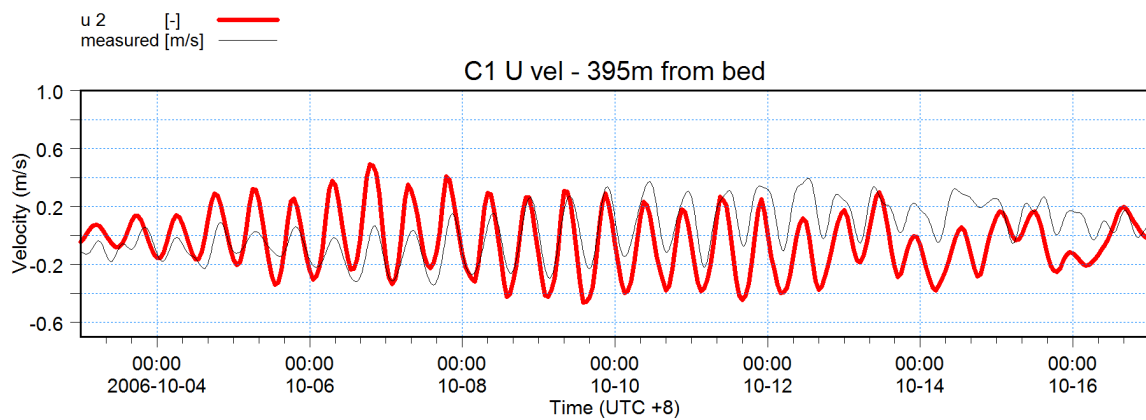
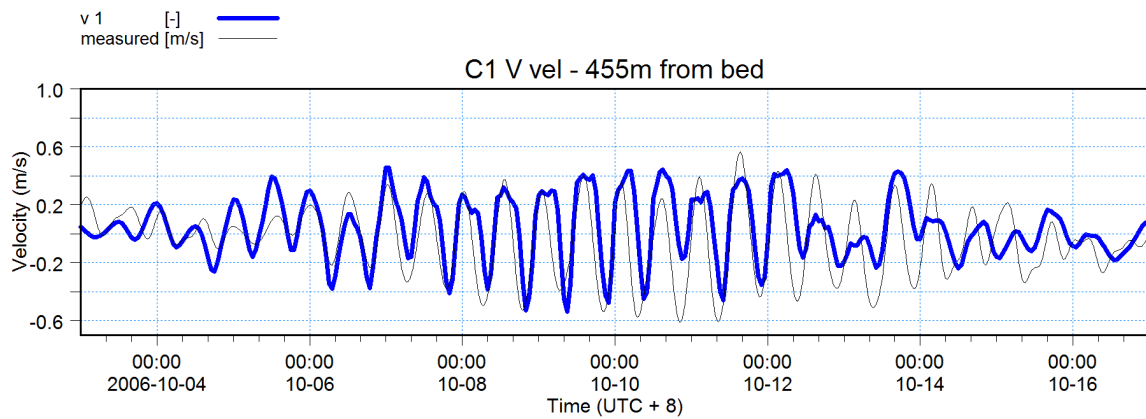
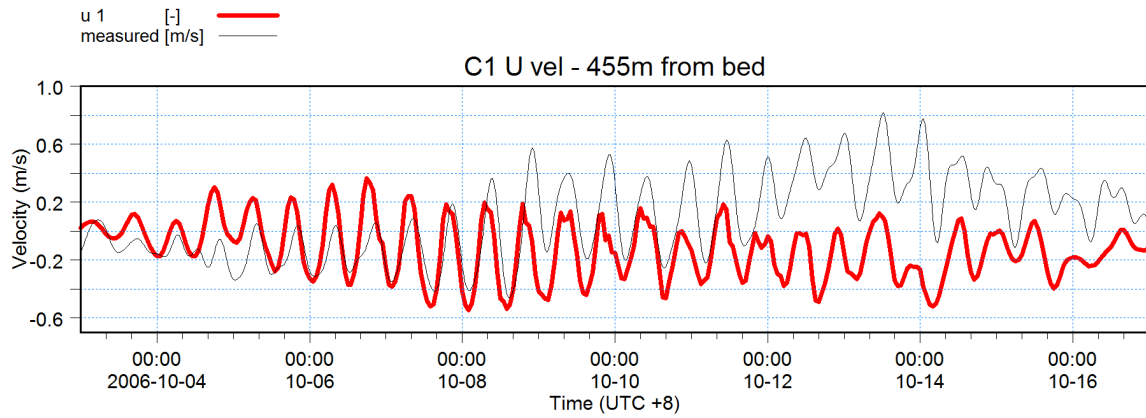


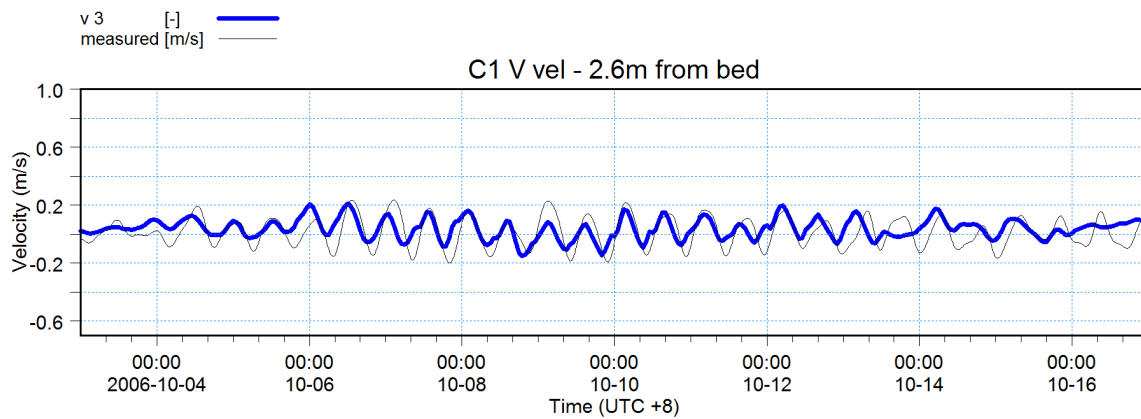
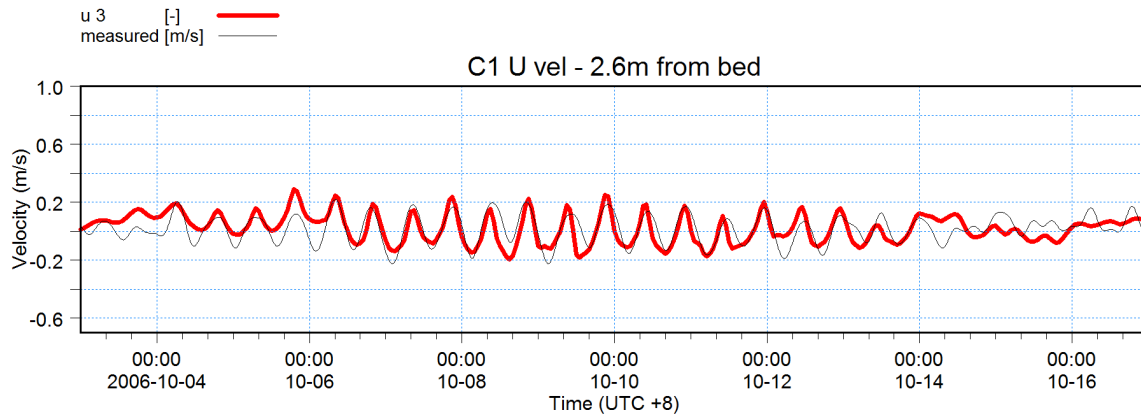


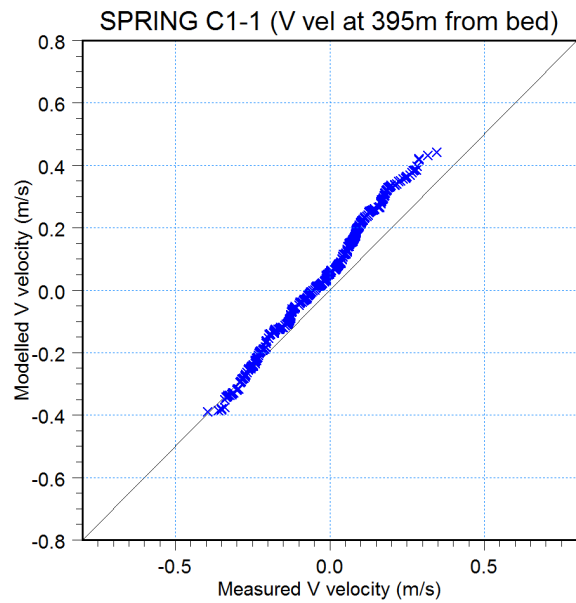
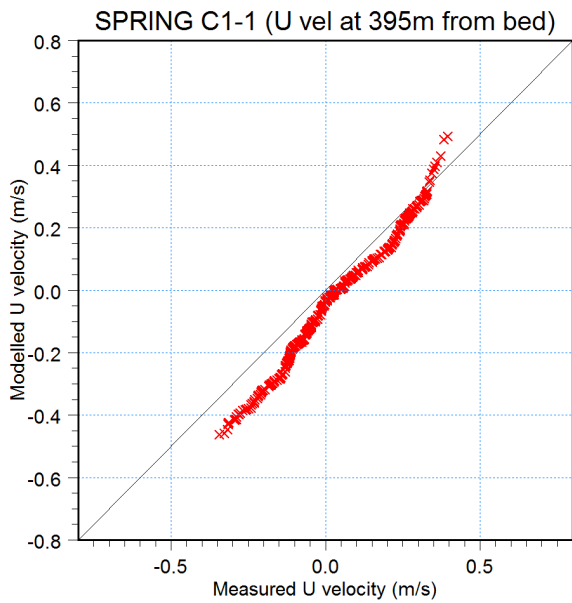
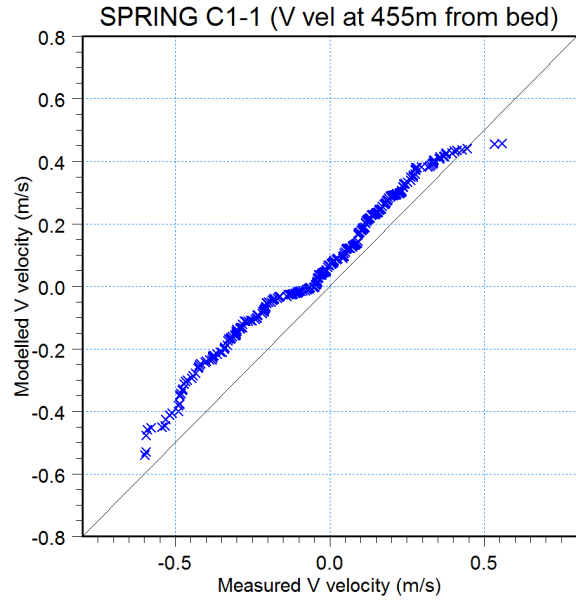
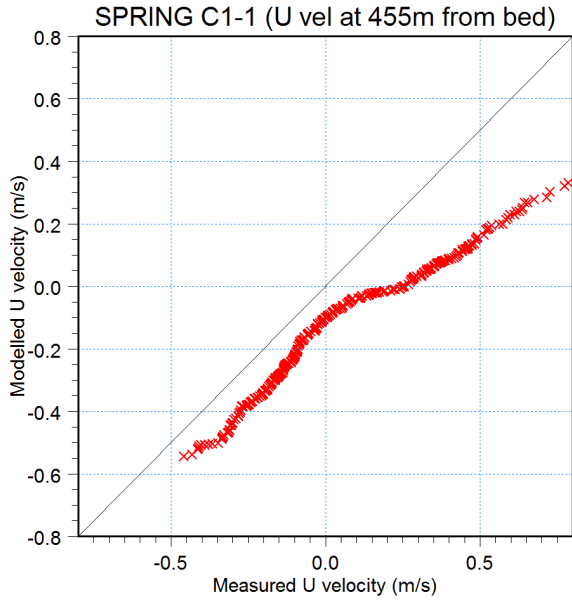
T at 455m × ×
T at 395m × ×
T at 2.6m × ×

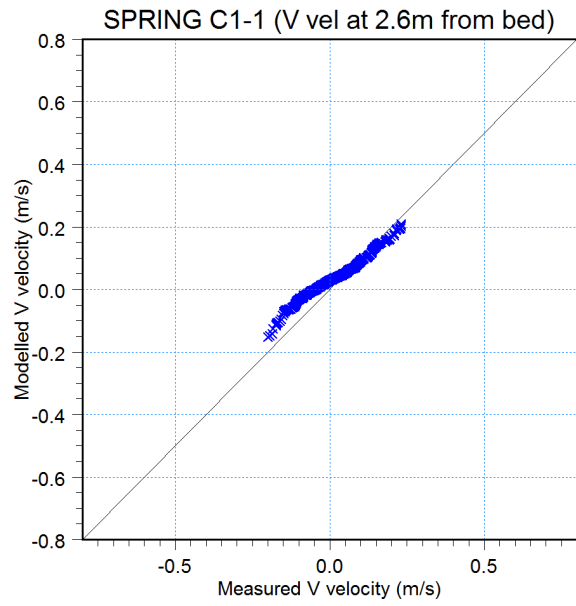
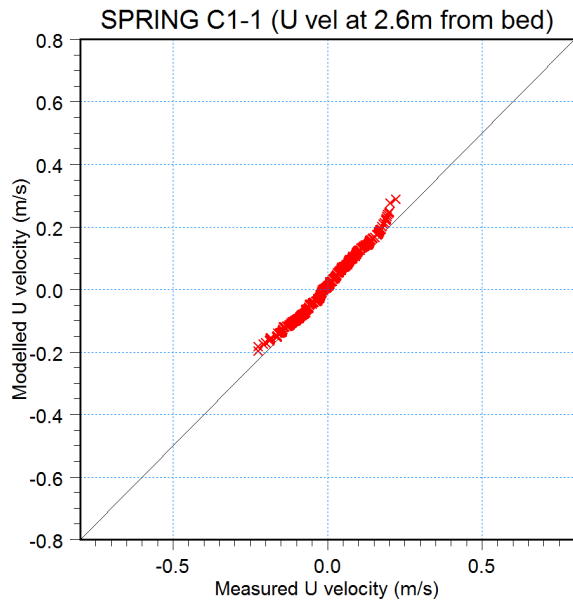


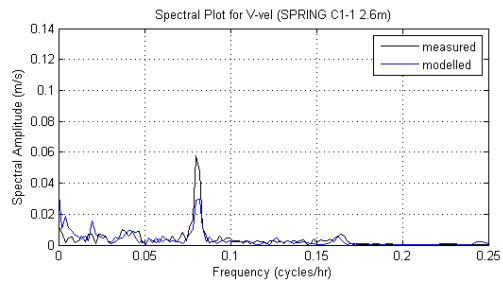
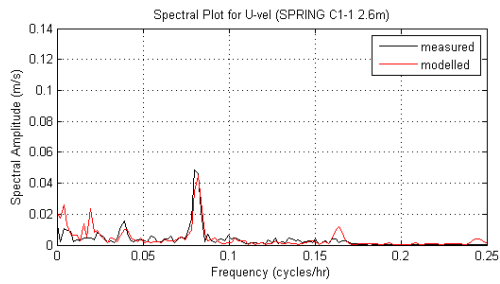
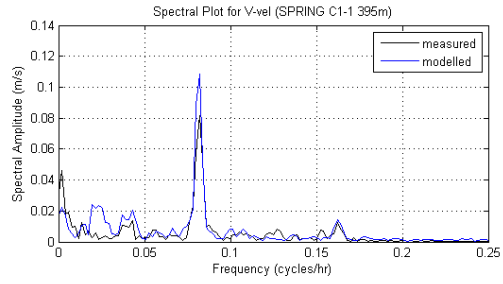
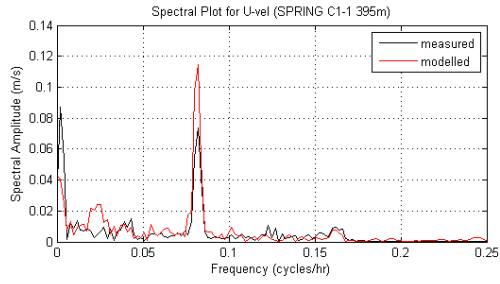
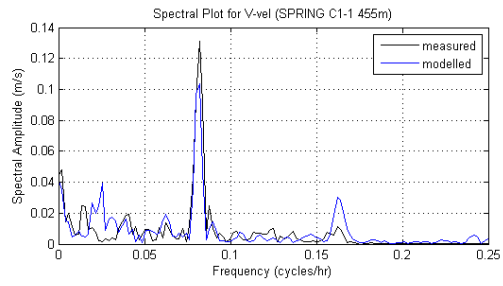
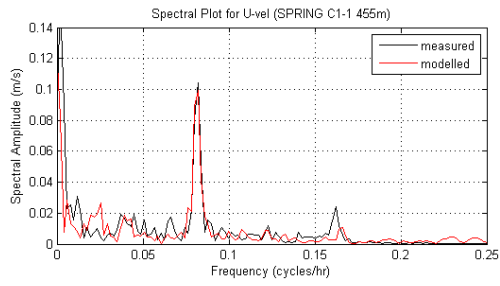


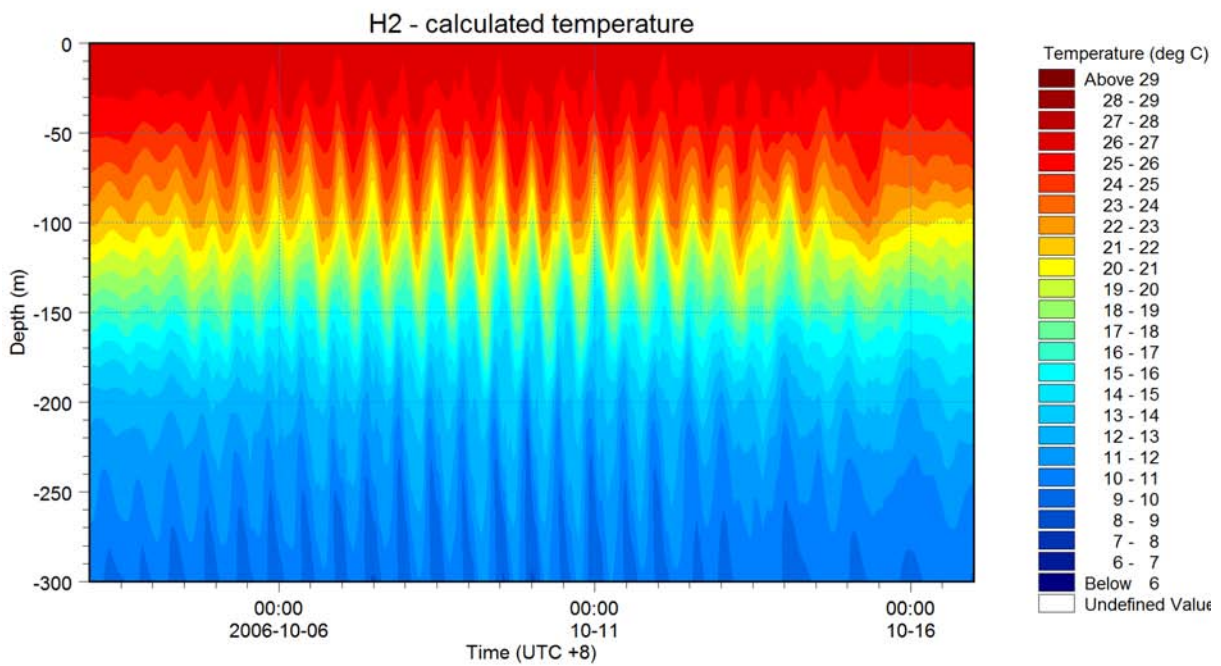
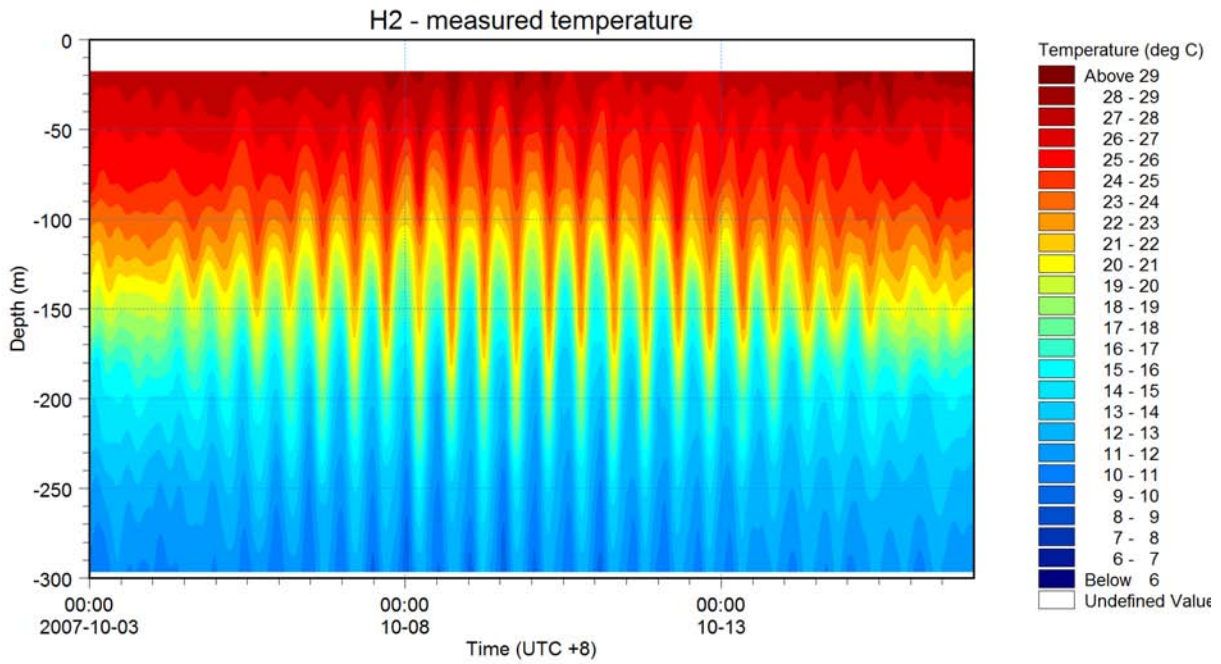








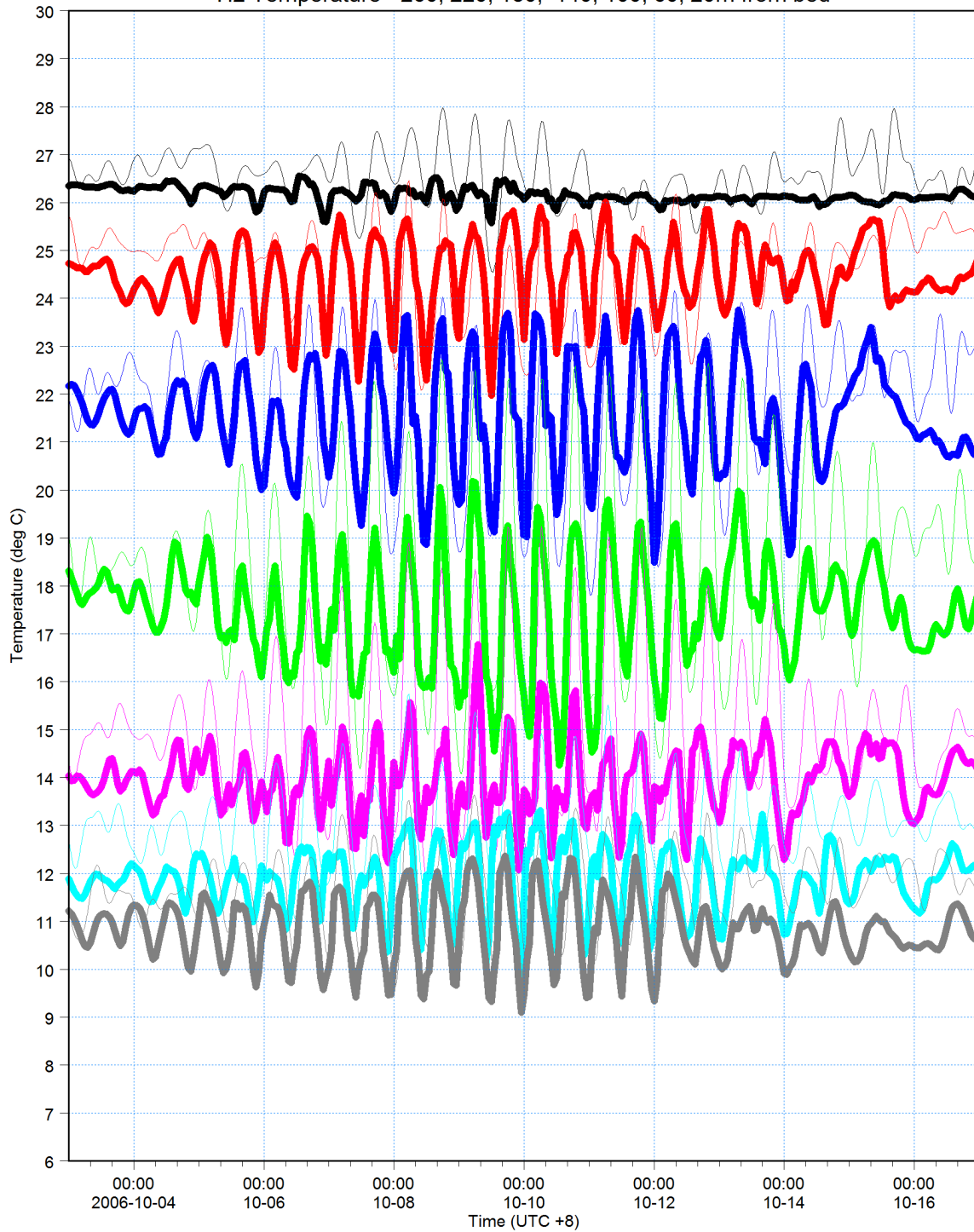






260m from bed: Temperature [C] [deg C] 
measured  [deg C]
220m from bed: Temperature [C] [deg C] 
measured  [deg C]
180m from bed: Temperature [C] [deg C] 
measured  [deg C]
140m from bed: Temperature [C] [deg C] 
measured  [deg C]
100m from bed: Temperature [C] [deg C] 
measured  [deg C]
60m from bed: Temperature [C] [deg C] 
measured  [deg C]
20m from bed: Temperature [C] [deg C] 
measured  [deg C]

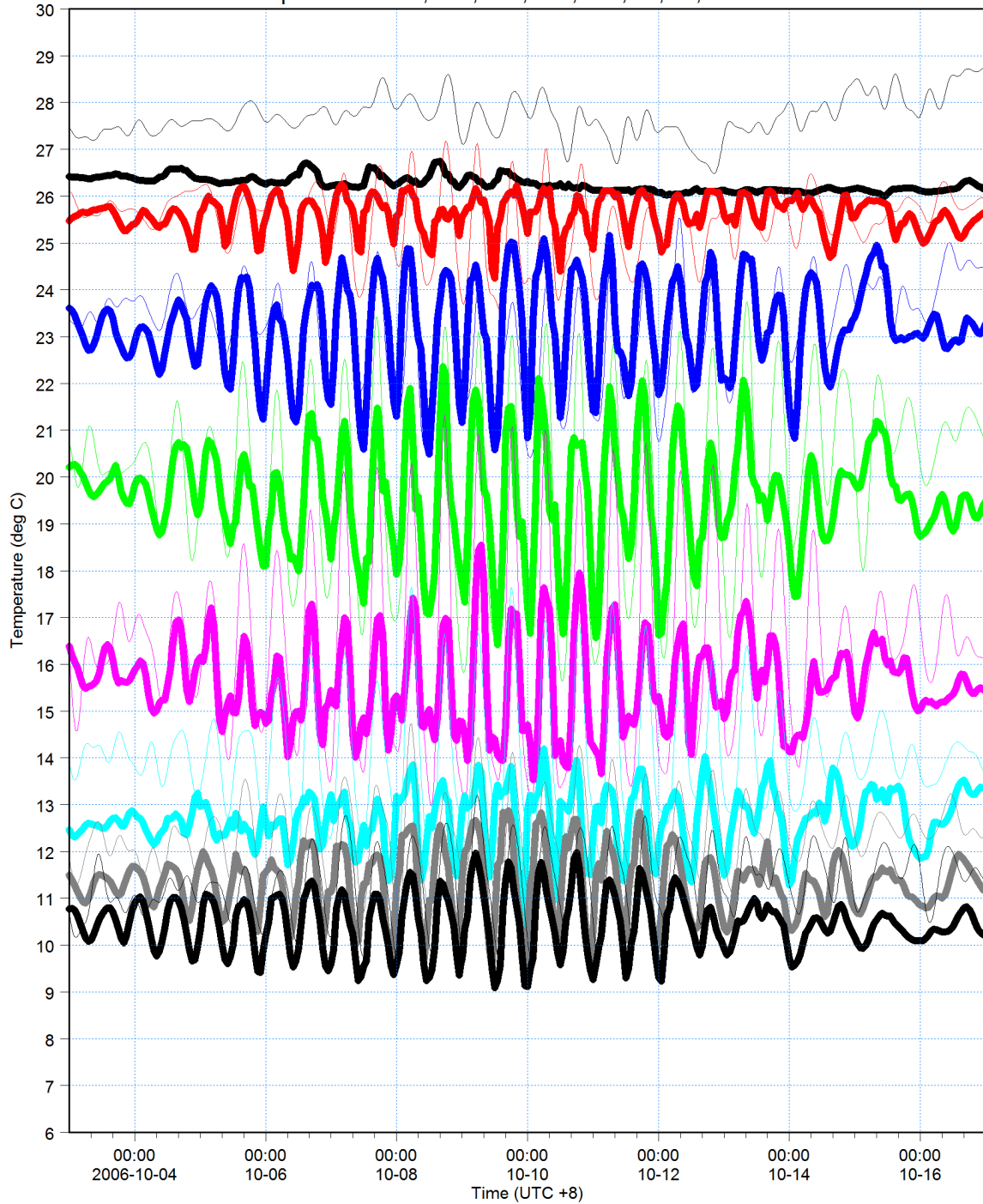
H2 Temperature - 260, 220, 180, 140, 100, 60, 20m from bed





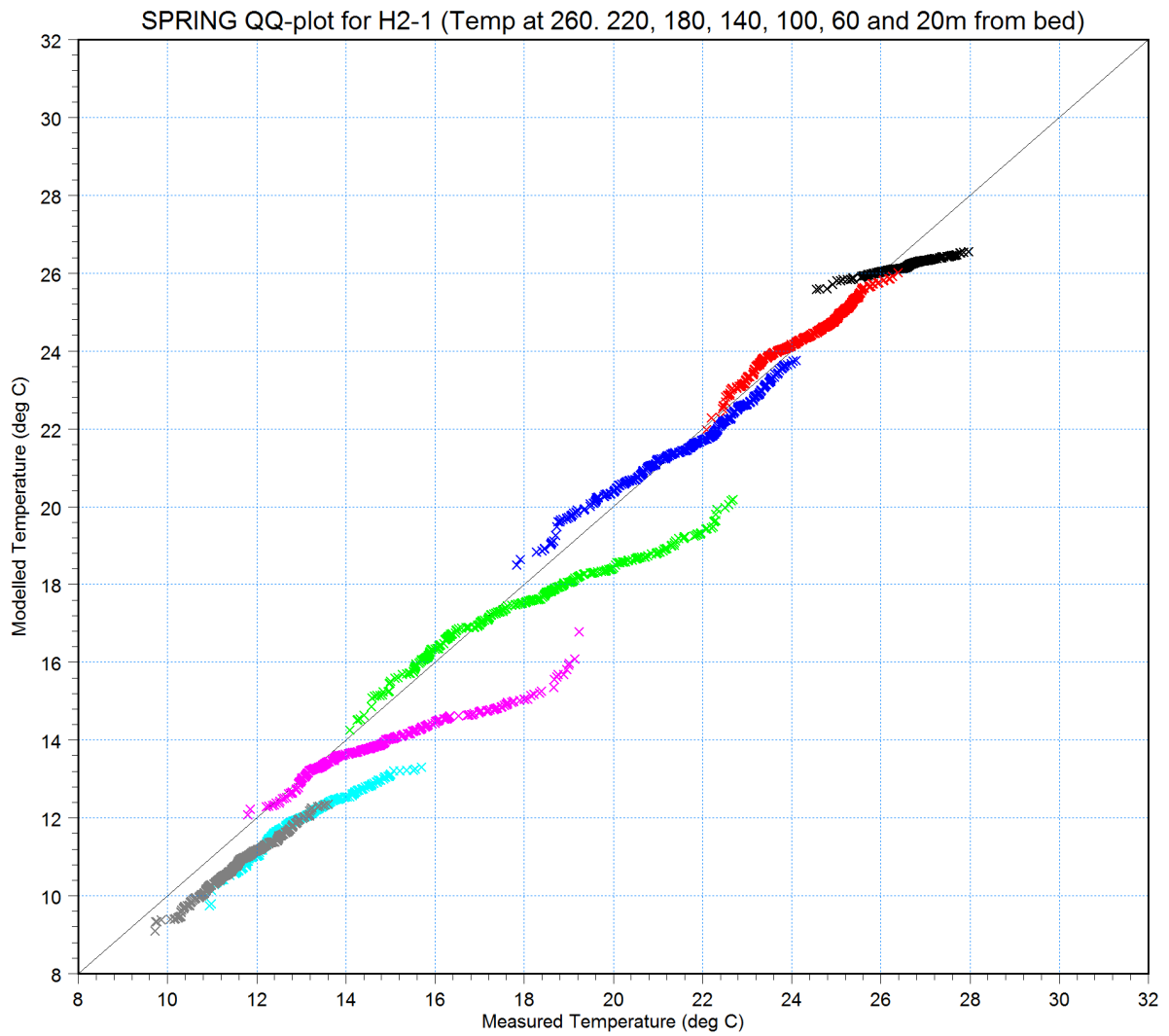
280m from bed: Temperature [C] [deg C] ———
measured [deg C] ———
240m from bed: Temperature [C] [deg C] ———
measured [deg C] ———
200m from bed: Temperature [C] [deg C] ———
measured [deg C] ———
160m from bed: Temperature [C] [deg C] ———
measured [deg C] ———
120m from bed: Temperature [C] [deg C] ———
measured [deg C] ———
80m from bed: Temperature [C] [deg C] ———
measured [deg C] ———
40m from bed: Temperature [C] [deg C] ———
measured [deg C] ———
2.6m from bed: Temperature [C] [deg C] ———
measured [deg C] ———

H2 Temperature - 280, 240, 200, 160, 120, 80, 40, 2.6m from bed



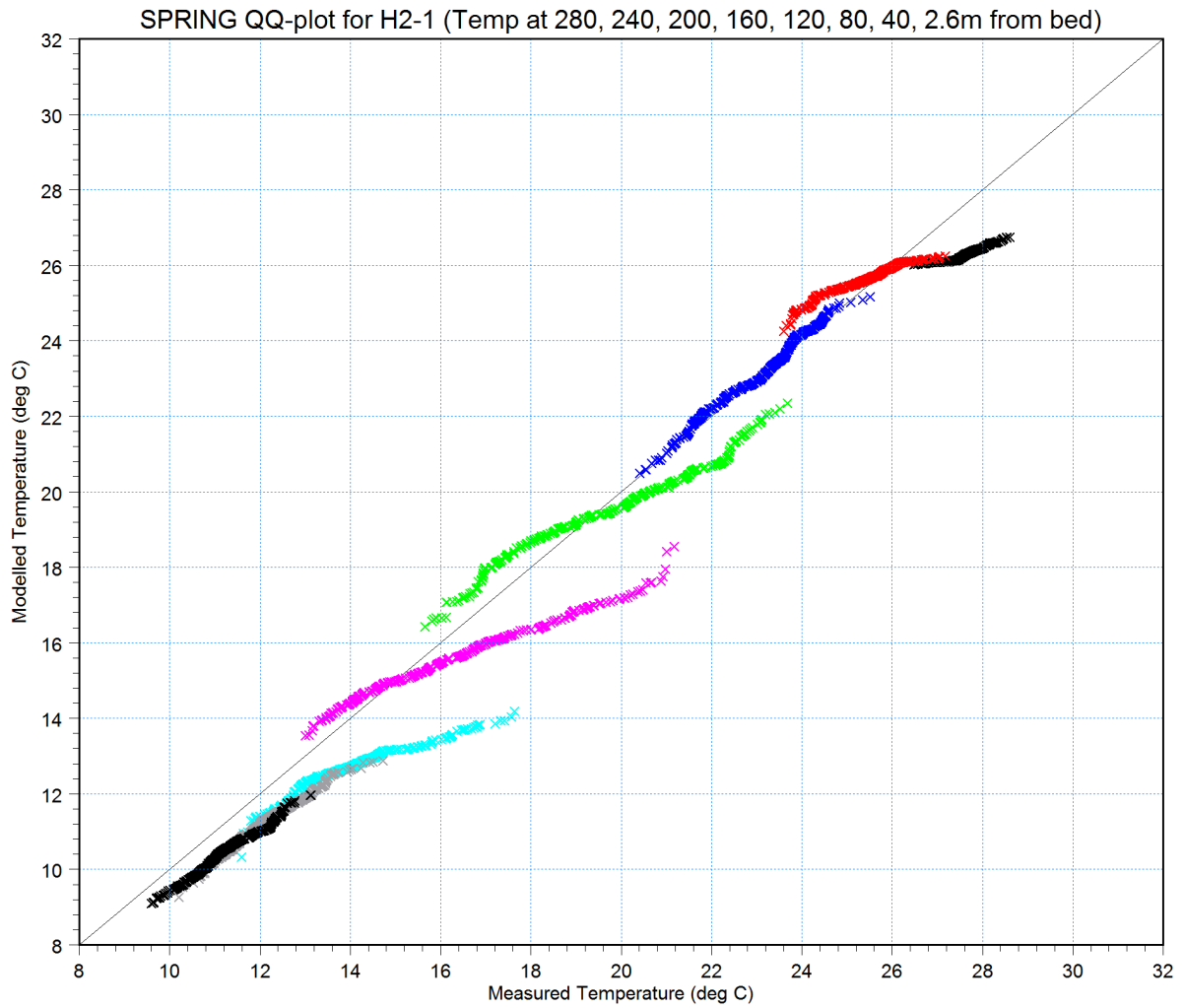


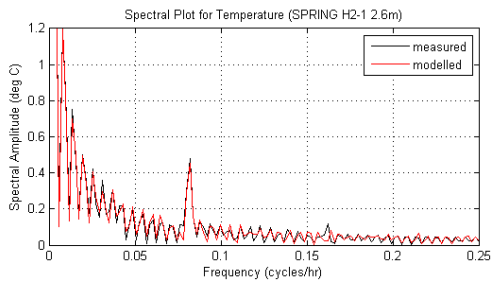
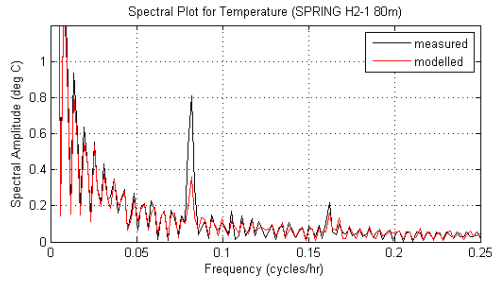
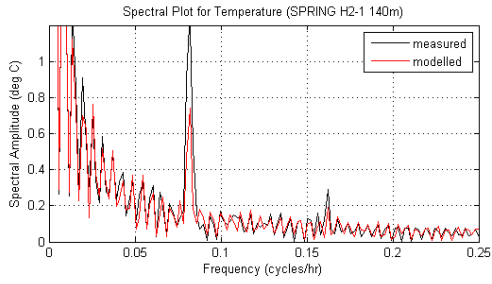
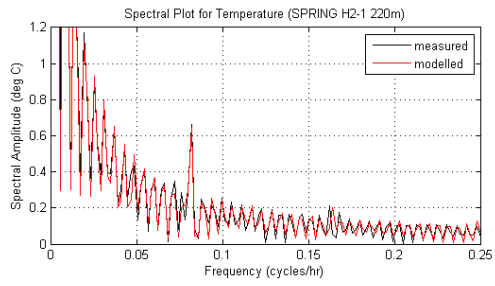
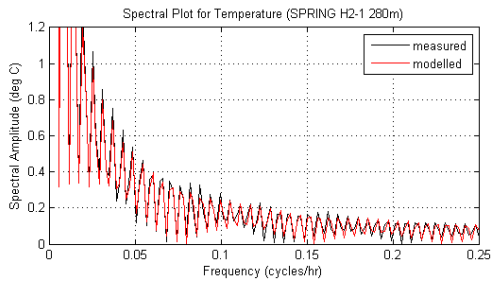
- T at 260m × ×
- T at 220m × ×
- T at 180m × ×
- T at 140m × ×
- T at 100m × ×
- T at 60m × ×
- T at 20m × ×

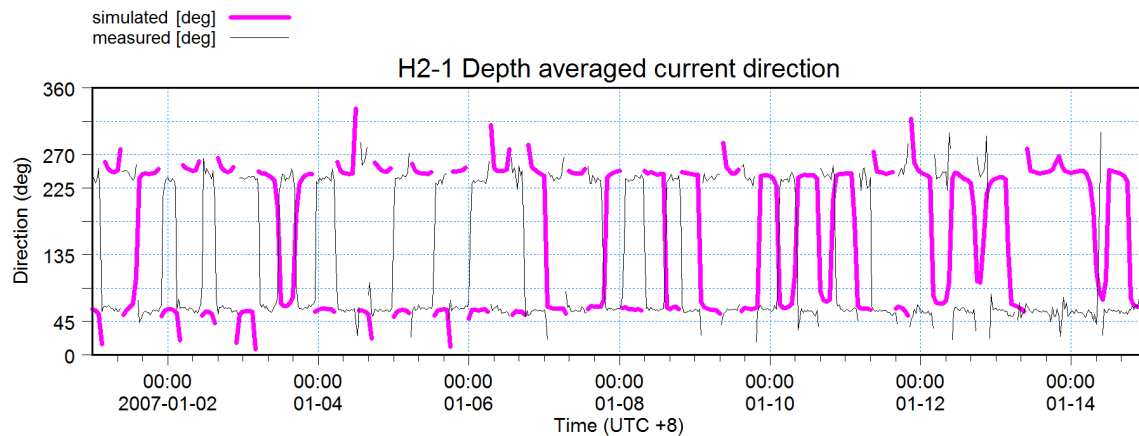
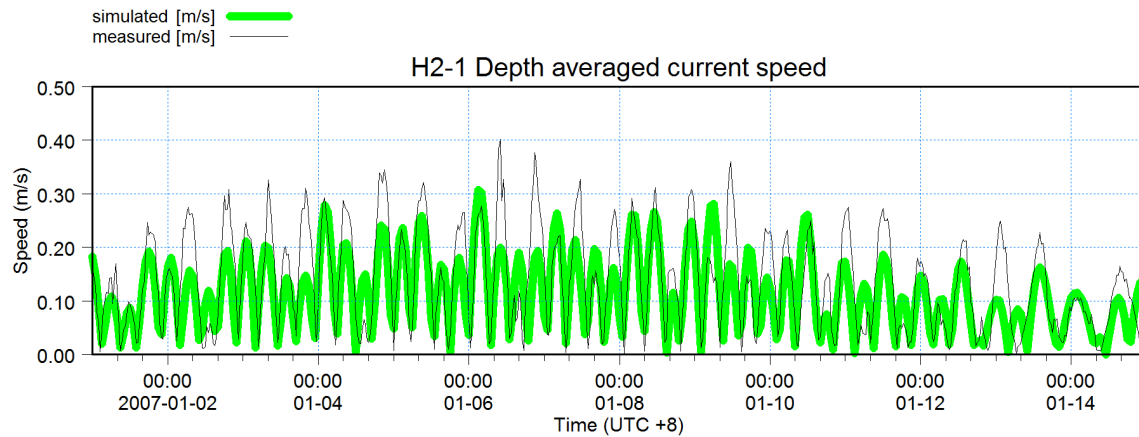
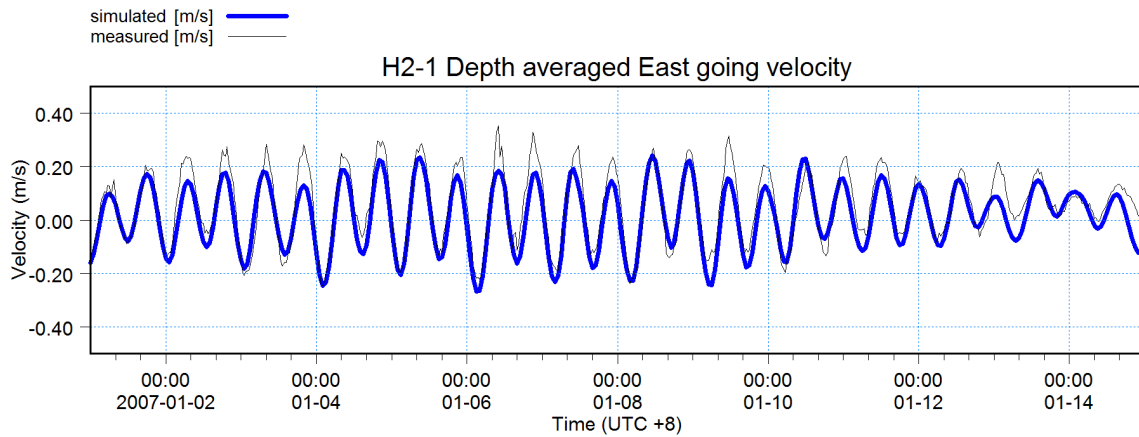
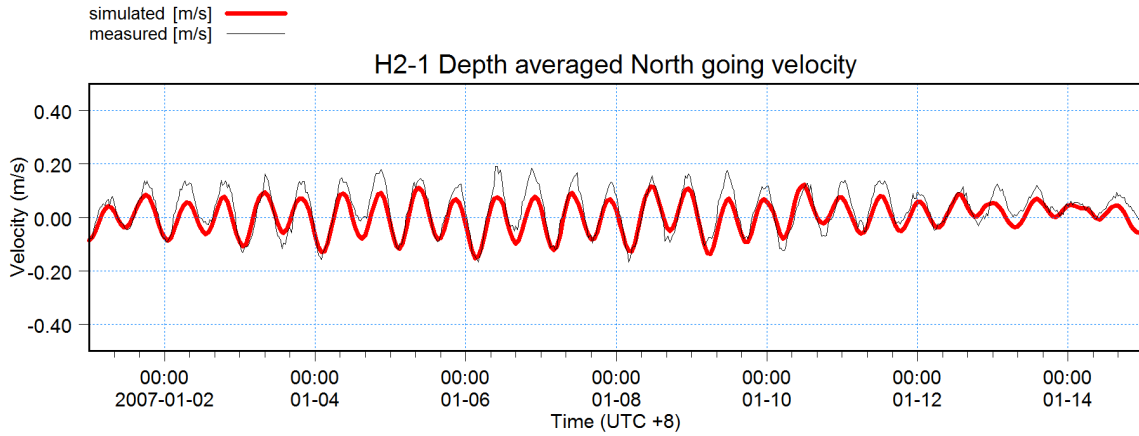




- T at 280m × ×
- T at 240m × ×
- T at 200m × ×
- T at 160m × ×
- T at 120m × ×
- T at 80m × ×
- T at 40m × ×
- T at 2.6m × ×

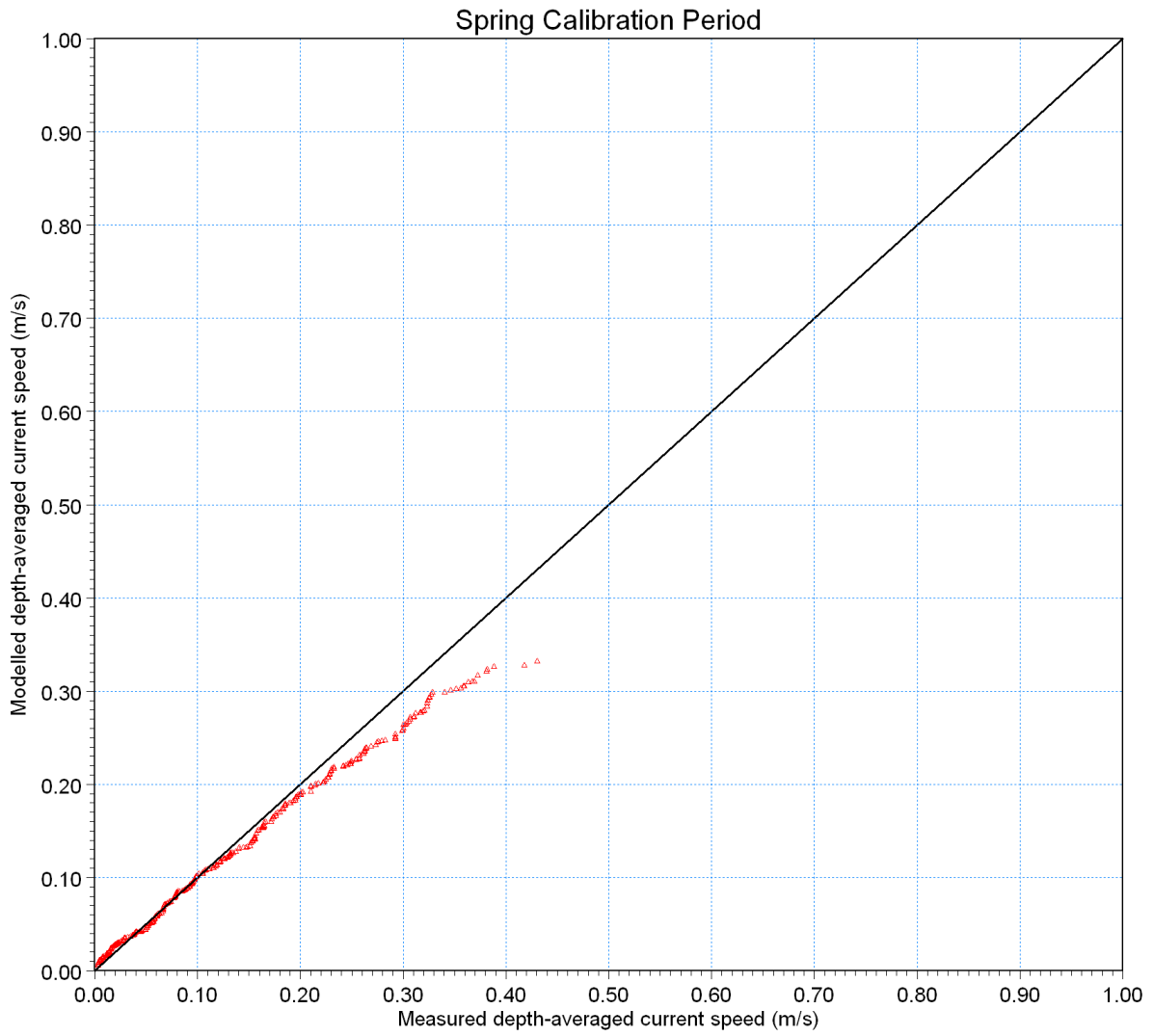


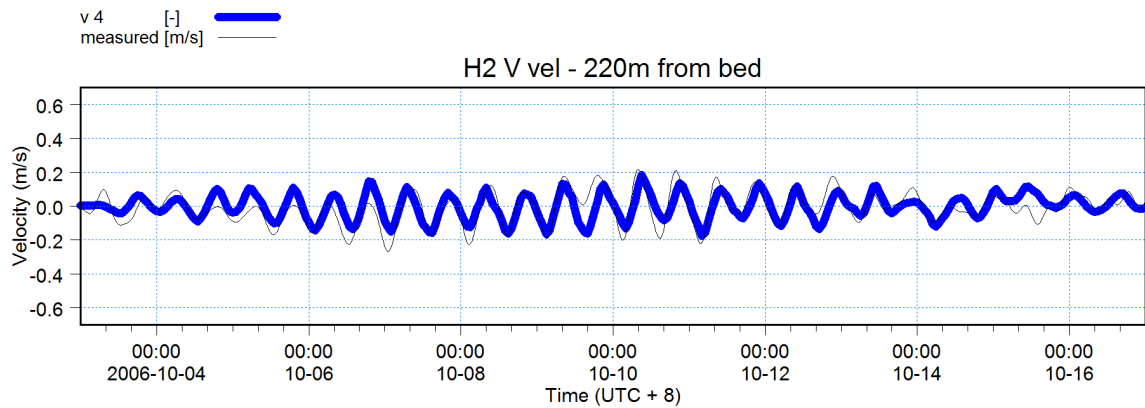
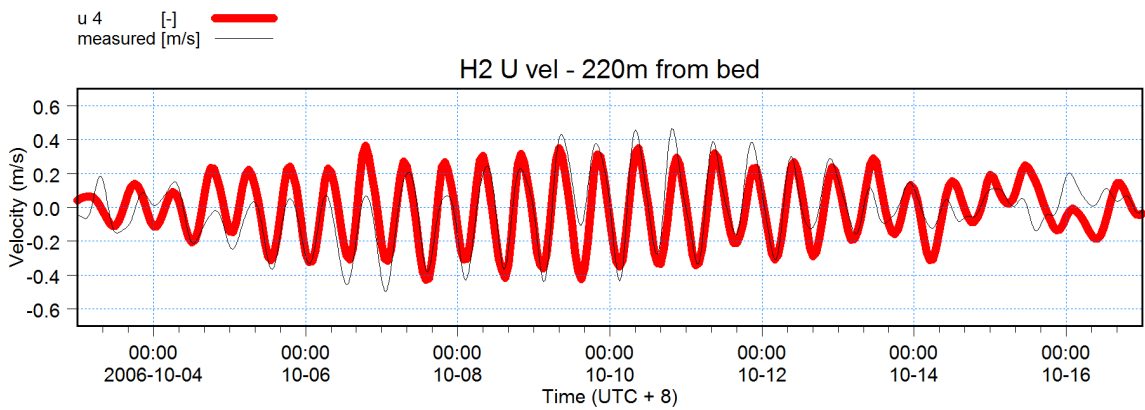
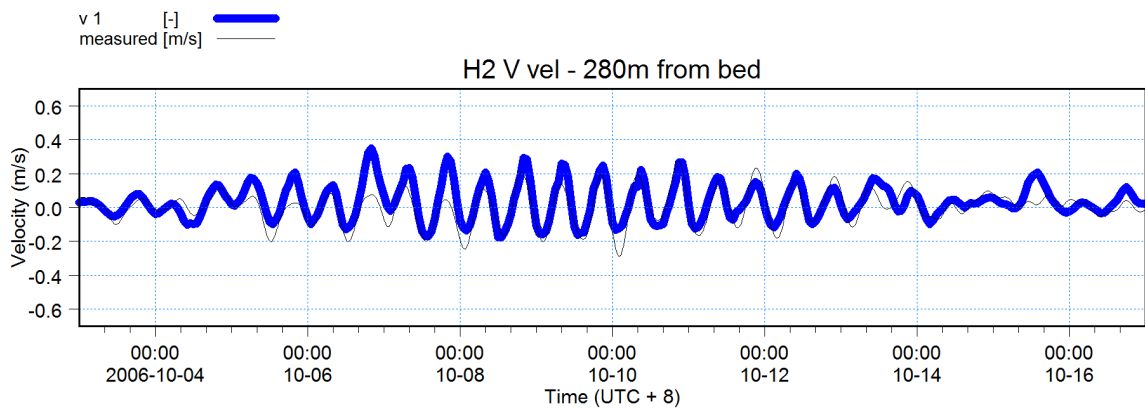
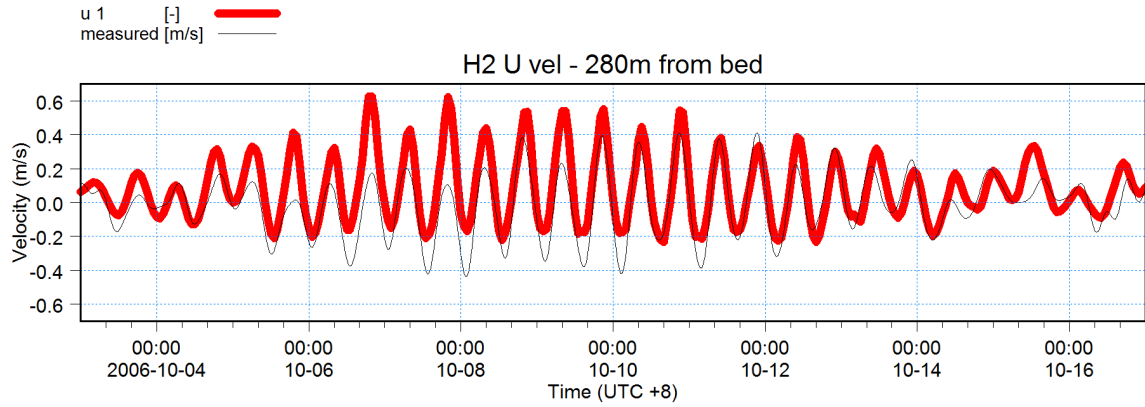


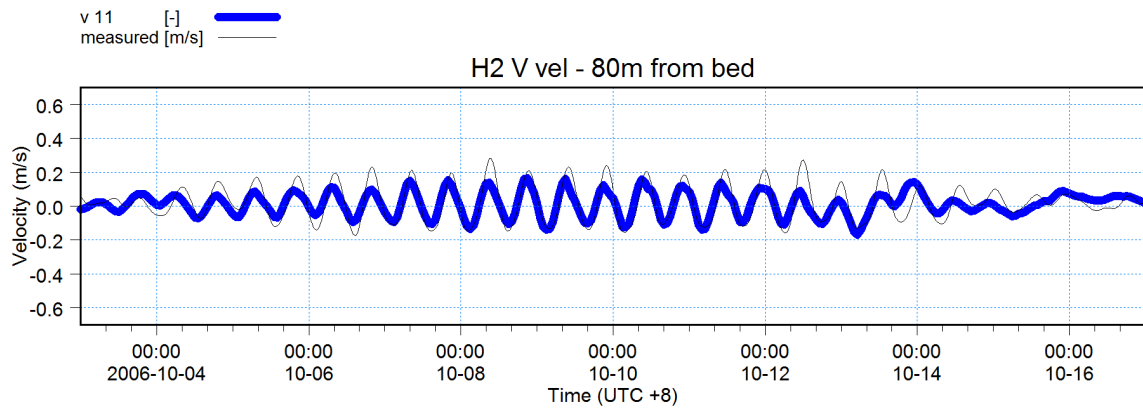
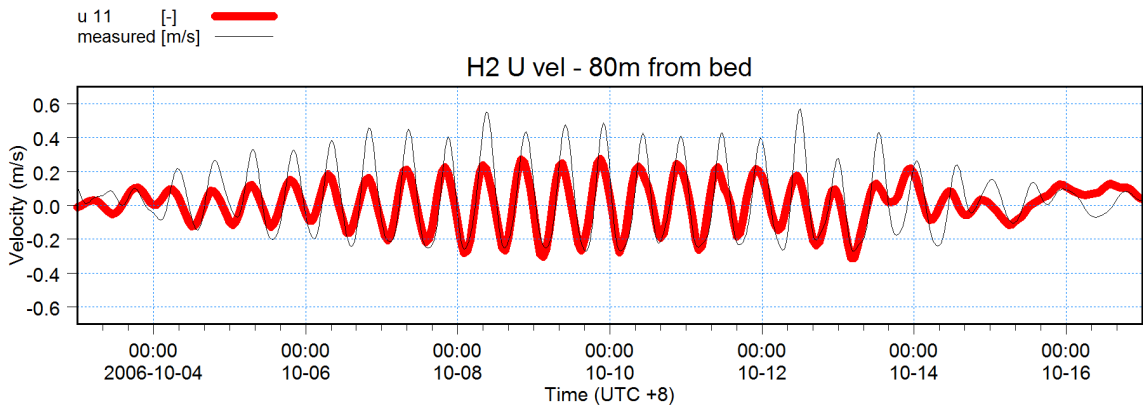
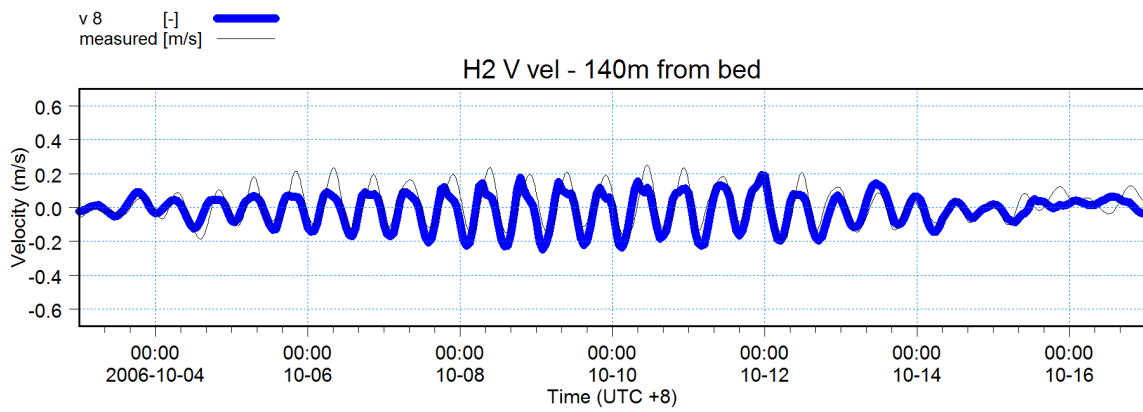
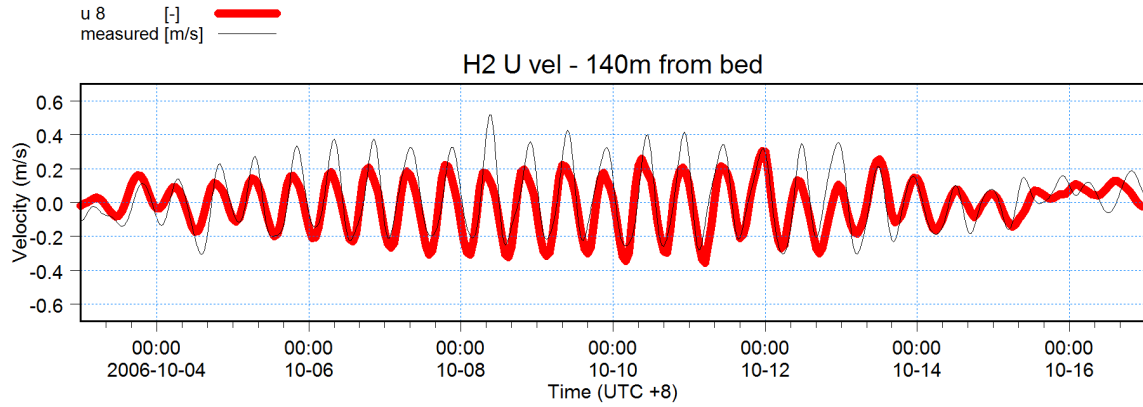


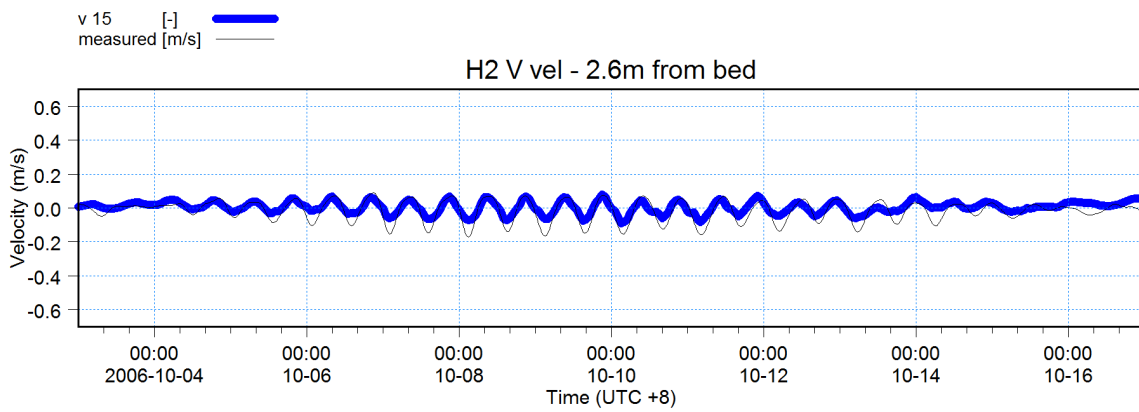
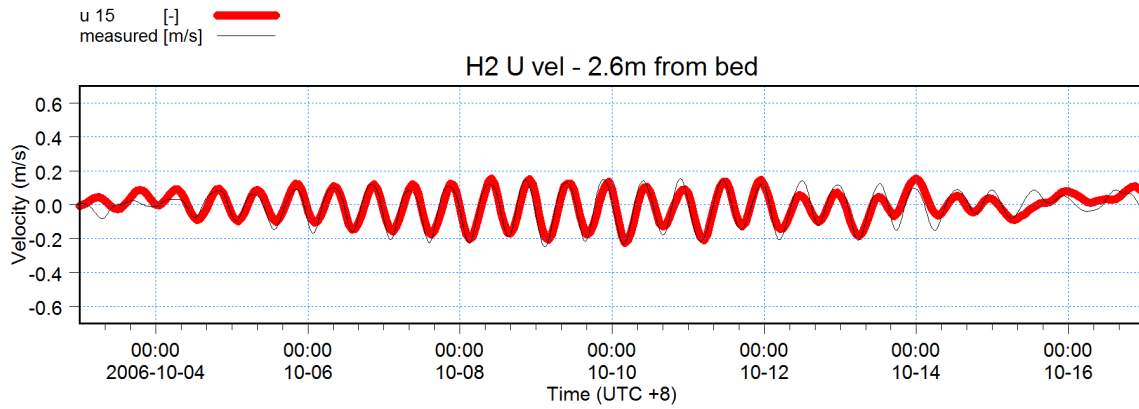


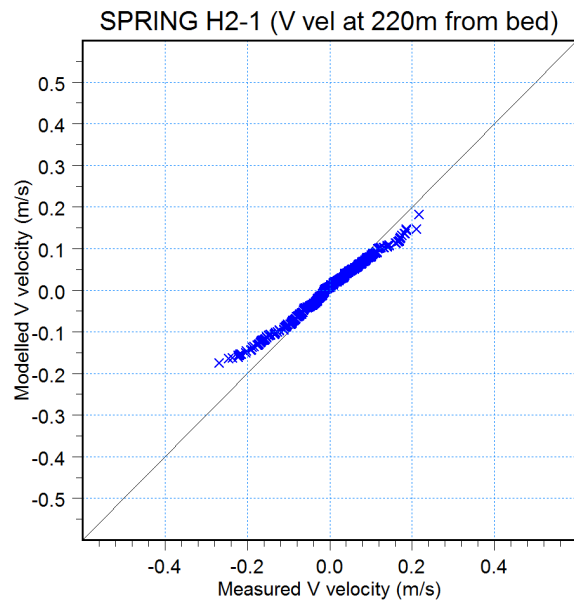
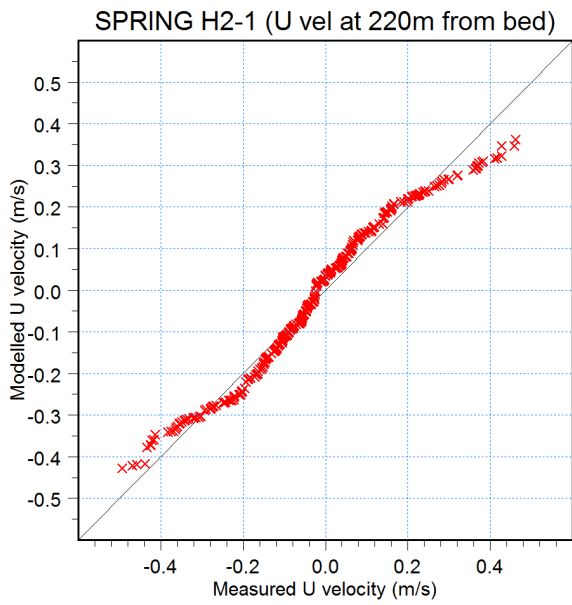
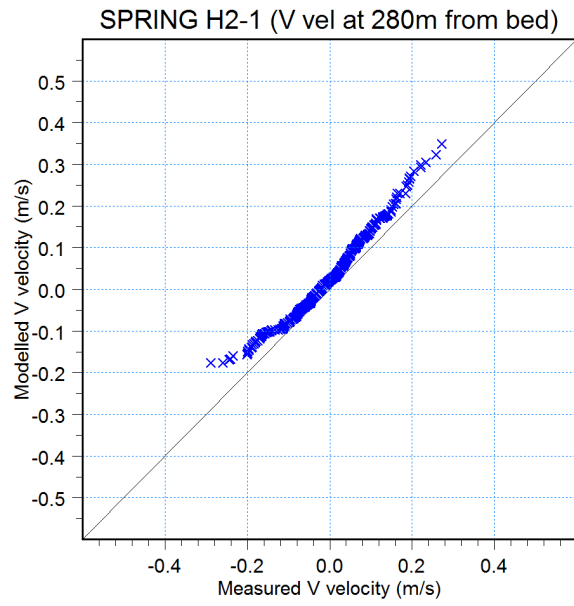
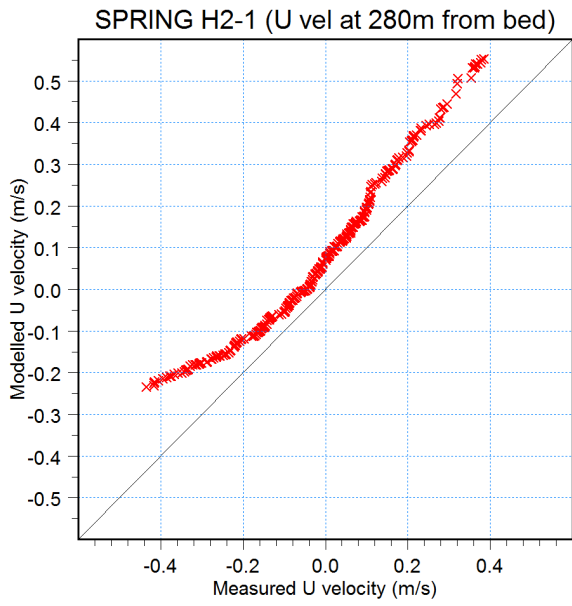
H2 △ △

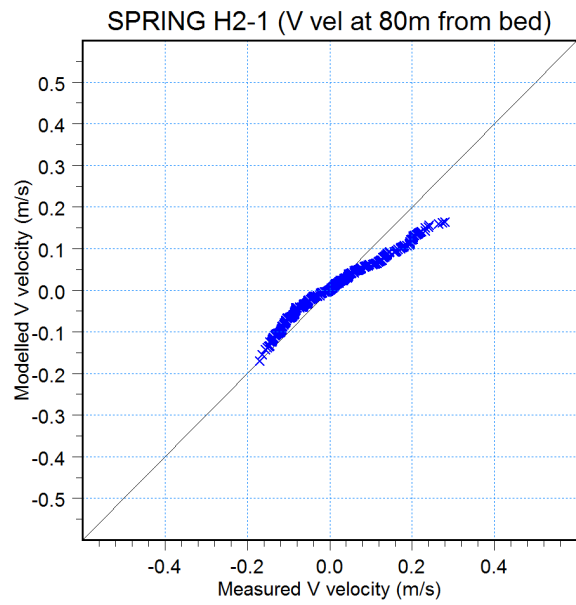
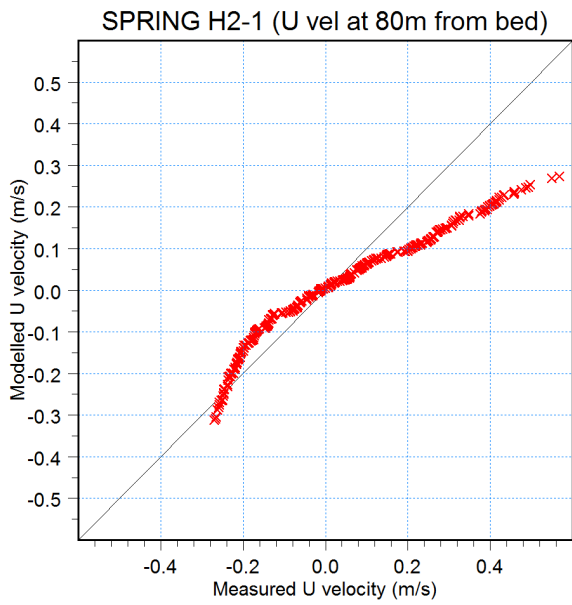
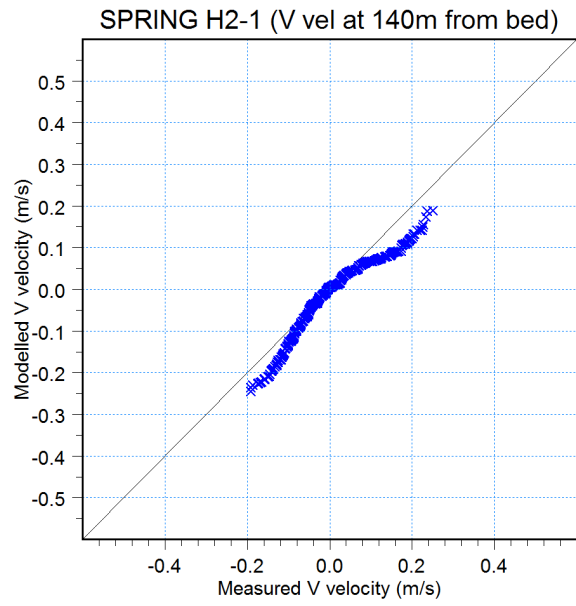
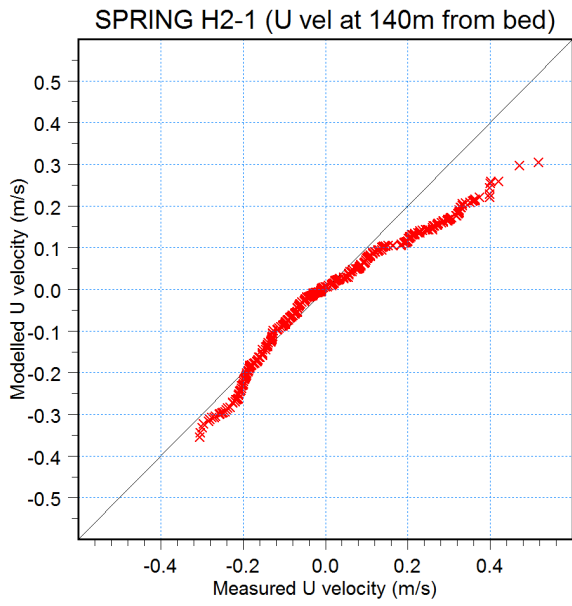


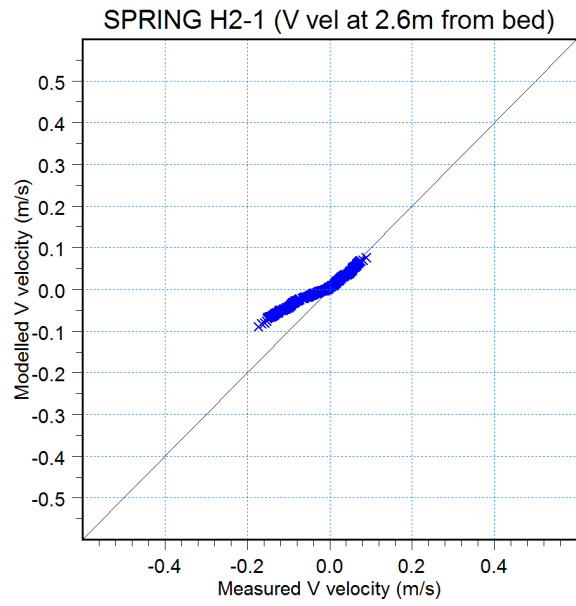
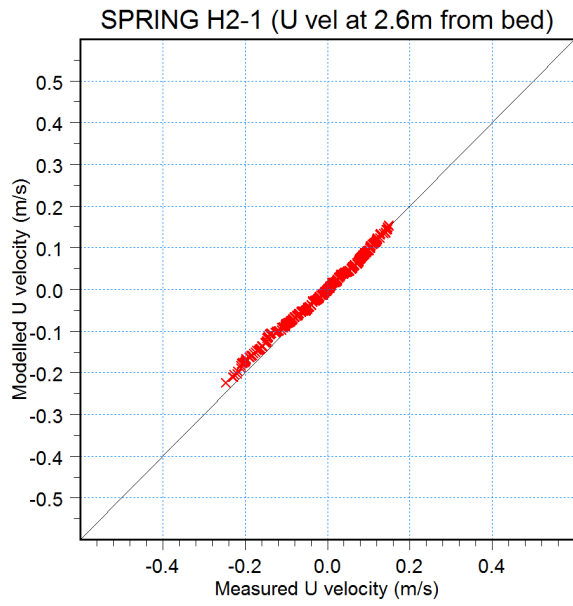


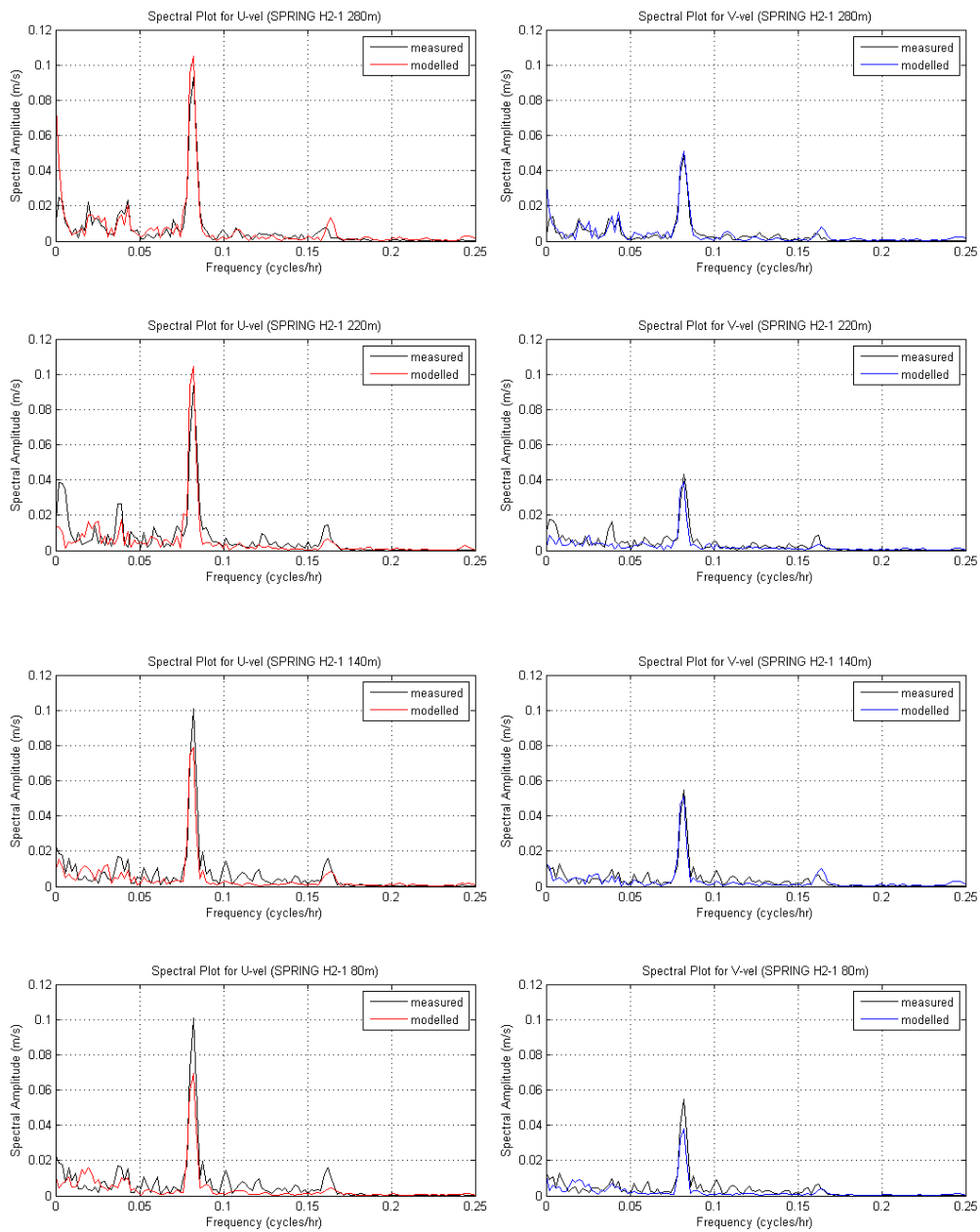


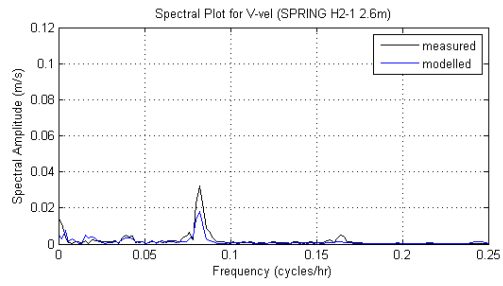
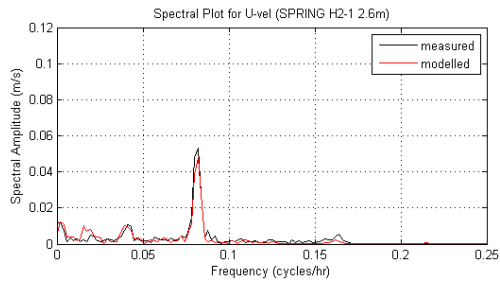


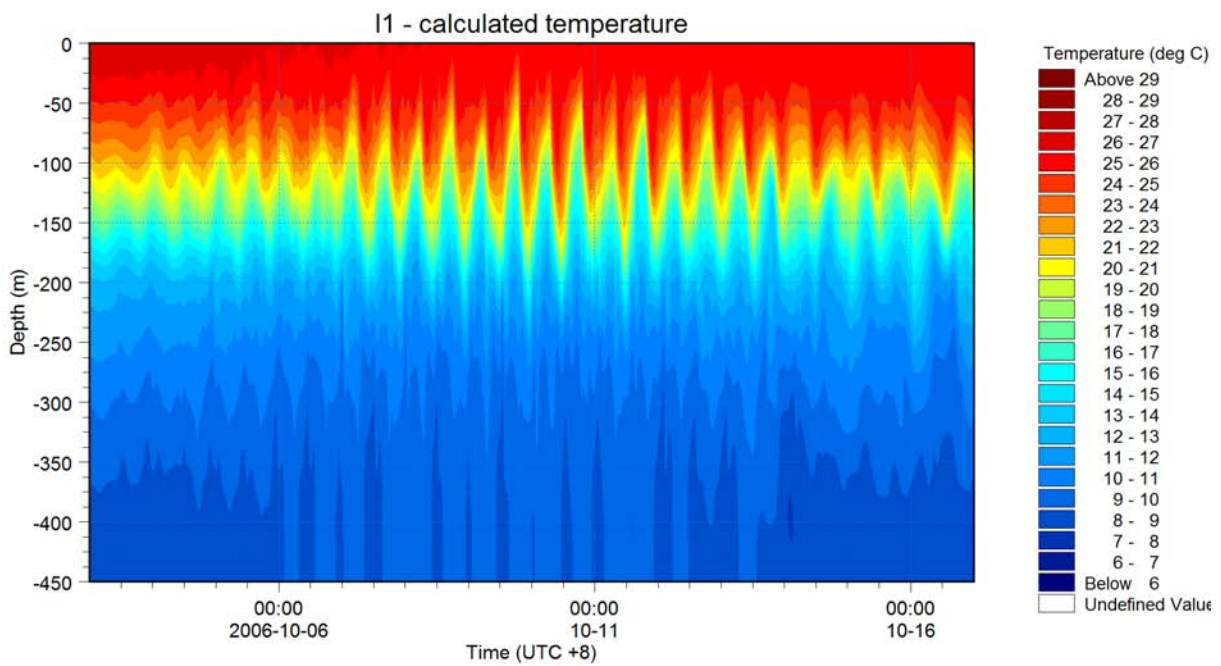
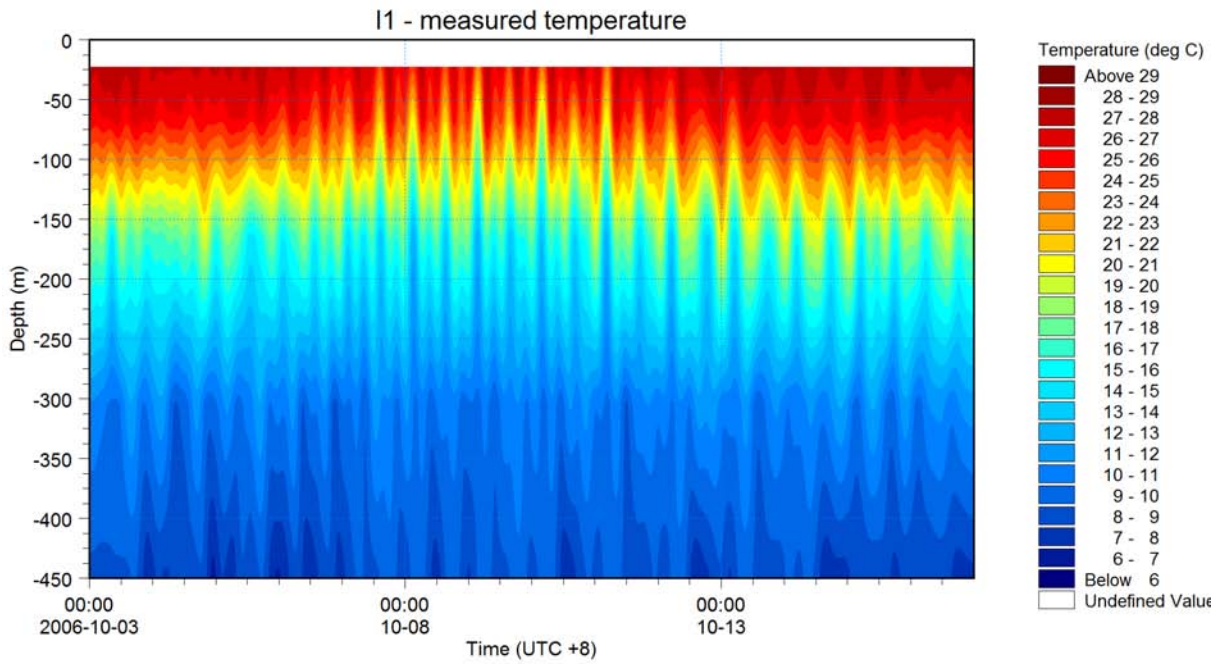








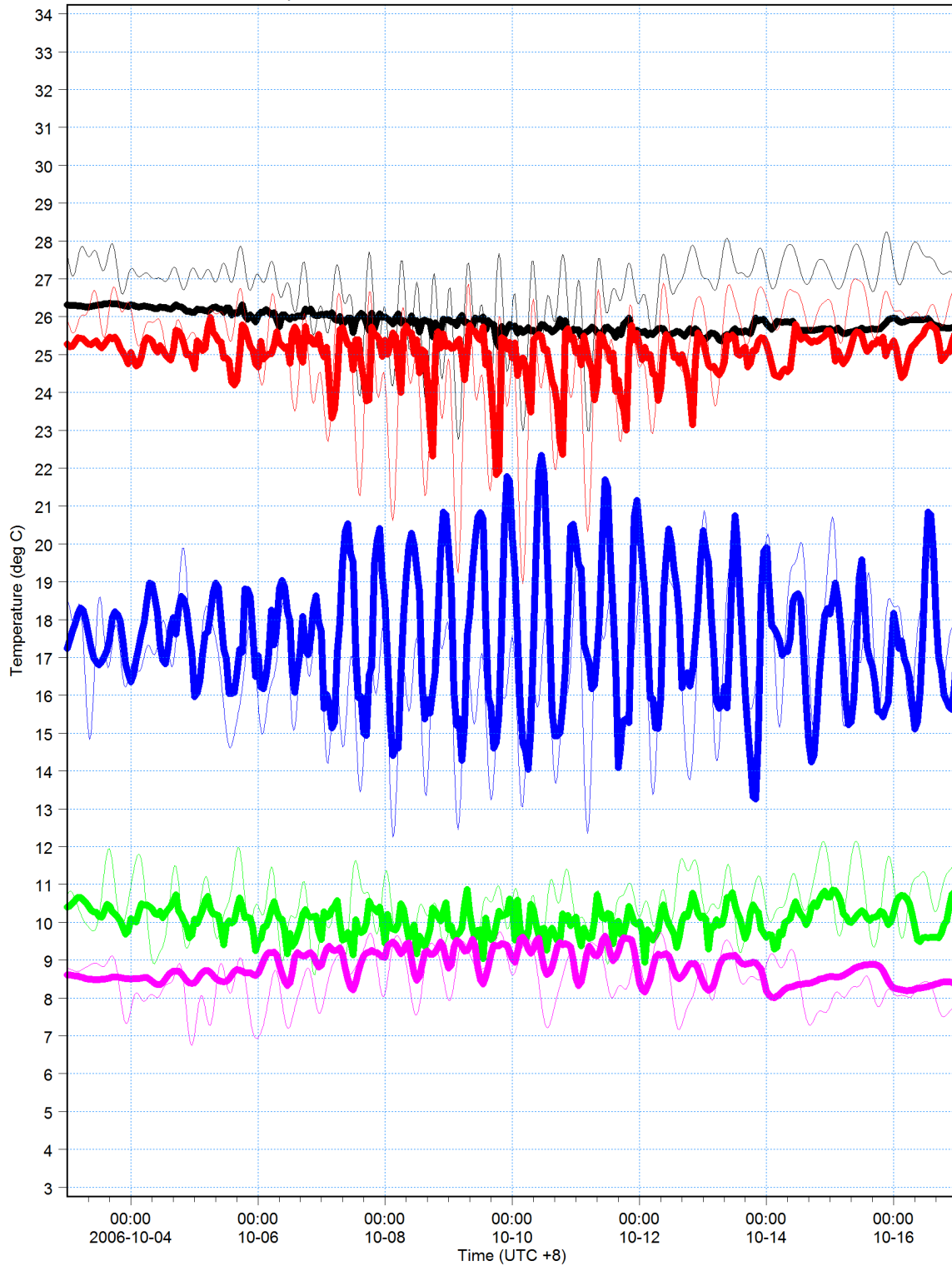






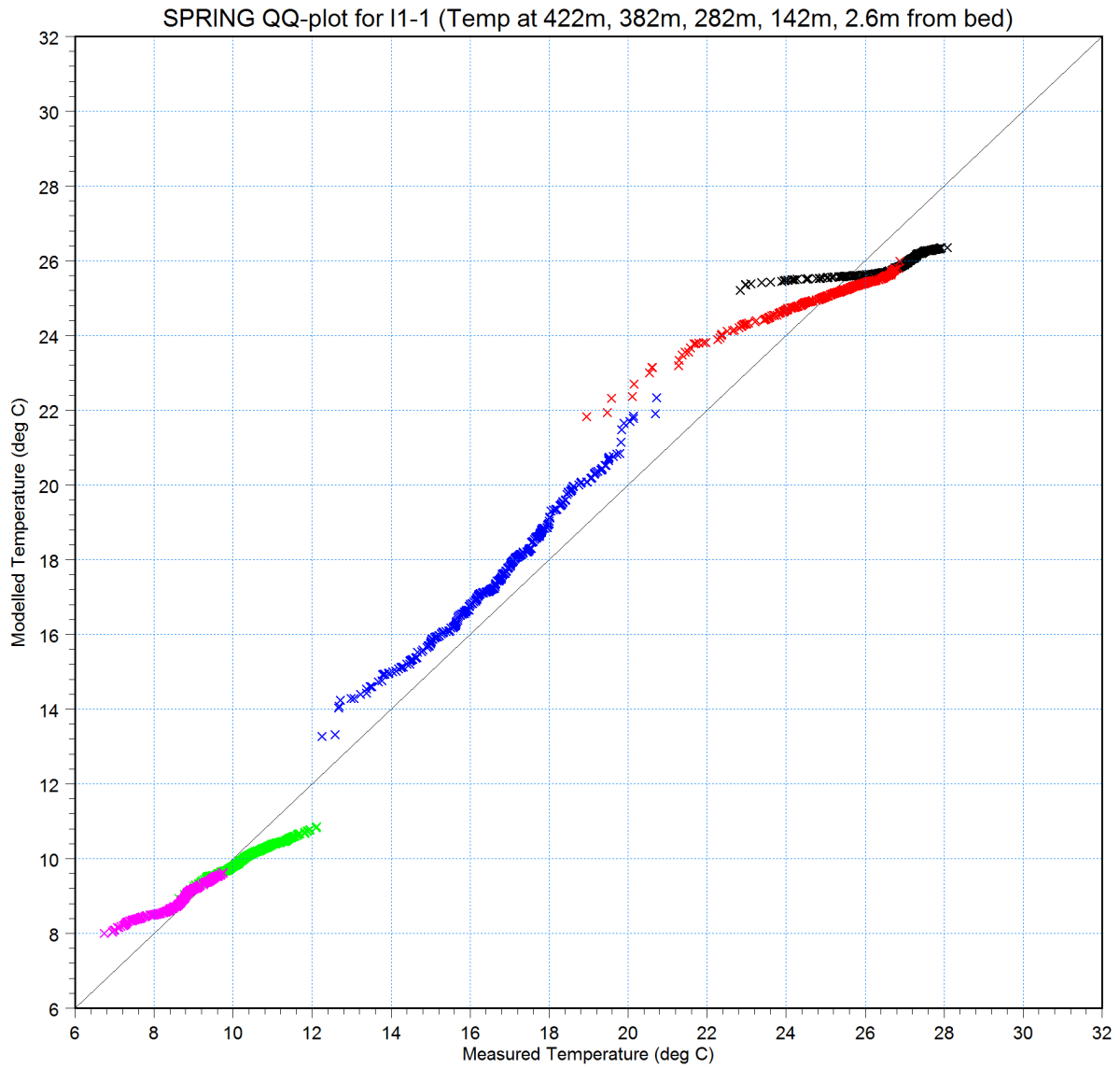
422m from bed: Temperature [deg C] 
measured [deg C] 
382m from bed: Temperature [deg C] 
measured [deg C] 
282m from bed: Temperature [deg C] 
measured [deg C] 
142m from bed: Temperature [deg C] 
measured [deg C] 
2.6m from bed: Temperature [deg C] 
measured [deg C] 

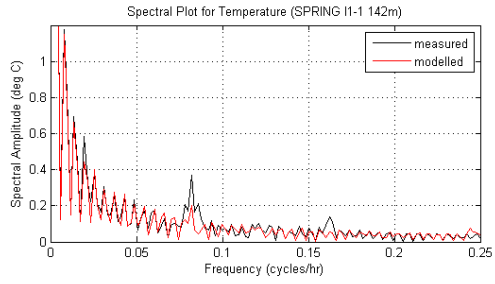
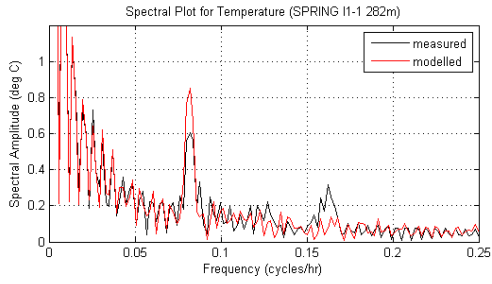
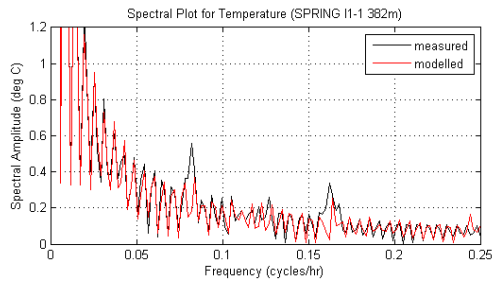
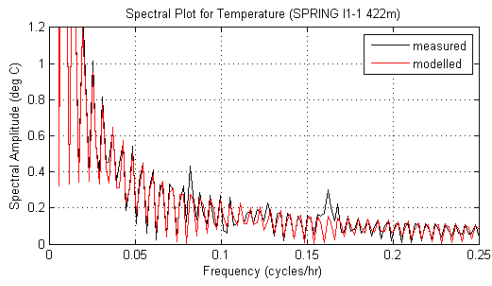
11 Temperature - 422m, 382m, 282m, 142m, 2.6m from bed

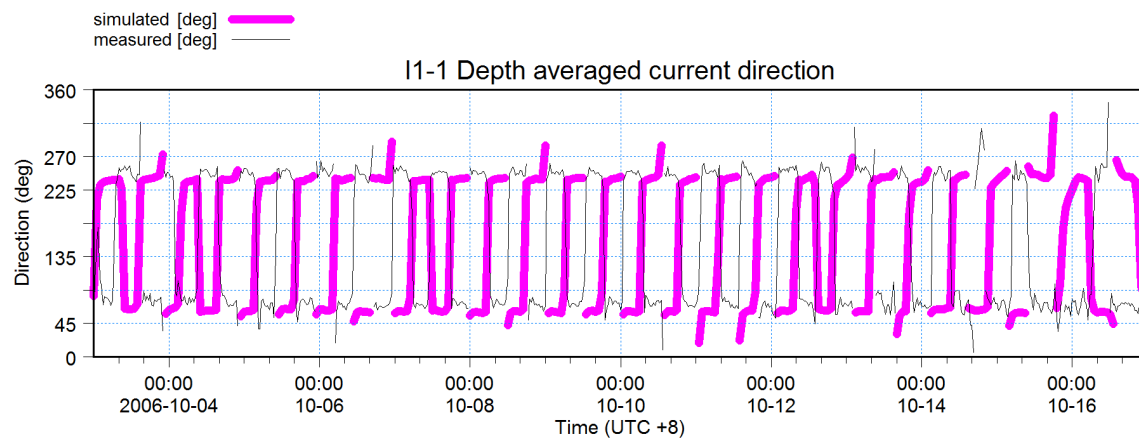
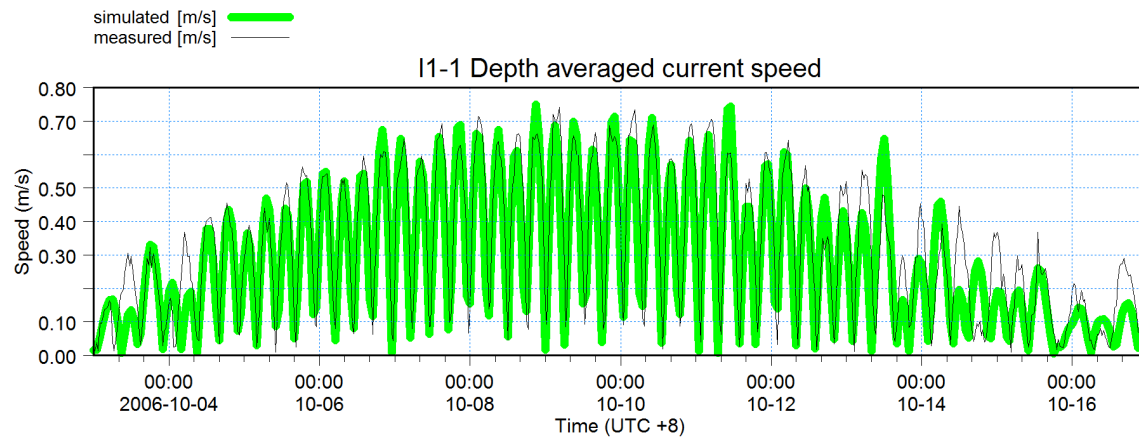
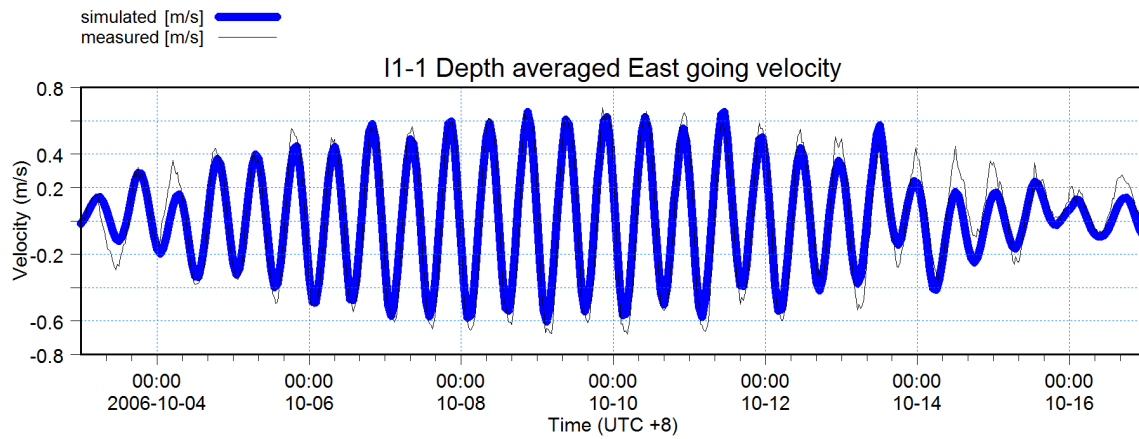
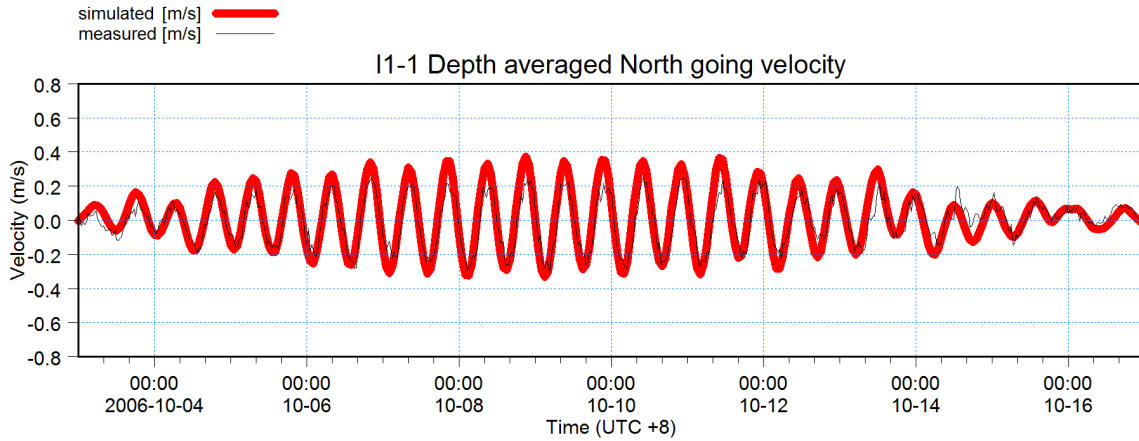


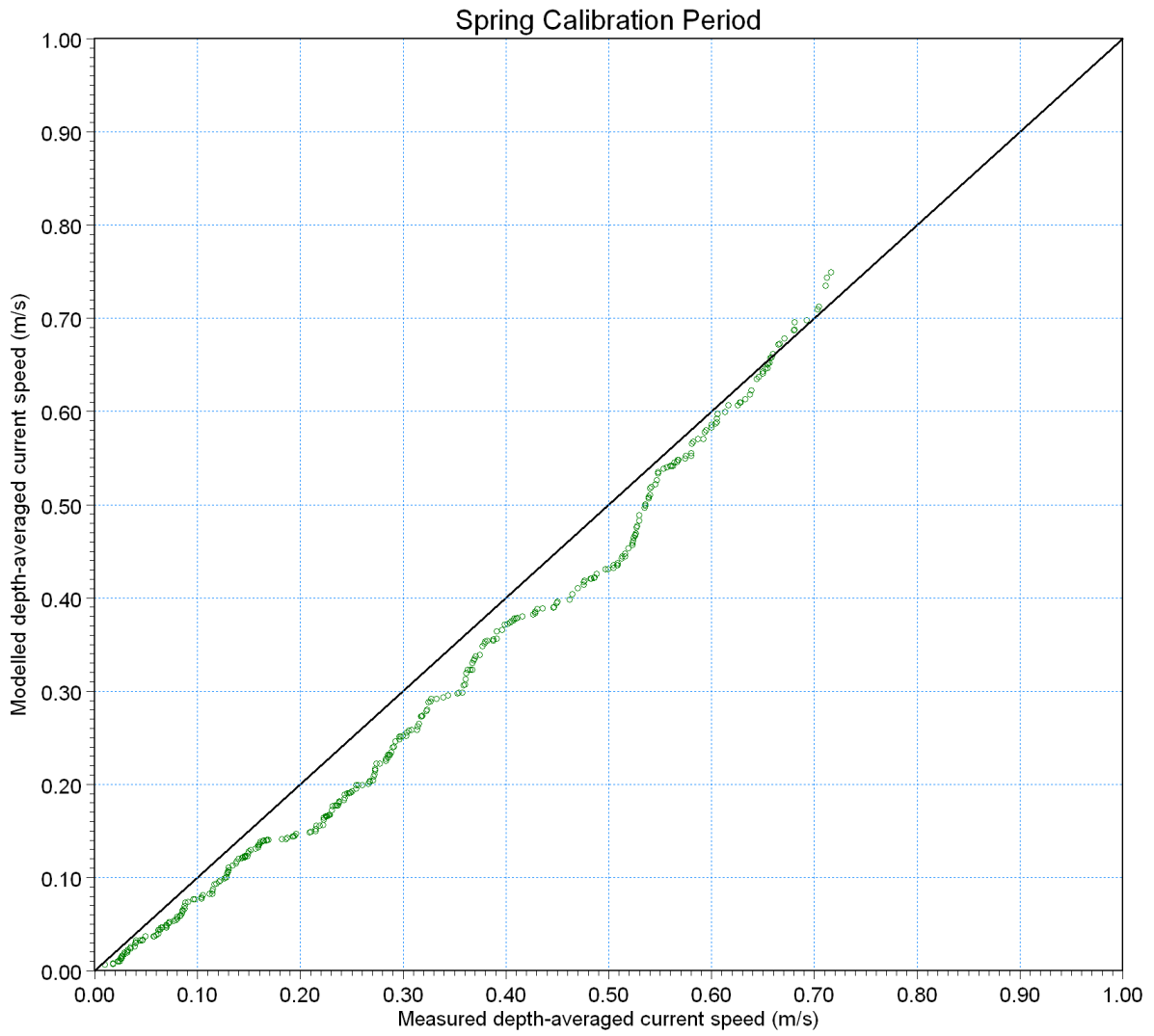


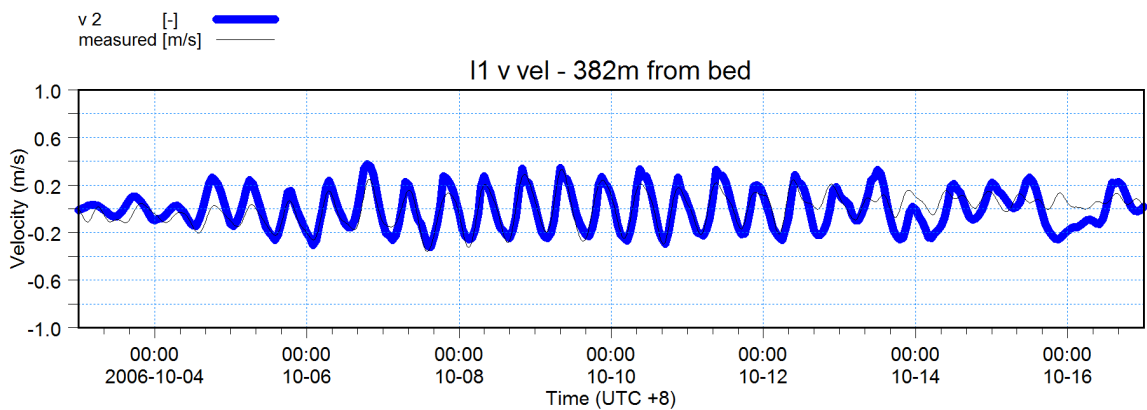
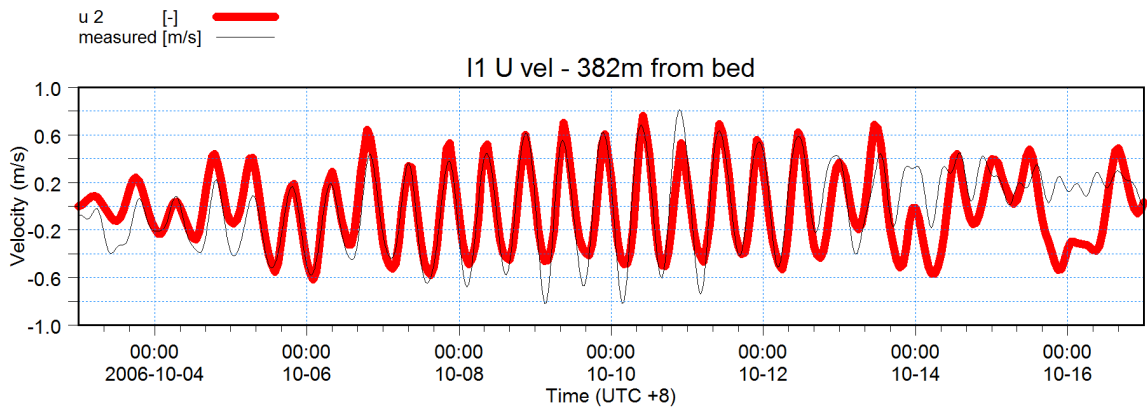
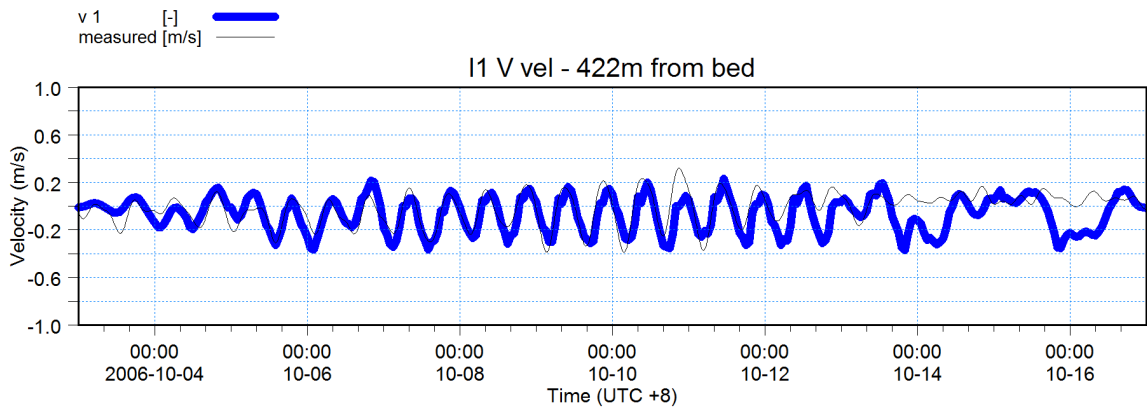
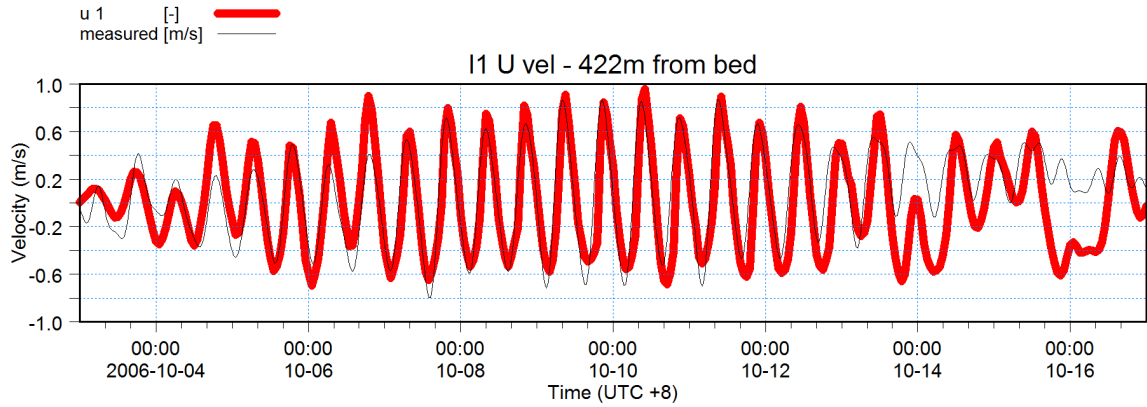
- T at 422m × ×
- T at 382m × ×
- T at 282m × ×
- T at 142m × ×
- T at 2.6m × ×

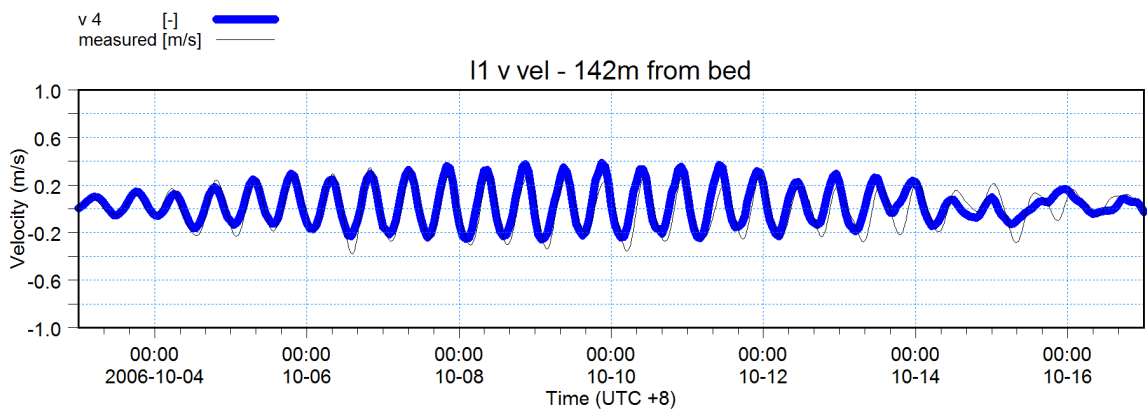
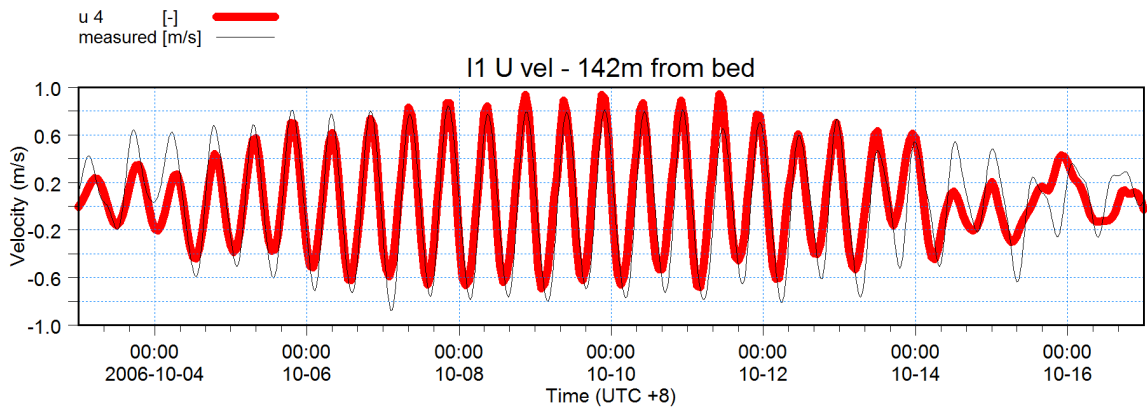
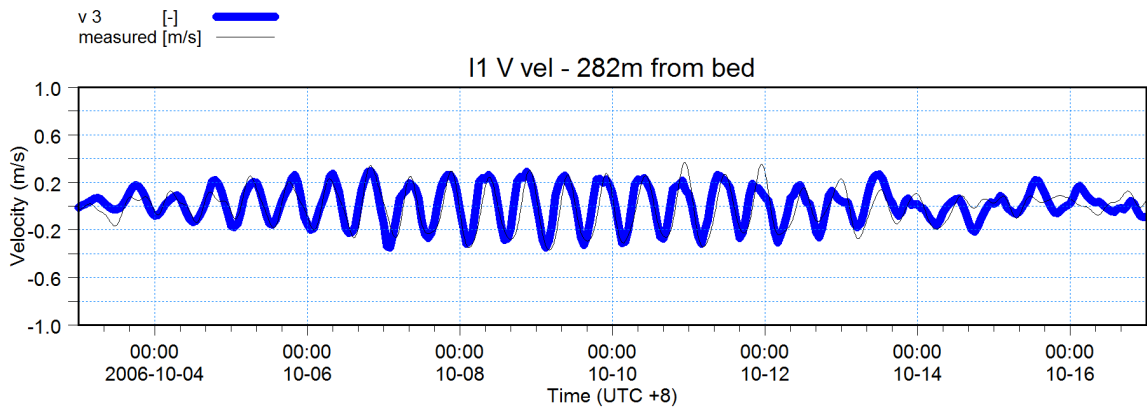
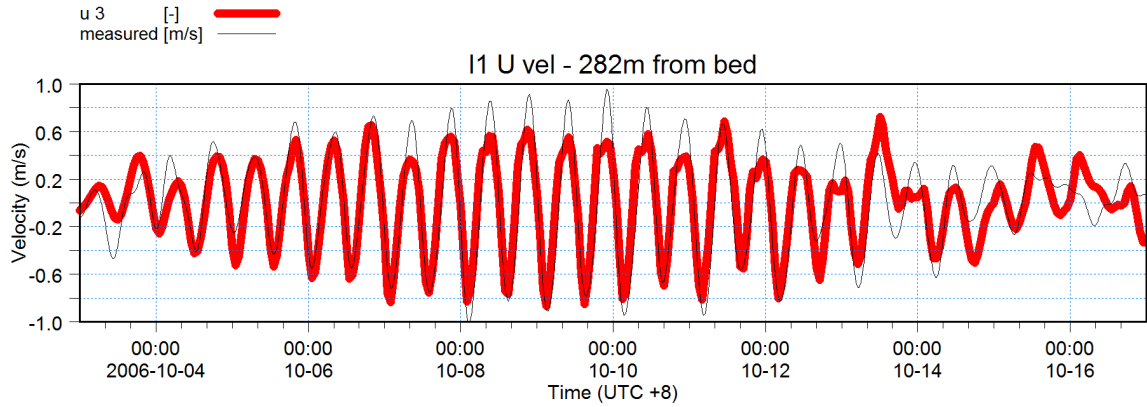


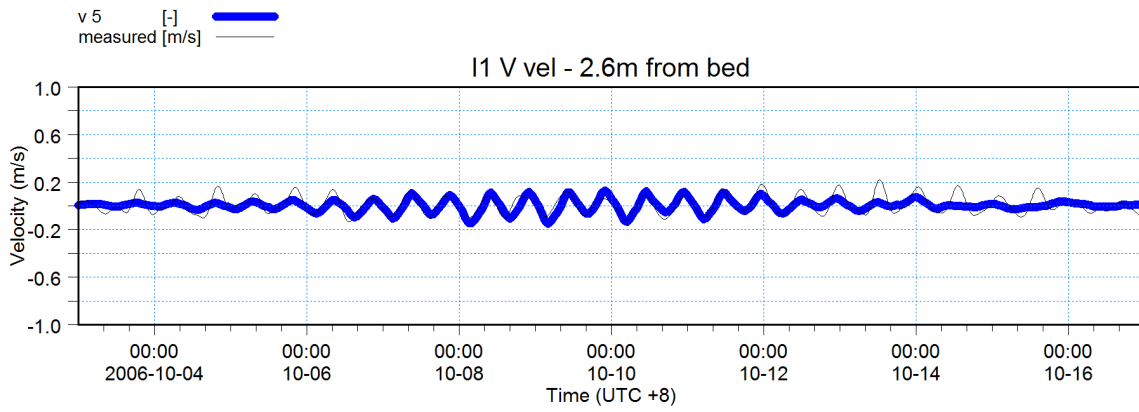
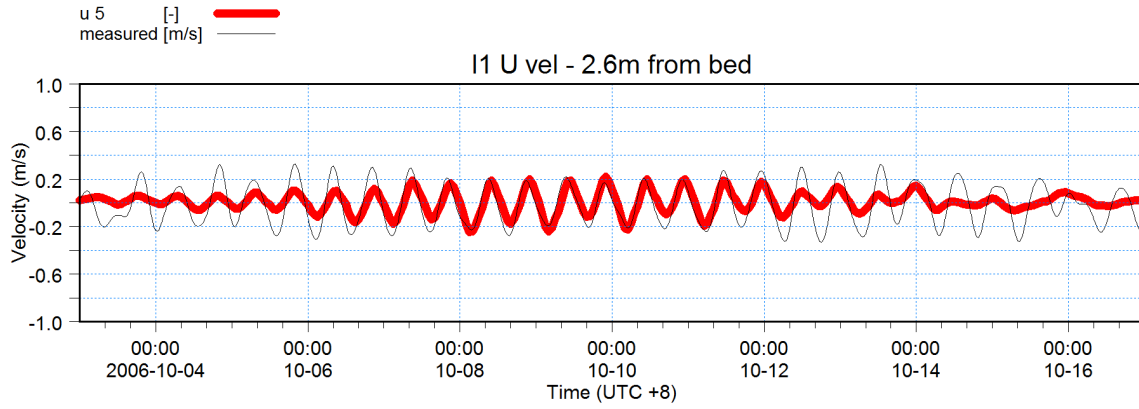


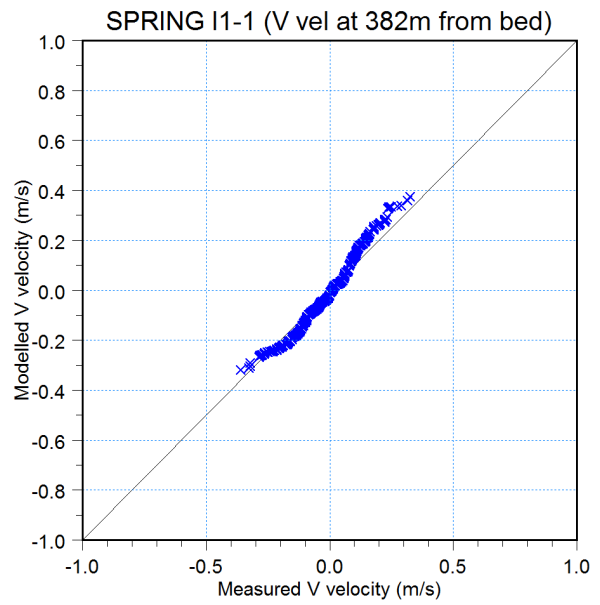
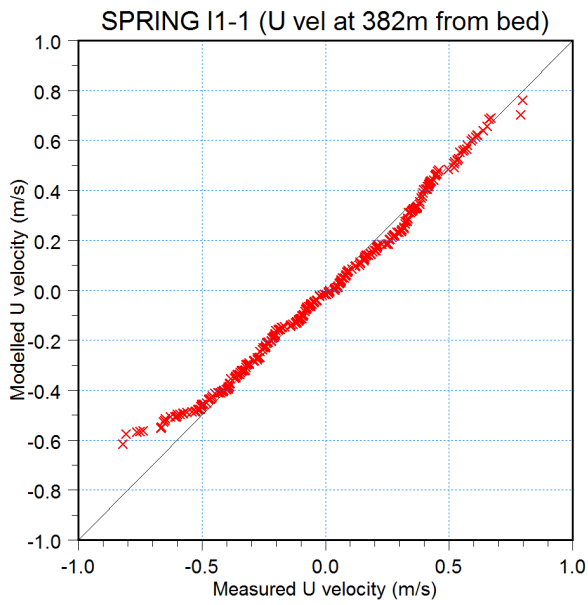
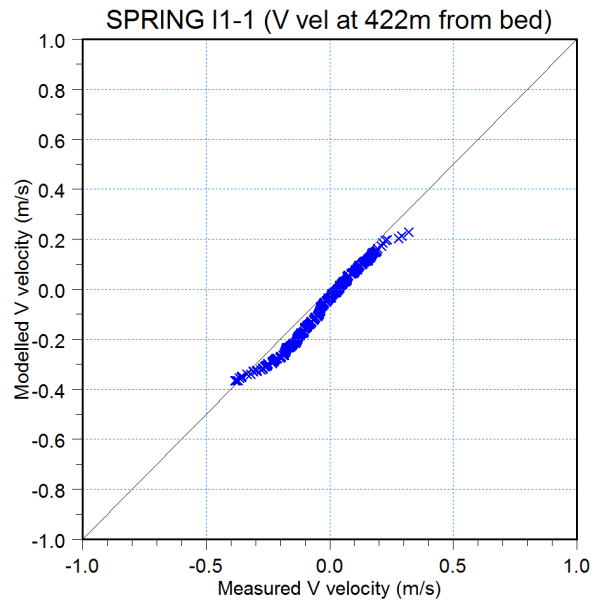
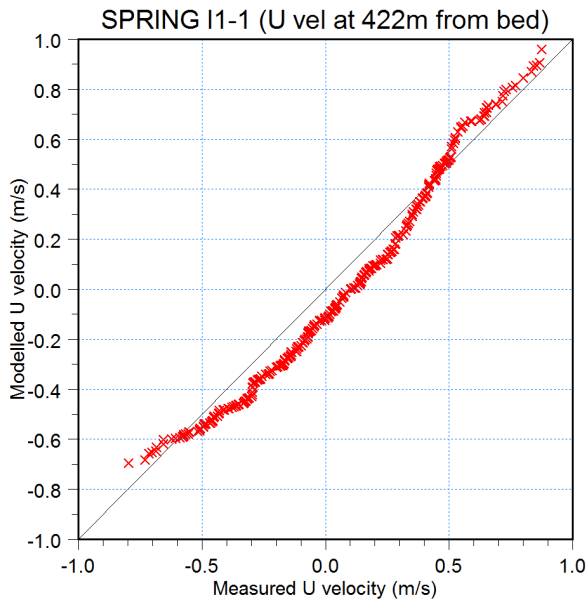


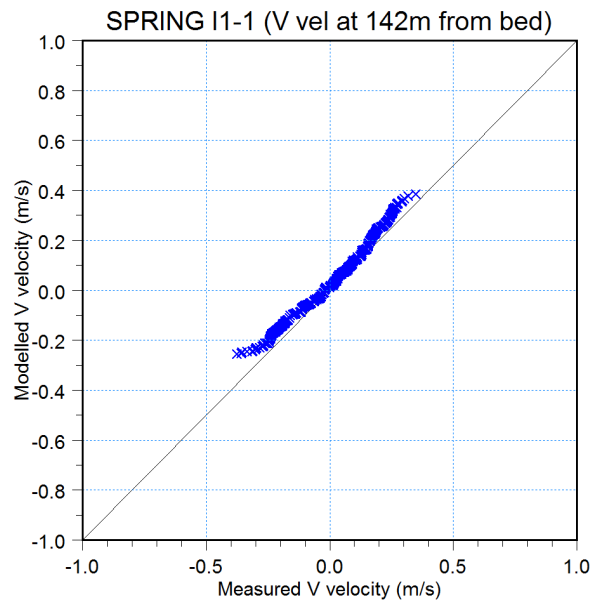
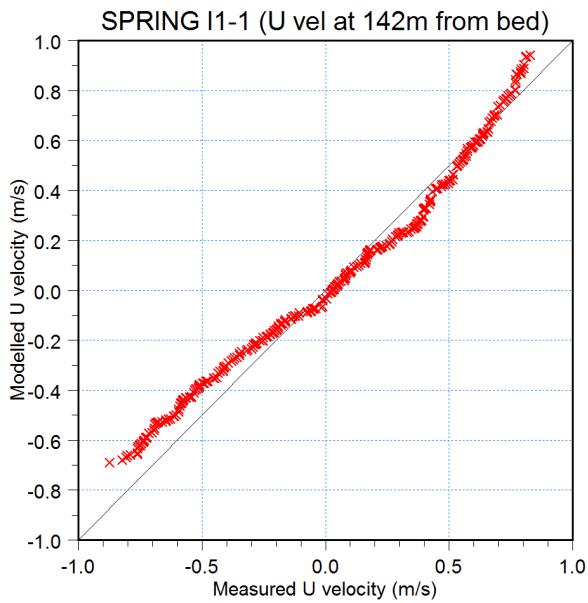
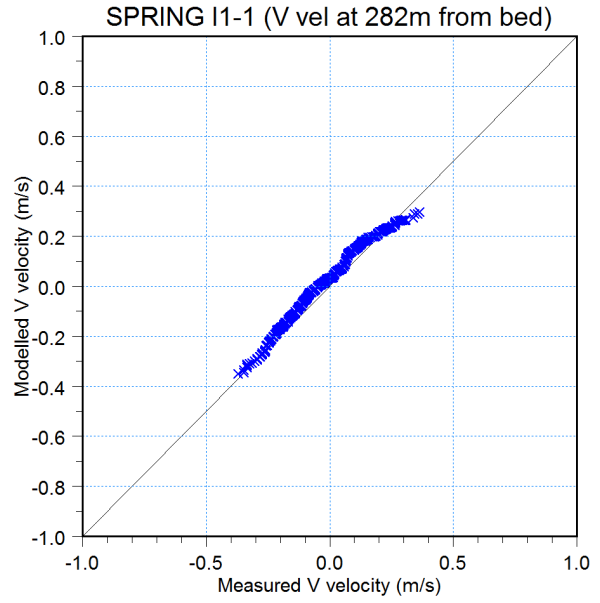
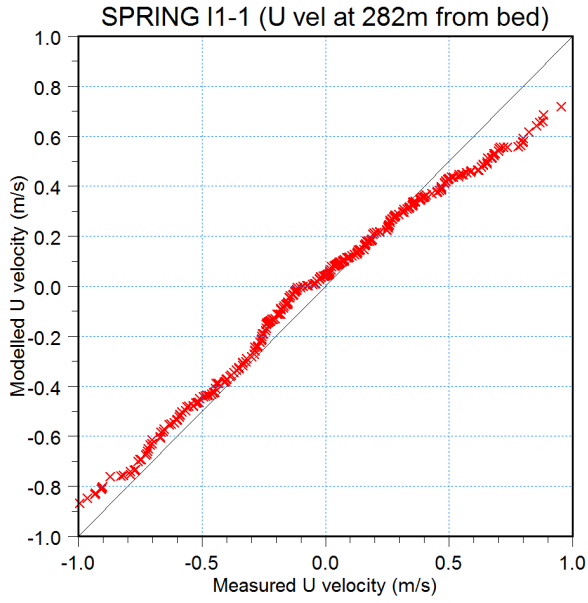


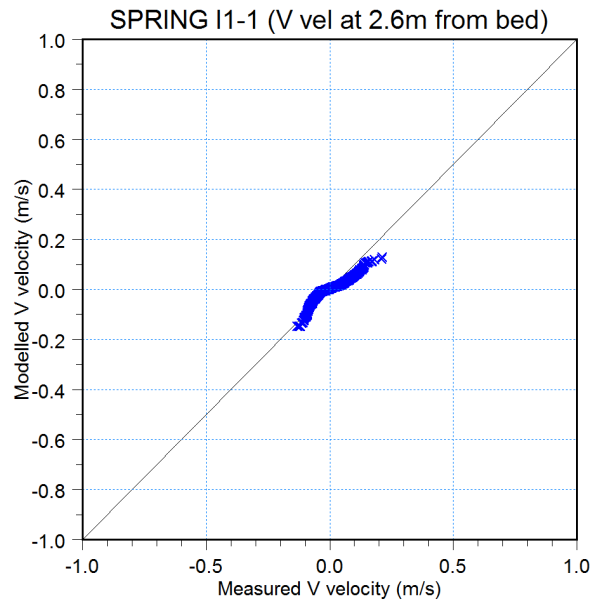
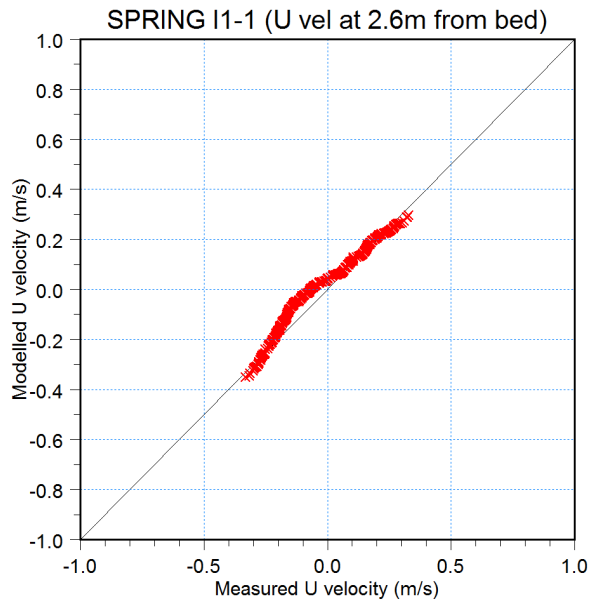


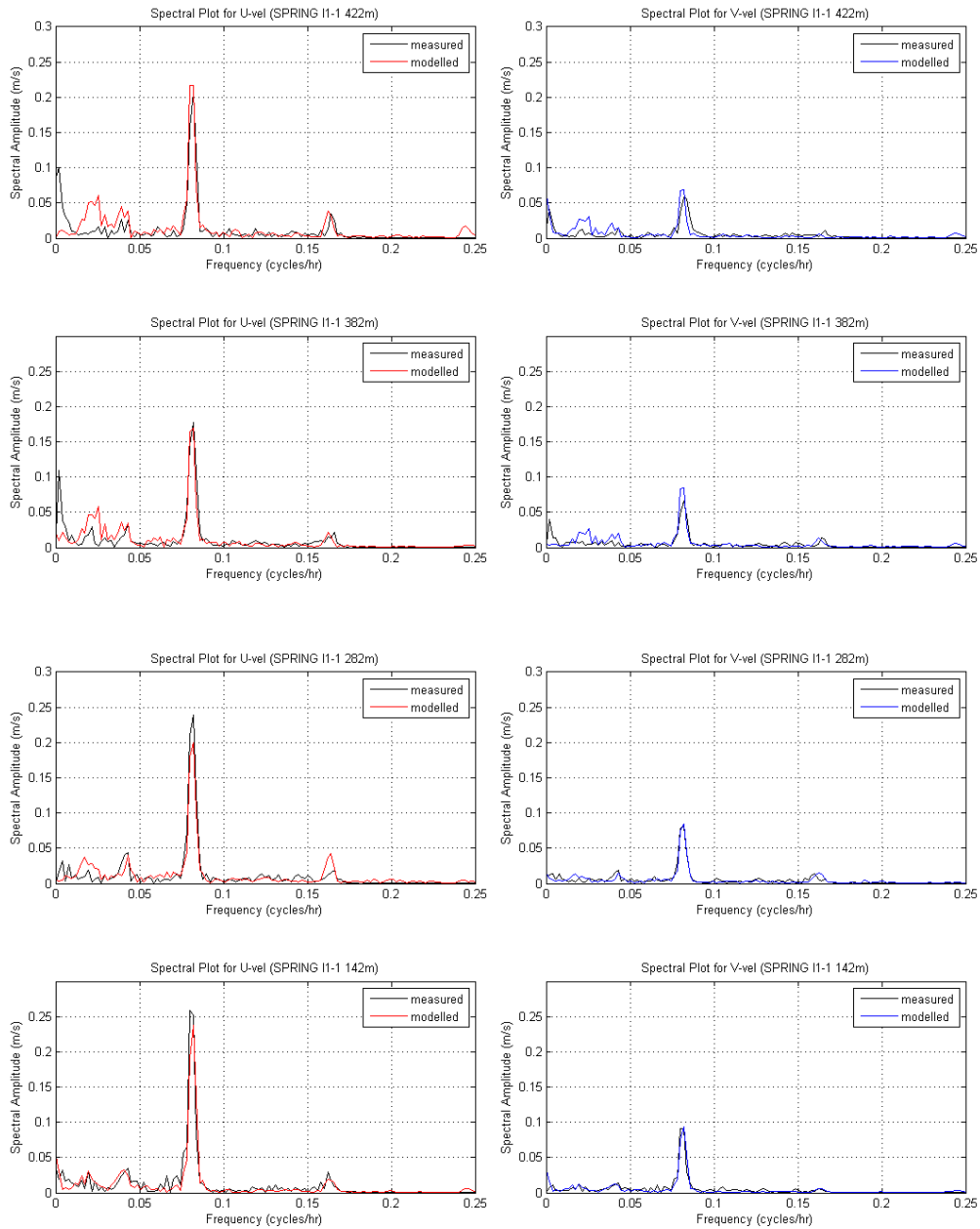


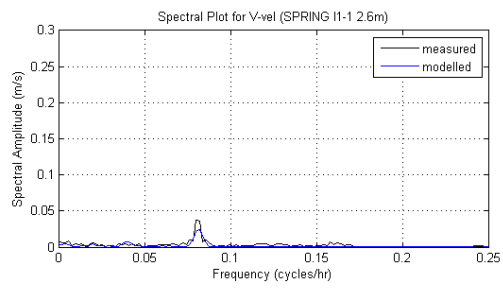
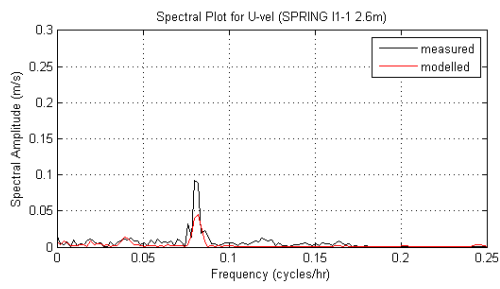










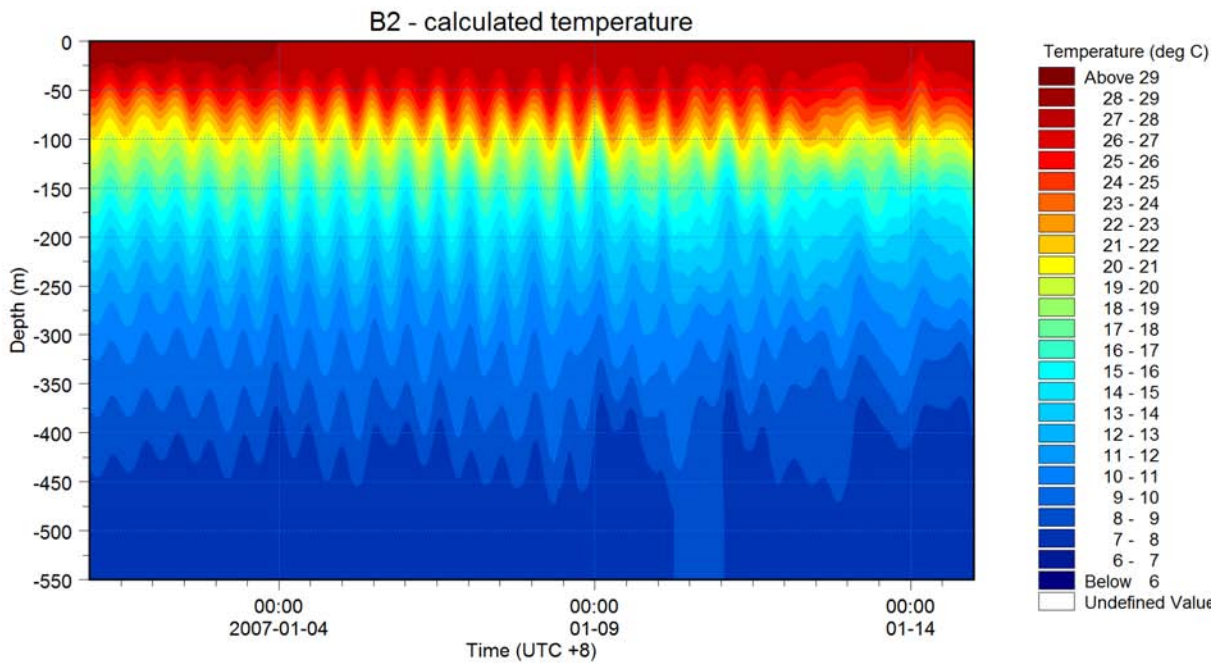
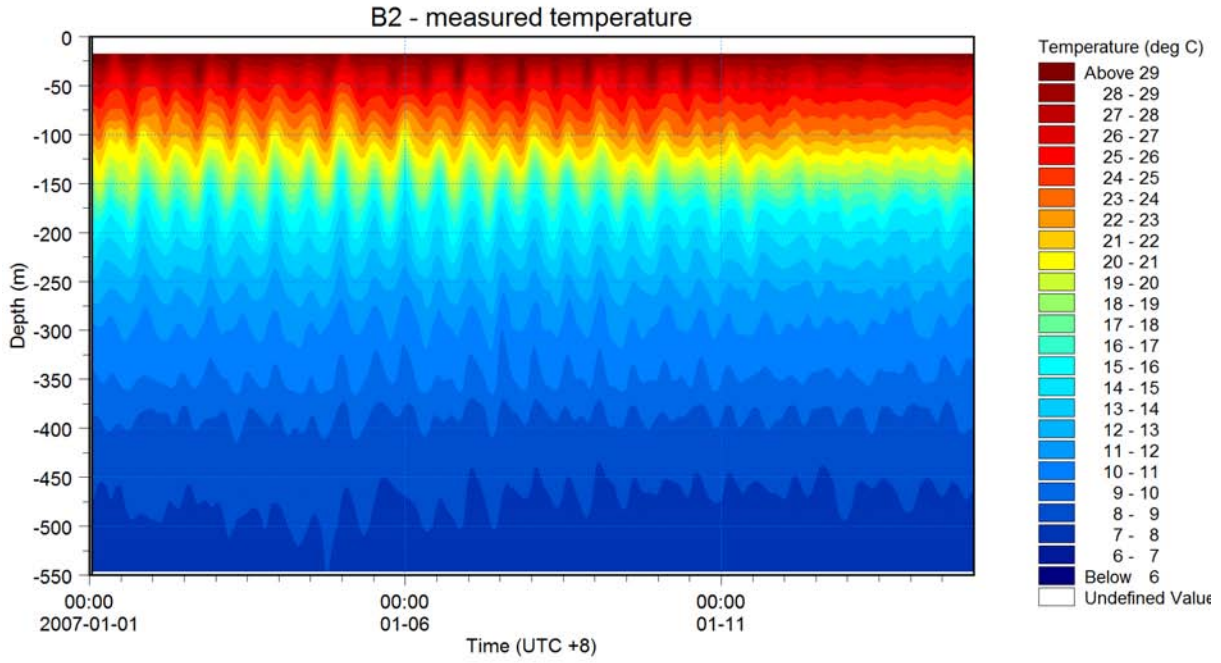




APPENDIX C

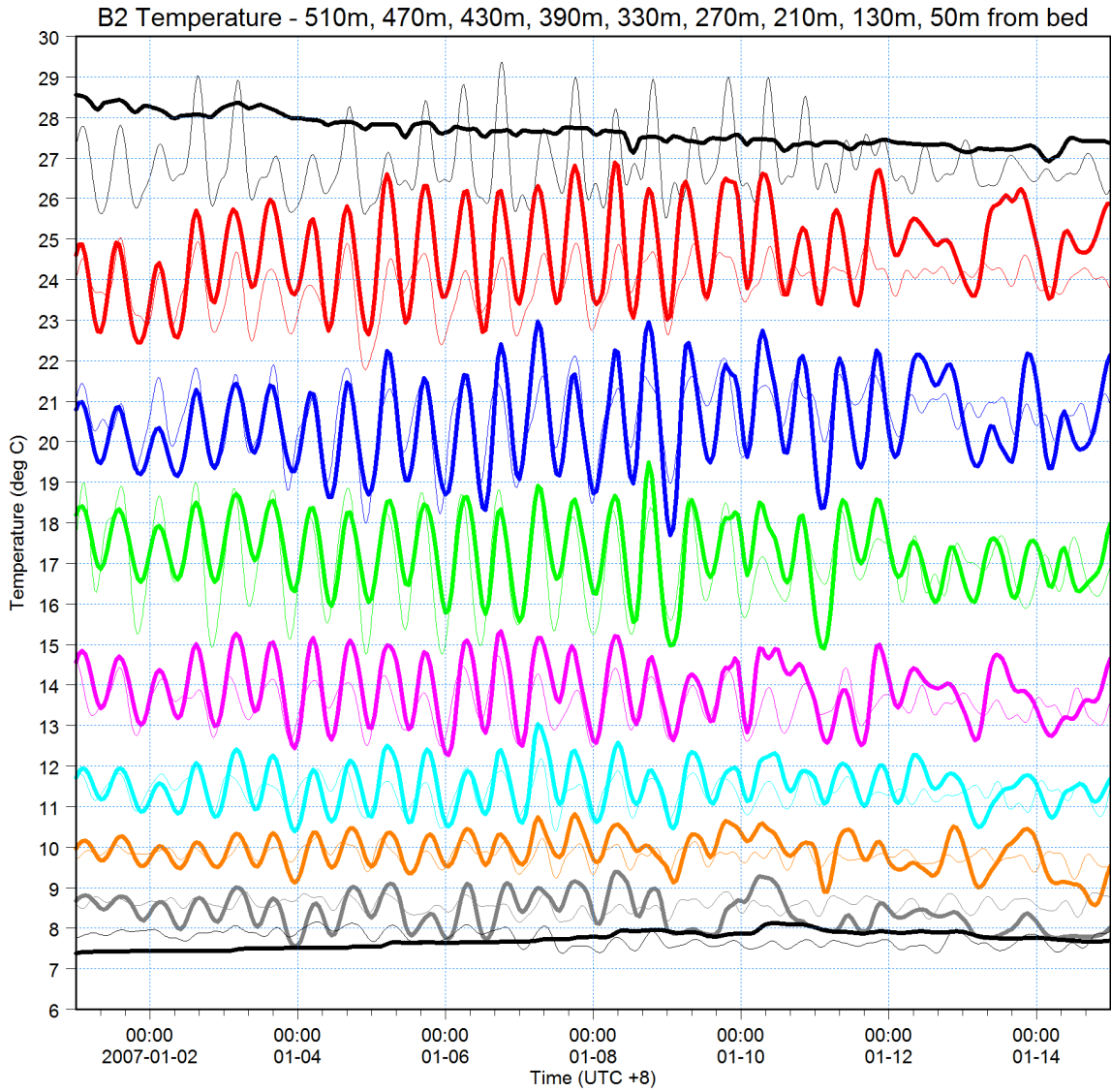
Summer Validation Period

Comparisons between Measurements and Model Simulation as Isopleth Plots, Time Series Plots, Q-Q Plots and Frequency Plots



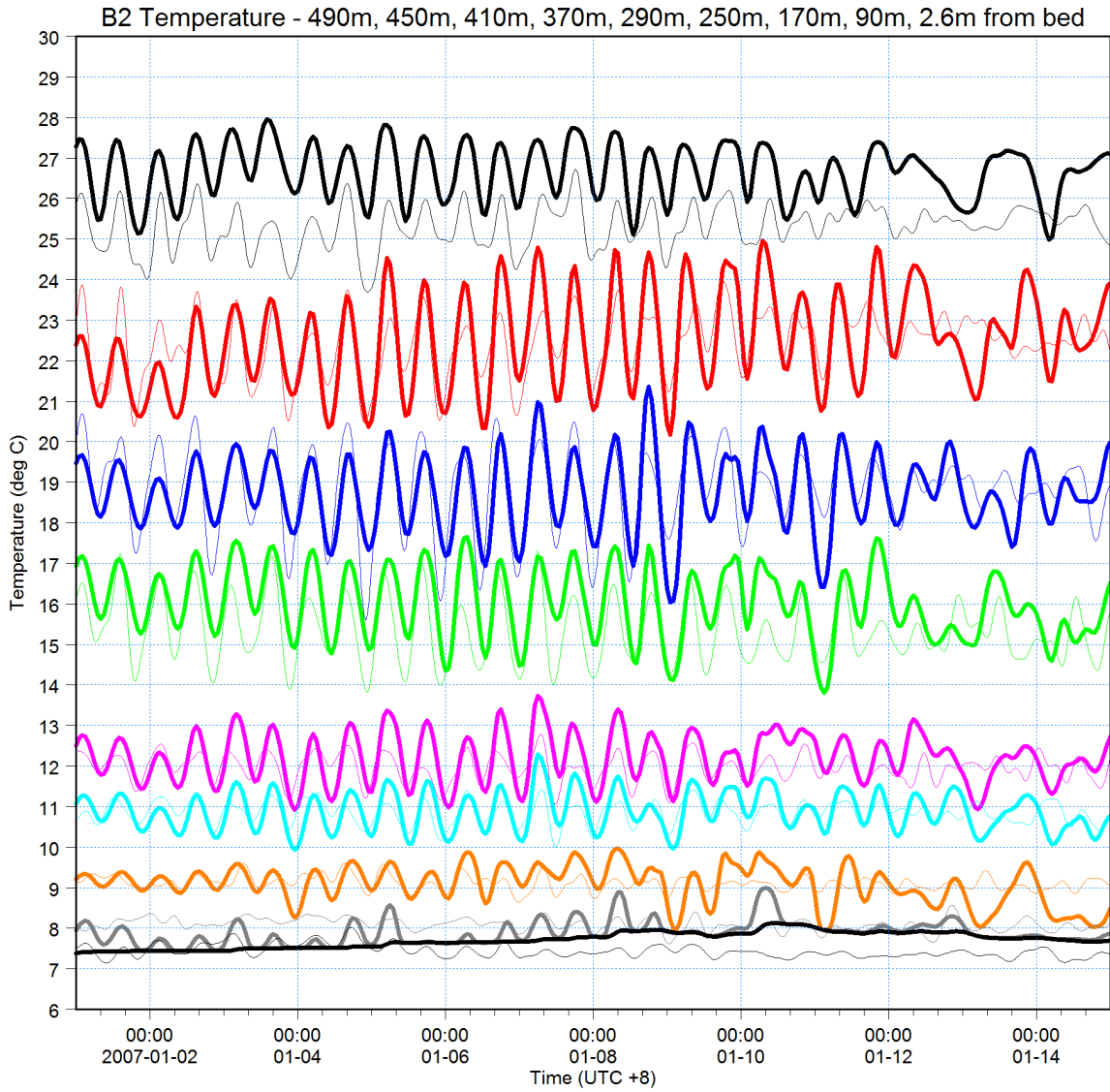


510m from bed: Temperature [C] [deg C] —
measured [deg C] —
470m from bed: Temperature [C] [deg C] —
measured [deg C] —
430m from bed: Temperature [C] [deg C] —
measured [deg C] —
390m from bed: Temperature [C] [deg C] —
measured [deg C] —
330m from bed: Temperature [C] [deg C] —
measured [deg C] —
270m from bed: Temperature [C] [deg C] —
measured [deg C] —
190m from bed: Temperature [C] [deg C] —
measured [deg C] —
130m from bed: Temperature [C] [deg C] —
measured [deg C] —
50m from bed: Temperature [C] [deg C] —
measured [deg C] —



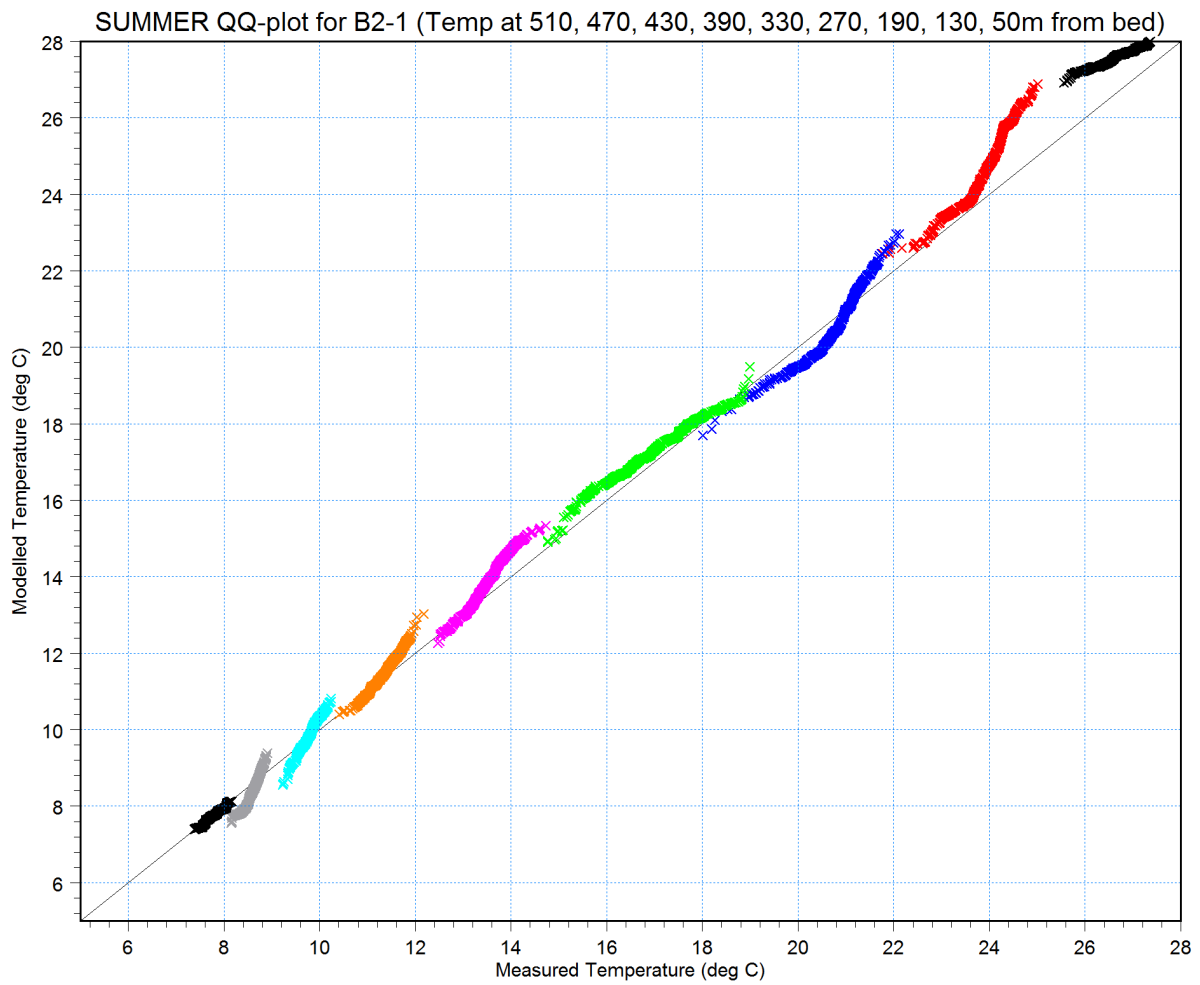


490m from bed: Temperature [C] [deg C] —
measured [deg C] —
450m from bed: Temperature [C] [deg C] —
measured [deg C] —
410m from bed: Temperature [C] [deg C] —
measured [deg C] —
370m from bed: Temperature [C] [deg C] —
measured [deg C] —
290m from bed: Temperature [C] [deg C] —
measured [deg C] —
250m from bed: Temperature [C] [deg C] —
measured [deg C] —
170m from bed: Temperature [C] [deg C] —
measured [deg C] —
130m from bed: Temperature [C] [deg C] —
measured [deg C] —
2.6m from bed: Temperature [C] [deg C] —
measured [deg C] —



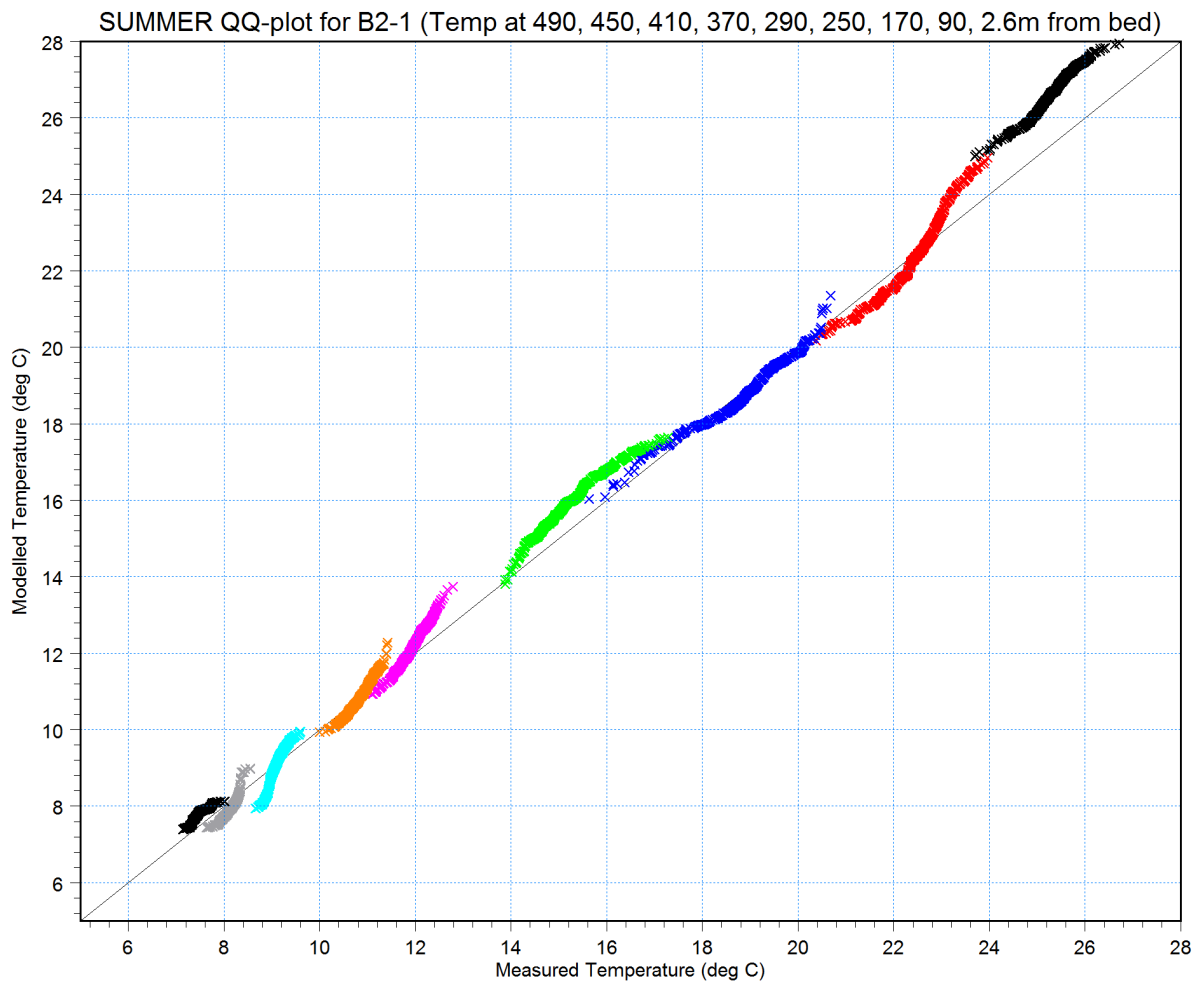


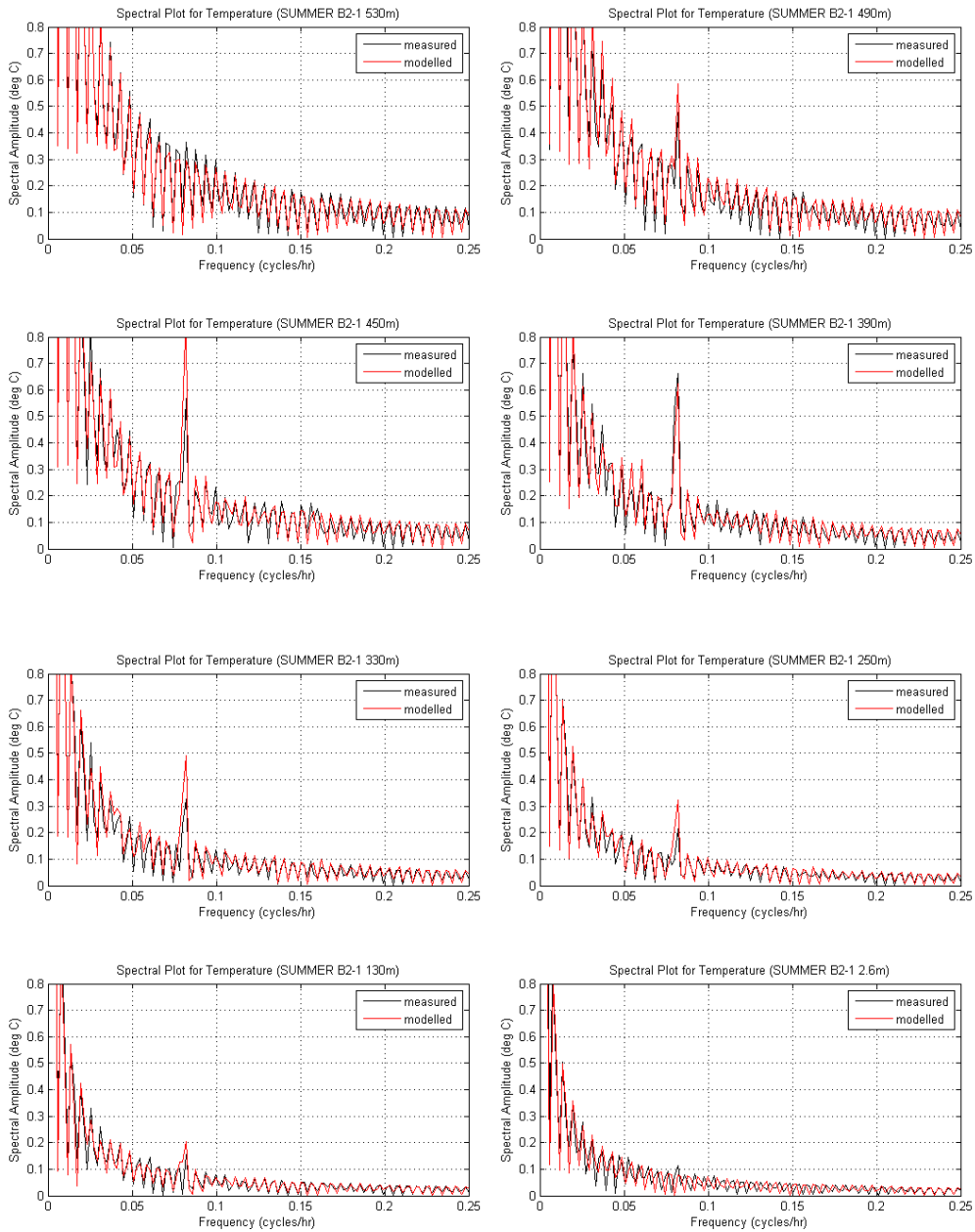
- T at 510m × ×
- T at 470m × ×
- T at 430m × ×
- T at 390m × ×
- T at 330m × ×
- T at 270m × ×
- T at 190m × ×
- T at 130m × ×
- T at 50m × ×

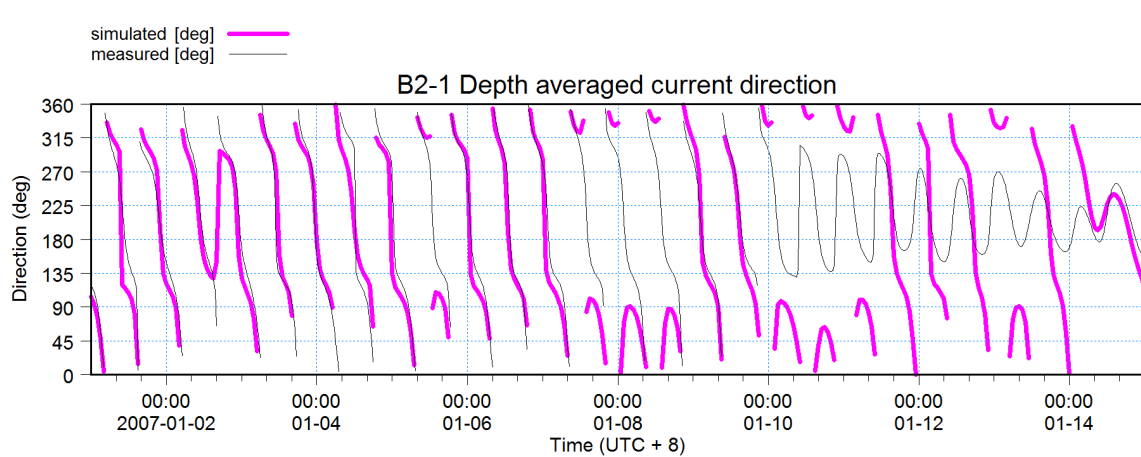
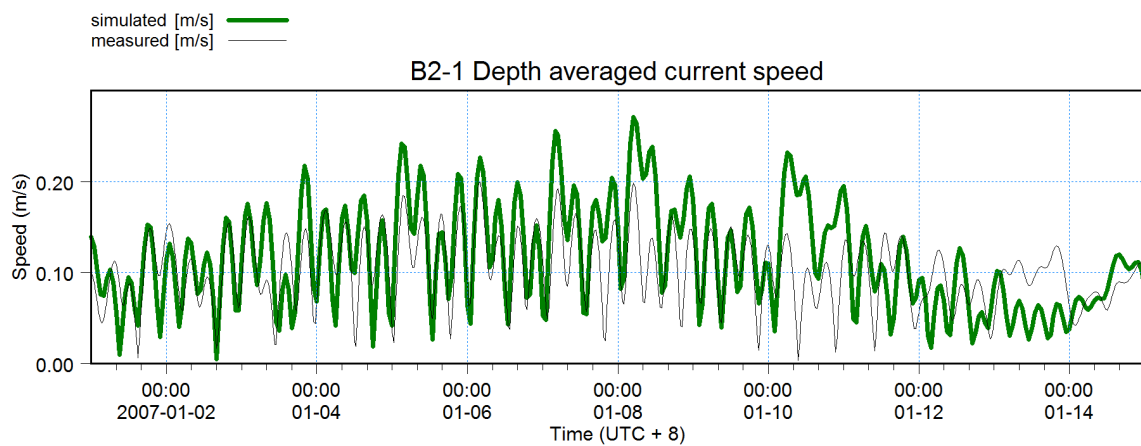
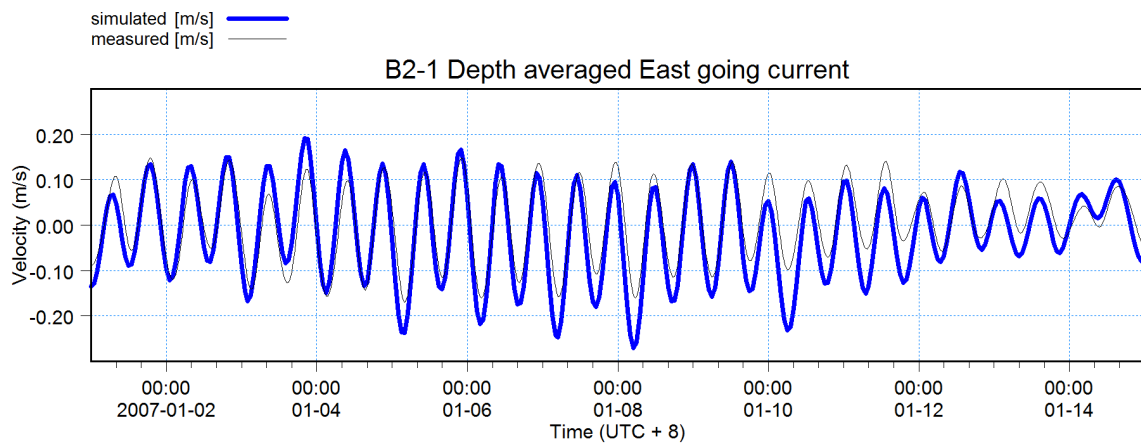
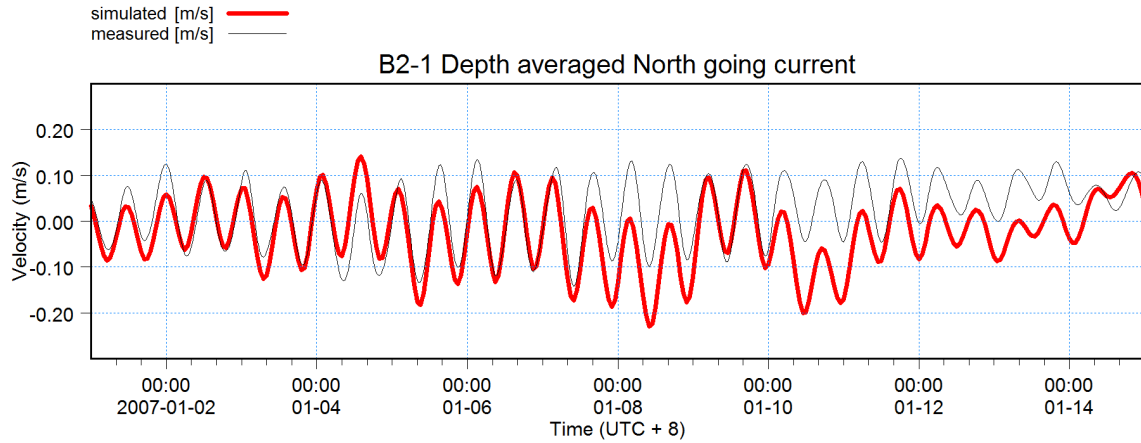




- T at 490m × ×
- T at 450m × ×
- T at 410m × ×
- T at 370m × ×
- T at 290m × ×
- T at 250m × ×
- T at 170m × ×
- T at 90m × ×
- T at 2.6m × ×

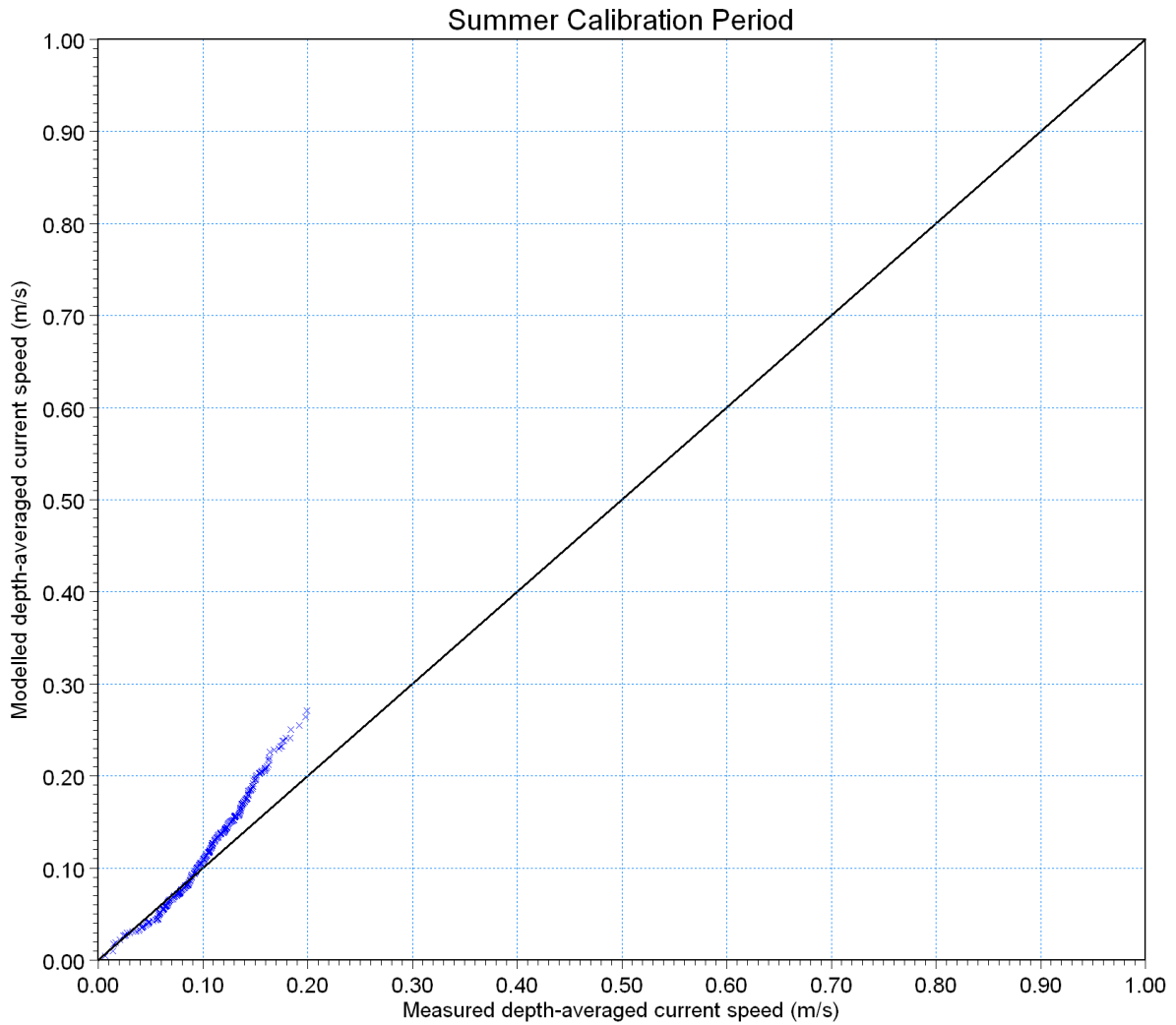


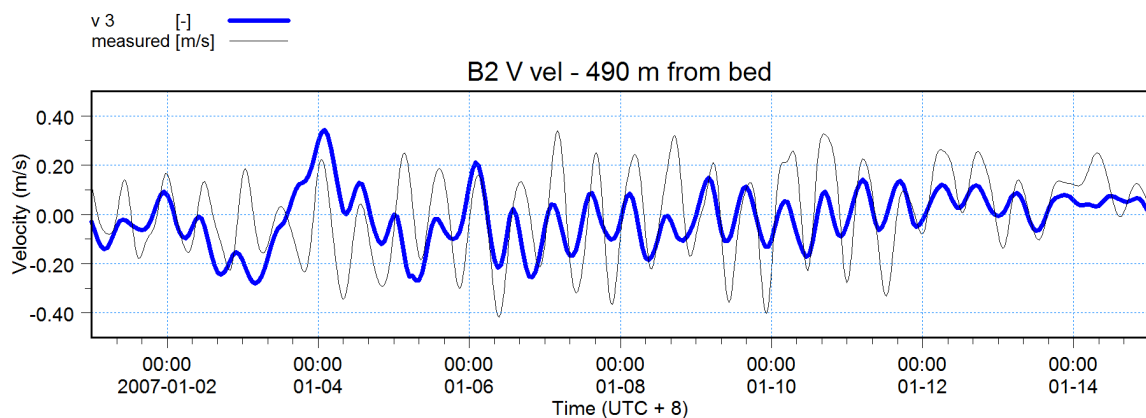
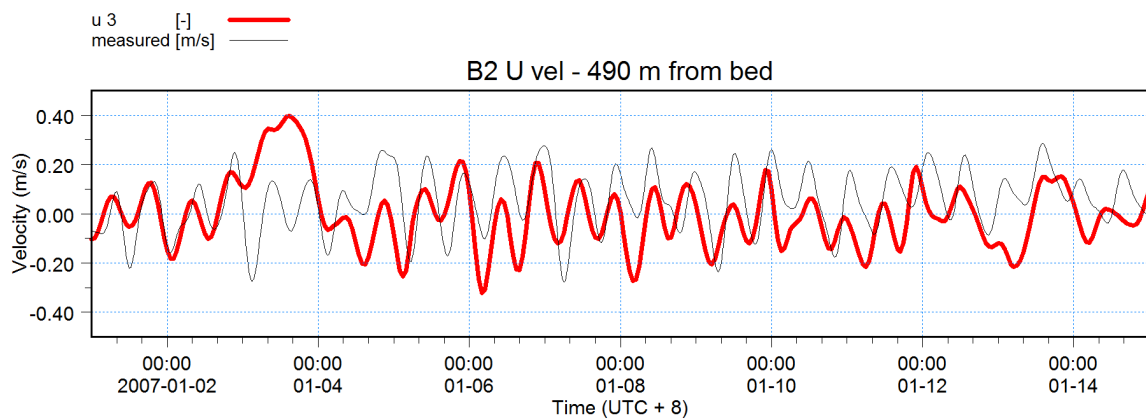
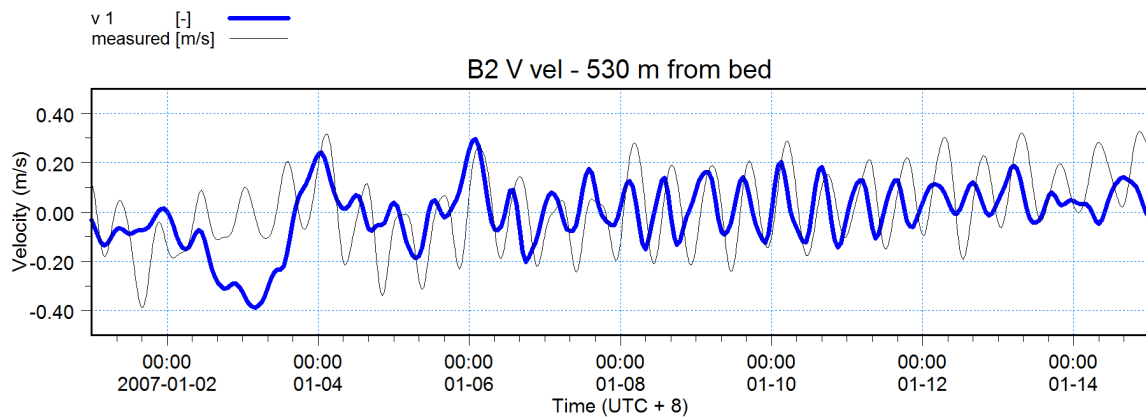
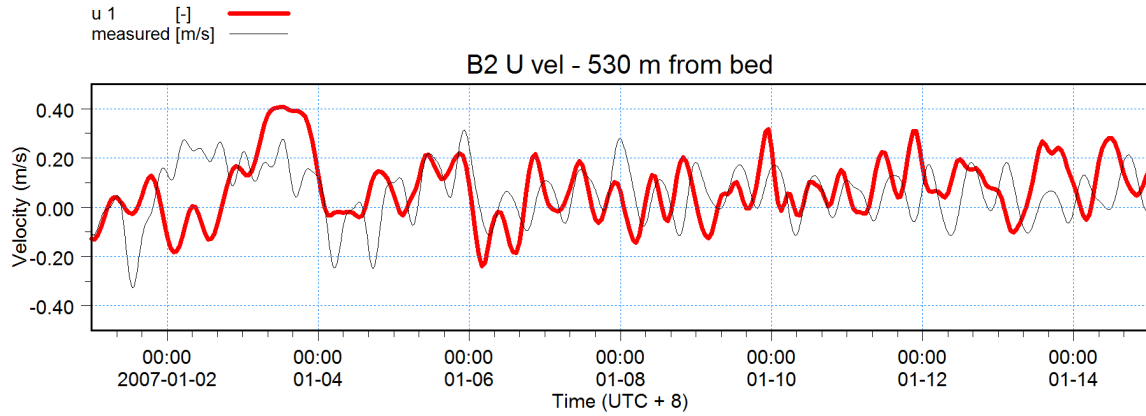


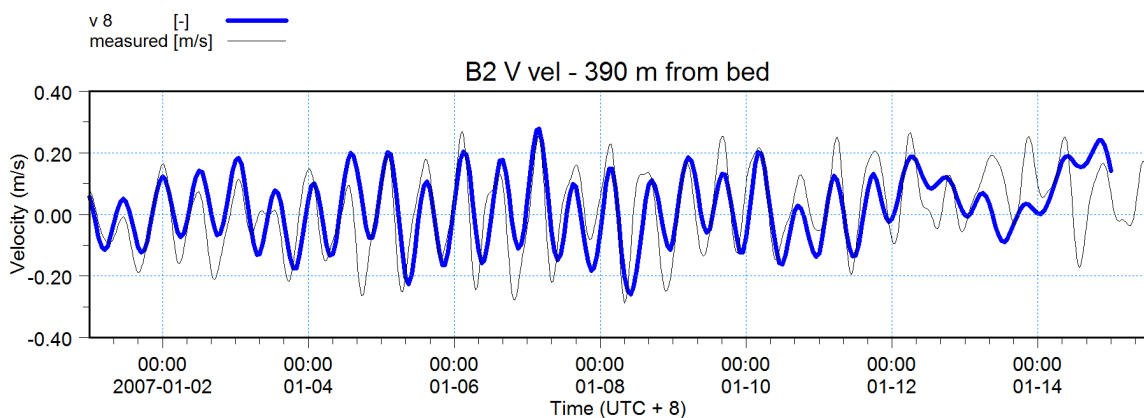
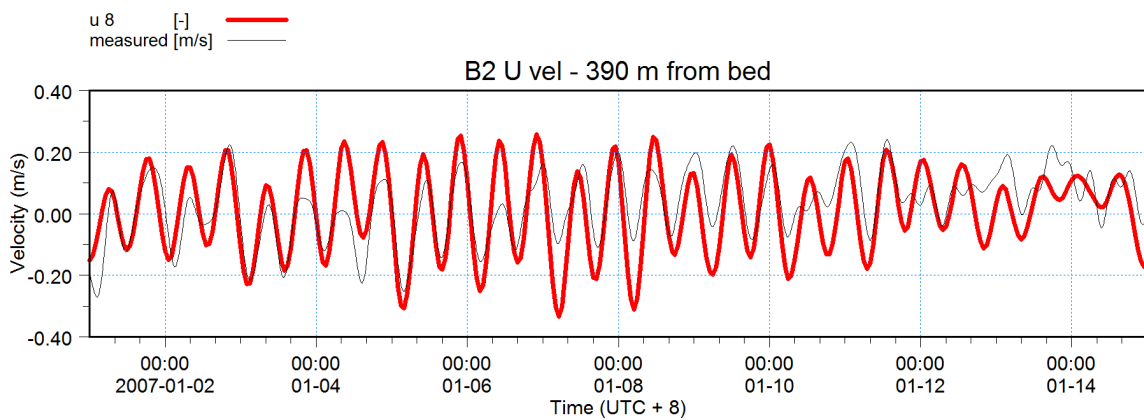
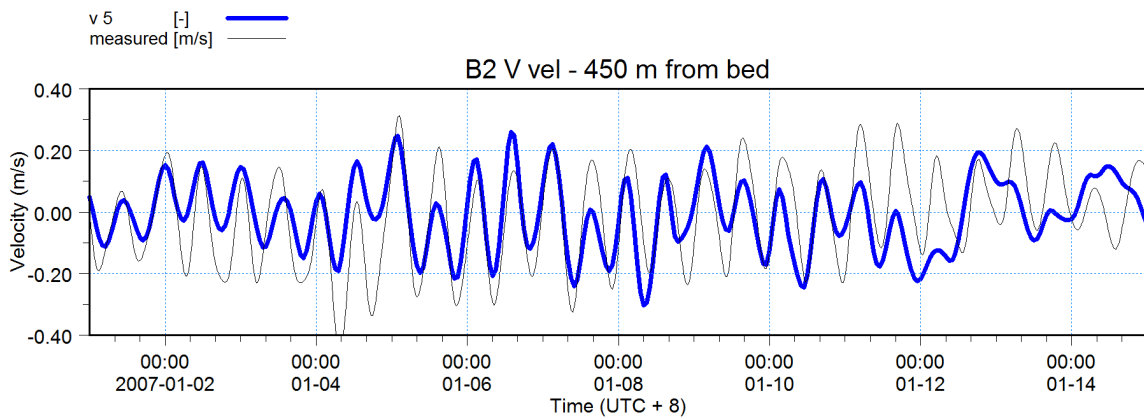
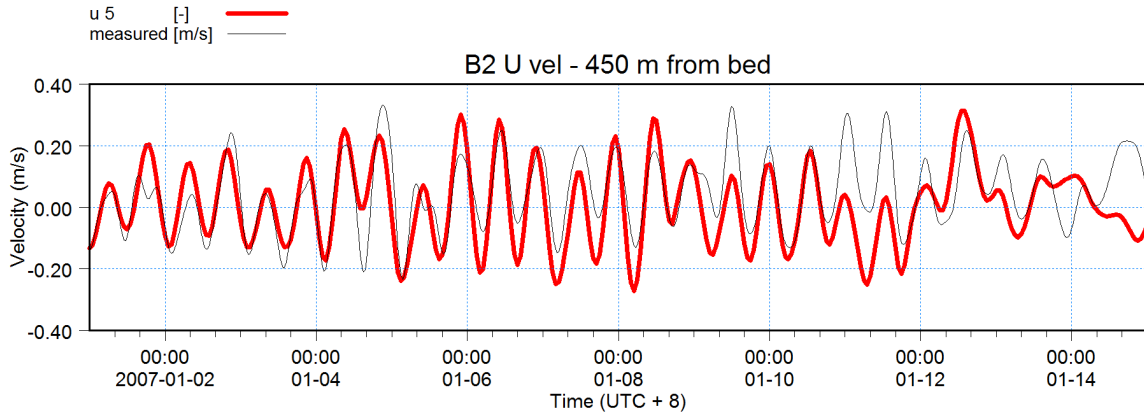


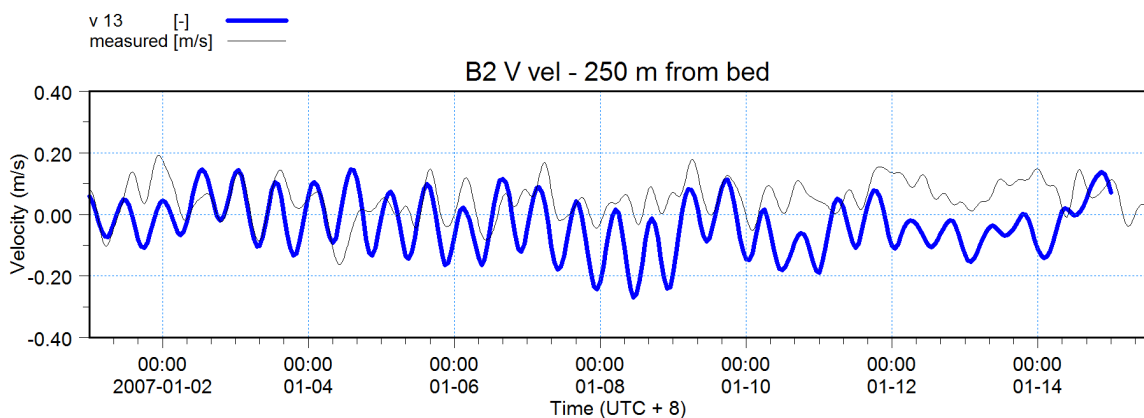
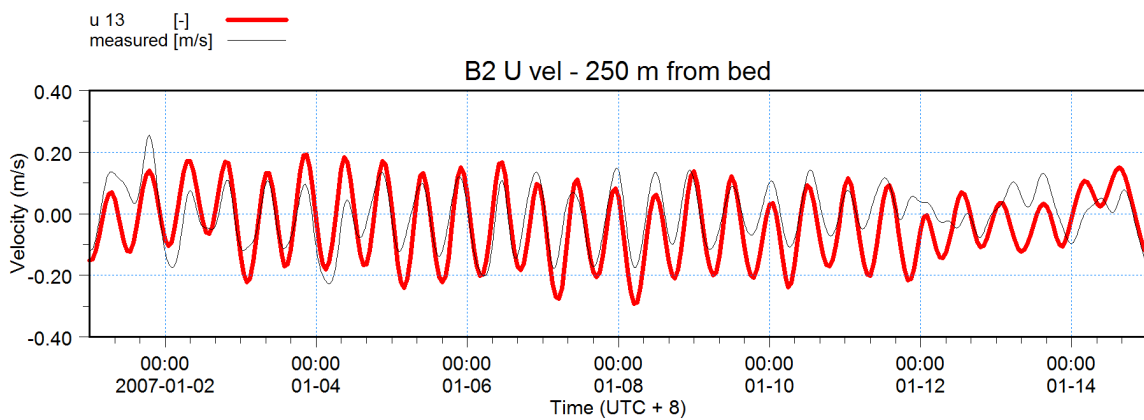
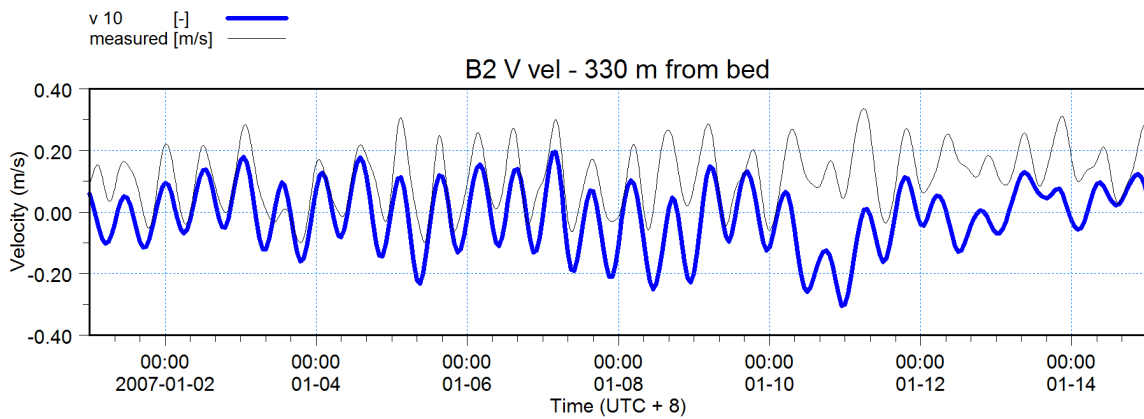
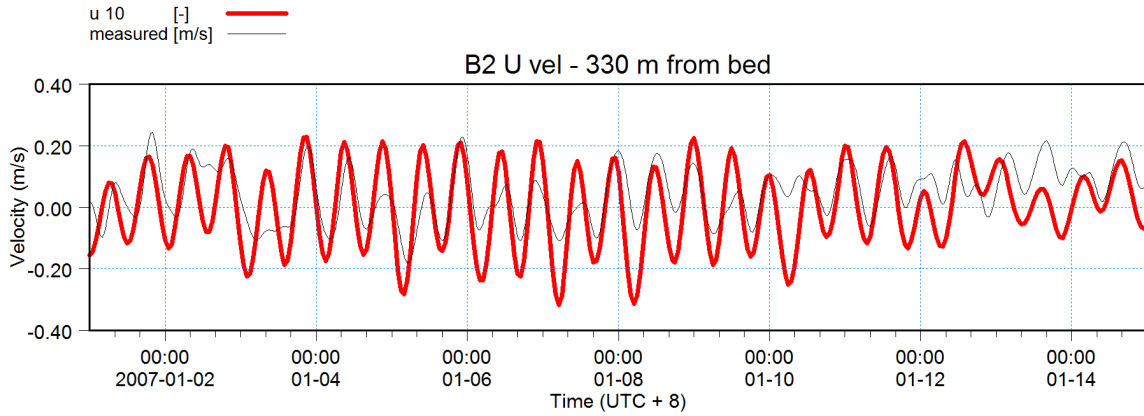


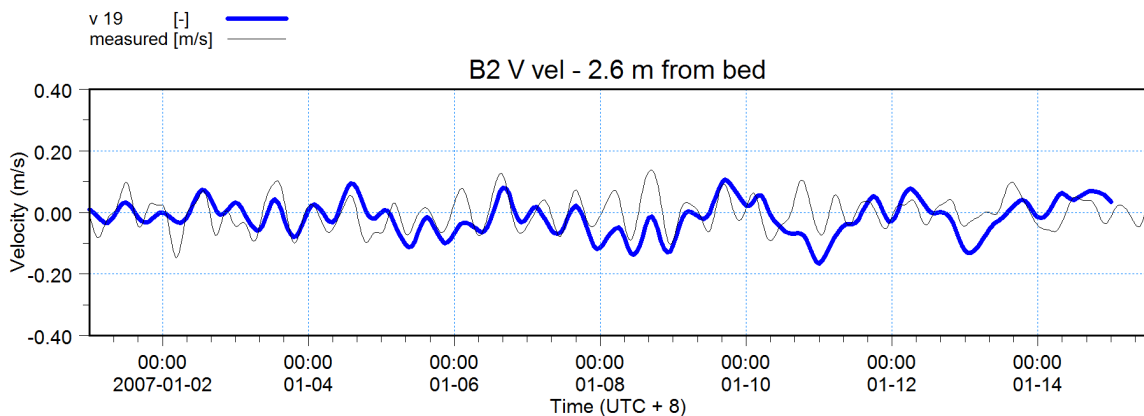
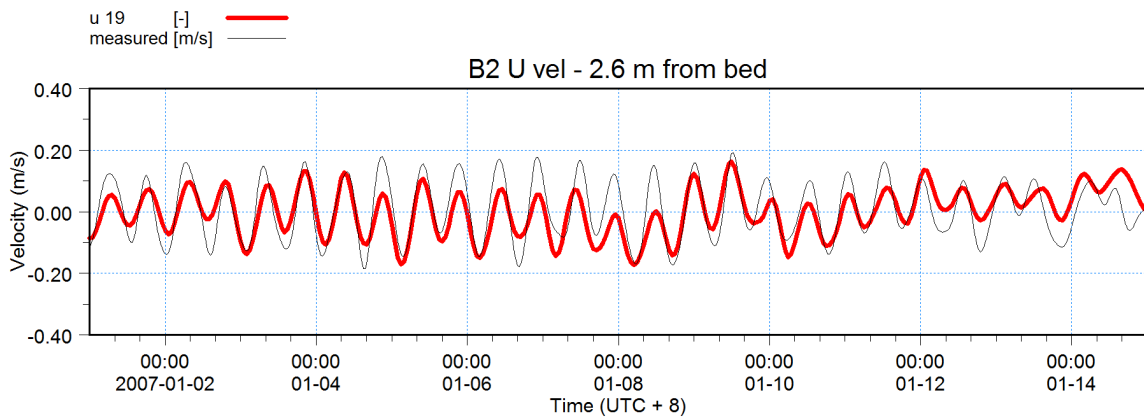
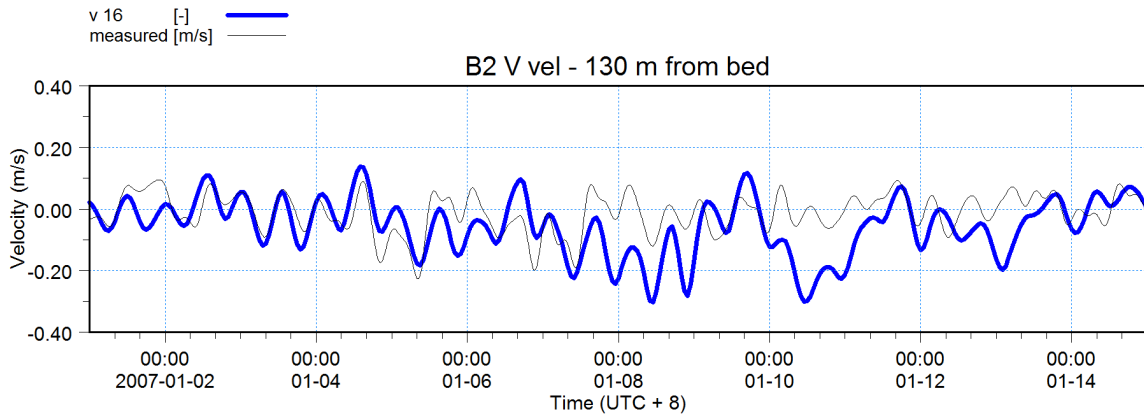
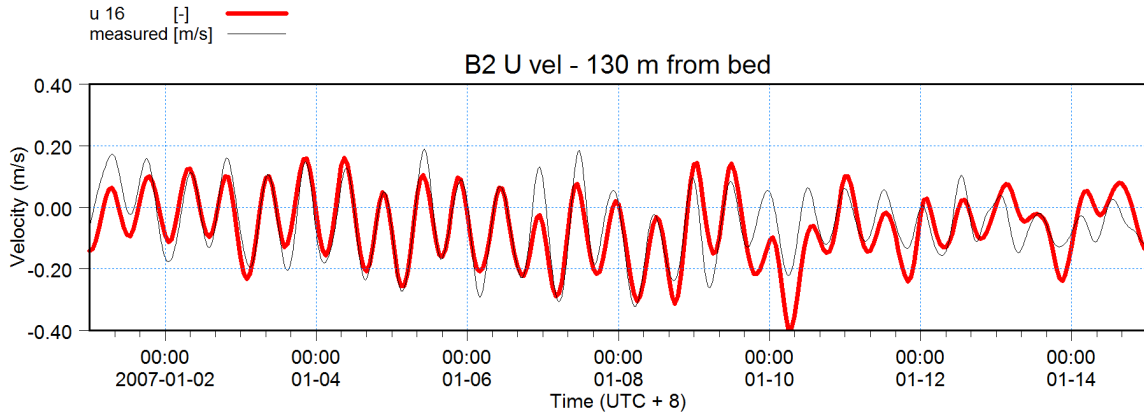
B2 × ×

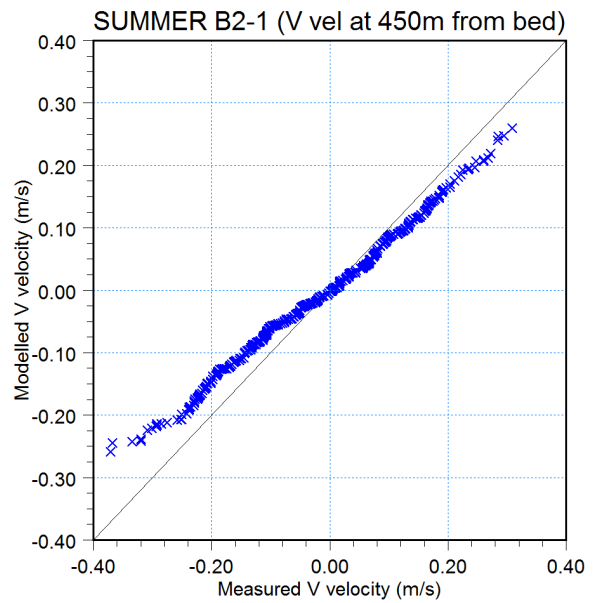
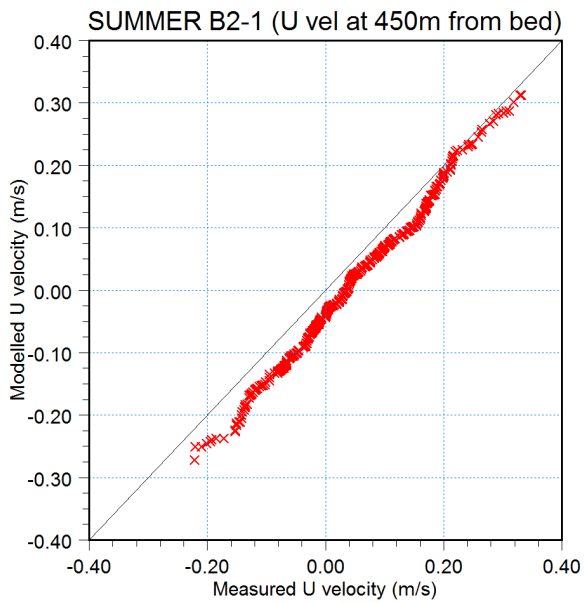
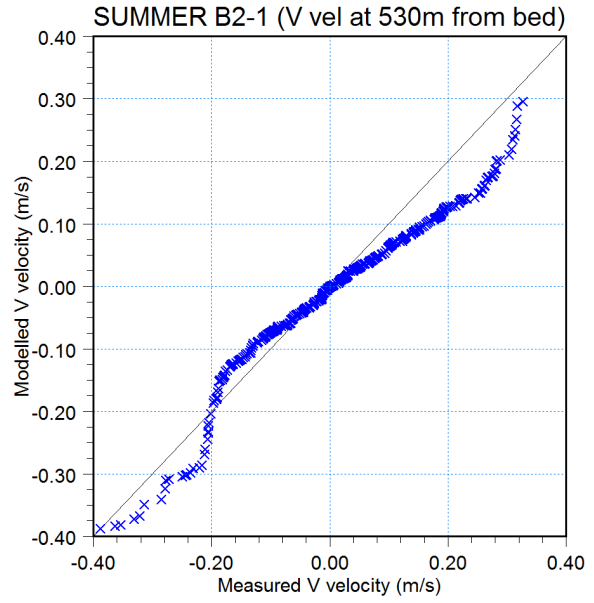
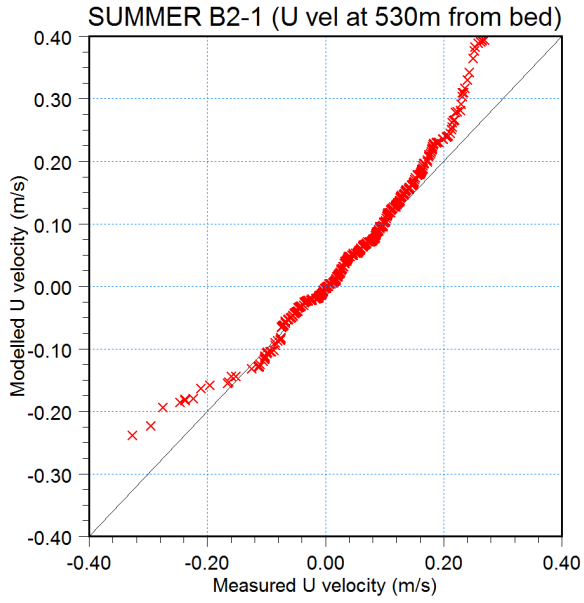


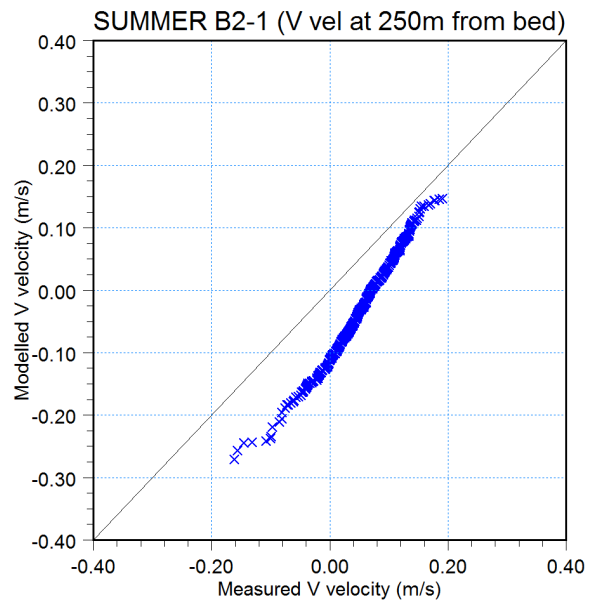
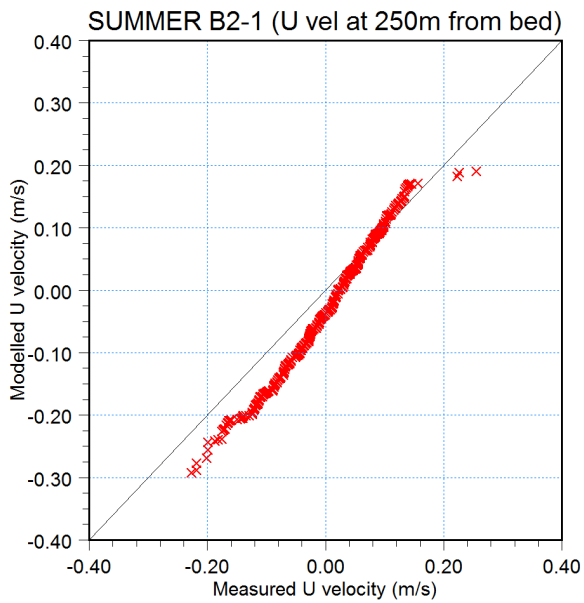
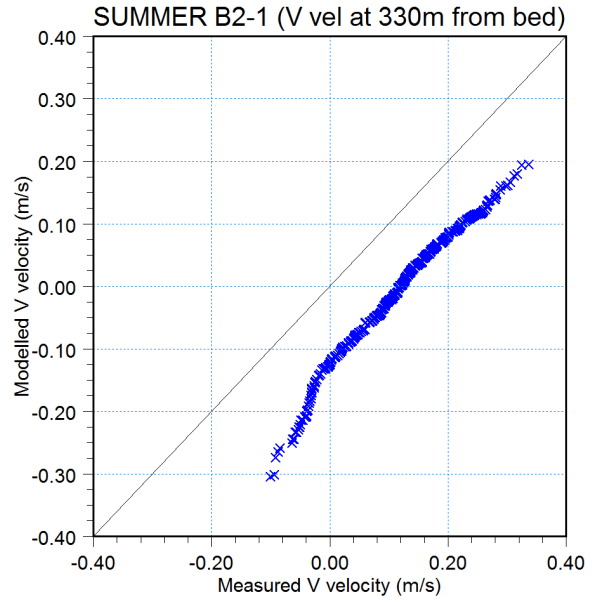
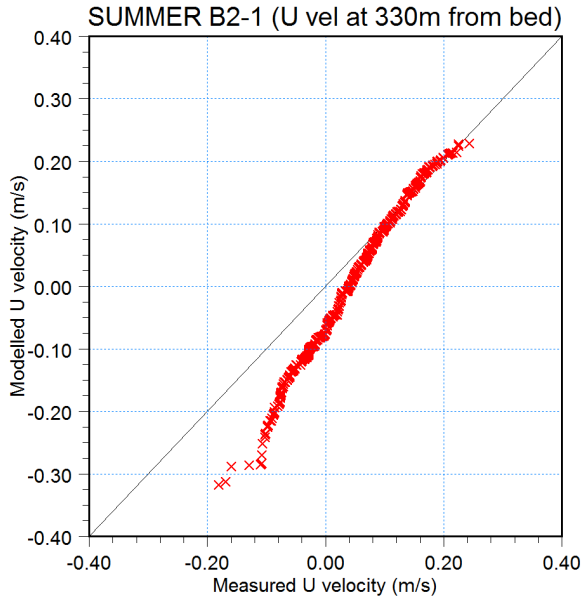


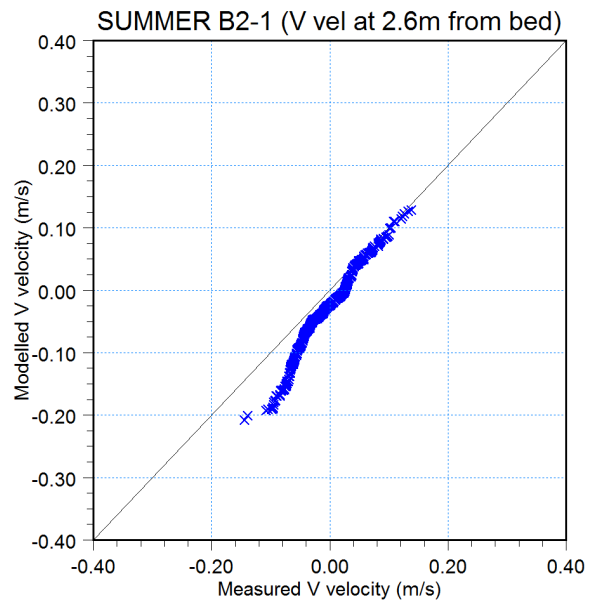
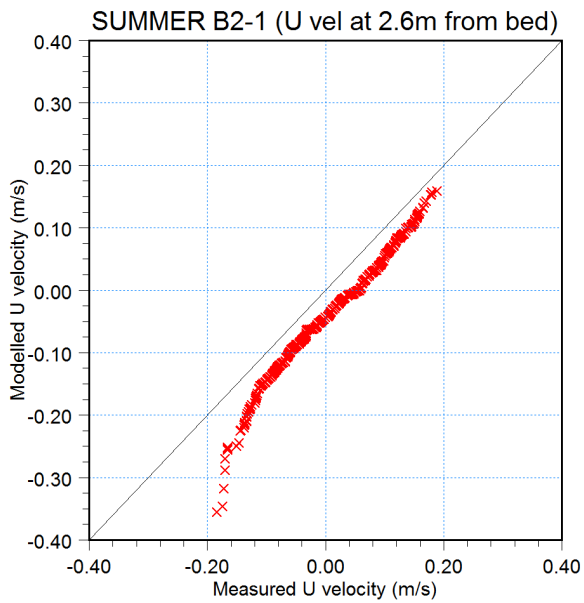
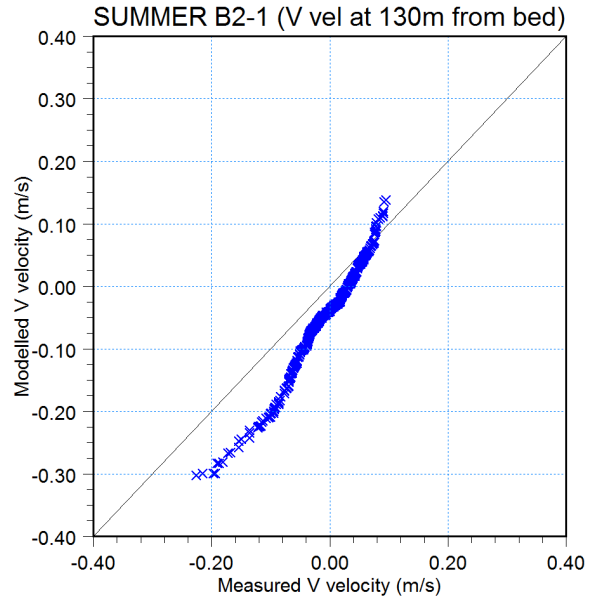
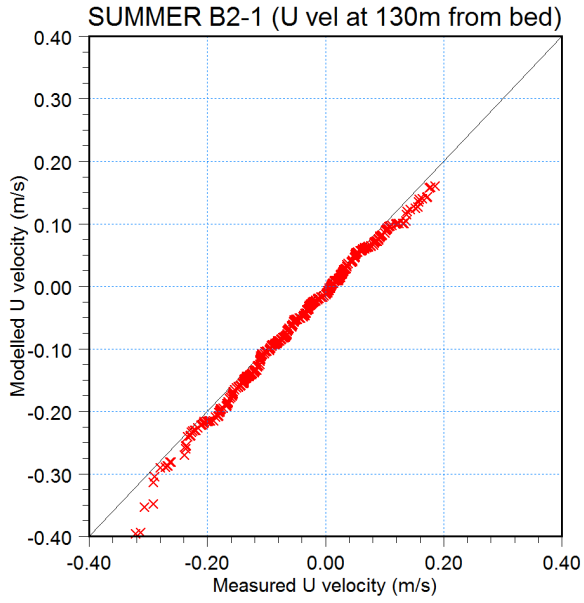


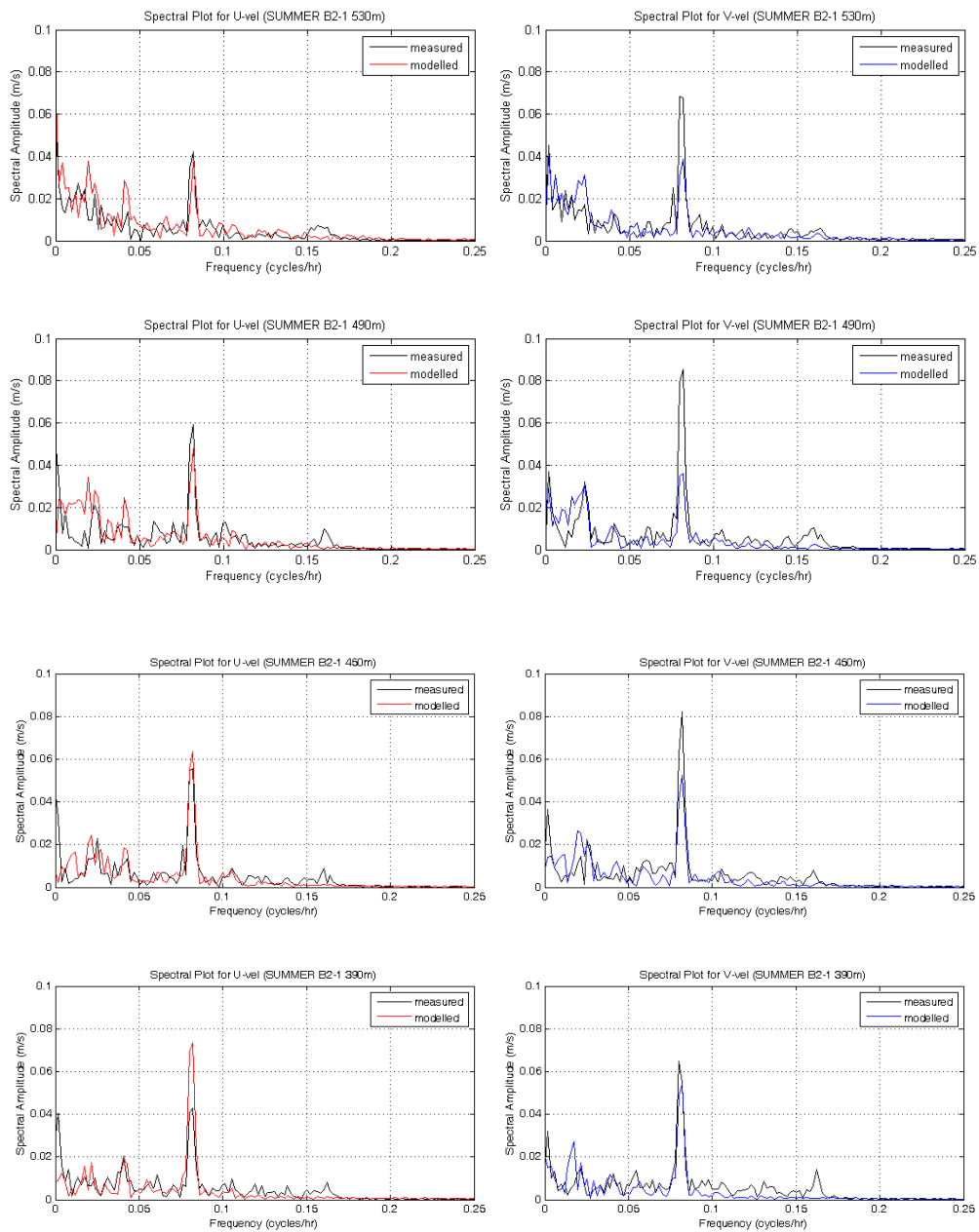


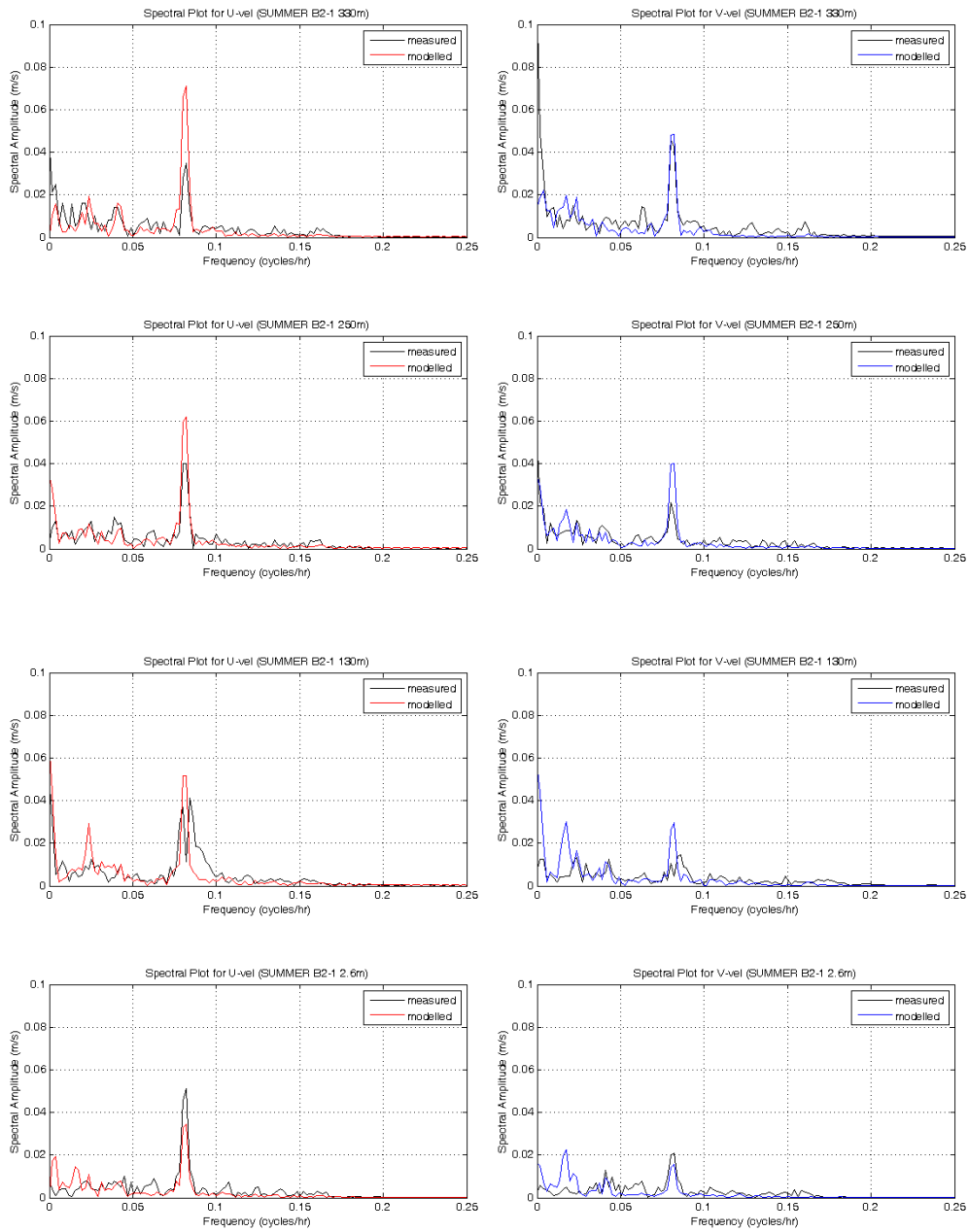








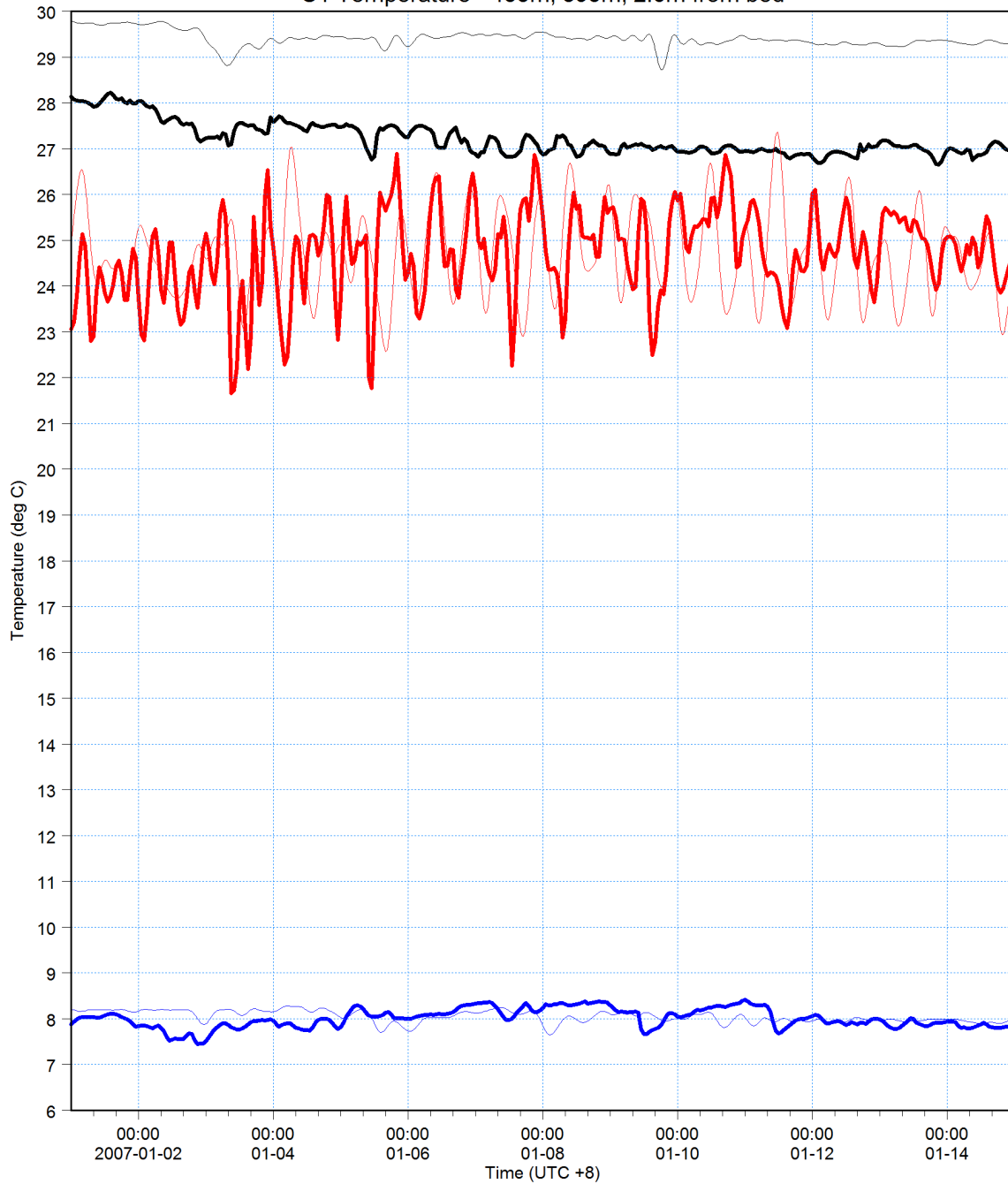






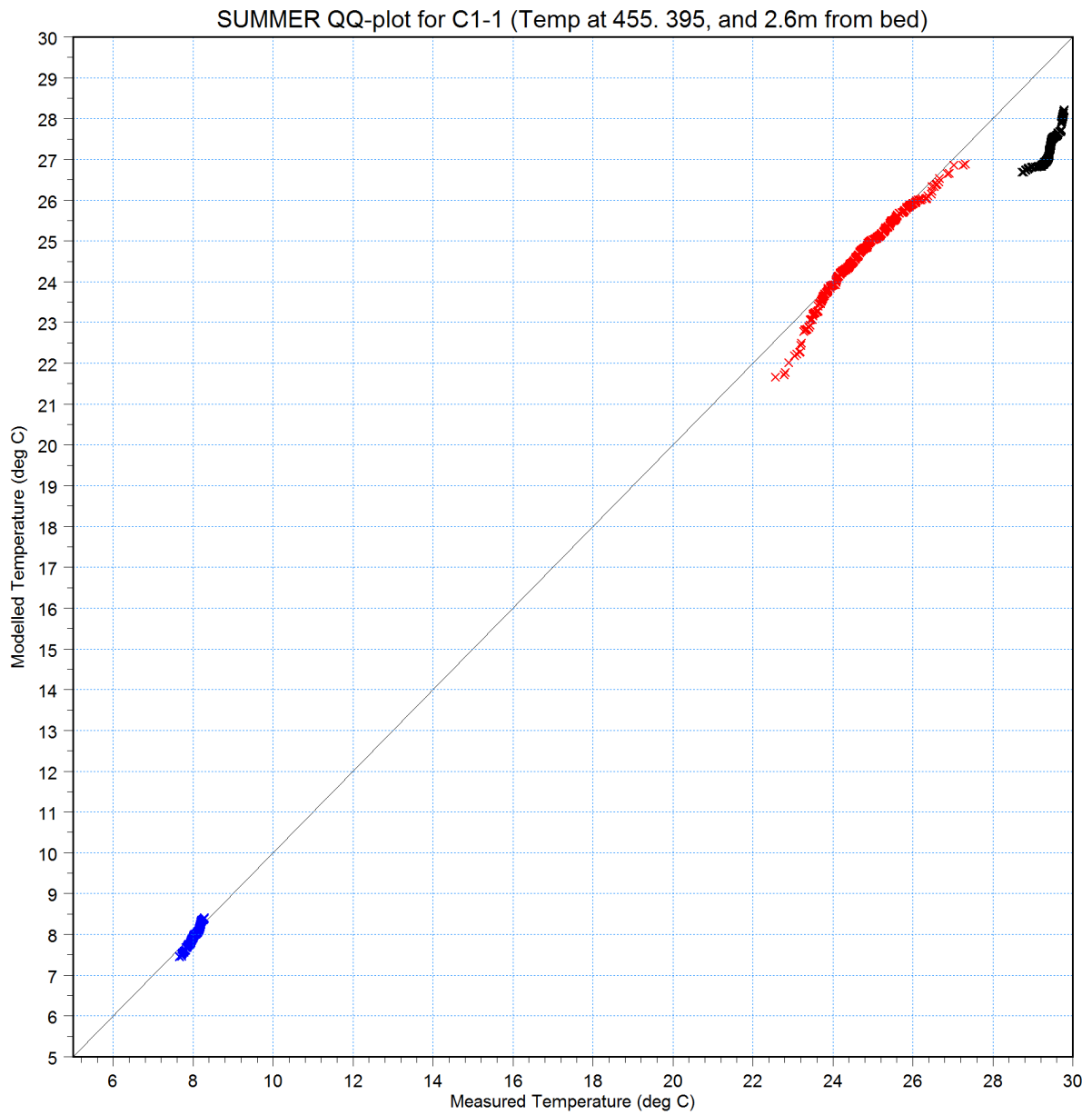
455m from bed: Temperature [C] [deg C] ———
measured [deg C] ———
395m from bed: Temperature [C] [deg C] ———
measured [deg C] ———
2.6m from bed: Temperature [C] [deg C] ———
measured [deg C] ———

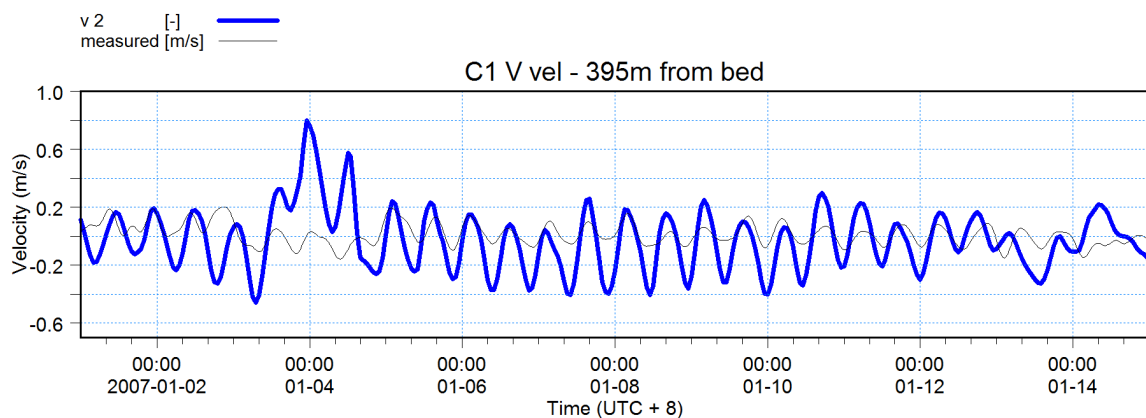
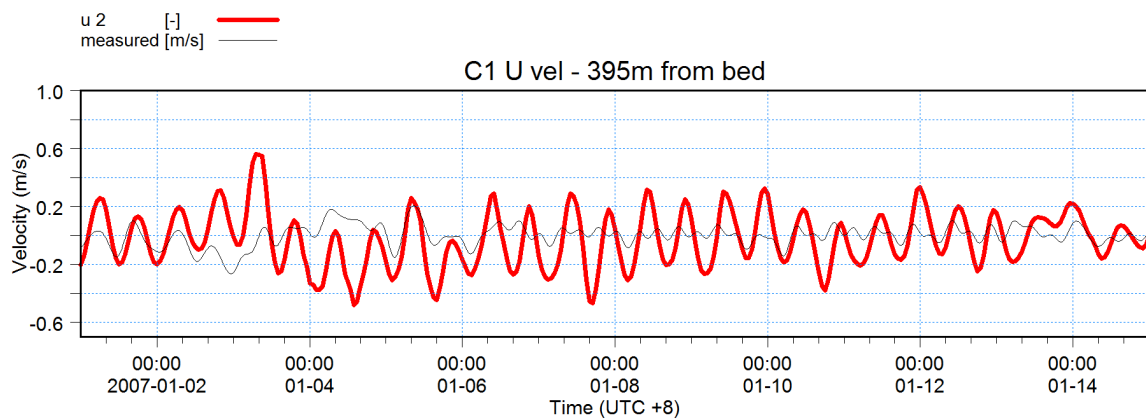
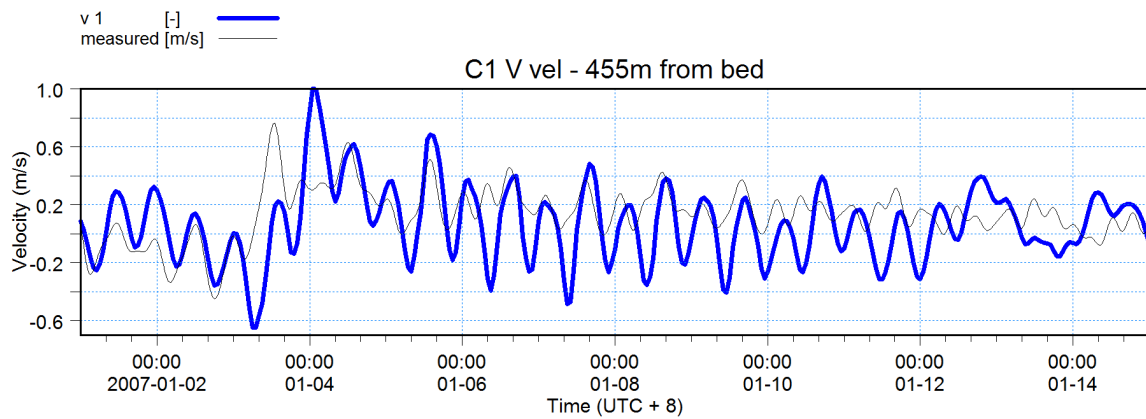
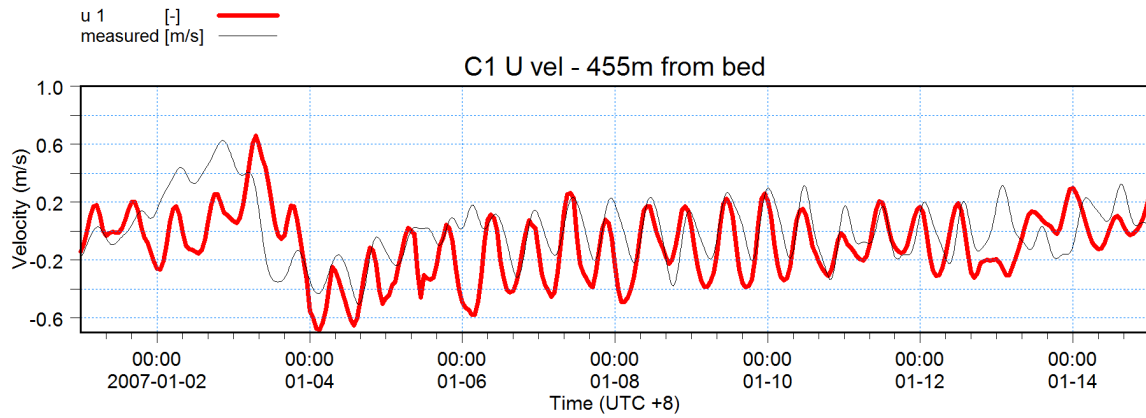
C1 Temperature - 455m, 395m, 2.6m from bed

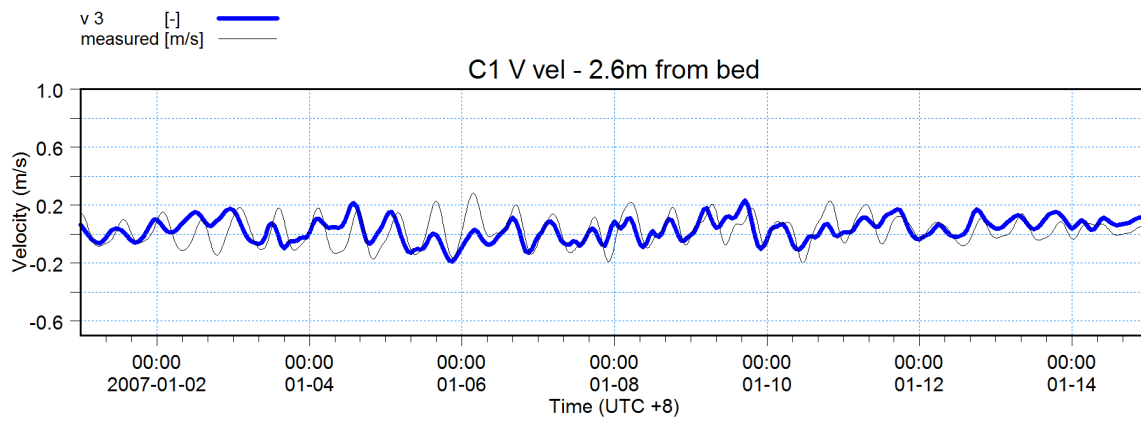
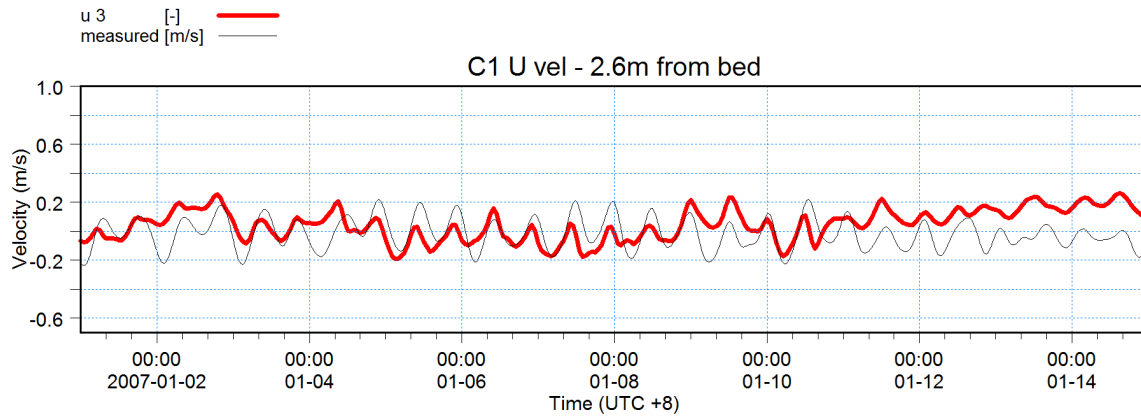


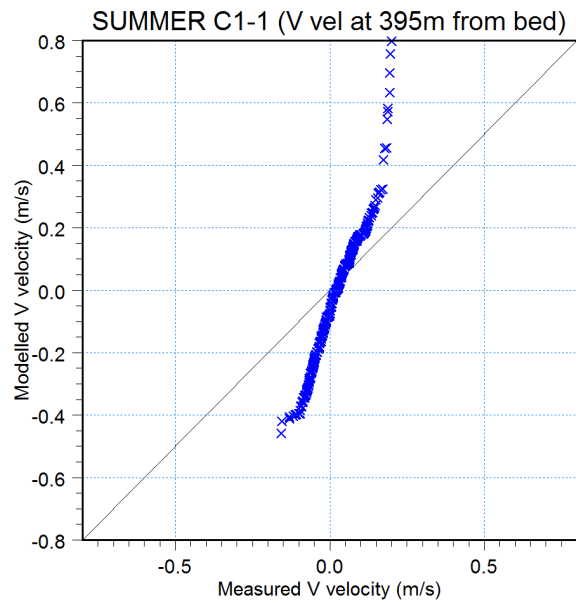
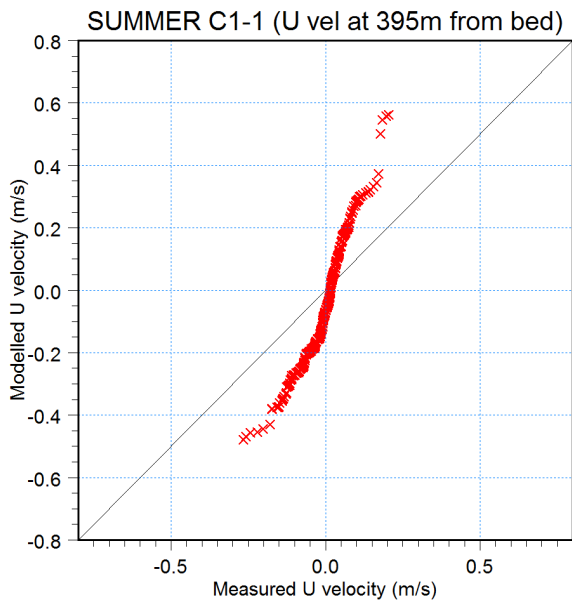
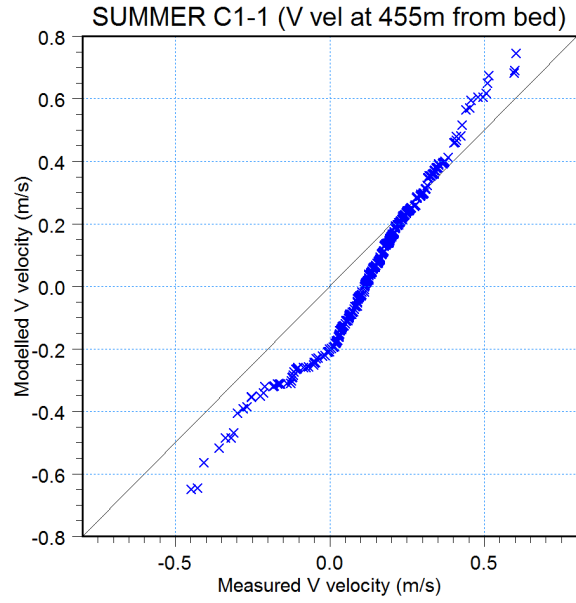
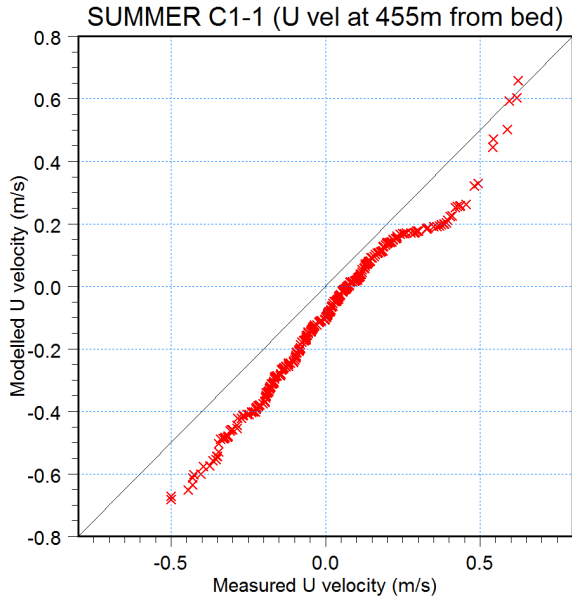


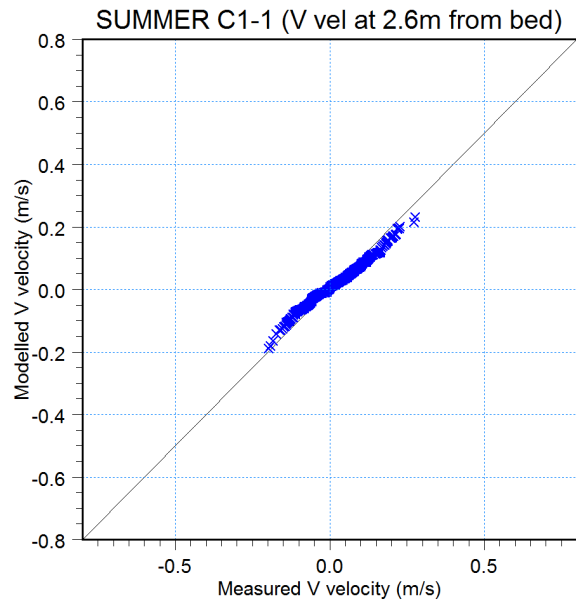
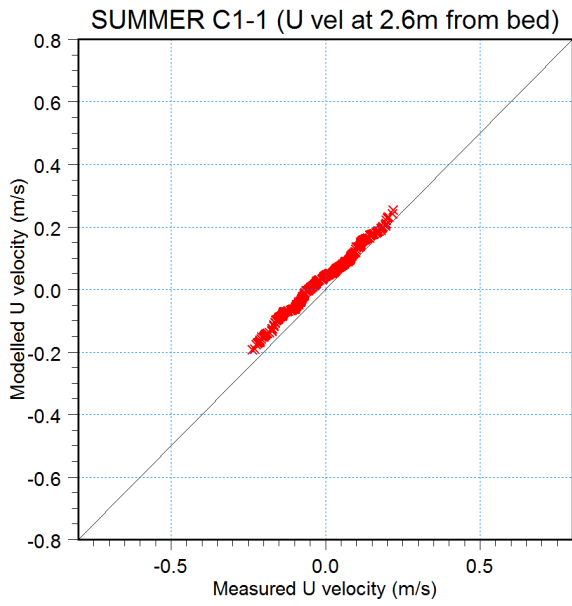
T at 455m × ×
T at 395m × ×
T at 2.6m × ×

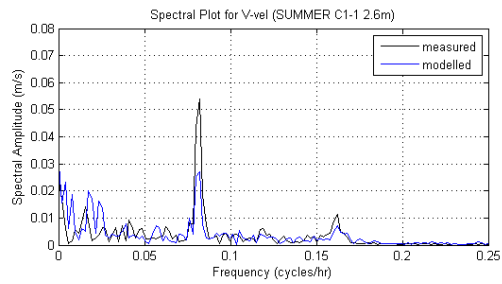
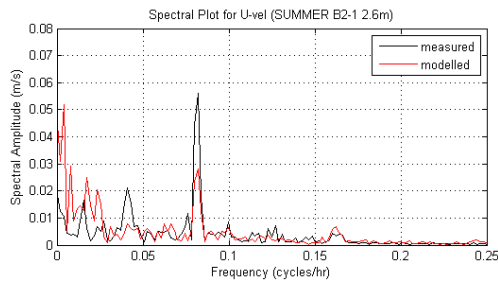
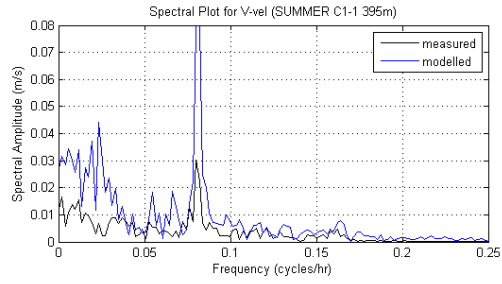
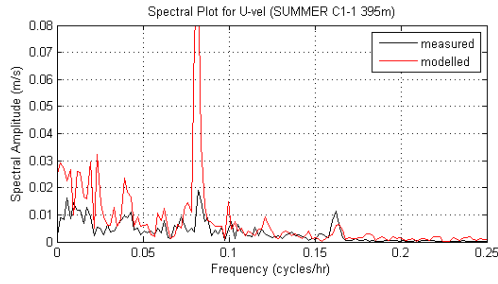
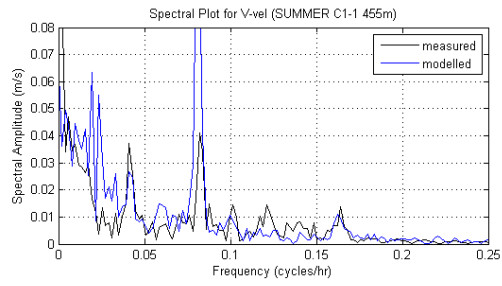
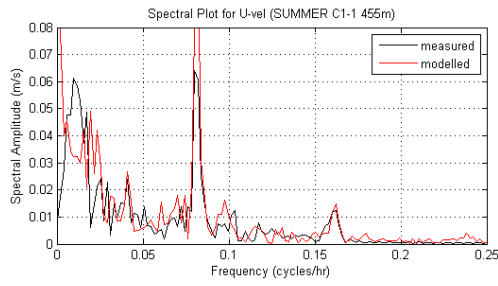


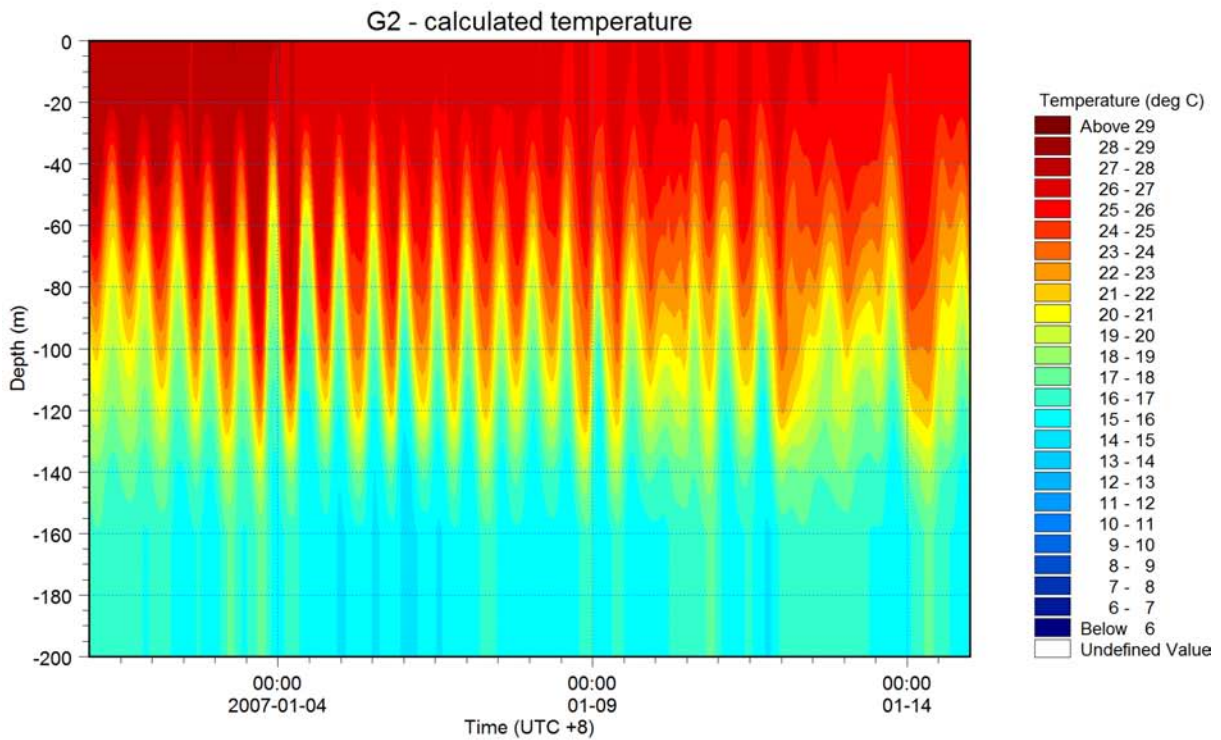
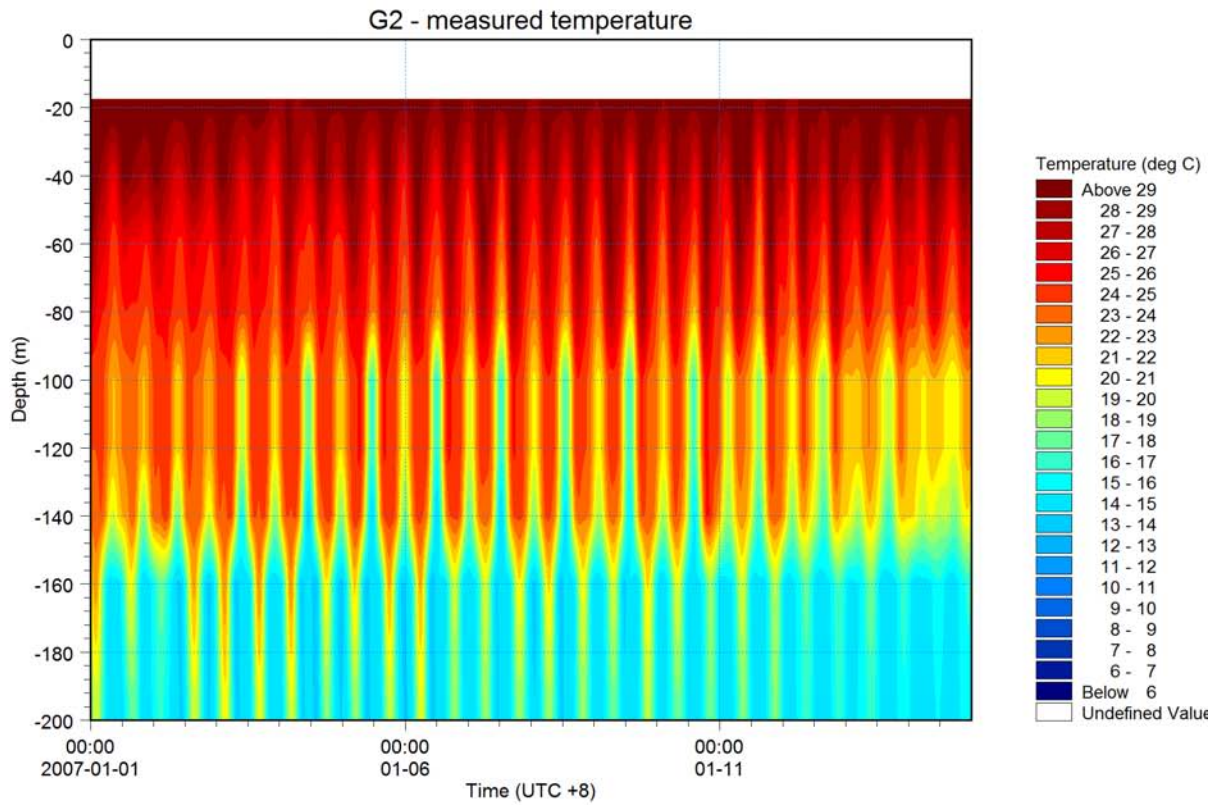








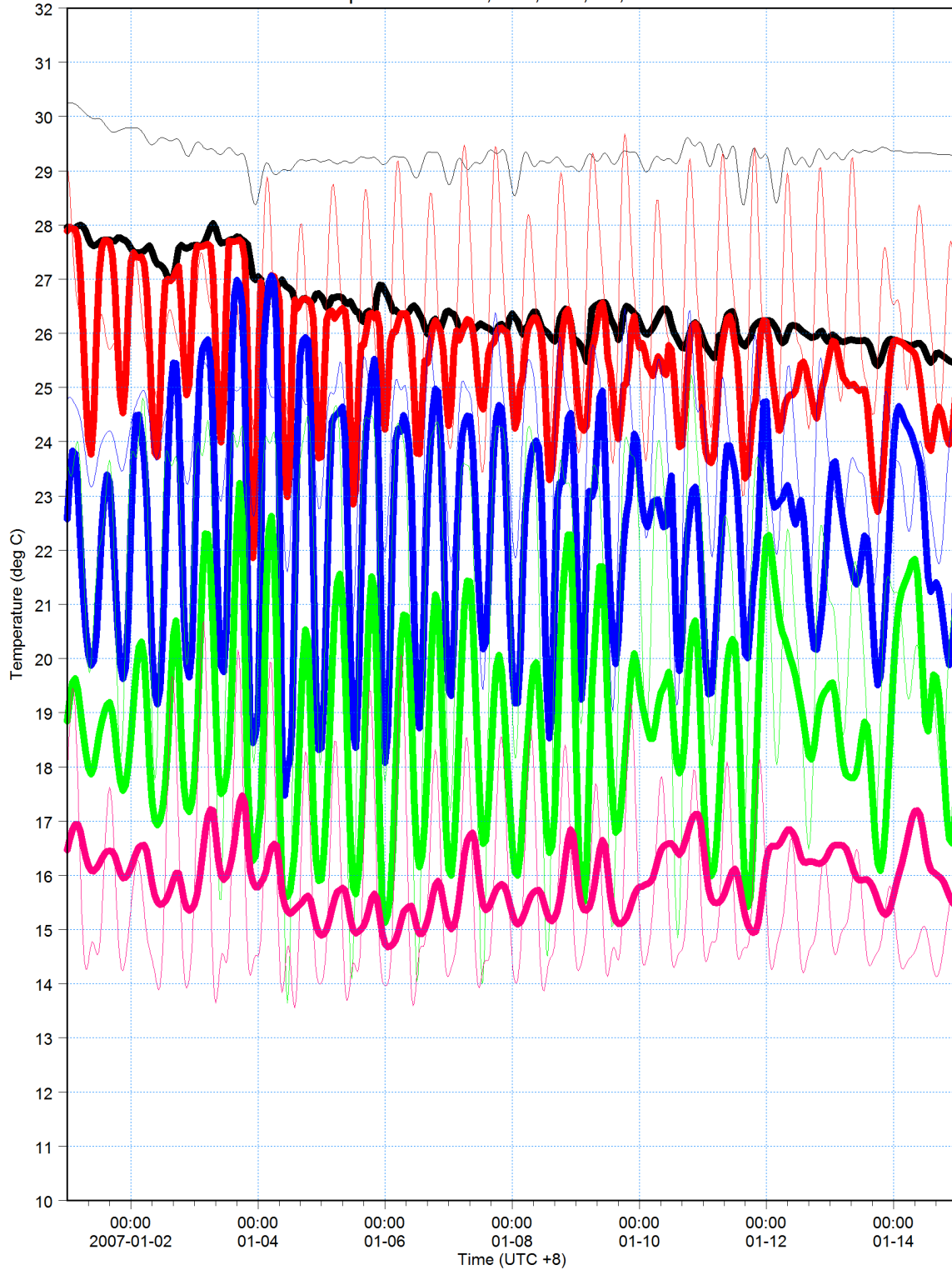






180m from bed: Temperature [C] [deg C] ———
measured [deg C] ———
140m from bed: Temperature [C] [deg C] ———
measured [deg C] ———
100m from bed: Temperature [C] [deg C] ———
measured [deg C] ———
60m from bed: Temperature [C] [deg C] ———
measured [deg C] ———
5m from bed: Temperature [C] [deg C] ———
measured [deg C] ———

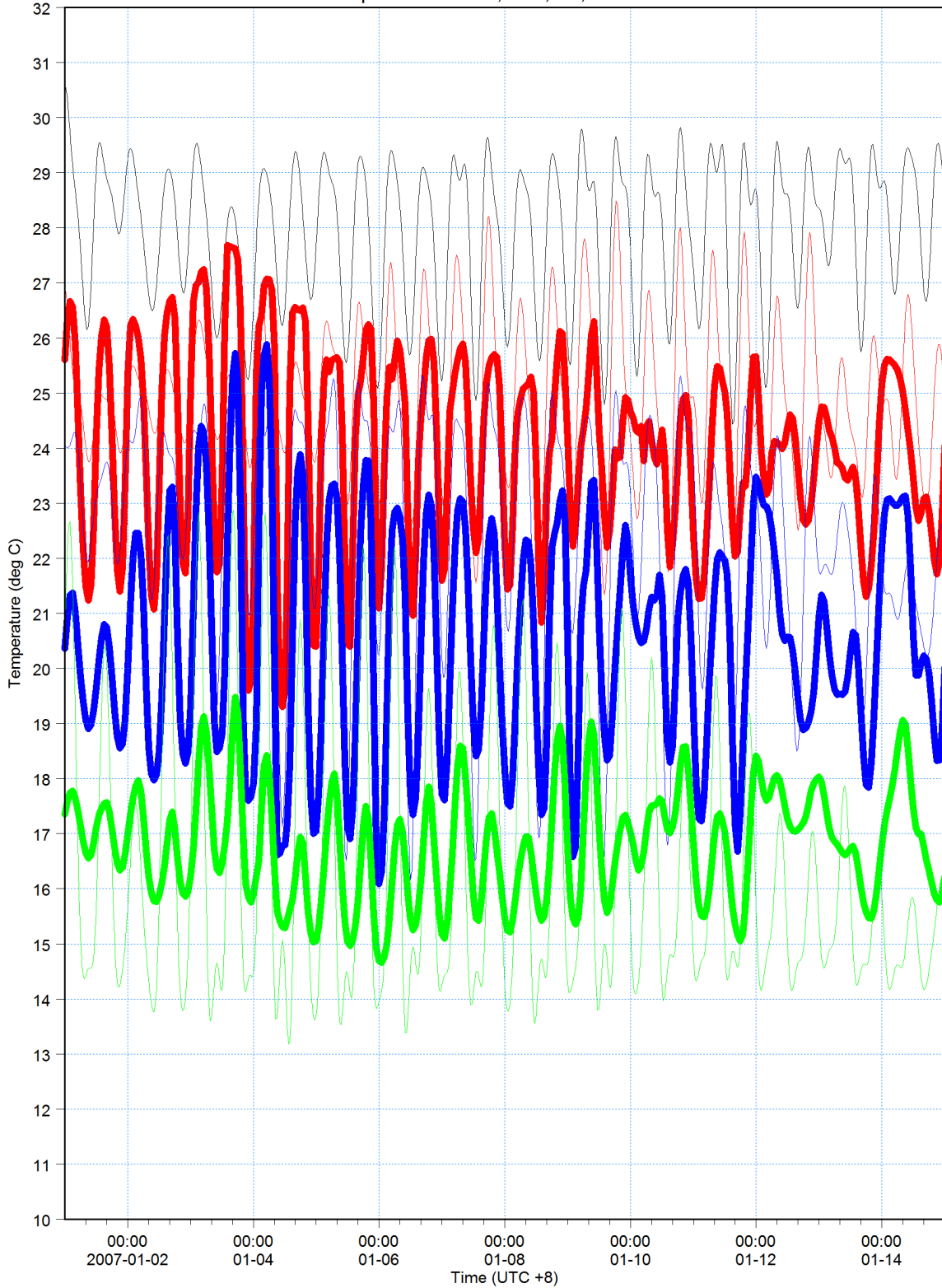
G2 Temperature - 180, 140, 100, 60, 5m from bed





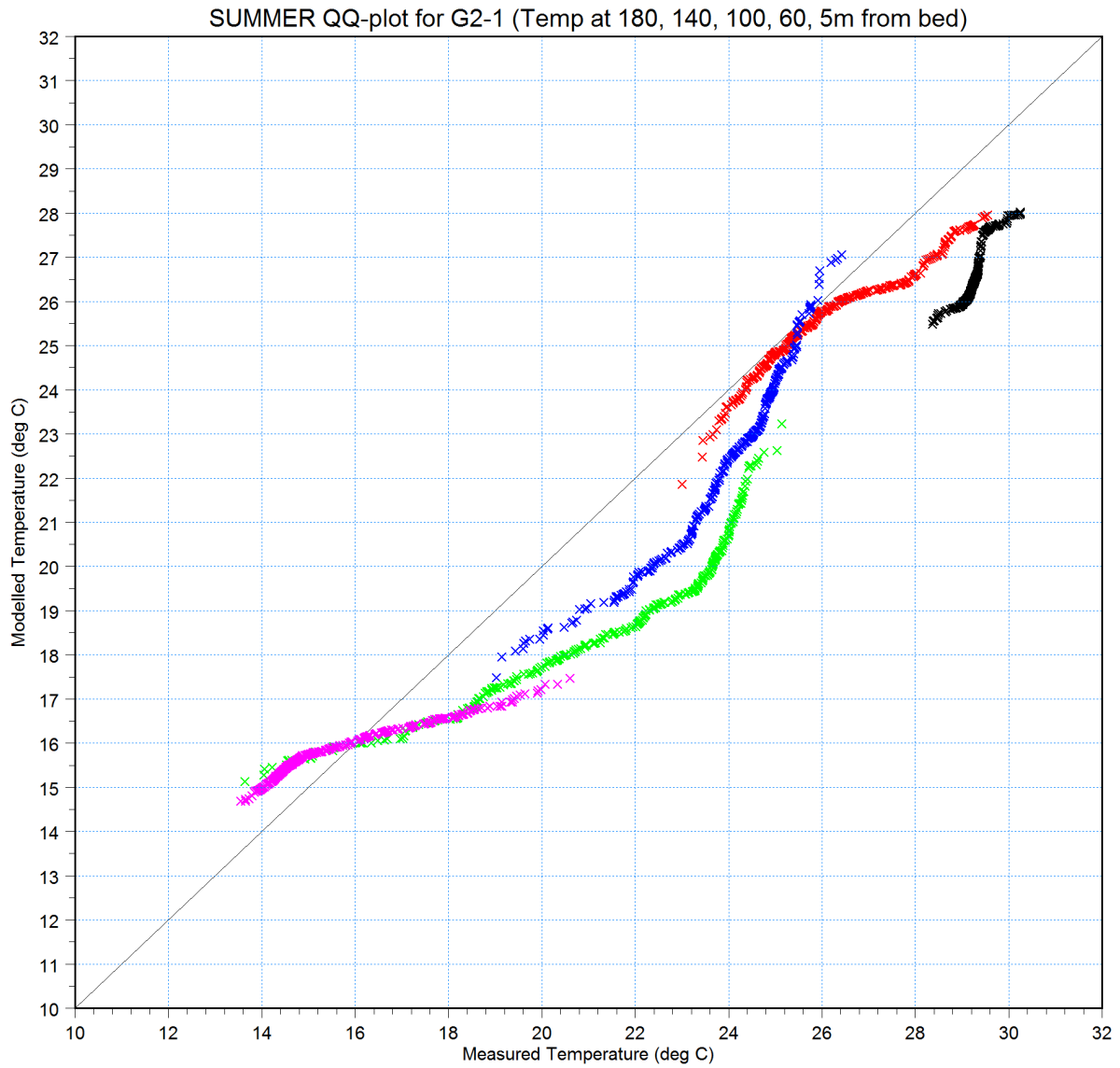
160m from bed: Temperature [C] [deg C] **—**
measured [deg C] **—**
120m from bed: Temperature [C] [deg C] **—**
measured [deg C] **—**
80m from bed: Temperature [C] [deg C] **—**
measured [deg C] **—**
40m from bed: Temperature [C] [deg C] **—**
measured [deg C] **—**

G2 Temperature - 160, 120, 80, 40m form bed



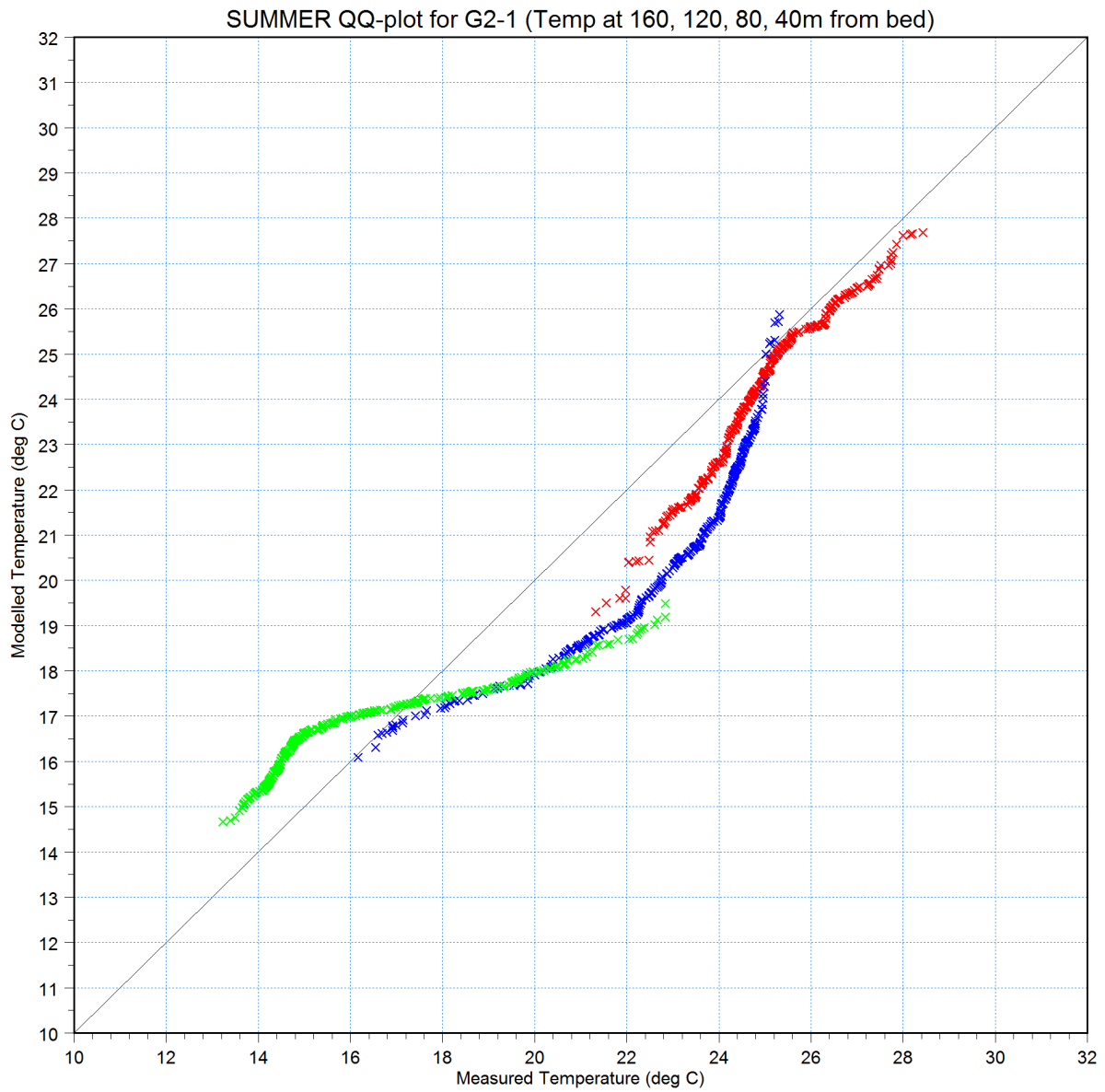


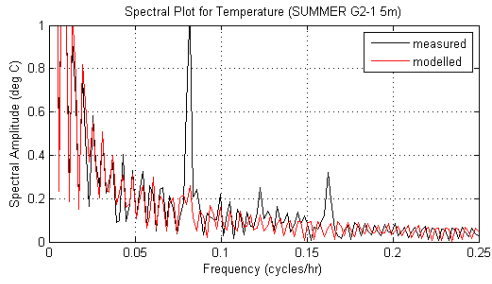
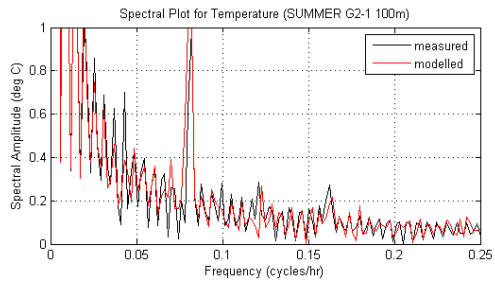
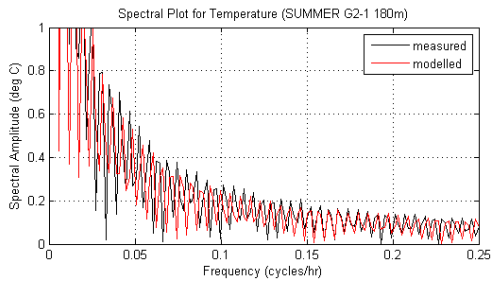
- T at 180m × ×
- T at 140m × ×
- T at 100m × ×
- T at 60m × ×
- T at 5m × ×

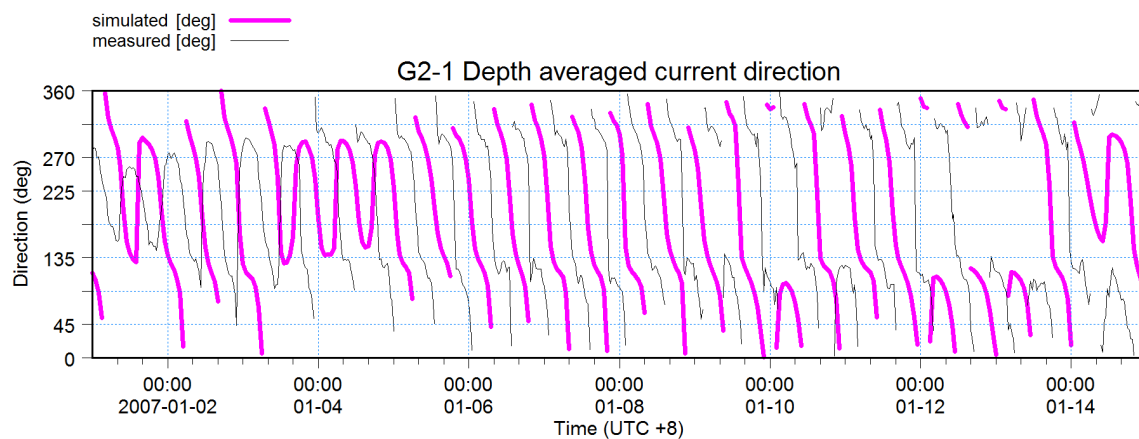
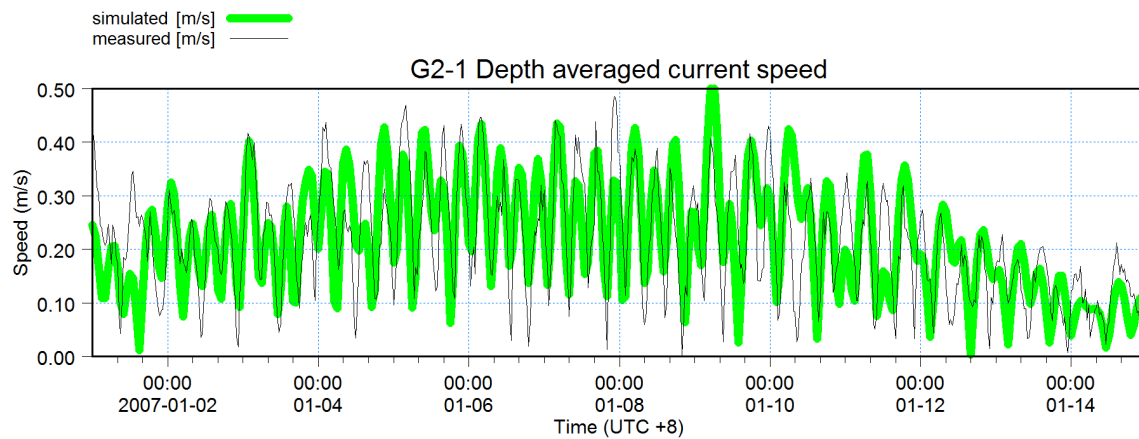
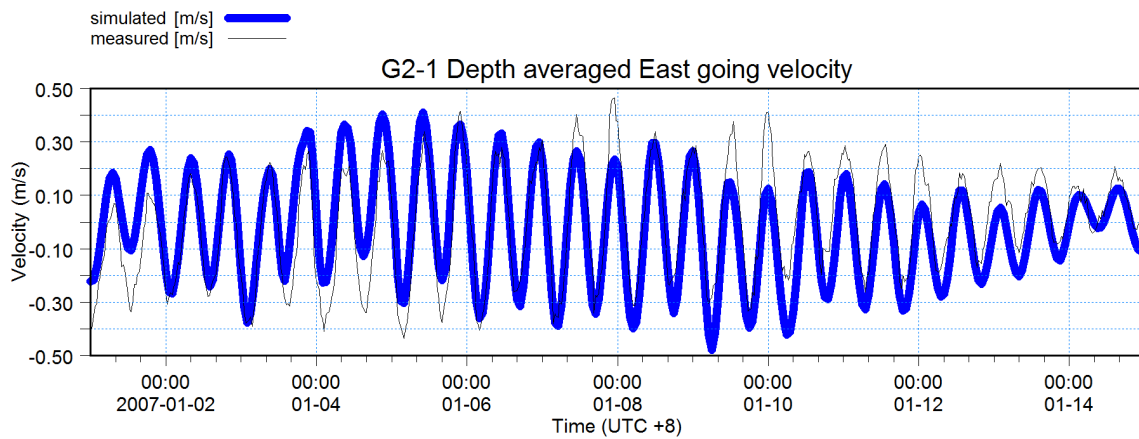
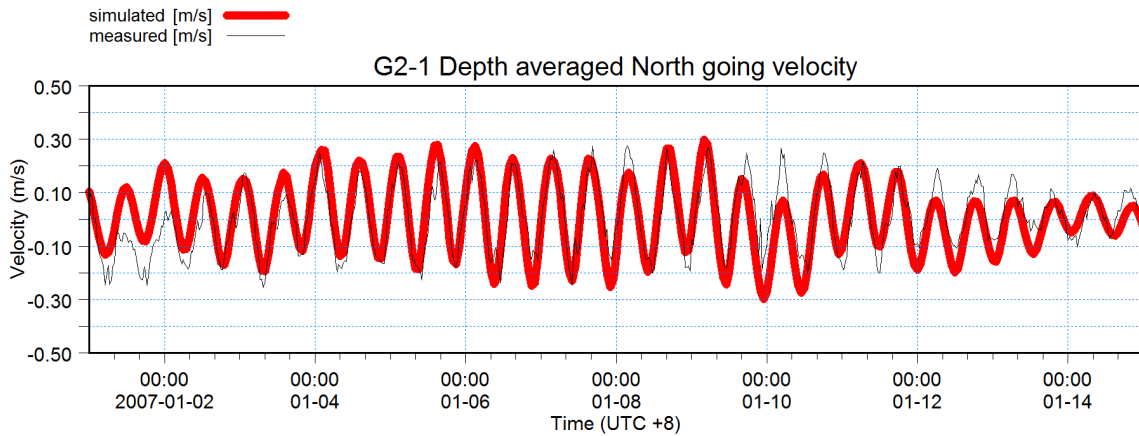




T at 160m × ×
T at 120m × ×
T at 80m × ×
T at 40m × ×



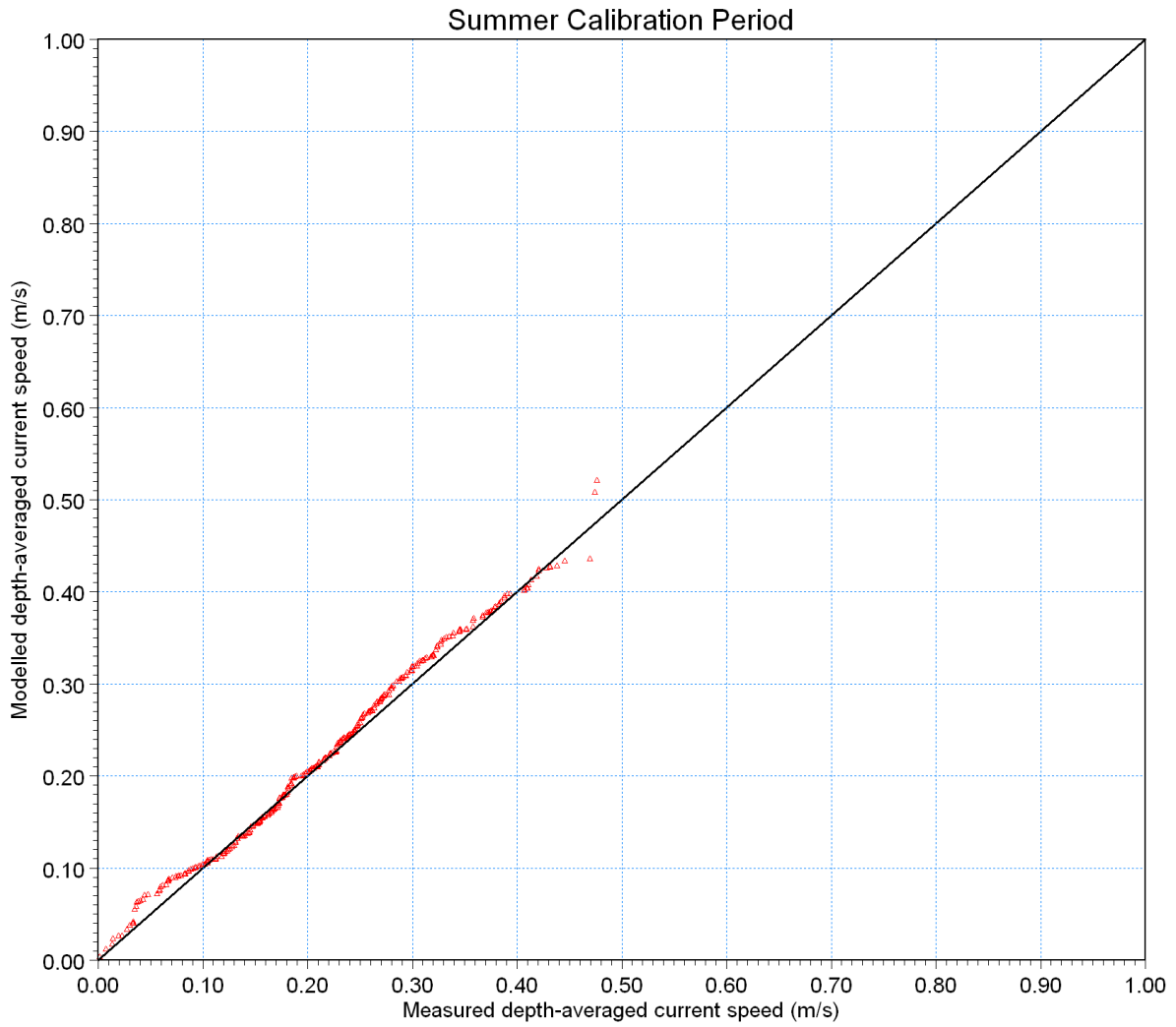


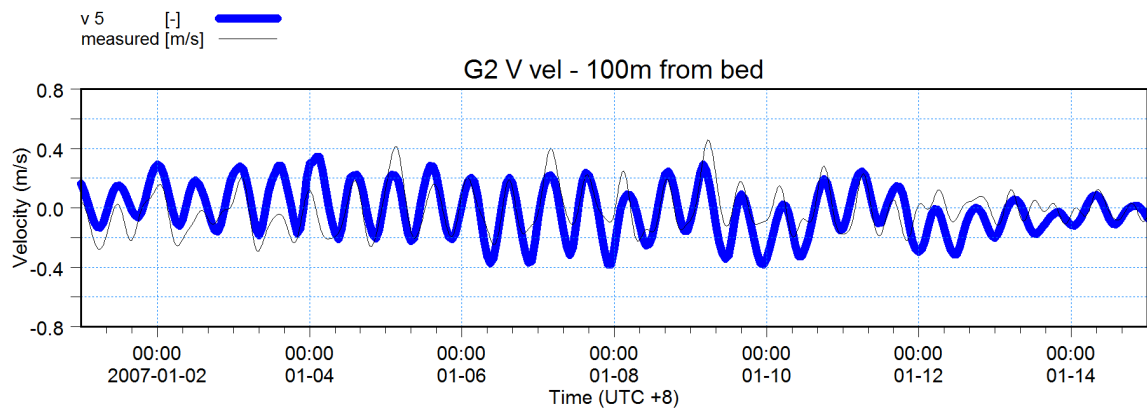
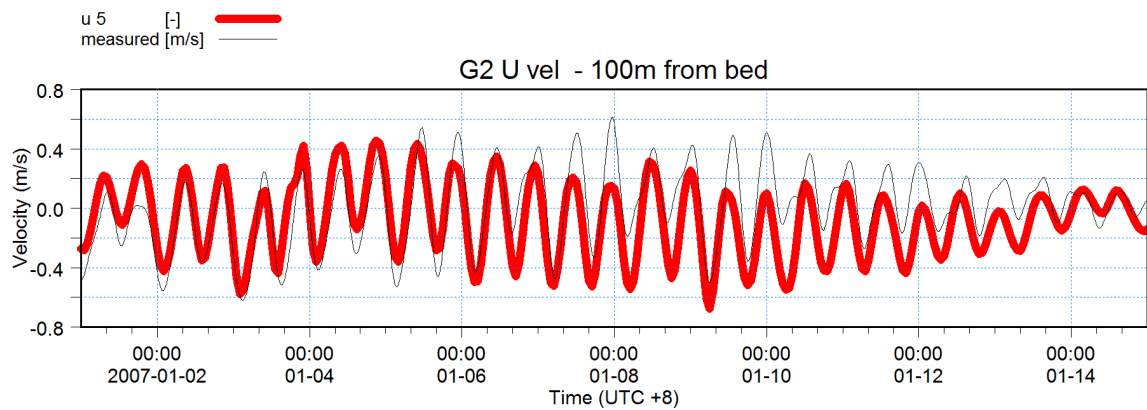
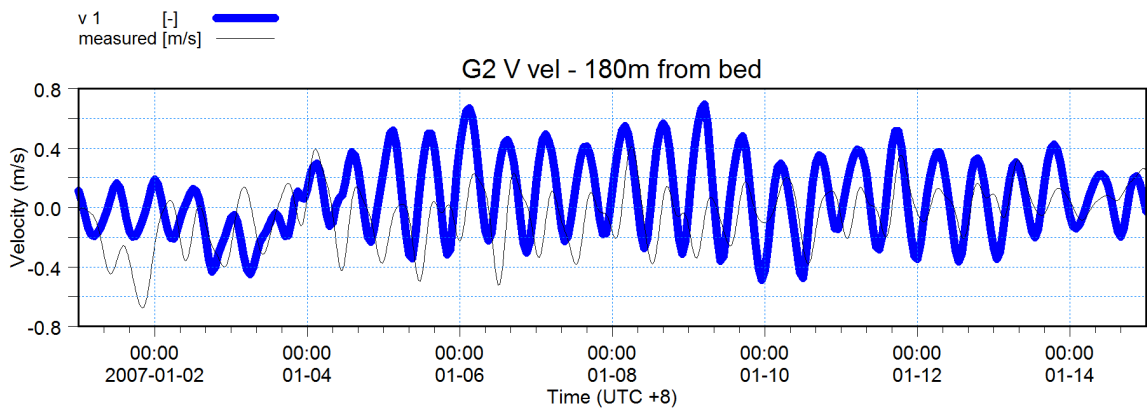
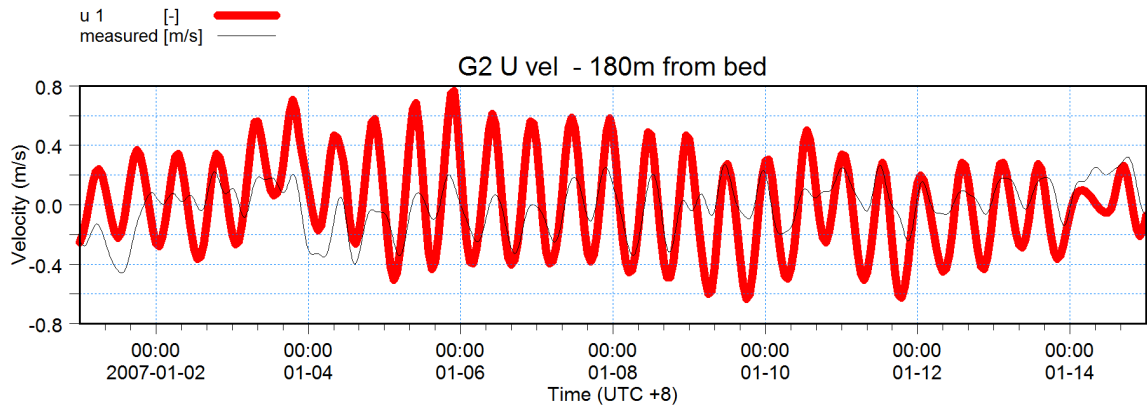


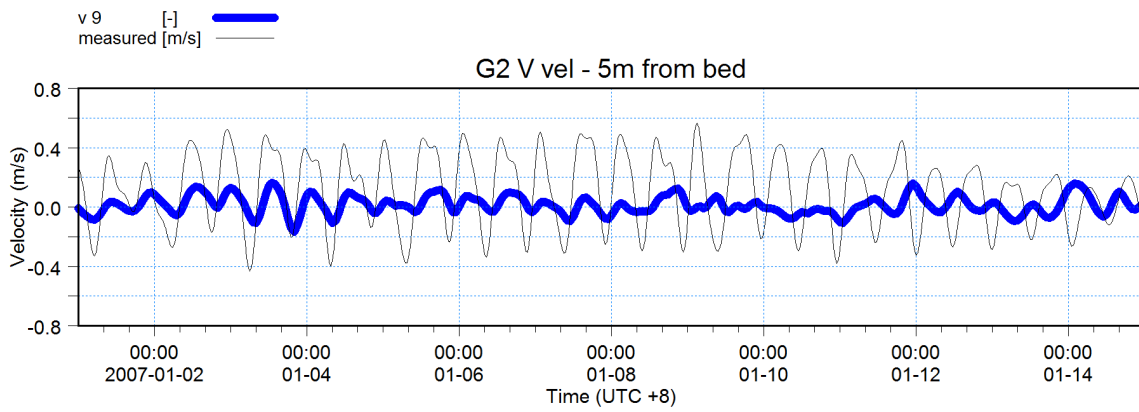
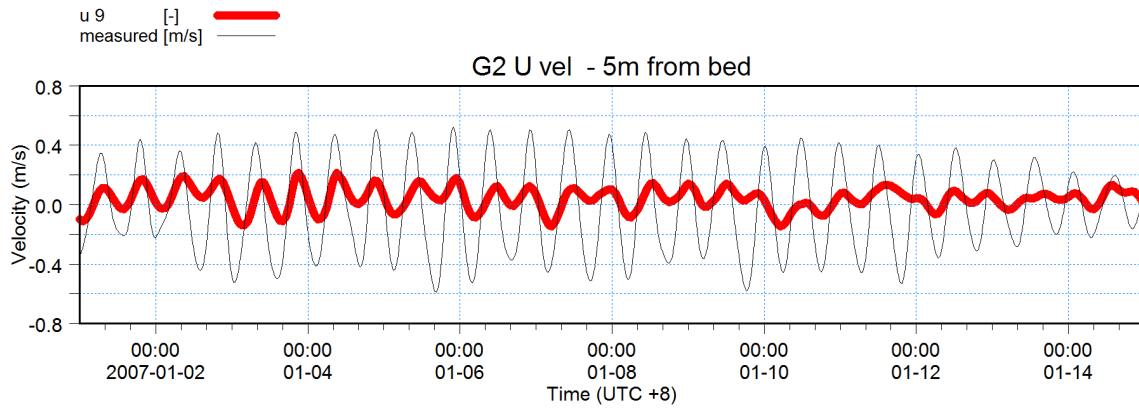


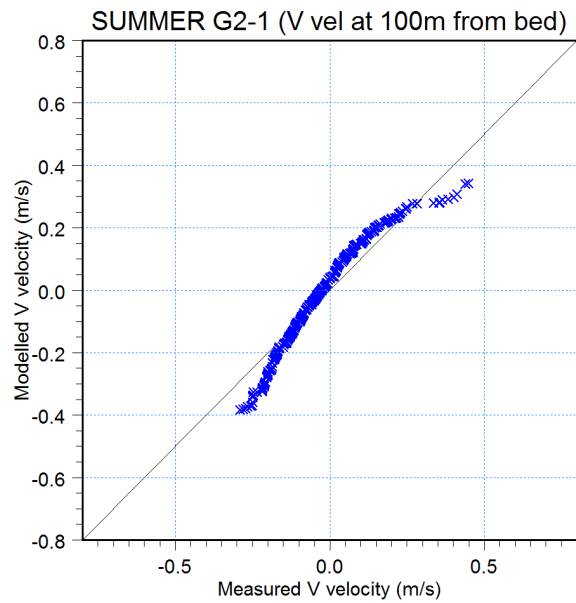
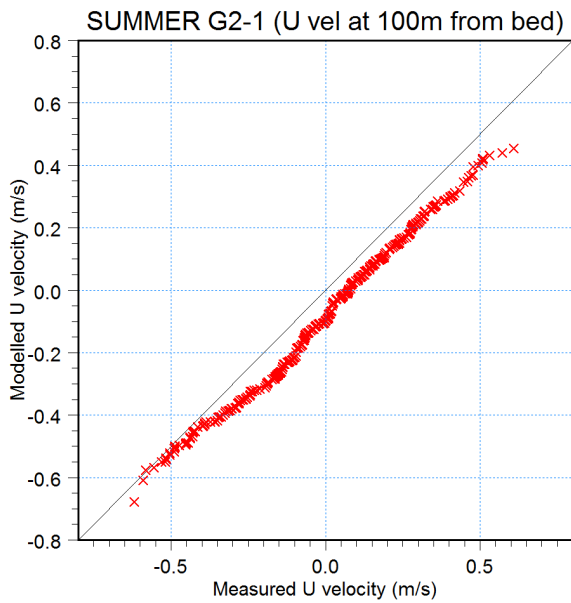
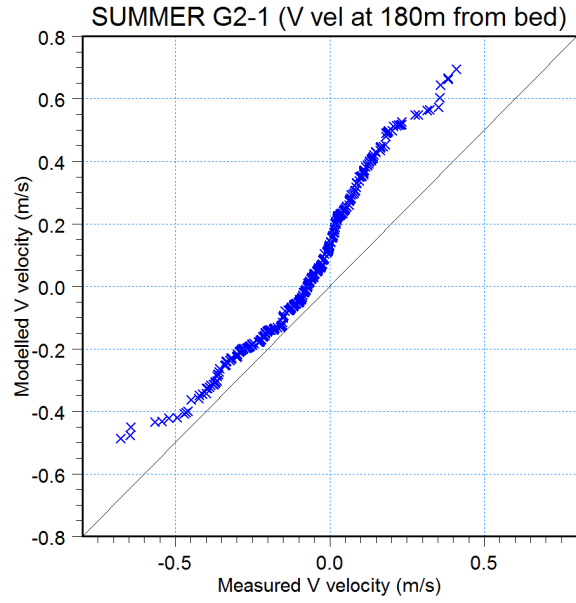
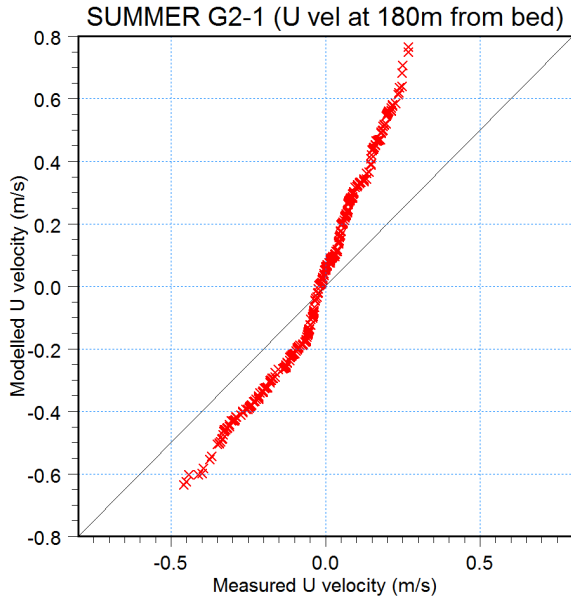
G2

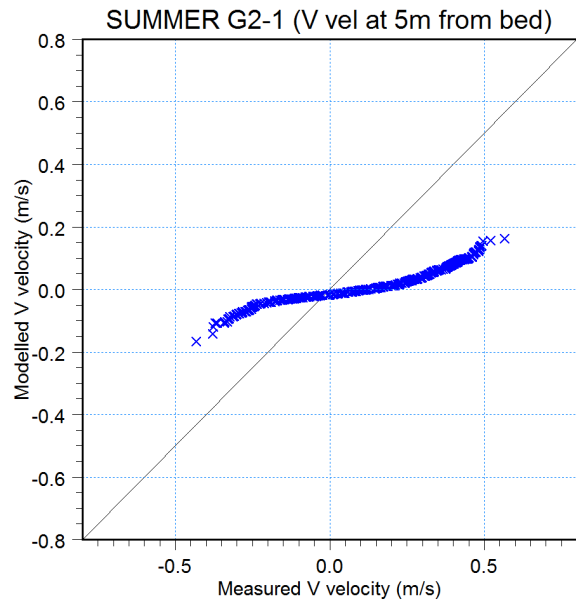
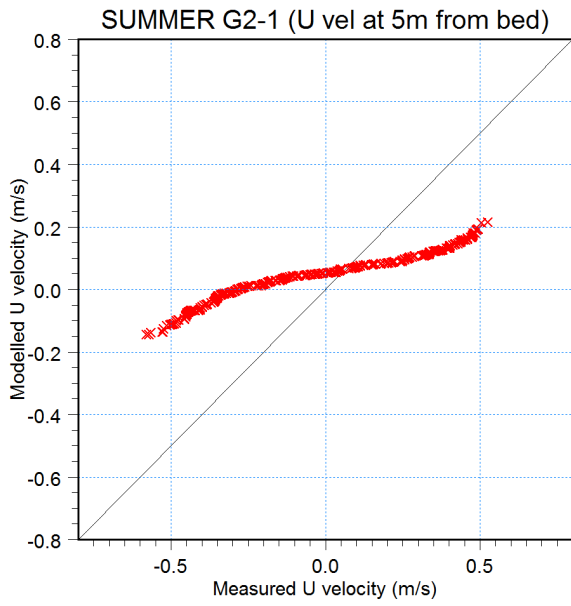
△ △

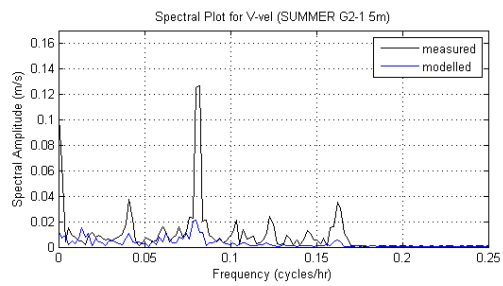
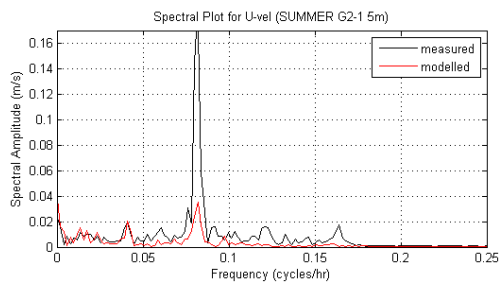
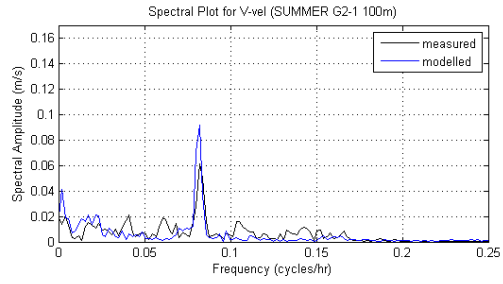
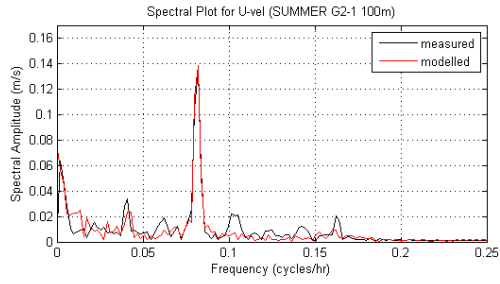
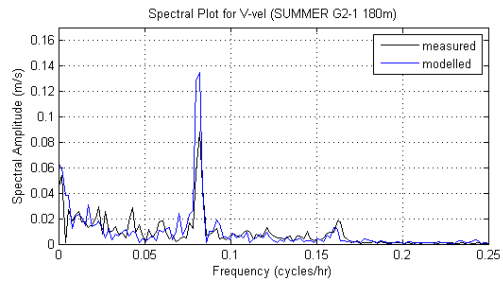
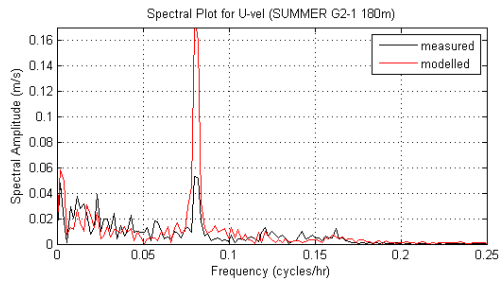


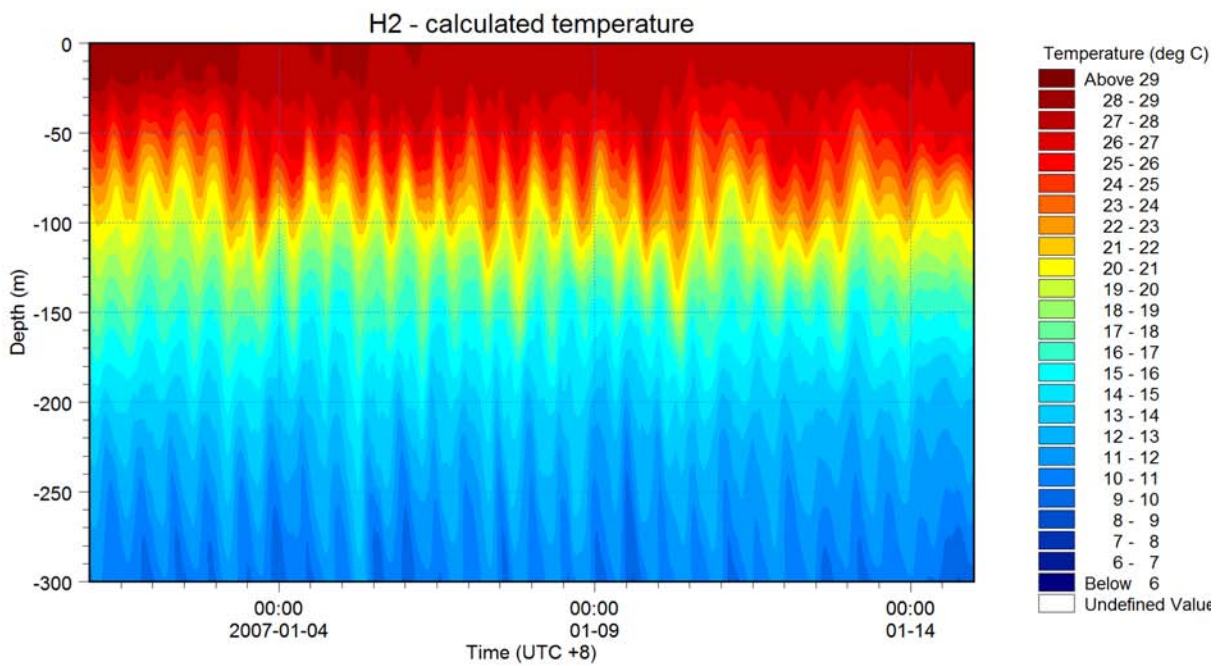
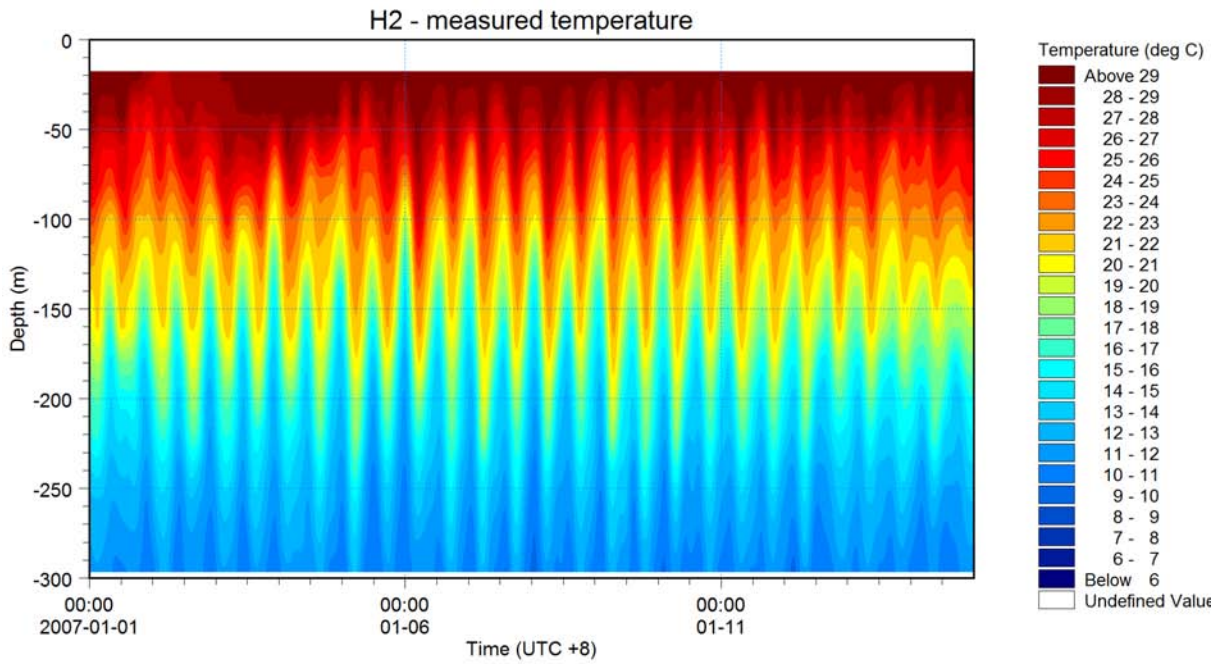








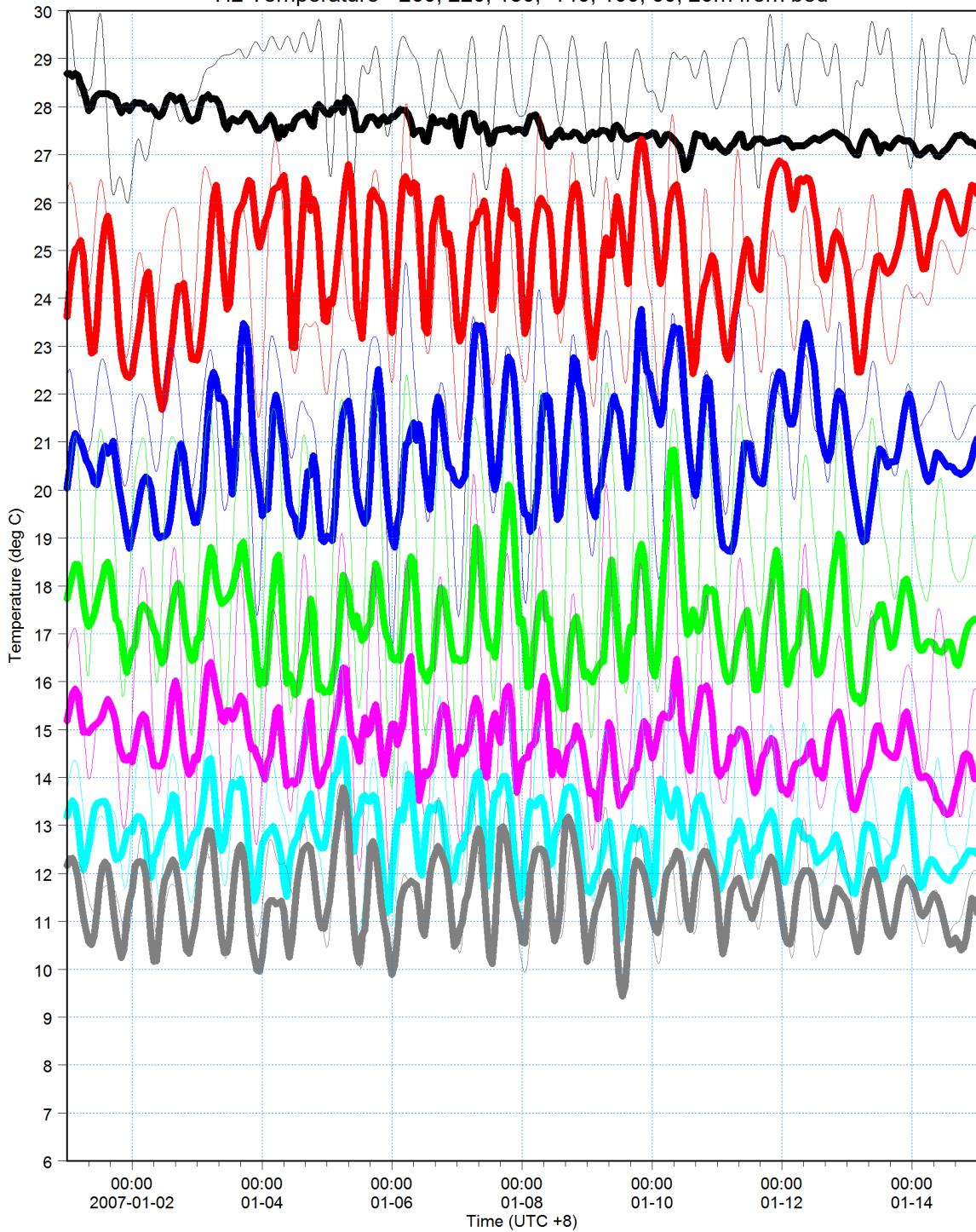






260m from bed: Temperature [C] [deg C] 
measured  [deg C]
220m from bed: Temperature [C] [deg C] 
measured  [deg C]
180m from bed: Temperature [C] [deg C] 
measured  [deg C]
140m from bed: Temperature [C] [deg C] 
measured  [deg C]
100m from bed: Temperature [C] [deg C] 
measured  [deg C]
60m from bed: Temperature [C] [deg C] 
measured  [deg C]
20m from bed: Temperature [C] [deg C] 
measured  [deg C]

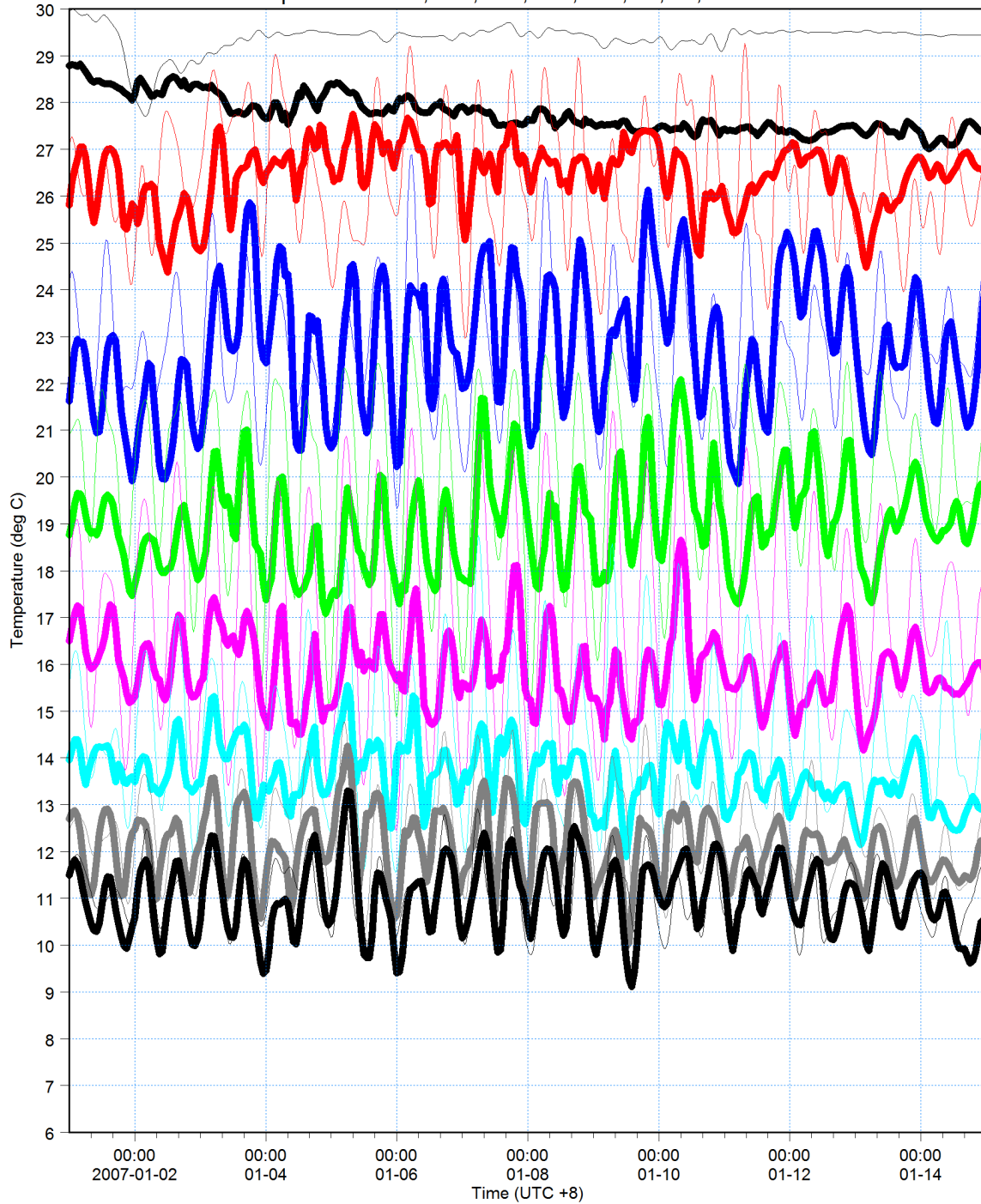
H2 Temperature - 260, 220, 180, 140, 100, 60, 20m from bed





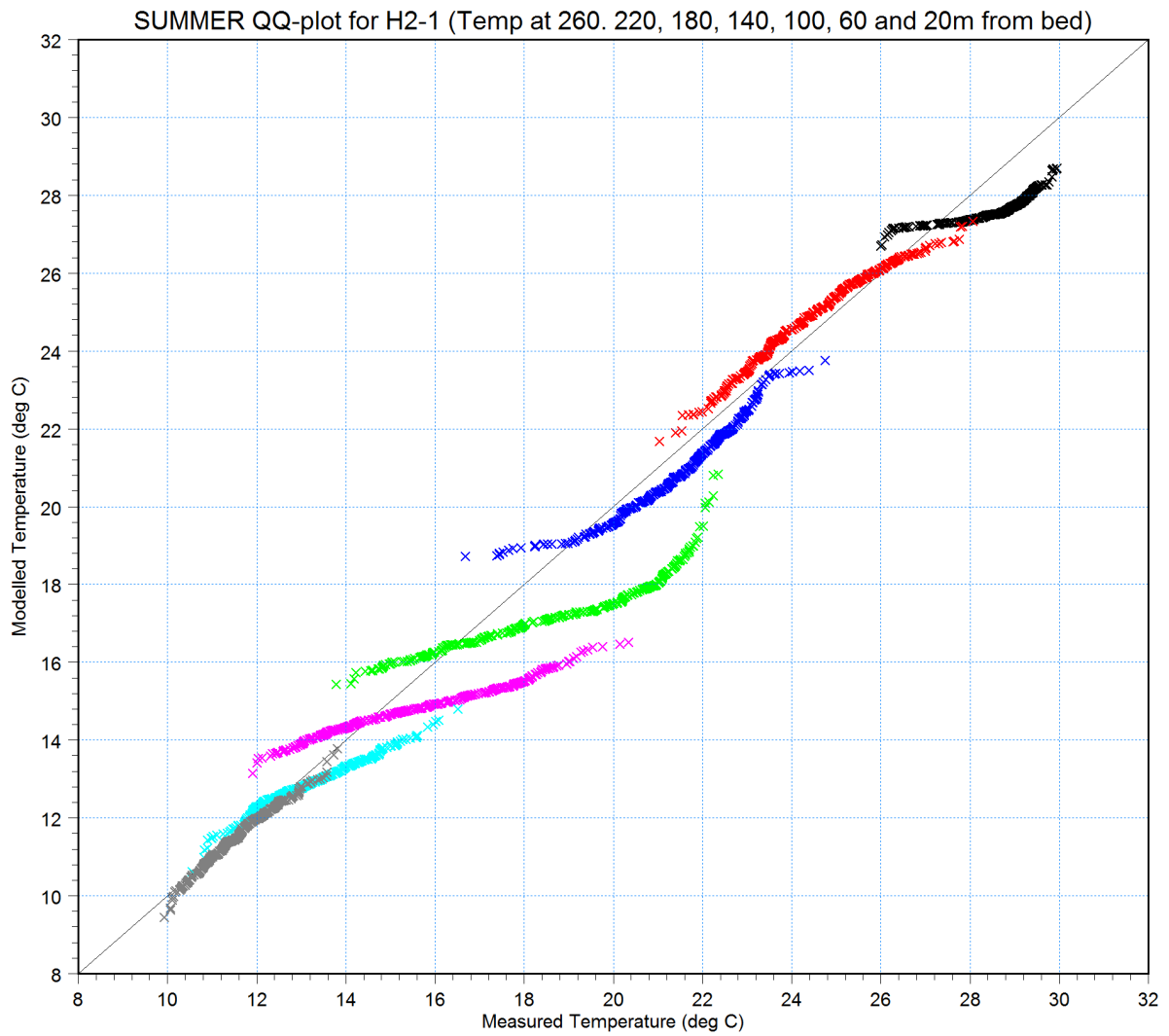
280m from bed: Temperature [C] [deg C] —
measured [deg C] —
240m from bed: Temperature [C] [deg C] —
measured [deg C] —
200m from bed: Temperature [C] [deg C] —
measured [deg C] —
160m from bed: Temperature [C] [deg C] —
measured [deg C] —
120m from bed: Temperature [C] [deg C] —
measured [deg C] —
80m from bed: Temperature [C] [deg C] —
measured [deg C] —
40m from bed: Temperature [C] [deg C] —
measured [deg C] —
2.6m from bed: Temperature [C] [deg C] —
measured [deg C] —

H2 Temperature - 280, 240, 200, 160, 120, 80, 40, 2.6m from bed



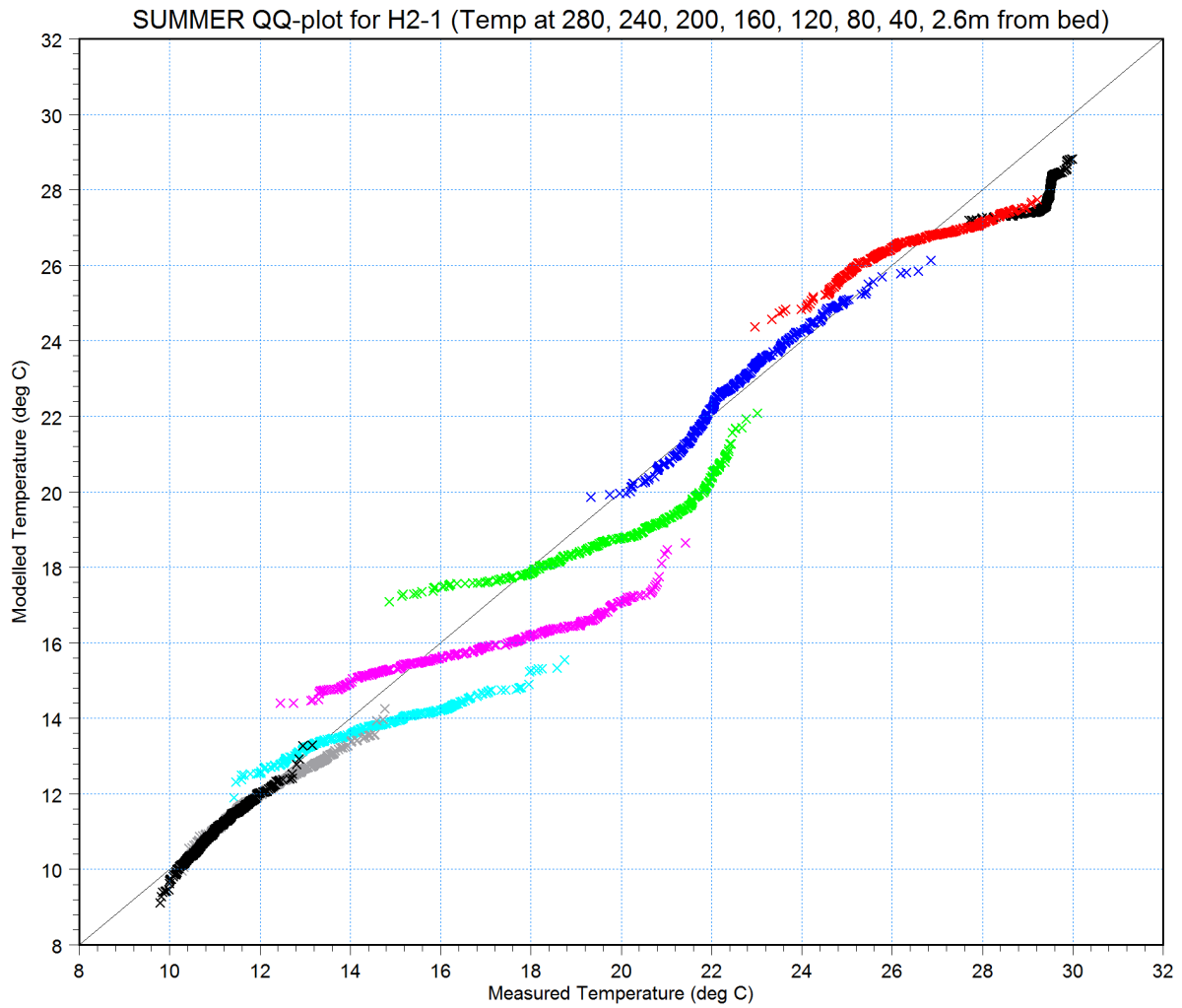


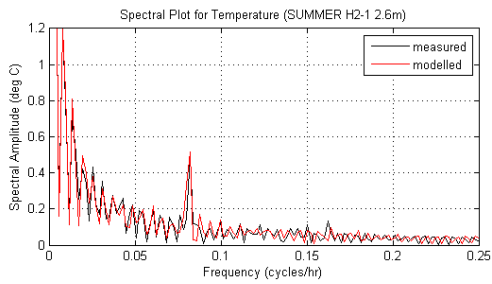
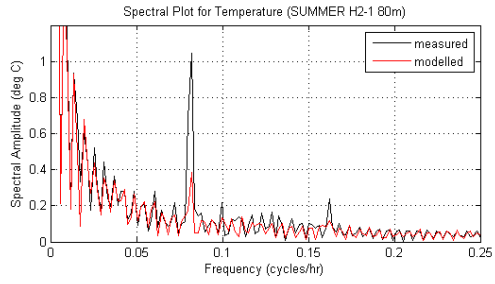
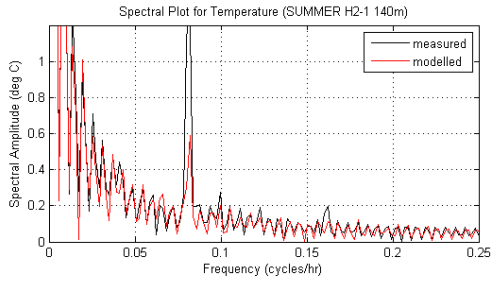
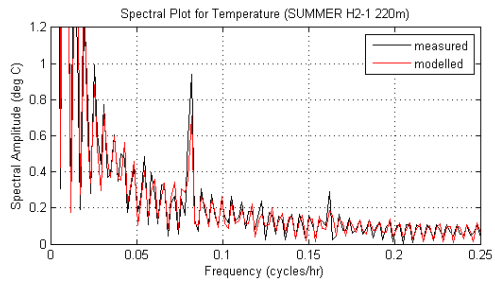
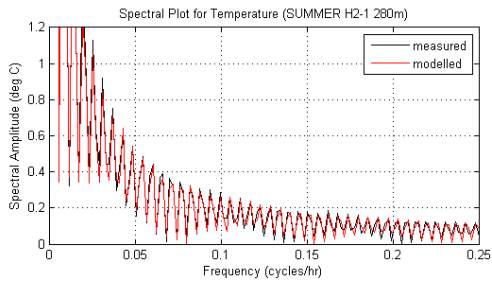
T at 260m × ×
T at 220m × ×
T at 180m × ×
T at 140m × ×
T at 100m × ×
T at 60m × ×
T at 20m × ×

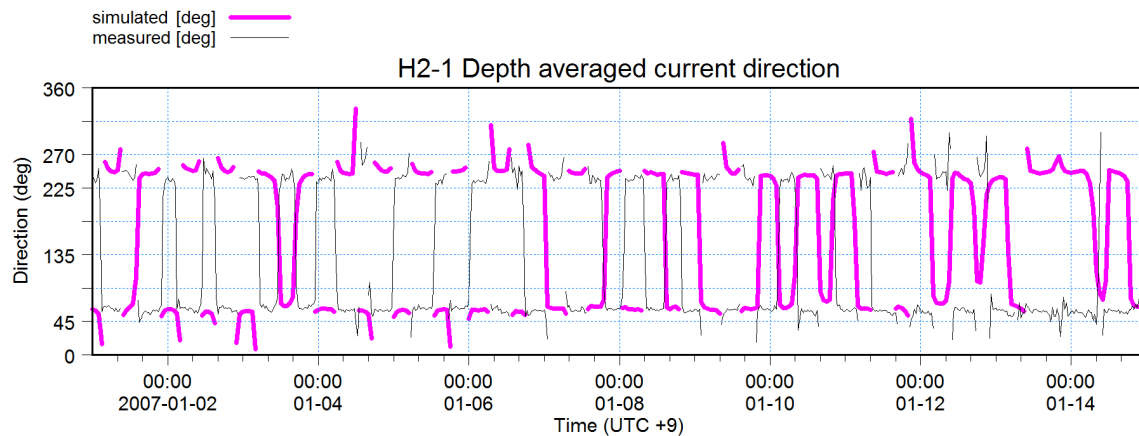
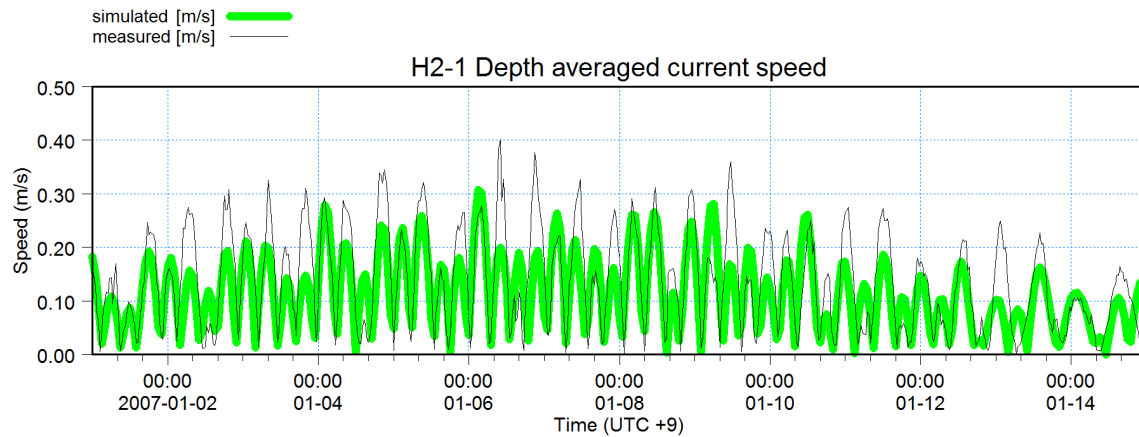
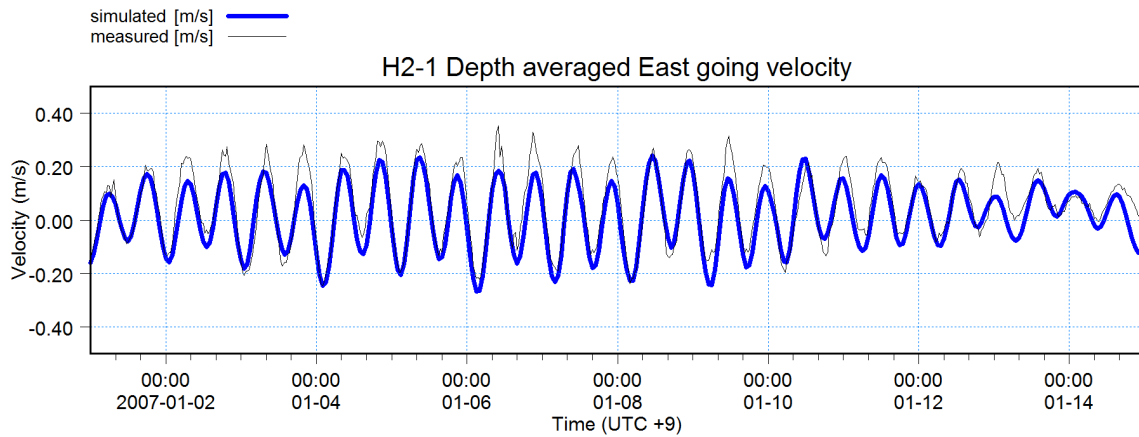
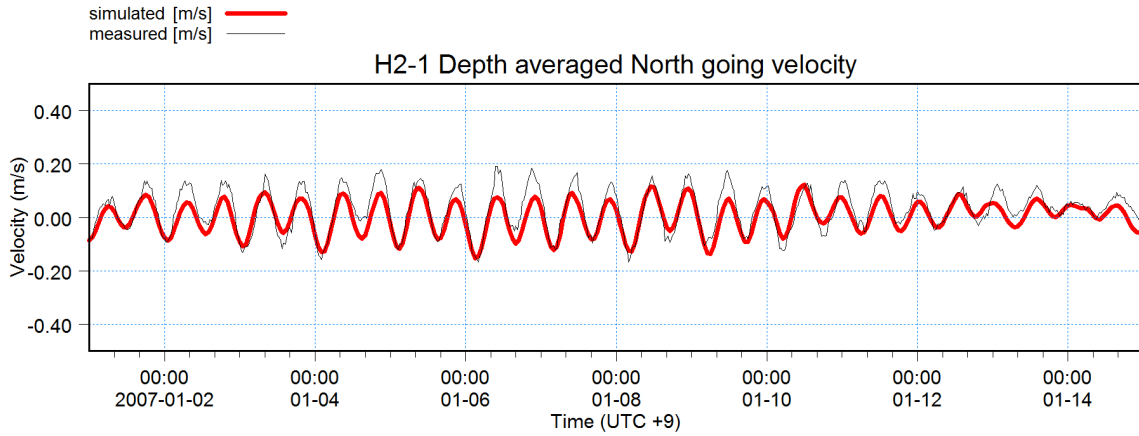




- T at 280m × ×
- T at 240m × ×
- T at 200m × ×
- T at 160m × ×
- T at 120m × ×
- T at 80m × ×
- T at 40m × ×
- T at 2.6m × ×

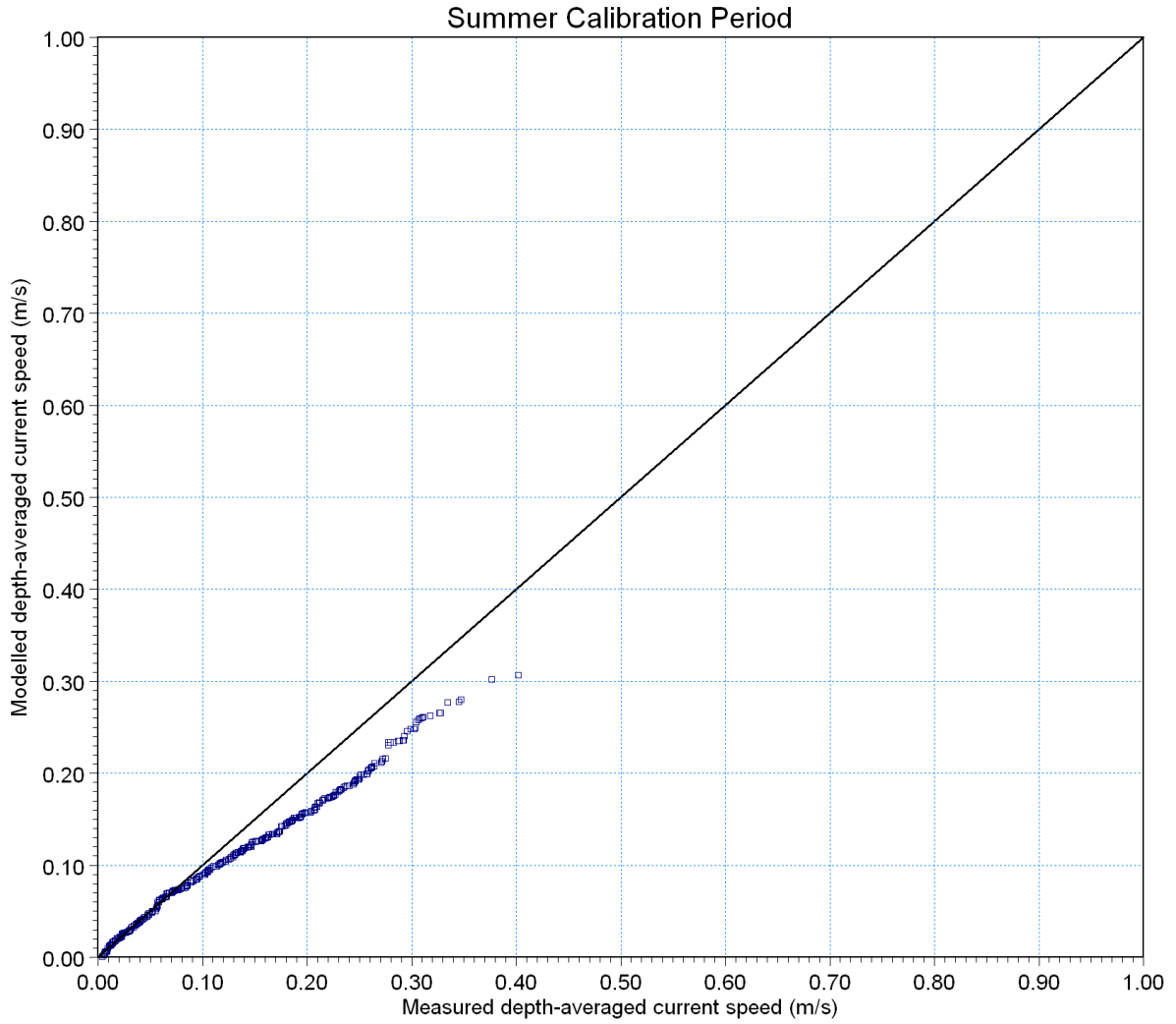


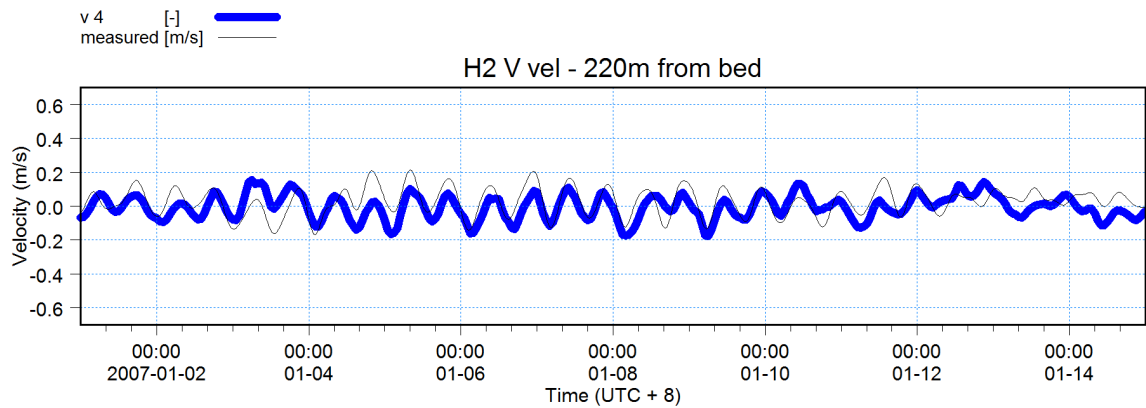
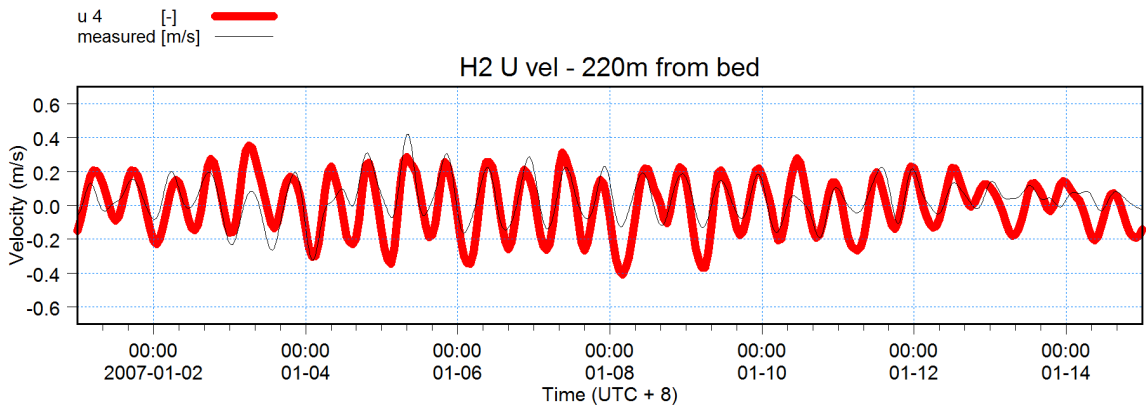
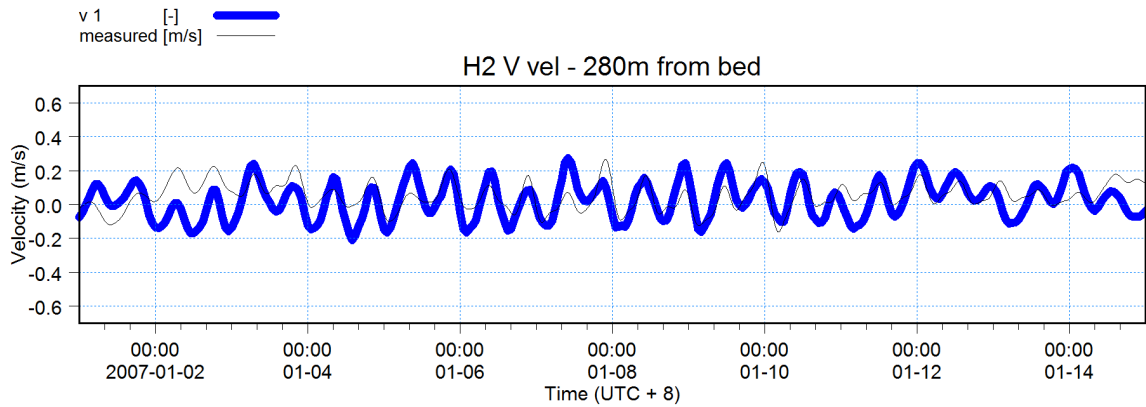
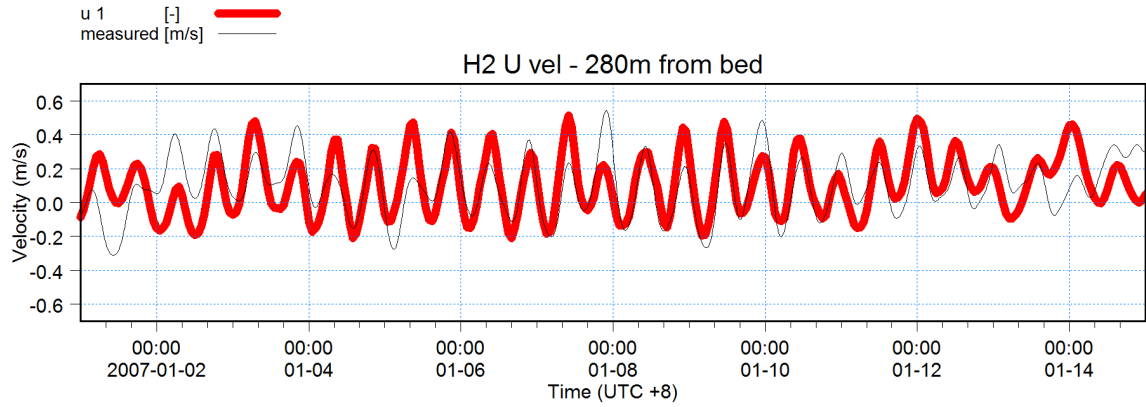


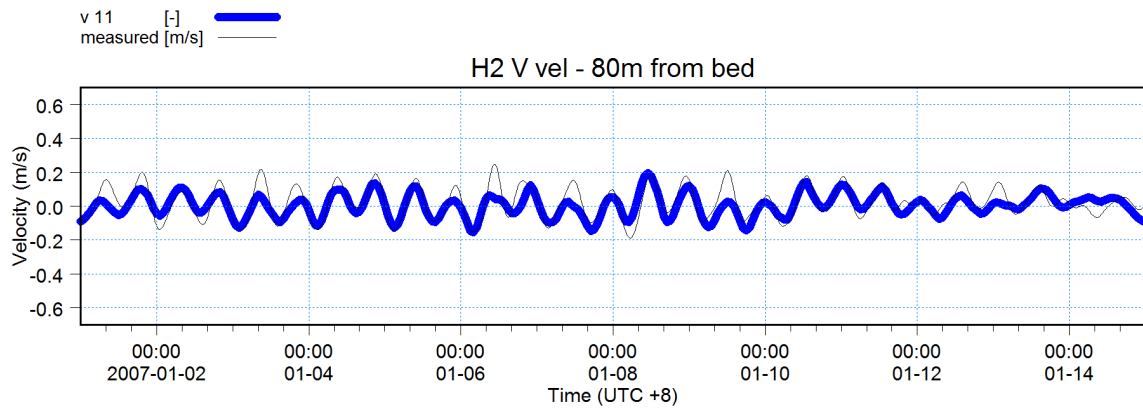
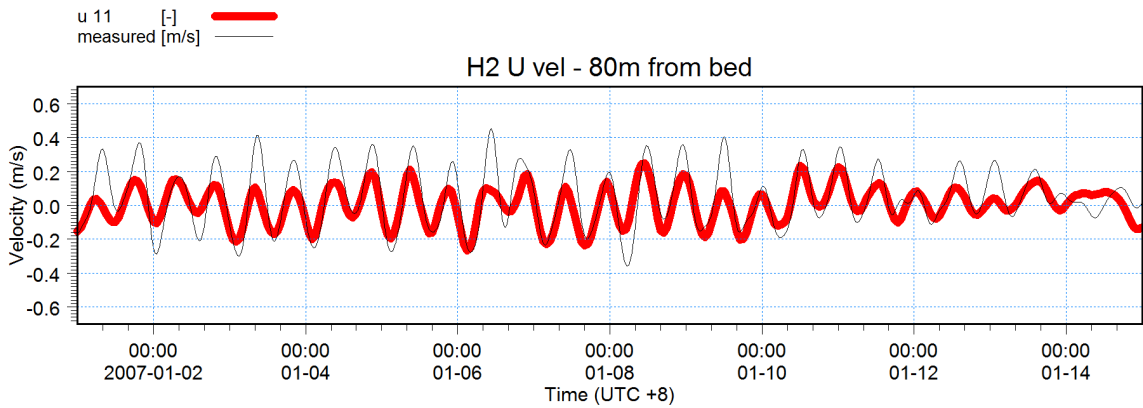
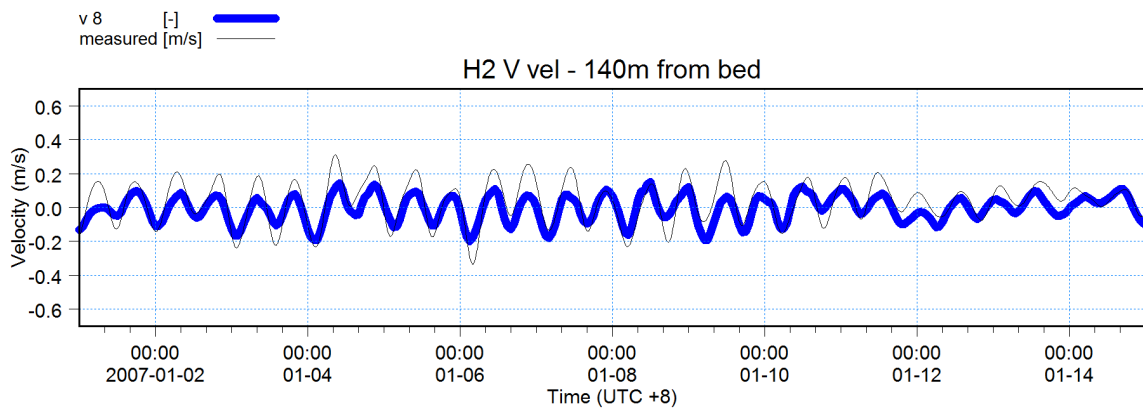
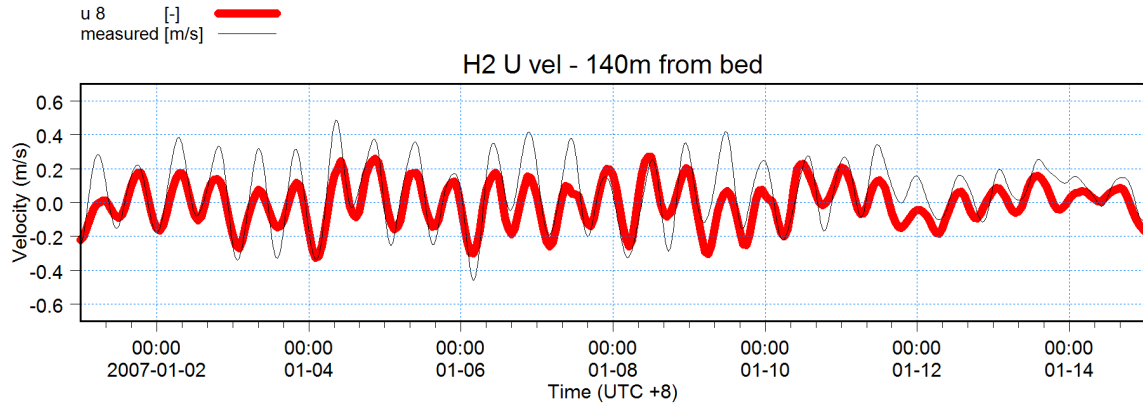


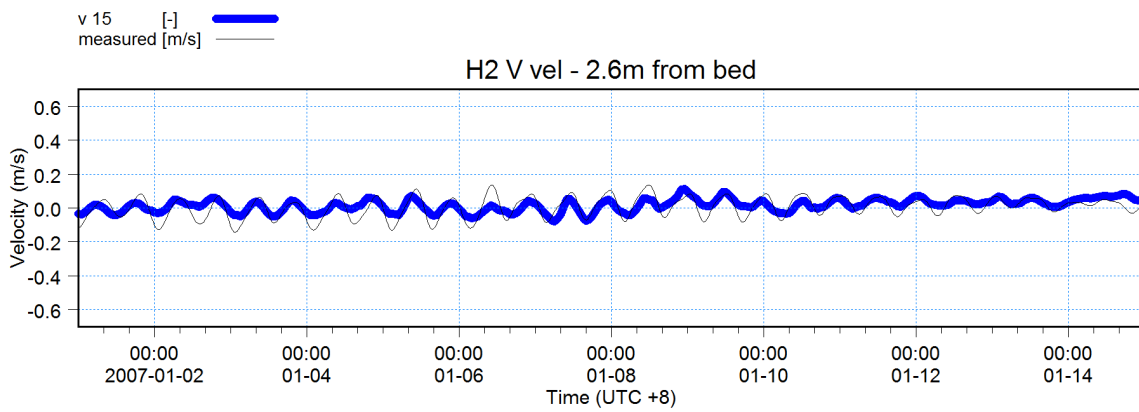
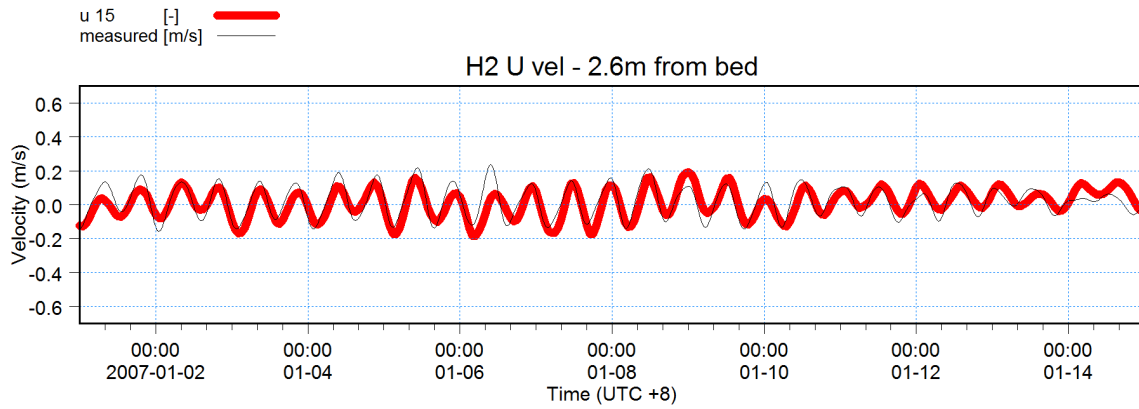


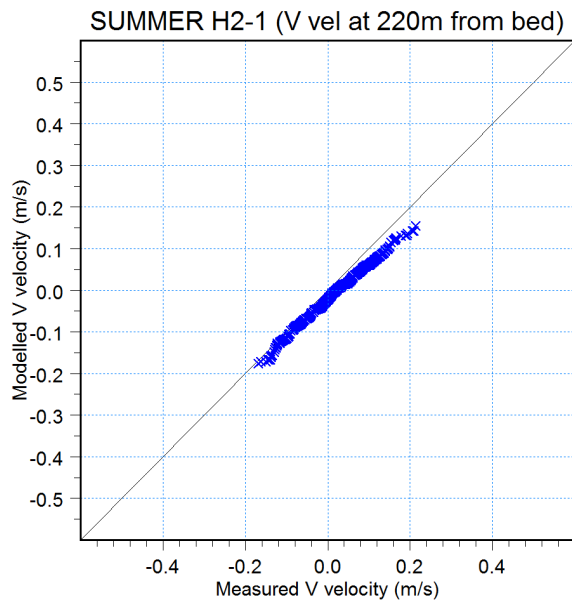
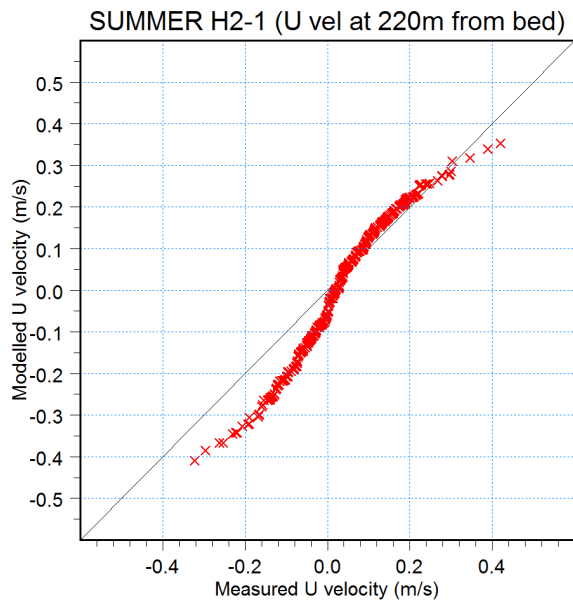
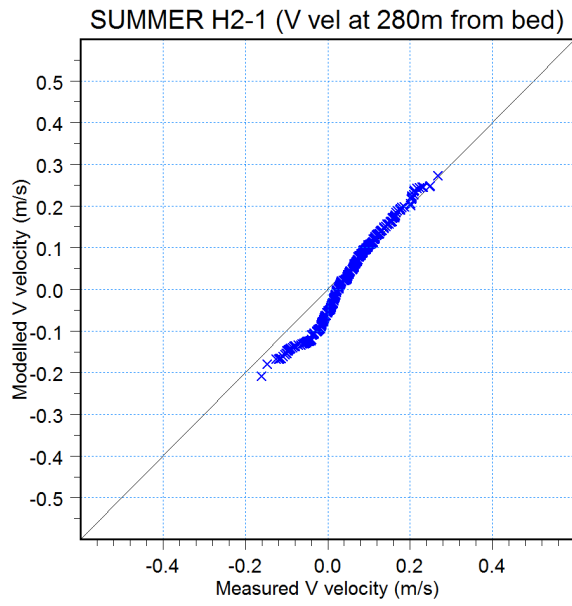
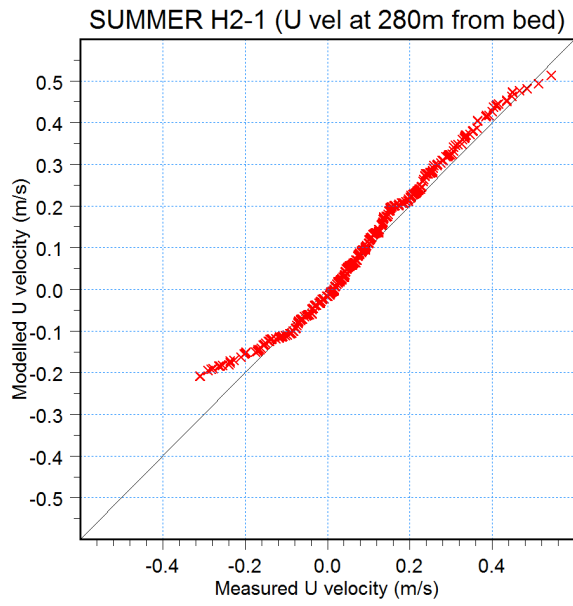
H2 □ □

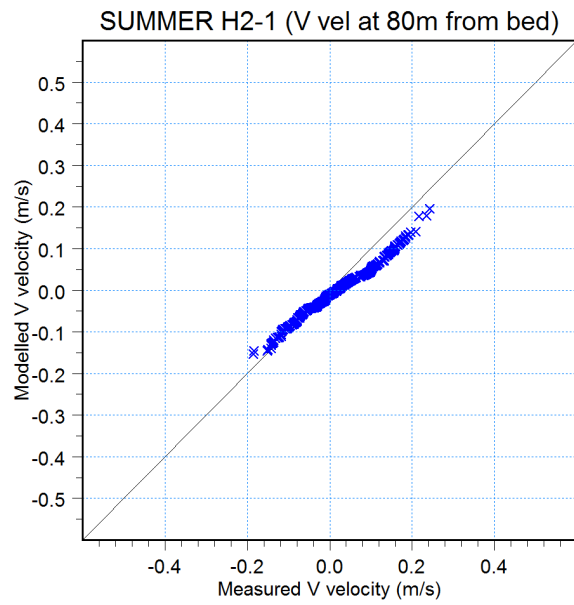
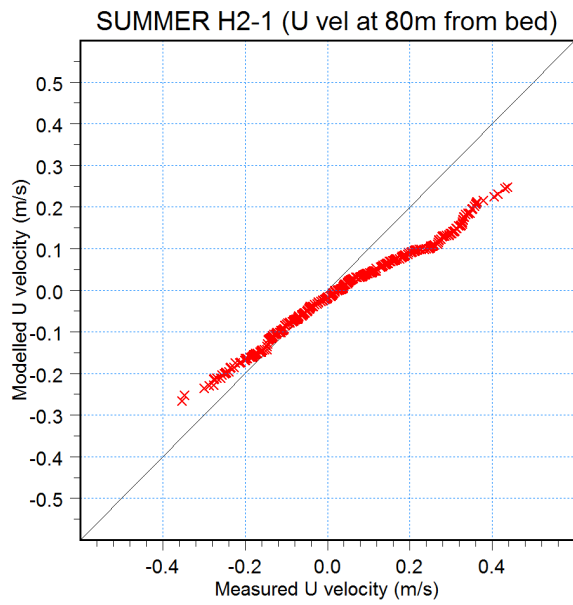
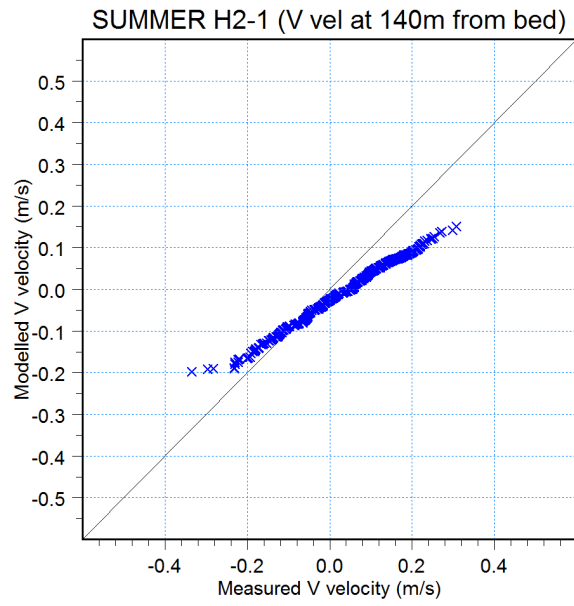
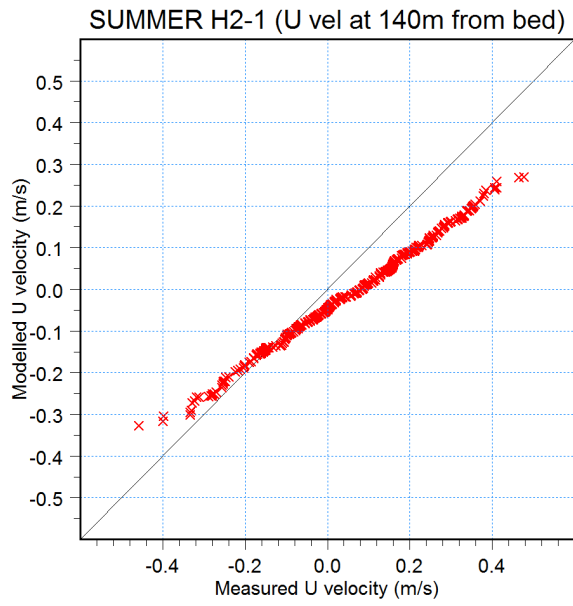


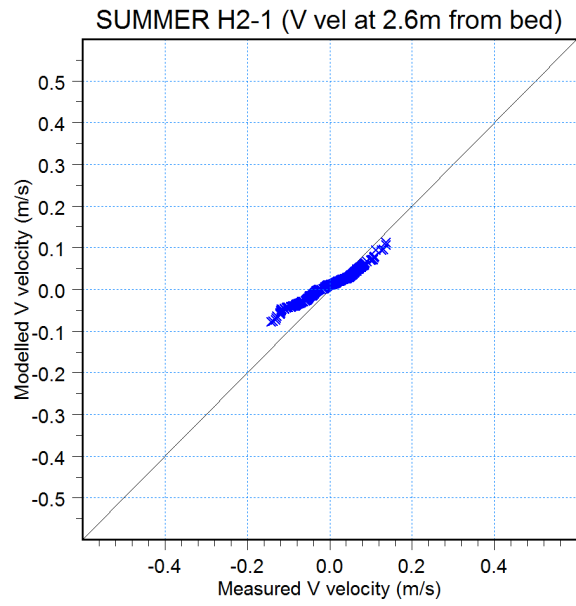
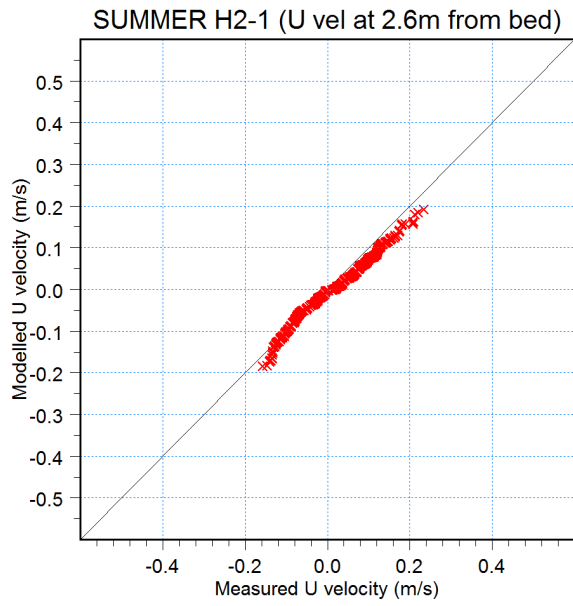


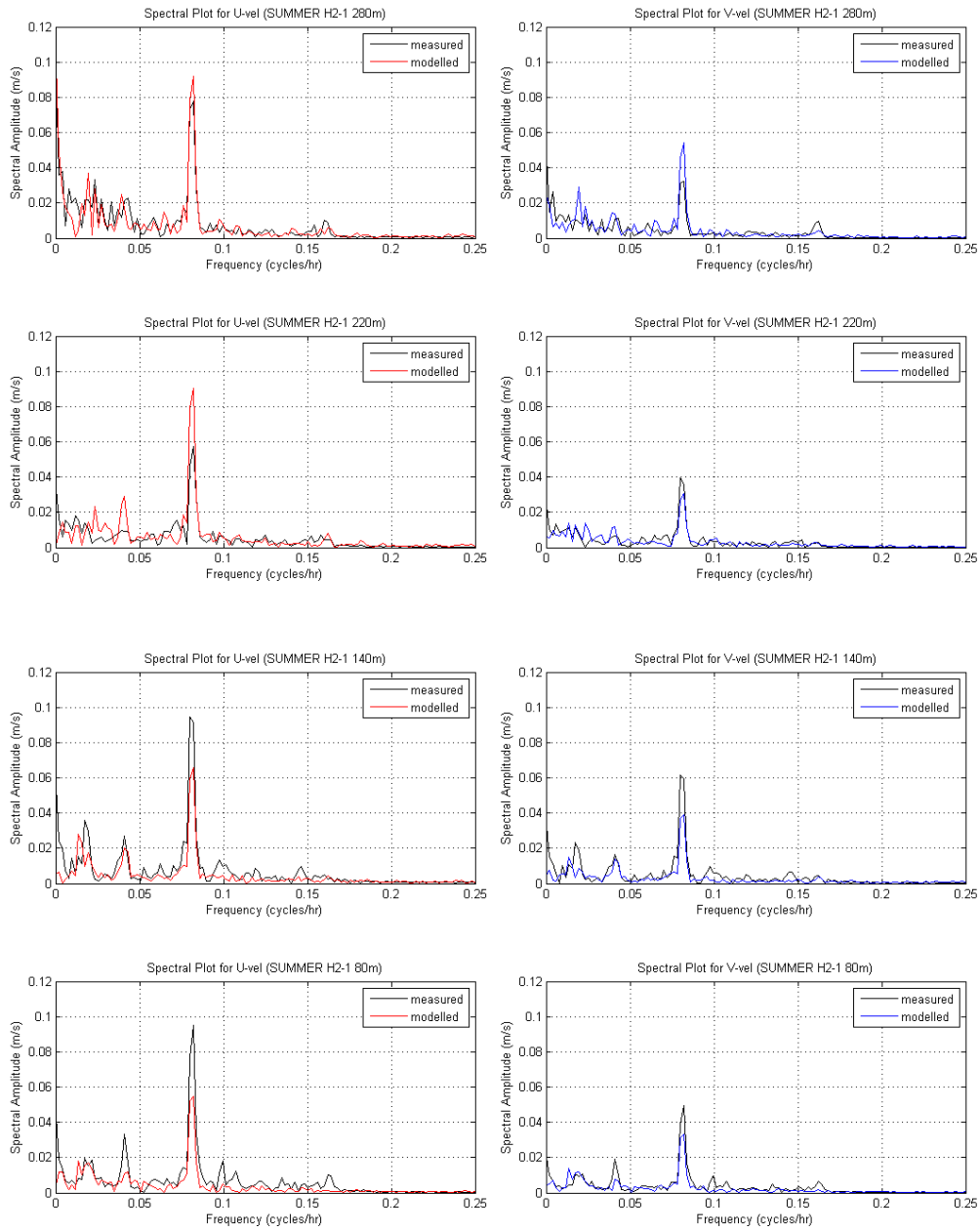


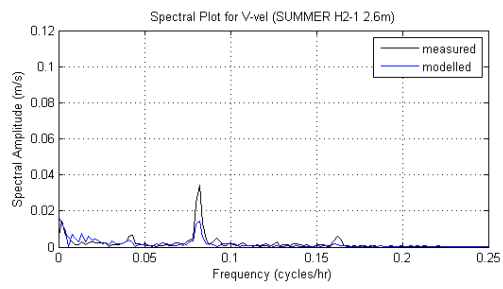
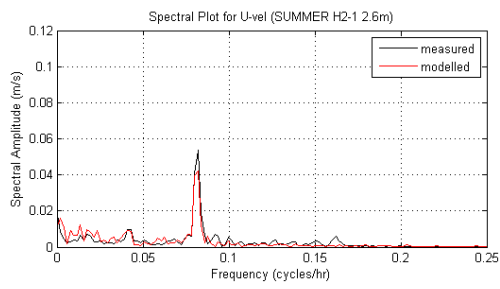


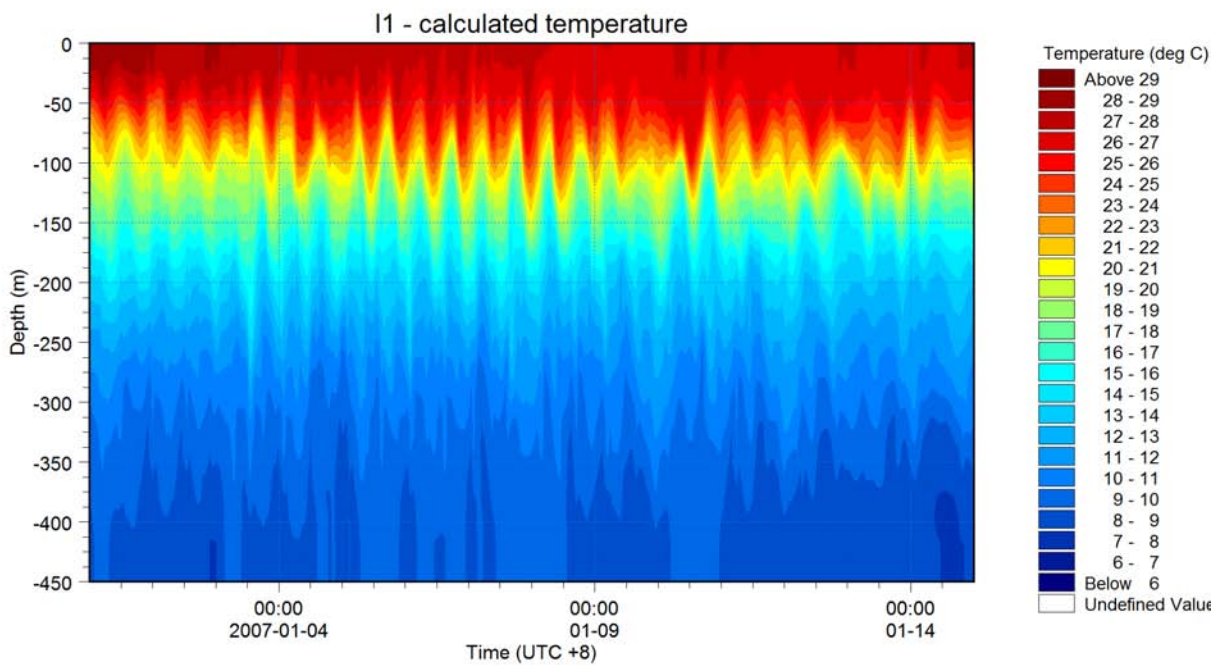
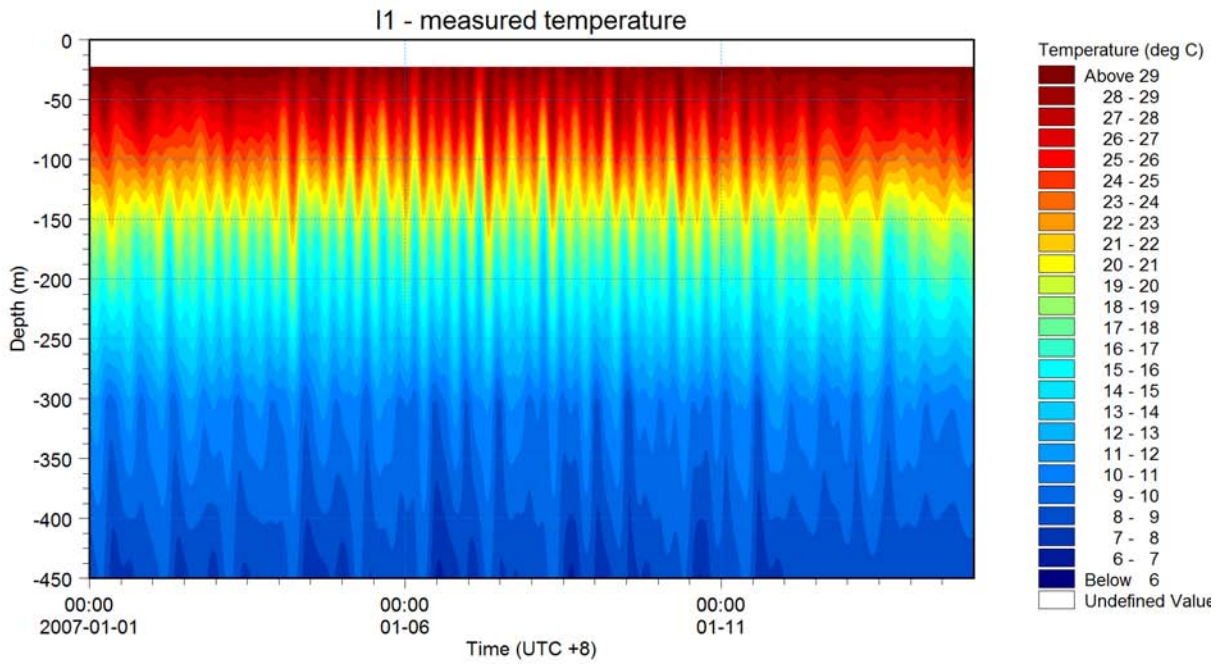








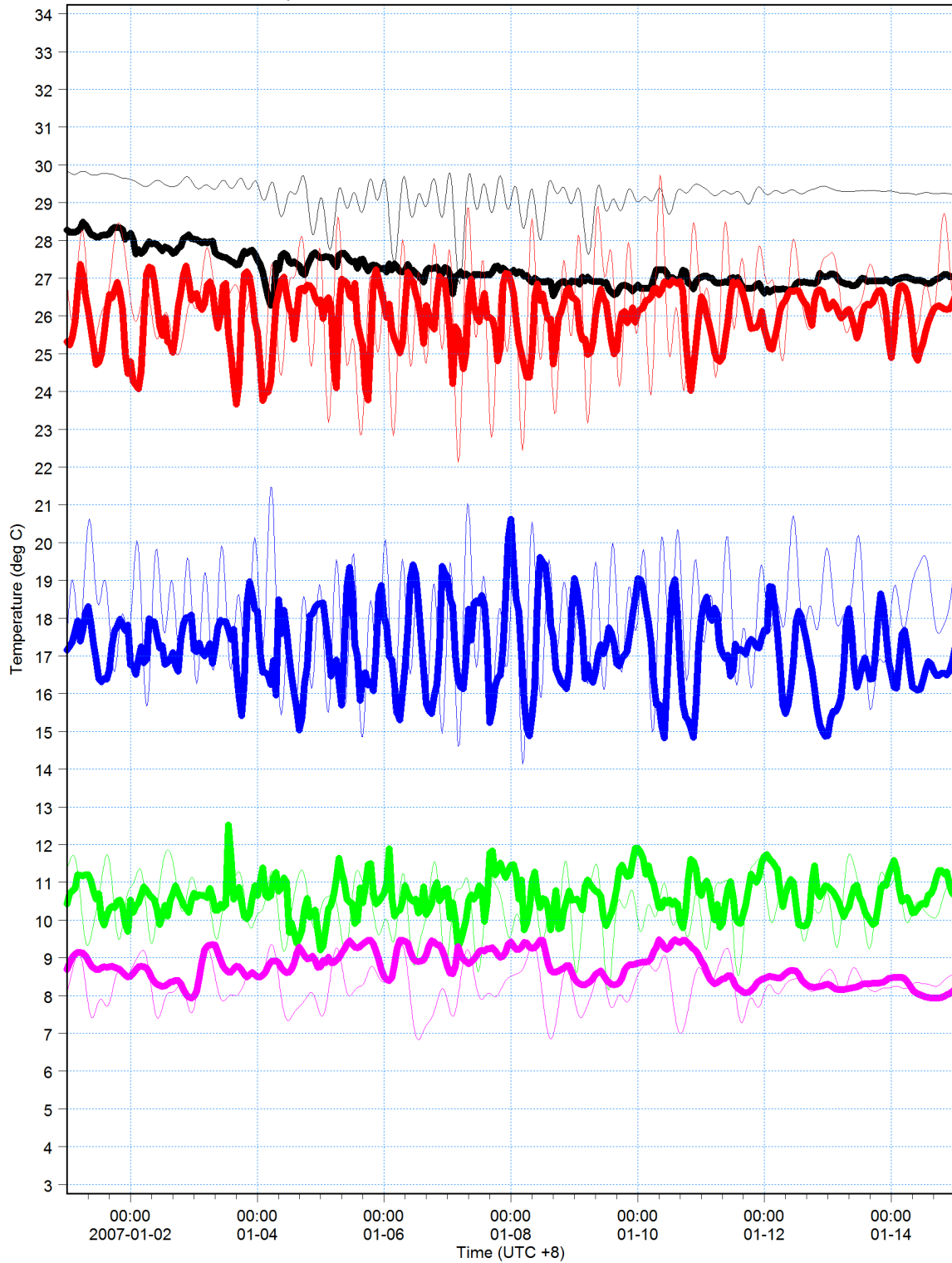






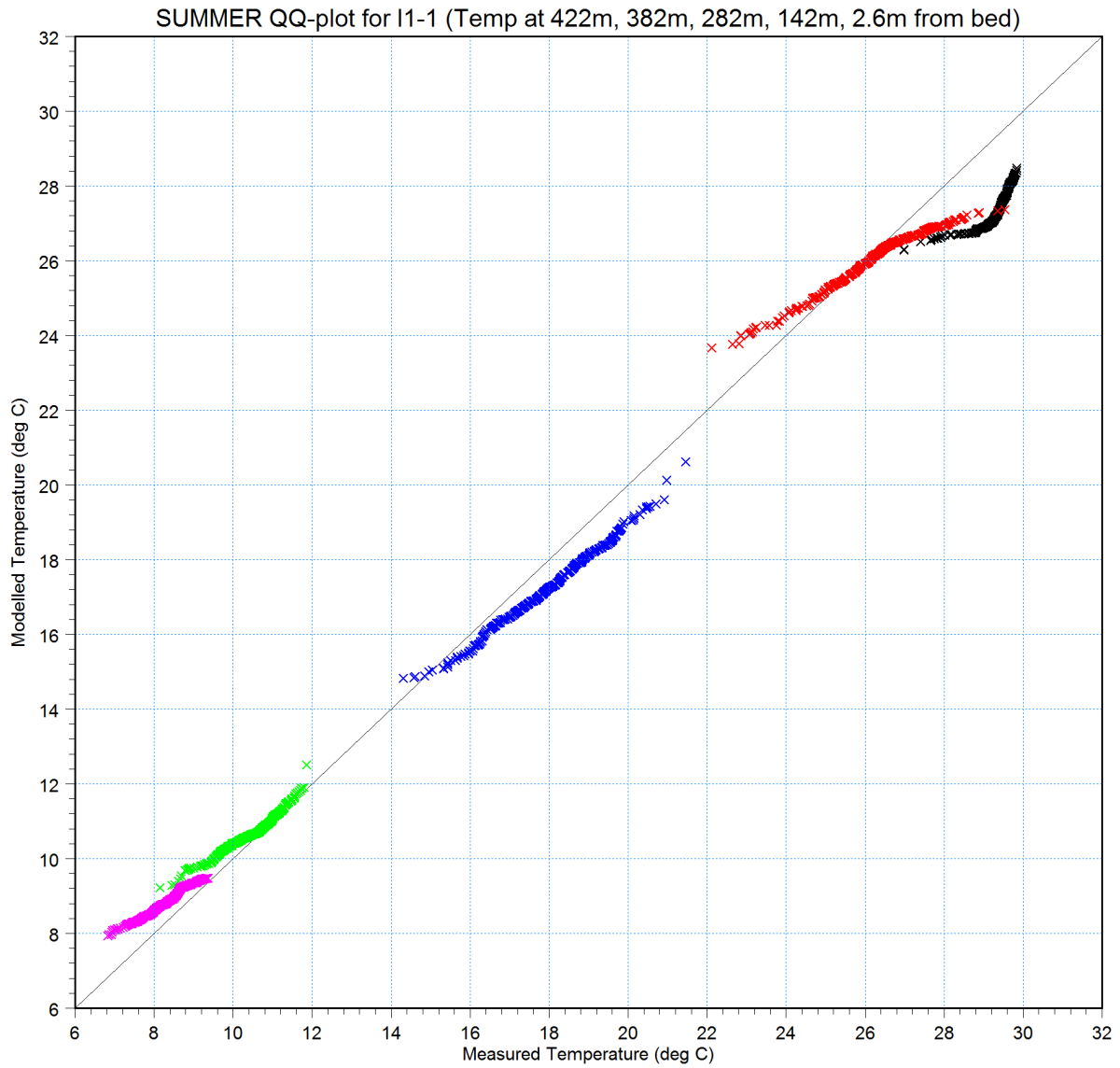
422m from bed: Temperature [deg C] 
measured [deg C] 
382m from bed: Temperature [deg C] 
measured [deg C] 
282m from bed: Temperature [deg C] 
measured [deg C] 
142m from bed: Temperature [deg C] 
measured [deg C] 
2.6m from bed: Temperature [deg C] 
measured [deg C] 

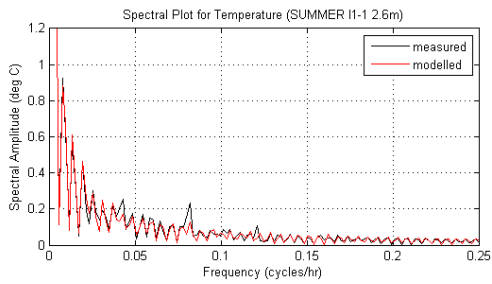
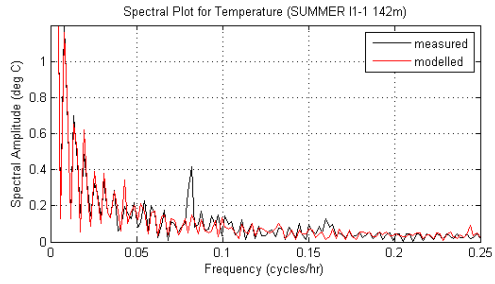
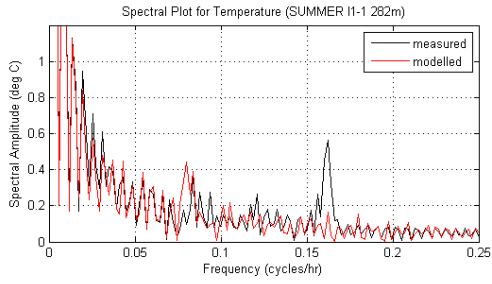
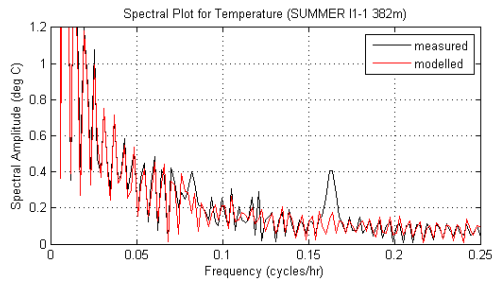
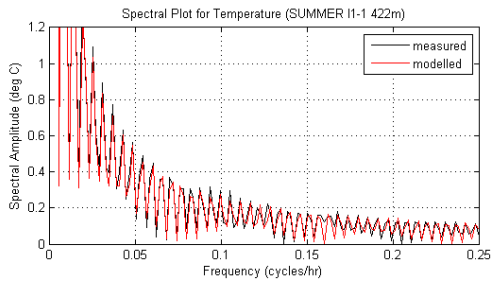
11 Temperature - 422m, 382m, 282m, 142m, 2.6m from bed

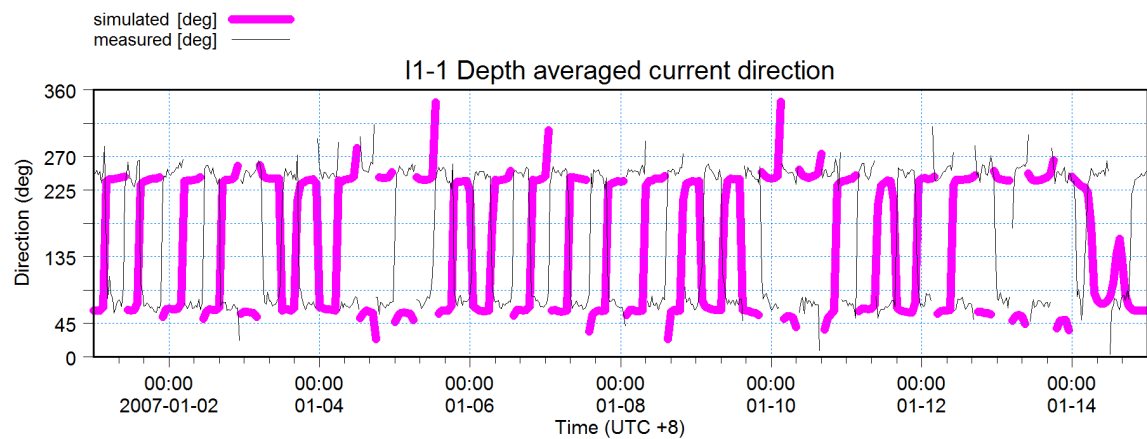
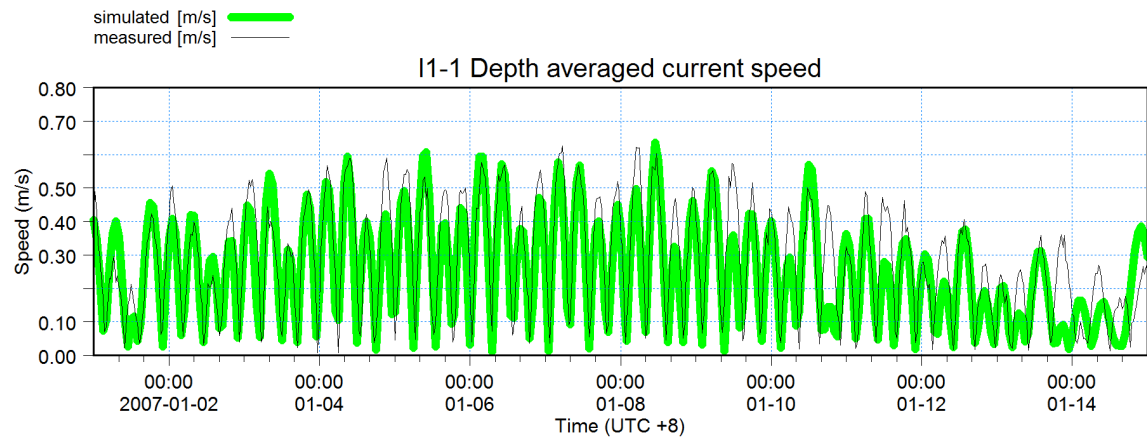
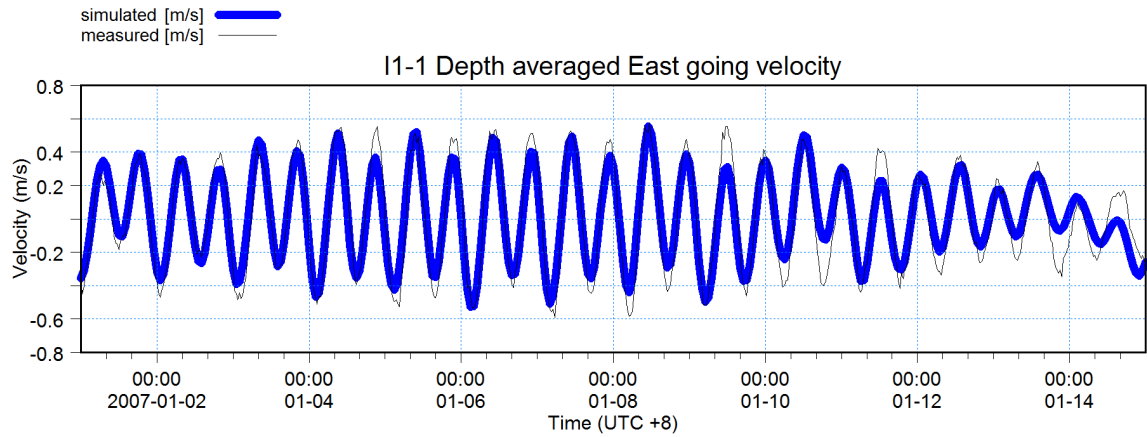
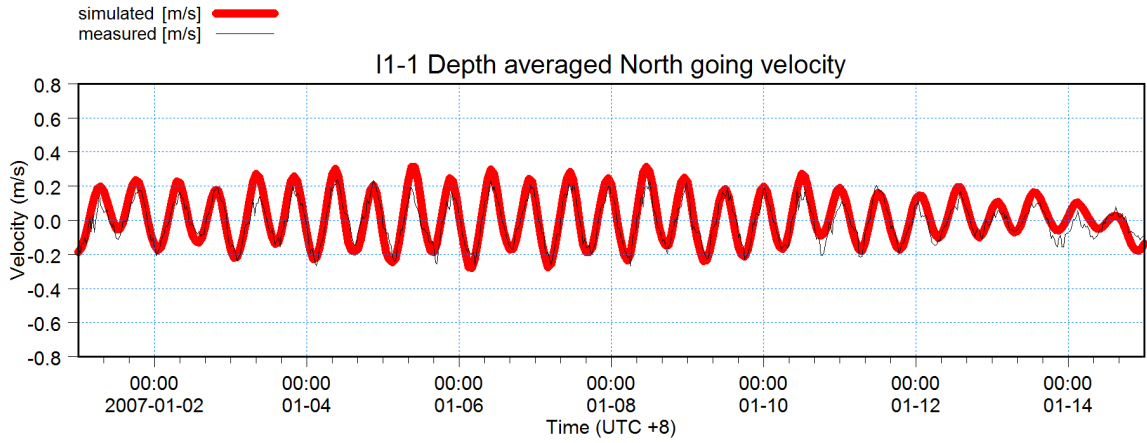


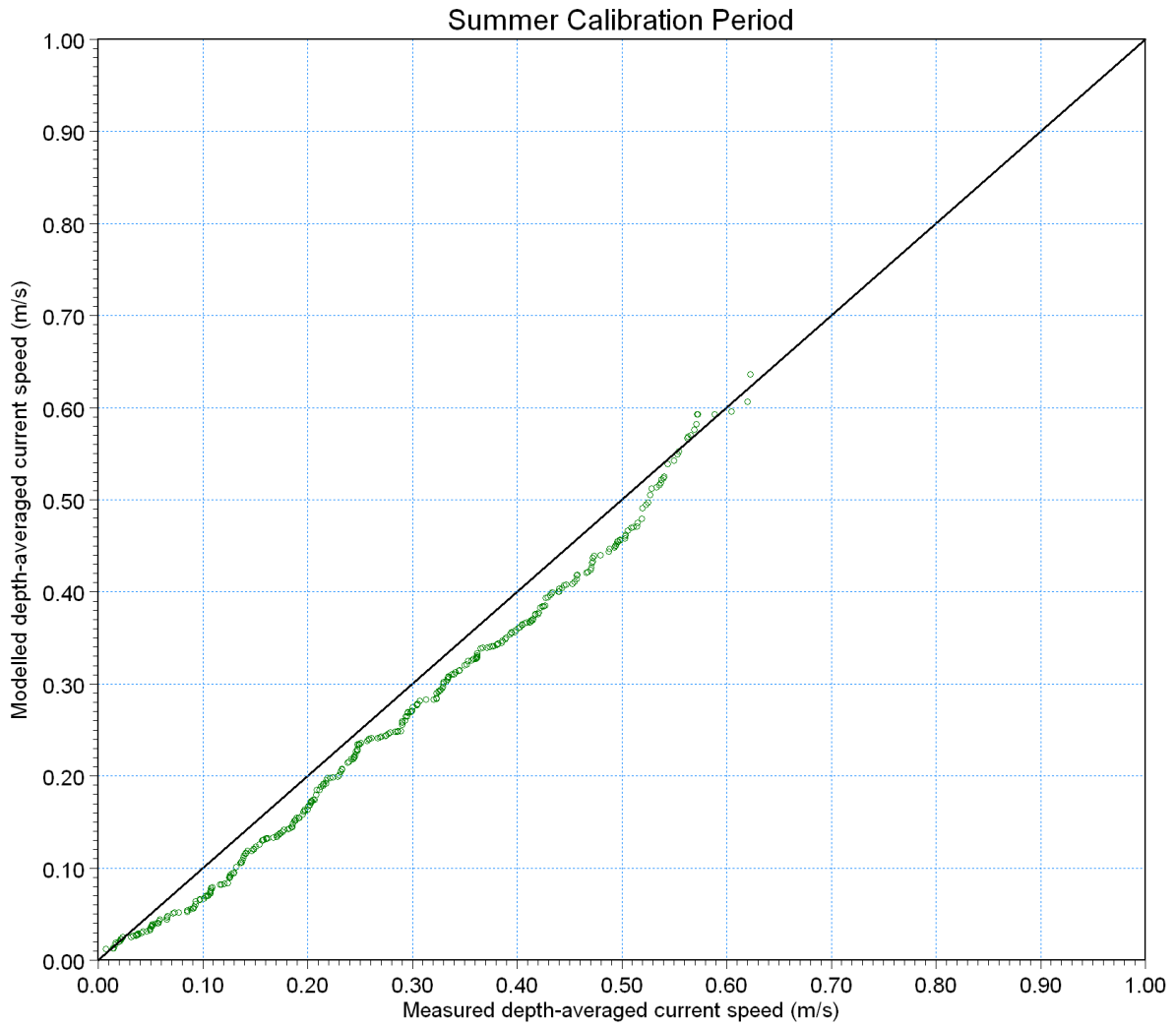


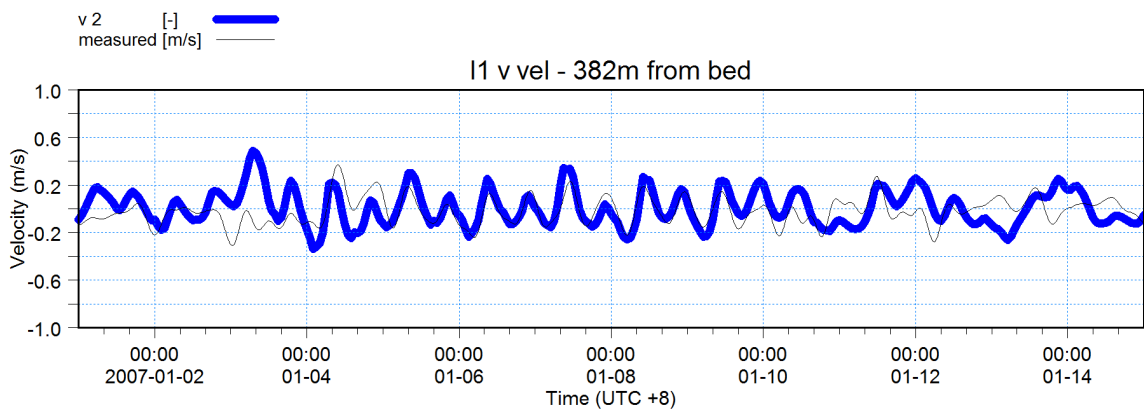
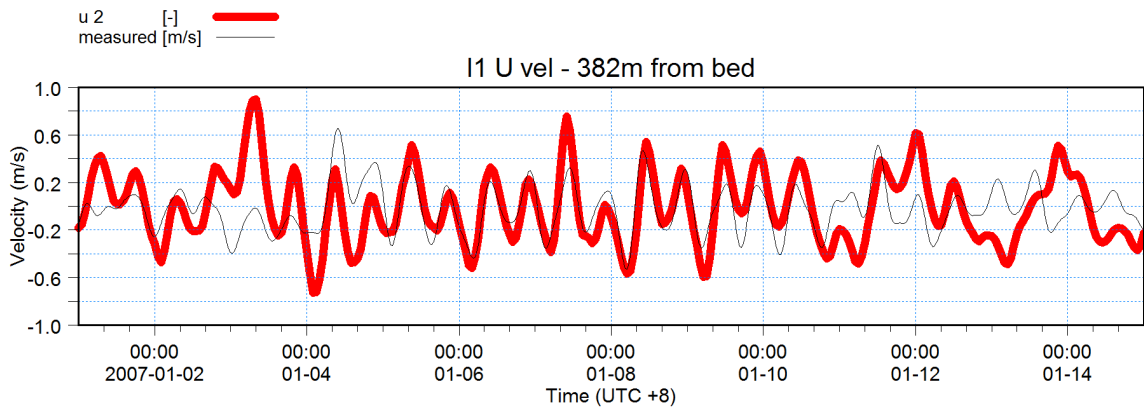
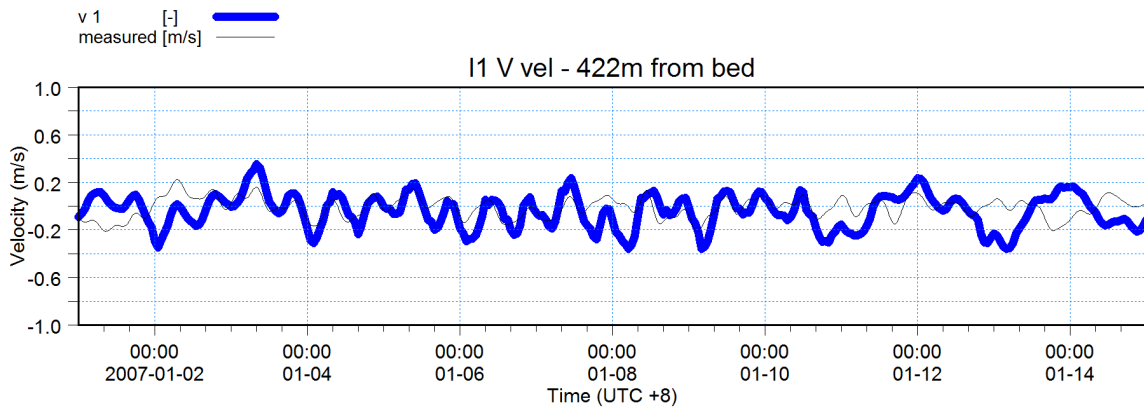
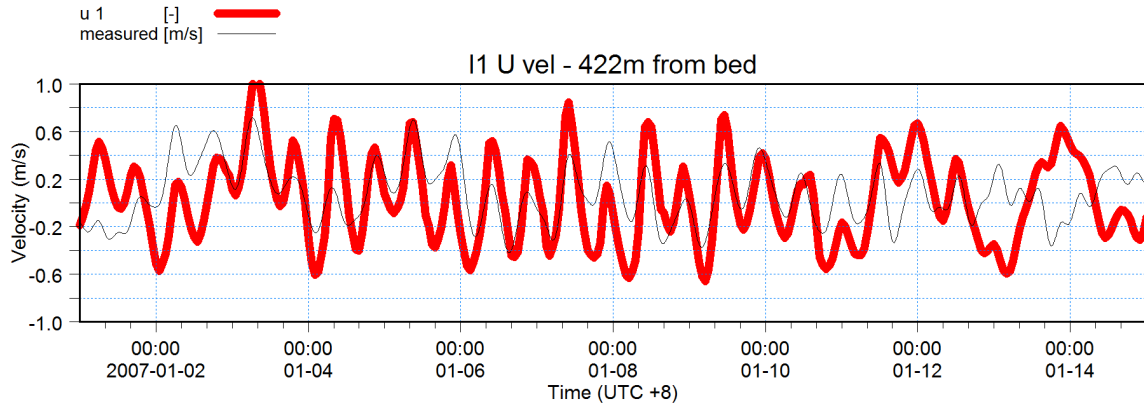
- T at 422m × ×
- T at 382m × ×
- T at 282m × ×
- T at 142m × ×
- T at 2.6m × ×

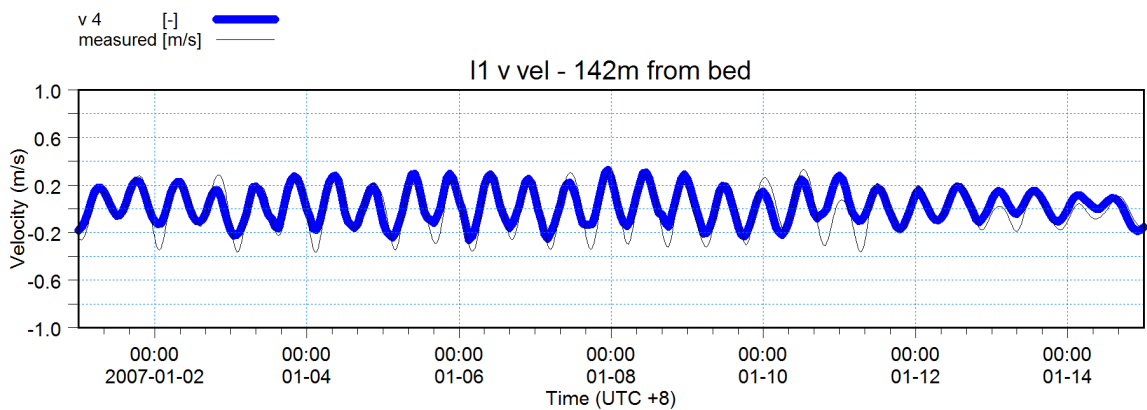
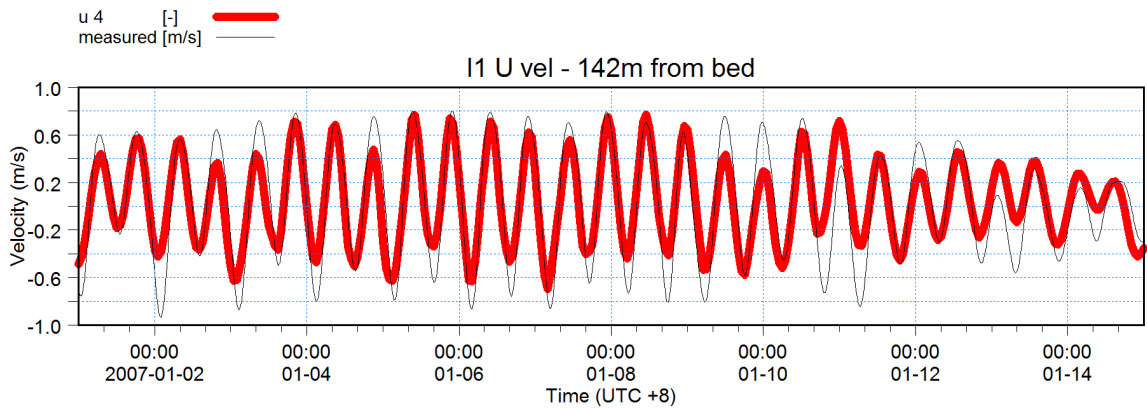
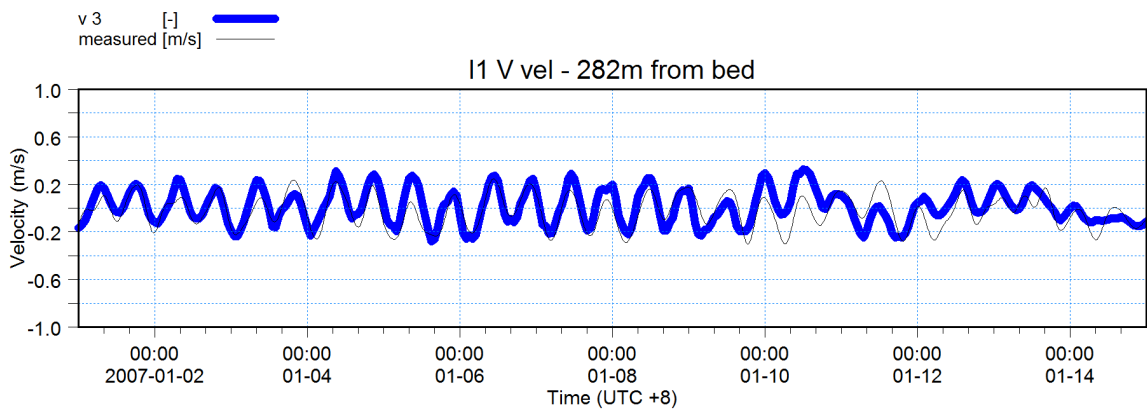
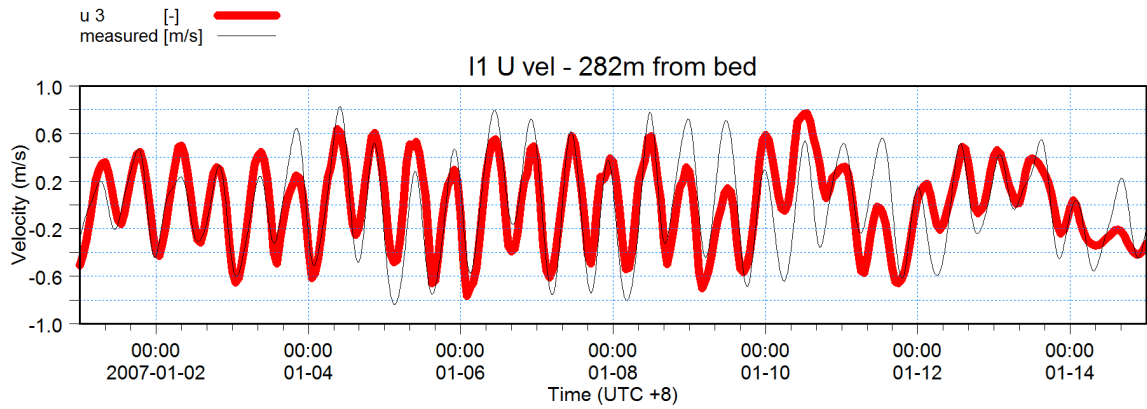


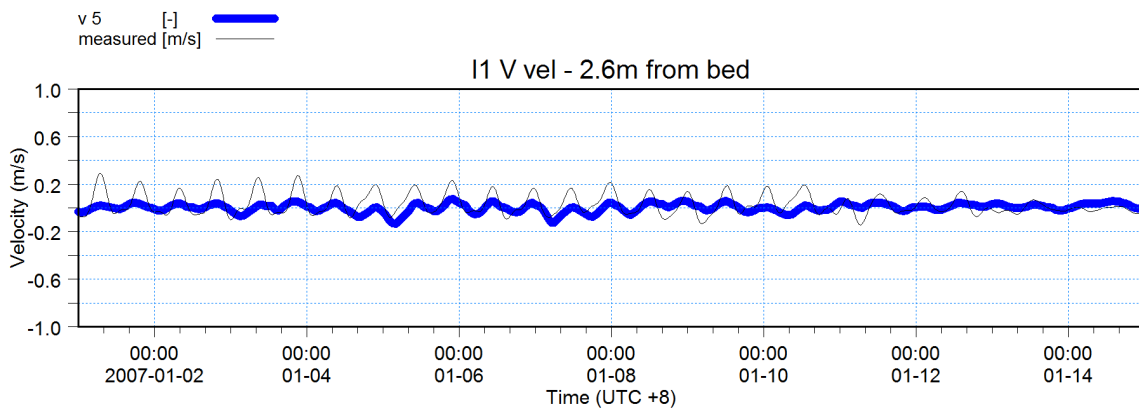
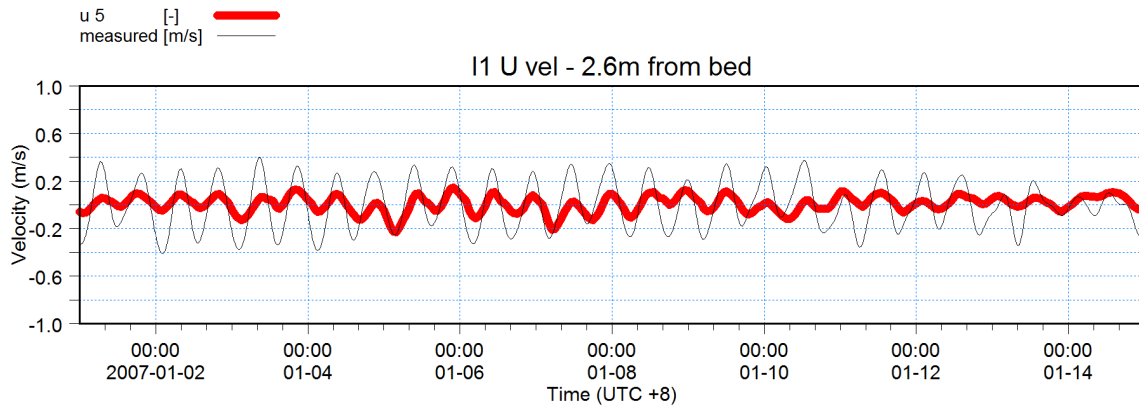


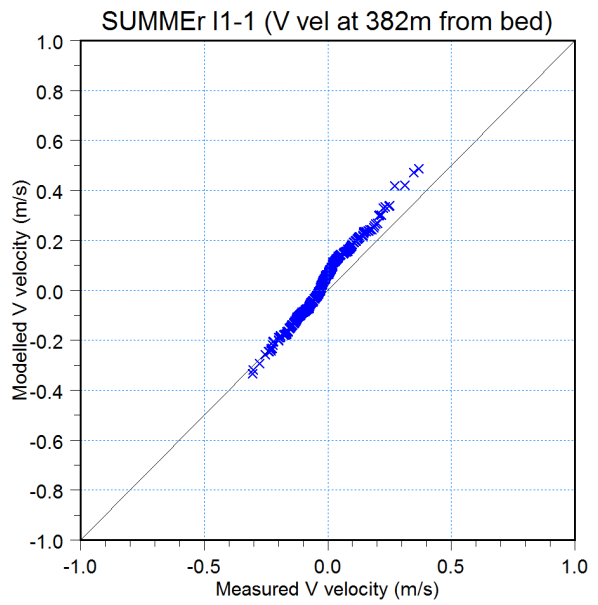
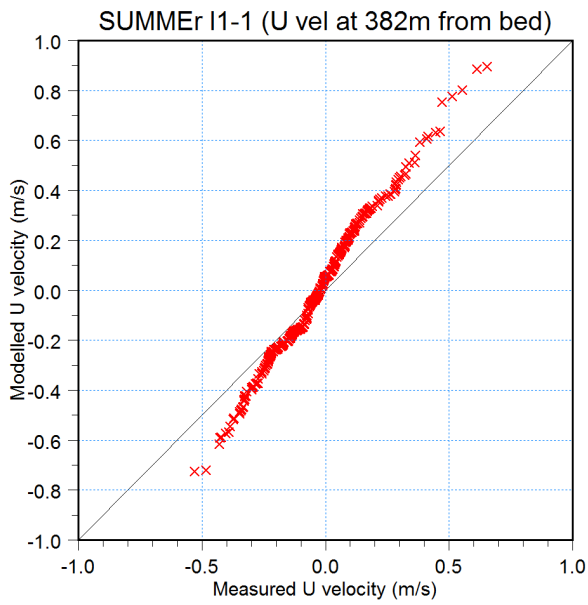
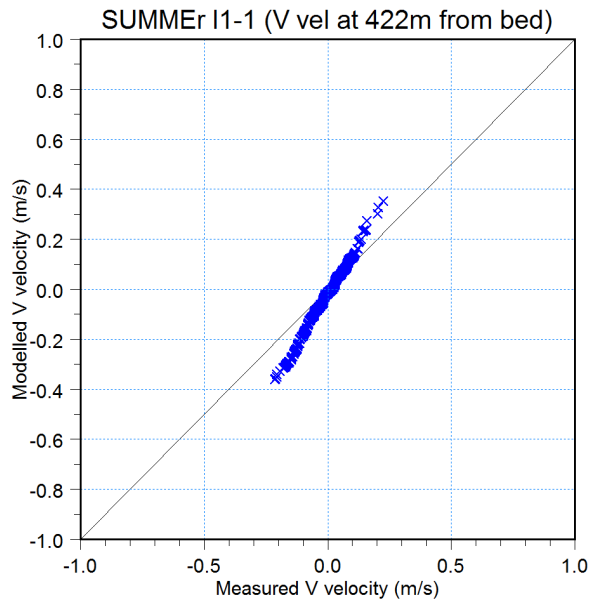
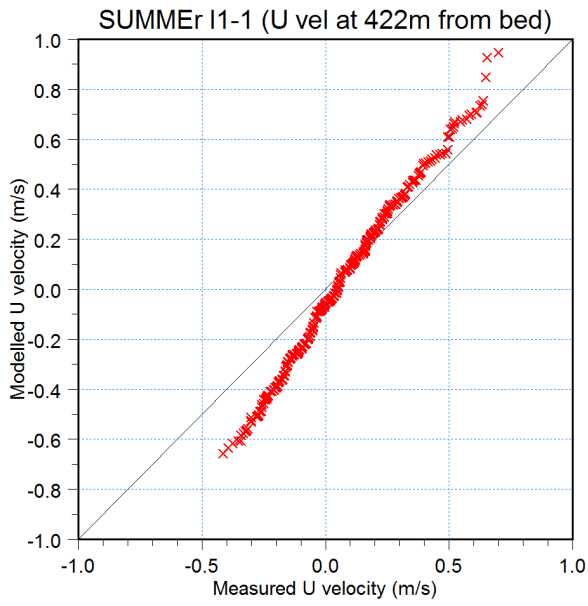


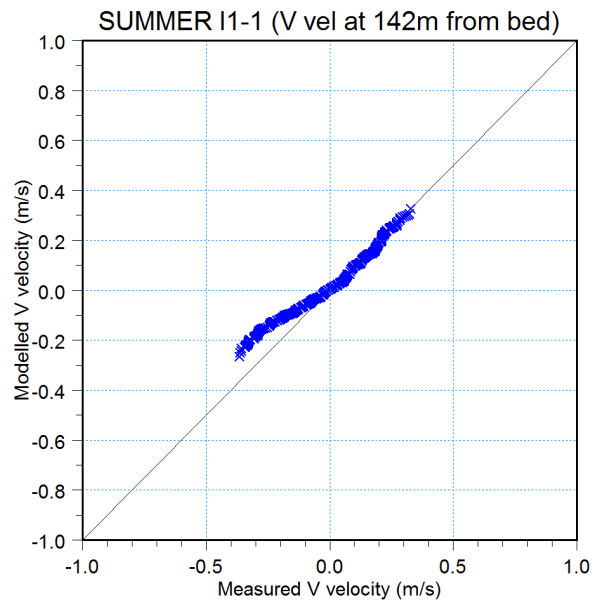
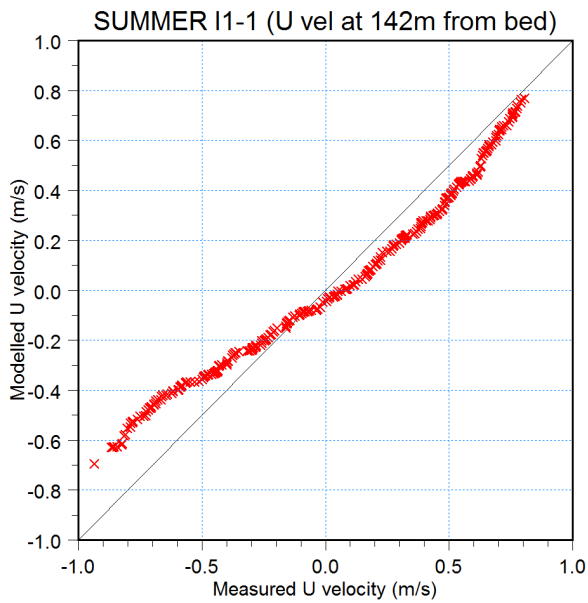
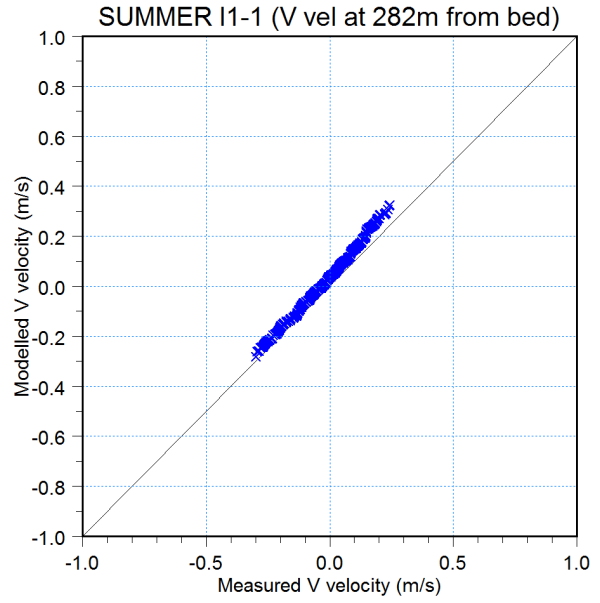
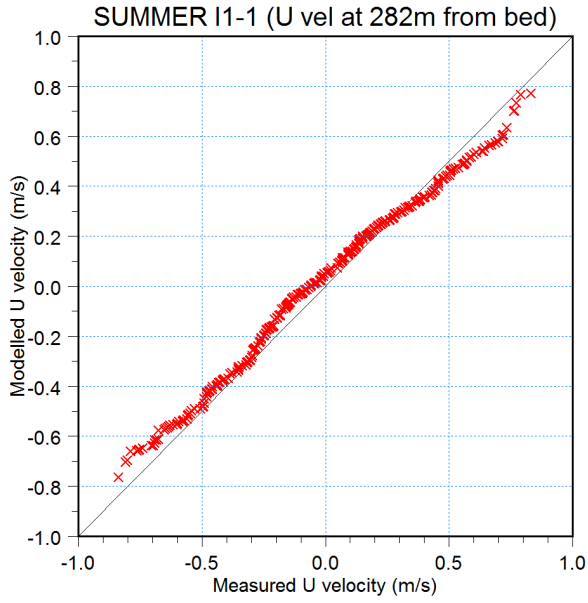


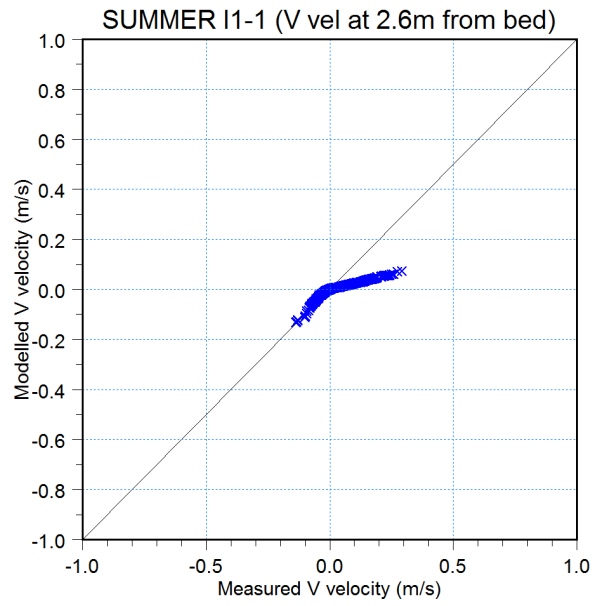
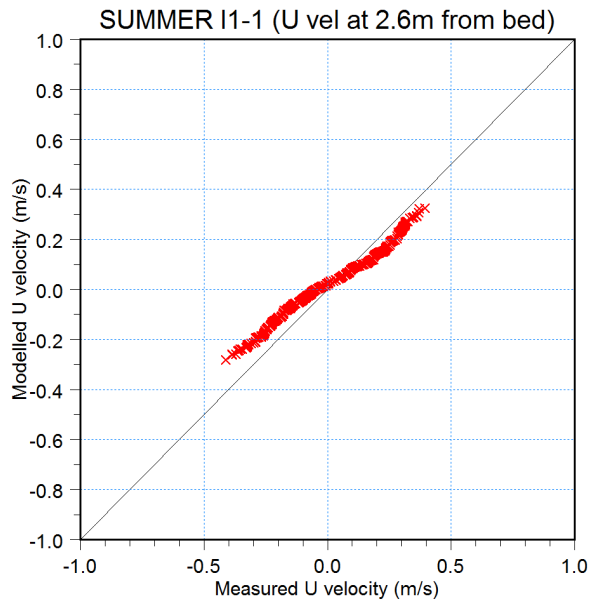


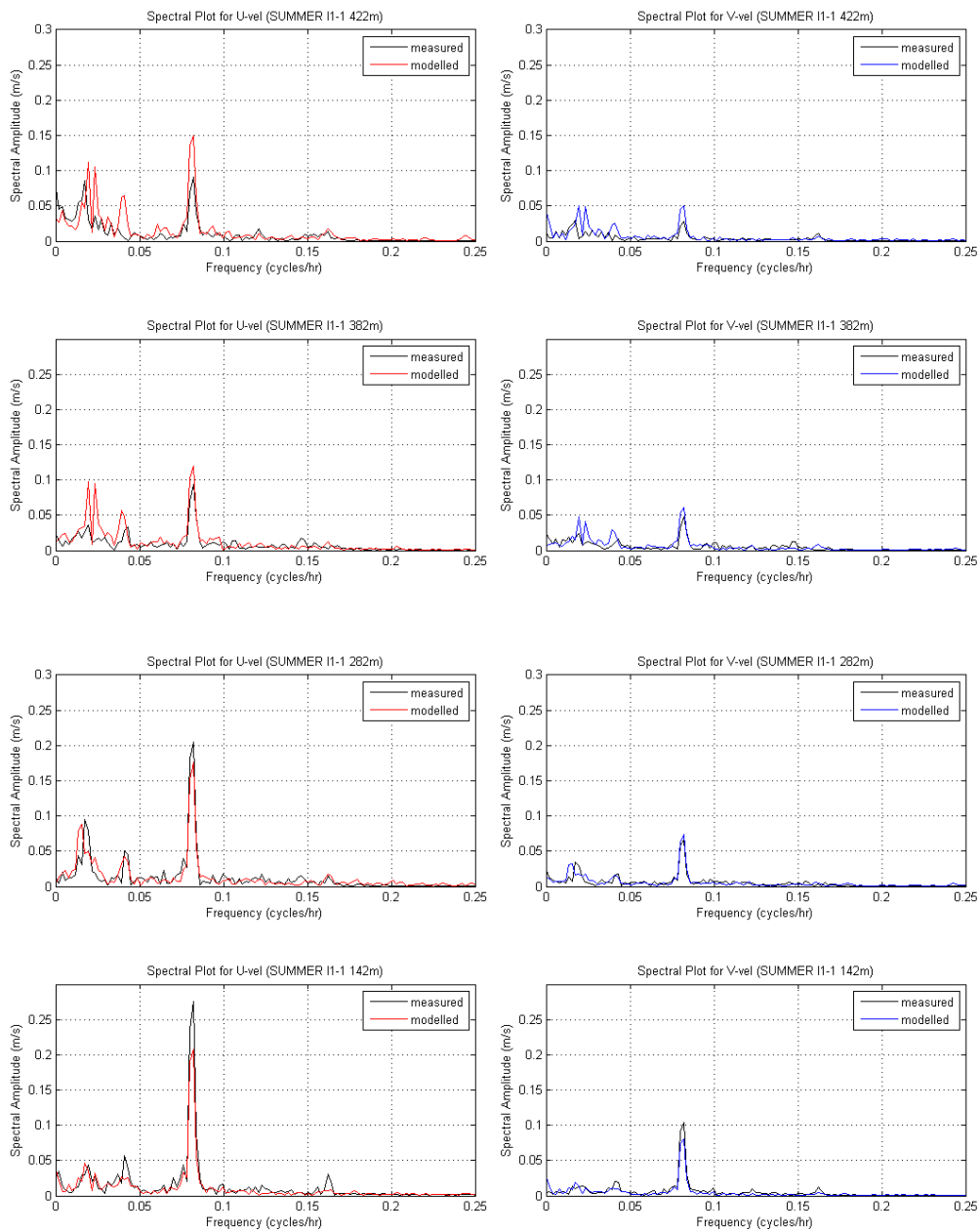


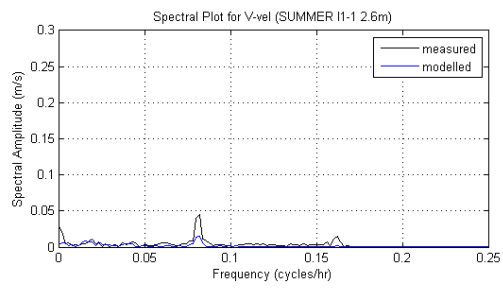
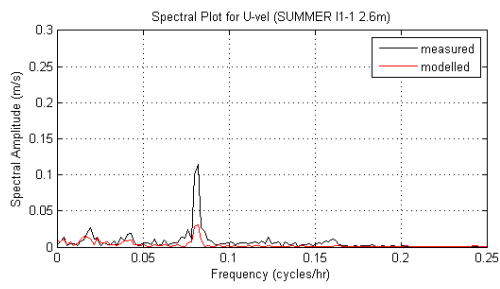










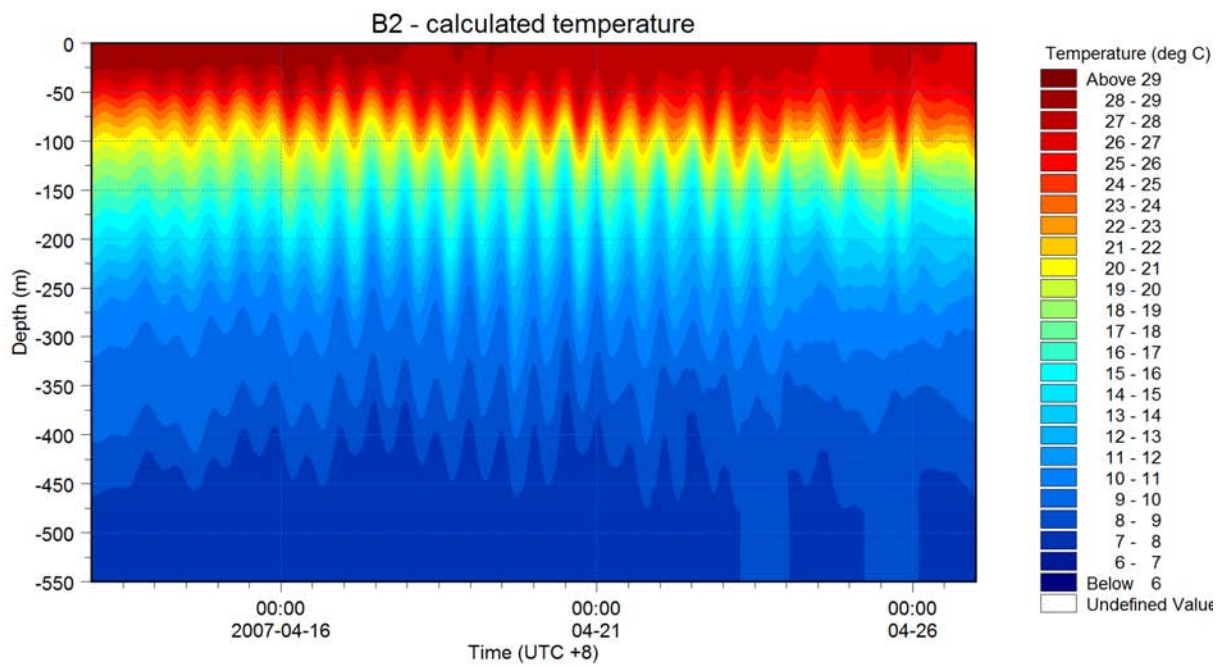
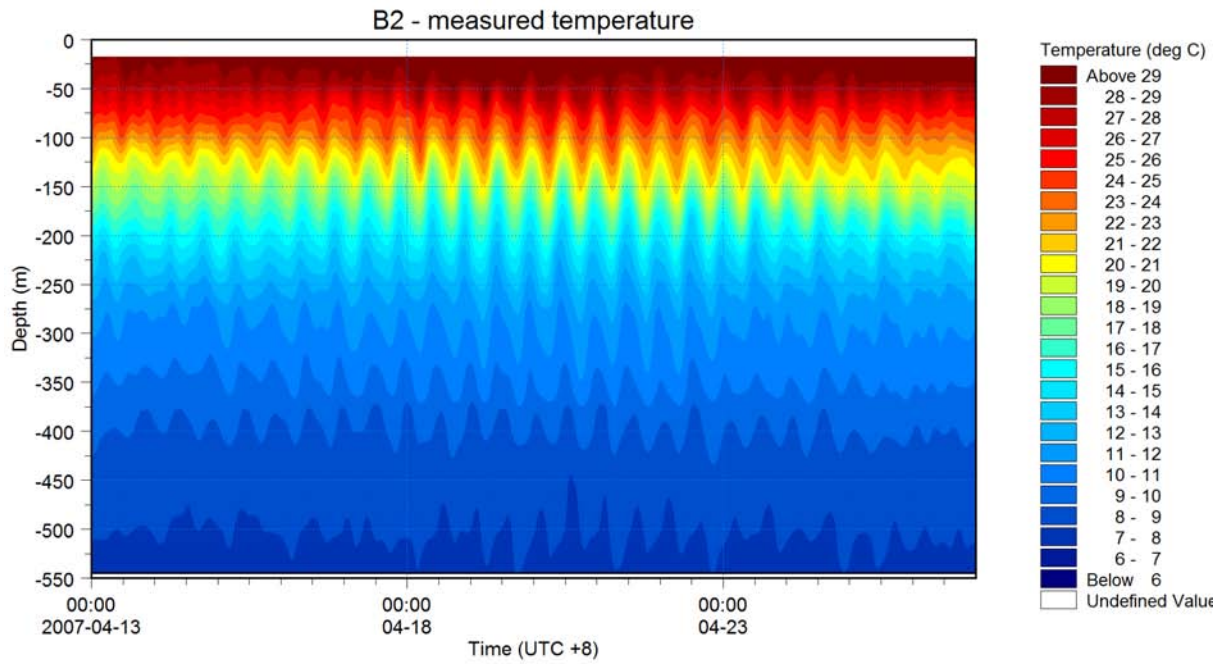




APPENDIX D

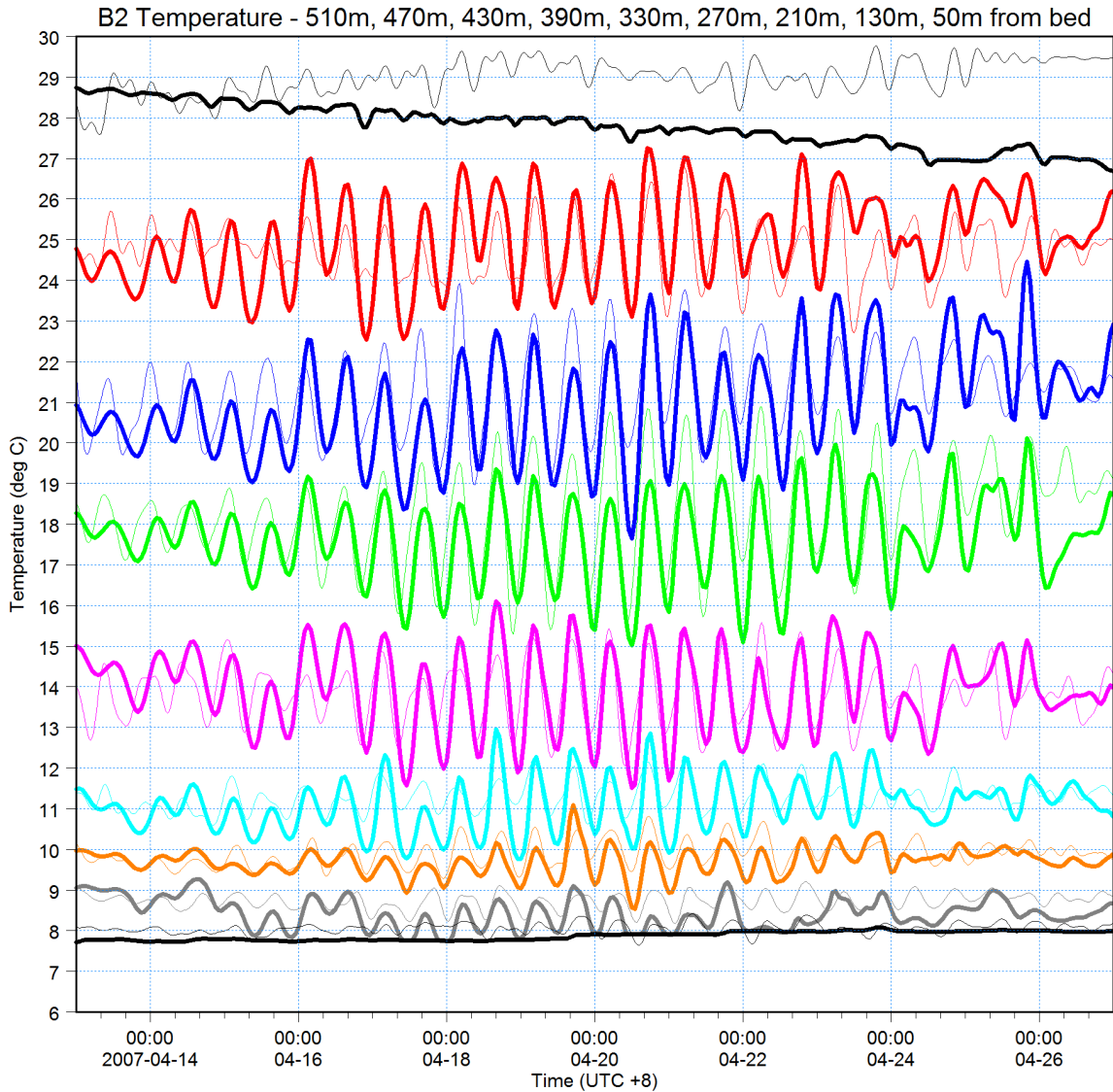
Autumn Validation Period

Comparisons between Measurements and Model Simulation as Isopleth Plots, Time Series Plots, Q-Q Plots and Frequency Plots



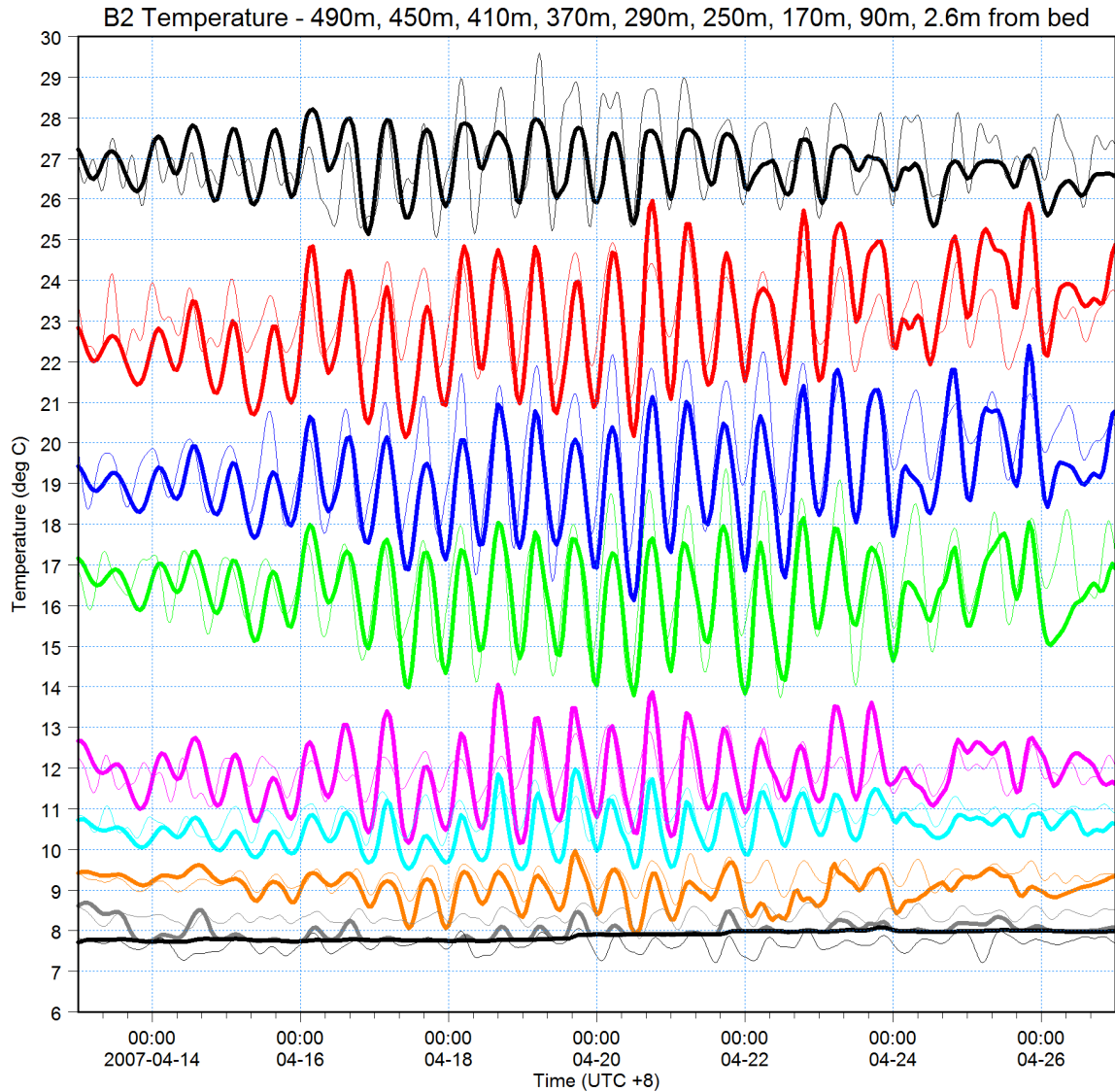


510m from bed: Temperature [C] [deg C] —
measured [deg C] —
470m from bed: Temperature [C] [deg C] —
measured [deg C] —
430m from bed: Temperature [C] [deg C] —
measured [deg C] —
390m from bed: Temperature [C] [deg C] —
measured [deg C] —
330m from bed: Temperature [C] [deg C] —
measured [deg C] —
270m from bed: Temperature [C] [deg C] —
measured [deg C] —
190m from bed: Temperature [C] [deg C] —
measured [deg C] —
130m from bed: Temperature [C] [deg C] —
measured [deg C] —
50m from bed: Temperature [C] [deg C] —
measured [deg C] —



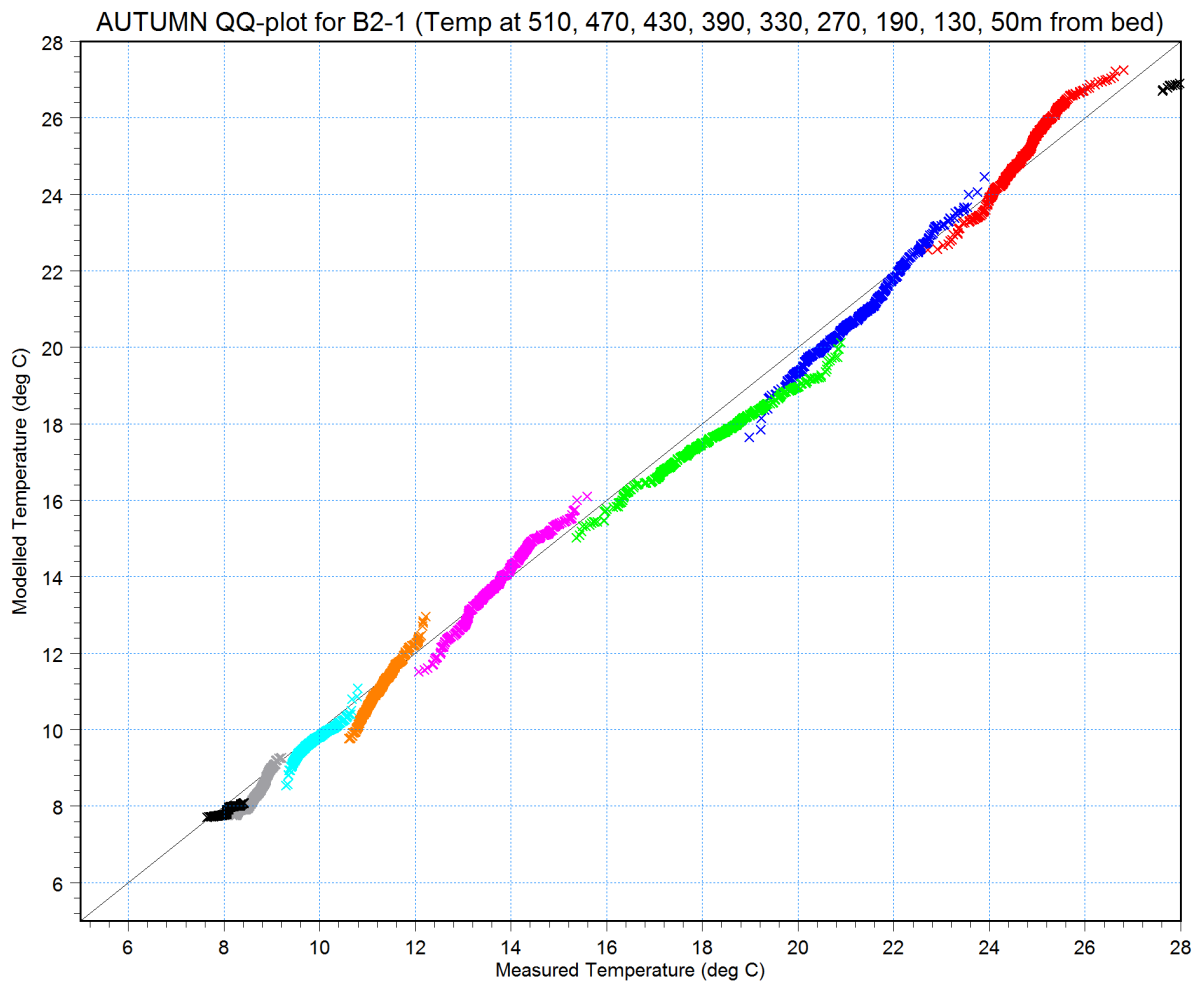


490m from bed: Temperature [C] [deg C] —
measured [deg C] —
450m from bed: Temperature [C] [deg C] —
measured [deg C] —
410m from bed: Temperature [C] [deg C] —
measured [deg C] —
370m from bed: Temperature [C] [deg C] —
measured [deg C] —
290m from bed: Temperature [C] [deg C] —
measured [deg C] —
250m from bed: Temperature [C] [deg C] —
measured [deg C] —
170m from bed: Temperature [C] [deg C] —
measured [deg C] —
130m from bed: Temperature [C] [deg C] —
measured [deg C] —
2.6m from bed: Temperature [C] [deg C] —
measured [deg C] —



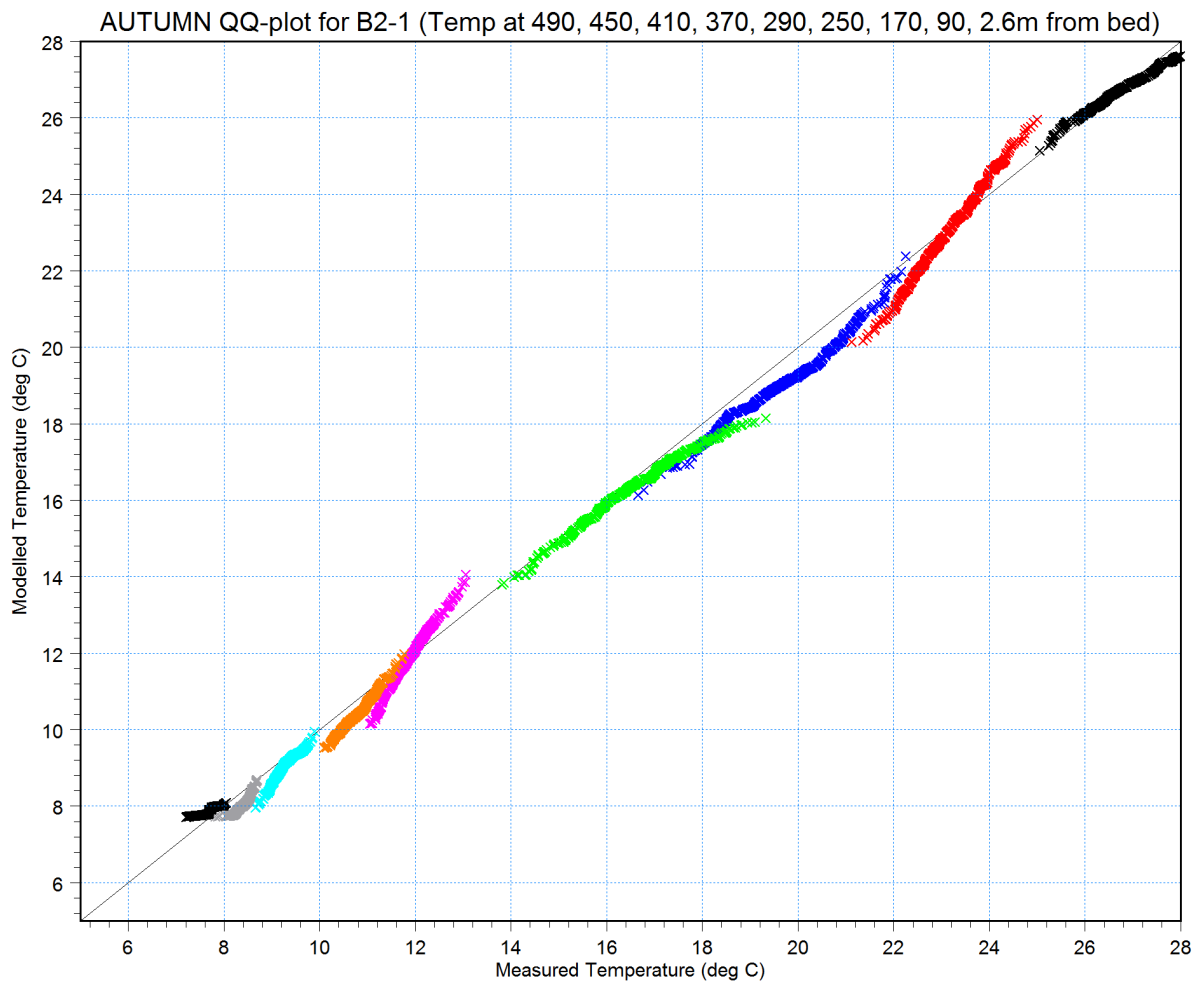


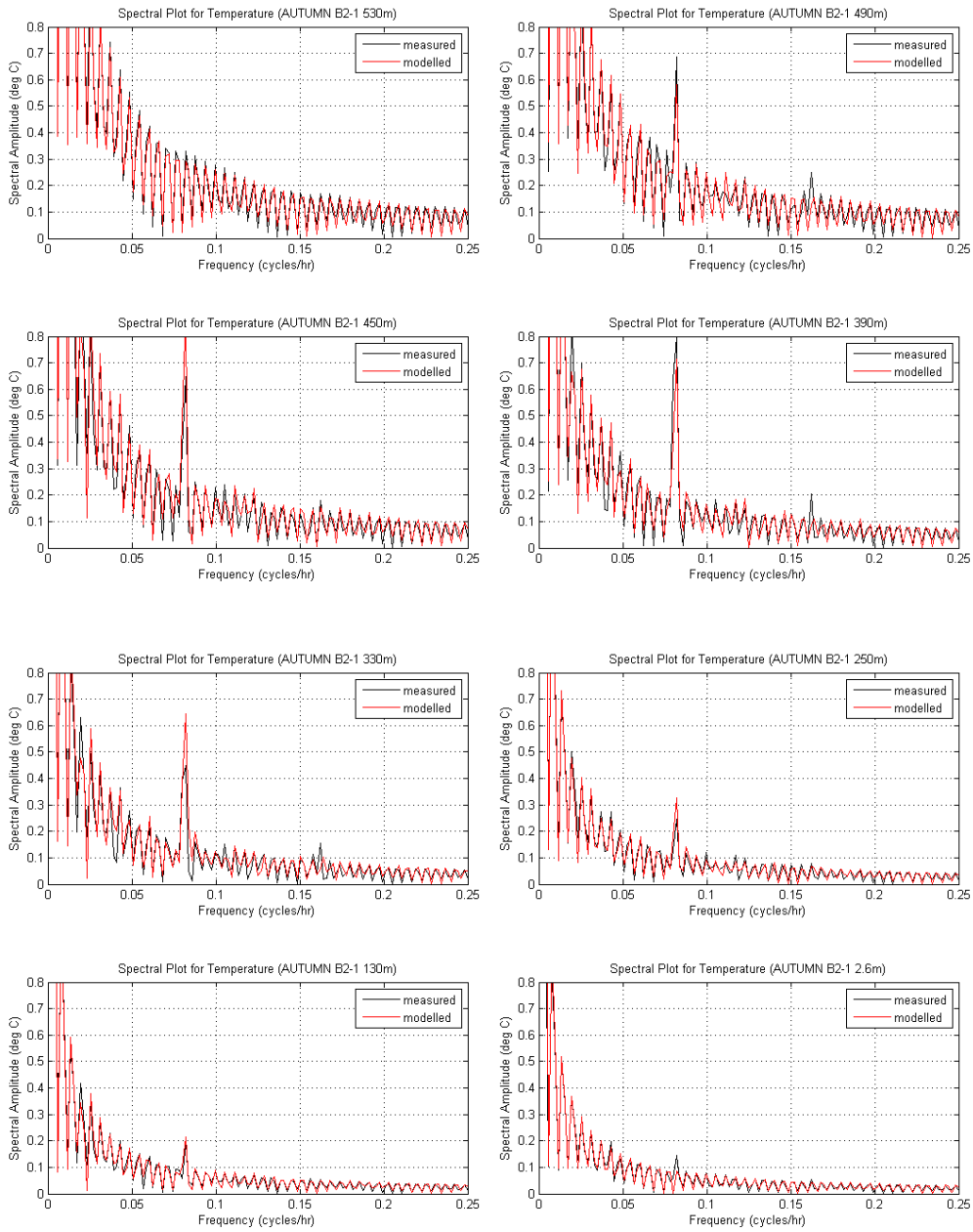
- T at 510m × ×
- T at 470m × ×
- T at 430m × ×
- T at 390m × ×
- T at 330m × ×
- T at 270m × ×
- T at 190m × ×
- T at 130m × ×
- T at 50m × ×

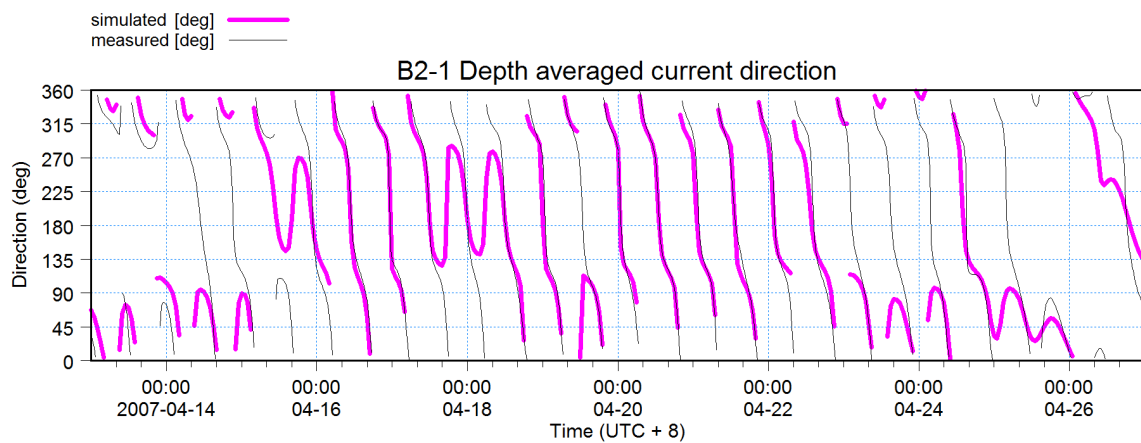
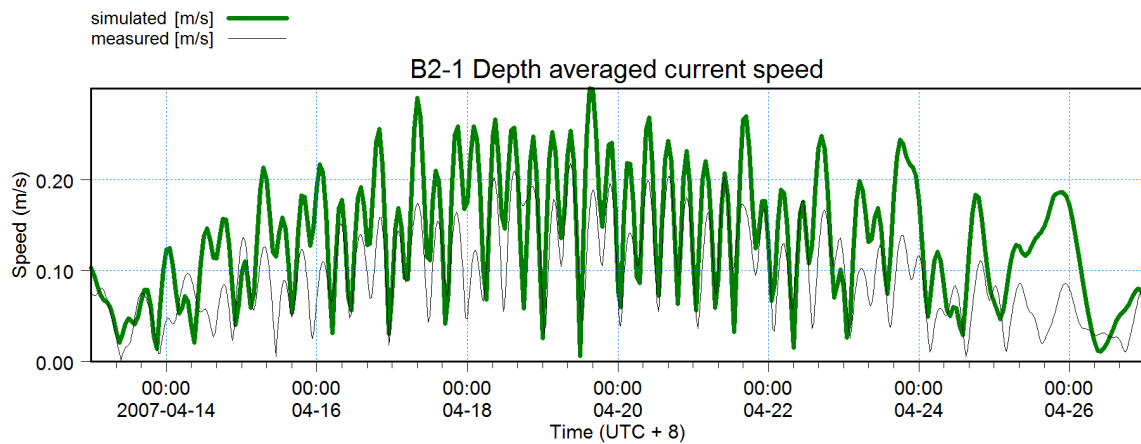
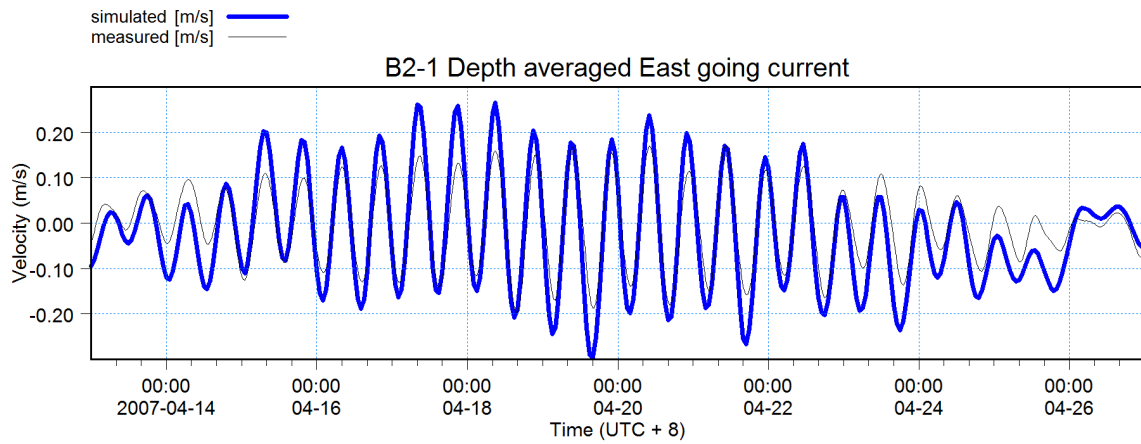
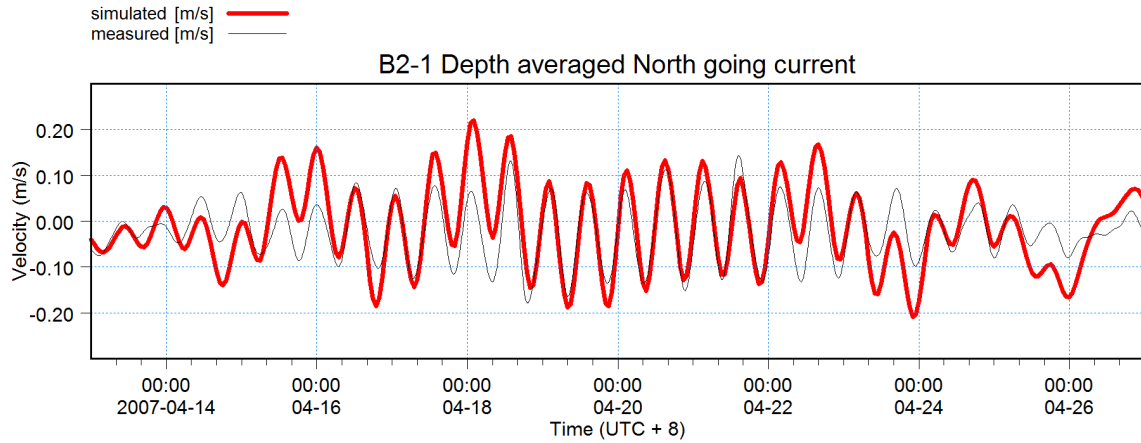




- T at 490m × ×
- T at 450m × ×
- T at 410m × ×
- T at 370m × ×
- T at 290m × ×
- T at 250m × ×
- T at 170m × ×
- T at 90m × ×
- T at 2.6m × ×

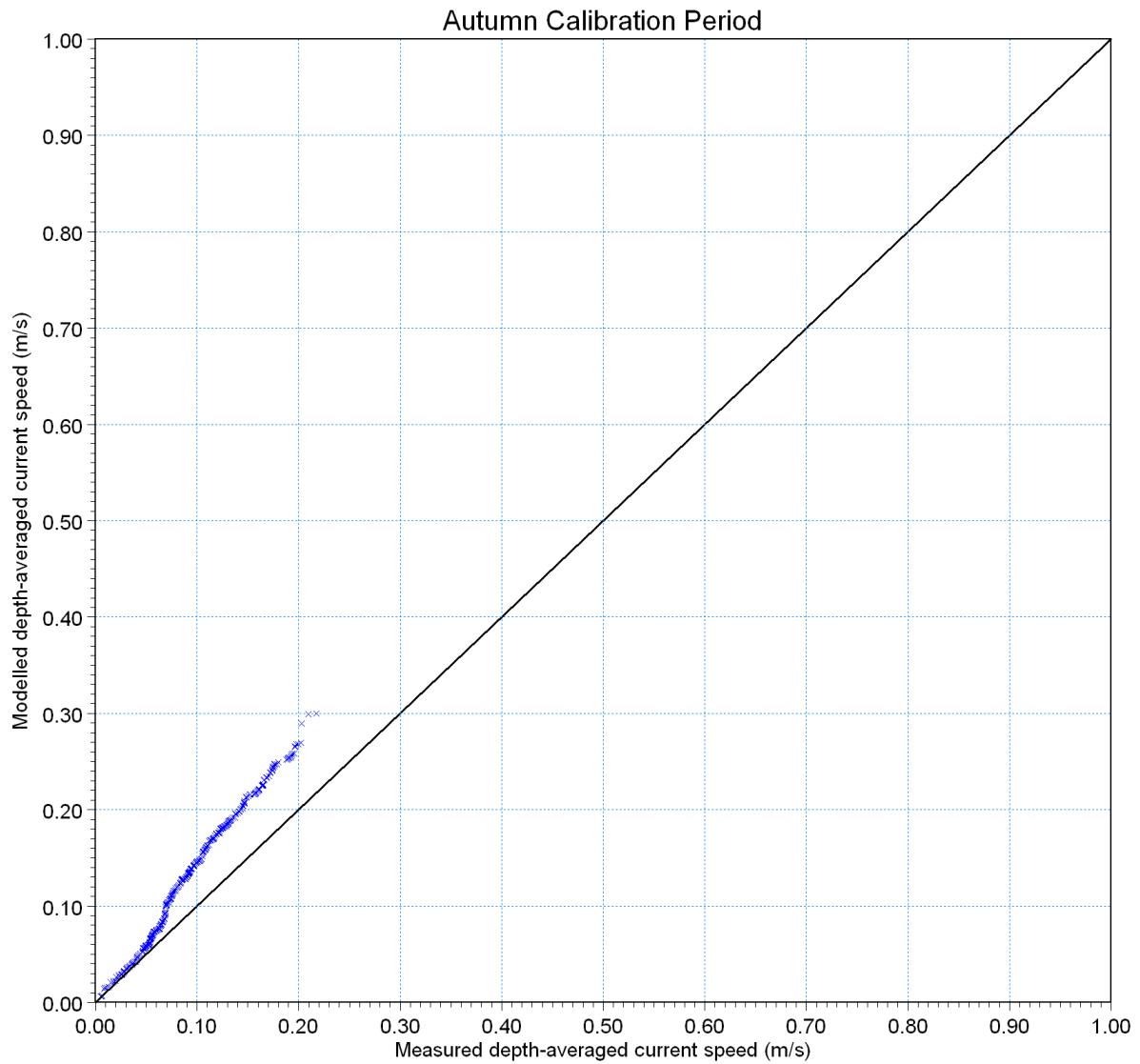


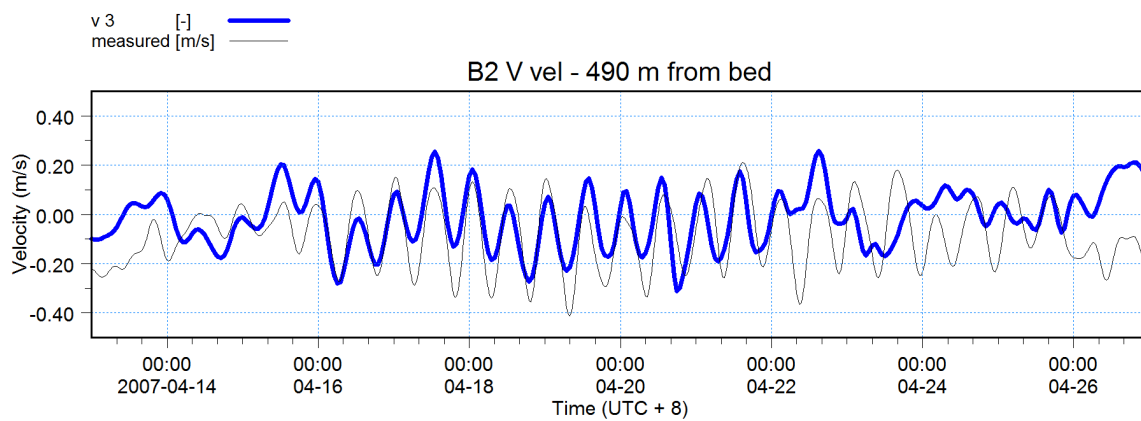
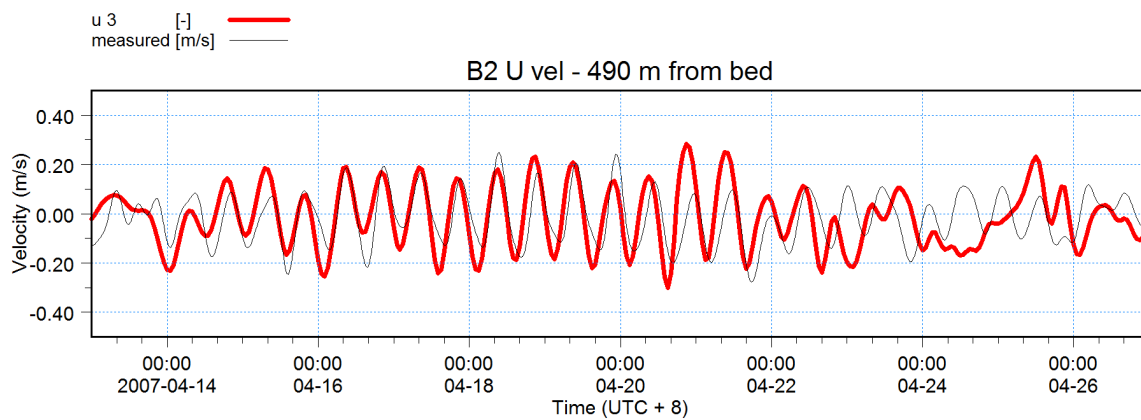
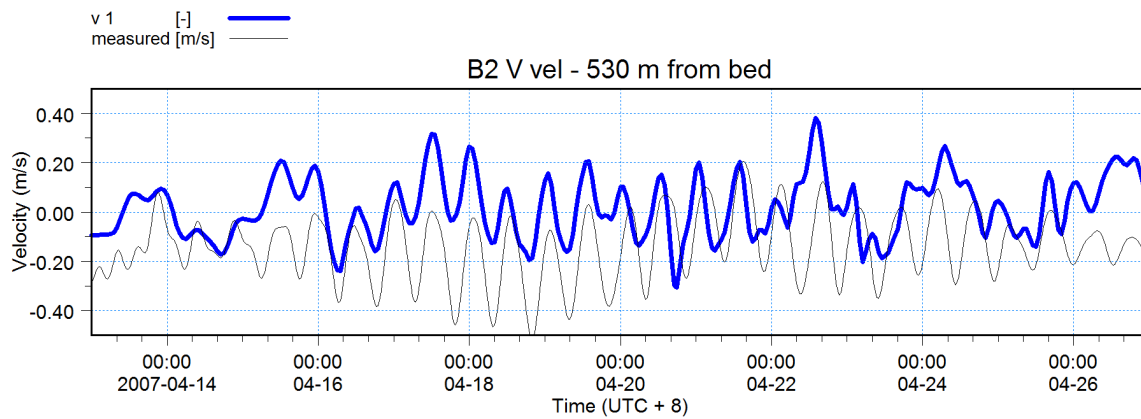
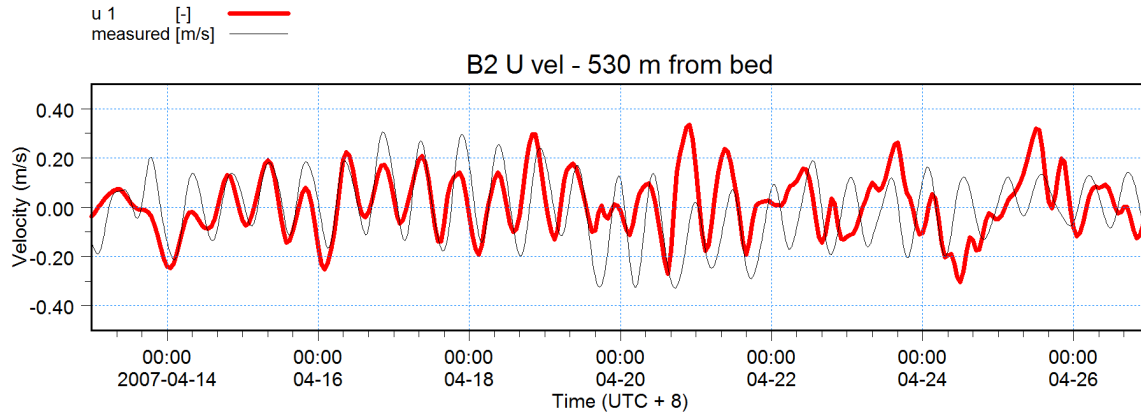


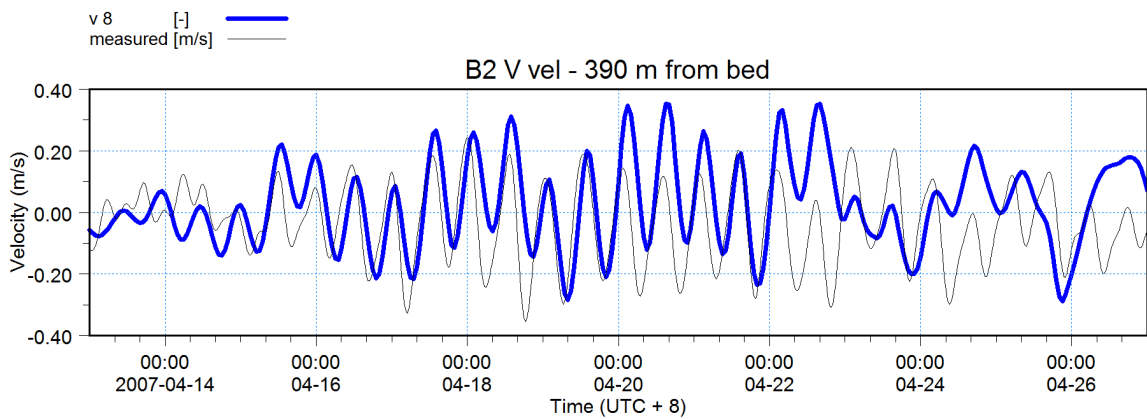
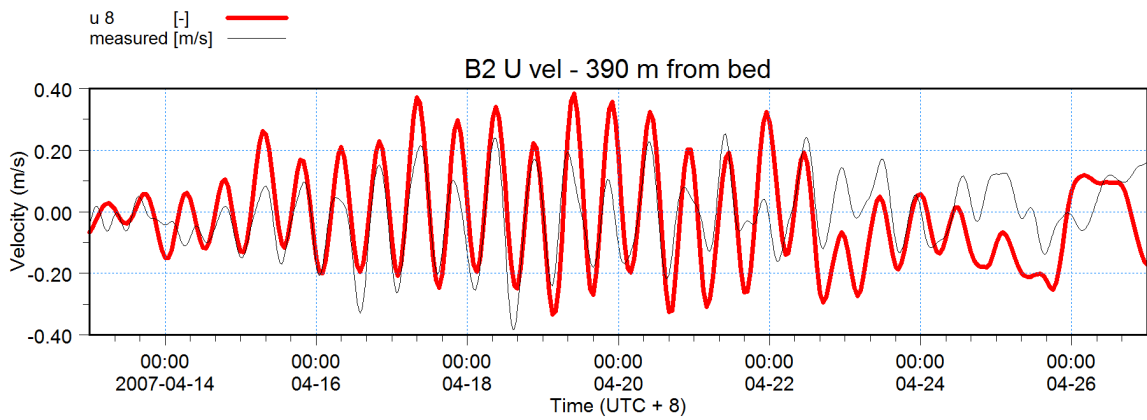
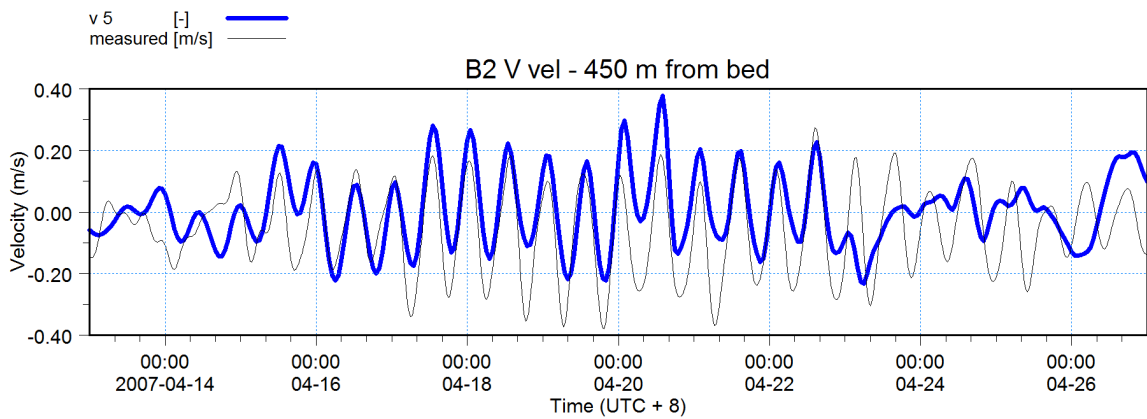
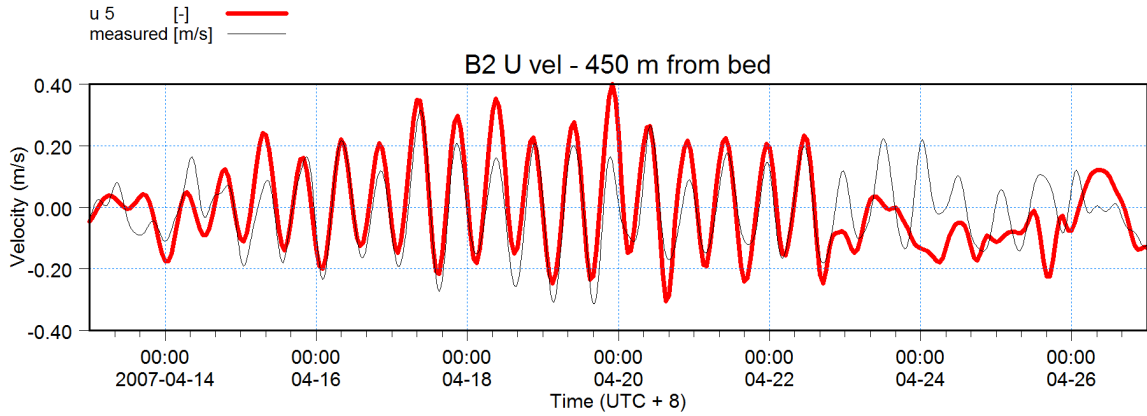


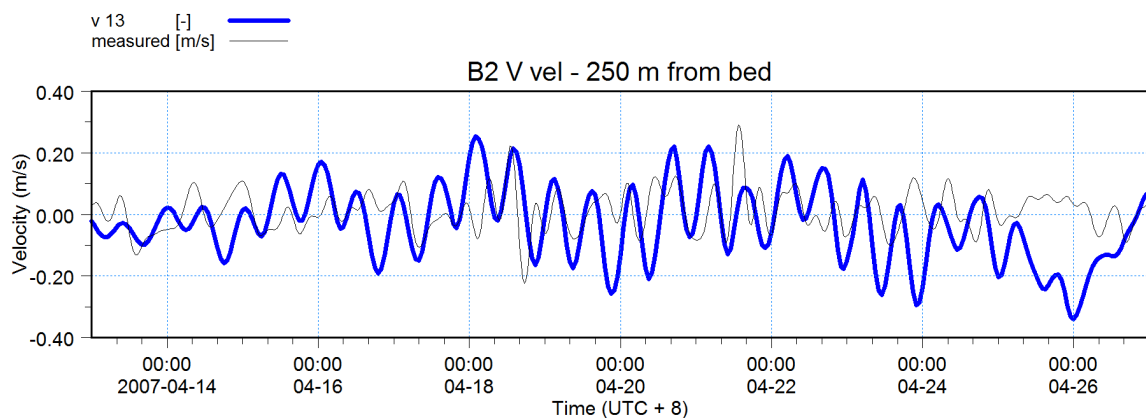
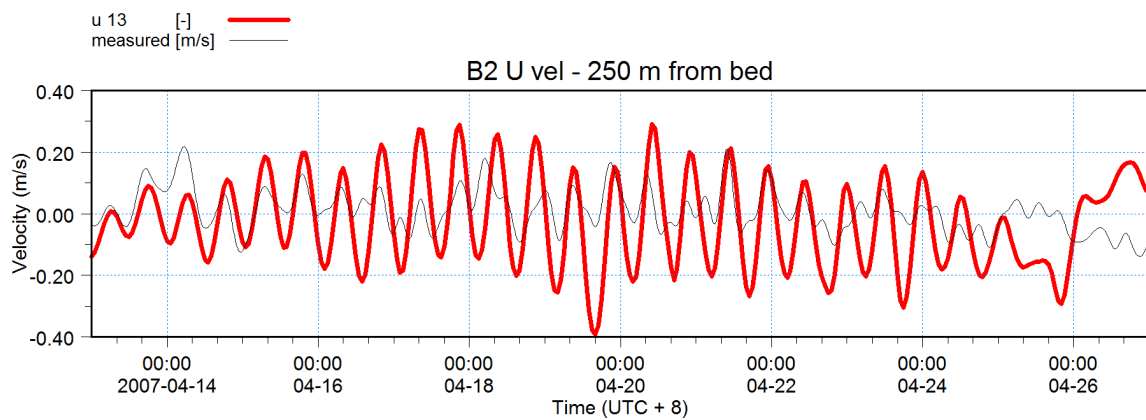
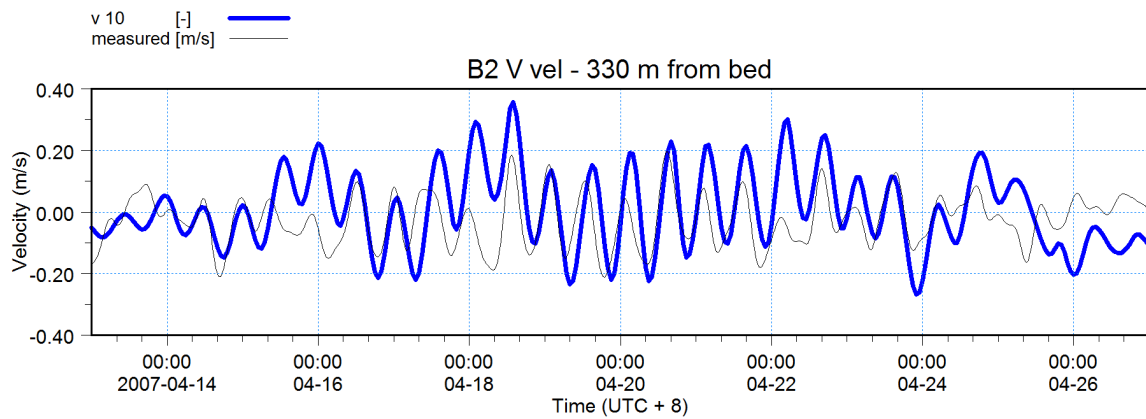
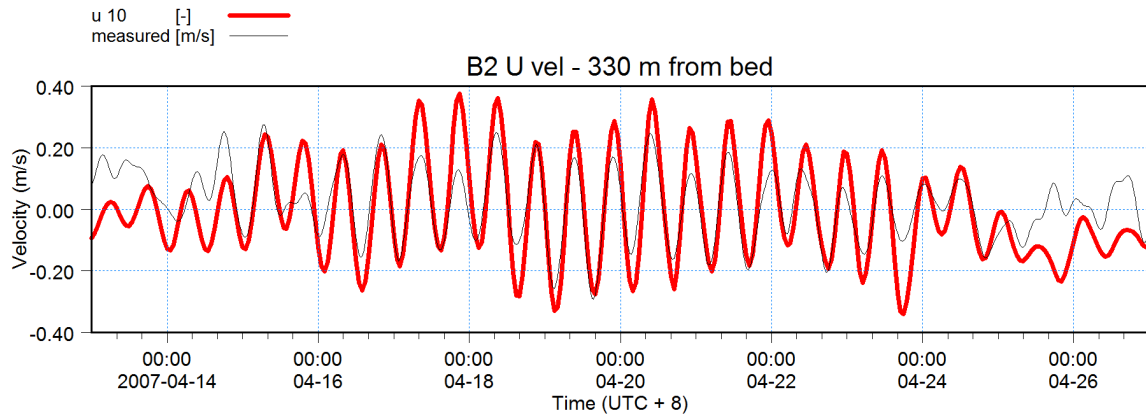


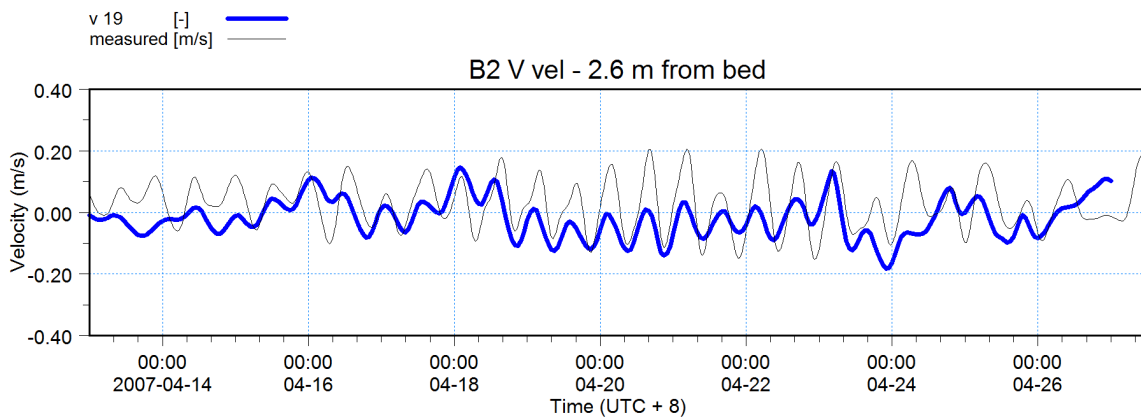
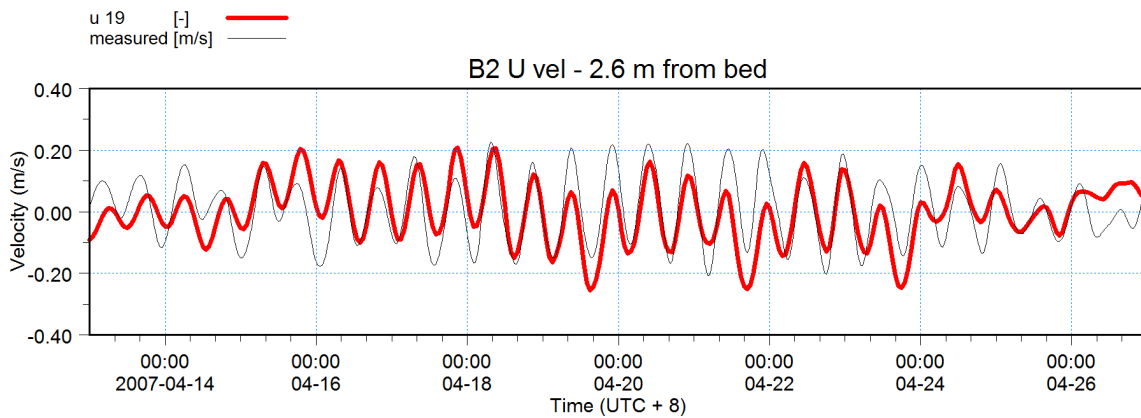
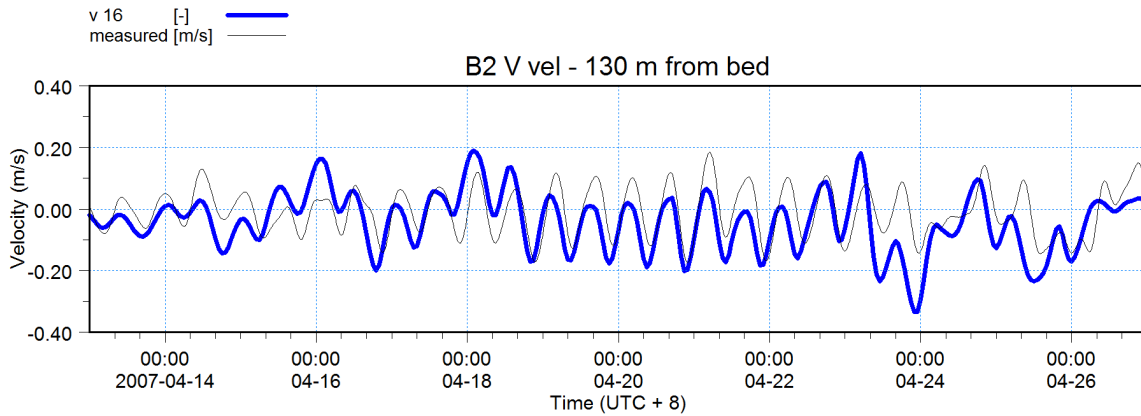
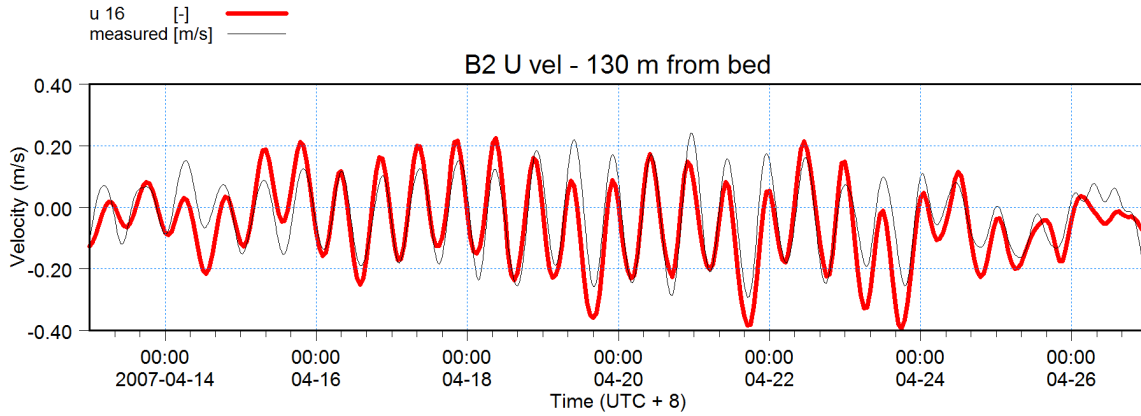
B2 × ×

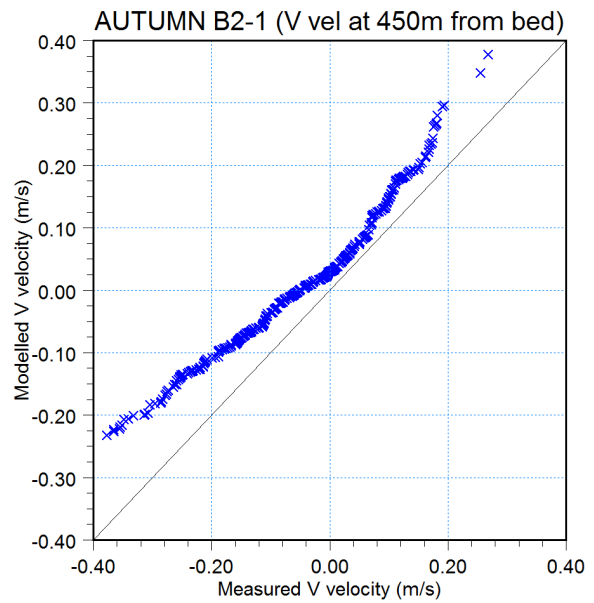
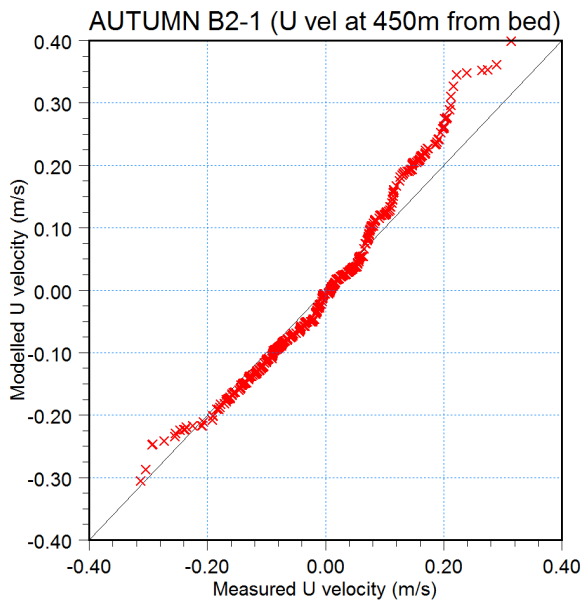
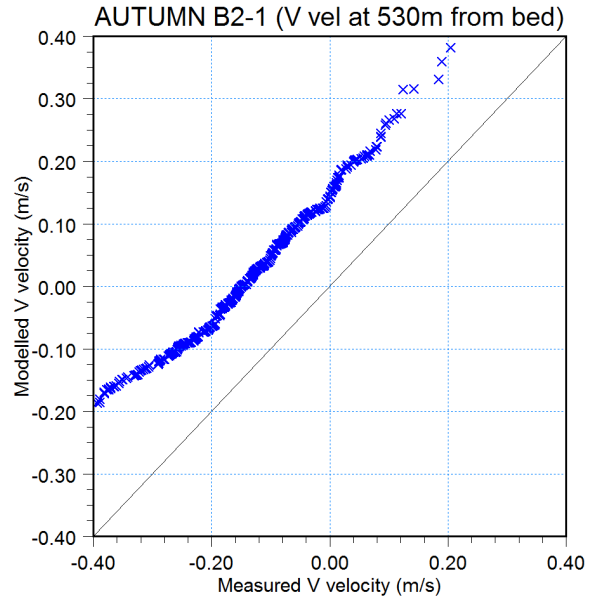
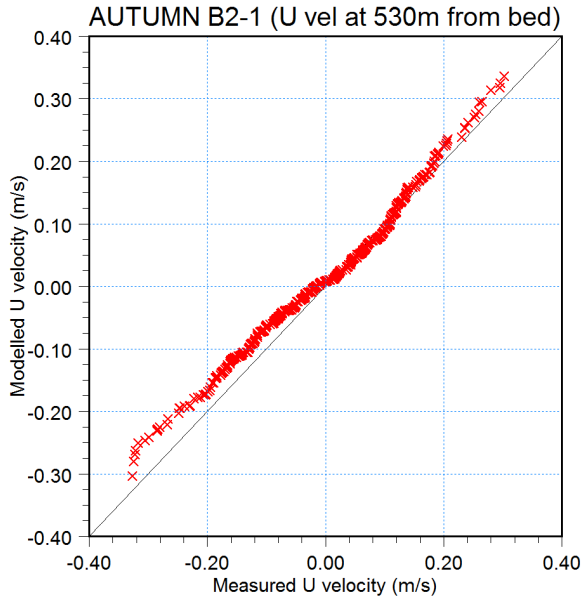


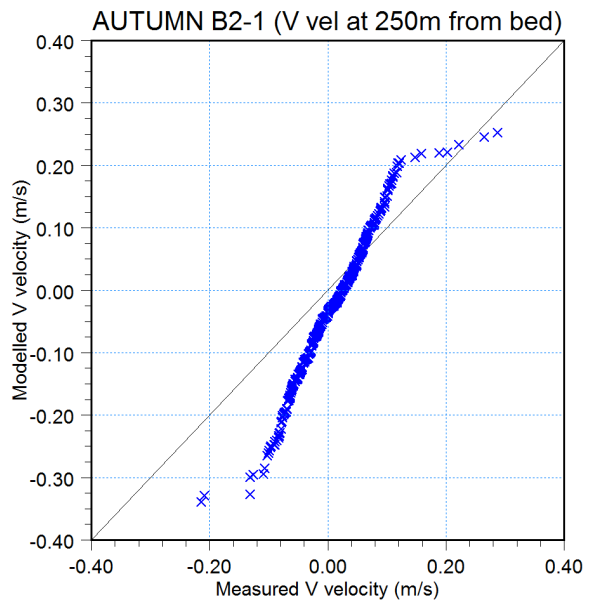
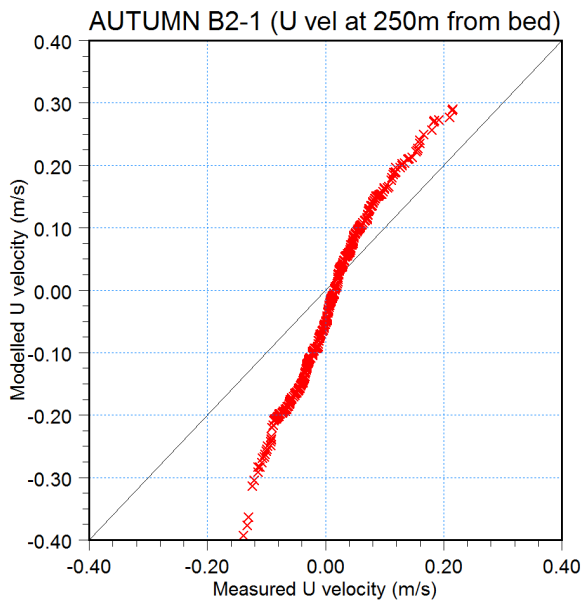
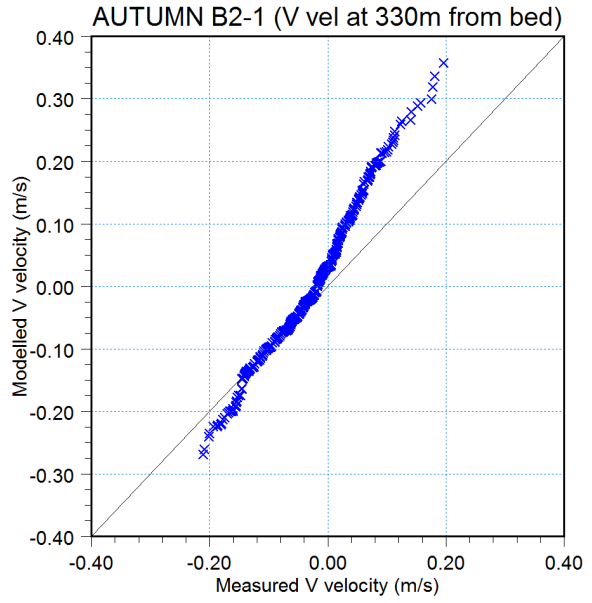
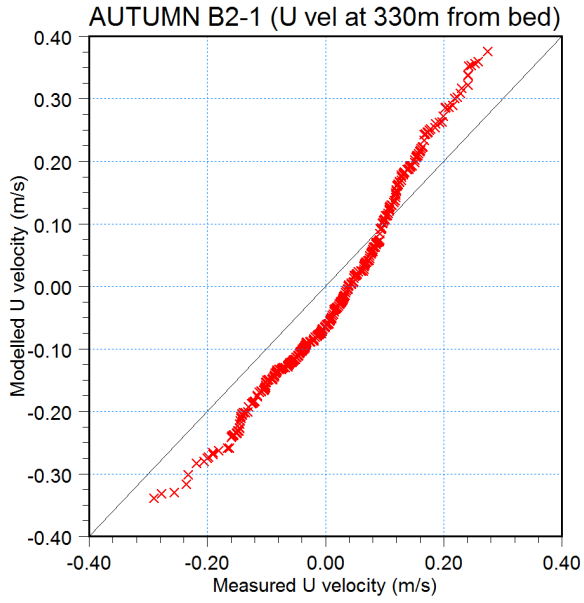


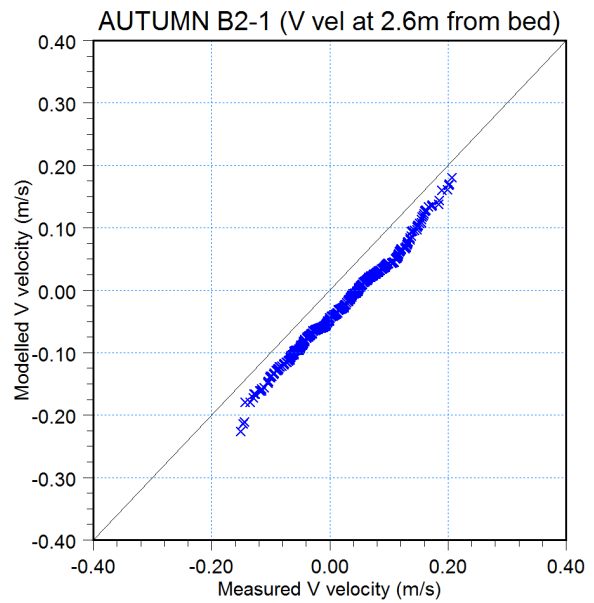
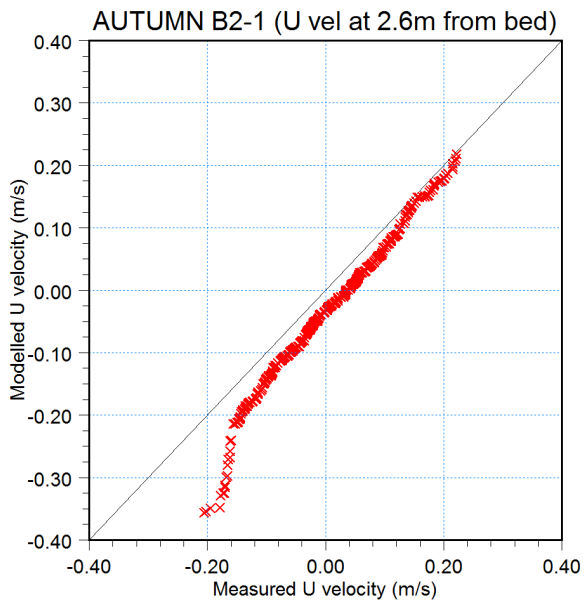
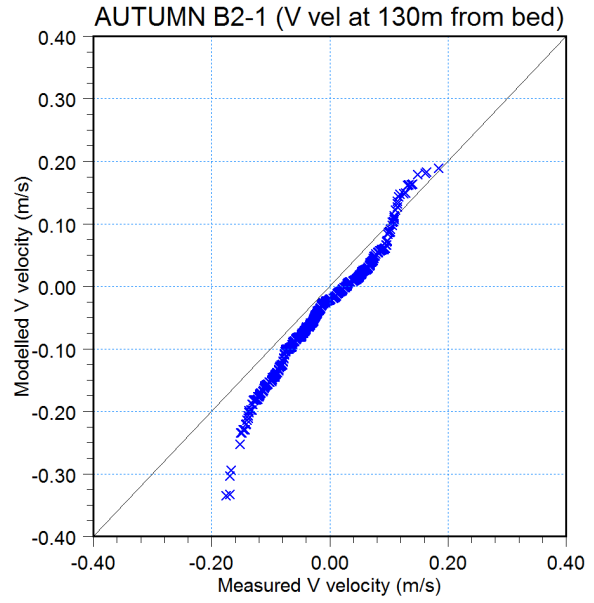
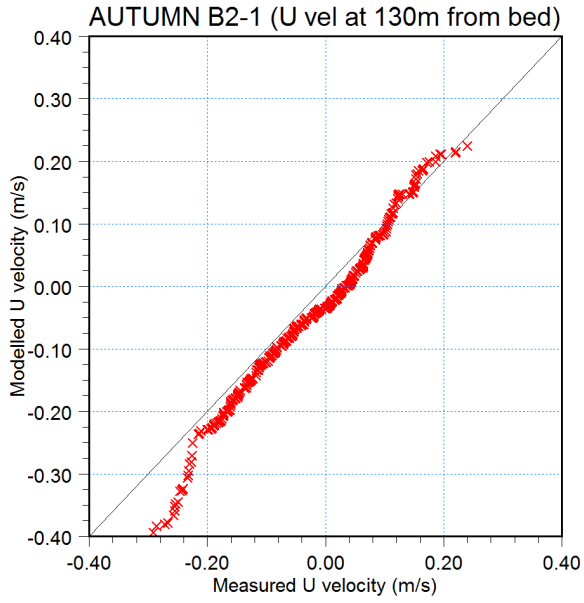


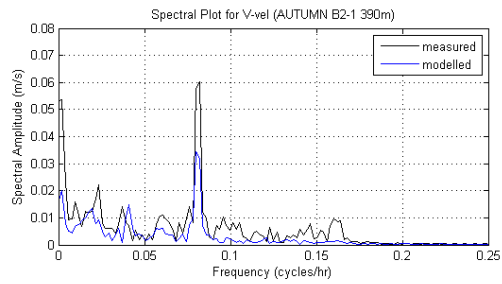
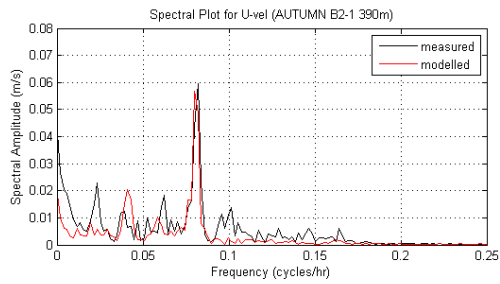
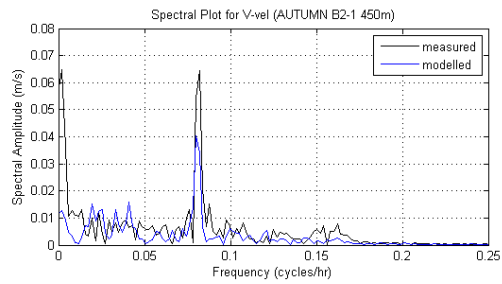
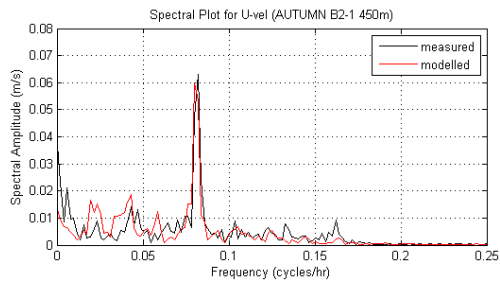
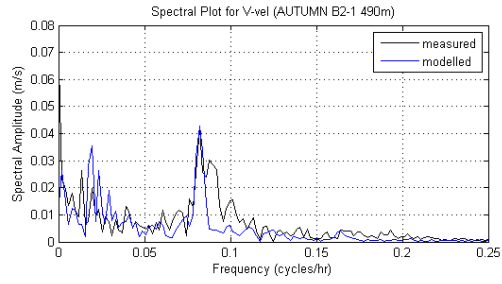
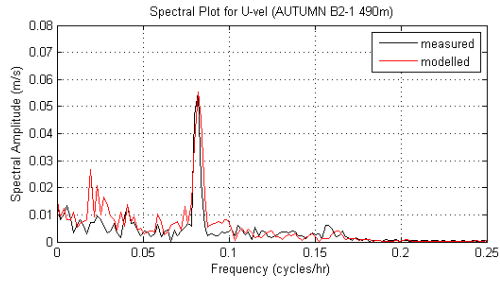
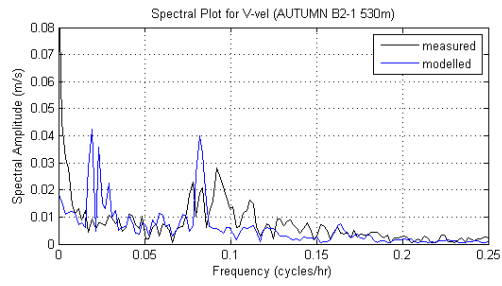
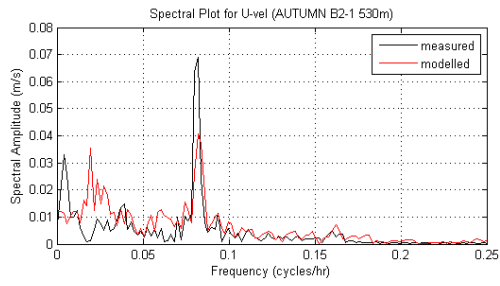


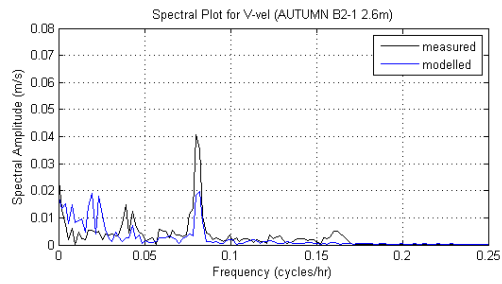
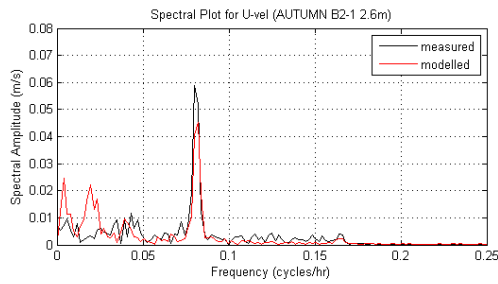
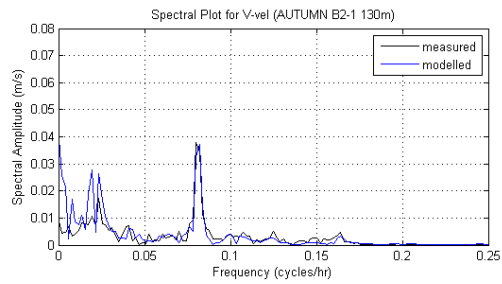
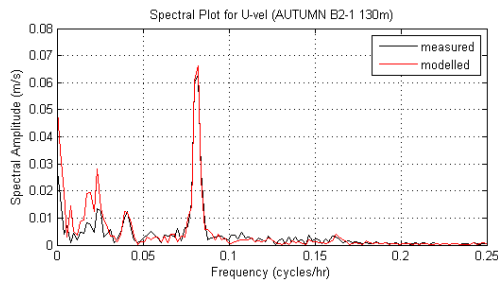
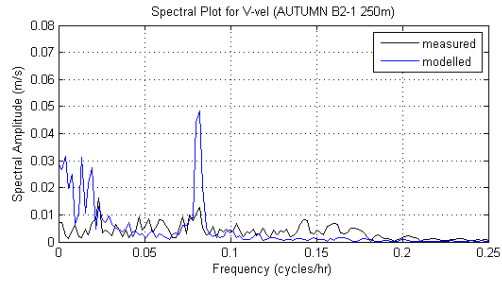
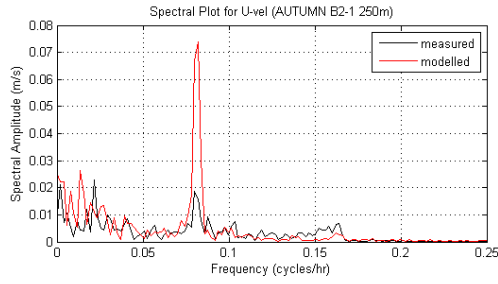
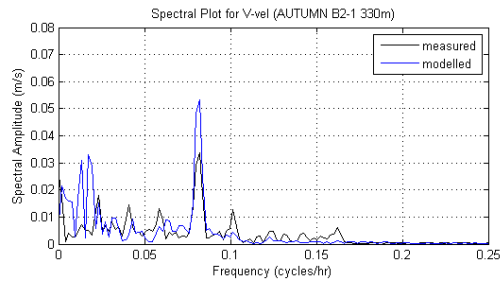
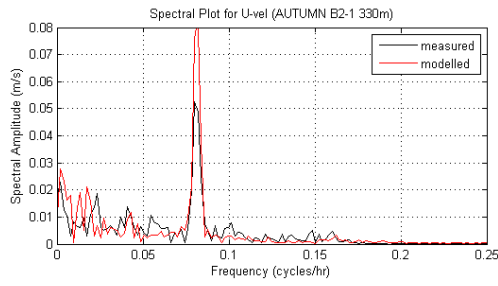








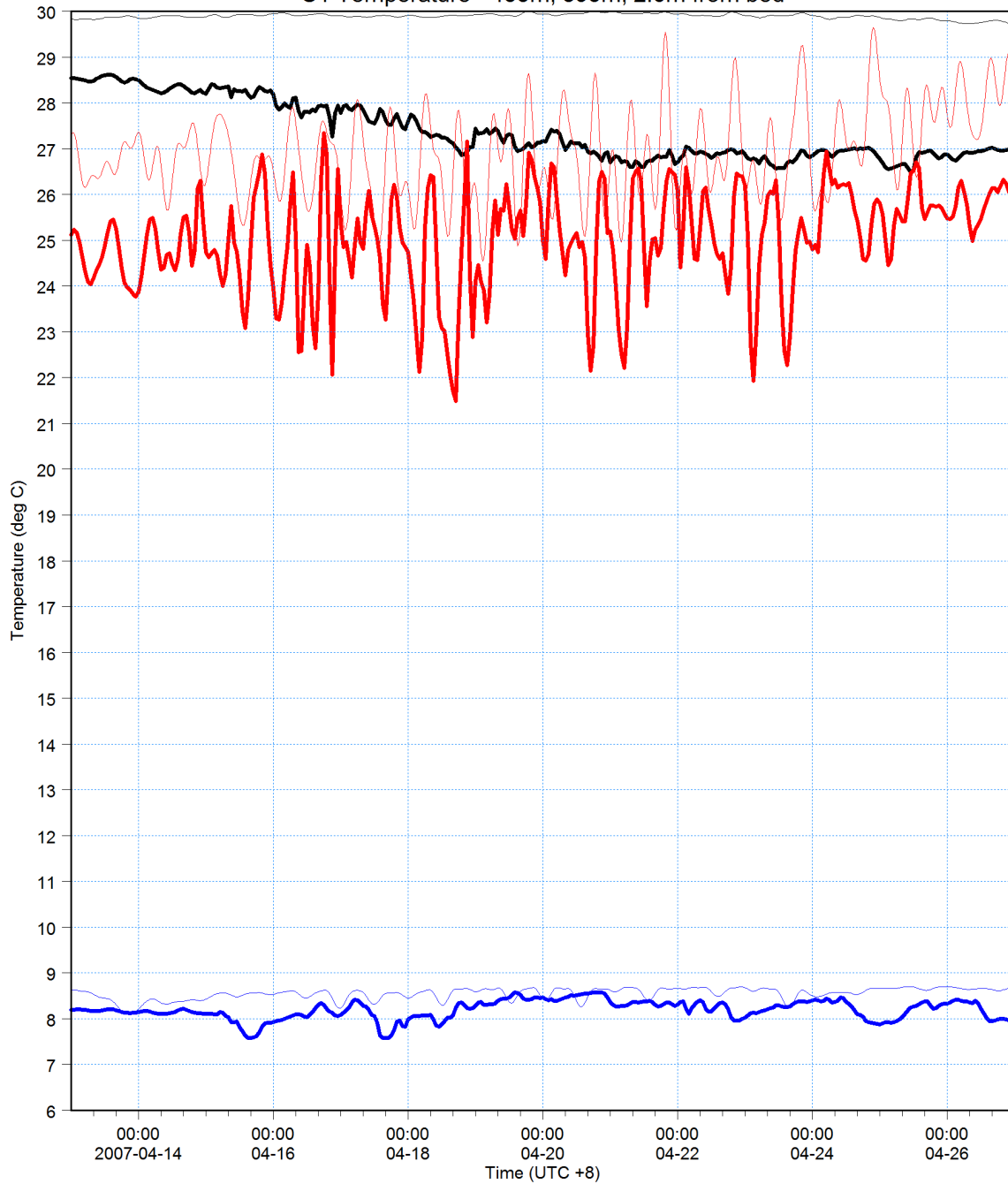






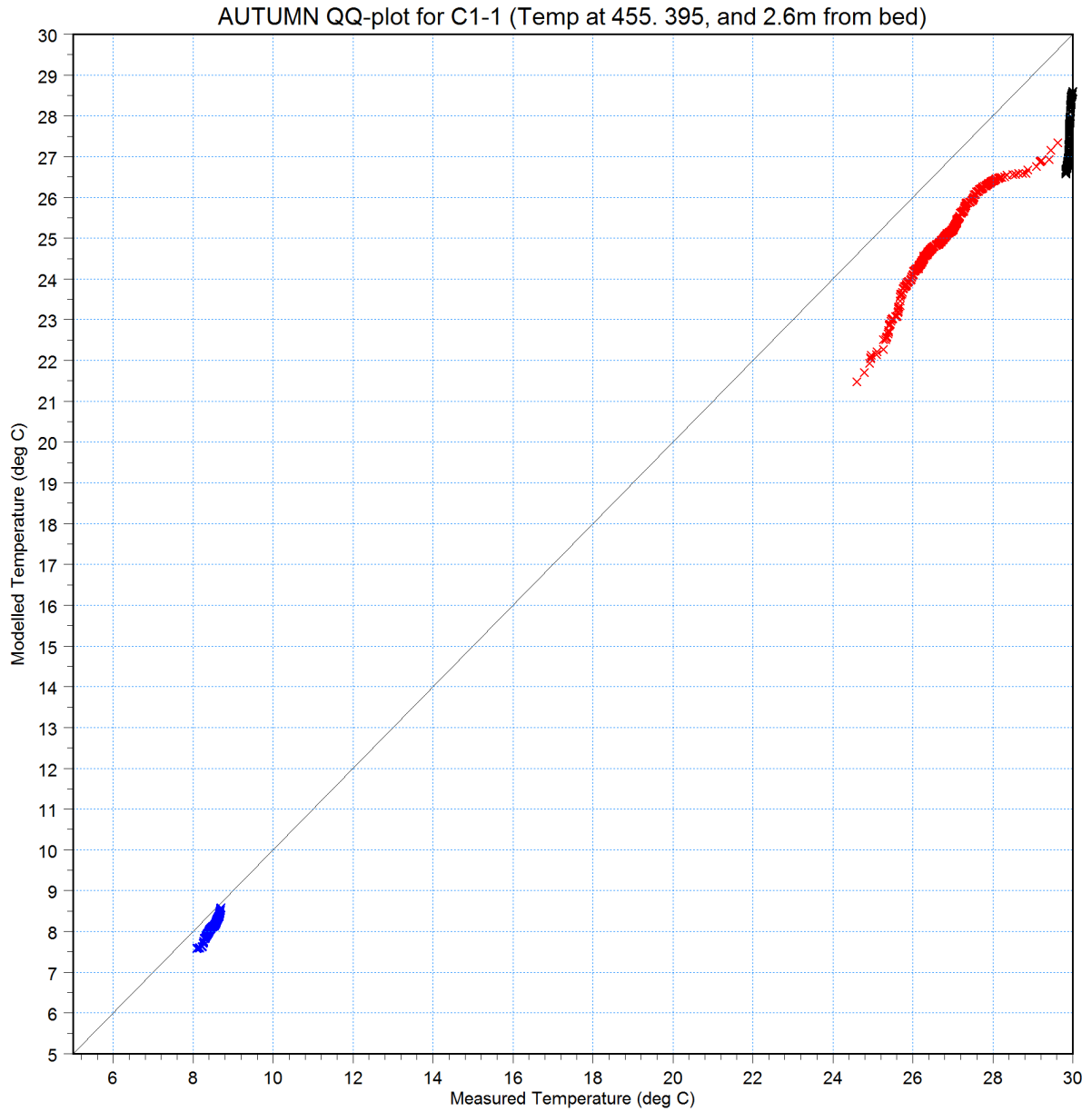
455m from bed: Temperature [C] [deg C] —
measured [deg C] —
395m from bed: Temperature [C] [deg C] —
measured [deg C] —
2.6m from bed: Temperature [C] [deg C] —
measured [deg C] —

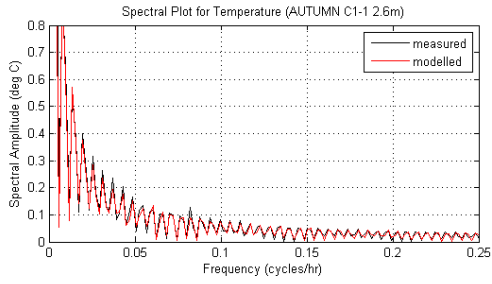
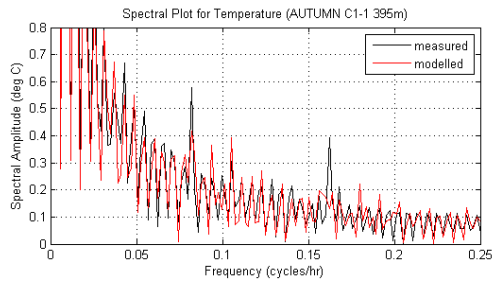
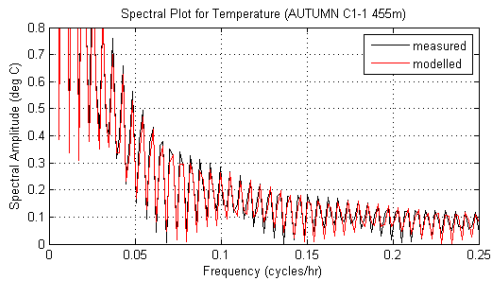
C1 Temperature - 455m, 395m, 2.6m from bed

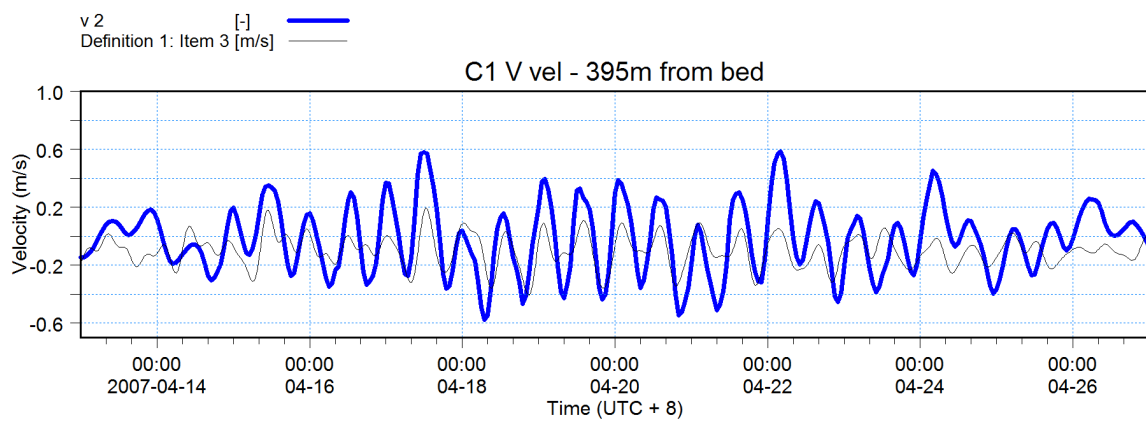
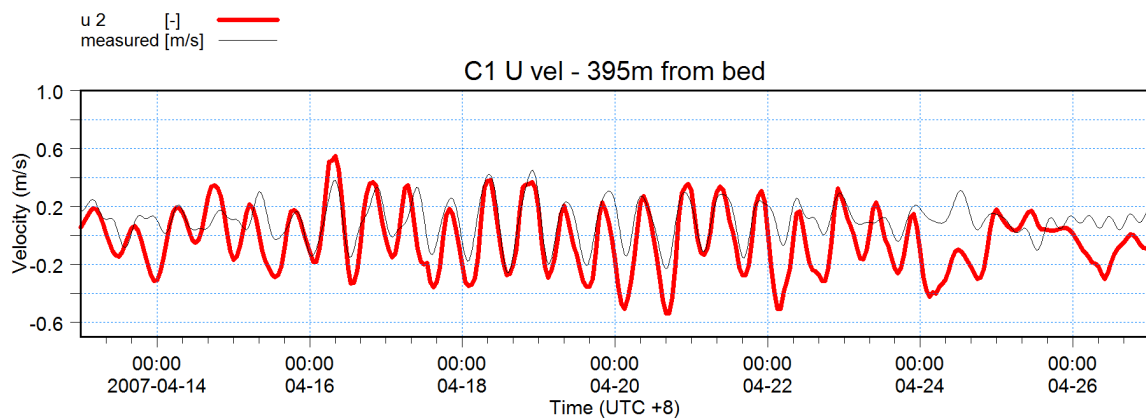
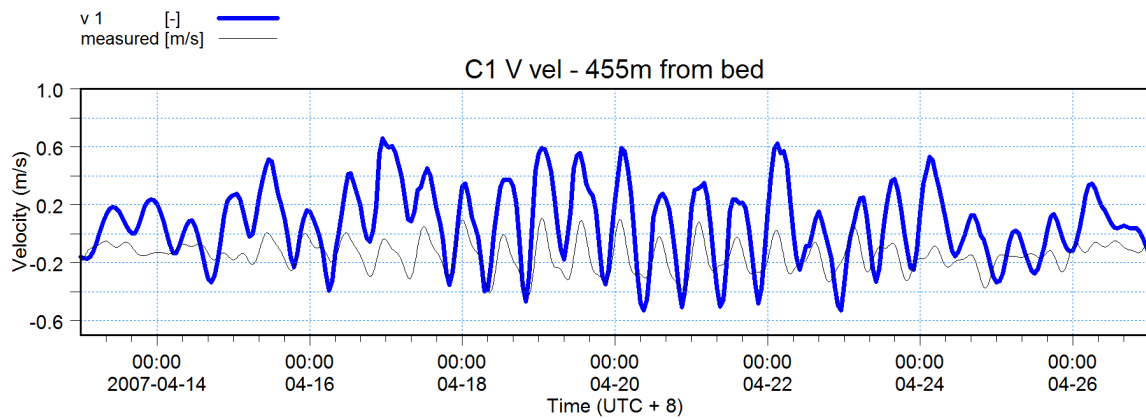
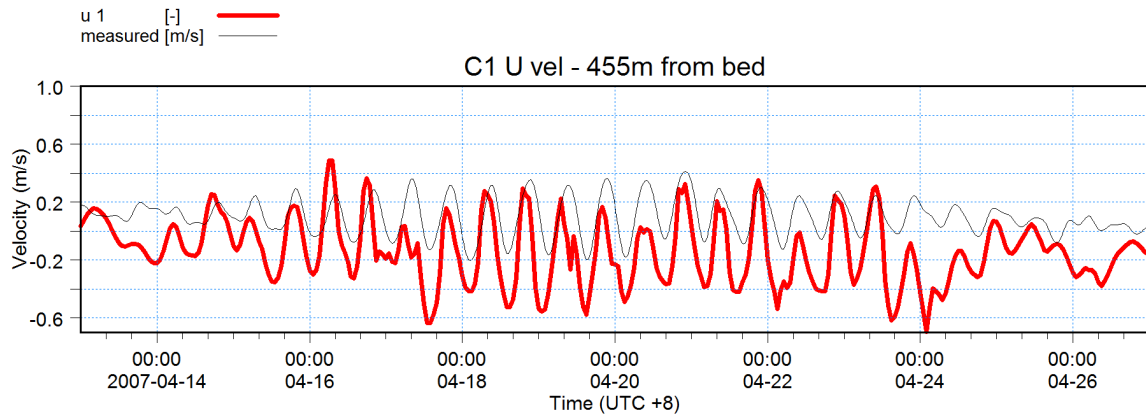


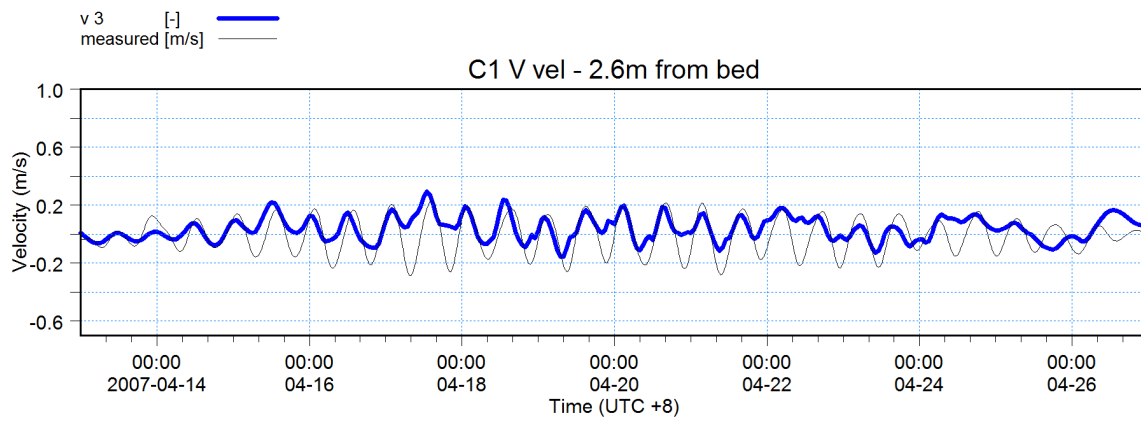
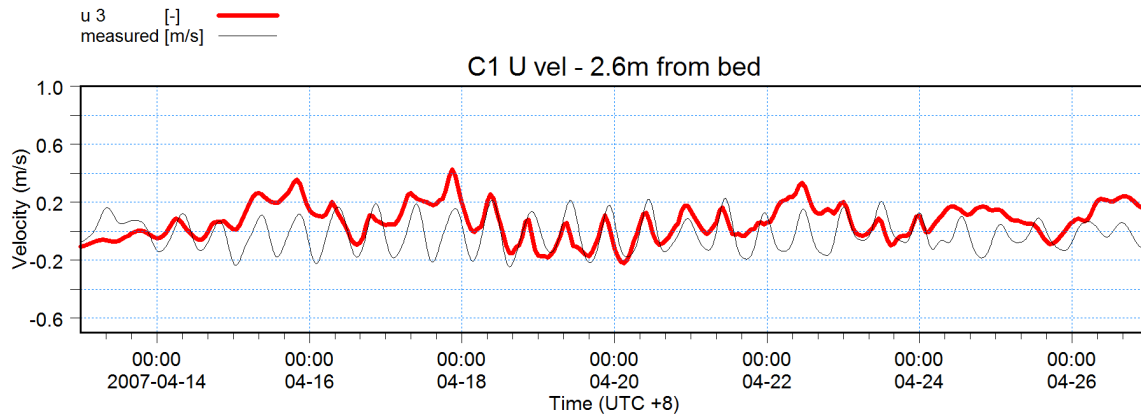


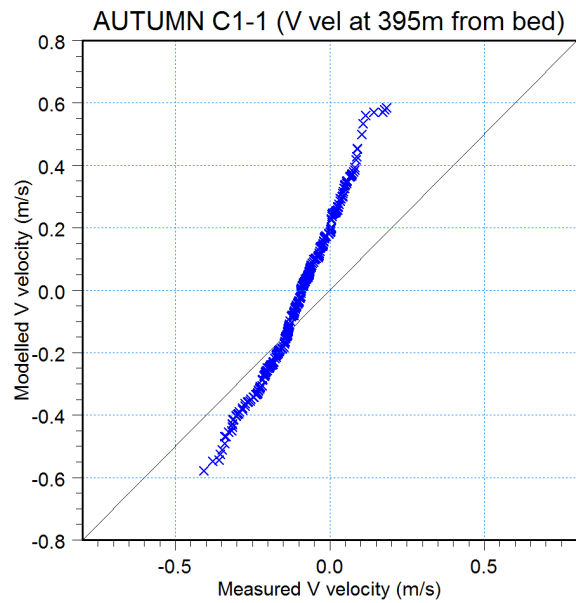
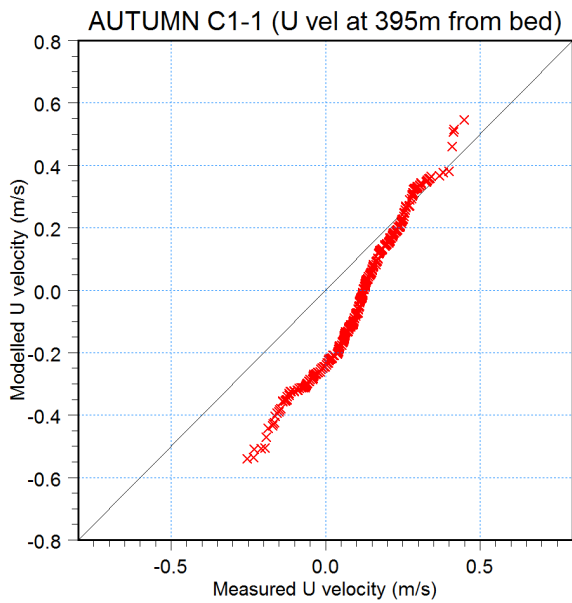
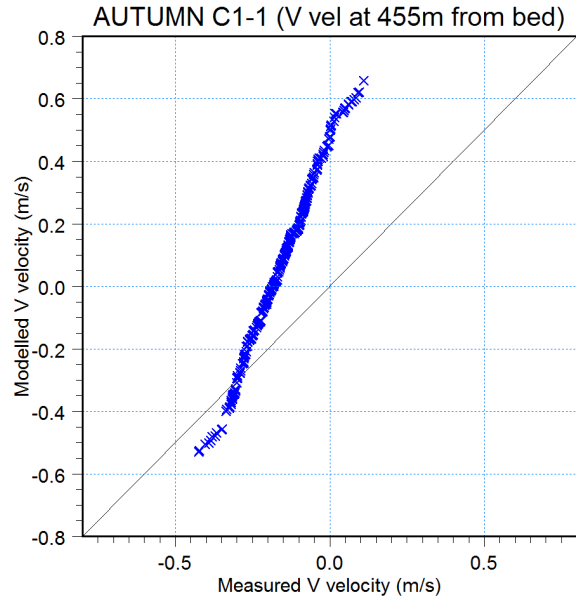
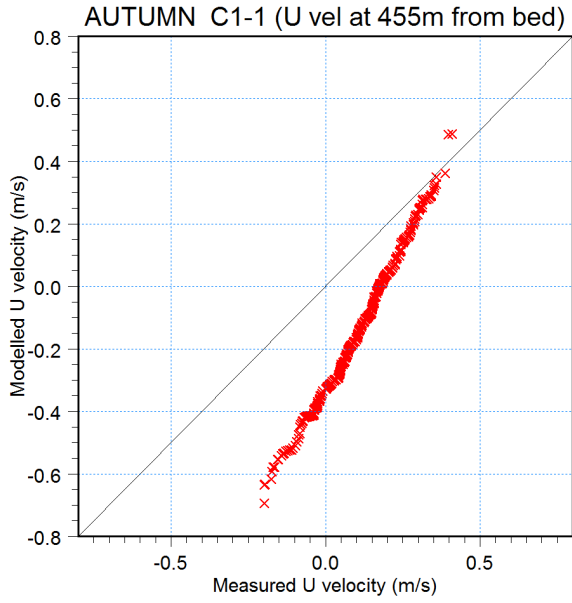
T at 455m × ×
T at 395m × ×
T at 2.6m × ×

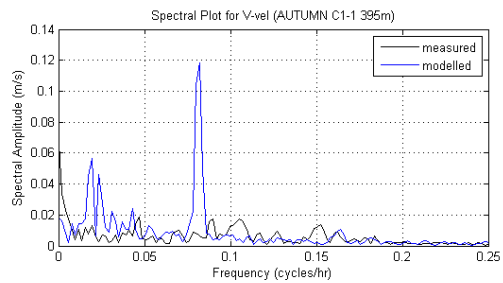
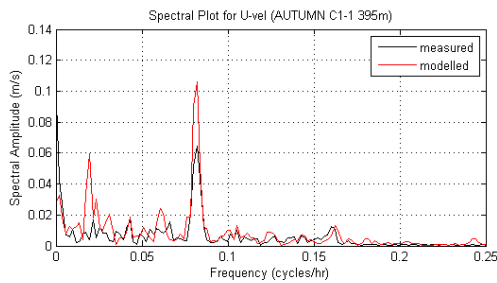
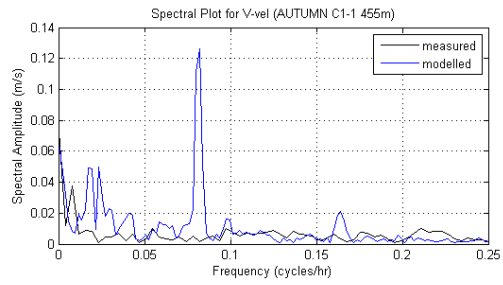
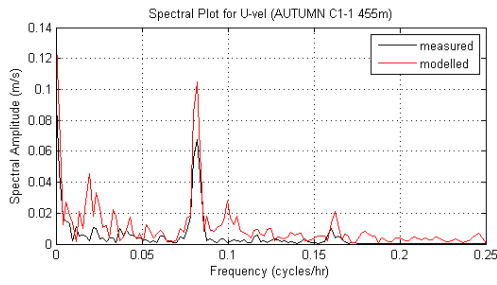
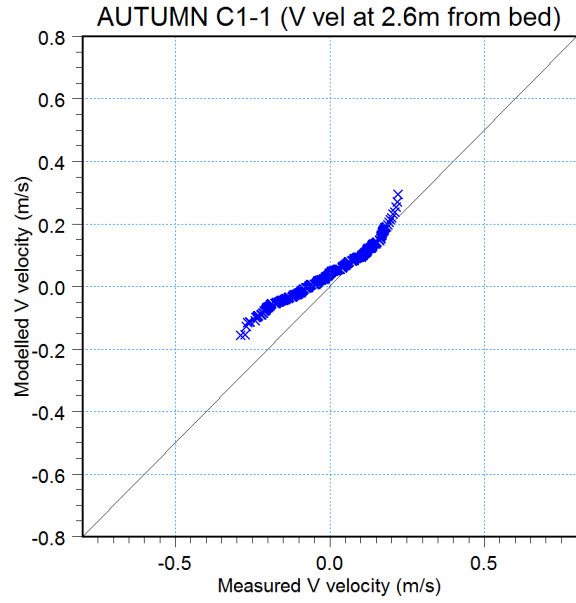
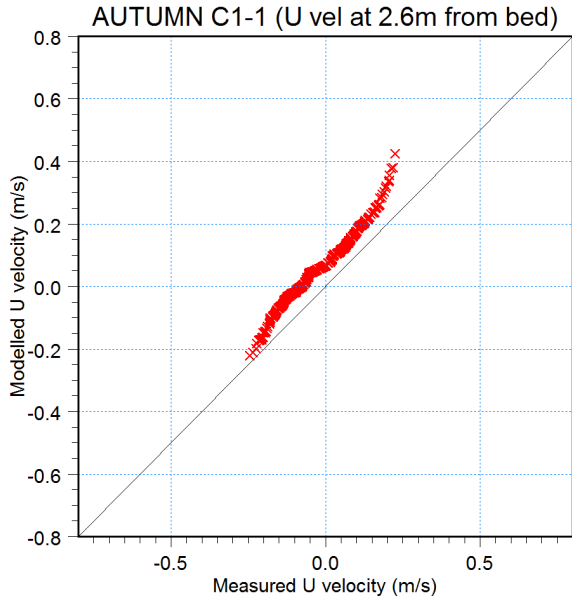


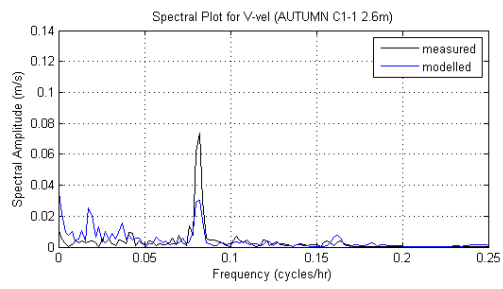
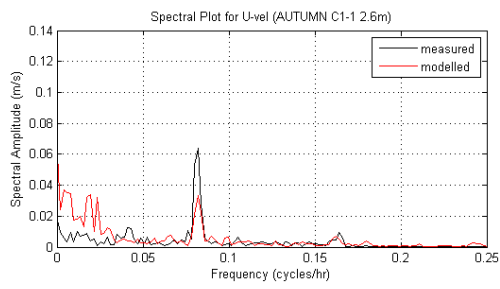










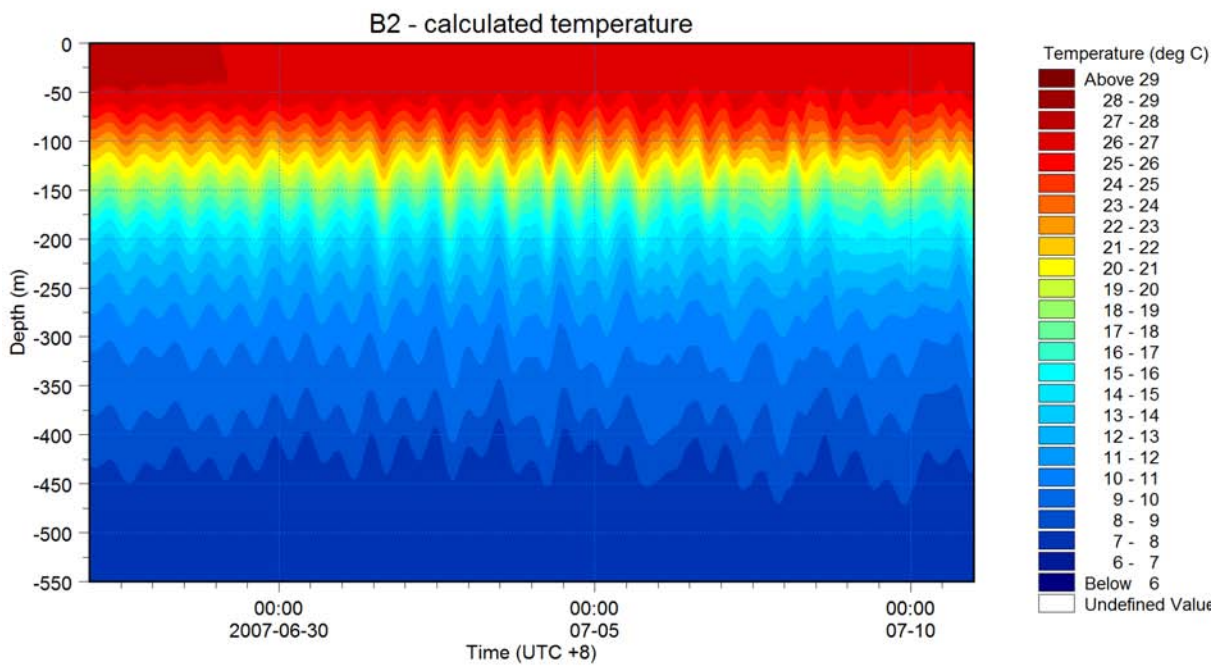
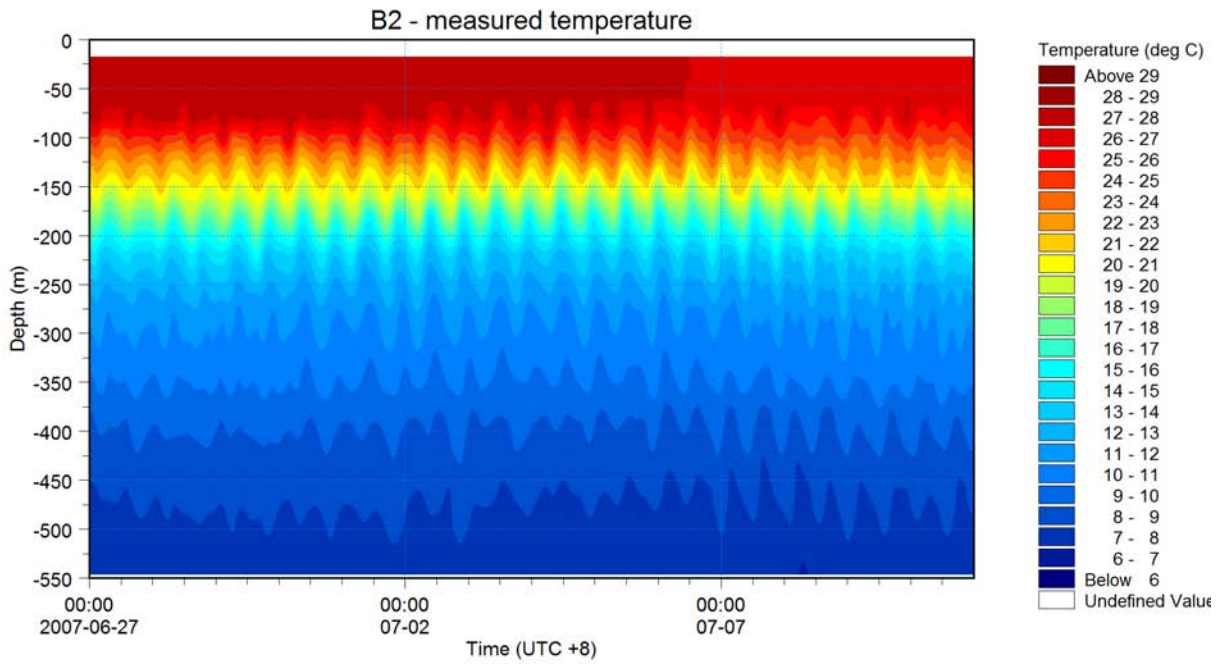




APPENDIX E

Summer Validation Period

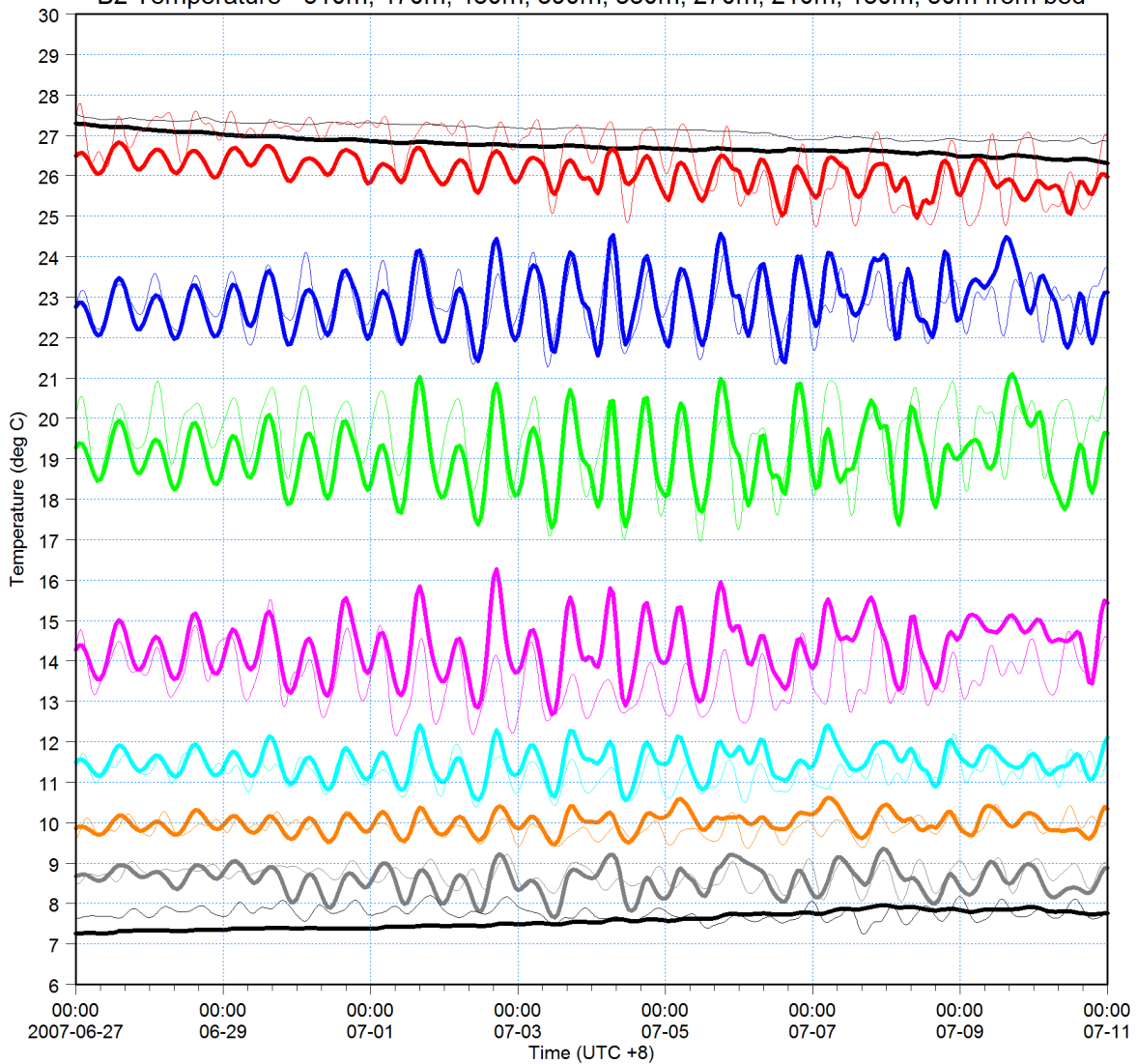
Comparisons between Measurements and Model Simulation as Isopleth Plots, Time Series Plots, Q-Q Plots and Frequency Plots





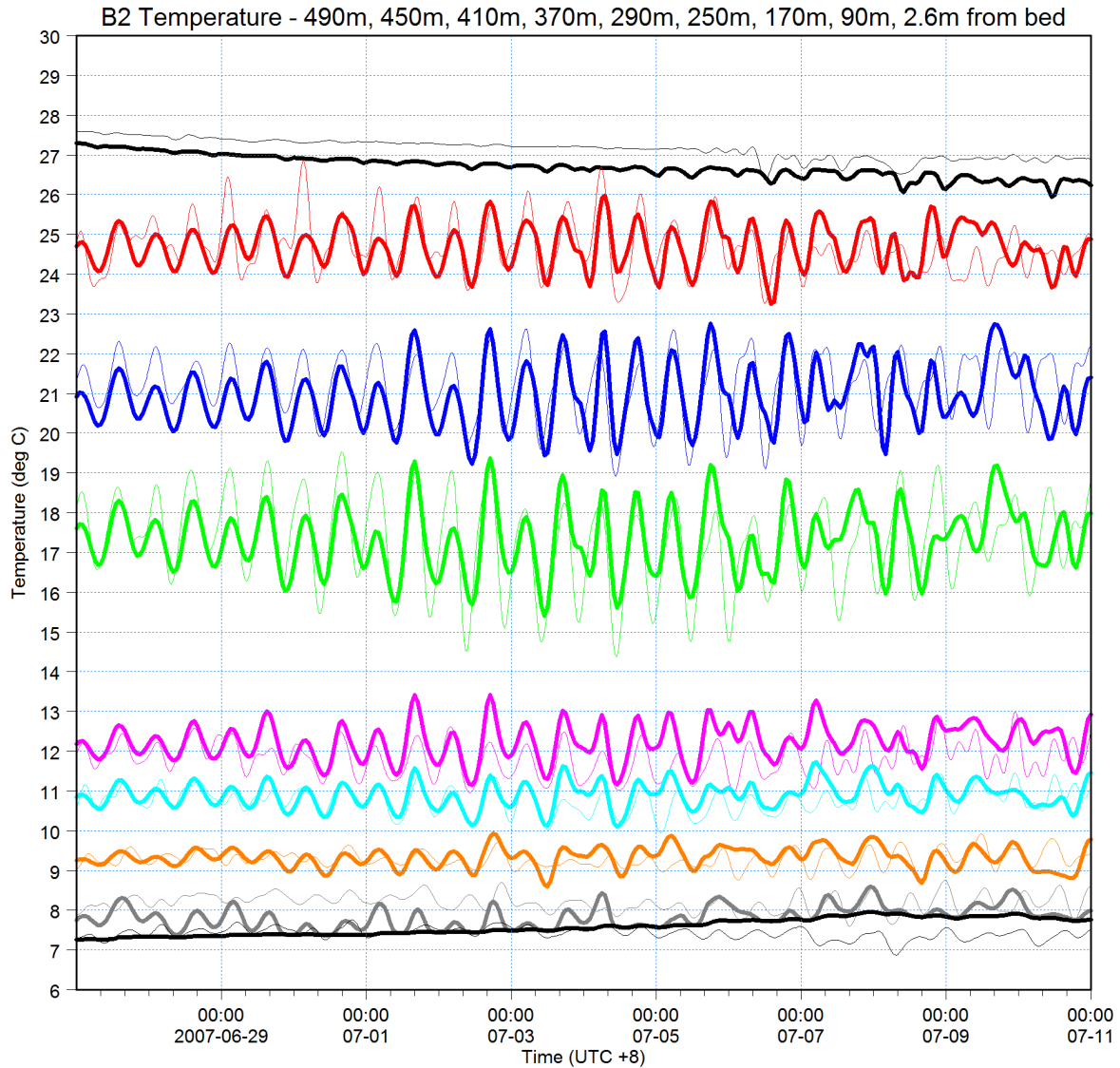
510m from bed: Temperature [C] [deg C] —
measured [deg C] —
470m from bed: Temperature [C] [deg C] —
measured [deg C] —
430m from bed: Temperature [C] [deg C] —
measured [deg C] —
390m from bed: Temperature [C] [deg C] —
measured [deg C] —
330m from bed: Temperature [C] [deg C] —
measured [deg C] —
270m from bed: Temperature [C] [deg C] —
measured [deg C] —
190m from bed: Temperature [C] [deg C] —
measured [deg C] —
130m from bed: Temperature [C] [deg C] —
measured [deg C] —
50m from bed: Temperature [C] [deg C] —
measured [deg C] —

B2 Temperature - 510m, 470m, 430m, 390m, 330m, 270m, 210m, 130m, 50m from bed



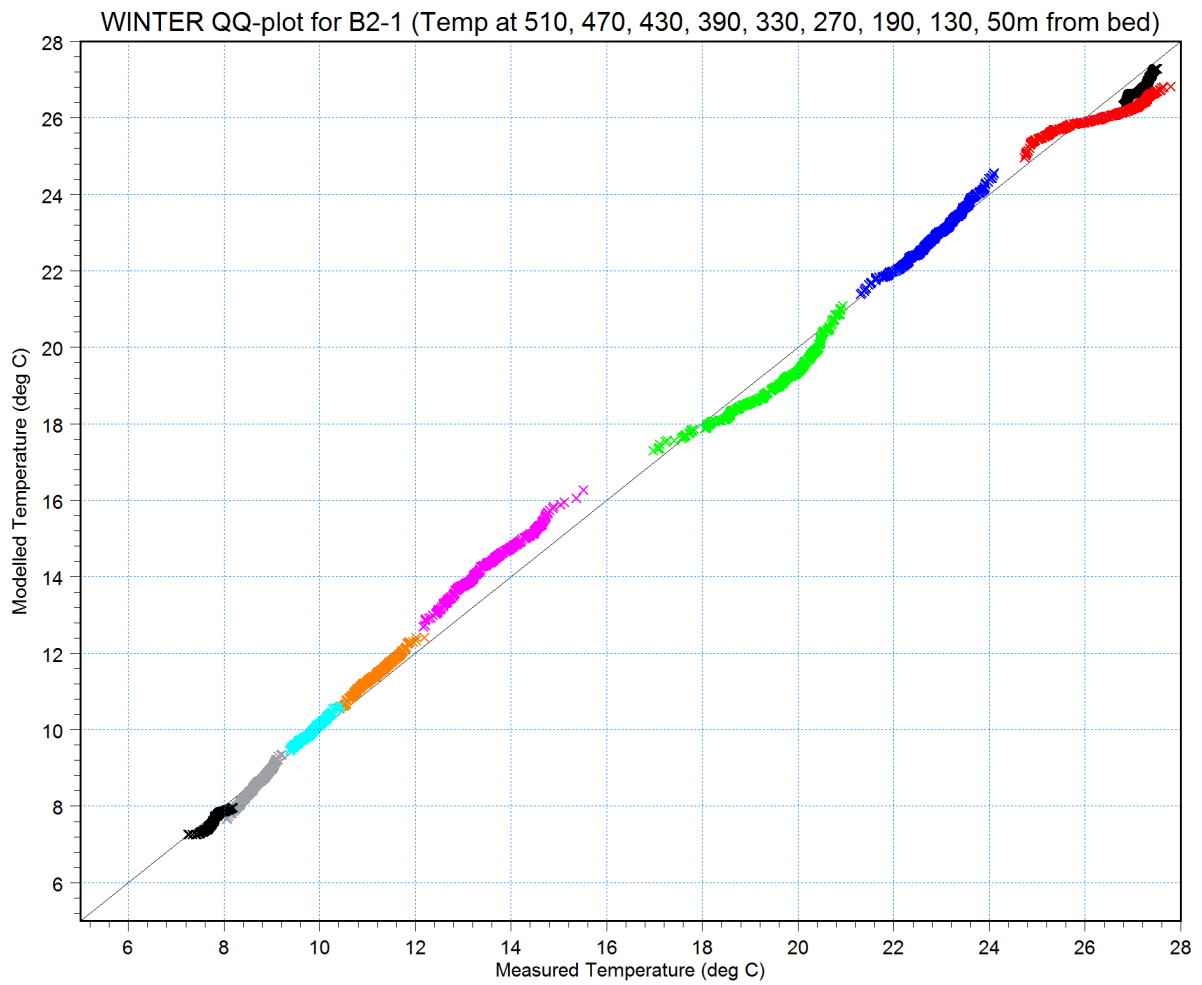


490m from bed: Temperature [C] [deg C] —
measured [deg C] —
450m from bed: Temperature [C] [deg C] —
measured [deg C] —
410m from bed: Temperature [C] [deg C] —
measured [deg C] —
370m from bed: Temperature [C] [deg C] —
measured [deg C] —
290m from bed: Temperature [C] [deg C] —
measured [deg C] —
250m from bed: Temperature [C] [deg C] —
measured [deg C] —
170m from bed: Temperature [C] [deg C] —
measured [deg C] —
130m from bed: Temperature [C] [deg C] —
measured [deg C] —
2.6m from bed: Temperature [C] [deg C] —
measured [deg C] —



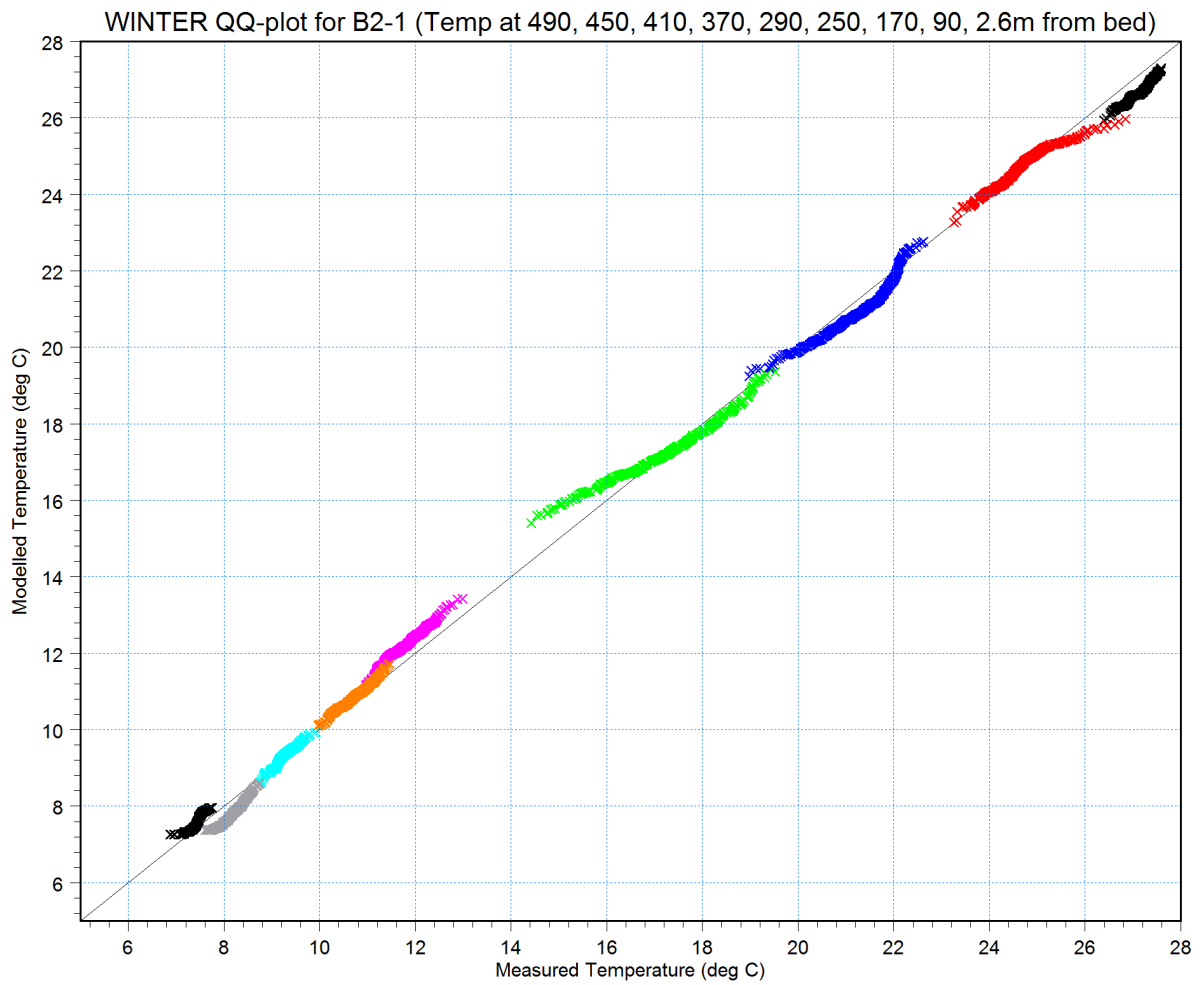


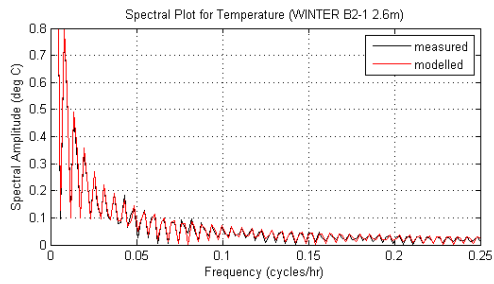
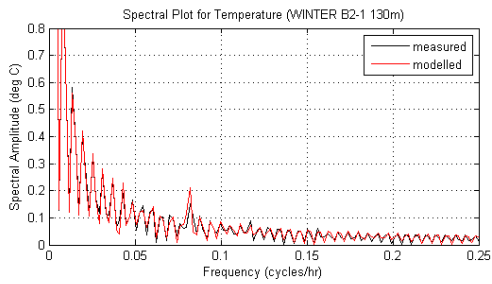
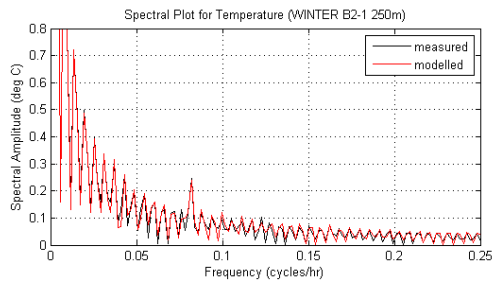
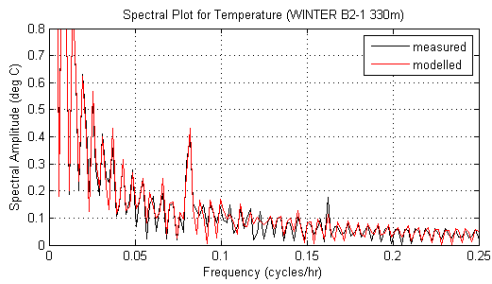
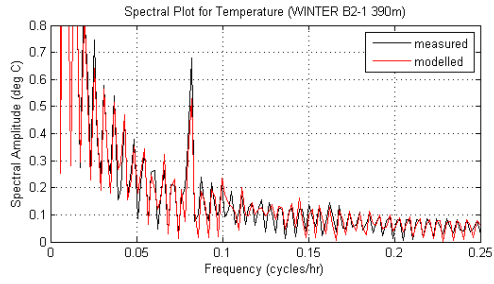
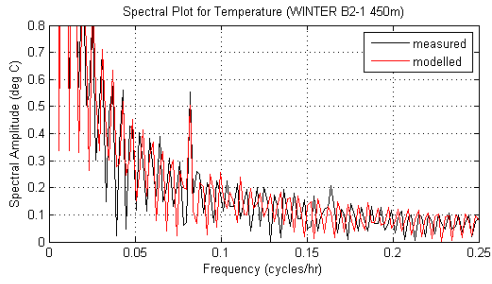
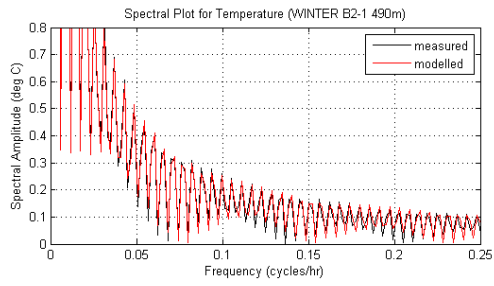
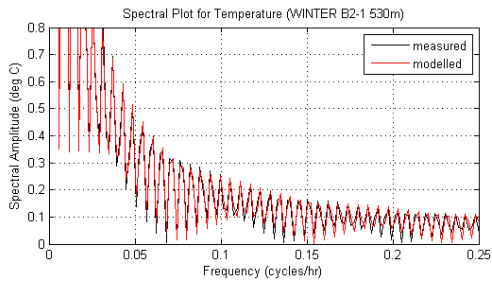
- T at 510m × ×
- T at 470m × ×
- T at 430m × ×
- T at 390m × ×
- T at 330m × ×
- T at 270m × ×
- T at 190m × ×
- T at 130m × ×
- T at 50m × ×

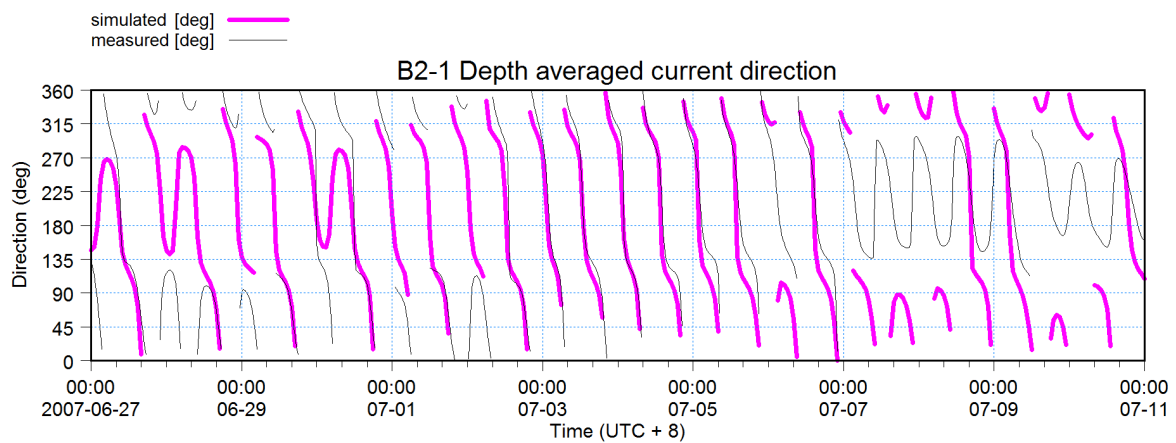
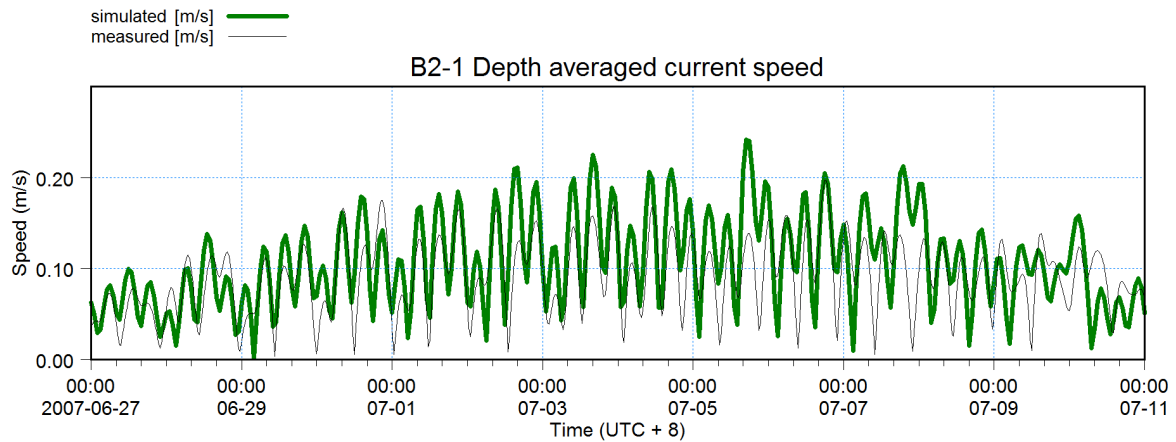
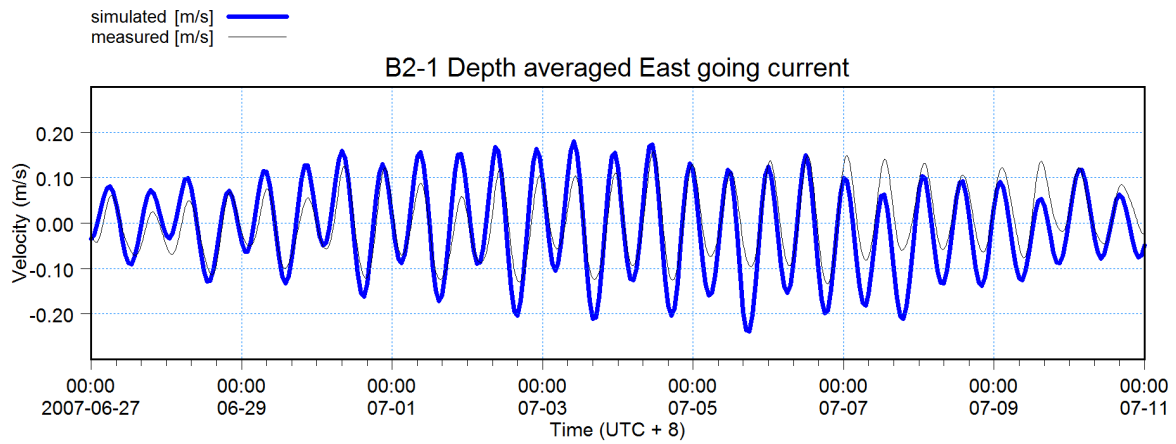
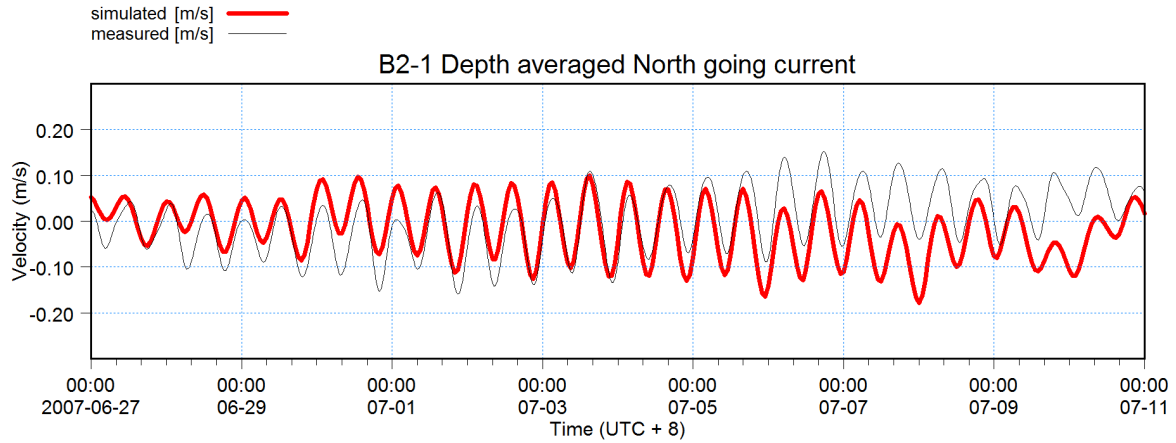




- T at 490m × ×
- T at 450m × ×
- T at 410m × ×
- T at 370m × ×
- T at 290m × ×
- T at 250m × ×
- T at 170m × ×
- T at 90m × ×
- T at 2.6m × ×

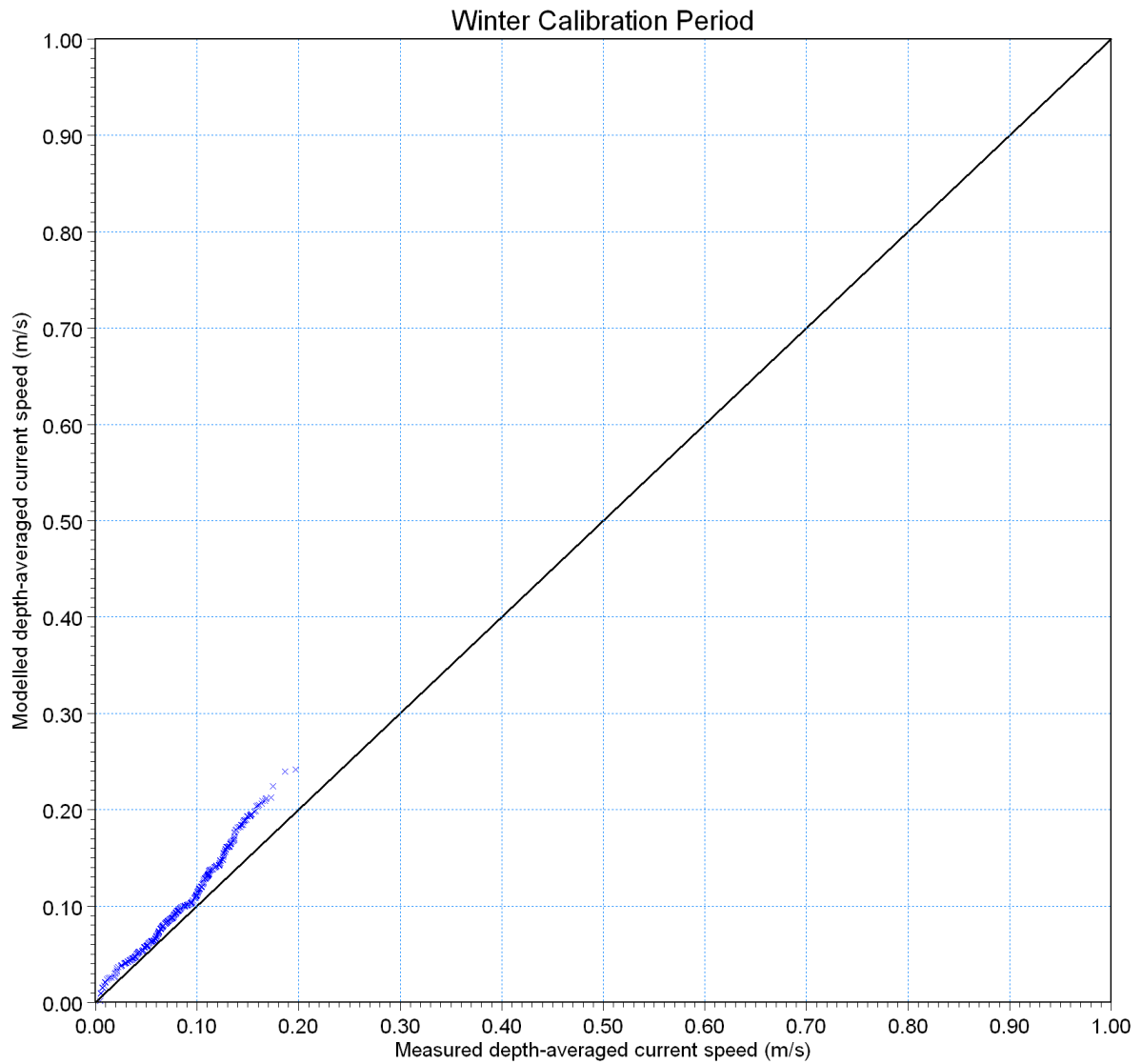


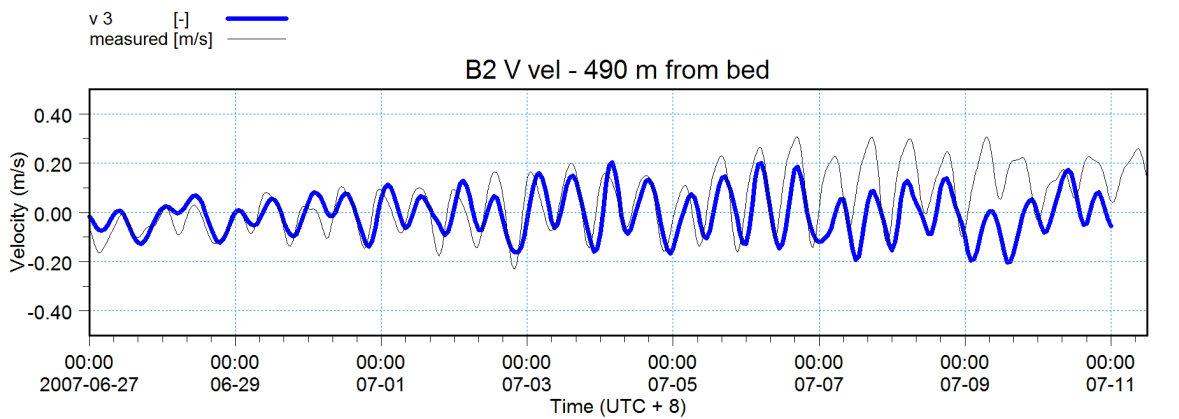
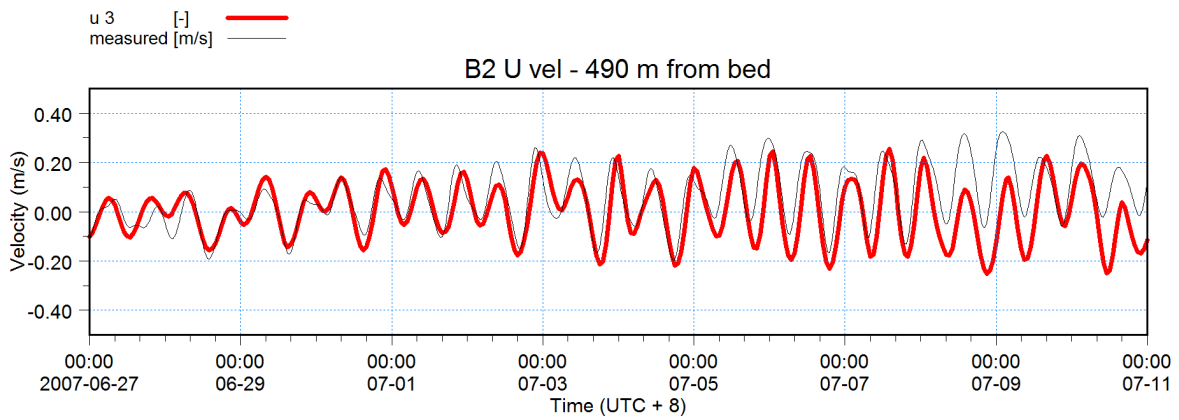
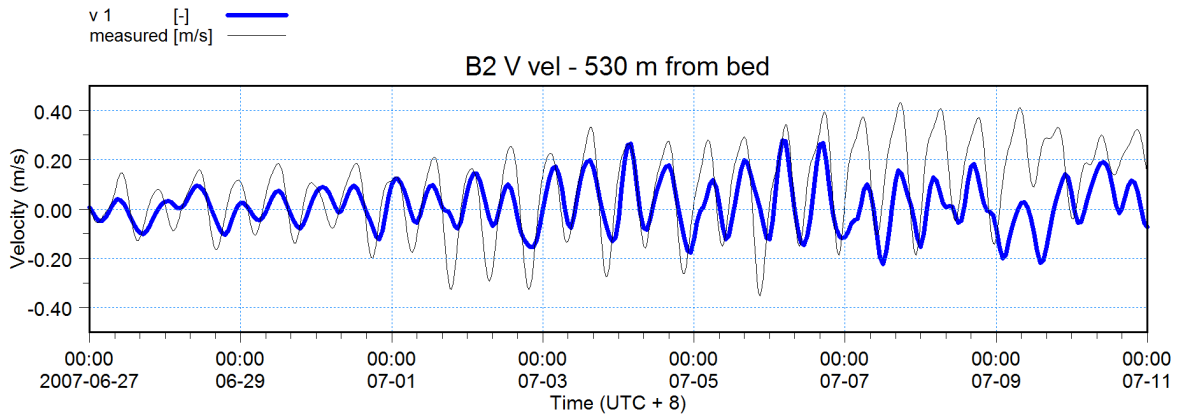
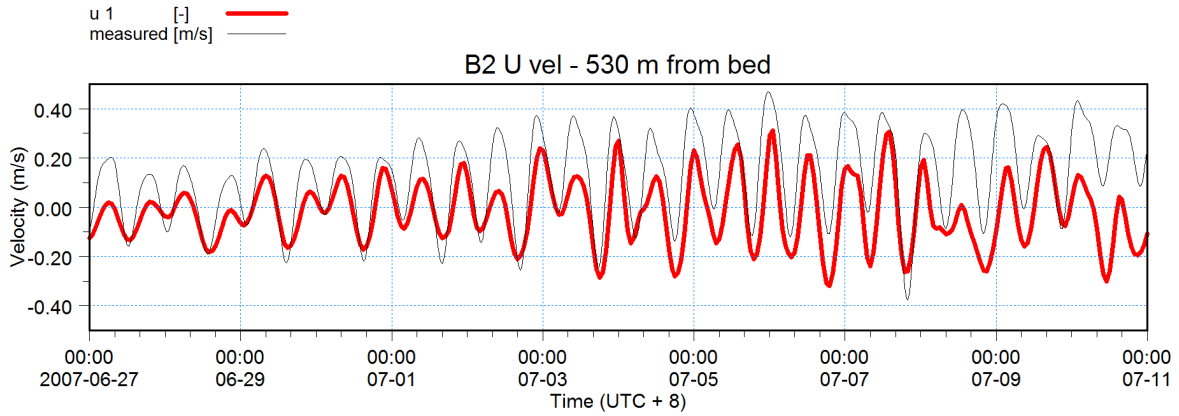


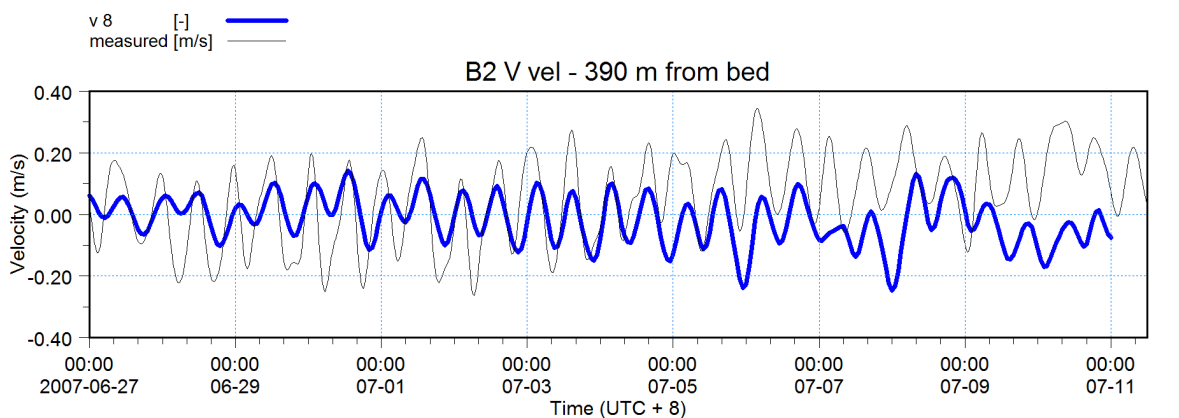
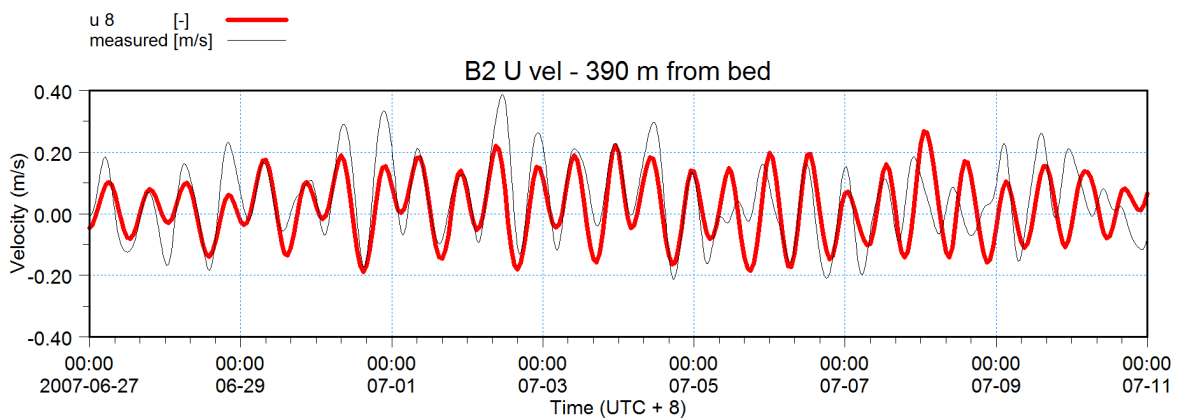
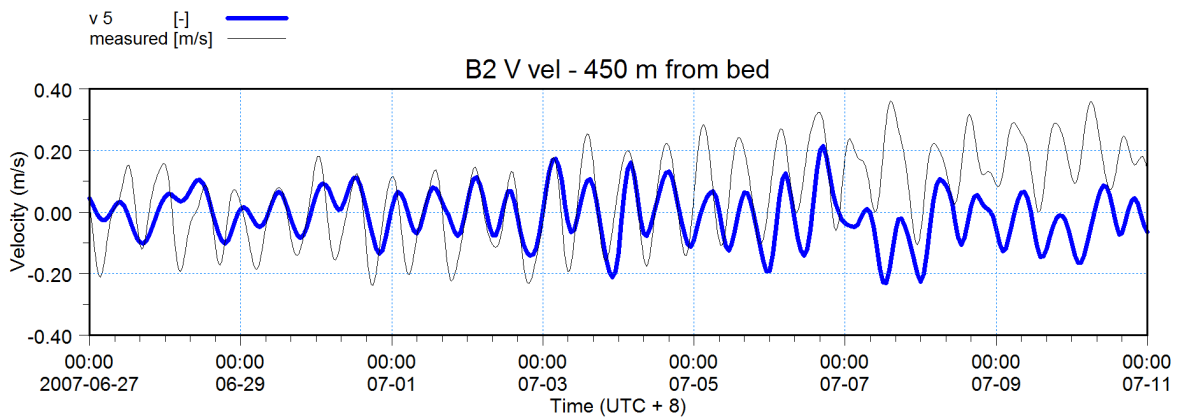
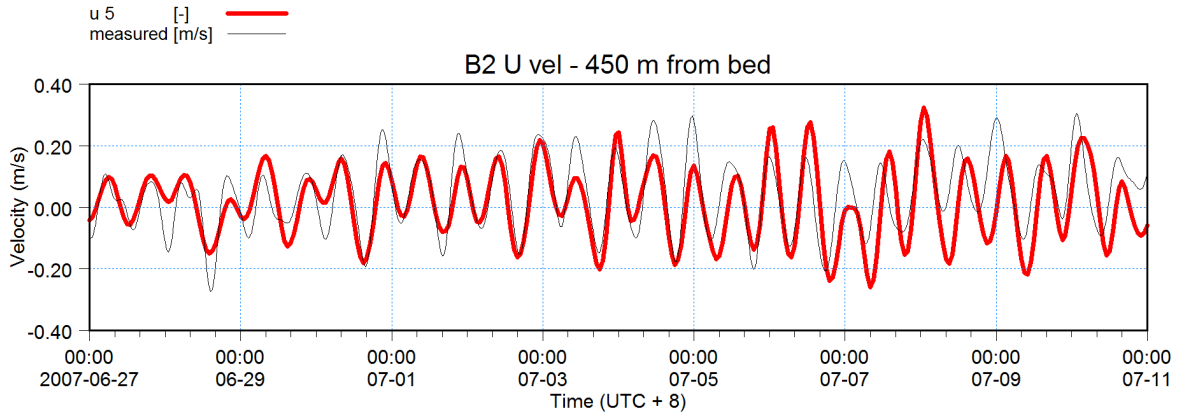


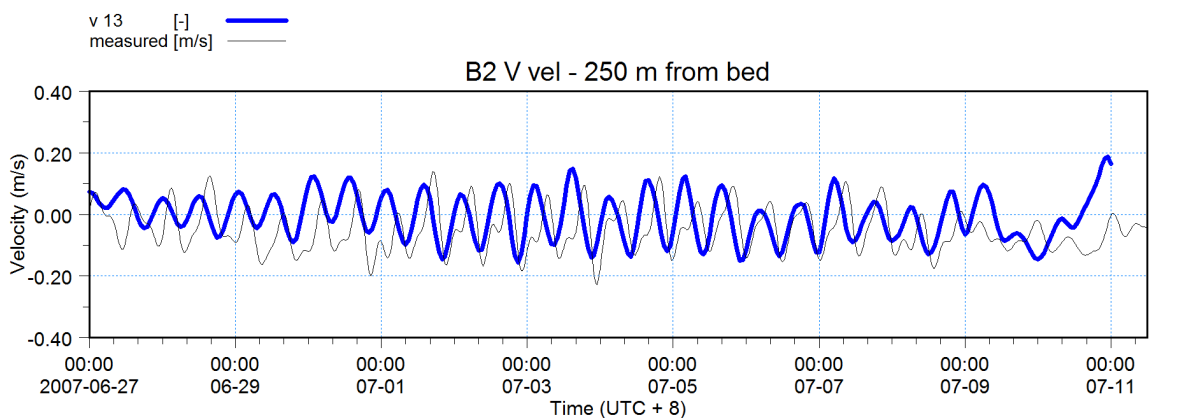
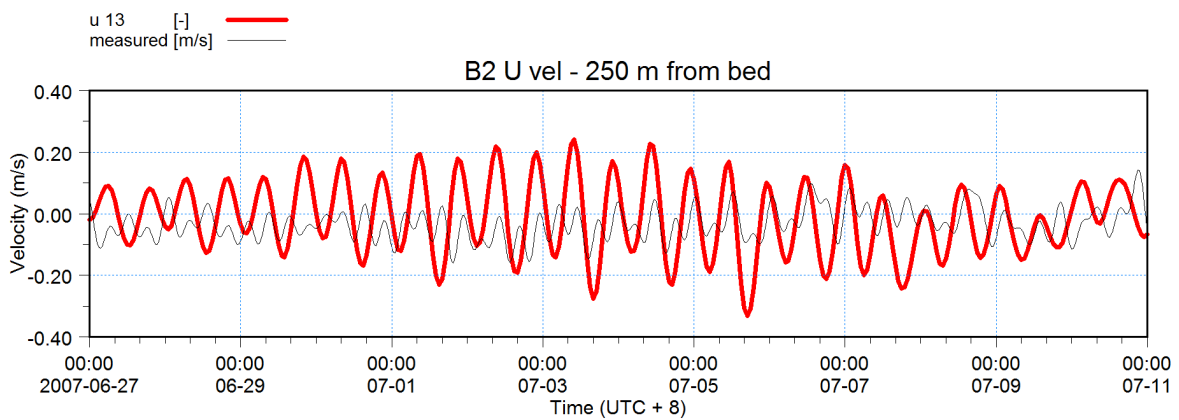
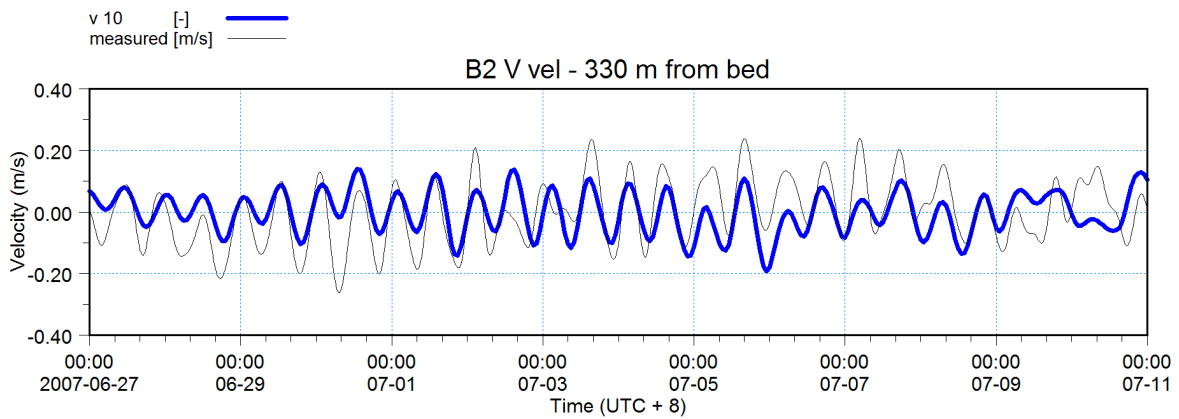
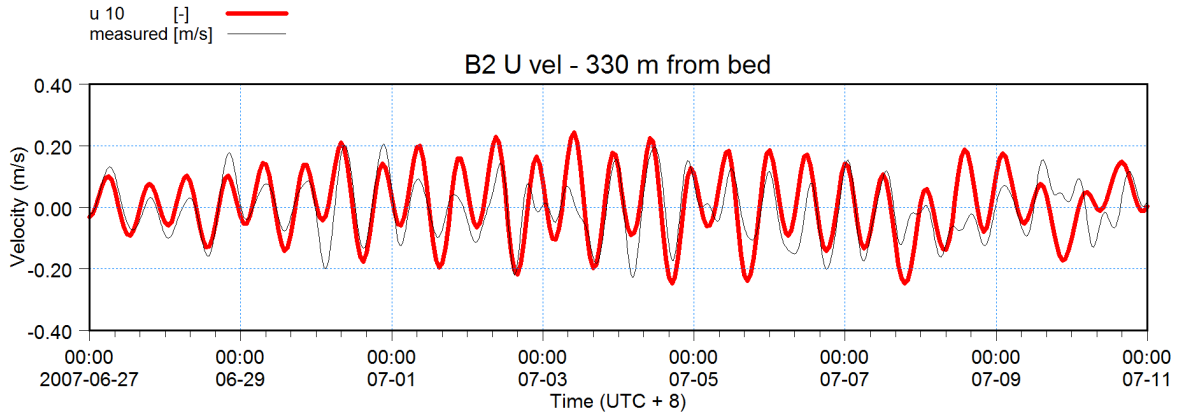


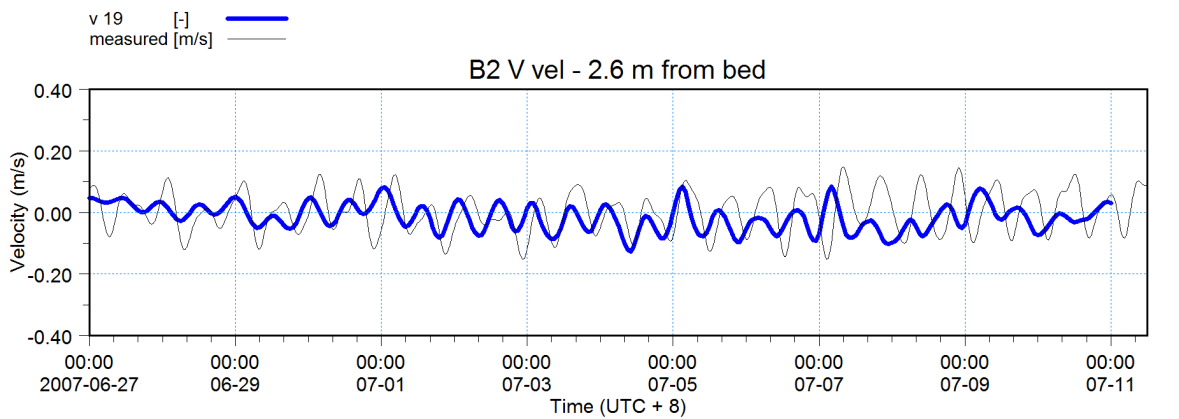
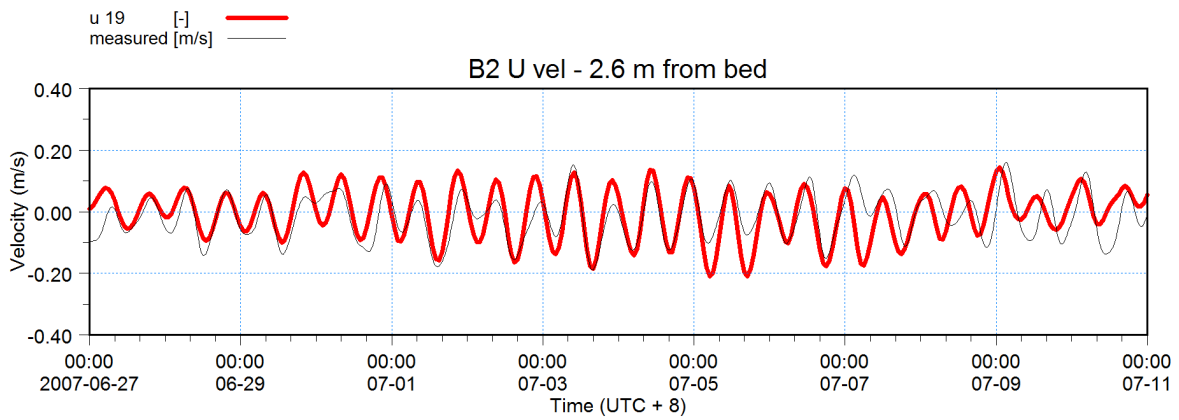
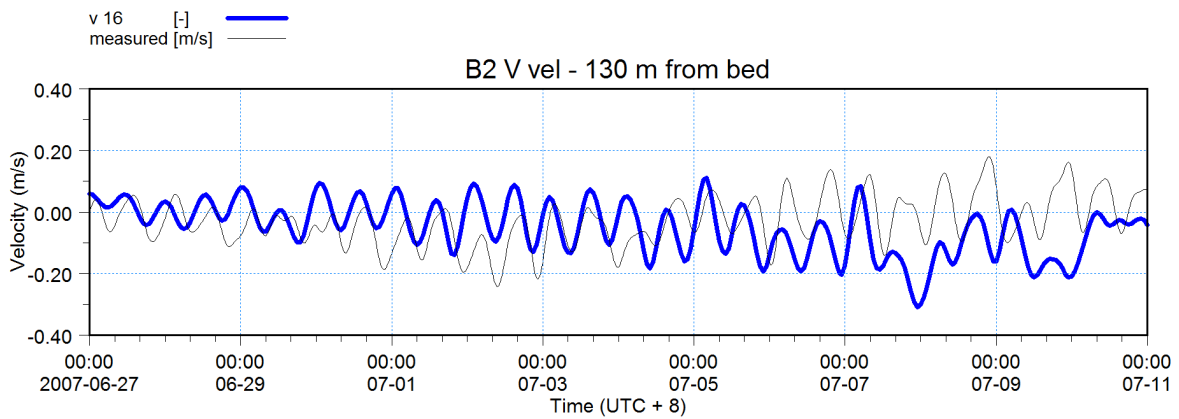
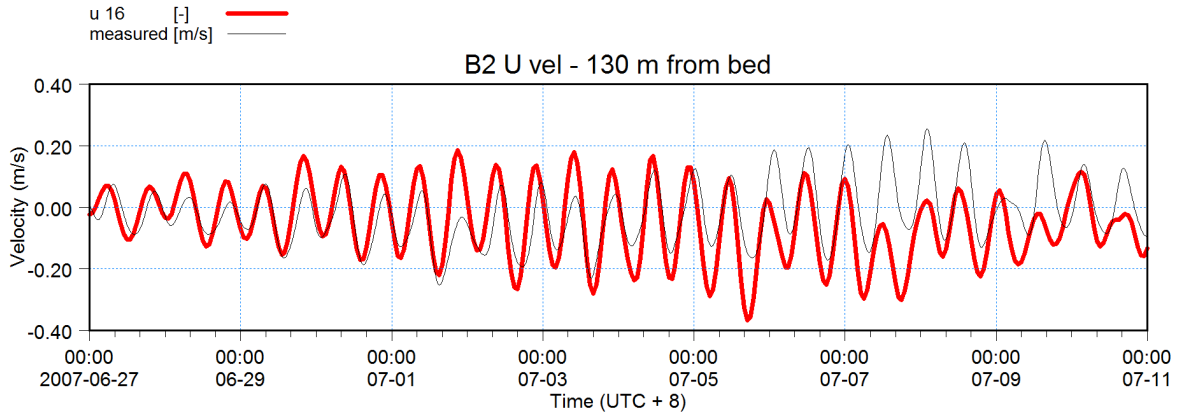
B2 × ×

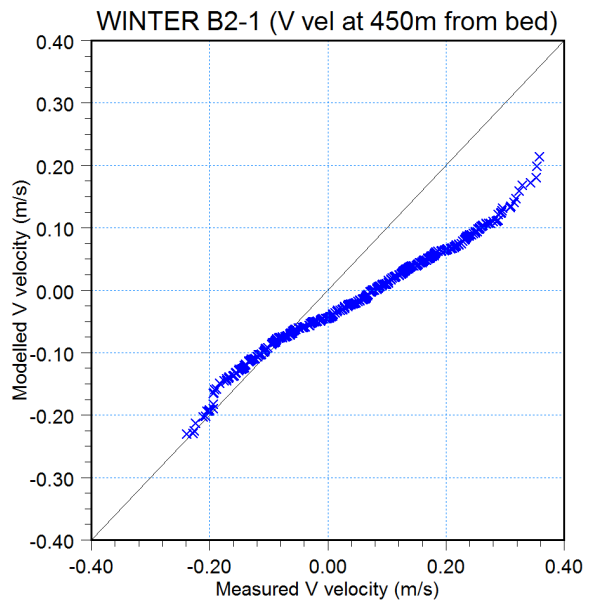
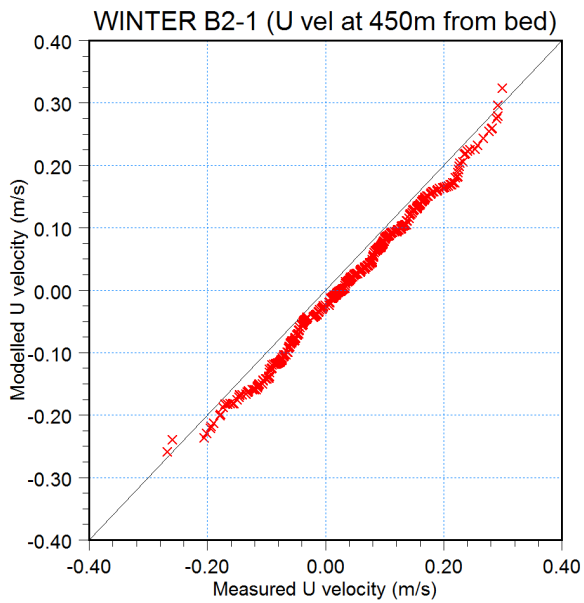
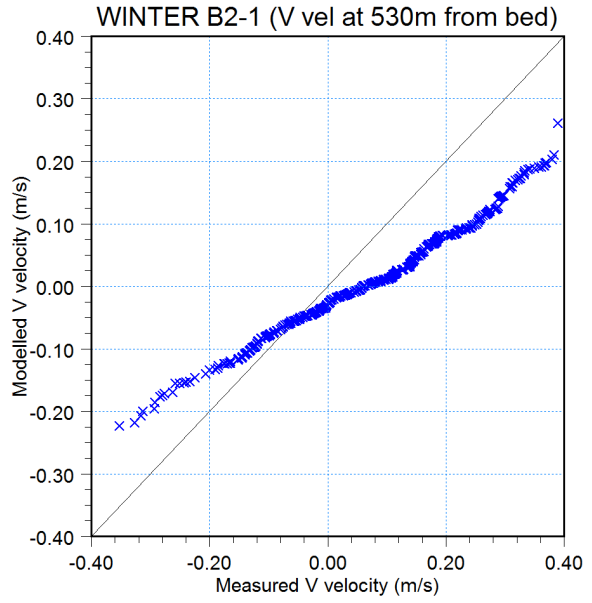
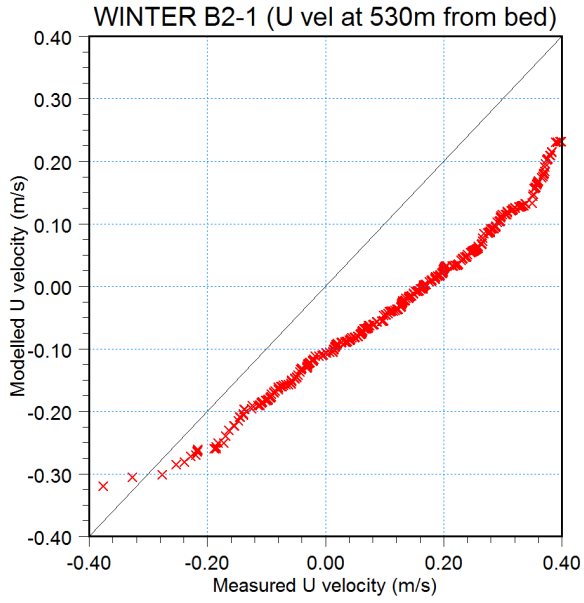


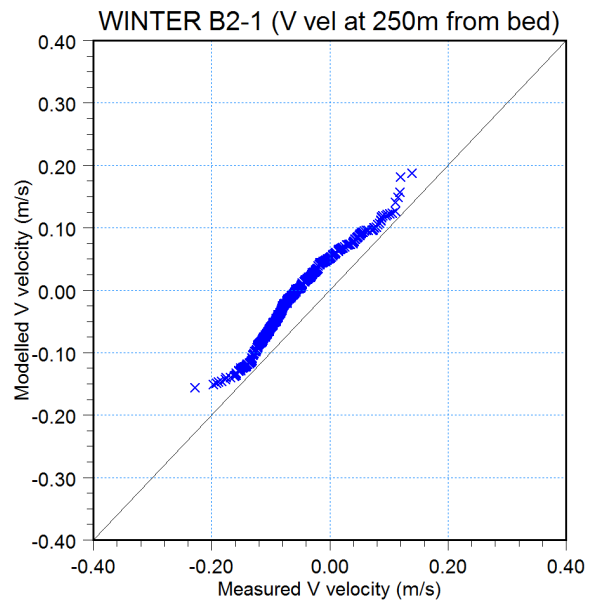
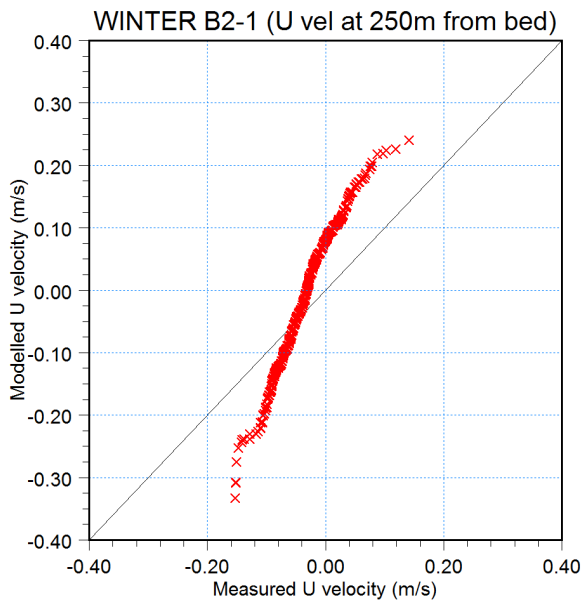
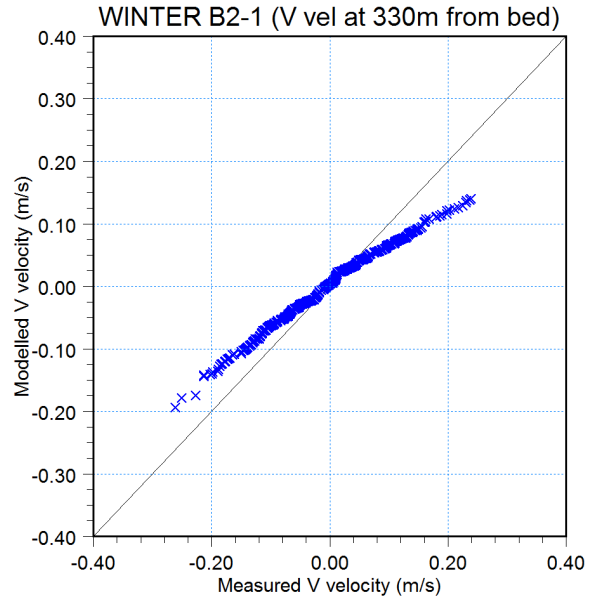
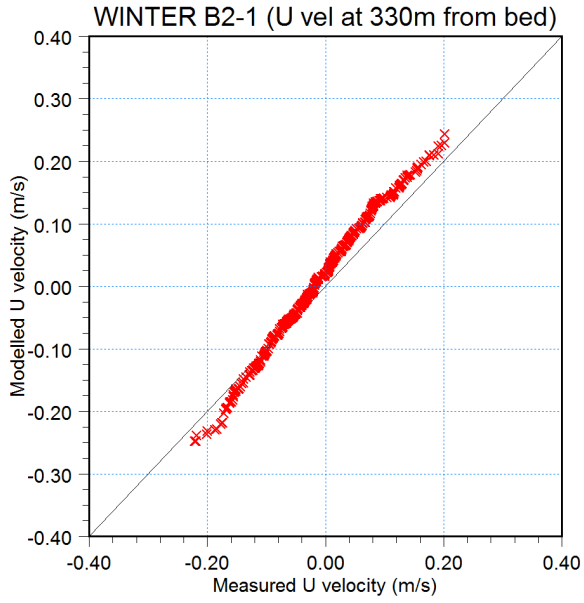


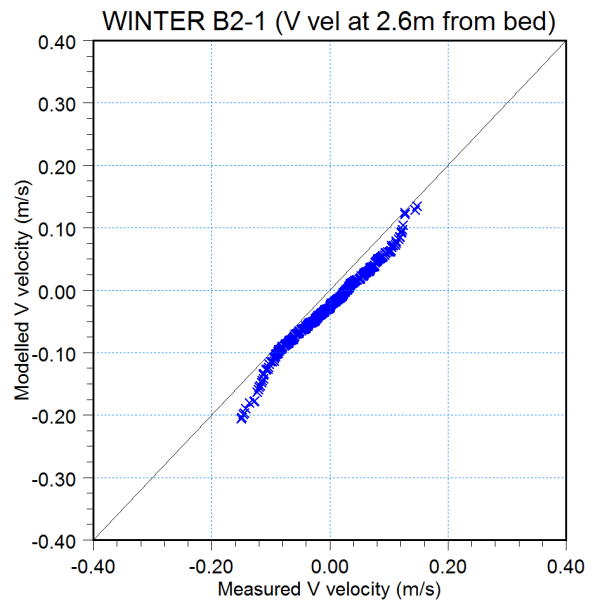
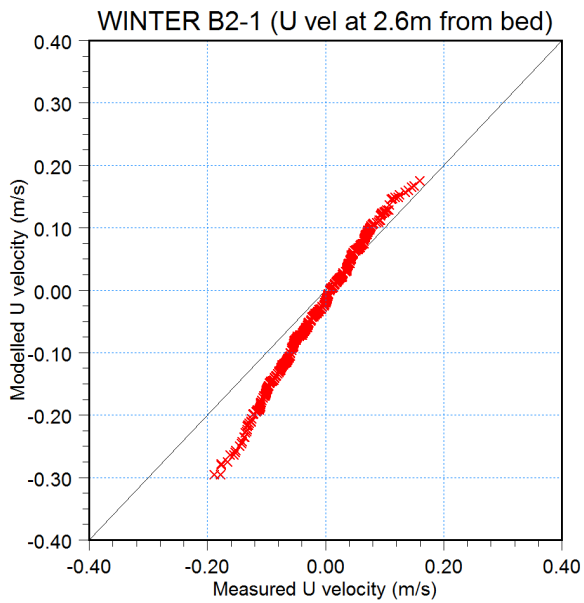
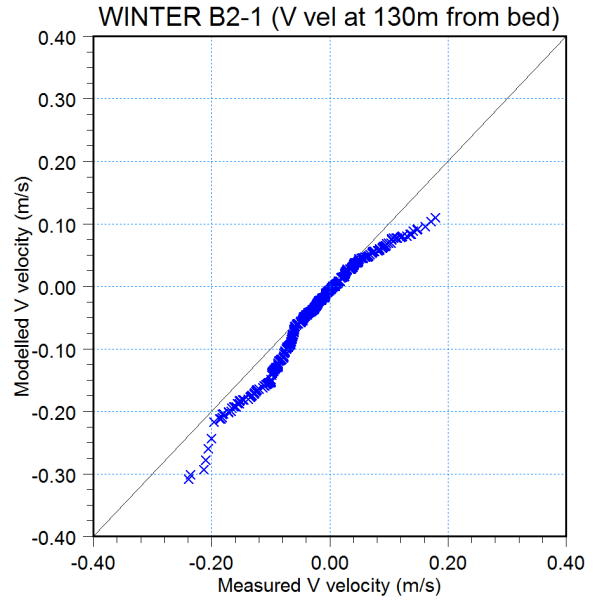
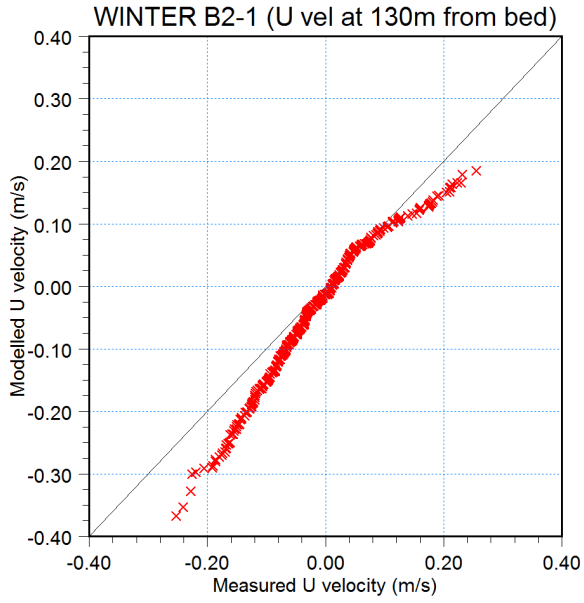


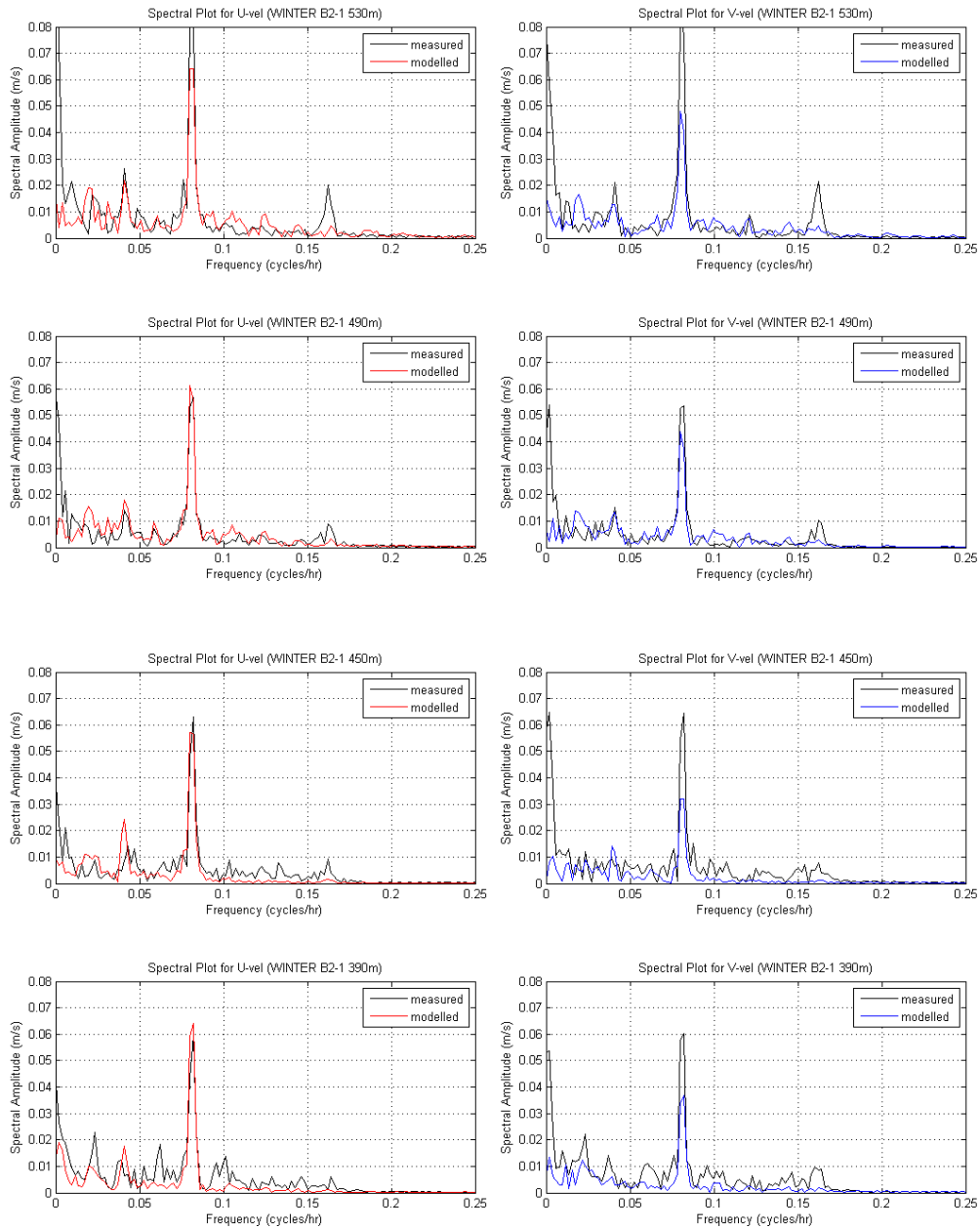


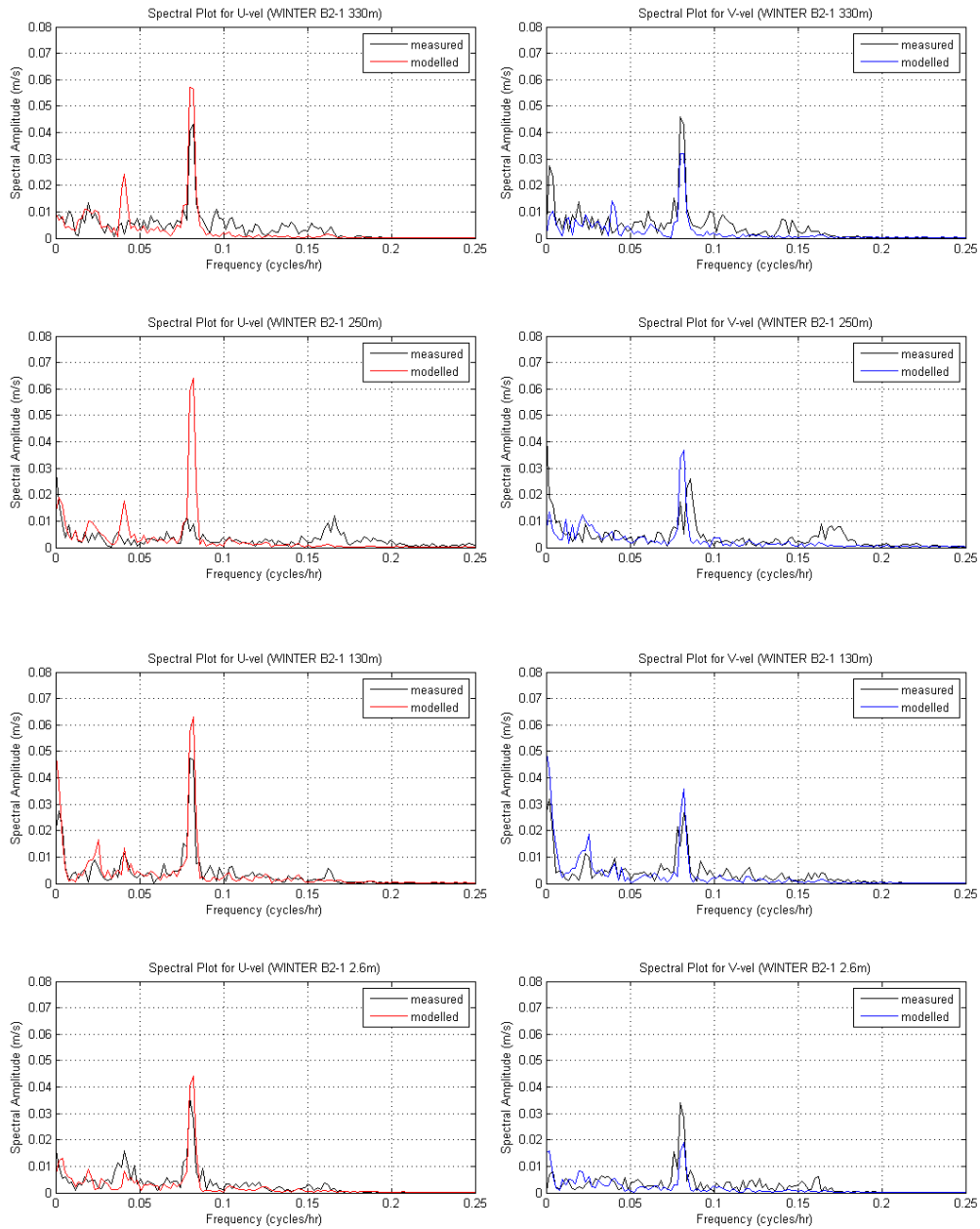








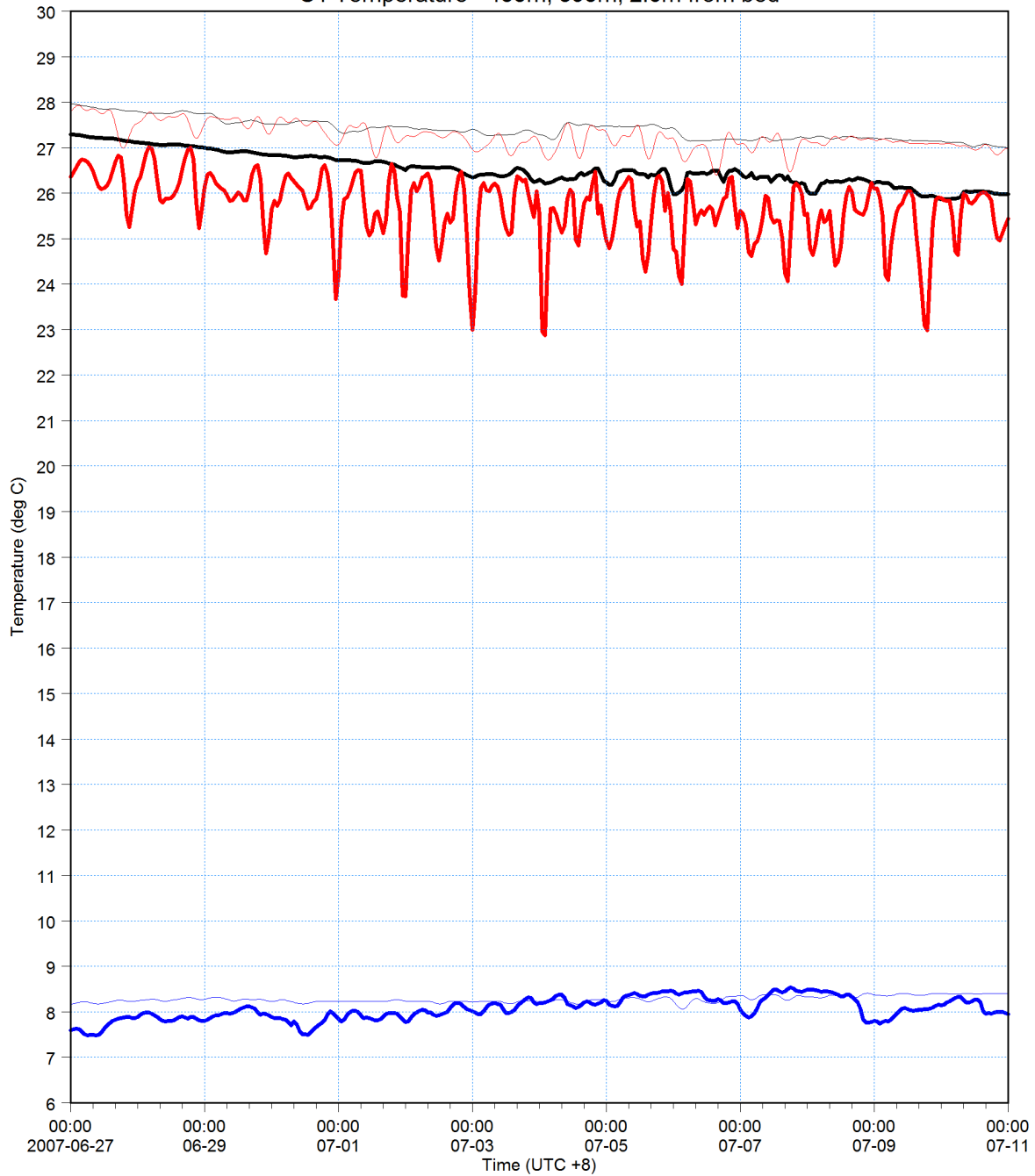






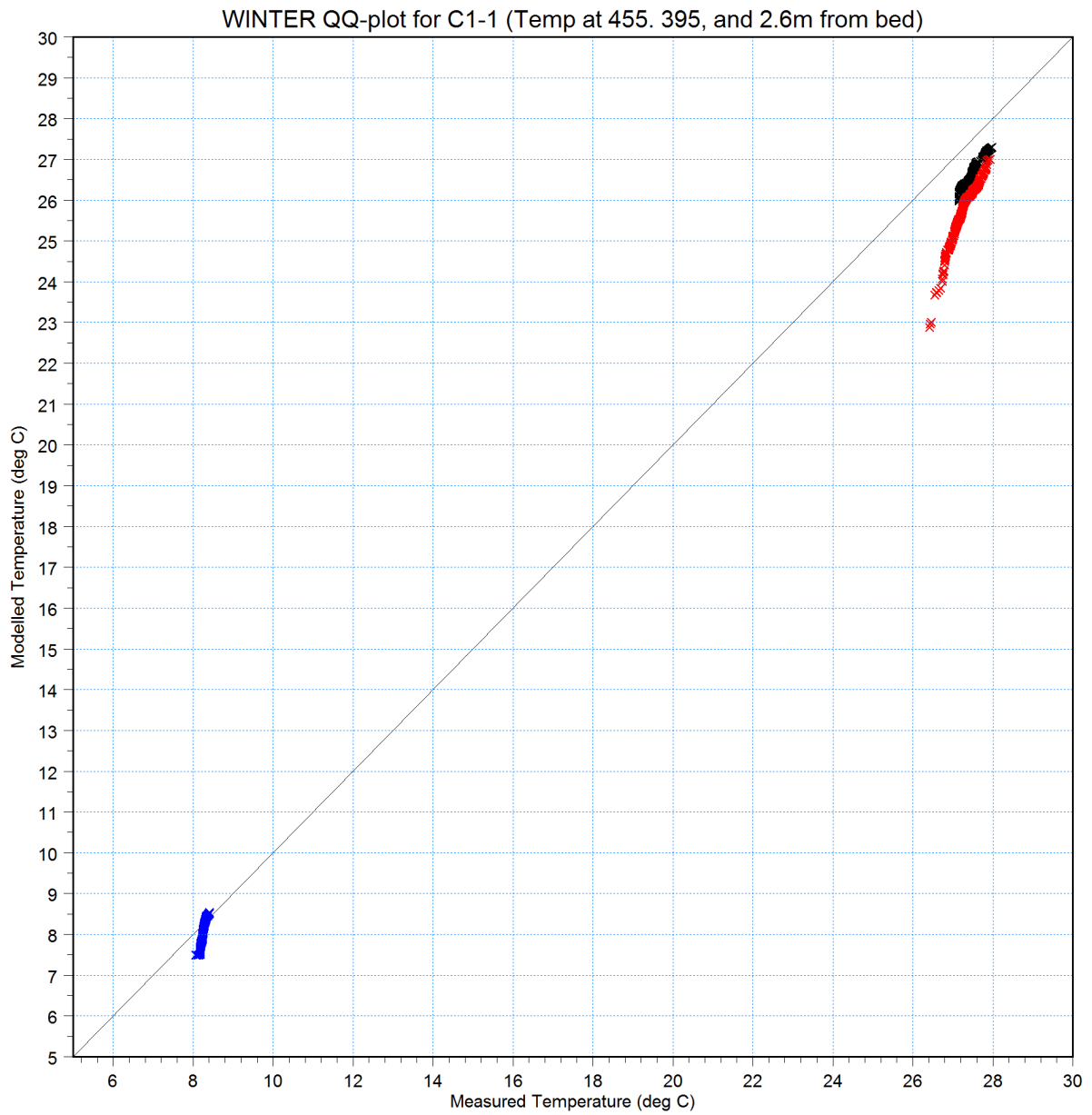
455m from bed: Temperature [C] [deg C] ———
measured [deg C] ———
395m from bed: Temperature [C] [deg C] ———
measured [deg C] ———
2.6m from bed: Temperature [C] [deg C] ———
measured [deg C] ———

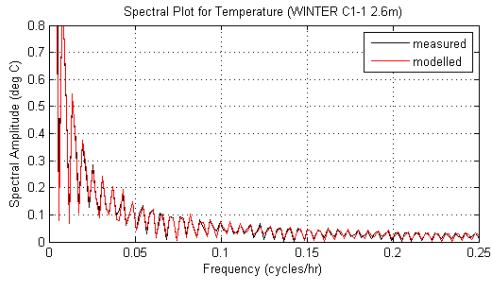
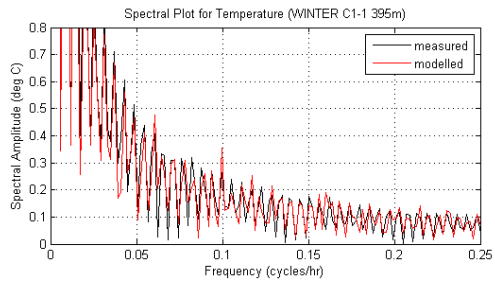
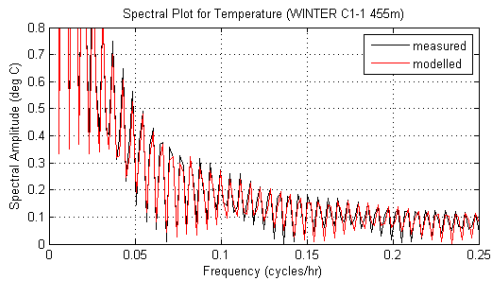
C1 Temperature - 455m, 395m, 2.6m from bed

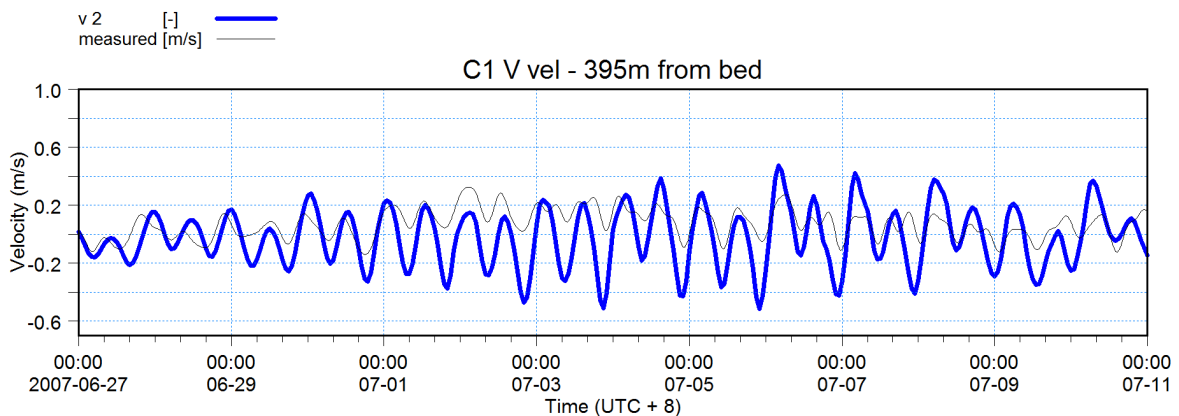
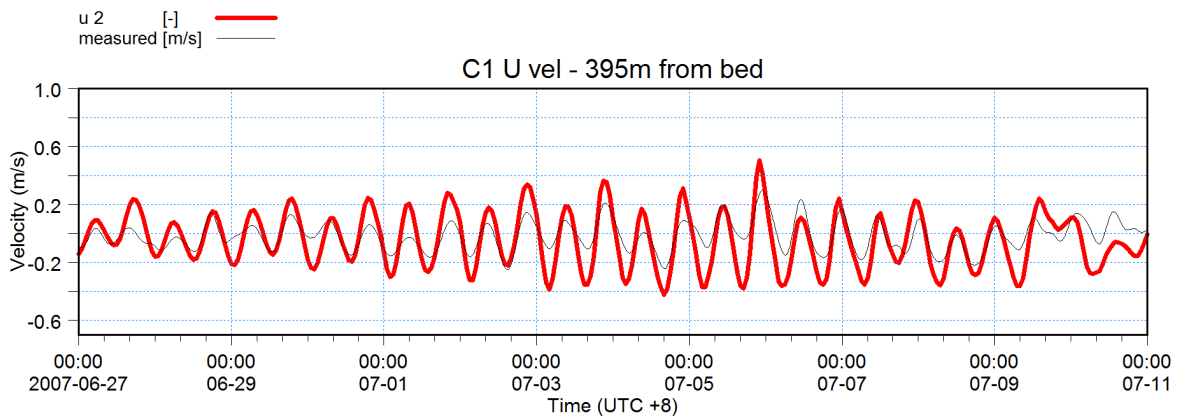
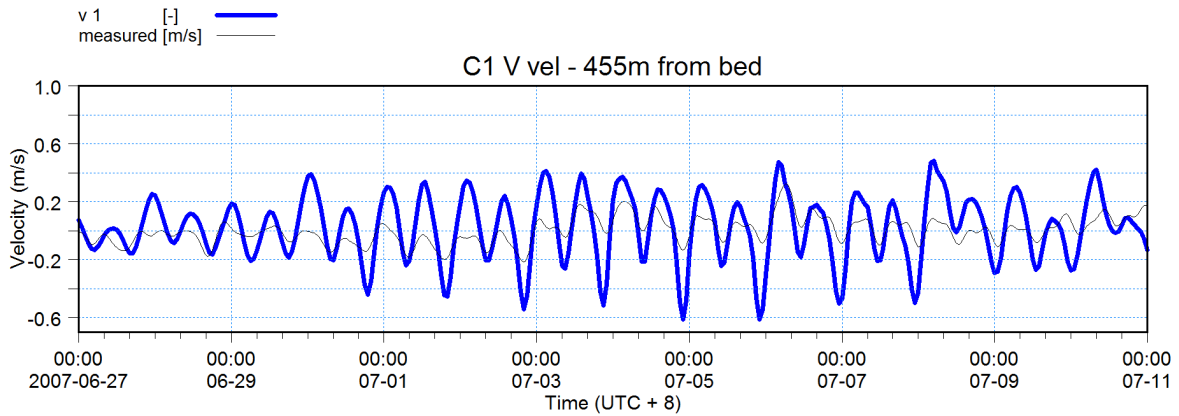
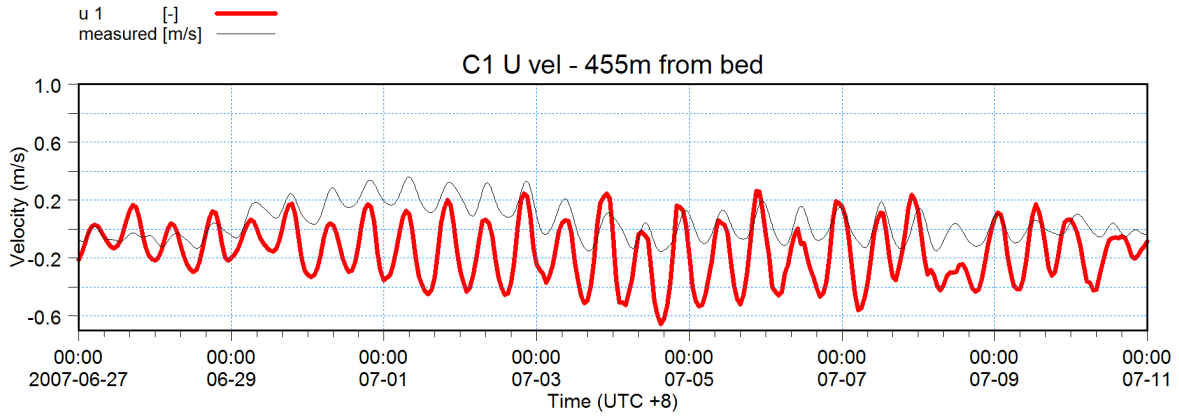


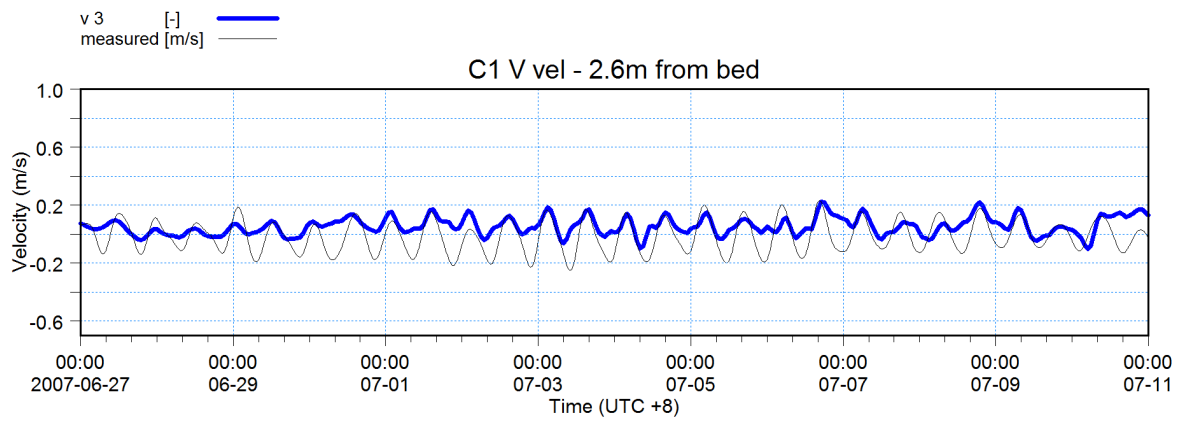
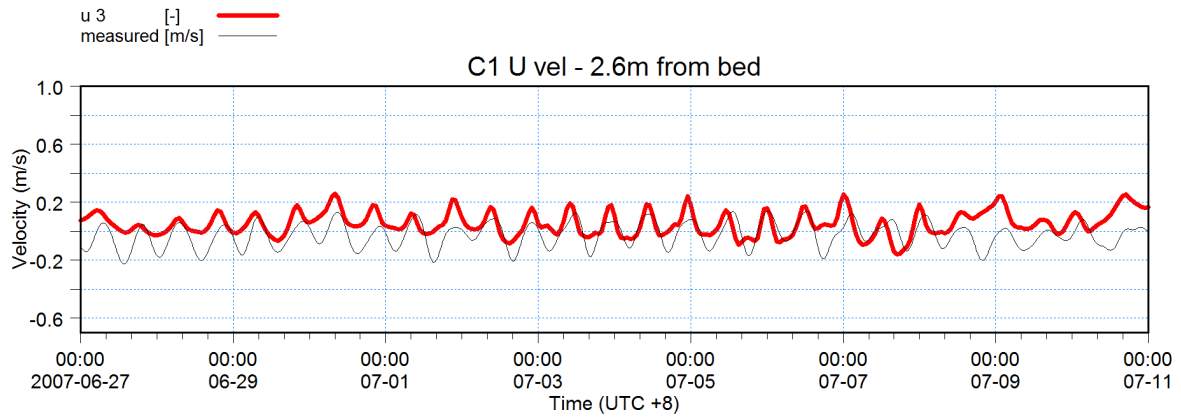


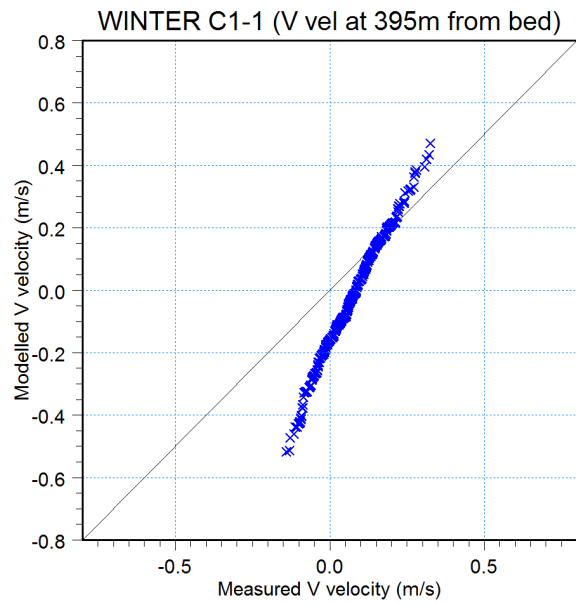
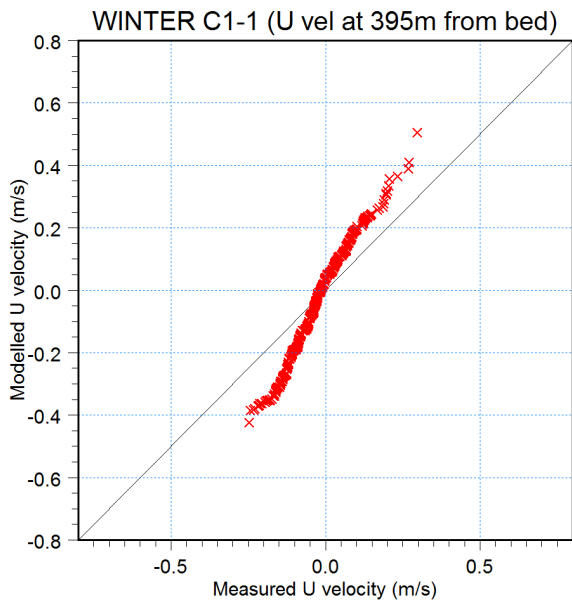
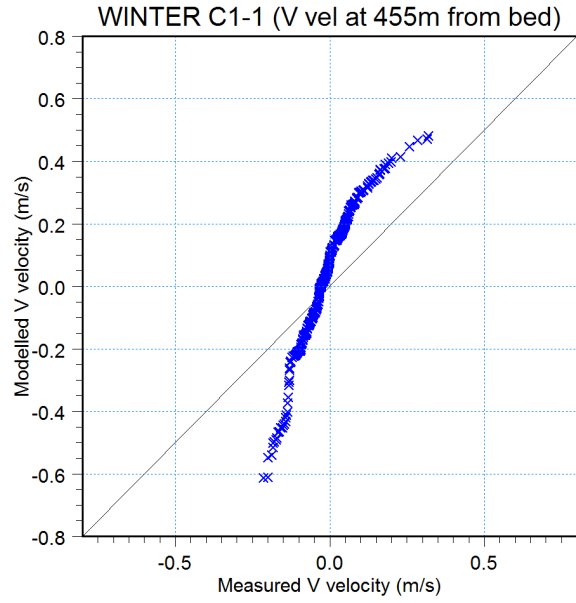
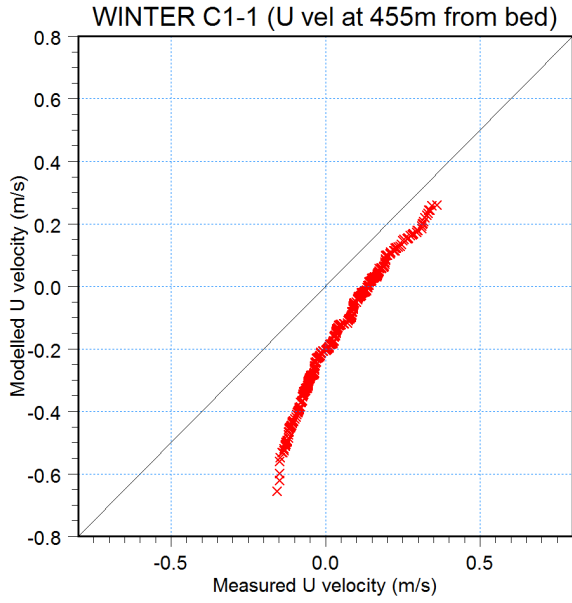
T at 455m × ×
T at 395m × ×
T at 2.6m × ×

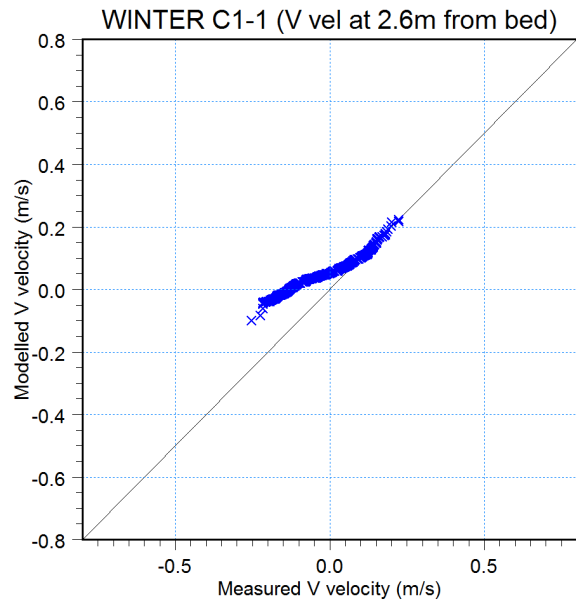
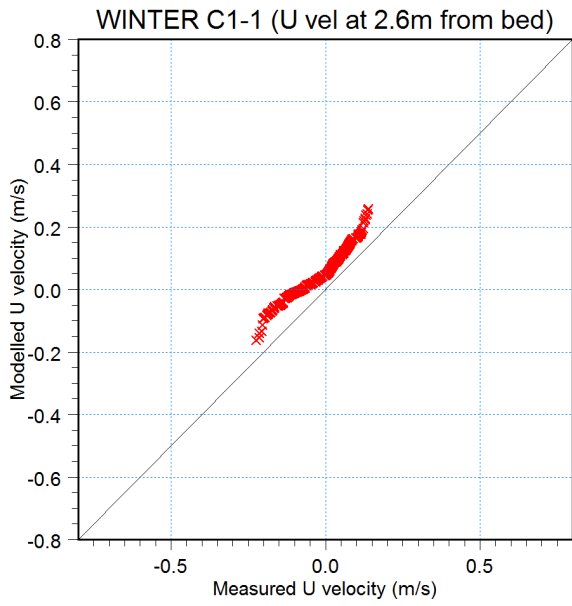


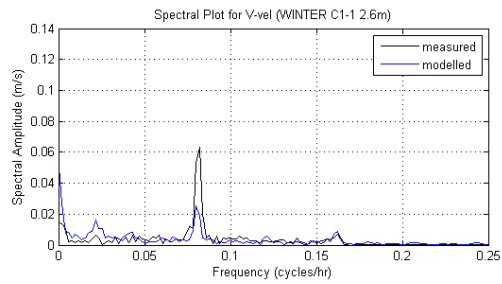
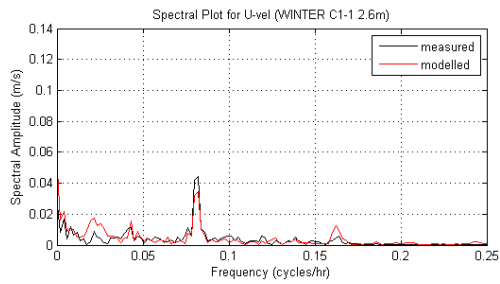
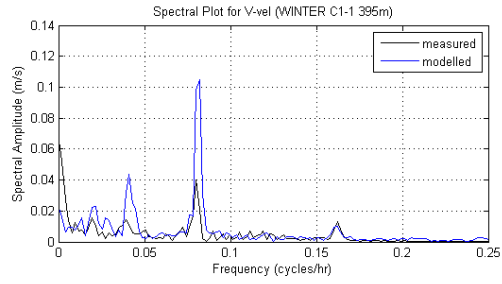
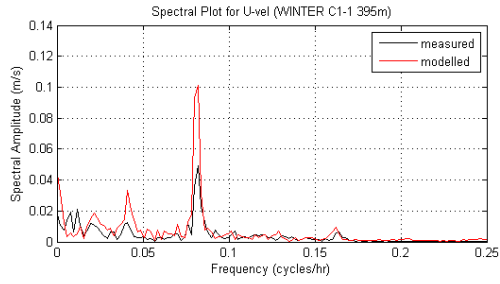
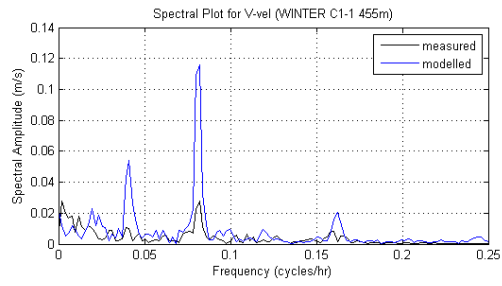
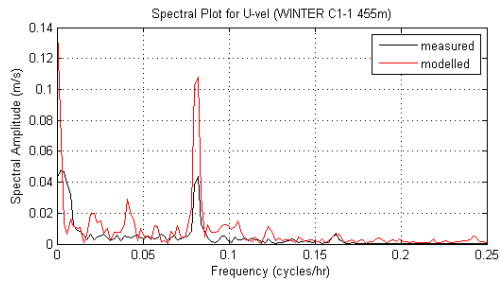












APPENDIX F

***PEER REVIEW OF
HYDRODYNAMIC MODEL AND
BRECKNOCK-4 APPLICATION
MODEL***



BROWSE LNG DEVELOPMENT

Peer Review of Hydrodynamic Model and Application Modelling

Document Cover Sheet

Phase:	Browse Environmental Modelling – Phase 1		
WEL Document No:	JB0006RH0118	Rev:	0
Contract No:	4510057734	Total # of Pages: (incl Doc Cover Sheet)	28
Equipment Tag No:			
Vendor Document No:	WV03795 – CTR9.303	Rev: (if applicable)	2

Vendor shall ensure that documents have been fully checked and approved prior to submittal to WPPL	Prepared	Ray Steedman	Checked	SKM -BSC	Approved	SKM -BSC
	Date	03/12/2009	Date	11/12/2009	Date	14/12/2009

Notes:	Supplier/Subcontractor Name, Address and Logo:
	<p>Sinclair Knight Merz 7th Floor, Durack Centre 263 Adelaide Terrace Perth WA 6001</p>

WOODSIDE REVIEW / STATUS INFORMATION					
			<input type="checkbox"/>	1. No Comments	
			<input type="checkbox"/>	2. Revise as noted see below	
			<input type="checkbox"/>	3. Revise & Resubmit for Review	
			<input checked="" type="checkbox"/>	4. Certified Final	
			<input type="checkbox"/>	5. Information Only	
			<input type="checkbox"/>	6. As Built	
0	Dec 2009	Issued for Approval	To be Returned at: (INFO, CF, AB or N/A)		
C	03/12/2009	Issued for Review	Vendor shall resubmit document in accordance with instructions accompanying returned document. This review and comments, if any, does not alter any of the terms and conditions of the purchase order nor relieve Supplier from any responsibility or liability for the accuracy and completeness of the document, nor shall it be interpreted so as to imply approval of such document nor shall it be interpreted as an assumption or imposition on the reviewer of any liability or responsibility as a result of such review.		
B	22/09/2009	Issued for Review			
A	05/08/2009	Issued for Review			
Rev	Date	Description	Responsible Engineer Name: S JARVIS		
Revisions to WEL Document No.			Signed:	Date	
			<i>S Jarvis</i>	18.1.10	



CLIENTS | PEOPLE | PERFORMANCE

SKM/Woodside

Report for Browse LNG Development,
Environmental Applications Modelling to
Upstream Approvals

Peer Review of Hydrodynamic Model
and Brecknock-4 Application Modelling

December 2009



Contents

Executive Summary	3
1. Introduction	1
1.1 The review	1
1.2 Scope of work for the peer review of hydrodynamic model and applications modelling	1
1.3 Particulars of the peer review of the hydrodynamic model and validation	1
1.4 Particulars for the peer review of the application modelling: oil spill and drill cuttings discharge for Brecknock-4 well	2
1.5 DHI reports reviewed	3
1.6 Study areas	3
2. MIKE 3 classic non- hydrostatic hydrodynamic model	4
2.1 Meteorologic and oceanographic measurements	4
2.2 Identification and reproduction of the dominant forcing mechanisms	4
2.3 MIKE 3 classic non-hydrodynamic mathematical modelling system	9
2.4 Model assumptions, parameters and data	10
2.5 Initial conditions	10
2.6 Model sensitivity tests	10
2.7 Model calibration	10
2.8 Model validation against <i>in situ</i> measurements	11
2.9 Applicability to Scott Reef and the other notional development areas	13
3. Review of models and application to Brecknock-4 oil spill and drill cutting discharge	15
3.1 Appropriateness of hydrodynamic and dispersion models	15
3.2 Oil spill and drill cutting discharge scenarios and results	16
3.3 Dispersion model parameters, inputs and assumptions	16
3.4 Limitations of the approach	17
3.5 Data used for validating the oil spill and drill cutting modelling	17



Executive Summary

The review

This report provides a review of DHI Water and Environment Pty Ltd: (a) Hydrodynamic Report: Browse Environmental Modelling – Phase 1, Hydrodynamic Model Validation at Scott Reef; and Surrounds Project No CTR9.301 and CTR9.303 Final Report, Revision 03; for SKM/ERM for Woodside Energy Ltd; June 2009; and (b) the Applications Report: Browse Environmental Modelling – Phase 1, Modelling of Oil Spill and Cuttings Discharge for the Brecknock-4 Well Report; for SKM/ERM for Woodside Energy Ltd; June 2009.

A summary of the review follows and is structured along the lines of the particulars of the peer review scope of work. Noting the review is constrained as the modelling is not intended for engineering purposes.

Suitability of MIKE 3 classic non-hydrostatic hydrodynamic modelling system

The MIKE 3 classic non-hydrostatic hydrodynamic and the oil spill and cuttings discharge models are well known and are part of a proven suite of numerical models, which have been applied to numerous environmental assessments requiring an understanding of coastal circulation, water level changes and dispersion.

The selection and set up of the specific models, the development of the bathymetry, computational grid, boundary and initial conditions, inputs of astronomical tidal and metrological forcing and heating, and the application to the Brecknock-4 oil spill and cuttings discharge dispersion, are considered to be within accepted practice. Model assumptions are clearly described within the reports.

The study shows the adjustment of various parameters and their coefficients (calibration factors), including the magnitudes of the coefficients for the parameterization of the turbulence scheme, compressibility, wind stress, bottom friction and heat exchange, and the accuracy of the amplitude and phase of the fit between the model and measured data over spring, summer, autumn and winter, 14 day neap to spring tidal simulation periods. The treatment of initial and boundary conditions are discussed.

The model performance is tested against criteria based on the UK Foundation for Water Research framework for marine and estuarine model specification, including the choice of simulated and measured time series from selected model grid and measurement locations.

The calibration method, each of the calibration and validation periods, the extensive comparisons of water levels, currents and seawater temperatures, which are plotted as time series, isopleths plots and the root mean square error and bias were calculated and compared to a hydrodynamic model acceptance framework criteria; including the comparison of time series, quantile-quantile plots (Q-Q plots) and spectral frequency plots, are extensive.

The nature of the buoy track simulation problem, which is designed to approximate a Lagrangian process is discussed. However, the complex nature of the movement of surface drifters is not fully described by the MIKE 3 model suit. In particular the advection and horizontal turbulence cannot be accurately simulated due to the stochastic nature of the surface drift. Consequently it is difficult to accurately simulate surface drogue tracks.



However reasonable comparisons are presented over certain sections the drogue tracks. Nevertheless these drifter tracks cannot be used to quantitatively calibrate the oil spill or cuttings discharge dispersion models.

It is concluded that the MIKE 3 classic non-hydrostatic hydrodynamic model and the oil spill and drill cutting discharge model are suitable for the purposes described in the original scope of work. The assumptions, parameters, model forcing, initial and boundary conditions, calibration, temporal and spatial nature and period of *in situ* data to force the model, or set the initial and boundary conditions, are appropriate for the calibration of the model and subsequent application.

It is concluded that the complex nature of the movement of surface drifters is not fully described by the model horizontal turbulence parameterisation. Consequently, the use of *in situ* drifter buoy tracks and model simulation of those tracks for validation purposes is inappropriate.

Identification and reproduction of the dominant forcing mechanisms

The study considers the complexity of continental shelf dynamic processes and metocean measurements, and identified the high importance phenomena as: (a) monsoonal winds; (b) surface wind driven currents; and (c) astronomical barotropic tidal currents.

The study analysis of the influence of the Indonesian Through Flow, synoptic scale eddies (or Rossby waves) at the shelf slope and longshore drift on the southern Northwest Shelf indicates that forcing driven by global scale processes (ie outside of the model boundaries) have little influence on the inner grid models. Some forcing and processes such as global scale steric height induced longshore drift, internal waves, baroclinic effects about steep topography and eddies shed off the lee side of islands or reefs in the presence of strong tidal currents are not considered to be dominant. However, these other forcing mechanisms and processes may be important for specific applications, and in particular about the Scott Reef area.

It is concluded that for practical modelling purposes the dominant forcing of the MIKE 3 model has been properly identified as: monsoonal winds (surface stress) driven by synoptic pressure gradients; surface wind driven currents (to 50 m depth); and astronomical tidal currents. These forces are admitted into the model by their mathematical description at appropriate regional and local scales.

However, two additional significant processes have been identified which require further consideration depending on the location and application. Firstly as seasonal drift (speed and direction) may play a significant role in the dispersion and fate of discharge plumes in regard to sensitive environments, the longshore drift should be further estimated from measurements and compared with the MIKE 3 model to ensure that the drift is adequately represented in the model results. Secondly, it is likely that eddies are present in the lee of Scott Reef, during periods of strong tidal currents. If these types of eddies are present it is possible for discharges to circulate around an eddy and come into contact with the sensitive fringing coral environment of Scott Reef.

It is recommended that: further analysis of the moored current meter data for longshore south west seasonal drift be undertaken and compared with model simulations; and an examination



of the measurements and model simulations for eddies shed in the lee of Scott Reef be undertaken to confirm the significance, or otherwise of these processes.

Model forcing, calibration, validation and sensitivity

The calibration adjustment of various parameters and their coefficients (calibration factors) and the fits between the model and measured data over spring, summer, autumn and winter, 14 day neap to spring tidal simulation periods are discussed. Extensive statistical comparisons between measure and model time series are presented as Q-Q plots, which show that the accuracy and reliability model simulation is variable depending on location. The model performance is tested against criteria based on the UK Foundation for Water Research framework.

The inner models about Brecknock and Scott Reef are generally insensitive to external forcing, particularly to global scale forcing of synoptic scale eddies (Rossby waves and longshore pressure gradients (eg. steric heights) through the open boundary conditions.

The simulation of the drift buoy track is considered to be part of the model validation.

It is concluded that MIKE 3 classic non-hydrostatic hydrodynamic model and the oil spill and drill cutting discharge models applied to Brecknock-4 are suitable for the purposes described in the original scope of work. The assumptions, parameters, model forcing, initial and boundary conditions and calibration, temporal and spatial nature and period of *in situ* data used to force the model or set the initial and boundary conditions are appropriate for the calibration of the model and subsequent application to Brecknock-4.

It is concluded the use of drifter buoy tracks for validation purposes is inappropriate (see above).

Model applicability to Scott Reef and the other notional development areas

Based on the discussion above, including the MIKE 3 hydrodynamic and dispersion models, the measurements from the model area, model nested grids, model set up, calibration and validation, and the application to Brecknock-4. It is concluded that the models are generally applicable to, Brecknock, Calliance, and outer open shelf and deeper water parts of the pipeline zones.

It is concluded that the models are generally applicable to Scott Reef and the other notional development areas, which includes Torosa North, Torosa South, subject to an improved understanding of the longshore drift, the horizontal density gradients about steep local topographic features and eddies shed off Scott Reef.

However in view of the complexity of the outer shelf bathymetry, dynamics, and the desired model reliability and accuracy, each area of interest and application should be examined to determine if there any site specific anomalies exist such as: global scale eastern boundary oceanic to shelf coupling forces, long shore drift; at a synoptic scale eddies (Rossby waves); and at a local scale density gradients, or large internal waves, or bottom boundary layer, or steep bathymetry. If site specific anomalies, such as synoptic scale eddies, are present then such forces and processes should be properly represented in the model.



Appropriateness of hydrodynamic and dispersion models

The Hydrodynamic Report and Application Report establishes the application of MIKE 3 hydrodynamic and oil spill and drill cutting discharge models in the Scot Reef and Bretnoch areas. Model parameters (coefficients) assumptions and their magnitudes, including properties of the oil (diesel) and drill cuttings, are based on other similar applications. The treatment of model forcing, including inter-annual wind variations is based on BoM 1992, 1993 and 1994 Scott Reef wind and tide measurements, which is a reasonable and practical approach to considering the possible influence of climatic variations. Generally based on the above the models and their forcing are appropriate for the application.

It is concluded that the use of the hydrodynamic and dispersion (applications) models are appropriate for the application to Brecknock-4 oil spill and drill cutting discharge modelling.

Oil spill and drill cutting discharge scenarios and results

The Hydrodynamic Report and Application Report establishes the application of MIKE 3 hydrodynamic and dispersion models. The scales of the simulated surface oil spill advection and plume spreading under various weather and tide conditions are comparable to other studies. The scales of the simulated drill cuttings advection and plume spreading under various weather and tide conditions are also comparable to other studies.

It is concluded that the scenarios used in the application to Brecknock-4 oil spill and drill cutting discharge modelling are appropriate.

Dispersion model parameters, inputs and assumptions

The Application Report lists the magnitude of the parameters, inputs and assumptions which appear reasonable. There is uncertainty associated with estimating oil and drill cutting properties from proposed wells. However the approximations made in the parameterisation of the dissipation processes appear reasonable for the environmental purposes of Brecknock-4 location.

It is concluded that the dispersion model parameters, inputs and assumptions are suitable for the application to both the Brecknock-4 oil spill and drill cutting discharge modelling.

Limitations of the approach for modelling at Brecknock-4

Any significant limitations of the approach rest with the MIKE 3 model set up, model parameterisation and dominant forcing selected to simulate conditions of interest. The nature of the dominant forcing and processes is possibly the cause of most uncertainty; eg inter-annual variation of surface wind climate, longshore drift and other global ocean effects. However for practical purposes the Brecknock-4 application model and application uncertainties appear to be understood and controlled.

It is concluded that there does not appear to be any significant limitations in the modelling approach taken that would prevent completion of for the scope of work for the Brecknock-4 oil spill and drill cuttings discharge modelling.



Data used for validating the oil spill and drill cutting modelling

The study assumes that the metocean measurements about Brecknock and Scott Reef are representative of the development area, including the inter-annual variations of wind and temperatures, the wind and astronomical tidal forcing. It is reasonable to assume that the Brechnock oceanographic data and Scott Reed wind and tide measurements are appropriate for validating the Brecknock-4 oil spill and drill cutting discharge modelling.

It is concluded that the data used for validating the Brecknock-4 oil spill and drill cutting discharge modelling are appropriate.



1. Introduction

1.1 The review

1. This report provides a review of DHI Water and Environment Pty Ltd hydrodynamic report: Browse Environmental Modelling – Phase 1, Hydrodynamic Model Validation at Scott Reef; and Surrounds Project No CTR9.301 and CTR9.303 Final Report, Revision 03; for SKM/ERM for Woodside Energy Ltd; June 2009 and the applications report: Browse Environmental Modelling – Phase 1, Modelling of Oil Spill and Cuttings Discharge for the Brecknock-4 Well Report; for SKM/ERM for Woodside Energy Ltd; June 2009.
2. The work was conducted for SKM by GHD in accordance with the scope of work for the peer review (file number I:\WVES\Projects\WV03795\Project Management\Modelling_Requests\Peer Review Request\DRIMS-#4944444-v3).
3. The following review report is structured along the lines of the scope of work, including particular requirements of the peer review peer for the hydrodynamic model and validation, and of the application modelling.

1.2 Scope of work for the peer review of hydrodynamic model and applications modelling

4. The scope of work for the peer review is described in the request form 1.
5. The Reviewer will provide expert opinion on the approach and data used to develop and validate the hydrodynamic model produced by DHI in response to the scope of work issued by Woodside (Appendix A). The Reviewer will also review the report of the application modelling undertaken using the hydrodynamic model, i.e. modelling of oil spill and cuttings discharge from the Brecknock-4 well).

1.3 Particulars of the peer review of the hydrodynamic model and validation

6. For this component, the Reviewer should review the hydrodynamic modelling and validation report prepared by DHI, and address the following:
 - (a) have the dominant forcing mechanisms (i.e. local as well as regional scale forcing functions such as the Indonesian Throughflow) been identified and then reproduced in the model at the appropriate scale, taking into account the intended use and application of the model?
 - (b) is the underlying hydrodynamic model used (MIKE 3 classic non- hydrostatic hydrodynamic model, nested with 25 z-layers) suitable for the purposes described in the original scope of work?

¹ Scope of work for the peer review is in file number I:\WVES\Projects\WV03795\Project Management\Modelling_Requests\Peer Review Request\DRIMS-#4944444-v3; Browse_LNG_Development__Upstream_Hydrodynamic_Model_Review_Scope_of_Work.DOC.



- (c) has the model been calibrated using appropriate assumptions, parameters and data, including those that are representative of the forcing functions? To produce the final model described in the report, this includes reviewing:
- ▶ the initial conditions of the model;
 - ▶ the period of *in situ* data used to calibrate the model as well as the resolution, temporal and spatial coverage of the data, e.g. the use of a global tidal model, and the use of Brecknock temperature profiles for use at the open boundaries; and
 - ▶ the sensitivity tests and analyses that have been undertaken (e.g. temperature);
- (d) has the model been adequately validated against *in situ* measurements?
7. The Reviewer should consider both the approach taken to validate the model performance, and the amount/period of data that has been used for validation.
8. In addition, the Reviewer should consider the different validation approaches separately (i.e. use of *in situ* profile measurements and drifter buoy tracks) as they provide insight into the ability of the model to reproduce different processes that will be required to different extents when undertaking the different application modelling.
9. Is the hydrodynamic model developed considered to have applicability to Scott Reef and the other notional development areas, which includes Torosa North, Torosa South, Brecknock, Calliance, Shelf and Pipeline Zones?

1.4 Particulars for the peer review of the application modelling: oil spill and drill cuttings discharge for Brecknock-4 well

10. The Reviewer should review the application modelling report for Brecknock-4 and address the following:
- (a) is the use of the hydrodynamic model appropriate for these applications?
 - (b) are the scenarios used in the application modelling appropriate?
 - (c) are the parameters, inputs and assumptions used to undertake these modelling applications suitable?
 - (d) are there any limitations in the approach taken that would not allow for the scope of work (for the oil spill and cuttings discharge modelling) to be completed? and
 - (e) is the data used for validating the modelling appropriate?
11. The review of the modelling applications should be completed in the context and confines of what they are to address. For example, the modelling applications that the hydrodynamic model will be applied to are for environmental activities or operational discharges that will not be undertaken in extreme weather conditions, such as cyclonic activity, and as such, there is not a need to address extreme weather events.



12. The modelling was not intended for engineering design purposes where extreme or continuous loading assessments would be required. In addition, the hydrodynamic model was developed on 12 months data, while the application modelling considers inter-annual variation in conditions.

1.5 DHI reports reviewed

13. The following reports were reviewed:
 - (a) DHI Water and Environment Pty Ltd report: Browse Environmental Modelling – Phase 1 Hydrodynamic Model Validation at Scott Reef and Surrounds²; and
 - (b) DHI Water and Environment Pty Ltd report: Browse Environmental Modelling – Phase 1 Modelling of Oil Spill and Cuttings Discharge for the Brecknock-4 Well Report³.

1.6 Study areas

14. The Browse development area is located on the edge of the continental shelf about 400 km north of Broome with depths varying from 200 m in the shelf platform zone to more than 500m around Scott Reef. The nested model areas are shown in figure 4.2 of the hydrodynamic modelling report² and figure 3.6 of the applications report³.

² DHI Water and Environment Pty Ltd report: Browse Environmental Modelling – Phase 1, Hydrodynamic Model Validation at Scott Reef and Surrounds Project No CTR9.301 and CTR9.303 Final Report, Revision 03; for SKM/ERM for Woodside Energy Ltd; June 2009

³ DHI Water and Environment Pty Ltd Browse Environmental Modelling – Phase 1, Modelling of Oil Spill and Cuttings Discharge for the Brecknock-4 Well Report; for SKM/ERM for Woodside Energy Ltd; June 2009



2. MIKE 3 classic non- hydrostatic hydrodynamic model

2.1 Meteorologic and oceanographic measurements

15. During the period, September 2006 to September 2007, wind, water level current and temperature measurements were made for six locations within the study area. The measurements and their durations are described in section 3, figure 3.1, and tables 3.2 and 3.3 of the hydrodynamic model report², and the locations shown in figure 3.1 of the applications report³.

2.2 Identification and reproduction of the dominant forcing mechanisms

16. DHI have produced a practical hydrodynamic circulation model which describes the Significant forcing mechanisms and other physical oceanographic processes. In doing so various simplifying assumptions have been made, thereby reducing the number of possible driving forces to the following: monsoonal surface wind stress and atmospheric pressure gradients; surface wind driven currents; and barotropic tidal levels and currents. The significant forcing and physical oceanographic processes are summarized in section 2.4 and tables 2.1, 2.2 and 3.1. In addition, as a result of this review, it is suggested that further consideration should be given to the global scale longshore steric height and resultant longshore drift and local scale eddies thought to be shed off Scott Reef.
17. The forcing of the physical processes on the outer continental shelf and slope are often complex and take place across global to local scales, which vary from region to region (eg^{4,5}; and figures 2.3, 2.4 and 2.5²). Well established circulation models, such as MIKE 3², can reasonably resolve the process across regional to local scales, such as circulation and water levels forced by the surface wind stress and atmospheric pressure gradients, barotropic tides, small amplitude internal waves, and horizontal and vertical density gradients (tables 2.1, 2.2 and 3.1).
18. However some forcing and physical processes are difficult to simulate due to large and expensive data requirements, availability of information, parametric estimations of diffusion surface wind stress and other processes, and general high costs of modelling. Therefore judgment has to be made on the processes which should be simulated for the purposes of the application.
19. Consider for example the northern boundaries of the DHI model, which lie to the south of Timor and borders the Timor Sea and eastern Indian Ocean. In this region the ocean, and continental slope dynamics are forced by global scale

⁴ A R Robinson and K H Brink eds, *The Sea Volume 11 The Global Coastal Ocean - Regional Syntheses*, John Wiley and Sons 1998.

⁵ J S Allen et al, *Physical oceanography of continental shelves* *Rev Geophys and Space Phys*, 21 (5), 1149-1181 1983.



Indonesian Through Flow, thermohaline gradients and a persistent meridional steric height gradient along the Western Australian coast and astronomical tidal water levels. At synoptic scales these forces are mainly through surface wind stress and atmospheric pressure gradients. These forces generate a range of processes^{4,5} such as longshore poleward currents on the continental shelf and slope, eddies (Rossby waves), which are known to form at the edge of the Northwest Australian shelf (eg^{6,7}), shelf Kelvin and arrested topographic waves, and tidal currents and water levels. The understanding of the oceanic forcing on the continental slope and shelf is rapidly improving⁴, but much remains unknown.

20. The complexity of the coupling between the deep ocean, continental slope and continental shelf, is known⁴. The coupling of the deep ocean to continental shelf is likely to affect the magnitude and seasonality of the longshore drift currents about the Brecknock area. The drift may result from global and synoptic scale processes which reach far beyond the boundaries of the model. The problem of decomposing the cause and scales of the longshore drift is difficult.
21. It is known that warm equatorial waters pile up on the northern margin of Western Australia, due to the Indonesian Through Flow component of the global thermohaline circulation. A resultant longshore oceanic pressure gradient drives water masses on to the continental slope and outer shelf, forms the southwest drift currents observed on the southern North West Shelf and ultimately forms the Leeuwin current, which flows poleward along the Western Australian coast. As the current flows south the steric height drops maintaining the meridional pressure gradient, which suggests open ocean processes, rather than complex responses to wind forcing, drive the flows poleward.
22. One analysis¹⁰ shows one form of coupling between the ocean and shelf, where the steady state adjustment between the oceanic pressure gradients and the coastal zone can be interpreted in terms of an arrested topographic wave⁸.
23. Another explanation of longshore drift arises from the oceanic sea level gradient that is physically due to meridional drop in steric height arising from a fall in ocean temperatures polewards^{9,10}. In this circumstance, when zonally orientated density surfaces interact with a meridional sloping boundary the dynamic adjustment of density induces a pressure gradient to the bottom slope, which is called the joint effect of baroclinicity and relief or pycnobathic forcing.
24. Another different interpretation of the poleward eastern boundary current, applied to the southern part of the North West Shelf¹¹, is made in terms of the rectification of time dependant motions over a sloping boundary. Rectification of the cross slope component of oscillatory barotropic and internal tides can induce

⁶ F Fang and R Morrow, 2003, Deep-Sea Research II, 50, 2245–2261.

⁷ G R Cresswell and T J Golding, 1980, Deep Sea Research, 27A, 6A, 449-466.

⁸ G T Csanady, J Phys Oceanogr 8(1), 47-62, 1978.

⁹ J M Huthnance Prog Oceanogr, 10, 193-226, 1984.

¹⁰ J M Huthnance Prog Oceanogr, 35, 353-431, 1995

¹¹ P. E. Holloway, J Geophys Res., 92 (C5), 5405-5416, 1987.



longshore Eulerian flow in the direction of the topographic wave propagation (eg ¹²). The ever present sub-inertial time dependant flows over irregular topography are rectified by form stress along the sloping continental shelf can also produce a longshore flow in the direction of the topographic wave direction under general conditions. This process is thought to be applicable to the North West Shelf ^{4,12,13}.

25. The Australian northwest region has relatively little freshwater run off, but evaporation is large enough to generate strong coastal density gradients. Thermohaline forcing of the eastern boundary current and longshore poleward flow (drift) has also been applied to Western Australian coast ¹⁴.
26. To better understand the influence of synoptic or global scale forcing originating outside of the model area, comparisons have been made between the mean monthly currents generated by MIKE 3 regional model and the global scale BlueLink model. Both the MIKE 3 and BlueLink models produce the regional wind driven north and south flowing seasonal drift currents. In principal BlueLink also estimates the global scale circulation contribution to the longshore drift. The comparison shows that MIKE 3 monthly mean currents (drift) are comparable to those of BlueLink throughout the year 2007, except during June and July, where MIKE 3 drift estimates are lower than those of BlueLink. Given the available information it is not practical to include the effects of global scale forcing at the MIKE 3 boundaries.
27. Surface wind stress and its daily and seasonal variations are significant in driving the coastal circulation. The seasonal synoptic, regional and local winds have been analysed from the satellite surface wind data, Bureau of Meteorology (BoM), records of Adele Island and Woodside's measurements at Scott Reef.
28. Adele Island, Scott Reef and the satellite measurements appear to be made at different levels above MSL. The report would be enhanced if reference was made to the adjustment of wind speeds and directions to a standard reference level, which is usually set at 10 m AMSL.
29. As the model application is offshore about the shelf break, land or sea breeze, and sea to shore surface roughness changes, as they influence the surface wind stress, are reasonably reoriented in the model.
30. The Browse measurement programme (section 2.4) and various studies of the North West Shelf ^{13,15} show that there are large amplitude internal waves generated by the steepening of the internal tide on the North West Shelf extending from strongly stratified summer conditions to weakly stratified winter conditions. DHI state that in the context of the model applications the simulation of large amplitude internal waves require dedicated models, extensive data and

¹² J M Loader, J. Phys. Oceangr, 10, 1399-1416, 1980.

¹³ P. E. Holloway, J Geophys Res., 92 (C5), 5405-5416, 1987.

¹⁴ J P McCreary, J. Mar. Res., 44, 71-92.

¹⁵ P V Gastel, G N. Ivey, M J. Meuleners, J P. Antenucci and O Fringer, Continental Shelf Res 29, 15, , 1373-1383 2009



are unlikely to influence the transport and dispersion processes. DHI have reasonably omitted the simulation large amplitude internal waves from the model.

31. Other field measurements and modelling¹⁶ about Scott Reef have shown that tidal currents reached 0.6 ms^{-1} and the internal wave amplitude was about 60m (peak to trough). Numerical model and data suggest that the internal tidal waves were generated locally by the interaction of tidal currents and steeply sloping bathymetry. It is thought that trapped barotropic and internal waves rotated clockwise about the island with maximum amplitude found along the island slopes¹⁶. DHI have omitted the generation of large amplitude internal waves from the processes, which appears reasonable for Brecknock applications, but this approach need careful consideration for Scott Reef applications.
32. It is possible that internal waves increase the shear within the bottom boundary layer (BBL), which in turn increases the bottom stress and turbulent mixing in the BBL, and enhances the dispersion of any drill cuttings or heavier than water substances within the BBL. DHI have omitted the BBL from the model which appears reasonable.
33. The influence of synoptic scale eddies on the nested models was considered. DHI reviewed unpublished UWA ROMS numerical model simulations, moored instrument arrays, XBT's and satellite altimeter observations show the formation of Rossby waves along the shelf slope and break. Brecknock B2-1 moored current and temperature measurements² shows that eddies occur in this region. It is not known if these measured eddies at Brecknock are propagating past the site or being generated nearby.
34. However, current and temperature measurements from a moored array at C1-1 North Scott Reef do not show any evidence of synoptic scale eddies (Rossby waves) either propagating south west along the shelf break or being formed about Scott Reef, which is consistent with other studies¹⁶.
35. Based on this review and measurements and model boundary condition sensitivity tests, DHI suggest that it is unlikely that synoptic scale eddies regularly influence the ocean circulation and properties about Scott Reef. Accordingly DHI have not imposed synoptic eddies on the model.. As a first order approximation this assumption appears reasonable, particularly over the time scales over which the application modelling is performed.
36. Longshore drift currents are not included in the important oceanographic phenomena of tables 2.2 or 3.1. However, it is known that longshore drifts^{4,5,11} occur over most continental shelves and that velocity and direction of the drift often varies with the seasons. The analysis of drift is complicated. There are many causes of longshore drift over continental shelves; eg. the drift may be forced by: global steric height differences; regional longshore pressure fields caused by seasonal water density changes driven by evaporation or freshwater runoff; regional atmospheric pressures and surface wind field; and atmospheric

¹⁶ E Wolanski and E Deleersnijder, Continental Shelf Res. 18, 1649-1666, 1998.



pressures and local surface wind fields. North West Shelf surface current maps of figures 2.3 and 2.4 show a seasonal longshore drift flowing south west long the continental shelf. Holloway's analysis¹¹ of current observations southern Northwest Shelf (figure 2.6) shows a seasonal longshore drift at speeds of up to 0.3 ms^{-1} flowing in a south west direction. It is likely that a longshore drift is present about the C2-1 and H2-1 Scott Reef, B2-1 Brecknock and (G2-1) shelf locations (figure 3). The south west drift current is likely to be strengthened by the winter southeast monsoon.

37. It is known that eddies are shed from islands in presence of strong (tidal) currents¹⁷. Scaling analysis suggests that during spring tides a deep water form of eddies should form in the lee of Scott Reef. Although the phase of the tide is not stated, figure 5.6 suggests that eddies may be present in the lee of Scott Reef. However, internal wave studies of Scott Reef¹⁶ indicate that eddies may not form the lee of the island. The reason for differing interpretation concerning the presence, or absence, remains unresolved.
38. At the sea bed the benthic habitat and the fate of heavier than water drill cuttings will depend on bottom boundary layer (BBL) dynamics. The BBL is forced by the local pressure barotropic tidal and internal wave gradients and the free stream velocity just above the sea bed. The forcing determines the shape (shear) of the BBL velocity profile, bottom shear stress at the sea bed surface and turbulent mixing. The presence of barotropic tidal internal waves have been identified (table 3.1), but the influence of these waves on the BBL has not been included. Drill cuttings or heavier than water substances will sink to the sea bed, where they will come to rest or be dispersed, depending on the magnitude of the bottom stress, and the vertical and horizontal mixing processes. The logarithmic bottom velocity profile, roughness scales and other complexities of the BBL require a particular form of model, which is not included in this study. The omission of the BBL as significant processes in the model is reasonable in view of the application. However the report would be enhanced if the BBL is identified as physical process and its significance with respect to benthic habitat discussed particularly in relation to the dispersion of drill cuttings, or heavier than water substances.

39. Having particular regard to the application, complexity of continental shelf dynamic processes and metocean measurements, and identified the high importance phenomena (table 3.1) as being: (a) monsoonal winds; (b) surface wind driven currents; and (c) astronomical barotropic tidal currents. The study analysis of the influence of the Indonesian Through Flow, synoptic scale eddies (or Rossby waves) at the shelf slope and longshore drift on the southern Northwest Shelf, indicates that forcing driven by global scale process (ie outside of the model boundaries) have little influence on the inner grid models. Some "other" known forcing and processes such global scale steric height induced

¹⁷ E Wolanski, J Imberger, M L Heron, J Geophys Res, 89-C6, 10,553–10,569, 1984.

longshore drift and local scale processes including internal waves, baroclinic effects about steep topography and eddies shed off the lee side of islands or reefs in the presence of strong tidal currents are not considered to be dominant. However, these “other” forcing mechanisms and processes may be important for specific applications, and in particular applications about the Scott Reef area.

40. Accordingly it is concluded that the dominant forcing of the MIKE 3 model ² are: (a) monsoonal winds (surface stress) driven by synoptic pressure gradients; (b) surface wind driven currents (to 50 m depth); and (c) astronomical tidal currents; are properly identified, admitted into the model by their mathematical description and reasonably simulated by the model results at appropriate regional and local scales.
41. However, two additional significant processes have been identified which require further consideration depending on the location and application. Firstly as seasonal drift is likely to be present and may play a significant role in the dispersion and fate of discharge plumes in regard to sensitive environments. The seasonal longshore drift should be estimated from measurements. If present, the measured drift should be compared with relevant MIKE 3 model longshore drift. ,Secondly it is likely that eddies shed are present in the lee of Scott Reef, in presence of strong tidal currents. If these types of eddies are present it may be possible for discharges to circulate around an eddy and travel back to the reef coming into contact with the sensitive fringing corals of Scott Reef.
42. It is recommended that: further analysis of the moored current meter data for longshore south west seasonal drift be undertaken and compared with model simulations; and an examination of the measurements and model simulations for eddies shed in the lee of Scott Reef be undertaken to confirm the significance, or otherwise, of these processes.

2.3 MIKE 3 classic non-hydrodynamic mathematical modelling system

43. The finite difference non hydrostatic version of DHI’s 3-dimensional hydrodynamic modelling system, MIKE 3 Classic, was selected as the underlying hydrodynamic model (section 4.3) ^{2,3}. A series of nested models are set up about the proposed Brecknock development. The models span regional to local scales (figure 4.5) and cover the deep ocean to shallow coastal areas adjacent the Kimberly regional of Northwest Australia. The inner models span the outer continental shelf and slope regions, including Scott Reef and Brecknock locations of interest. The inner hydrodynamic models provide estimates of velocity fields (advection) and turbulent mixing for the projected Brecknock-4 oil spill and cuttings discharge and dispersion model ³. Brief mathematical descriptions are presented in hydrodynamic model report Appendix A ² and oil spill and drill cuttings model report Appendices B and C ³, respectively.



2.4 Model assumptions, parameters and data

44. The model calibration, assumptions, parameters and coefficients, and forcing functions were assessed, including the period of *in situ* data, the resolution, temporal and spatial coverage, and the boundary and initial conditions. A description of the parameters and their coefficients (calibration factors) and their adjustment as part of the calibration are discussed in section 5.3². The coefficients of the turbulence scheme, compressibility, wind stress, bottom friction and heat exchange parameterisation are described in section 5.3 and appendix A. The magnitude of these coefficients were systematically adjusted to give the best fit between the model and data (section 5.6 and Appendix B). The model calibration run simulated a 14 day period, which spanned a neap to spring tidal range.
45. The model assumes that the horizontal density gradients are small, such the density isopleths approximately parallel with the model grid surfaces. If the horizontal density gradients become too steep (eg about fronts) then the baroclinic component of the model are inaccurate.

2.5 Initial conditions

46. Concerning the initial and boundary conditions. The model is 'spun up' with initial conditions that may be regarded as a 'cold start', where a constant water level was set at MSL and Brecknock seasonal temperature profile with a constant salinity profile (ie density profile) were applied over the entire model area. Some tests results are discussed (section 4.4.4). The initial and boundary conditions appear appropriate for the application.
47. The phases and amplitudes of the six tidal largest constituents were estimated along the model open boundaries from the global tidal model. These tidal constituents were applied to the open boundary conditions allowing for amplitude and phases differences about the model boundaries. The application of the global model tidal constituents and phase differences along the open boundaries appear appropriate for deep water applications about the outer shelf.

Period of *in situ* data resolution, temporal and spatial coverage

2.6 Model sensitivity tests

48. DHI completed a series of sensitivity tests concerning initial and boundary conditions (section 5.4) and estimated that synoptic scale eddies and the initial condition density structure will only have a minor influence on the model results.

2.7 Model calibration

49. Model performance criteria were based on marine estuaries as criteria are not available for offshore areas and coral islands. DHI tested the model performance against the UK Foundation for Water Research publication: Reference FR0374, A framework for marine and estuarine model specification in the UK (section 5.5).



50. Time series from selected grid locations were extracted from the model results and compared to the measurements. The location of the measurement stations in the model grids are shown in Figure 5.10.
51. The calibration results are presented in section 5.6 and Appendix B, which includes the details of the spring period calibration, comparisons between measurement and model simulation as shown as isopleth, times series, quantile-quantile plots (Q-Q plots) and (power spectral) frequency plots.
52. Extensive comparisons of water levels, currents and seawater temperatures are presented to demonstrate the calibration results. Comparisons were plotted as time series, isopleths plots and the root mean square error and bias were calculated and compared to hydrodynamic model acceptance framework criteria. In addition a comparison of time series, Q-Q plots and spectral frequency plots are presented to further demonstrate of the accuracy of the amplitudes and to a lesser degree the phase of the simulations compared to measurement.
53. The variations in the calibration results between locations appear to represent the changing role of the dynamic processes both measured and simulated about the shelf, continental slope and Scott Reef. For example scaling analysis shows that the Ekman and Coriolis numbers vary significantly between the shallower continental shelf to the deeper waters of the slope; eg in the shallow water bottom friction plays an important role while in deep water bottom friction is diminished and Coriolis and geostrophic forces become important. The model and data appear to reflect these cross shelf changes in the dynamic processes. The cross shelf variations on the differences between model measured data are shown in the time series, rms error and Q-Q plots and power spectra. It is likely that the variations in the differences or errors between shelf and deeper slope measurement locations reflect the changes in the cross shore dynamics processes. Generally the calibration variations between model and measured data are reasonable and appear consistent with other studies.

2.8 Model validation against *in situ* measurements

54. The model validation runs simulated three seasonally distinct 14 day periods, during summer, autumn and winter (sections 5.6, 5.7 and 5.7, respectively), where these simulations were run with the magnitudes of the selected calibration coefficients held constant. The model validation runs each simulated a 14 day period, which spanned a neap to spring tidal range.
55. Similarly extensive details of further validations are found in the following sections and appendices: (a) section 5.7 and Appendix C: Summer period validation period, comparisons between measurement and model simulation as isopleth, times series Q-Q plots and (power spectral) frequency plots; (b) section 5.8 and Appendix D: Winter period calibration, comparisons between measurement and model simulation as isopleth, times series Q-Q plots and (power spectral) frequency plots; and (c) section 5.9 and Appendix E: Spring period calibration,



comparisons between measurement and model simulation as isopleth, times series Q-Q plots and (power spectral) frequency plots.

56. The coordinate system of the measured and model data appears to be orientated to the regular north south and east west system. However, as the longshore and cross shore dynamic processes are quite distinct it would have been far better to resolve the measured and model wind and current components to be parallel and perpendicular to the coast.
57. Lagrangian simulation of drifter buoy tracks is discussed in section 5.10. Although the simulated and measured tracks are in some agreement, such comparisons are unreliable. Numerical diffusion alone will displace the simulation in a manner that is very difficult to overcome or calibrate with the calibration parameters list in section 5.3. The complex nature of the movement of surface drifters is not fully described by the model advection and horizontal turbulence parameterization..Generally the advection and horizontal turbulence cannot be accurately simulated due to the stochastic nature of the surface drift. Consequently it is difficult to accurately simulate surface drogue tracks. However reasonable comparisons are presented over certain sections the drogue tracks. Nevertheless these drifter tracks cannot be used to quantitatively calibrate the oil spill or cuttings discharge dispersion models.

58. Having particular regard to the mathematical description of the MIKE 3 classic non- hydrostatic hydrodynamic model ² (Appendix A), and the oil spill and cuttings discharge model ³ (Appendices A and B) are part of a proven suit of models which have been applied to numerous environmental assessments requiring an understanding of coastal circulation, water level changes and dispersion. The selection and set up of the specific models (sections 4.3 and 4.4) ², the development of the bathymetry, computational grid (section 4.4.2) ², boundary and initial conditions (sections 4.4.4) ², inputs of astronomical tidal and metrological forcing and heating (section 4.4.5) ², and the application to the Brecknock-4 oil spill and cuttings discharge dispersion (section 3.3) ³, are considered to be within accepted practice. Model assumptions are clearly described within the reports.
59. The study shows the calibration adjustment of various parameters and their coefficients (calibration factors), including the magnitudes of the coefficients for the parameterization of the turbulence scheme, compressibility, wind stress, bottom friction and heat exchange parameterisation, the accuracy of the amplitude and phase of the fit between the model and measured data over spring, summer, autumn and winter, 14 day neap to spring tidal simulation periods. The treatment of the initial and boundary conditions are discussed.
60. The model performance is tested against criteria based on the UK Foundation for Water Research framework for marine and estuarine model specification in the UK, the choice of simulated and measured time series from selected model grid and measurement locations. The calibration method, calibration and validation

periods, extensive comparisons of water levels, currents and seawater temperatures, which are plotted as time series, isopleths plots and the root mean square error and bias were compared to hydrodynamic model acceptance framework criteria. The criteria included the comparison of time series, quantile-quantile plots (Q-Q plots) and spectral frequency plots. The model performance also considered the buoy track simulation problem, which is designed to simulate a Lagrangian process.

61. However the complex nature of the movement of surface drifters is not fully described by the MIKE 3 model suit. In particular the advection and horizontal turbulence parameterization cannot accurately simulate the stochastic nature of the surface drift. Any similarity between the actual and model tracks is at best qualitative
62. It is concluded that MIKE 3 classic non-hydrostatic hydrodynamic model ² and the oil spill and drill cutting discharge model ³ are suitable for the purposes described in the original scope of work. The assumptions, parameters, model forcing, initial and boundary conditions and calibration, temporal and spatial nature and period of *in situ data* used to force the model or set the initial and boundary conditions are appropriate for the calibration of the model and subsequent application.
63. It is concluded that the complex nature of the movement of surface drifters is not fully described by the model. Generally the advection and horizontal turbulence cannot be accurately simulated due to the stochastic nature of the surface drift. Consequently it is difficult to accurately simulate surface drogue tracks. However reasonable comparisons are presented over certain sections the drogue tracks. Nevertheless these drifter tracks cannot be used for a quantitative calibration of the oil spill or cuttings discharge dispersion models.

2.9 Applicability to Scott Reef and the other notional development areas

64. The MIKE 3 model ^{2,3} areas span the regions of Scott Reef and the other notional development areas, which includes Torosa North, Torosa South, Brecknock, Calliance, Shelf and the deeper water pipeline zones. Noting the measurements in the development areas and model results ^{2,3}, it is likely that the significant physical process described by DHI will be reasonably constant throughout the outer continental shelf and slope region about the development areas.
65. Further noting that it is recommended that further analysis longshore south west seasonal drift and eddies shed in the lee of Scott Reef be undertaken to confirm the significance, or otherwise of these processes. Assuming ocean waves and swell, and shallow water effects are not considered in the application.
66. Having particular regard to the assumptions of the MIKE 3 hydrodynamic and dispersion models ^{2,3}, the measurements from the general area, model area and nested grid, model set up, calibration and validation, and the application to Brecknock-4.



67. Accordingly it is concluded that the models ^{2,3} are generally applicable to, Brecknock, Calliance, and outer open shelf shelf and deeper water pipeline zones.
68. Accordingly it is concluded that the models ^{2,3} are generally applicable to Scott Reef and the other notional development areas, which includes Torosa North, Torosa South, subject to a better understanding of the longshore drift, the horizontal density gradients about steep local topographic features and eddies shed off Scott Reef.
69. However, in view of the complexity of the outer shelf bathymetry, ocean dynamics, and desired model reliability and accuracy,, each area of interest and application should be examined to determine if there any site specific anomalies exist such as: global scale eastern boundary oceanic to shelf coupling forces; at a synoptic scale eddies (Rossby waves); and at a local scale density gradients, or large internal waves, or bottom boundary layer, or steep bathymetry. If site specific anomalies, such as synoptic scale eddies, are present then such forces and processes should be properly represented in the model.



3. Review of models and application to Brecknock-4 oil spill and drill cutting discharge

3.1 Appropriateness of hydrodynamic and dispersion models

70. The oil spill modelling is described in section 4 and the transport equations are summarized in the spill analysis, appendix B. The oil properties of eight fractions, based on diesel, are listed in table 4³. The dispersion or entrainment is simulated (noting that the interfacial tension parameter units are expressed in dynes cm⁻¹ and not SI units which appears to be the basis of the model). Dissolution is set at the default value and the heat transport parameters through the albedo, air and water provided.
71. The environmental parameters, including Scott Reef wind and tide measurements, which force the local scale model, are described in section (4.1.3). Model simulations were carried out with Scott Reef tide and wind records from three separate 90 day periods of March to May, for each of the years 1992, 1993 and 1994. Any inter-annual wind variations are likely to be reasonably covered during these years, 1992, 1993 and 1994.
72. The model (advection) velocity components are estimated from MIKE3 hydrodynamic model (discussed above). The model turbulent diffusion process is anisotropic, where the magnitudes of longitudinal, transverse and vertical diffusion (m²s⁻¹) are proportional to the respective velocity components. There are no reported measurements of the *in situ* dispersion coefficients on the North West Shelf; hence the parameterization has been adopted from elsewhere. In the absence of anything else the parameterization is appropriate.
73. The MIKE 3 model surface layer is 30 m thick. The model calculates a vertically averaged velocity over this thickness. However oil floats over surface velocity profile which varies with depth. To improve the accuracy of the vertical velocity profile simulation, a parametric velocity profile is imposed over the surface layer (to a depth of 30 m).
74. The study establishes the application of MIKE 3 hydrodynamic model and oil spill and drill cutting discharge model, including the model area, nested grids, model set up, the model calibration and validation. Model parameters (coefficients) assumptions and magnitudes, including properties of the oil (diesel) and drill cuttings, are based on other similar applications. The treatment of inter annual wind variations is based on BoM 1992, 1993 and 1994 Scott Reef wind and tide measurements.
75. Accordingly it is concluded that the use of the hydrodynamic and dispersion models^{2,3} are appropriate for the application to Brecknock-4 oil spill and drill cutting discharge modelling.

3.2 Oil spill and drill cutting discharge scenarios and results

76. Oil spill model results are presented section 4.2 and shown in figures 4.6 to 4.14, where the maximum 'surface' concentrations are expressed in gm m² after 6, 12, 24 and 120 hours. The results are also expressed in time in hours to reach an exposure of concentration 0.1 gm m² and probability exceedance of 0.1 gm m².
77. Generally at larger time scales the scale of the dispersion appears reasonable. However, statistically the particle advection dominates the dispersion patterns at small time scales (< inertial period ~ 30 hours) and it is likely that the particle excursions would lie in the direction of the principle component of the tidal ellipse, particularly as the model has zero drift; eg figures 4.6 and 4.7 show no preferred alignment with the tidal ellipse, which suggest that the surface wind driven currents are far greater than the surface tidal currents.
78. The drill cutting discharge scenarios and results are present in section 5.2 and shown in figures 5.3 to 5.16, where various drill sections are analysed over a spring to neap tide period. Generally the sediment plume falls within an area of less than 1 to 1.5 km and is well away from any known sensitive environment such as Scott Reef. Interestingly the axes of the areas covered by drill cuttings appear to be aligned with the tidal ellipse. The scale of the dispersion pattern appears reasonable.

- | |
|---|
| <ol style="list-style-type: none">79. The study establishes the application of MIKE 3 hydrodynamic and dispersion models, including the scale of the simulated spreading, the treatment of seasonal and inter-annual surface wind variations and the surface velocity profile sub model. The estimated model parameters and estimated properties of the oil (diesel) and drill cuttings, are based on other studies. The oil spill spreading is simulated for the seasonal period March to May, where it is likely that southerly winds occur.80. Accordingly it is concluded that the scenarios used in the application to Brecknock-4 oil spill and drill cutting discharge modelling are appropriate. |
|---|

3.3 Dispersion model parameters, inputs and assumptions

81. The oil properties of eight listed fractions (table 4³) are based on diesel. The dispersion or entrainment is simulated. Dissolution is set at the default value and the heat transport parameters through the albedo, air and water provided.
82. The drill cutting parameters estimates, for different drill sections, are given in table 5.2³. Various mass flux and material properties, including particle size distributions are quantified.
83. The dispersion coefficients are discussed which are the same magnitude as those applied to oil spill. The sediment suspension and resuspension rates are discussed.

84. The report lists the magnitude of the parameters, which appear reasonable. There is uncertainty associated with estimating oil and drill cutting properties from proposed wells. The approximations made in the parameterisation of the dissipation processes appear reasonable for the environmental purposes of Brecknock-4 location.
85. Accordingly it is concluded that the dispersion model parameters, inputs and assumptions are suitable for the application to Brecknock-4 oil spill and drill cutting discharge modelling.

3.4 Limitations of the approach

86. The limitations of the model are discussed above, where it is shown that much of the outer shelf dynamic processes are the subject of national and international ocean research. Generally the application of the model and the accuracy of the forecasts and environmental impact assessment on sensitive receptors and habitats will necessarily be limited. Thus it would be prudent to better understand the limitations by carefully considering each area of interest. The application should be examined to determine if there any site specific anomalies exist. If site specific anomalies are present, then such forces and processes should be properly represented in the model.

87. The study shows the Brecknock-4 application, the assumptions and estimations of the parameters concerning the properties of oil and drill cuttings. Any significant limitations of the approach rest with the MIKE 3 model set up, model parameterisation and dominant forcing selected to simulate conditions of interest. The nature of the dominant forcing and processes is possibly the cause of most uncertainty; eg inter-annual variation of surface wind climate, longshore drift and other global ocean effects. However for practical purposes the Brecknock-4 application model and application uncertainties appear to be understood and controlled.
88. Accordingly there does not appear to be any significant limitations in the modelling approach taken that would prevent completion of the scope of work for the Brecknock-4 oil spill and drill cuttings discharge modelling.

3.5 Data used for validating the oil spill and drill cutting modelling

89. During a one year period, September 2006 to September 2007, wind, water level current and temperature measurements were made for six locations within the study area. The measurements and their durations are described in section 3, tables 3.2 and 3.3 of the hydrodynamic model report ², and the locations shown in figure 3.1.
90. The hydrodynamic model calibration and validation have used appropriate mathematical assumptions, parameters and measured data, and as a first approximation the astronomical tidal (barotropic) and surface atmospheric



barometric pressure gradients are reasonably representative of the forcing functions (refer to above).

91. The Brecknock-4 location falls between the Brecknock (figure 3²) measurement locations. These data will represent the major processes occurring about the open shelf waters about Brecknock-4 and consequently the Brecknock-4 application model.

92. The study assumes that the metocean measurements about Brecknock and Scott Reef are representative of the development area, including the inter-annual variations of wind and temperatures, the wind and astronomical tidal forcing. It is reasonable to assume that the Brecknock oceanographic data and Scott Reed wind and tide measurements are appropriate for validating the Brecknock-4 oil spill and drill cutting discharge modelling.
93. Accordingly it is concluded that the data used for validating the Brecknock-4 oil spill and drill cutting discharge modelling are appropriate.



GHD

GHD House, 239 Adelaide Tce. Perth, WA 6004
P.O. Box Y3106, Perth WA 6832
T: 61 8 6222 8222 F: 61 8 6222 8555 E: permail@ghd.com.au

© GHD 2009

This document is and shall remain the property of GHD. The document may only be used for the purpose for which it was commissioned and in accordance with the Terms of Engagement for the commission. Unauthorised use of this document in any form whatsoever is prohibited.

Document Status

Rev No.	Author	Reviewer		Approved for Issue		
		Name	Signature	Name	Signature	Date
	R STEEDMAN	David Horn		R STEEDMAN		02.12.09
				D. Horn		3.12.09

APPENDIX G

**DHI'S REPLY TO
REVIEWERS
COMMENT**

We would like to first thank the reviewer for their helpful comments and suggestions. Generally, the reviewer was very supportive of the modelling methodology and model outcomes but raised four specific concerns. The reviewers comments are in italics followed by DHI’s response.

1. Reviewers Comment: *DHI have omitted the generation of large amplitude internal waves from the processes, which appears reasonable for Brecknock applications, but this approach needs careful consideration for Scott Reef applications.*

DHI Reply: DHI investigated whether the passage of internal waves through the Scott Reef region can affect the stability of submarine pipelines in the channel between North and South Scott Reef and concluded that the passage of internal waves did not generate above ambient seabed currents. DHI did this by reviewing the findings of a numerical modeling study conducted for WEL by UWA in 2007. The study examined the internal wave dynamics of the Browse Basin focusing on the Scott Reef region and its surrounds. We have extended the findings of the study by using the numerical solution to specifically examine the internal wave dynamics within the channel.

A conceptual sketch summarizing the generation, propagation and dissipation of the internal wave field of the Browse Basin is shown in Figure 1.

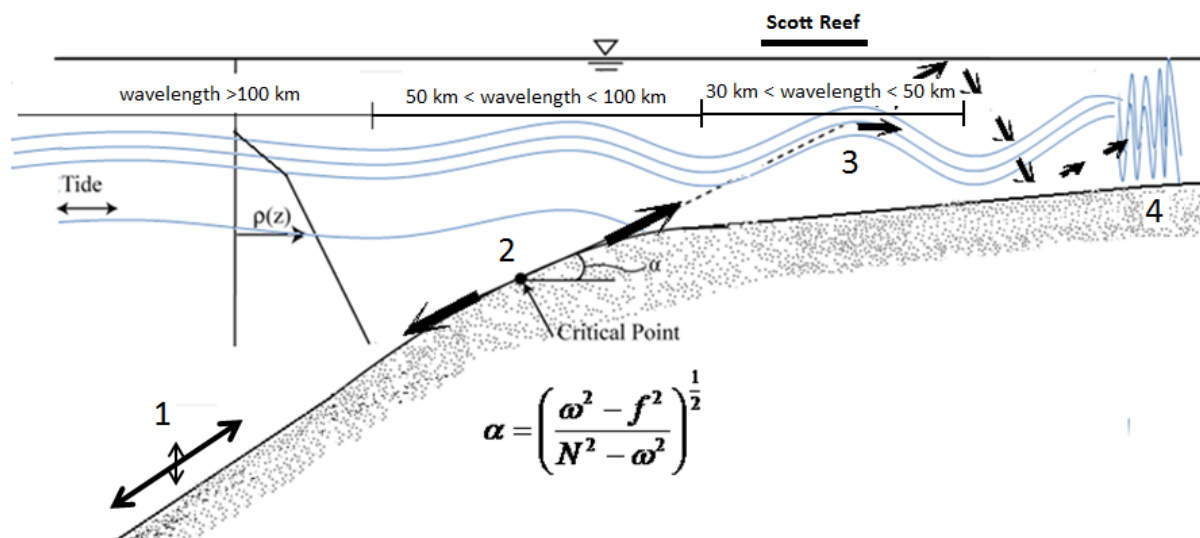


Figure 1: Schematic of the generation, propagation and dissipation of the internal wave.

Figure 1 shows weakly non-linear waves form as a result of the sloshing of the tide west of Scott Reef along the outer continental slope – the generation of the internal tide (‘1’ in Fig. 1). Internal wave rays are generated to the west of Scott Reef at critical points (‘2’ in Fig. 1), where the depth is of order 600 m or greater. They then propagate obliquely in both an

offshore and inshore direction. The inshore propagating wave rays pass by Scott Reef region before intercepting the thermocline to the east of Scott Reef - they can now be described as horizontally propagating modes that can undergo considerable steepening and can acquire very large vertical amplitudes and relatively short wavelengths as shown ('3' and '4' in Fig 1). Eventually these highly non-linear waves can no longer be supported inducing the onset of a high frequency large amplitude internal wave train (4) before dissipating in water where the rising seabed intersects the seasonal thermocline. Associated with the generation of these wave trains is the formation of strong near seabed currents.

So from this description we conclude the following:

1. The wave field passing through the channel is the near-linear internal tide. The results show that the horizontal scale of motion (wavelength) of the wave field is between 30 km and 50 km and that the vertical amplitude is ~40 m (near the seabed). The phase speed of the waves are approximately equivalent to the depth average tidal current and although small high frequency motions are induced by the passage of the internal tide, there is no evidence of significant higher frequency motions generating a strong near seabed current response that could destabilize marine infrastructure. The modelled near seabed current speeds are $< 0.3\text{m/s}$ within the channel, and secondly
 2. Due to the linear nature of the internal tide, the modelled near seabed current speeds and the associated scale of motions, it is suggested that the passing of the internal tide over the submarine pipelines will not increase the turbulent motions within the bottom boundary layer and therefore have no affect on pipeline stability.
2. Reviewers Comment: *The logarithmic bottom velocity profile, roughness scales and other complexities of the BBL require a particular form of model, which is not included in this study. The omission of the BBL as significant processes in the model is reasonable in view of the application. However the report would be enhanced if the BBL is identified as physical process and its significance with respect to benthic habitat discussed particularly in relation to the dispersion of drill cuttings, or heavier than water substances.*

DHI Reply: DHI omitted from the report references to the bottom boundary layer dynamics (BBL) as motions on these scales are not resolved by the model. Although DHI acknowledges the role of the BBL dynamics in the near seabed circulation, we consider the tides to be the dominant forcing mechanism and any turbulent mixing within the BBL to be a secondary process in the movement of drill cuttings. The model's primary application was to resolve the tidally induced flow field throughout the water column focusing on the circulation dynamics in the upper water column.

3. Reviewers Comment: *The seasonal longshore drift should be estimated from measurements. If present, the measured drift should be compared with relevant MIKE 3 model longshore drift.*

DHI Reply: Alongshore flows/drift is either driven by the wind or by the setup of large scale horizontal density gradients that is setup by the pooling of warm low salinity Pacific Ocean waters off the Kimberley coast through the Indonesian Archipelago. These currents can advect coherent fluid masses over large distances (Fig. 1) and therefore their influence on the dispersion of contaminants cannot be ignored.

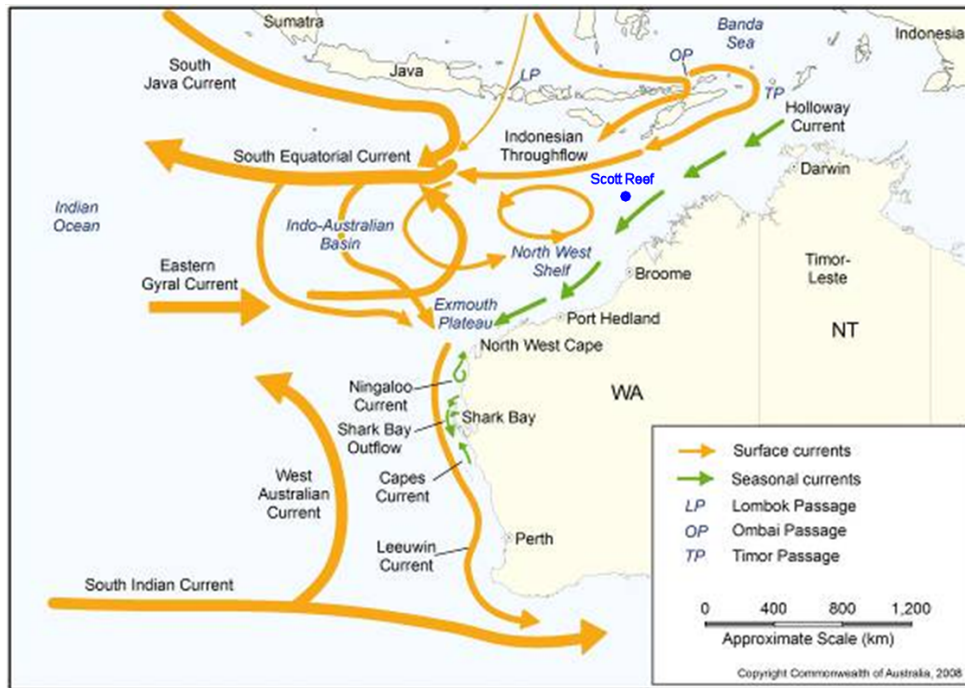


Fig 1: From “The North-west Marine Bioregional Plan, Bioregional Profile, A Description of the Ecosystems, Conservation Values and Uses of the North-west Marine Region, Department of the Environment, Water, Heritage and the Arts, 2008”

Discussing each flow type separately:

1. Comparing the MIKE3 model’s performance (for January 2007 and July 2007) with that of the BOM/CSIRO’s BLUElink model solution shows that the MIKE3 solution reproduces the magnitude and direction of the wind-driven north-going and south-going currents.
2. If we now consider the density driven low frequency flows. As suggested by the reviewer, the boundary forcing of the MIKE3 solution does not include the existence of these flows and therefore limits the model’s applicability to any contaminant modelling within the Browse Basin. For this reason a second hydrodynamic (HD) model specifically designed for spill trajectory modelling was developed. The HD model was run for a single year, September 2008 to August 2009 and validated against DSP’s AWAC field deployment sites. The HD model was forced solely by the tides. Wind forcing and seasonal and inter-annual variability of the surface velocity field is introduced through the addition of the daily averaged velocity components from the BLUElink solution. The BLUElink solution is a wind driven global circulation model that does not include the tides. The one-way coupling of the models ensures that the three main driving mechanisms in spill trajectory modeling have been

incorporated i.e. tides, winds and the low frequency density driven flows. The coupling will be achieved by the vector addition of the surface profile of the daily averaged U and V velocity components from BLUElink global circulation model to the surface velocity profile of the MIKE CLASSIC 2D tidal model of the region.

To ensure we simulate the influence of the inter-annual variability, possibly linked to the ENSO cycle, two year long simulations were run. The first simulation was forced by a strong La Nina ENSO event and the second forced by an extreme El Niño pattern. La Nina is the warming of tropical waters enhances the alongshore density gradient between the waters of the Indonesian Archipelago and those off Australia's North West coastline, enhancing response in the regional scale oceanographic currents. The El Niño pattern is a state where the tropical waters to the North of Australia cool and setup a weakened alongshore density gradient reducing the response in the regional scale currents.

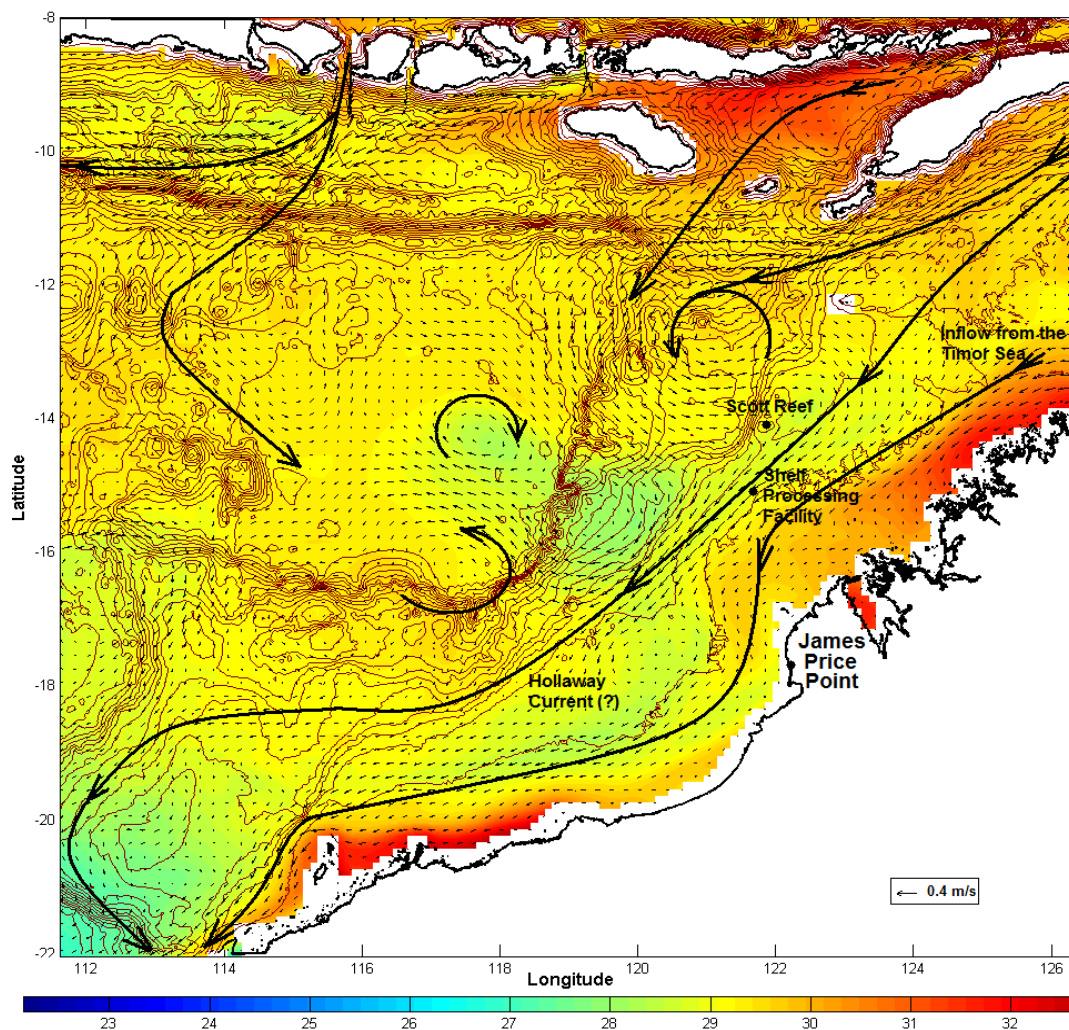


Fig 2: A three year summer average (January February) of the non tidally driven mean flow characteristics off Australia's North West coast.

Incorporating both these ENSO patterns ensures we simulate the two extreme global scale processes that drive the setup and inter-annual variability of the large scale regional flows off Australia's North West coast. An example of this can be seen in Fig. 2.3 which shows the

mean flow field over three years for January and February extracted from the Bluelink ReAnalysis (BRAN) v2.1 model solution and shows strong spatial variability consisting of meandering currents and eddies.

Reviewers Comment: *It is likely that eddies shed are present in the lee of Scott Reef, in presence of strong tidal currents. If these types of eddies are present it may be possible for discharges to circulate around an eddy and travel back to the reef coming into contact with the sensitive fringing corals of Scott Reef. It is recommended that: further analysis of the moored current meter data for longshore south west seasonal drift be undertaken and compared with model simulations; and an examination of the measurements and model simulations for eddies shed in the lee of Scott Reef be undertaken to confirm the significance, or otherwise, of these processes.*

DHI Reply: Although not discussed in the report the model solution reproduces the eddying features shed along the eastern boundary of South Scott Reef and therefore the eddy induced migration of contaminants will be well represented in the model. It is suspected the eddy features are generated by topographically induced horizontal shear and appear to direct the circulation along the eastern extent of the south Scott Reef lagoon (Fig. 3).

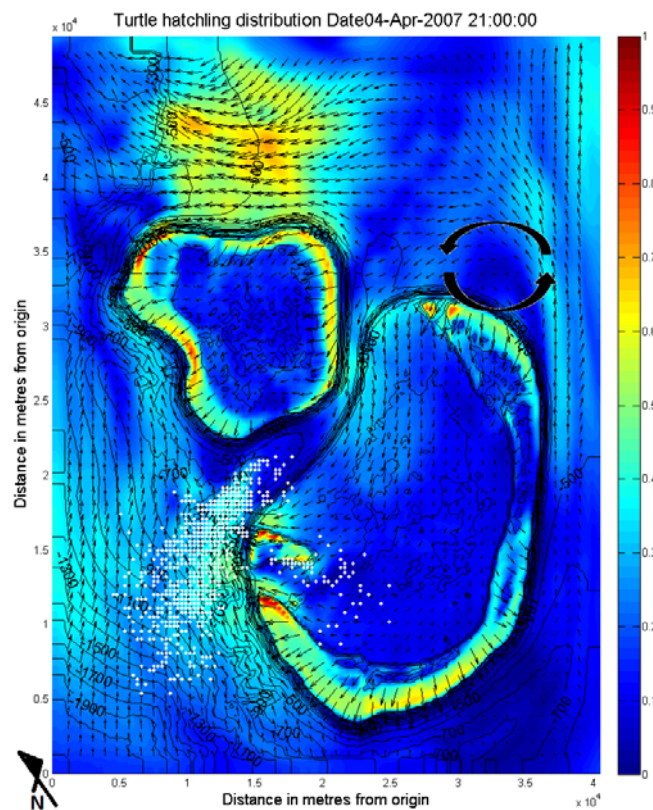


Fig. 3: A snapshot in time of the tidally induced circulation around Scott Reef. An eddying structure has formed along the eastern edge of South Scott Reef.